ISSI

Period.

VOL. 546 NOS. 1 + 2 JUNE 21,

COMPLETE IN ONE ISSUE

Int. Ion Chromatography Symp. 1990
San Diego, CA, Sept. 30–Oct. 3, 1990

JOURNAL OF CHROMATOGRAPHY

INCLUDING ELECTROPHORESIS AND OTHER SEPARATION METHODS

SYMPOSIUM VOLUMES

ELSEVIER

Scope. The *Journal of Chromatography* publishes papers on all aspects of chromatography, electrophoresis and related methods. Contributions consist mainly of research papers dealing with chromatographic theory, instrumental development and their applications. The section *Biomedical Applications*, which is under separate editorship, deals with the following aspects: developments in and applications of chromatographic and electrophoretic techniques related to clinical diagnosis or alterations during medical treatment; screening and profiling of body fluids or tissues with special reference to metabolic disorders; results from basic medical research with direct consequences in clinical practice; drug level monitoring and pharmacokinetic studies; clinical toxicology; analytical studies in occupational medicine.

Submission of Papers. Manuscripts (in English; *four* copies are required) should be submitted to: Editorial Office of *Journal of Chromatography*, P.O. Box 681, 1000 AR Amsterdam, The Netherlands, Telefax (+31-20) 5862 304, or to: The Editor of *Journal of Chromatography, Biomedical Applications*, P.O. Box 681, 1000 AR Amsterdam, The Netherlands. Review articles are invited or proposed by letter to the Editors. An outline of the proposed review should first be forwarded to the Editors for preliminary discussion prior to preparation. Submission of an article is understood to imply that the article is original and unpublished and is not being considered for publication elsewhere. For copyright regulations, see below.

Publication. The *Journal of Chromatography* (incl. *Biomedical Applications*) has 38 volumes in 1991. The subscription prices for 1991 are:

J. Chromatogr. (incl. *Cum. Indexes, Vols. 501–550*) + *Biomed. Appl.* (Vols. 535–572):
Dfl. 7220.00 plus Dfl. 1140.00 (p.p.h.) (total *ca.* US$ 4519.00)

J. Chromatogr. (incl. *Cum. Indexes, Vols. 501–550*) only (Vols. 535–561):
Dfl. 5859.00 plus Dfl. 810.00 (p.p.h.) (total *ca.* US$ 3604.75)

Biomed. Appl. only (Vols. 562–572):
Dfl. 2387.00 plus Dfl. 330.00 (p.p.h.) (total *ca.* US$ 1468.75).

Subscription Orders. The Dutch guilder price is definitive. The US$ price is subject to exchange-rate fluctuations and is given as a guide. Subscriptions are accepted on a prepaid basis only, unless different terms have been previously agreed upon. Subscription orders can be entered only by calender year (Jan.–Dec.) and should be sent to Elsevier Science Publishers, Journal Department, P.O. Box 211, 1000 AE Amsterdam, The Netherlands, Tel. (+31-20) 5803 642, Telefax (+31-20) 5803 598, or to your usual subscription agent. Postage and handling charges include surface delivery except to the following countries where air delivery via SAL (Surface Air Lift) mail is ensured: Argentina, Australia, Brazil, Canada, Hong Kong, India, Israel, Japan*, Malaysia, Mexico, New Zealand, Pakistan, PR China, Singapore, South Africa, South Korea, Taiwan, Thailand, USA. * For Japan air delivery (SAL) requires 50% additional charge of the normal postage and handling charge. For all other countries airmail rates are available upon request. Claims for missing issues must be made within three months of our publication (mailing) date, otherwise such claims cannot be honoured free of charge. Back volumes of the *Journal of Chromatography* (Vols. 1–534) are available at Dfl. 208.00 (plus postage). Customers in the USA and Canada wishing information on this and other Elsevier journals, please contact Journal Information Center, Elsevier Science Publishing Co. Inc., 655 Avenue of the Americas, New York, NY 10010, USA, Tel. (+1-212) 633 3750, Telefax (+1-212) 633 3990.

Abstracts/Contents Lists published in Analytical Abstracts, Biochemical Abstracts, Biological Abstracts, Chemical Abstracts, Chemical Titles, Chromatography Abstracts, Clinical Chemistry Lookout, Current Contents/Life Sciences, Current Contents/Physical, Chemical & Earth Sciences, Deep-Sea Research/Part B: Oceanographic Literature Review, Excerpta Medica, Index Medicus, Mass Spectrometry Bulletin, PASCAL-CNRS, Pharmaceutical Abstracts, Referativnyi Zhurnal, Research Alert, Science Citation Index and Trends in Biotechnology.

See inside back cover for Publication Schedule, Information for Authors and information on Advertisements.

0021-9673/91/$03.50

Printed in The Netherlands

For Contents see p. VII

FOR ADVERTISING INFORMATION PLEASE CONTACT OUR ADVERTISING REPRESENTATIVES

USA/CANADA

Weston Media Associates
Mr. Daniel S. Lipner
P.O. Box 1110, GREENS FARMS, CT 06436-1110
Tel: (203) 261-2500, Fax: (203) 261-0101

GREAT BRITAIN

T.G. Scott & Son Ltd.
Tim Blake
Portland House, 21 Narborough Road
COSBY, Leicestershire LE9 5TA
Tel: (0533) 753-333, Fax: (0533) 750-522

Mr. M. White or Mrs. A. Curtis
30-32 Southampton Street, LONDON WC2E 7HR
Tel: (071) 240 2032, Fax: (071) 379 7155,
Telex: 299181 adsale/g

JAPAN

ESP - Tokyo Branch
Mr. S. Onoda
20-12 Yushima, 3 chome, Bunkyo-Ku
TOKYO 113
Tel: (03) 3836 0810, Fax: (03) 3839-4344
Telex: 02657617

REST OF WORLD

ELSEVIER SCIENCE PUBLISHERS
Ms. W. van Cattenburch
P.O. Box 211, 1000 AE AMSTERDAM,
The Netherlands
Tel: (20) 515.3220/21/22, Telex: 16479 els vi nl
Fax: (20) 683.3041

Selective Sample Handling and Detection in High-Performance Liquid Chromatography

Journal of Chromatography Library, 39

part A

edited by **R.W. Frei†**, *Free University, Amsterdam, The Netherlands, and* **K. Zech**, *Byk Gulden Pharmaceuticals, Konstanz, FRG*

Part A of this two-volume project attempts to treat the sample handling and detection processes in a liquid chromatographic system in an integrated fashion. The need for more selective and sensitive chromatographic methods to help solve the numerous trace analysis problems in complex samples is undisputed. However, few workers realize the strong interdependence of the various steps - sample handling, separation and detection - which must be considered if one wants to arrive at an optimal solution. By introducing a strong element of selectivity and trace enrich- ment in the sample preparation step, fewer demands are placed on the quality of the chromatography and often a simple UV detector can be used. By using a selective detection mode, i.e. a reaction detector, the sample handling step can frequently be simplified and more easily automated. The impact of such a "total system" approach on handling series of highly complex samples such as environmental specimens or biological fluids can be easily imagined.

1988 xii + 458 pages
US$ 123.00 / Dfl. 240.00
ISBN 0-444-42881-X

part B

edited by **K. Zech**, *Byk Gulden Pharmaceuticals, Konstanz, FRG, and* **R.W. Frei†**, *Free University, Amsterdam, The Netherlands*

Part B completes the treatment of the handling, separation and detection of complex samples as an integrated, interconnected process. On the basis of this philosophy the editors have selected those contributions which demonstrate that optimal sample preparation leads to a simplification of detection or reduced demands on the separation process. Throughout the book emphasis is on chemical principles with minimum discussion of the equipment required - an approach which reflects the editors' view that the limiting factor in the analysis of complex samples is an incomplete knowledge of the underlying chemistry rather than the hardware available. This lack of knowledge becomes more evident as the demands for lower detection limits grow, as solving complex matrix problems requires a greater understanding of the chemical interaction between the substance to be analysed and the stationary phase.

1989 xii + 394 pages
US$ 136.00 / Dfl. 265.00
ISBN 0-444-88327-4

Written by experienced practitioners, these volumes will be of interest to investigators in many areas of application, including environmental scientists and those active in the clinical, pharmaceutical and bioanalytical fields.

For more information, please write to:

Elsevier Science Publishers
P.O. Box 211, 1000 AE Amsterdam, The Netherlands
P.O. Box 882, Madison Square Station, New York, NY 10159, USA

(Data Handling in Science and Technology, 5)

PCs for Chemists

edited by: **J. Zupan**, *University of Ljubljana, Yugoslavia*

PCs for Chemists is a handbook on how, when and with what kind of software a chemist should use a PC. Being a beginners' guide, it does not require any specific knowledge about computers. The book covers word processors, spreadsheets, compilers and databases for chemical applications, and it comprises ten contributions each describing one or two different applications and a suggestion for the best choice. Information on how a PC can be linked to instruments, other computers and data networks is also provided.

PCs for Chemists should prove invaluable for all courses covering computer applications to chemistry, pharmacy, biology, and metallurgy.

1990 xvi + 212 pages
Price: US$ 100.00 / Dfl. 195.00
ISBN 0-444-88623-0

Contents:

ELSEVIER SCIENCE PUBLISHERS

P.O. Box 211, 1000 AE Amsterdam, The Netherlands
P.O. Box 882, Madison Square Station, New York, NY 10159, USA

JOURNAL OF CHROMATOGRAPHY

VOL. 546 (1991)

JOURNAL of CHROMATOGRAPHY

INCLUDING ELECTROPHORESIS AND OTHER SEPARATION METHODS

SYMPOSIUM VOLUMES

ELSEVIER
AMSTERDAM — OXFORD — NEW YORK — TOKYO

J. Chromatogr., Vol. 546 (1991)

San Diego: Hotel del Coronado, Eastern view, main entrance

0021-9673/91/$03.50

Printed in The Netherlands

SYMPOSIUM VOLUME

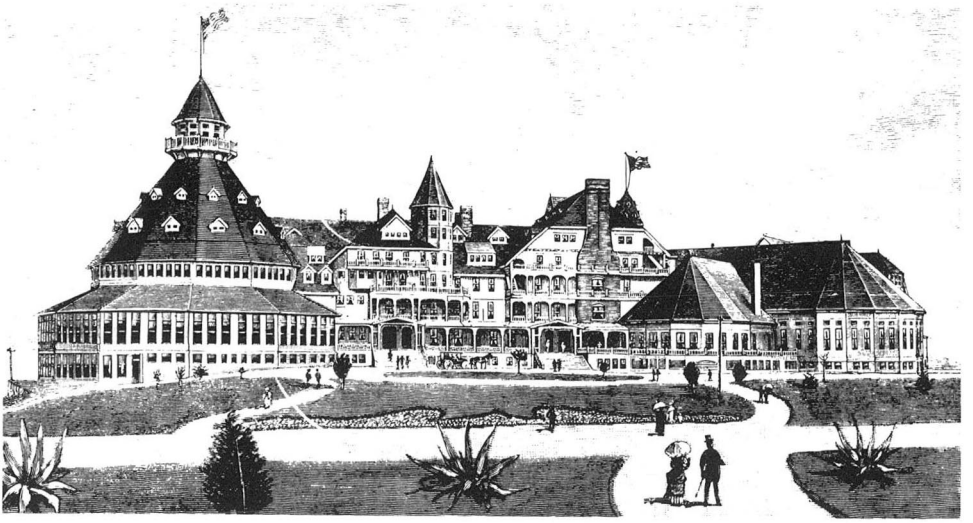

INTERNATIONAL ION CHROMATOGRAPHY SYMPOSIUM 1990

San Diego, CA (U.S.A.), September 30–October 3, 1990

Guest Editor

PAUL R. HADDAD

(Kensington)

VOL. 546, NOS. 1+2 JOURNAL OF CHROMATOGRAPHY JUNE 21, 1991

CONTENTS

INTERNATIONAL ION CHROMATOGRAPHY SYMPOSIUM 1990, SAN DIEGO, CA, SEPTEMBER 30–OCTOBER 3, 1990

In articles with more than one author, the name of the author to whom correspondence should be addressed is indicated in the article heading by a 6-pointed asterisk (*)

Journal of Chromatography, 546 (1991) I
Elsevier Science Publishers B.V., Amsterdam

FOREWORD

The *International Ion Chromatography Symposium 1990* (IICS '90) was held at the historic and beautiful Hotel del Coronado in Coronado, CA, U.S.A. from 1–3 October, 1990. IICS '90 was the largest meeting on ion chromatography (IC) yet held and was attended by over 250 scientists from 13 countries and featured 65 oral presentations and 20 posters. In the past, a number of smaller IC conference series have been offered, including the Sils-Maria meetings organized by the late Professor Roland Frei, the Ion Chromatography Forums held in Boston, and other regional meetings. IICS '90 arose as an amalgamation of these conferences and was designed to be a focus meeting for ion chromatographers by bringing together the world leaders in the field and by offering a comprehensive coverage of all aspects of the technique.

The symposium opened with a plenary lecture by Dr. Hamish Small, who presented a personal account of the historical development of IC. The remainder of the symposium agenda was organized around nine session topics, which included detection, stationary phases and separations, sample handling methods, ion-exclusion chromatography, gradient elution, post-column reaction detection, and applications. One novel feature of the technical program was the dedication of a session to the area of inorganic capillary electrophoresis. The scientific sessions were opened with review lectures presented by internationally renowned experts in IC.

A highlight of the meeting was the recognition of two scientists for their outstanding contributions to the development of the methodology of IC. The recipients of achievement awards were Dr. Petr Jandik, Manager of Ion Analysis R&D at the Waters Chromatography Division of Millipore, and Dr. Christopher Pohl, Technical Director of Polymer Chemistry at Dionex Corporation. Dr. Jandik presented a keynote lecture on "Optimization of detection sensitivity in the capillary electrophoresis of inorganic ions", whilst Dr. Pohl gave a keynote lecture on "Development of moderate capacity pellicular ion-exchange packing materials for ion chromatography".

IICS '90 was a highly successful and stimulating meeting, due chiefly to the originality and quality of the technical presentations and the lively contributions of other participants. I would like to thank the members of the scientific committee (G. K. Bonn, R. M. Cassidy, J. S. Fritz, D. T. Gjerde, P. Jandik, J. D. Lamb, D. J. Pietrzyk, G. Schmuckler, H. Small and J. R. Stillian) for their valuable contributions to the design of the symposium. Special thanks are also due to Janet Strimaitis of Century International for the superb organization of the meeting, and to Dr. Erich Heftmann of the *Journal of Chromatography* for his meticulous efforts in editing the proceedings volume. On behalf of all attendees of the symposium, I would also like to express my appreciation to the joint corporate sponsors, Dionex Corporation and Waters Chromatography Division of Millipore, for the provision of financial support. We look forward to IICS '91, to be held in the Denver area under the chairmanship of John D. Lamb of Brigham Young University.

Kensington, Sydney (Australia)

PAUL R. HADDAD
Symposium Chairman

Journal of Chromatography, 546 (1991) 3–15
Elsevier Science Publishers B.V., Amsterdam

CHROMSYMP. 2124

Review

Twenty years of ion chromatography

HAMISH SMALL
4176 Oxford Drive, Leland, MI 49654 (U.S.A.)

ABSTRACT

This historical account of the development of ion chromatography traces the evolution of conductometric detection, shows how its problems created the need for new ion exchangers, describes how these materials were developed and relates how many of the innovations came from research that was unconnected to the original mission of extending chromatography to inorganic ions.

CONTENTS

1. INTRODUCTION

In the twenty or so years that encompass its birth and development, ion chromatography (IC) has undergone enormous changes. In its earliest embodiments IC was focused primarily on the analysis of inorganic ions; it used ion exchange to separate the ions and conductometric monitoring to detect them. Today IC has a much wider scope. It now has an important role in the analysis of organic ions as well as inorganic, it employs several separation modes besides ion exchange, and although conductometric detection is still a particularly versatile tool it is nowadays augmented with a variety of other detection methods. IC has undergone such an expansion in the past twenty years that to cover all of its aspects adequately in the alloted space and time is impossible. Fortunately, much of the task is in the capable hands of the various reviewers in the symposium so I will confine my remarks to just two topics: the evolution of conductometric detection and the development of stationary phases for IC. The technical background to these areas has received abundant discussion in many books and publications [1,2] and is by now familiar to most of the attendees. My purpose here is not to repeat much of what has already been said but rather to give an

0021-9673/91/$03.50

account of some of the historical background to the development of IC and to show how some serendipitous events played an important role. And to illustrate the tempo of development I will provide some benchmarks of progress from those early days to the present time.

2. THE EVOLUTION OF CONDUCTOMETRIC DETECTION

Those familiar with the development of chromatography will be aware that in the early seventies chromatography was firmly entrenched in organic analysis. Gas chromatography was by then a mature technique and liquid chromatography was beginning to show its great potential for those organics beyond the capabilities of gas chromatography. In contrast, the impact of chromatography in inorganic analysis was comparatively slight even though the existing methods for a great number of common and important inorganic species were often relatively insensitive, non-selective and invariably laborious and time consuming.

I had joined Dow in the Physical Research Laboratory in 1955 and during the late fifties and through the late sixties a small number of us talked frequently, and often wistfully, of extending chromatography to inorganic analysis. By the early seventies we were aware of the power of ion exchange to separate ions but recognized a major barrier to applying this in a broadly analytical way, namely, the inability in many instances to provide prompt detection of ions in the column effluent. Progress in the liquid chromatography of organic species was convenienced by their being UV absorbers in many cases. In contrast, many inorganic ions were transparent to UV and were not thought at that time to be detectable by the widely used spectrophotometers. The alkali and alkaline earth metal ions, the ammonium ion, and a great many inorganic anions such as the halides, sulfate, sulfite, nitrate, nitrite, phosphate and carbonate, etc., were just a few examples of these "problematical" ions.

One of our early attempts to solve the detection problem, while it had a very limited scope, is worth mentioning because it had an interesting sequel. In working with hydrodynamic chromatography I had become very aware of the exceptional sensitivity of spectrophotometers in detecting colloidal dispersions. So I devised a method of analysis for halides and "pseudo" halides such as thiocyanate that involved their separation by anion exchange and their photometric detection following post-column precipitation with silver nitrate. The first attempts used the high capacity anion exchanger Dowex 1 and the separation was lengthy and inefficient. Many years later when low-capacity resins became available we were able to obtain good chromatograms such as illustrated in Fig. 1. It was while doing some routine evaluation of this method for the determination of chromate ion, which is also precipitated by silver nitrate, that the idea occurred of employing chromate ion as a displacing ion in anion-exchange chromatography and using the UV detector to reveal the deficiencies in the chromate ion as non-UV-absorbing ions were eluted. This of course was the beginning of what we went on to call indirect photometric detection [3].

Besides turbidimetric detection there were other schemes that we considered from time to time but they too were usually hampered by having a rather limited range of applicability. But one property of ions that stood out as having special appeal was electrical conductivity; it was a property of all ions in solution and it was anticipated

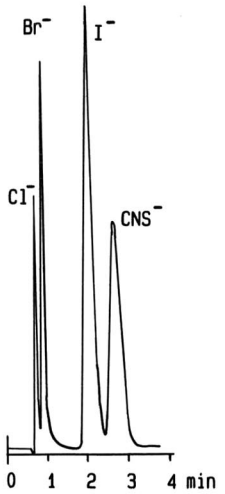

Fig. 1. Ion chromatographic separation of anions with turbidimetric detection. Stationary phase: pellicular anion-exchange resin. Eluent: 0.1 *M* sodium nitrate. Post-column precipitation with 0.01 *M* silver nitrate with gelatin. Detection: UV spectrophotometer at 280 nm.

that a conductivity detector ought to be fairly simple to fabricate and reliable in operation. But ion-exchange separation required that we use electrolytes as eluents and we were concerned that the uncertainty or noise in the very conducting background might obscure the oftentimes slight perturbations in conductivity due to the analyte species. It was to get around this problem of background noise that my colleague Bill Bauman and myself came up with the innovation that became known as "eluent suppression". For more details on the events leading up to the invention I refer readers to an earlier account [4].

The first demonstration of eluent suppression involved the separation of the three alkali metal ions lithium, sodium and potassium. It was carried out on a low-capacity cation exchanger followed by a bed of Dowex 1 in the hydroxide form to remove the hydrochloric acid eluent and convert the metal ions to their respective hydroxides. The effluent from the suppressor column, or as we called it in those days the stripper, then passed to a conductivity cell which monitored the analyte hydroxide peaks as they eluted. Fig. 2 is a photograph of this first ion chromatogram. The capacity of the separator bed was much higher than was necessary and the chromatogram took over two hours to develop but the separation was excellent, sensitivity of detection was good and we had successfully demonstrated that the concept worked. Since this is an historical account it is appropriate to mention that this occurred on November 9th, 1971.

A few days later we had demonstrated that the new technique worked also for anions (Fig. 3) but with an interesting twist in that a membrane suppressor was used to remove the sodium hydroxide eluent. Some years prior to this, while pursuing the idea of Donnan dialysis as a means of extracting magnesium out of seawater, I had developed hollow tubular cation-exchange membranes by sulfonating polyethylene surgical tubing. In the first anion separation I tried the idea of continuously

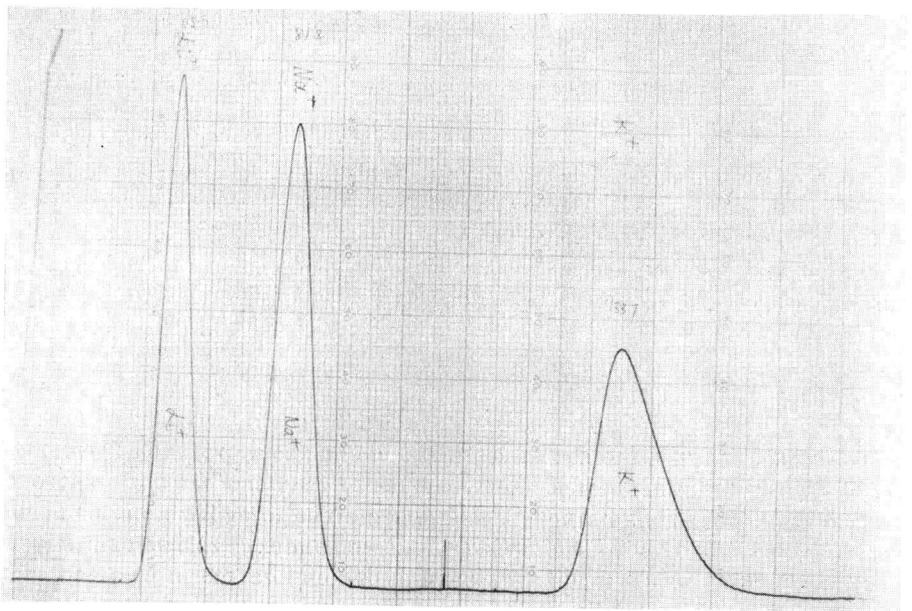

Fig. 2. First ion chromatogram using suppressed conductometric detection. Separation of cations on a surface sulfonated separator column followed by a strong base resin in the hydroxide form and conductometric detection.

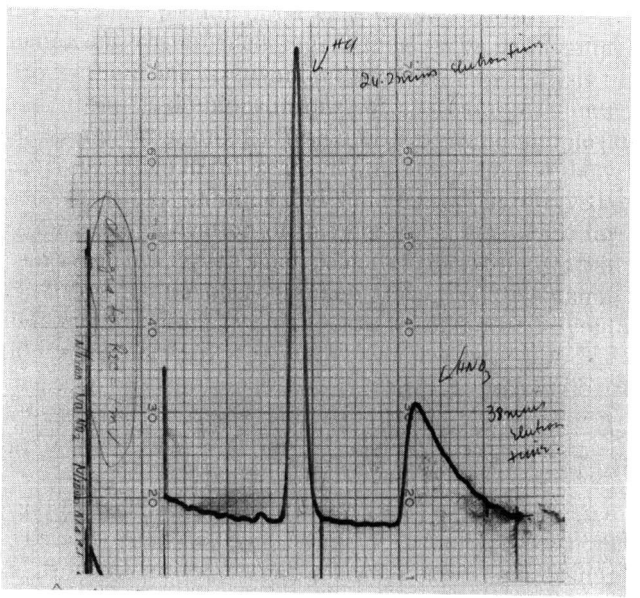

Fig. 3. First ion chromatogram of an anion separation using suppressed conductometric detection. Stationary phase: surface agglomerated anion exchanger. Tubular membrane suppressor. Conductometric detection.

suppressing eluent by allowing the effluent from the separator bed to flow down one of these sulfonated tubes that was immersed in a bath of acid. The acid was actually a stirred suspension of Dowex 50 cation-exchange resin in the hydrogen form which provided hydronium ions through "bumping" contacts with the membrane. I had considered simply using a solution of a mineral acid exterior to the tubular membrane but was concerned about acid leakage into the lumen of the fiber. This perfectly non-diffusible "solid" acid eliminated that problem. These membrane devices were very effective in removing the sodium hydroxide in anion analysis but their relatively large void volume impaired efficiency and they tended to burst under mild excess pressure. In subsequent work we used column suppressors since the resin packings were readily available, the beds were easier to prepare in a reproducible fashion and did not have the pressure limitations of the membrane devices. The idea of continuous membrane suppressors lay dormant for a time but was revived in later years when problems with column suppressors became critical [5].

Tim Stevens joined our project in early 1972 to explore the potential of the new technique for routine ion analysis. In a relatively short time Tim had achieved significant reductions in run times and had explored a variety of applications for alkali metals and ammonia analysis on some real world samples such as urine, blood serum, etc. Alkaline earth ions proved problematical for the hydronium ion based eluents and we developed the silver nitrate eluent system for these more intractable ions. Sometime around the middle of 1972 Tim had done enough to convince the analytical people that the technique had promise and he left our lab to pursue development of IC in an analytical-laboratory environment.

From the earliest tests on anion analysis it had become apparent that some major modification was necessary if one wished to extend the technique to a wide range of anions which would include those that were tightly bound to anion exchangers. For example, in these early attempts we were never able to elute anions like iodide or phosphate from the columns using sodium hydroxide as eluent. So in late 1972 we set about exploring the idea of using more potent displacing ions than hydroxide.

For an eluent to be suitable, in addition to having favorable displacing power, it had to be amenable to suppression. This considerably limited our choice but on examining a selection of ions and their anion-exchange affinity coefficients relative to the hydroxide ion, phenate looked like a good candidate. It had a high affinity and it formed a very weak acid in the suppressor. Originally we considered removing the phenol entirely by passing the effluent from the resin bed through yet another bed of charcoal but we never adopted the idea. We established elution conditions using the phenate eluent and carried out several separations that showed it to be greatly superior to the hydroxide system. It was our workhorse eluent for quite a time and was used for a great deal of anion analysis. Nowadays phenate eluents are rarely used having been displaced by the more versatile and acceptable carbonate system. Carbonate-based eluents were discovered in an interesting way.

When we were developing low-capacity resins for anion analysis we had among our tests one in which we measured the separation of chloride and bromide using sodium hydroxide as eluent. Depending on the resin's capacity, which varied over a wide range, we used one or other of two eluents —0.01 *M* and 0.05 *M* sodium hydroxide. We were bewildered at first on finding that the weaker solution was just as effective as the stronger in displacing chloride and bromide. In solving the mystery, we

got our major clue when it became apparent that the 0.01 *M* solution could have become contaminated by absorbing carbon dioxide from the air while the more concentrated eluent happened to be much better protected from such contamination. The unusual potency of the more dilute eluent was proved to be due to the superior displacing power of the divalent carbonate ion that it contained. This happy accident set us on the way to a systematic study of the carbonate–bicarbonate eluent system and its eventual adoption as the eluent of choice for anion analysis by suppressed IC.

Fig. 4 represents the state of the art for anion analysis in 1975. That was a landmark year for IC; following a licensing agreement with Dow, Dionex launched its commercial development of the technique by exhibiting the first IC instrument at the fall ACS meeting in Chicago and we simultaneously published the first paper on the new technique [6]. In the years immediately following, Dionex in collaboration with its customers established the market for IC, often in areas that could not be foreseen by the original inventors. This combination of invention and marketing changed the face of inorganic ion analysis and much of organic ion analysis as well, for now instruments were available that could determine a wide diversity of ions with a speed and sensitivity that had been unattainable by the older classical methods of analysis.

As the market for IC grew, so also did alternative methods. The separation and conductometric detection of ions without the use of a suppressor was first reported in 1979 [7,8]. Subsequently, Fritz and co-workers published a series of papers and a monograph describing the new method and prescribing conditions for its application to the analysis of both cation and anion mixtures. In the non-suppressed approach, or single-column ion chromatography (SCIC) as it was originally termed, detection depends, in the first place, on their being a significant difference in conductivity between the eluting analyte ions and the prevailing eluent ions. Sensitivity of detection

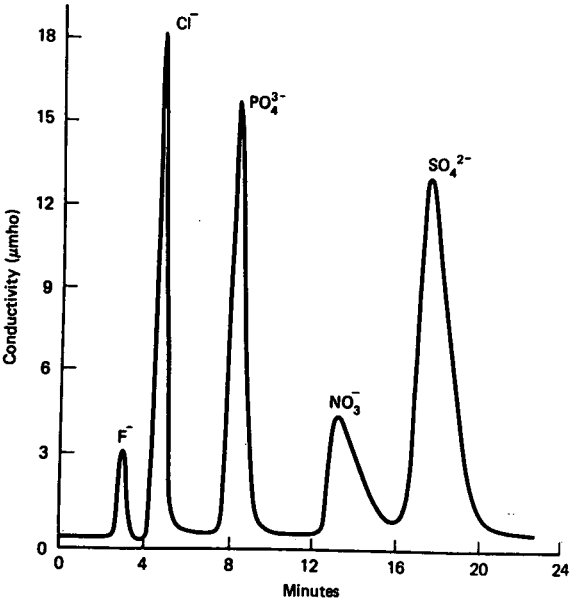

Fig. 4. Example of state-of-the-art ion chromatography *ca.* 1975.

hinges on how the perturbation of the ambient conductivity by the analyte stands out against the prevailing noise on the background conductivity. To reduce the effect of noise, the practitioners of non-suppressed IC adopted low-capacity ion exchangers and low concentration eluents. They also noted that the requirements of low eluent concentration and adequate displacing power could be more easily met if they used potent displacing ions. Organic acid ions such as benzoate, phthalate and sulfobenzoate had this property and had conductances that differed significantly from those of common inorganic analyte ions that were the focus of their interest. Choosing among the various eluents was influenced principally by the affinities of the analyte species, benzoate being preferred for mixtures such as acetate, bicarbonate, fluoride, chloride, etc. Divalent analytes and other intractable ions were more effectively eluted by phthalate or sulfobenzoate containing eluents. Analogous schemes were developed for cation analysis.

Shortly after publication of the non-suppressed approach in 1979 commercialization of the technique began, first by the Wescan Company and later by Waters, Shimadzu, Metrohm and others. At about the same time there was an evolutionary change in the meaning of the term "ion chromatography". Previously it had been applied solely to the eluent suppression technique, but with the increasing prominence of other techniques for the chromatography of ions, the name, logically, and happily, came to embrace a much wider range of methods. Nowadays the term "ion chromatography" includes any chromatographic method applied to the determination of ions.

The appearance of non-suppressed IC as well as providing an alternative way to using conductometric detection also ignited the "great debate" as to which of the two conductometric modes was the superior. For my most recent comments on the matter I refer the reader to my book on IC [1].

While column-based suppressors were employed in the earliest commercial IC instruments and many applications developed around their use, they suffered from a number of drawbacks; the interruptions to regenerate, the drifting of certain analyte peaks as the suppressor exhausted, reduced response of some species such as nitrite and the additional void volume of the second column detracted significantly from the efficiency of the newer separators. There were sufficient arguments therefore for developing an alternative means of suppression that would remove or at least minimize these undesirable effects. In the late seventies when the drawbacks of column suppressors were becoming more acute, the tubular membrane concept that had been set aside in the early days of IC was revived and developed to provide much more robust and practical devices.

The first of these new devices [5] employed a bundle of fibers in a tube and shell arrangement. They were somewhat more detrimental to efficiency than a typical column suppressor but they eliminated most of the other problems. In a later embodiment of the hollow fiber approach a single fiber was used with its lumen packed with inert polymer spheres of styrene–divinylbenzene copolymer [9]. These tiny beads essentially formed a necklace inside the lumen and led to two beneficial effects; they reduced the void volume and hence bandspreading contributed by the suppressor and they improved mass transfer within the lumen so that shorter lengths of device could supply the requisite amount of suppression. As a result of these developments, column suppressors were gradually phased out of commercial suppressed IC instruments to be replaced by both anion and cation versions of the packed hollow fiber design.

In late 1985 Dionex introduced another significant improvement in suppressor design [10]. This too was a membrane device operating under the same principles as the original, but with markedly improved suppression capacity and reduced void volume. It employed two flat membranes with effluent from the separator flowing between the membranes and regenerant flowing in the two spaces outside of the membranes. The addition of sulfonated screens to the various fluid-carrying compartments reduced void volume and enhanced mass transfer in the solution phases. The use of this low-void-volume suppressor led to notable improvements in overall efficiency but even more remarkable was its greatly improved suppression capacity, so much so that it could cope with relatively very high concentrations of sodium hydroxide and enable separations such as exemplified by Fig. 5. This is in marked contrast to the very earliest attempts to use sodium hydroxide eluents when even orthophosphate was inaccessible. This high suppression capacity also opened the door to gradient elution for the conductometric mode of IC and enabled chromatography such as is illustrated in Fig. 6.

In the continuing evolution of the suppressor technique, two very recent developments are worthy of note. Gjerde and Benson [11] have used post-separator addition of finely divided cation exchanger in the hydronium form to suppress carbonate eluents to carbonic acid. The finely divided sodium form resin particles are carried into the conductivity cell but contribute little to the overall conductivity in keeping with our understanding of the conductance of conducting particles suspended in a conducting medium [12]. In the other development, Slingsby *et al.* [13] have just recently extended the application of suppressors beyond conductometric detection. They have used a suppressor to modify eluents in order to make them more acceptable for injection into a mass spectrometer.

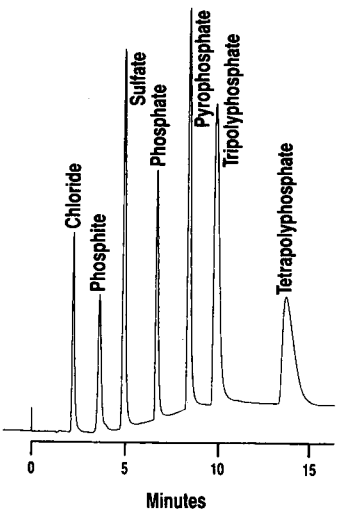

Fig. 5. Ion chromatography of anions using micromembrane suppressor. Courtesy Dionex Corporation.

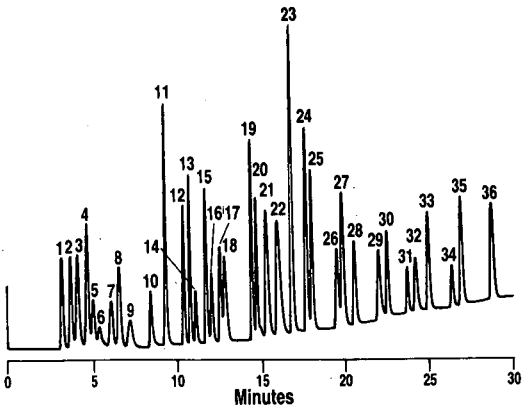

Fig. 6. Gradient elution of inorganic and organic anions on a pellicular anion-exchange resin. Eluent: gradient of 0.75 m*M* to 100 m*M* sodium hydroxide. Detection: suppressed conductometric; anion micromembrane suppressor. All anions 10 ppm unless noted otherwise. Peaks: 1 = F^- (1.5 ppm); 2 = α-hydroxybutyrate; 3 = acetate; 4 = glycolate; 5 = butyrate; 6 = gluconate; 7 = α-hydroxyvalerate; 8 = formate (5 ppm); 9 = valerate; 10 = pyruvate; 11 = monochloroacetate; 12 = BrO_3^-; 13 = Cl^- (3 ppm); 14 = galacturonate; 15 = NO_2^- (5 ppm); 16 = glucuronate; 17 = dichloroacetate; 18 = trifluoroacetate; 19 = HPO_3^{2-}; 20 = SeO_3^{2-}; 21 = Br^-; 22 = NO_3^-; 23 = SO_4^{2-}; 24 = oxalate; 25 = SeO_4^{2-}; 26 = α-ketoglutarate; 27 = fumarate; 28 = phthalate; 29 = oxalacetate; 30 = PO_4^{3-}; 31 = AsO_4^{3-}; 32 = CrO_4^{2-}; 33 = citrate; 34 = isocitrate; 35 = *cis*-aconitate; 36 = *trans*-aconitate. Courtesy Dionex Corporation.

3. STATIONARY PHASES FOR ION CHROMATOGRAPHY

Of all the elements in a chromatographic system, the stationary phase is the key. It is the stationary phase that determines what separation mechanism is operative, what the composition of the mobile phase should be and often what detection methods may be appropriately applied. Ion-exchange resins are the most widely used stationary phase in IC at the present time. They are in most cases of the low-capacity pellicular type, they are polymer based and usually derivatives of cross-linked polystyrene. This part of the article will describe how these materials were developed and show how their evolution, at least in the early stages of IC, was closely entwined with the concurrent development of conductometric detection.

When we first considered the idea of eluent suppression, we proposed a model separation of alkali metals using a system comprising a column of Dowex 50 cation-exchange resin, followed by an approximately equal-sized bed of Dowex 44, a weak base resin, and terminating in a conductivity cell. The eluent would be hydrochloric acid which the Dowex 44 would remove, leaving the analytes as peaks of metal chlorides to be conductometrically detected in a background of essentially deionized water. There was however a serious problem with this particular approach that halted progress for some time. What we were proposing to do was radical for chromatography, that is add a second bed which would exhaust during use and require replacement or regeneration. Interruptions to perform this operation could clearly become a considerable drawback if they occurred too frequently and calculation revealed that this would be the case in the first system we proposed. An alternative was to use a very large suppressor column but that solution, for obvious reasons, was out of

the question. The idea that solved the problem was to use a resin in the separator with a much lower specific capacity than that in the suppressor. In this way the very small amounts of eluent required for separation would consume but a small fraction of the suppressor and permit the analysis of many samples per regeneration of the suppressor. So an early challenge in IC was how to prepare ion exchangers of requisitely low capacity.

Several years before the research on ion chromatography began, I had been exploring a concept that I called "gel–liquid extraction". It was a separation process that attempted to combine the selective chemistry of some solvent extraction systems with the superior efficiency of working in a chromatographic mode [14]. Accordingly I was swelling styrene–divinylbenzene copolymer beads with water immiscible organic extractants such as tributyl phosphate, packing them in columns and carrying out chromatographic separations using aqueous mobile phases. An aggravating property of these solvent-swollen, very hydrophobic beads was their tendency to aggregate into clusters when placed in an aqueous environment. Used in this way they packed very poorly into the columns and penalised the separation efficiency rather severely. I got around the problem by sulfonating a thin outer skin of the polymer bead leaving the mass of the core still available for swelling. Given this treatment, the beads, although swollen with solvent, gave the superficial appearance of being very hydrophilic and like an ion-exchange resin dispersed nicely when added to water. I had saved a quantity of this surface sulfonated resin from that earlier work and used it in the first cation separation (Fig. 2). Though the amount chosen was much larger than necessary, the size, capacity and crosslinking proved to be remarkably appropriate and this resin was subsequently used in a good deal of our early exploratory work.

Having demonstrated that the suppressed IC worked for cation analysis I was anxious to try the idea as soon as possible for inorganic anions for it was in this area that I anticipated it would have its greatest utility —there were other good methods, atomic absorption for example, that could be applied to inorganic cations but not to inorganic or organic anions. Anion exchangers of low capacity were available in 1971; they were being fairly widely used in high-performance liquid chromatography in conjunction with UV detectors to determine a wide range of organic ions. However, not working in an analytical laboratory I did not have immediate access to these materials and since I was very impatient to try out the idea I decided to try to prepare a resin myself. Furthermore I had doubts about the chemical stability of the commercial materials; they were based on silica and I was proposing to use them in very basic media. At first I thought of quaternizing a thin skin on the surface of the same styrene–divinylbenzene beads, analogously to the surface sulfonation procedure, but was deterred from doing this by not having any good ideas on how I might confine the ion-exchange functionality to a *sharp* surface zone (more on this point later). The solution that proved to be a very satisfactory one was again prompted by some work from many years prior on behavior that was peculiar to mixed-bed ion-exchange resins.

An old problem in mixed-bed resins was the tendency of the cation- and anion-exchange resins to clump together. It was problematical for two reasons; it gave poorly packed beds and when it was time to regenerate the resins they could be separated only with great difficulty. The experience of studying the clumping phenomenon and finding a successful means of counteracting it left me with an

appreciation of the tenacious way in which cationic and anionic materials hold together, so I took substrate cation-exchange particles and exposed them to a suspension of very finely divided anion-exchange particles. The substrate particles were actually the surface sulfonated beads I had used in cation analysis —superficial functionality was all that was necessary— and the finely divided anion exchanger was some ground up IRA 400, a Rohm & Haas resin. This was the resin used in the separation of Fig. 3. Thereafter we used a variety of finely ground Dowex anion-exchange resins of various functionalities and degrees of cross-linking but eventually this proved to be an unsatisfactory and non-reproducible source of the anion-exchange material and we abandoned it in favor of the emulsion polymerization synthesis of resins. In this process, vinyl benzyl chloride and divinylbenzene are copolymerized by emulsion techniques to yield particles anywhere from 0.01 to 1 μm in diameter. These particles are then derivatised to yield anion-exchanging particles by reacting with appropriate amines at which stage they are ready for electrostatic coupling with the cation exchange substrate to form what we termed "surface-agglomerated resins".

These resins have a number of advantages over other chromatographic materials, particularly those based on silica or glass. The pellicular nature of these materials provides for excellent mass transfer properties; the electrostatic attachment of the pellicle to its substrate and the polymeric nature of both assure chemical and physical stability, particularly in the high-pH aqueous environments where silica-based materials rapidly degrade. This method of preparing pellicular resins also provides a number of advantages. The fact that the substrate and the colloidal resin are distinctly separate entities until they are agglomerated, greatly facilitates the research and development of new materials. The process provides relatively facile means for controlling those properties of the colloidal resin that impinge on the selectivity and efficiency of the final column; the functionality and cross-linking of the resin and its particle size are the most important ones. The manufacture of columns with reproducible behavior is also simplified; preparation of a large batch of colloidal resin assures that at least the chemistry of the pellicle will be the same from one column to another.

This method of preparing pellicular resins has an important advantage over the polymer-modification approach as exemplified by surface-sulfonated cation exchangers. In the latter case the boundary between the functionalized shell and the non-functionalized core is unavoidably a diffuse one. Consequently ion-exchange sites in this boundary region are not as hydrated as in the bulk of the pellicle and transport of ions in this region must necessarily be impeded. This in turn has a detrimental effect on the performance of the resins. Surface agglomerated resins do not suffer from this drawback; the outer layer of resin microparticles are uniformly swollen, the transition from functionalized to non-functionalized polymer is extremely sharp with beneficial effects on mass transfer in the pellicle region. In light of this, Dionex in recent years have applied the surface agglomeration technique to the preparation of cation exchangers thus supplanting the surface sulfonation method.

These forms of surface-agglomerated resins do have at least one drawback however; the substrate particle has a tendency to swell in organic solvents, indeed to swell a great deal in solvents with the appropriate solubility parameter. This is not a problem when aqueous eluents are used but in recent years as IC has expanded more

and more into the realm of organic ion analysis where organic solvents must often be employed it has become more of a liability. It was mainly for this reason that workers at Dionex recently developed a new series of pellicular resins still using the electrostatic bonding approach but with a core that is much less susceptible to swelling. And in a very radical departure from earlier embodiments where the core is entirely inert they now involve the core as well as the pellicle in the chromatography [15]. They have done this by using macroporous polymer particles as the substrate on which to attach the ion-exchange microparticles of ion exchanger. Adding appropriate reagents, electrolytes and solvents to the mobile phase gives a hybrid form of chromatography that has components of ion-exchange and ion-pairing chromatography.

While the bulk of the research on improving resins for IC has been focused on anion analysis, there has also been significant progress in cation analysis. An interesting development in the evolution of cation exchangers has been the appearance in recent years of materials that facilitate the chromatography of alkali and alkaline earth metal ions. Surface-sulfonated, styrene-based resins permit isocratic elution of either alkali metal ions or alkaline earth ions but not of mixtures of ions from the two groups. Finding solutions to this problem has been one of the major challenges in the IC of cations and recently two successful attempts have been reported [16,17].

Kolla *et al.* [16] describe an ion exchanger prepared by copolymerizing a thin layer of butadiene and maleic acids onto a porous silica substrate. This has been applied to the isocratic separation of the more important alkali and alkaline earth metal ions using weak acid eluents and non-suppressed conductometric detection (Fig. 7). Stillian *et al.* [17] have adopted a different approach. Arguing from the basis that a resin with a lower density of sulfonated sites should display less affinity for divalent ions than a fully sulfonated version, they prepared copolymers wherein one of the monomers was comparatively inactive to sulfonation. The resulting sulfonated resins have ion-exchange sites dispersed uniformly among inert sites and enable isocratic elution of the subject ions within very acceptable time frame using suppressed conductometric detection (Fig. 8).

Although low-capacity ion exchangers for IC were initially developed as a means of getting around the various problems of conductometric detection and continue to

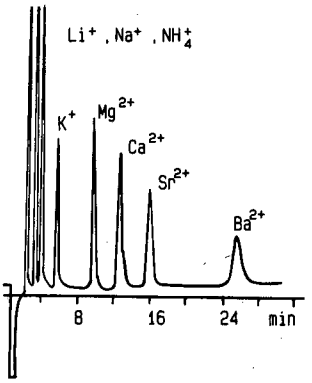

Fig. 7. Isocratic separation of alkali and alkaline earth metal ions. Stationary phase: poly(butadiene–maleic acid) on silica. Eluent: 0.01 *M* tartaric acid. Detection: non-suppressed conductometric. Ref. 16.

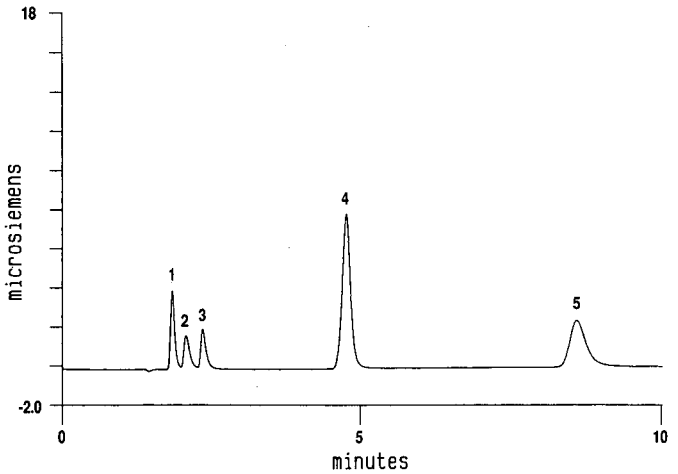

Fig. 8. Isocratic separation of alkali and alkaline earth metal ions. Stationary phase: Dionex IonPac CS10. Eluent: 60 m*M* HCl–6 m*M* diaminopropionic acid. Detection: suppressed conductometric. Peaks: 1 = sodium; 2 = ammonium; 3 = potassium; 4 = magnesium; 5 = calcium. Ref. 17.

do so, recent years have seen them being widely used with other detection modes. And capacity is no longer the only property of concern. More and more we see an increased understanding of resin selectivity being translated into materials with separation capabilities that are remarkably different from the early resins. We can anticipate further developments along these lines as research and development people continue to respond to the analytical challenges of ion chromatography.

REFERENCES

1 H. Small, *Ion Chromatography*, Plenum Press, New York, 1989.
2 D. T. Gjerde and J. S. Fritz, *Ion Chromatography*, Hüthig, Mamaroneck, NY, 2nd ed., 1987.
3 H. Small and T. E. Miller, Jr., *Anal. Chem.*, 54 (1982) 462.
4 H. Small, in J. T. Stock and M. V. Orna (Editors), *The History and Preservation of Chemical Instrumentation*, Reidel, Dordrecht, 1986, pp. 97–107.
5 T. S. Stevens, J. C. Davis and H. Small, *Anal. Chem.*, 53 (1981) 1488.
6 H. Small, T. S. Stevens and W. C. Bauman, *Anal. Chem.*, 47 (1975) 1801.
7 K. Harrison and D. Burge, presented at the *Pittsburgh Conference on Analytical Chemistry, Cleveland, OH, 1979*, abstract No. 301.
8 D. T. Gjerde, J. S. Fritz and G. Schmuckler, *J. Chromatogr.*, 186 (1979) 509.
9 T. S. Stevens, G. L. Jewett and R. A. Bredeweg, *Anal. Chem.*, 54 (1982) 1206.
10 J. Stillian, *LC Mag.*, 3(9) (1985) 802.
11 D. T. Gjerde and J. V. Benson, *Anal. Chem.*, 62 (1990) 612.
12 H. Small, *Some Electrochemical Properties of an Ion Exchanger, M.Sc. Thesis*, Queen's University of Belfast, Belfast, 1953.
13 R. W. Slingsby, M. A. Brown, J. Hsu and R. J. Joyce, *Anal. Chem.*, in press.
14 H. Small, *J. Inorg. Nucl. Chem.*, 18 (1961) 232.
15 J. R. Stillian and C. A. Pohl, *J. Chromatogr.*, 499 (1990) 249.
16 P. Kolla, J. Kohler and G. Schomburg, *Chromatographia*, 23 (1987) 465.
17 J. Stillian, C. Pohl, A. Woodruff and C. R. Devasa, presented at the *Pittsburgh Conference on Analytical Chemistry, New York, 1990*, paper No. 628.

Journal of Chromatography, 546 (1991) 17–25
Elsevier Science Publishers B.V., Amsterdam

CHROMSYMP. 2258

Charged surface and mass transfer in dynamic ion exchangers

R. BAILEY and R. M. CASSIDY*
Department of Chemistry, University of Saskatchewan, Saskatoon, Saskatchewan S7N 0W0 (Canada)

ABSTRACT

Ion-interaction reagents (IIR) were used in both static (presorbed as fixed-site charges) and dynamic modes on C_{18} silica bonded phases to evaluate the sorption mechanisms for inorganic ions in "ion pairing systems". Column break-through techniques were used to determine the shifts in the sorption equilibria of the IIR as a result of the sorption of the analyte. The results showed that the changes in the sorption isotherm of the IIR were linearly related to the amount of analyte retained on the stationary phase, even for loadings up to 25% of the total capacity (0.26 mequiv. of IIR per ml of column volume); this behaviour is consistent with theoretical models previously reported for a dynamic ion-exchange mechanism. Studies of the ion-exchange constant, K_{IEX}, for the sorption of inorganic ions onto the charged surface of the reversed-phase, have shown that the magnitude of K_{IEX} depends on the amount of IIR sorbed. The relationship was essentially the same for both static and dynamic separation modes, and was similar to patterns reported for K_{IEX} for inorganic ions as a function of ion-exchange capacity in conventional resins.

INTRODUCTION

Dynamic ion-exchange or ion-pairing techniques have been used extensively for the separation of organic and inorganic analytes. Studies on the mechanism of sorption of organic analytes in these systems has been the subject of several papers. Experimental results reported by Schill and co-workers [1–3] have shown that the equilibration of an organic analyte and an ion interaction reagent (IIR) with the stationary phase (SP) are related to each other in a complex fashion. The most important features of these expermental studies are that the introduction of the analyte ion (A^{n+}) causes changes in the concentration of the IIR relative to the mobile phase (MP) concentration; and that the magnitude and sign of these changes is dependent upon A^{n+} and system peak (IIR) retention. Other experimental studies on these systems have reported unusual peak behaviour such as peak splitting and deformations, and these effects have been explained with a model based on multiple retention mechanisms or a gradient in the IIR during the elution of the analyte peak [4–6].

Several mathematical treatments that predict some of the features of dynamic ion-exchange systems have been reported [7–13], but these treatments have not provided a complete chemical interpretation of the mechanism of the sorption process. Theoretical studies by Stranahan and Deming [9] have provided an explanation of the direction of the peak response for the IIR observed by indirect detection, but did not

0021-9673/91/$03.50

explain the changes in the signal intensity with retention of A^{n+} and system peak. Other theoretical studies have developed mathematical expressions relating the signal intensity to the retention of A^{n+} and the system peak [10–13], but these treatments have not provided a clear chemically based description as to why these changes occur.

Recently, we have made use of selective detection of the IIR (indirect detection method) and A^{n+} (inorganic ions) to provide a better understanding of the equilibria occurring in these systems [14]. With the results of these experimental measurements and simulations based on a simple Craig distribution model it was possible to provide a chemically based explanation for the peak response patterns and signal intensity changes in the IIR as a function of retention of the IIR and A^{n+}. The model was also used to explain how separation problems such as peak splitting could be eliminated. These studies also examined the relationship of the amount of excess IIR adsorbed, which is caused by injection of A^{n+}, with the amount of A^{n+} injected. However, the results were not accurate enough to clearly define how the ratio, moles excess IIR_{SP} to moles A^{n+} injected, changed with retention of A^{n+} and IIR (system peak). Consequently one aim of our present studies was to determine, using column breakthrough techniques with selective detection for the analyte and IIR, how the adsorption of excess IIR changed with amount of A^{n+}_{SP} and retention of A^{n+}.

Recent studies by Liu and Cantwell [15] on a model based on an electrical double layer for dynamic ion exchange have shown that for small organic analytes the dominant mechanism of sorption is ion exchange rather than adsorption. For the small organic solutes studied by Liu and Cantwell the coefficient for ion exchange, K_{IEX}, was determined to be a constant with amount of IIR adsorbed. However, Fritz and Story [16] have shown that K_{IEX} for inorganic ions on conventional ion-exchange resins changes with the ion-exchange capacity. Consequently, we wanted to determine K_{IEX} by direct detection methods to see if similar changes in the ion-exchange constant could occur in dynamic and fixed-site ion-exchange systems, and if these changes in K_{IEX} might alter the sorption process.

EXPERIMENTAL

Equipment and chemicals

The detector was a Waters 990 photodiode array detector (Waters Division of Millipore, Missauga, Canada). The pumps were Waters 510 pumps and the injector was a Rheodyne 7125 (Rheodyne, Cotati, CA, U.S.A.). The column was a Supelcosil 5-μm LC-18 column (150 × 4.6 mm I.D., C_{18} bonded to silica, Supelco, Oakville, Canada) or Waters 5-μm Radial-Pak C_{18} column (100 × 8.0 mm I.D., C_{18} bonded to silica). The IIR was 4-octylbenzenesulfonic acid (4-OBS) (Aldrich, Milwaukee, WI, U.S.A.). Complexing agents, which were added to the mobile phase, were tartaric acid (Aldrich) and α-hydroxyisobutyric acid (Sigma, St. Louis, MO, U.S.A.). The postcolumn reagent used for detection of metal ions was 4-(2-pyridylazo)resorcinol monosodium salt ($2.0 \cdot 10^{-4}$ mol l^{-1} PAR, 1.0 mol l^{-1} ammonium acetate, 2.0 mol l^{-1} ammonium hydroxide, Aldrich).

PROCEDURE AND CALCULATIONS

Mole ratio IIR to A^{n+} studies

A mobile phase containing 1.71 m*M* 4-octylbenzenesulfonic acid, 0.10 *M* α-hydroxyisobutyric acid ($pK_a = 4.03$ [17]), at pH 3.90 and sodium chloride was passed through a Supelcosil 5-μm C_{18} column at 1.0 ml min^{-1}. The ionic strength of the mobile phase was selected to be $1.225 \cdot 10^{-1}$ *M*. Sodium chloride was used to compensate for varying amounts of metal ion present in the mobile phase. Equilibration of the column with mobile phase was verified by the breakthrough curve for the IIR reagent by monitoring the absorbance of the IIR (4-octylbenzenesulfonic acid) at 260 nm with a photodiode array detector. Once equilibration was reached the mobile phase was changed to one containing metal ion (at constant ionic strength) and the breakthrough curve for the IIR was determined. The breakthrough curve for A^{n+} was determined by monitoring the absorbance of the metal–PAR complex after postcolumn reaction with PAR (at 520 nm). Helium gas was used to introduce the postcolumn reagent into the eluent at a flow-rate of 0.5 ml min^{-1} via a low-dead-volume mixer. The analyte ions (Cd, Mg and Mn) were selected as analytes on basis of their retention characteristics and solubility properties in surfactant solutions.

Fixed-site ion exchangers

Fixed-site ion exchangers were prepared by coating a 5-μm C_{18} Supelcosil (at 1.0 ml min^{-1}) or a Waters Radial-Pak column (at 2.0 ml min^{-1}) with an arachidyl sulfate (C_{20} sulfate) acetonitrile solution, followed by equilibration with a mobile phase containing a complexing agent ($\approx$ 150 ml). The column was stripped with acetonitrile–deionized water (50:50, v/v) solution and measurements of the dry mass of arachidyl sulfate adsorbed onto the stationary phase were made by constant weight analysis.

Preparation of dynamic ion exchangers

The dynamic ion exchangers were prepared by equilibration of a mobile phase containing 4-octylbenzenesulfonic acid and a complexing agent (α-hydroxyisobutyric acid). The concentration of α-hydroxyisobutyric acid, pH, and column (LC-18 5-μm C_{18} column, Supelcosil) were selected to be the same as one of the fixed-site systems for purposes of comparison of different types of ion exchangers. The mass of 4-octylbenzenesulfonic acid loaded onto the stationary phase was determined from the breakthrough curve of 4-octylbenzenesulfonic acid.

CALCULATIONS

Relative ion-exchange constant ($K_{IEK,R}$)

A relative ion-exchange constant, $K_{IEX,R}$, which can be used to evaluate relative changes in selectivity with ion-exchange capacity for a given set of eluent conditions, was calculated as follows:

$$K_{IEX,R} = \frac{K_{IEX}}{[E^+]^n_{MP}} = \frac{[A^{n+}]_{SP}}{[E^+]^n_{SP}\,[A^{n+}]_{MP}} = \frac{k'_A}{(m_{IX})^n} \qquad (1)$$

where K_{IEX} is the ion-exchange selectivity constant; MP and SP are mobile and stationary phase respectively; A^{n+} is the uncomplexed analyte ion; n is the charge of the analyte ion; k'_A is the capacity factor of the analyte ion; E^+ is the counterion of the ion exchanger; $[E^+]_{MP}$ was held constant under the experimental conditions selected by maintaining constant pH and complexing agent concentration; and m_{IX} is the concentration (g per column volume) of the ion-exchange reagent (arachidyl sulfate or 4-octylbenzenesulfonate) adsorbed onto the stationary phase. The loading of metal ion was small and thus

$$[E^+]_{SP} = \text{total capacity} - [A^{n+}]_{SP} \approx \text{total capacity} = m_{IX} \quad (2)$$

Since the concentration of the complexing reagent in the eluent was held constant, the relative distribution of the different metal species was also constant, and thus, the effect of this is also included in $K_{IEX,R}$. The capacity factors (k'_A) were determined by injection of 100 ng of metal ion onto a column containing known amounts of arachidyl sulfate or 4-octylbenzene sulfonate sorbed on the packing.

RESULTS AND DISCUSSION

Mole ratio IIR to A^{n+}

The breakthrough curve for the metal ion and IIR (4-OBS) in the presence of a metal ion is shown in Fig. 1. The absorbance of the metal–PAR complex remains at baseline until equilibration of the metal ion between the mobile and stationary phase is reached. At equilibrium of the metal ion, the absorbance from the metal–PAR complex increases to a maximum ($\approx$ 40 min) and then remains constant, as shown in Fig. 1. The absorbance of the IIR decreases ($\approx$ 40 min) when equilibration of the metal

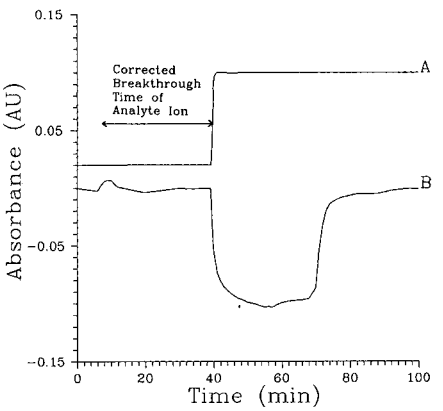

Fig. 1. Breakthrough curves for analyte ion and 4-octylbenzene sulfonic acid. Experimental conditions: 150 × 4.6 mm I.D. Supelcosil 5-μm C_{18} column; flow-rate mobile phase is 1.0 ml min^{-1}; flow-rate PAR for curve A is 0.5 ml min^{-1}; time = 0 eluent, 1.71 m*M* 4-octylbenzenesulfonic acid–0.1 *M* α-hydroxyisobutyric acid–78.59 m*M* sodium chloride, pH 3.90 with NH_4OH; time = 5.0 min eluent, 1.71 m*M* 4-octylbenzene sulfonic acid–0.1 *M* α-hydroxyisobutyric acid–1.09 m*M* manganese–74.33 m*M* sodium chloride, pH 3.90 with NH_4OH. Curve A analyte ion; curve B 4-octylbenzenesulfonic acid; *Y*-scale for curve A reduced by factor of 5.

ion is reached. This corrected breakthrough time, as labelled in Fig. 1, can be used to determine the moles of analyte ion adsorbed onto the stationary phase per column volume as follows:

$$A_{SP}^{n+} = \text{corrected breakthrough time} \cdot \text{flow-rate} \cdot [\text{analyte ion}]$$

The decrease in absorbance of the IIR (40–80 min) is caused by adsorption of excess IIR when A^{n+} is sorbed onto the stationary phase. The absorbance returns to the baseline when an equilibrium of the IIR is reached between mobile and stationary phases. Under normal elution conditions when $k'A^{n+} < k'$system peak a negative response or a decrease in the concentration of the IIR is observed [4–6], but these results show that excess IIR is adsorbed onto the stationary phase in the presence of analyte, even when $k'A^{n+} < k'$system peak. The amount of excess IIR_{SP} per column volume was determined from the absolute area of the rectangular breakthrough curve by converting the absorbance scale to concentration with Beer's law. The data obtained from these measurements are given in Fig. 2 for analyte ion concentrations ranging from 0.66 mM to 15.3 mM.

Fig. 2 (curves E, F, G and H) show that IIR_{SP} increases with A_{MP}^{n+} and with the capacity factor of A^{n+} (k'Cd < k'Mg < k'Mn for $k'A^{n+} < k'$sytem peak at mobile phase pH 3.90, and k'Mn > k'system peak at pH 3.15). These results show that the introduction of A^{n+} into the mobile phase causes an enhanced adsorption of IIR on the stationary phase as a result of partial neutralization of the charge at the eluent–sorbent interface by A^{n+}. As the retention of A^{n+} increases A_{SP}^{n+} increases, and, consequently, the amount of excess IIR_{SP}. Fig. 2 also shows that these curves become non-linear at higher analyte ion loadings, which is the result of overload conditions.

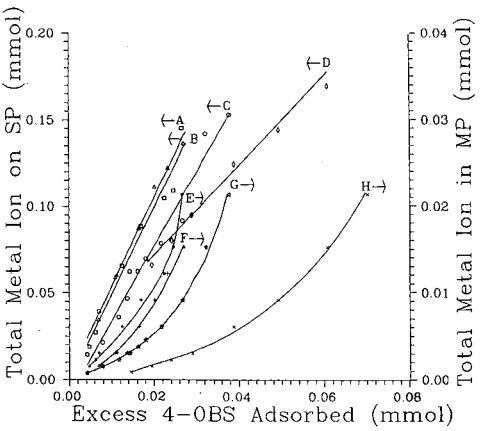

Fig. 2. The variation of moles metal ion with excess moles 4-octylbenzene sulfonic acid adsorbed on sorbent. Curves A, B, C and D Y-scale is total metal ion present on column; curves E, F, G and H Y-scale total metal ion present in the mobile phase. Curve A, E k'Cd = 13.7; curve B, F k'Mg = 23.1; Curve C, G k'Mn = 26.0; k'system peak = 37.3; Curve D, H k'Mn = 61.0 and k'system peak = 37.7. Experimental conditions: 150 × 4.6 mm I.D. Supelcosil 5-μm C_{18} column; flow-rate 1.0 ml min^{-1}; eluent, 1.71 mM 4-octylbenzenesulfonic acid–0.1 M α-hydroxyisobutyric acid, (78.59 − 4x) mM sodium chloride–x mM analyte ion, pH adjusted with NH_4OH to 3.90 for $k'_A < k'$system peak and 3.15 for $k'_A > k'$system peak.

TABLE I

AVERAGE MOLE RATIO EXCESS IIR_{SP} TO A_{SP}^{n+}

A^{n+} [a]	$k'A^{n+}$ [b]	k'sys [b]	Ionic strength (mM)	Mole ratio excess IIR_{SP}/A_{SP}^{n+} (± S.D.)	No. of data points
Manganese	26.0	37.3	122.5	0.23 ± 0.01	11
Cadmium	13.7	37.3	122.5	0.21 ± 0.03	8
Magnesium	23.1	37.3	122.5	0.19 ± 0.01	7
Manganese	61.0	37.7	91.8	0.34 ± 0.05	7

[a] Analytes were added to the mobile phase in the concentration range of 0.66 to 15.3 mM.
[b] Analyte retention times under elution conditions with a mobile phase containing no metal ion.

However, Fig. 2 (curves A, B, C and D) shows that, even for loadings up to 25% of the total capacity (0.26 mequiv. of IIR per ml of column volume), there is a linear relationship between the excess IIR_{SP} and A_{SP}^{n+}. Thus the mole ratio of excess 4-octylbenzene sulfonate sorbed to A_{SP}^{n+} is independent of the amount of analyte sorbed on the stationary phase. Table I shows the average mole ratio of excess IIR_{SP} to A_{SP}^{n+}. This table shows that for conditions of constant ionic strength that the mole ratio is to a first approximation independent of retention of A^{n+}. This is due to the fact that the sorption of A^{n+} onto the stationary phase causes a fixed amount of IIR to be adsorbed onto the stationary phase in order compensate for the partial neutralization of the charge at the eluent–sorbent interface, which is caused by sorption of A^{n+} onto the stationary phase.

Changes in the mole ratio of IIR_{SP} to A_{SP}^{n+} can be observed when the ionic strength of the mobile phase is changed. Table I shows that the mole ratio for manganese increases when the retention time for manganese is adjusted to elute after the system peak. The changes in the mole ratio are due to a decrease in ionic strength of the mobile phase from $1.225 \cdot 10^{-1}$ M to $9.180 \cdot 10^{-2}$ M when the pH of the mobile phase was adjusted from 3.90 to 3.15 to increase the retention time of manganese. When the ionic strength is decreased the metal ion is more effective at neutralizing the charge at the eluent–sorbent interface, and thus a large amount of excess IIR is adsorbed onto the sorbent, which causes the mole ratio of excess IIR to A_{SP}^{n+} to increase.

Equilibrium constants for ion exchange in fixed-site and dynamic ion-exchange systems

The retention of small organic ions in dynamic ion-exchange systems has been described by Liu and Cantwell [15] based on a model of an electrical double-layer that exists between the mobile phase and the stationary phase. His model showed that the retention of these analytes was controlled primarily by ion-exchange rather than by adsorption processes. In his model it was determined that the coefficient for ion exchange, K_{IEX}, for small organic solutes studies was approximately constant with the loading of IIR on the sorbent.

Figs. 3 and 4 show the variation in $K_{IEX,R}$ (see Calculations) with loading of surfactant for fixed-site ion exchange on two reversed-phase systems. The magnitude of $K_{IEX,R}$ decreases to a minimum at capacities of 0.1 to 0.3 μmol g^{-1} and then begins to

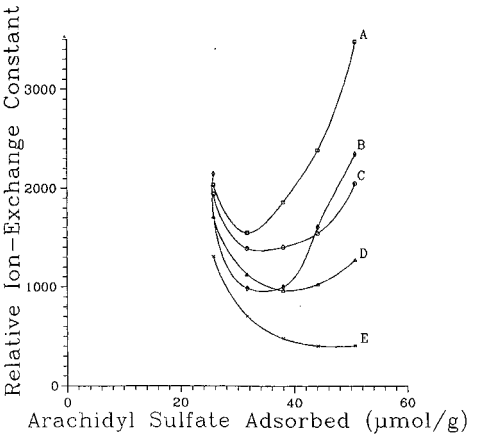

Fig. 3. Change in the relative ion-exchange constant with ion-exchange capacity (loading of ion-interaction reagent) for a fixed-site ion exchanger. Experimental conditions: 100 × 8 mm I.D. 5-μm C_{18} Waters Radial-Pak column; flow-rate 2.0 ml min^{-1}; eluent, 0.05 *M* tartaric acid, pH 3.40; sample size approximately 100 ng metal ion, Curves: A = manganese, B = lanthanum, C = nickel, D = lead, E = ytterbium. *Y*-scale for La and Yt reduced by factor of 40 and for manganese by factor of 1.5.

increases at higher capacities. The general shape of these curves are in agreement with the results reported by Fritz and Story [16] for sulfonated highly cross-linked macroporous polystyrene resins with capacities 0.23 to 3.70 μmol g^{-1}. The differences between the two curves in Figs. 3 and 4 are due to variation in pH, and complexing agent (tartaric acid and α-hydroxyisobutyric acid present in the mobile phase) and the resulting changes in $[E^+]_{MP}$ and consequently the value of $K_{IEX,R}$. The different reversed-phase columns may by also cause changes in the magnitude of $K_{IEX,R}$.

Fig. 5 shows that in dynamic ion-exchange systems the relative ion-exchange

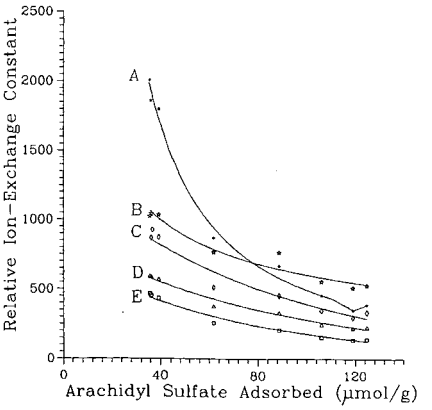

Fig. 4. Change in the relative ion-exchange constant with ion-exchange capacity for a fixed-site ion exchanger. Experimental conditions: 150 × 4.6 mm I.D. 5-μm C_{18} Supelcosil column; flow-rate 1.0 ml min^{-1}; eluent, 0.20 *M* α-hydroxyisobutyric acid pH 3.92; sample size approximately 100 ng metal ion, Curves: A = lanthanum, B = manganese, C = lead, D = cobalt, E = nickel. *Y*-scale La reduced by factor of 20.

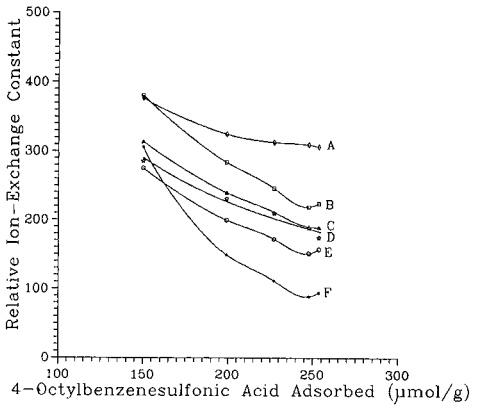

Fig. 5. Change in the relative ion-exchange constant with ion-exchange capacity for dynamic ion exchanger. Experimental conditions: 150 × 4.6 mm I.D. 5-μm C_{18} Supelcosil column; flow-rate 1.0 ml min^{-1}; eluent, x mM 4-octylbenzenesulfonic acid–0.20 M α-hydroxyisobutyric acid, pH 3.90; sample size approximately 100 ng metal ion, Curves: A = lead (scale factor 0.5), B = nickel, C = cobalt (scale factor 0.5), D = manganese (scale factor 0.2), E = zinc, F = copper (scale factor 4).

constant is also not constant with loading of surfactant. Comparison of Figs. 4 and 5 show that the relationship of $K_{IEX,R}$ to IIR loading is similar for both fixed-site and dynamic ion exchangers.

Determination of retention mechanism for inorgaic analytes

In Liu and Cantwell's [15] electrical double layer model the ion-exchange distribution coefficient, $K_{S,IEX}$, is calculated as follows:

$$K_{S,IEX} = K_{IEX} A_{SP} \Gamma_{TBA+}/c \tag{3}$$

where K_{IEX} for the small organic anion p-nitrobenzenesulfonate (NBS^-) was determined to be a constant; A_{SP} is the area of the stationary phase; Γ_{TBA+} is the surface excess of tetrabutylammonium ion; and c is the ionic strength. However, from the results reported here, K_{IEX} for inorganic solutes does not remain constant. Consequently the potential effect of a variation inK_{IEX} on the distribution coefficient for ion exchange was determined using the maximum variation in K_{IEX} found with the dynamic ion-exchange system. The maximum variation in $K_{IEX,R}$ was that found for Cu which is given by $K_{IEX,R} = -0.0152x + 3.8691$ where x is the amount of 4-octylbenzenesulfonic acid adsorbed.

Curves A, B, and D of Fig. 6 shows the results obtained by Liu and Cantwell [15] for NBS^- on a column coated with tetrabutylammonium ion. The overall distribution coefficient, K_S, is calculated as follows:

$$K_S = K_{S,IEX} + K_{S,ADS} \tag{4}$$

where $K_{S,IEX}$ and $K_{S,ADS}$ are the contributions to the distribution coefficient from ion-exchange and adsorption processes. Curve C of Fig. 6 shows the distribution coefficient for ion exchange, $K_{S,IEX,R}$, corrected for potential variation in $K_{IEX,R}$ ob-

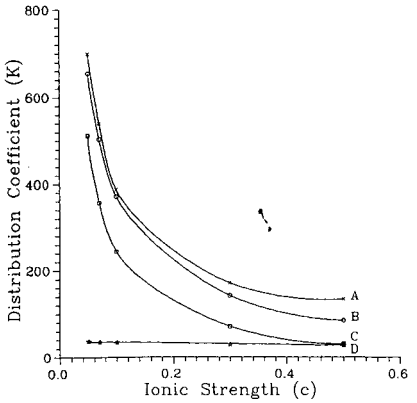

Fig. 6. Variation of distribution coefficient of NBS^- on octyldecylsilane packing with ionic strength. Experimental conditons: eluent, 0.010 *M* tetrabutylammonium chloride; Curves: A = K_S, B = $K_{S,IEX}$ (corrected for variation in K_{IEX}), D = $K_{S,ADS}$ (Curve A, B and D from ref. 15).

served for inorganic cations. From Fig. 6 it is clear that the variations in $K_{IEX,R}$ do not effect the conclusions made by Liu and Cantwell [15] that ion exchange is the dominant process in the retention of the analyte, except at high ionic strengths where adsorption and ion-exchange distribution coefficients are of approximately the same magnitude. In addition, the changes in $K_{S,IEX,R}$ due to corrections for variation of $K_{IEX,R}$ with ion-exchange capacity for inorganic cations were determined to be more important at higher concentrations of surfactant in the mobile phase (higher loadings of surfactant).

REFERENCES

1 M. Denkert, L. Hackzell and G. Schill, E. Sjorgren, *J. Chromatogr.*, 218 (1981) 31.
2 L. Hackzell, T. Rydberg and G. Schill, *J. Chromatogr.*, 282 (1983) 179.
3 L. Hackzell and G. Schill, *Chromatographia*, 15 (1982) 437.
4 R. M. Cassidy, M. Frazer, *Chromatographia*, 18 (1984) 369.
5 G. K. C. Low, A. M. Duffield and P. R. Haddad, *Chromatographia*, 15 (1982) 289.
6 G. K. C. Low, P. R. Haddad and A. M. Duffield, *J. Chromatogr.*, 336 (1984) 15.
7 J. E. Eble, R. L. Grob, P. E. Antle and L. R. Snyder, *J. Chromatogr.*, 384 (1987) 25.
8 D. J. Solms, T. W. Smuts and V. Pretorious, *J. Chromatogr. Sci.*, 9 (1971) 600.
9 J. J. Stranahan and S. N. Deming, *Anal. Chem.*, 54 (1982) 1540.
10 J. Stahlberg and M. Almgren, *Anal. Chem.*, 67 (1989) 1109.
11 T. Takeuchi, S. Watanabe, K. Murase and D. Ishii, *Chromatographia*, 25 (1988) 107.
12 A. Yamamoto, A. Matsunga, M. Ohto, E. Mizukami, K. Hayakawa and M. Miyazaki, *J. Chromatogr.*, 482 (1989) 107.
13 J. Crommen, G. Schill, D. Westerlund and L. Hackzell, *Chromatographia*, 24 (1987) 252.
14 R. Michaelis and R. M. Cassidy, in P. Jandic and R. M. Cassidy (Editors), *The Chemistry of Dynamic Ion Exchangers, Proceedings of 2nd International Ion Chromatography Forum, Boston, 1989; Advances in Ion Chromatography*, Vol. 2, Century International, Medfield, MA, 1989, p. 21.
15 H. Liu and F. Cantwell, *Anal. Chem.*, submitted for publication; and in H. Liu, *Ph.D. Thesis*, University of Alberta, Edmonton.
16 J. S. Fritz and J. N. Story, *J. Chromatogr.*, 90 (1974) 267.
17 G. Kortum, W. Vogel and K. Andrussow, *Dissociation Constants of Organic Acids in Aqueous Solution*, Butterworths, London, 1961, p. 309.

Journal of Chromatography, 546 (1991) 27–36
Elsevier Science Publishers B.V., Amsterdam

CHROMSYMP. 2091

Peak interactions under concave isotherm conditions in preparative ion chromatography

CHARLES A. LUCY*, THI-LUONG LUONG and STEVE ELCHUK
General Chemistry Branch, AECL Research, Chalk River Laboratories, Chalk River, Ontario K0J 1J0 (Canada)

ABSTRACT

There have been recent improvements in the understanding of the behaviour occurring when chromatographic columns are severely overloaded and neighbouring peaks start to interact. However, these studies have concentrated exclusively on convex non-linear isotherms (*e.g.* Langmuir). In many preparative separations concave isotherms are operative and result in fronting peaks.

The separation of lanthanides on an ion-exchange column, with α-hydroxyisobutyric acid (HIBA) as eluent, is used as a model system for the study of peak interactions under concave isotherm conditions. Experimental evidence suggests that the concave isotherm results from the HIBA in the mobile phase being unable to complex all of the lanthanide injected. Two types of peak interaction have been identified: the retainment effect, where a more retained peak shifts to greater retention times due to the overloading of an earlier peak, and the pull-back effect, where a peak is smeared into a more retained peak due to the overloading of the later peak.

INTRODUCTION

Ion chromatography is increasingly being looked upon as a means of separating commercial quantities of a variety of products. One of its advantages for such preparative separations is the wide variety of modes of separation which have become available: ion-exclusion chromatography has been used for the large-scale separation of sugars from molasses [1], and ion-pair chromatography has been used to purify tripeptides [2]. However, despite preparative ion-exchange chromatography dating back to the Manhattan project [3], there is still little understanding of the peak interaction behaviour which often affects the quality of the separation.

It has been recognized that productivity and throughput in preparative chromatography can best be achieved by overloading the column. Under these conditions, the distribution isotherm of the sample between the stationary and mobile phases will be non-linear. The non-linearity may be either convex, as for the Langmuir isotherm, in which case the peak will tail when the column is overloaded, or concave for which fronting peaks are observed. Theoretical [4–6] and experimental [7–10] studies have been made of the interactions between adjacent peaks under convex isotherm conditions. These studies have identified "displacement" and "tag-along" effects which affect the productivity and purities obtained from a preparative system.

0021-9673/91/$03.50

On the other hand, the interaction between adjacent peaks under concave isotherm conditions has received essentially no attention, despite this behaviour having been observed in almost every branch of chromatography [8,11–13]. In this work, the separation of binary solutions of lanthanides is used as a model system for the study of peak interactions in preparative chromatography under concave isotherm conditions.

BACKGROUND

Convex isotherm

A convex isotherm results when the sample adsorption capacity of the stationary phase becomes limited. Under these conditions the solute molecules in the band centre will remain in the mobile phase longer and thus migrate faster than those molecules at the edges of the peak where the solute concentration is lower. This results in a steepening of the peak front and a broadening of the tail.

Analytical chromatography operates under linear isotherm conditions and thus the overlap of adjacent peaks does not alter the original peak shape. This will not be true under non-linear convex isotherm conditions, since the overlapping of peaks will exacerbate the already limited capacity of the stationary phase. Theoretical studies using the numerical "semi-ideal" model have identified two types of interaction operating between adjacent bands [4,5,14]. The first is "sample self-displacement", where the more strongly retained component of a pair of solutes has a stronger interaction with the stationary phase. Consequently, when the bands overlap the less retained component is displaced by the more retained component. In severe cases this leads to an earlier and sharper elution of the first component[a]. This displacement behaviour has been observed experimentally in a number of preparative chromatographic separations [8–10].

The second type of interaction predicted is the "tag-along" effect. For adjacent peaks the strength of the solute interaction with the stationary phase is similar. Therefore, while the more retained solute has a slightly stronger interaction with the stationary phase, it can still be displaced by the less retained solute if the localized concentration of the latter is large enough. The "tag-along" effect appears then as a smearing forward of the more retained solute into the peak of the less retained solute. This behaviour is enhanced by increases in the relative concentration of the less retained solute and results in decreases in the separation between the two bands. Experimental verification of the tag-along effect was recently obtained by Katti and Guiochon [10].

Concave isotherm

Concave isotherms are observed less frequently than convex isotherms discussed above. A concave isotherm results when the sample capacity in the mobile phase becomes limited. Under these conditions the resultant peak shape is a fronting peak, with a broad gradual upward slope culminating in a steep tail (Fig. 1). Profiles of peaks fronting due to a concave isotherm have been generated using the fundamental models

[a] Similar behaviour has been modelled using a Craig counter-current simulation of preparative chromatography assuming Langmuir isotherms [6].

of Houghton [12,15] and Haarhoff and Van der Linde [16], and by the numerical semi-ideal model (using an S-shaped isotherm) [17]. However, no theoretical or experimental studies of the interaction of adjacent peaks under concave isotherm conditions have been made. Thus, no theoretical or experimental guidelines exist regarding the behaviour to be expected.

In this work, the separation of lanthanides by ion-exchange chromatography with α-hydroxyisobutyric acid (HIBA) is used as a model system for the study of peak interactions under concave isotherm conditions. The fronting behaviour of the lanthanides under preparative isocratic elution conditions was first noted by Campbell and Buxton [13]. They ascribed this behaviour to the formation of a precipitate which they observed on their glass columns. In addition, however, the lanthanide separations are particularly well suited to the study of peak interactions under concave isotherm conditions because of their narrow, sharply-defined spectral peaks. The sharp absorption bands result from f–f transitions within the 4f shell, which is well shielded from distortions from the surroundings of the ion, and so the transitions take on a free atom like character. Many of these bands are characteristic to a particular lanthanide [18], and UV–visible spectroscopy can be used to selectively monitor the behaviour of an individual lanthanide in the presence of another. While it is possible to perform such a study using pairs of organic solutes having differing absorption spectra, these solutes would have dissimilar adsorption isotherms and so little general understanding of the processes involved would be gained.

EXPERIMENTAL

The high-performance liquid chromatography (HPLC) equipment consisted of a Shimadzu LC-610 solvent delivery system, a Rheodyne 7125 sample injection valve fitted with a 100-μl loop, a Shimadzu 6AV variable-wavelength UV–visible detector and an IBM-XT computer containing a LAB MASTER data acquisition board. All data handling was performed with Lotus 1-2-3. The column was a 150 × 4.6 mm I.D. stainless-steel jacket packed with 30–45 μm Dowex AG 50W-X8 sized by elutriation [19]. The column was slurry packed at 1500 p.s.i. from 1.0 *M* HIBA pH 4.6 solution. The injector and column were thermostatted at 30.0°C using a Haake water bath.

The HIBA (Aldrich, Milwaukee, WI, U.S.A.) was purified with a 200 × 3 cm AG 50W-X8 cation-exchange column and filtered with a 0.8 μm/0.4 cartridge filter (Nalge Co.). The eluents and solutions were prepared from quartz-distilled and deionized water (Milli-Q system). All eluents were filtered through 0.45-μm Millipore filters before use. The eluent was 0.30 *M* HIBA, pH 4.6, and was pumped at a flow-rate of 1.0 ml/min. Neodymium and praseodymium standards were prepared in distilled water from their nitrate salts (Aldrich). Calibration curves for Nd at 575 nm and Pr at 444 nm were linear (correlation coefficients of 0.9997 and 0.9994, respectively) over the absorbance ranges used in this study, with zero intercepts (within the 95% confidence interval).

RESULTS AND DISCUSSION

Individual peak profiles

The changes in peak profiles with increasing amounts of neodymium and

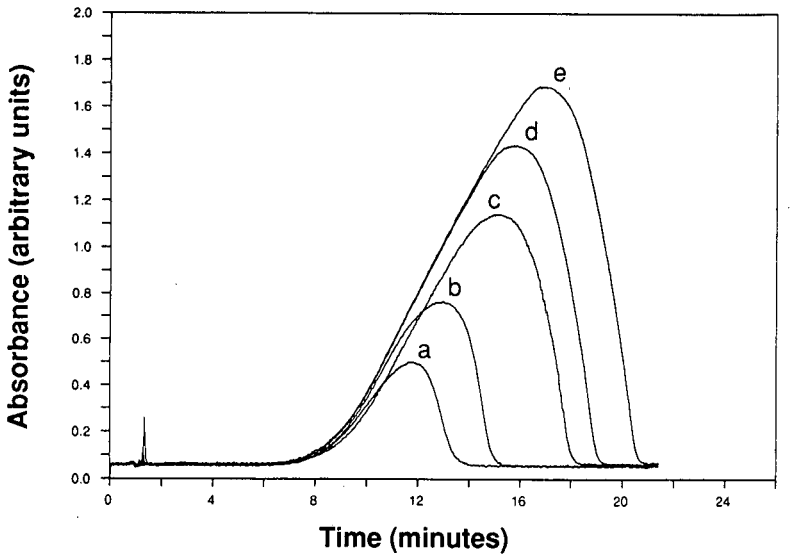

Fig. 1. Peak profiles for neodymium under concentration overload conditions. Nd loadings: a = 1 mg; b = 2 mg; c = 4 mg; d = 6 mg; e = 8 mg. Nd monitored at 575 nm.

praseodymium injected onto the Dowex AG 50W-X8 cation-exchange column are shown in Figs. 1 and 2. These figures illustrate the effect of column overload on the individual peak shapes. In both cases the profiles are asymmetrical with a gradual rise at the front of the peak followed by a sharp drop. The degree of the asymmetry

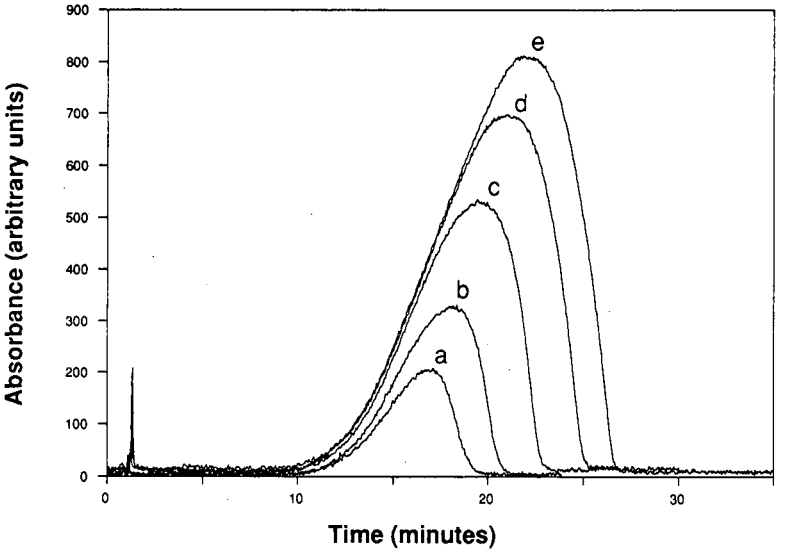

Fig. 2. Peak profiles for praseodymium under concentration overload conditions. Pr loadings: a = 1 mg; b = 2 mg; c = 4 mg; d = 6 mg; e = 8 mg. Pr monitored at 444 nm.

increases with the degree of loading, with a resultant increased retention time for the peak maximum. This indicates that the migration rate of the solute decreases with increasing solute concentration in the mobile phase.

However, the fronting behaviour and increased retention time for the peak maximum are not sufficient, by themselves, to assure that the isotherm is concave. Indeed, similar peak shapes have been observed in both theoretical and experimental studies of adsorption chromatography with binary eluents containing a strongly sorbed additive [20,21]. In the adsorption chromatography case, the peak profiles result from competition between the molecules of the strong solvent component and those of the sample for the adsorbent surface (*i.e.*, competitive Langmuir isotherms). When the mobile phase additive is more strongly retained than the sample, the resultant peak profiles display a diffuse front and a sharp tail [20], and increases in the sample loading result in increased peak asymmetry and movement of the peak front to earlier retention times. This last characteristic is unlike the behaviour resulting from a concave isotherm, where the peak front does not change retention time when the loading is changed. In Figs. 1 and 2 it can be seen that the peak front does not move when the loading of either neodymium or praseodymium is increased. Thus, both lanthanides follow true concave isotherms.

Fig. 3 shows a plot of the lanthanide concentration measured at the peak maximum *versus* the retention time for the peak maximum. Theoretical relationships derived from the Houghton model of non-linear chromatography predict that such a plot fundamentally follows an orthogonal hyperbola [12]. However, over a small concentration range such a plot would appear rectilinear as observed in Fig. 3 for both neodymium ($r = 0.989$) and praseodymium ($r = 0.998$). Thus for both lanthanides studied, no discontinuities exist in the isotherm behaviour, unlike other concave isotherm systems studied previously [12].

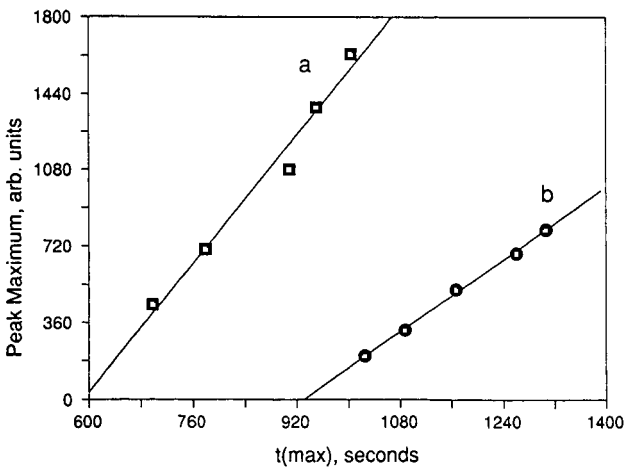

Fig. 3. Variation of retention time of peak maximum [t(max)] with concentration measured at peak maximum for (a) neodymium and (b) praseodymium. Lines are the best-fit linear regression of the points.

Binary mixture: effect of overload on trailing peak

Fig. 4a shows a composite of the retention behaviour of neodymium and praseodymium when each is injected alone. The concentrations are such that neodymium is severely overloaded (*i.e.*, exhibiting extreme fronting) while praseodymium is only slightly overloaded. When the two lanthanides are injected together, the praseodymium is pushed backwards to longer retention times (Fig. 4b). This behaviour is analogous to the "displacement" effect observed in convex (Langmuir)

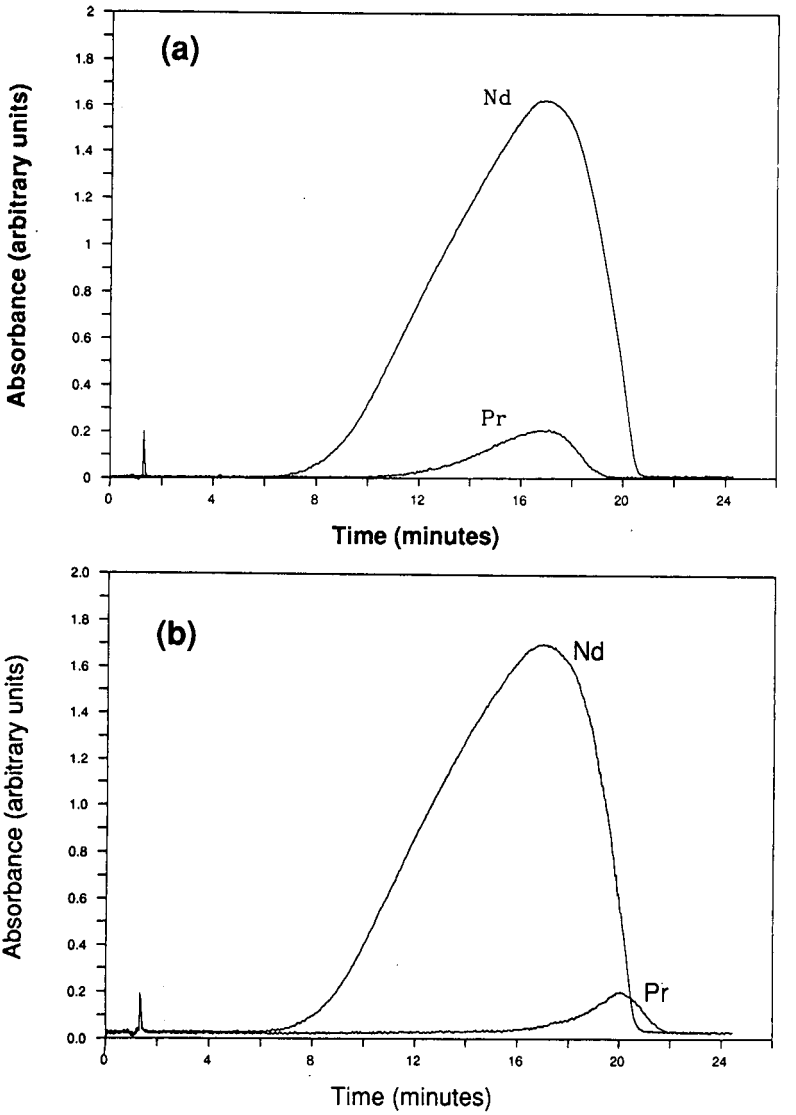

Fig. 4. Effect of neodymium loading on later-eluting praseodymium: (a) composite of retention behaviour of praseodymium (1.0 mg monitored at 444 nm) and neodymium (8.0 mg monitored at 575 nm) injected separately; (b) retention behaviour of 0.5 mg praseodymium and 8.0 mg neodymium when injected together.

isotherm conditions [8–10], and in keeping with the terminology of Golshan-Shirazi and Guiochon [22], it will be referred to as the *retainment effect*.

The behaviour of the praseodymium peak when increasing loadings of neodymium are co-injected with the praseodymium is shown in Fig. 5. As the neodymium loading is increased, the praseodymium peak shifts to longer retention times and becomes sharper. A plot of the retention time for the praseodymium peak maximum *versus* the neodymium loading was linear [r = 0.994, intercept of 15.6 min (95% confidence interval is 0.2 min)]. This behaviour is similar to that predicted and observed for the displacement effect in convex isotherm systems [4,5,8–10].

The cause of the concave isotherm can be determined based on the behaviour observed in Figs. 4 and 5. Assuming that the cause of the concave isotherm is precipitation of the lanthanide–HIBA complex, as had been postulated by Campbell and Buxton [13], one would expect praseodymium to be unaffected by the neodymium precipitation, since the praseodymium concentration is still below its solubility limit. However, since the retainment effect was observed this expectation must be modified. The extra retention of praseodymium could be due to praseodymium co-precipitating with the neodymium–HIBA complex. However, upon redissolving, such a precipitate would liberate both neodymium and praseodymium at the same rate, which would result in comparable peak shapes and peak maxium shifts for both neodymium and praseodymium. This is not what is observed in Figs. 4 and 5. Therefore, the concave isotherm behaviour exhibited by the lanthanides does not result from the formation of a precipitate.

An alternative hypothesis is that the concave isotherm behaviour results from a shortage of HIBA in the mobile phase. At the highest loadings studied, 0.55 *M* Nd is injected into an eluent stream containing only 0.30 *M* HIBA. Using this assumption, the retainment effect can be explained in an analogous fashion to the displacement

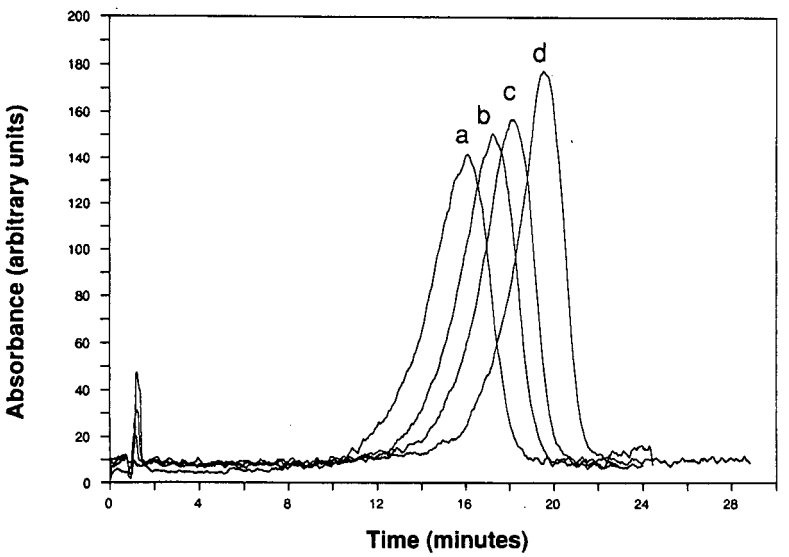

Fig. 5. Behaviour of later-eluting praseodymium with increasing loadings of neodymium. Nd loading: a = 1.0 mg; b = 3.0 mg; c = 5.0 mg; d = 7.0 mg. Pr loading: 0.5 mg. Detector wavelength: 444 nm.

effect observed when overloading a convex isotherm. The less retained of the pair of solutes (Nd) forms a stronger complex with the eluent, HIBA [23]. Consequently, when the peaks overlap the Nd will be preferentially complexed by the HIBA, leaving the more retained solute (Pr) stranded on the stationary phase and resulting in increased retention for the more retained solute (Pr). In cases of greater relative concentration of the less retained solute to the more retained (*i.e.*, Nd *vs.* Pr), the situation will be exacerbated such that the degree of the retainment effect will increase, and the more retained peak (Pr) will become sharper. This is the behaviour observed in Fig. 5. Therefore it is concluded that the concave isotherm results from the limited capacity of the mobile phase, brought on by the limited concentration of HIBA in the eluent.

Binary mixture: effect of overload on leading peak

Fig. 6 shows the neodymium peak profiles observed for the injection of 0.5 mg neodymium along with various larger loadings of praseodymium. The neodymium peak shape broadens and undergoes a transition from a fronting to a tailing peak as the praseodymium concentration is increased. Some increase in the retention time is also observed. This behaviour is analogous to that in the convex isotherm situation. In this case, the results mirror the "tag-along effect" [10,14], and have been termed the *pull-back effect* [22].

This pull-back effect can be explained by assuming that limited complexation capacity in the mobile phase is the cause of the concave isotherm. The less retained component, neodymium, forms a more stable complex with the eluent, HIBA, than does praseodymium. While this difference in complex stability causes the retainment effect, this difference is small. Thus, increasing the concentration of praseodymium will result in shifting the equilibrium away from the neodymium–HIBA complex,

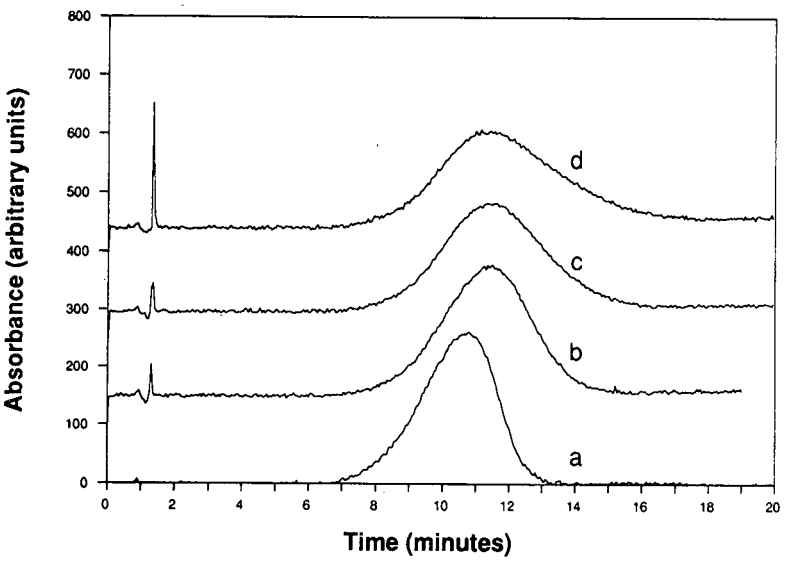

Fig. 6. Behaviour of earlier-eluting neodymium with increased loading of praseodymium. Nd loading: 0.5 mg. Pr loading: a = 1.0 mg; b = 3.0 mg; c = 5.0 mg; d = 7.0 mg. Detector wavelength: 575 nm.

leading to greater retention for neodymium. Concurrently, the neodymium peak broadens due to the praseodymium concentration gradient (*i.e.*, the praseodymium peak front) which is spread across the width of the neodymium peak. The praseodymium, present in high concentrations, complexes the available HIBA with the result that the "free" HIBA concentration across the neodymium peak also varies. This non-uniform eluent concentration across the neodymium peak leads to varied migration rates and thus peak broadening.

CONCLUSIONS

Fronting peaks are observed when ion-exchange columns are concentration overloaded by a lanthanide while using HIBA as eluent. This is typical of preparative chromatography under concave non-linear isotherm conditions. The peak profiles display consistent behaviour over the full concentration range studied, indicating that no secondary phenomenon are occurring which would complicate the observed behaviour. The concave isotherm could result from either precipitation of the lanthanides on the column or limited complexation capacity of the mobile phase. The peak interaction behaviour indicates that the latter mechanism is most probable.

The experimental studies have identified two types of peak interactions which occur when peaks overlap under concave isotherm conditions. These are the *retainment* and *pull-back* effects, which result from the two solutes competing for the limited complexation capacity of the mobile phase. The retainment effect appears as a delay and sharpening of the more retained peak when the less retained peak is severely overloaded. The intensity of the effect is proportional to the concentration of the less retained solute injected. The pull-back effect is the smearing of the less retained peak when the more retained peak is severely fronting. The severity of the effect is related to the concentration of the more retained solute injected.

The peak interaction behaviour observed under concave isotherm conditions is analogous to that observed in convex isotherm system, allowing for the mobile phase having the limited capacity rather than the stationary phase. Thus it is possible to take the wealth of understanding available for convex isotherm systems [4–10] and use it as a guide for the behaviour expected in preparative chromatographic separations which follow a concave isotherm.

ACKNOWLEDGEMENTS

The authors are grateful to Fred Cantwell (University of Alberta) for his helpful discussions and to Paul Leeson (Chalk River Laboratories) for writing the software for data acquisition.

REFERENCES

1 H. Heikkila, *Chem. Eng.*, (1983) 50.
2 W. S. Hancock and R. L. Prestidge, in B. A. Bidlingmeyer (Editor), *Preparative Liquid Chromatography*, Elsevier, Amsterdam, 1987, p. 217.
3 F. H. Speeding, E. I. Fulmer, T. A. Butler, E. M. Gladrow, M. Gobush, P. E. Porter, J. E. Powell and J. M. Wright, *J. Am. Chem. Soc.*, 69 (1947) 2812.
4 S. Ghodbane and G. Guiochon, *J. Chromatogr.*, 440 (1988) 9.

5 S. Ghodbane and G. Guiochon, *J. Chromatogr.*, 444 (1988) 275.
6 J. E. Eble, R. L. Grob, P. E. Antle and L. R. Snyder, *J. Chromatogr.*, 405 (1987) 1.
7 J. E. Eble, R. L. Grob, P. E. Antle, G. B. Cox and L. R. Snyder, *J. Chromatogr.*, 405 (1987) 31.
8 J. Newburger, L. Liebes, H. Colin and G. Guiochon, *Sep. Sci. Technol.*, 22 (1987) 1933.
9 J. Newburger and G. Guiochon, *J. Chromatogr.*, 484 (1989) 153.
10 A. M. Katti and G. Guiochon, *J. Chromatogr.*, 499 (1990) 21.
11 A. Jaulmes, I. Ignatiadis, P. Cardot and C. Vidal-Madjar, *J. Chromatogr.*, 395 (1987) 291.
12 A. Jaulmes, C. Vidal-Madjar, H. Colin and G. Guiochon, *J. Phys. Chem.*, 90 (1986) 207.
13 D. O. Campbell and S. R. Buxton, *Ind. Eng. Chem. Process Des. Develop.*, 9 (1970) 89.
14 G. Guiochon and S. Ghodbane, *J. Phys. Chem.*, 92 (1988) 3682.
15 G. Houghton, *J. Phys. Chem.*, 67 (1963) 84.
16 P. C. Haarhoff and H. J. van der Linde, *Anal. Chem.*, 38 (1966) 573.
17 G. Guiochon, S. Golshan-Shirazi and A. Jaulmes, *Anal. Chem.*, 60 (1988) 1856.
18 D. C. Stewart and D. Kato, *Anal. Chem.*, 30 (1958) 164.
19 C. D. Scott, *Anal. Biochem.*, 24 (1968) 292.
20 S. Golshan-Shirazi and G. Guiochon, *J. Chromatogr.*, 461 (1988) 1.
21 S. Golshan-Shirazi and G. Guiochon, *J. Chromatogr.*, 461 (1988) 19.
22 S. Golshan-Shirazi and G. Guiochon, *Anal. Chem.*, 61 (1989) 2373.
23 A. E. Martell and R. M. Smith, *Critical Stability Constants, Vol. 3, Other Organic Ligands*, Plenum Press, New York, 1977, p. 36.

Journal of Chromatography, 546 (1991) 37–59
Elsevier Science Publishers B.V., Amsterdam

CHROMSYMP. 2148

Computer optimization in ion chromatography

II. A systematic evaluation of linear retention models for anions

ANDREW D. SOSIMENKO and PAUL R. HADDAD*
Department of Analytical Chemistry, University of New South Wales, P.O. Box 1, Kensington, N.S.W. 2033 (Australia)

ABSTRACT

Extensive retention data for non-suppressed ion chromatography of anions have been acquired for 17 analytes (halides, oxohalides, nitrite, nitrate, sulfite, sulfate, bisulfite, thiosulfate, phosphate, thiocyanate, carbonate, acetate and oxalate) on three stationary phases (Waters IC Pak A, Hamilton PRP-X100 and Vydac 302.IC 4.6) using 7 eluent types (benzoate, phthalate, hydroxide, carbonate/bicarbonate, gluconate/borate, *p*-toluenesulfonate and phosphate). These retention data are used to assess the validity of retention models which predict a linear relationship between the logarithm of solute capacity factor and the logarithm of the activity of the eluent competing anion. The linearity of these plots is uniformly good, but the slopes differ markedly from those predicted from theory. When the eluent contains two competing anions, neither the dominant equilibrium approach nor the effective charge approach give reliable prediction of the slopes. Optimization of one eluent parameter at a time (*e.g.* the concentration of the competing anion in the eluent) can be successful if the slope of the retention plot is determined by measurement of analyte retention times at two eluent compositions falling at the extremes of the range of eluent compositions under consideration. An example of this "end points" method is provided, in which the concentration of a phthalate eluent is optimized.

INTRODUCTION

Computer optimization procedures have been applied extensively in liquid chromatography and one of the most successful of these applications has been the computer-assisted selection of mobile phase composition in reversed-phase liquid chromatography. Despite this success, computer optimization techniques have found only limited usage in ion chromatography (IC).

The most important parameter to be considered in an optimization procedure is the chromatographic selectivity; that is, the ability of the chromatographic system to differentiate between two solutes. In IC there are several variables which can be used to change chromatographic selectivity. These can be divided into two classes, namely, hardware variables (*e.g.* stationary phase composition, ion-exchange capacity, temperature and detection method) and eluent variables (*e.g.* the nature and

0021-9673/91/$03.50

concentration of the competing ions, and the pH). Whilst hardware variables must be taken into consideration in the initial selection of the chromatographic system to be used, it is often more appropriate to select a specific combination of these variables and to then concentrate on modifying the eluent composition.

We have recently reviewed the use of computer optimization in IC [1] and we have shown that two distinct approaches exist. The first of these is the algorithmic method, in which a suitable searching algorithm, such as the Simplex procedure, is applied to the optimization of a designated number of experimental variables until the separation is optimized. This approach is time consuming due to the large number of experiments required, but has the attributes that no theoretical insight into the chromatographic retention mechanism is necessary, and that several experimental parameters can be optimized simultaneously.

The second approach to optimization involves the modelling of solute retention over a specified range of experimental parameters (called the "search area"). The aim is to enable the retention time of any solute to be determined for any eluent composition within the search area. That is, solute retention times are derived from the retention model and are used to calculate the optimal eluent composition. The model used may be *experimental* or *theoretical*. Experimental models fit measured retention times to a mathematical equation, which is then used to calculate retention times for any desired eluent composition within the search area. The accuracy of this calculation is generally dependent on the number of data points used to define the retention equation, and the geographic distribution of these data points over the search area. Accurate calculation of retention times results only when the number of measured data points is large, so that the use of experimental models normally requires considerable exploration. On the other hand, theoretical models use an abstract understanding of retention behaviour to predict solute retention times over the designated search area. This prediction can be made solely on the basis of theory, but it is more usual to perform a small number of experiments using eluent compositions from within the search area and to then base predictions on these measured points.

All chromatographic techniques are relatively slow to produce data, especially when the composition of the mobile phase is varied. The reason for this is that the stationary phase must become fully equilibrated with the new mobile phase before reliable retention data can be measured. Relatively slow equilibration to changes in eluent composition is a characteristic of ion-exchange chromatography in general, and IC in particular. It therefore becomes desirable to restrict the number of experiments performed in an optimization process, and to this end, a reliable theoretical model would be preferable. In this paper, we provide a detailed evaluation of the suitability of simple, linear retention models as predictive tools for the retention of anions in non-suppressed IC. Our goal in performing this evaluation is to determine if any linear retention model can be used with confidence in a theoretical optimization strategy for IC.

THEORY

Linear retention models for IC

Consideration of fundamental equilibrium and chromatographic theory enables a retention equation for IC to be derived. The full derivation of this equation has been

presented earlier by several authors [2–4], and when applied to the ion-exchange equilibrium between a solute anion, A^{x-}, and an eluent anion, E^{y-}, the final equation takes the form:

$$\log k'_A = \frac{1}{y}\log K_{A,E} + \frac{x}{y}\log\frac{Q}{y} + \log\frac{w}{V_m} - \frac{x}{y}\log[E_m^{y-}] \quad (1)$$

where k'_A is the capacity factor for a solute A^{x-}, $K_{A,E}$ is the ion-exchange selectivity coefficient for the solute and eluent, Q is the ion-exchange capacity of the stationary phase, w is the weight of stationary phase used in the column, V_m is the volume of mobile phase existing in the column, x is the charge on the solute anion, y is the charge on the eluent anion, and $[E_m^{y-}]$ is the concentration of the eluent ion in the mobile phase.

Although shown for the case of anion-exchange, eqn. 1 applies also to cation-exchange [5].

Some of the terms in eqn. 1 are constant for a particular column and type of mobile phase, so that under these conditions, eqn. 1 can be simplified to:

$$\log k'_A = \text{Constant} - \frac{x}{y}\log[E_m^{y-}] \quad (2)$$

Eqn. 2 predicts that a linear relationship exists between $\log k'_A$ and $\log [E_m^{y-}]$, with a slope of $-x/y$. The literature of IC abounds with examples in which measured retention data obtained with eluents containing a single type of eluting ion are shown to produce linear plots with approximate agreement between the predicted and measured slopes. The only caveats which apply are that activity effects should be considered for eluents in which the ionic strength is sufficient to give activity coefficients less than unity, and that ions carrying a charge greater than 2 give slopes which are less than the theoretical value. The latter aspect can be rationalized by considering that the low ion-exchange capacities of typical IC stationary phases would make it improbable that a polyvalent ion will closely approach a stoichiometric number of exchange sites.

Problems arise with the above linear retention model when there are two or more eluent ions present, as typified by the use of phthalate eluents at pH values where both the singly charged hydrogen phthalate ion (HP^-) and the doubly charged phthalate ion (P^{2-}) co-exist. In these cases, experience shows that the linearity of the retention plots is maintained, but to predict the theoretical slope of the plot, an appropriate value of eluent charge must be inserted into the equation. Two possibilities exist; the first is to assume that the eluent ion with the higher charge dominates solute elution and the lesser charged eluent species can be disregarded, whilst the second possibility is to calculate a weighted average charge on the eluent ion by considering the concentrations and charges on each eluent species. The former will be referred to as the *dominant equilibrium approach*, and the latter as the *effective charge approach*. The effective charge on the eluent can be calculated according to:

$$y = \alpha_1 + 2\alpha_2 + 3\alpha_3 + \ldots + n\alpha_n \quad (3)$$

where α_n is the mole fraction of eluent species carrying a charge of n^-. When the effective charge approach is used, the total eluent concentration, C_E, replaces the $[E_m^{y-}]$ term in eqn. 2.

EXPERIMENTAL

Instrumentation

The liquid chromatograph consisted of a Millipore Waters (Milford, MA, U.S.A.) M6000A pump, a WISP M712 autoinjection unit, two six-port column switching valves and a Model M730 data module. The chromatographic columns were housed in a Waters temperature control module and were maintained at a constant 35 ± 0.1°C to minimize the effects of temperature fluctuations on analyte response [6]. The operating temperature was lowered to 25 ± 0.1°C for the Hamilton PRP-X100 column when used with eluents having a pH greater than 8. Two detectors were used throughout this study, these being a Waters M430 conductivity detector and a Waters M450 variable-wavelength UV detector. The conductivity detector was used wherever possible because of its wide applicability, but in cases where the background conductance of the eluent was high (especially with the phosphate and carbonate/bicarbonate eluents), the UV detector was also utilised. The UV detector was set at a wavelength of 195 nm, since it has been shown that a large majority of the anions studied show absorbance at this wavelength [7].

Columns

Three anion-exchange columns were used. A Waters IC Pak A (50 × 4.6 mm I.D.) column packed with 10 μm functionalised polymethacrylate with an ion-exchange capacity of 0.03 mequiv./ml. A Vydac (The Separations Group, Hesperia, CA, U.S.A.) 302 IC 4.6 (250 × 4.6 mm I.D.) column packed with 10 μm functionalised silica with an ion-exchange capacity of 0.10 mequiv./g. A Hamilton (Reno, NV, U.S.A.) PRP-X100 (150 × 4.1 mm I.D.) column packed with functionalised 10 μm polystyrene–divinylbenzene copolymer with an ion-exchange capacity of 0.19 mequiv./g.

The three columns were connected in parallel and housed in the temperature controlled oven. Two manually operated column switching valves were used to direct the eluent flow through the desired column. All three columns could therefore be equilibrated with the same eluent, as required.

Eluents

For each eluent used in this study, a stock solution of approximately 100 m*M* was prepared by dissolution of an accurately weighed amount of the appropriate analytical grade reagents in pure water. Working eluents were prepared daily by dilution of a suitable volume of the stock solution to approximately 900 ml, followed by adjustment of the pH (where necessary) by the dropwise addition of 0.1 *M* LiOH, using a magnetic stirrer. The solution was then made up to volume (1 l) and the pH measured accurately using an Activon (Sydney, Australia), Model 101 mV/pH meter with a glass electrode. Finally the solution was passed through a Millipore solvent clarification apparatus using 0.45-μm membrane filters and degassed in an ultrasonic bath before use.

The actual eluent compositions used are given in Tables II–VIII. The general preparation of these eluents was as follows:

Benzoate eluents. The stock solutions were prepared from sodium benzoate.

Carbonate/bicarbonate eluents. The stock solutions were prepared from sodium carbonate and sodium bicarbonate, mixed in the appropriate proportions.

Gluconate/borate eluents. The stock solution was prepared by dissolving 16 g sodium gluconate, 18 g boric acid and 25 g sodium tetraborate in 1 l of pure water. The working eluents were prepared by combining the appropriate aliquot of stock solution with glycerol solution (10 ml, 25%), acetonitrile (120 ml, UV grade), followed by dilution to 1 l.

Hydroxide eluents. The stock solution was prepared by dissolving AR grade LiOH in pure water under an inert atmosphere of argon. Working eluents were prepared under argon by dilution of an appropriate aliquot of the stock solution, with the concentration of OH^- being determined by titration with standardized HCl. During use, these eluents were maintained under an atmosphere of nitrogen to limit the absorption of carbon dioxide.

p-Toluenesulfonate eluents. The stock solutions were prepared from *p*-toluenesulfonic acid.

Phthalate eluents. The stock solutions were prepared from either potassium hydrogen phthalate or, where the mobile phase was to be buffered at a pH of 4.0 or below, from phthalic acid.

Phosphate eluents. The stock solutions were prepared from sodium dihydrogen phosphate.

Analytes

The analytes (see Table I) were prepared as 1000 ppm stock solutions by dissolving the appropriate amount of the sodium salt in pure water in a volumetric flask. A working standard (100 ppm) of each analyte was prepared daily by dilution of the stock solution. Where the retention time of the analyte being studied was found to occur in the water dip or the solvent front peak, a fresh standard was prepared by

TABLE I

ANALYTES, ELUENTS AND COLUMNS USED IN THIS STUDY

Anions: F^-, Cl^-, Br^-, I^-, ClO_3^-, BrO_3^-, IO_3^-, NO_2^-, NO_3^-, HSO_3^-, SO_3^{2-}, SO_4^{2-}, $S_2O_3^{2-}$, SCN^-, phosphate, carbonate, oxalate and CH_3COO^-.

Eluent	Column		
	Hamilton PRP-X100	Vydac 302 IC 4.6	Waters IC Pak A
Benzoate	Yes	Yes	Yes
Carbonate/bicarbonate	No	No	Yes
Gluconate/borate	Yes	No	Yes
Hydroxide	No	No	Yes
p-Toluenesulfonate	Yes	Yes	Yes
Phthalate	Yes	Yes	Yes
Phosphate	Yes	No	Yes

TABLE II

RETENTION TIMES FOR ANIONS USING BENZOATE ELUENTS ON THREE COLUMNS (HAMILTON PRP-X100, VYDAC 302 IC 4.6 AND WATERS IC PAK A)

	Hamilton				Vydac							Waters			
Concentration (m*M*):	2.00	3.00	4.00	5.00	2.38	2.66	3.53	4.49	4.67	5.88	7.71	2.99	3.99	4.99	5.99
pH:	6.4	6.4	6.4	6.4	4.0	4.0	4.0	4.0	4.0	4.0	4.0	6.4	6.4	6.4	6.4
Fluoride	3.06	2.26	1.69	1.39	–	–	–	–	–	–	–	3.21	2.85	2.42	2.15
Chloride	3.88	2.83	2.08	1.75	12.69	9.69	7.50	–	6.99	4.69	3.85	5.37	4.46	3.61	3.23
Bromide	5.26	3.75	2.76	2.32	15.47	11.75	9.01	7.68	8.45	5.54	4.46	8.10	6.65	5.47	4.75
Iodide	13.74	9.49	6.38	4.69	27.10	20.06	15.21	–	14.23	8.87	6.89	23.66	18.62	14.37	12.91
Chlorate	7.06	4.98	3.51	2.78	15.72	11.84	9.14	–	8.58	5.60	4.51	8.81	7.01	5.74	4.99
Bromate	3.98	2.89	2.16	1.80	–	8.91	6.94	6.04	–	4.47	3.69	4.59	3.86	3.24	2.85
Iodate	2.80	2.11	1.61	1.46	9.18	7.15	5.63	–	5.34	3.75	3.16	2.85	2.55	2.20	1.95
Nitrite	4.30	3.12	2.29	1.90	14.26	10.86	–	–	7.80	5.28	4.29	6.92	5.57	4.61	4.00
Nitrate	5.88	4.18	2.95	2.36	–	13.28	10.18	–	9.49	6.13	4.90	10.09	8.05	6.55	5.68
Bisulfite	–	–	–	–	–	8.24	–	–	6.02	4.37	3.69	–	–	–	2.36
Sulfite	38.18	17.66	7.78	4.54	–	–	–	57.14	–	–	13.91	41.33	28.34	18.51	13.29
Sulfate	36.88	18.81	7.06	5.01	–	–	–	57.97	41.46	25.10	13.98	42.42	28.85	18.80	13.50
Thiosulfate	65.34	31.61	10.68	8.56	–	–	–	77.87	–	33.14	18.13	79.56	51.76	32.89	23.81
Phosphate	5.58	3.66	1.76	1.54	–	13.68	–	11.13	10.28	–	–	5.49	5.49	4.59	3.35
Thiocyanate	–	–	–	–	–	30.48	23.15	19.37	–	13.25	10.08	–	–	–	–
Acetate	3.06	2.30	1.80	1.55	–	3.66	–	3.16	3.09	2.84	2.59	3.24	2.87	2.46	2.17
Oxalate	78.15	18.86	–	9.93	–	–	–	–	–	–	–	–	–	–	–
System	42.56	–	26.90	–	–	–	–	–	–	–	–	–	–	–	–
Void vol. eq.	0.75	0.77	0.81	0.83	1.65	1.65	1.65	1.65	1.65	1.65	1.65	0.77	0.78	0.79	0.80

dilution of the stock solution in the eluent being used. The limited stability of the bisulfite ion in aqueous solutions [8] required that the standards containing this ion also contain a preservative. In the low pH eluent studies the bisulfite ion was preserved by the addition of formaldehyde to give a final concentration in the sample of 0.2% (v/v). Under these conditions, the bisulfite ion is chromatographed as the hydroxymethanesulfonate ion.

RESULTS AND DISCUSSION

Selection of analytes, eluents and stationary phases

In order to systematically evaluate the suitability of linear retention models for predicting solute retention times, an experimental design was formulated to permit the acquisition of extensive retention data for a variety of anions, eluents and stationary phases. Table I shows the scope of this study. The range of analytes covers most of the common inorganic anions, and includes some species (such as phosphate, oxalate, carbonate and nitrite) which show changes in form as the pH is altered. Similarly, the eluents cover most of those commonly used in non-suppressed IC and include those which can be expected to show prominent pH effects (such as phthalate, benzoate, carbonate/bicarbonate and phosphate). The stationary phases are representative of the three main types of substrate used in columns for non-suppressed IC, namely silica, polystyrene–divinylbenzene and polymethacrylate. It was necessary to impose some limitations concerning the various combinations of eluents and stationary phase that could be used. For example, high pH eluents were unsuitable for use with the silica based column. Table I details the combinations of eluents and stationary phases that

TABLE III

RETENTION TIMES FOR ANIONS USING CARBONATE ELUENT ON A WATERS IC PAK A COLUMN

Concentration (m*M*):	0.49	0.99	1.49	1.49	1.99	1.98	2.49	2.48	2.99	2.98
pH:	10.3	8.5	8.5	10.3	8.5	10.3	8.5	10.3	8.5	10.3
Fluoride	3.85	7.75	5.76	3.09	4.60	2.46	4.01	2.26	3.70	2.01
Chloride	6.03	12.11	9.47	4.91	7.49	3.94	6.51	3.58	6.01	3.15
Bromide	10.66	24.06	17.42	9.60	13.71	7.14	11.83	6.61	10.86	5.61
Iodide	30.09	53.02	38.62	27.37	26.72	21.31	21.91	18.82	20.56	16.23
Chlorate	11.18	26.68	19.41	10.31	14.99	7.64	12.93	7.07	12.01	6.02
Bromate	5.37	12.61	9.30	4.51	7.33	3.46	6.35	3.34	5.90	2.92
Iodate	3.04	7.42	5.14	2.61	3.72	2.13	3.27	2.00	3.48	1.81
Nitrite	7.95	18.03	13.12	7.77	10.38	5.81	8.92	5.42	8.43	4.64
Nitrate	12.73	26.65	19.72	11.93	15.02	8.65	12.92	8.01	13.35	6.82
Bisulfite	4.20	9.76	7.24	3.53	5.70	2.84	4.98	2.51	4.64	2.32
Sulfite	41.90	49.35	37.34	29.77	24.47	16.81	20.14	14.42	18.97	10.41
Sulfate	42.16	51.51	34.59	29.78	24.08	16.82	19.43	14.39	18.41	10.41
Thiosulfate	79.16	–	139.98	54.25	82.93	30.60	61.32	27.23	53.05	18.97
Phosphate	36.75	51.05	32.14	23.90	20.62	13.60	16.64	11.49	18.33	8.45
Thiocyanate	57.73	57.33	40.73	50.58	29.83	40.94	24.79	38.32	23.02	20.47
Acetate	3.59	8.92	6.22	3.09	5.53	–	4.16	2.30	4.10	–
System	9.23	–	–	7.06	–	5.28	–	4.65	–	3.86
Void vol. eq.	0.85	0.81	0.79	0.85	0.80	0.86	0.80	0.84	0.81	0.86

were employed. Since retention times for each analyte were measured in triplicate, more than 8500 data points were acquired in this study.

Retention data

The retention times collected for the anions using the various combinations of eluents and stationary phases are presented in full in Tables II–VIII. It should be noted that some of the solutes were either unretained or were retained too strongly on the column to be eluted within a reasonable period of time (*i.e.* 4 h). In these cases, retention data are not shown. Tables II–VIII comprise a comprehensive database which will be used for the evaluation of further retention models in subsequent papers in this series.

Applicability of linear retention models

Plots of $\log k'_A$ *versus* $\log\{E_m^{y-}\}$ were prepared (where { } represents activity), in accordance with eqn. 2, for each combination of analyte, eluent and stationary phase. In each case, the points were fitted to a line of best fit using a linear regression analysis technique, giving correlation coefficients of 0.98 or higher. The observed slopes of these plots are presented in Tables IX–XV, together with theoretical slopes calculated using both the dominant equilibrium approach and the effective charge approach. These Tables show that neither of the above-mentioned approaches shows good agreement with the observed slopes.

TABLE IV

RETENTION TIMES FOR ANIONS USING GLUCONATE/BORATE ELUENTS ON TWO COLUMNS (HAMILTON PRP-X100 AND WATERS IC PAK A)

	Hamilton					Waters				
Concentration (mM)[a]:	1.10	1.46	1.83	2.20	2.56	1.10	1.46	1.83	2.20	2.56
pH:	8.5	8.5	8.5	8.5	8.5	8.5	8.5	8.5	8.5	8.5
Fluoride	2.15	1.90	1.70	1.63	1.47	2.05	1.78	1.58	1.51	1.49
Chloride	4.37	3.75	3.27	3.07	2.72	3.40	2.85	2.48	2.30	2.30
Bromide	11.15	10.72	8.22	7.33	6.73	5.16	4.29	3.71	3.40	3.35
Iodide	–	–	–	–	–	14.23	11.59	9.77	8.90	8.93
Chlorate	26.71	24.24	23.03	17.87	17.70	5.71	4.69	4.05	3.70	3.66
Bromate	5.98	5.09	4.63	4.41	3.81	3.03	2.52	2.26	2.11	2.07
Iodate	2.11	2.07	1.74	1.54	1.46	1.82	1.62	1.60	1.17	1.07
Nitrite	6.39	5.69	4.89	4.78	4.00	4.15	3.51	3.04	2.79	2.76
Nitrate	17.30	12.56	13.09	11.86	9.91	6.05	5.06	4.33	4.02	3.85
Sulfite	30.03	20.50	15.04	12.92	10.13	14.29	9.52	6.88	5.67	5.15
Sulfate	30.60	20.57	14.80	12.55	10.10	14.29	9.53	6.89	5.61	5.08
Thiosulfate	–	72.10	–	57.03	29.83	30.08	19.90	14.17	11.36	9.91
Carbonate	2.80	2.41	2.11	1.97	1.76	2.61	2.23	1.96	1.83	1.72
Phosphate	17.05	13.62	8.77	7.20	6.02	10.19	6.73	5.03	4.18	3.75
Acetate	2.42	2.41	2.05	1.88	1.67	2.06	1.85	1.68	1.57	1.51
Oxalate	–	–	–	–	–	–	–	–	7.38	5.24
System	–	–	–	–	–	–	–	–	4.12	–
Void vol. eq.	0.77	0.82	0.81	0.83	0.82	0.90	0.89	0.88	0.89	0.91

[a] Refers to gluconate.

TABLE V

RETENTION TIMES FOR ANIONS USING HYDROXIDE ELUENT ON A WATERS IC PAK A COLUMN

Concentration (m*M*):	1.02	2.05	2.76	4.60
pH:	11–12	11–12	11–12	11–12
Fluoride	6.22	3.81	2.92	2.04
Chloride	10.38	5.63	4.31	2.89
Bromide	15.92	7.88	6.15	4.01
Iodide	45.09	19.82	15.62	9.65
Chlorate	14.57	8.14	6.38	4.13
Bromate	8.36	4.95	3.85	2.61
Iodate	5.32	3.31	2.68	1.92
Nitrite	11.82	6.75	5.22	3.43
Nitrate	16.83	9.19	7.23	4.64
Bisulfite	6.94	4.18	3.30	2.29
Sulfite	–	44.84	30.60	11.64
Sulfate	74.05	47.98	31.43	11.91
Thiosulfate	230.76	96.83	55.85	23.30
Carbonate	57.72	23.81	19.50	8.63
Phosphate	63.58	29.08	18.94	9.40
Thiocyanate	64.57	32.62	25.02	17.03
Acetate	5.42	3.24	3.07	2.08
Oxalate	60.86	26.04	20.77	9.05
System	–	36.20	23.59	10.63
Void vol. eq.	0.91	0.91	0.91	0.91

The data shown in Tables IX–XV were subjected to statistical analysis to determine the reliability to which retention times could be predicted. In each case, the retention time for a particular analyte, eluent and stationary phase combination, obtained at the lowest eluent concentration, was used as the basis for the prediction of other retention data. The plot of $\log k'_A$ *versus* $\log\{E_m^{y-}\}$ was assumed to be linear and the theoretical slope derived from either the dominant equilibrium approach or the effective charge approach was used to predict retention times at other eluent concentrations. The predicted and observed retention times were then compared using a paired data Student's *t*-test. The *t*-test was also applied to the retention times calculated using the slope of the line of best fit. Table XVI gives a summary of the *t*-test statistics and shows the percentage success of predicting retention times at the 95% confidence level.

From Table XVI it can be seen the success rate is variable, but the following trends emerge. First, prediction is most successful when the eluent contains a single competing anion (*e.g.* benzoate or phthalate at pH 4). Second, the effective charge approach gives slightly better prediction of retention times than the dominant equilibrium approach for eluents containing two competing anions (*e.g.* phthalate at pH 5). Third, neither the dominant equilibrium approach nor the effective charge approach can be considered to provide sufficient reliability in predicting solute retention times to permit their use as a theoretical model for optimization in IC.

TABLE VI

RETENTION TIMES FOR ANIONS USING PHOSPHATE ELUENTS ON TWO COLUMNS (HAMILTON PRP-X100 AND WATERS IC PAK A)

	Hamilton														
Concentration (m*M*):	1.98	2.96	4.00	4.00	3.93	4.84	6.00	8.00	7.84	10.00	9.77	15.00	20.00	25.00	30.00
pH:	10.0	10.0	5.0	7.2	10.0	10.0	7.2	5.0	7.2	5.0	7.2	5.0	5.0	5.0	5.0
Fluoride	1.75	1.50	3.91	1.85	1.35	1.30	1.41	1.44	–	1.08	1.34	–	–	–	–
Chloride	3.12	2.66	8.55	3.02	2.39	2.27	2.66	8.02	2.44	7.01	2.18	5.48	4.82	4.18	3.74
Bromide	7.14	5.93	23.04	6.93	5.27	5.00	6.16	19.89	5.58	17.44	5.35	13.15	11.62	9.91	8.72
Iodide	–	–	–	–	47.70	36.70	48.26	170.90	47.54	108.40	38.69	–	–	76.60	75.02
Chlorate	12.52	10.55	51.63	14.77	9.09	8.37	9.20	30.75	8.80	24.70	10.99	18.81	15.88	9.82	13.24
Bromate	5.70	4.92	17.74	5.17	4.32	4.07	4.98	16.30	4.40	14.07	4.05	11.01	9.37	8.10	7.17
Iodate	1.74	1.55	5.58	1.76	1.41	1.34	1.55	3.96	1.42	3.44	1.36	2.80	2.48	2.19	1.99
Nitrite	4.66	4.02	16.01	4.54	3.55	3.32	4.09	13.41	3.65	12.02	3.52	9.48	8.13	7.04	6.21
Nitrate	10.76	8.91	35.82	9.59	7.69	7.12	8.60	25.86	7.91	23.64	–	17.77	15.28	14.93	12.63
Bisulfite	2.34	2.02	7.47	5.03	1.81	1.72	3.57	5.70	2.84	5.26	2.37	4.21	3.68	3.23	2.89
Sulfite	–	–	–	–	–	–	22.05	–	13.50	–	–	–	–	–	–
Thiosulfate	44.76	31.25	–	39.50	18.64	19.26	28.23	–	21.07	–	18.32	–	–	–	–
Acetate	2.36	2.03	6.90	2.45	1.83	1.74	2.14	5.59	1.63	4.94	1.82	4.03	3.60	3.26	3.01
Oxalate	12.70	11.58	–	–	9.49	8.09	57.31	–	44.89	–	–	–	74.53	41.59	41.11
System	31.65	25.51	31.06	11.58	20.47	–	9.84	31.02	8.64	28.35	12.57	19.66	16.18	12.83	10.34
Void vol. eq.	0.79	0.79	0.75	0.80	0.79	0.79	0.80	0.74	0.80	0.76	0.80	0.76	0.78	0.76	0.76

	Waters											
Concentration (m*M*):	2.00	3.99	3.99	5.84	6.00	8.00	7.83	8.00	10.02	9.78	15.04	19.99
pH:	10.0	7.2	10.0	7.2	10.0	5.0	7.2	10.0	5.0	7.2	5.0	5.0
Fluoride	–	1.90	1.45	1.65	1.27	–	1.46	–	–	1.31	–	–
Chloride	3.45	3.27	2.86	3.08	2.43	10.12	2.76	2.02	8.45	2.57	6.73	5.89
Bromide	6.26	6.48	5.83	5.94	4.64	23.35	5.51	3.47	19.22	4.94	14.78	12.94
Iodide	24.58	25.84	19.71	23.26	17.57	103.43	21.03	11.94	84.37	6.32	65.65	56.76
Chlorate	7.21	7.39	6.18	6.82	5.07	27.03	6.08	3.80	20.62	5.62	17.36	12.94
Bromate	3.05	3.00	2.67	2.80	2.26	9.63	2.61	1.84	7.92	2.34	6.52	5.39
Iodate	1.61	1.52	1.50	1.49	1.28	3.69	1.44	1.16	3.22	1.28	2.73	2.31
Nitrite	5.01	5.08	4.31	4.61	3.61	17.58	4.25	2.74	14.27	3.79	11.83	9.61
Nitrate	8.62	8.64	7.38	8.01	6.12	35.78	7.29	4.39	29.30	6.58	21.62	18.30
Bisulfite	2.25	2.16	2.02	2.06	1.72	6.13	1.93	1.43	5.19	1.76	4.22	3.63
Sulfite	–	9.24	6.09	8.43	4.62	84.50	5.76	–	–	4.42	–	–
Thiosulfate	24.59	22.84	16.75	16.95	11.33	–	13.09	6.15	–	11.04	–	–
Thiocyanate	47.72	54.39	43.33	32.04	36.30	220.40	–	24.90	169.20	–	143.00	126.11
Acetate	1.85	1.78	1.78	1.76	1.45	3.84	1.66	1.35	3.41	1.47	2.79	2.44
Oxalate	8.95	–	7.41	–	6.34	–	–	–	113.22	6.91	–	–
System	17.13	2.03	14.01	2.18	4.07	29.50	1.90	6.61	21.01	1.63	17.78	13.16
Void vol. eq.	0.83	0.80	0.83	0.80	0.83	0.80	0.80	0.83	0.80	0.80	0.80	0.80

End-points approach

The data listed in Tables IX–XV give linear plots and this linearity is further confirmed in Table XVI which shows that the success rate (using *t*-statistics) obtained when the observed slope is used to calculate retention times was 100%. However, this

TABLE VII

RETENTION TIMES FOR ANIONS USING PHTHALATE ELUENTS ON THREE COLUMNS (HAMILTON PRP-X100, VYDAC 302 IC 4.6 AND WATERS IC PAK A)

	Hamilton								
Concentration (m*M*):	1.00	1.00	1.00	2.00	2.00	2.00	4.00	4.00	4.00
pH:	4.0	5.0	6.0	4.0	5.0	6.0	4.0	5.0	6.0
Fluoride	2.96	2.10	1.65	2.02	1.52	0.81	1.45	1.37	0.82
Chloride	4.02	2.61	2.16	2.60	1.82	1.65	1.75	1.41	1.33
Bromide	5.14	3.41	2.94	3.25	2.32	2.19	2.11	1.69	1.70
Iodide	11.16	7.95	8.00	6.60	5.18	5.71	4.01	3.36	4.11
Chlorate	6.65	4.57	4.36	3.97	2.99	3.15	2.50	2.08	2.39
Bromate	3.93	2.62	2.26	2.49	1.85	1.74	1.75	1.42	1.40
Iodate	2.97	1.85	1.58	1.97	1.43	1.26	1.41	1.17	1.11
Nitrite	4.40	2.92	2.45	2.80	2.04	1.86	1.97	1.52	1.49
Nitrate	5.91	3.82	3.47	3.54	2.62	2.52	2.32	1.87	1.93
Sulfite	39.21	13.94	8.31	14.10	6.26	4.26	5.60	3.02	2.42
Sulfate	39.37	14.15	8.35	14.07	6.29	4.30	5.58	3.04	2.42
Thiosulfate	71.81	23.32	14.08	23.47	10.01	6.97	8.93	4.54	3.70
Phosphate	3.01	1.96	2.01	2.01	1.49	1.51	1.39	1.20	1.22
Acetate	2.13	2.01	1.81	1.95	1.66	1.45	1.67	1.45	1.23
Oxalate	53.78	13.54	8.96	–	6.36	5.04	4.04	3.66	3.40
System	55.00	43.33	–	46.00	22.96	–	30.00	13.64	–
Void vol. eq.	0.71	0.74	0.77	0.75	0.78	0.79	0.78	0.83	0.81
	Vydac								
Concentration (m*M*)	1.00	1.00	1.00	2.00	2.00	2.00	4.00	4.00	4.00
pH:	4.0	5.0	6.0	4.0	5.0	6.0	4.0	5.0	6.0
Chloride	10.92	6.34	5.05	6.84	4.51	3.49	4.63	3.33	2.70
Bromide	13.20	7.85	6.77	8.15	5.43	4.13	5.30	3.75	3.02
Iodide	22.49	14.36	15.45	13.30	9.29	6.90	7.91	5.53	4.30
Chlorate	13.26	7.96	7.12	8.27	5.53	4.15	5.41	3.90	3.07
Bromate	9.97	5.83	4.67	6.36	4.27	3.32	4.52	3.20	2.65
Iodate	8.07	4.37	3.29	5.30	3.50	2.83	3.86	2.96	2.41
Nitrite	11.93	7.55	6.43	7.57	5.28	3.97	5.10	3.70	2.95
Nitrate	14.59	8.82	6.90	8.93	6.04	4.53	5.81	4.05	3.21
Sulfite	48.00	35.63	19.22	54.35	17.18	8.56	22.90	8.12	4.40
Sulfate	48.00	35.42	18.52	53.40	17.17	8.61	22.68	8.13	4.42
Thiosulfate	86.40	55.76	29.32	70.61	22.48	11.26	28.05	10.01	5.33
Phosphate	10.02	5.59	4.84	6.35	4.03	4.05	4.51	4.03	3.23
Acetate	3.83	4.40	3.73	3.27	3.76	3.28	2.76	2.98	2.70
Oxalate	37.45	27.63	21.81	24.00	22.63	12.26	18.00	12.34	5.96
System	48.00	39.55	–	24.00	–	–	18.00	12.34	–
Void vol. eq.	1.45	1.62	1.78	1.60	1.68	1.75	1.52	1.79	1.87

TABLE VII (*continued*)

	Waters								
Concentration (m*M*):	1.00	1.00	1.00	2.00	2.00	2.00	4.00	4.00	4.00
pH:	4.0	5.0	6.0	4.0	5.0	6.0	4.0	5.0	6.0
Fluoride	3.76	2.07	1.67	2.29	1.42	1.26	1.69	1.27	1.15
Chloride	6.26	3.93	3.61	3.99	2.53	2.29	2.70	1.94	1.85
Bromide	9.81	8.10	6.53	6.25	4.12	4.07	3.96	2.97	2.92
Iodide	28.14	28.13	23.18	17.58	12.79	13.60	10.42	9.35	8.95
Chlorate	10.43	6.81	5.69	6.83	4.67	4.26	4.07	3.15	3.37
Bromate	5.18	3.26	2.66	3.62	2.38	2.08	2.29	1.76	1.74
Iodate	3.16	2.11	1.66	2.29	1.56	1.32	1.86	1.28	1.07
Nitrite	7.91	5.37	5.26	5.03	3.70	3.25	3.22	2.57	2.35
Nitrate	11.85	9.14	8.83	7.72	6.26	5.29	4.73	3.75	3.61
Sulfite	53.60	17.19	10.44	24.62	8.27	5.63	10.74	4.21	2.85
Sulfate	53.28	17.92	10.62	24.29	8.05	5.72	10.76	4.10	2.81
Thiosulfate	109.77	34.00	18.68	–	14.62	9.36	16.71	7.10	5.14
Phosphate	3.43	2.23	2.10	2.14	1.61	1.55	2.45	1.26	1.30
Acetate	1.69	1.98	1.92	1.36	1.55	1.50	1.08	1.29	1.31
Oxalate	36.39	22.20	15.84	17.30	10.04	6.99	7.33	4.63	3.50
System	35.00	26.78	–	22.00	15.86	–	12.00	9.72	–
Void vol. eq.	0.72	0.65	0.77	0.65	0.68	0.60	0.66	0.76	0.71

success rate is of limited practical value in optimization procedures since it can be attained only after retention data are measured for at least 5 points across the search area. As stated earlier, acquisition of these data would be a time consuming process.

One possible compromise between the theoretical approaches (*i.e.* the dominant equilibrium and the effective charge methods) and the experimental technique is to define the slope of the retention plot by measuring retention data at the extremes of the search area. Retention times for eluent compositions which are intermediate between the measured points could then be calculated by assuming linearity of the retention plot. This method can be termed the "end points" approach. The success rate for this approach is shown in Table XVI, from which it can be seen that the end points method is certainly more successful than either of the theoretical methods and so can be considered more appropriate for use in an optimization routine for IC. The main advantage of this method is that only two experiments are necessary to permit prediction of solute retention times for any eluent composition in the search area.

Optimization of eluent composition using the end points approach

A limited optimization of the separation of a mixture of inorganic anions using the "end points" approach was performed. The optimization strategy employed has been described in detail earlier [1]. Since this approach enables one parameter to be optimized at a time, only the concentration of the competing ions in the eluent was optimized. Phthalate eluents at pH 5.0 were employed since at this pH value, both the singly and doubly charged forms are present. Two initial experiments were performed in which retention times for each solute ion were obtained at two limiting eluent concentrations, namely 1 m*M* and 4 m*M*. This defined the search area of eluent

TABLE VIII

RETENTION TIMES FOR ANIONS USING *p*-TOLUENESULFONATE ELUENTS ON THREE COLUMNS (HAMILTON PRP-X100, VYDAC 302 IC 4.6 AND WATERS IC PAK A)

	Hamilton				Vydac				Waters			
Concentration (m*M*):	1.00	2.00	3.00	4.00	2.00	3.00	4.00	5.00	2.00	3.00	4.00	5.00
pH:	4.0	4.0	4.0	4.0	4.0	4.0	4.0	4.0	4.0	4.0	4.0	4.0
Fluoride	2.74	1.85	1.52	1.32	–	–	–	–	3.54	2.74	2.35	1.96
Chloride	4.15	2.34	1.80	1.57	6.45	5.15	4.04	3.55	6.88	4.59	3.70	3.14
Bromide	4.81	2.77	2.15	1.79	6.97	4.99	4.07	3.59	10.02	6.89	5.74	4.61
Iodide	9.30	5.66	4.03	3.31	8.76	5.92	4.50	3.96	29.04	19.65	14.91	12.68
Chlorate	6.18	3.45	2.53	2.13	6.97	5.24	4.09	3.61	10.69	7.21	6.03	4.92
Bromate	3.85	2.26	1.75	1.52	6.55	4.74	3.88	3.46	5.54	3.93	3.33	2.77
Iodate	2.98	1.85	1.61	1.44	6.34	4.76	3.82	3.41	3.56	2.64	2.29	1.95
Nitrite	4.03	2.53	1.98	1.71	7.42	5.14	4.14	3.56	7.66	5.56	4.65	3.71
Nitrate	5.41	3.08	2.28	1.95	7.52	5.53	4.27	3.76	12.40	8.47	6.75	5.64
Bisulfite	–	1.70	–	–	–	–	–	–	–	–	2.44	–
Sulfite	9.99	7.77	5.08	3.51	75.23	38.94	16.43	13.85	60.75	26.70	16.77	11.16
Sulfate	9.70	7.71	5.06	3.52	81.87	34.21	16.51	13.99	59.29	26.87	16.18	11.25
Thiosulfate	38.73	14.08	8.45	5.17	92.85	66.54	20.89	14.36	114.57	48.97	32.25	19.38
Phosphate	2.95	1.98	1.43	1.53	10.14	7.07	5.41	4.10	3.42	2.62	2.24	1.86
Thiocyanate	–	12.49	–	–	–	–	–	–	–	–	30.49	–
Acetate	1.97	1.80	1.61	1.39	3.40	3.20	2.94	2.49	1.64	1.66	1.50	1.28
Oxalate	8.43	6.08	3.85	–	74.17	–	–	11.68	–	49.40	17.73	8.04
System	10.63	9.45	10.66	–	36.00	28.10	18.30	13.88	41.70	42.54	18.81	12.10
Void vol. eq.	0.75	0.82	0.88	0.93	1.47	1.58	1.66	1.70	0.74	0.75	0.77	0.72

TABLE IX

OBSERVED AND PREDICTED SLOPES OF LOG *k'* *VERSUS* LOG{BENZOATE} PLOTS FOR ANIONS ON THREE COLUMNS (HAMILTON PRP-X100, VYDAC 302 IC 4.6 AND WATERS IC PAK A)

Model:	pH 4.0				pH 6.4					
	Dominant equilibrium	Effective charge	Vydac		Dominant equilibrium	Effective charge	Hamilton		Waters	
			Observed slope	End points			Observed slope	End points	Observed slope	End points
Fluoride	–	–	–	–	−1.000	−1.000	−1.705	−1.703	−0.953	−0.946
Chloride	−1.000	−2.564	−1.334	−1.426	−1.000	−1.000	−1.515	−1.493	−1.033	−1.009
Bromide	−1.000	−2.564	−1.314	−1.411	−1.000	−1.000	−1.387	−1.367	−0.989	−0.982
Iodide	−1.000	−2.564	−1.297	−1.398	−1.000	−1.000	−1.486	−1.482	−1.045	−1.011
Chlorate	−1.000	−2.564	−1.311	−1.411	−1.000	−1.000	−1.452	−1.441	−1.040	−1.033
Bromate	−1.000	−2.564	−1.250	−1.239	−1.000	−1.000	−1.486	−1.474	−0.993	−0.987
Iodate	−1.000	−2.564	−1.325	−1.422	−1.000	−1.000	−1.488	−1.441	−0.942	−0.939
Nitrite	−0.880	−2.256	−1.302	−1.385	−1.000	−1.000	−1.482	−1.466	−1.040	−1.036
Nitrate	−1.000	−2.564	−1.250	−1.248	−1.000	−1.000	−1.494	−1.481	−1.035	−1.026
Bisulfite	−0.990	−2.538	−1.165	−1.148	–	–	–	–	–	–
Sulfite	−1.980	−2.538	−2.914	−2.914	−1.140	−1.140	−2.745	−2.721	−1.832	−1.821
Sulfate	−2.000	−5.128	−2.754	−2.932	−2.000	−2.000	−2.657	−2.547	−1.847	−1.834
Thiosulfate	−2.000	−5.128	−2.956	−2.956	−2.000	−2.000	−2.669	−2.508	−1.929	−1.911
Phosphate	−0.990	−2.538	−0.553	−0.612	−1.140	−1.140	−2.431	−2.283	−0.935	−0.979
Thiocyanate	−1.000	−2.564	−1.214	−1.202	–	–	–	–	–	–
Acetate	−0.150	−0.384	−0.741	−0.745	−0.980	−0.980	−1.440	−1.427	−0.939	−0.937
Oxalate	−1.380	−3.538	–	–	−1.990	−1.990	−2.489	−2.529	–	–
System	–	–	–	–	–	–	−0.815	−0.815	–	–

TABLE X

OBSERVED AND PREDICTED SLOPES OF LOG *k' VERSUS* LOG{CARBONATE} PLOTS FOR ANIONS ON A WATERS IC PAK A COLUMN

Model:	pH 8.5				pH 10.3			
	Dominant equilibrium	Effective charge	Waters		Dominant equilibrium	Effective charge	Waters	
			Observed slope	End points			Observed slope	End points
Fluoride	−0.500	−1.000	−0.832	−0.812	−0.500	−0.667	−0.521	−0.553
Chloride	−0.500	−1.000	−0.744	−0.719	−0.500	−0.667	−0.441	−0.468
Bromide	−0.500	−1.000	−0.796	−0.778	−0.500	−0.667	−0.387	−0.418
Iodide	−0.500	−1.000	−0.959	−0.901	−0.500	−0.667	−0.342	−0.370
Chlorate	−0.500	−1.000	−0.803	−0.776	−0.500	−0.667	−0.370	−0.400
Bromate	−0.500	−1.000	−0.802	−0.779	−0.500	−0.667	−0.425	−0.451
Iodate	−0.500	−1.000	−0.931	−0.839	−0.500	−0.667	−0.452	−0.483
Nitrite	−0.500	−1.000	−0.784	−0.757	−0.500	−0.667	−0.330	−0.363
Nitrate	−0.500	−1.000	−0.734	−0.671	−0.500	−0.667	−0.368	−0.396
Bisulfite	−0.500	−1.000	−0.813	−0.788	−0.500	−0.667	−0.460	−0.477
Sulfite	−1.000	−2.000	−0.985	−0.912	−1.000	−1.333	−0.783	−0.831
Sulfate	−1.000	−2.000	−1.036	−0.981	−1.000	−1.333	−0.787	−0.835
Thiosulfate	−1.000	−2.000	−1.502	−1.485	−1.000	−1.333	−0.782	−0.834
Phosphate	−1.000	−2.000	−1.090	−0.977	−1.000	−1.333	−0.842	−0.885
Thiocyanate	−0.500	−1.000	−0.905	−0.866	−0.500	−0.667	−0.456	−0.609
Acetate	−0.500	−1.000	−0.867	−0.836	−0.500	−0.667	−0.355	−0.388
System	–	–	–	–	–	–	−0.550	−0.588

TABLE XI

OBSERVED AND PREDICTED SLOPES OF LOG *k' VERSUS* LOG{GLUCONATE} PLOTS FOR ANIONS ON TWO COLUMNS (HAMILTON PRP-X100 AND WATERS IC PAK A) AT pH 8.5

Model:	Dominant equilibrium	Effective charge	Hamilton		Waters	
			Observed slope	End points	Observed slope	End points
Fluoride	−1.000	−1.000	−0.943	−0.980	−0.848	−0.832
Chloride	−1.000	−1.000	−0.825	−0.851	−0.754	−0.725
Bromide	−1.000	−1.000	−0.817	−0.759	−0.710	−0.690
Iodide	−1.000	−1.000	–	–	−0.658	−0.628
Chlorate	−1.000	−1.000	−0.627	−0.586	−0.713	−0.694
Bromate	−1.000	−1.000	−0.697	−0.750	−0.758	−0.755
Iodate	−1.000	−1.000	−1.048	−0.970	−2.074	−2.138
Nitrite	−1.000	−1.000	−0.720	−0.766	−0.725	−0.699
Nitrate	−1.000	−1.000	−0.686	−0.801	−0.700	−0.692
Sulfite	−1.960	−1.960	−1.430	−1.466	−1.434	−1.409
Sulfate	−2.000	−2.000	−1.471	−1.492	−1.457	−1.430
Thiosulfate	−2.000	−2.000	−1.426	−1.640	−1.455	−1.439
Phosphate	−1.960	−1.960	−1.519	−1.461	−1.460	−1.453
Acetate	−1.000	−1.000	−0.897	−0.886	−0.818	−0.824
Oxalate	−2.000	−2.000	–	–	−2.927	−2.927
Carbonate	−1.010	−1.010	−1.003	−1.035	−0.901	−0.914

TABLE XII

OBSERVED AND PREDICTED SLOPES OF LOG *k'* *VERSUS* LOG{HYDROXIDE} PLOTS ON A WATERS IC PAK A COLUMN AT pH 11–12

Model:	Dominant equilibrium	Effective charge	Waters	
			Observed slope	End points
Fluoride	−1.000	−1.000	−1.058	−1.058
Chloride	−1.000	−1.000	−1.070	−1.069
Bromide	−1.000	−1.000	−1.077	−1.079
Iodide	−1.000	−1.000	−1.103	−1.108
Chlorate	−1.000	−1.000	−0.983	−0.987
Bromate	−1.000	−1.000	−1.010	−1.013
Iodate	−1.000	−1.000	−1.003	−1.007
Nitrite	−1.000	−1.000	−1.000	−1.003
Nitrate	−1.000	−1.000	−0.987	−0.992
Bisulfite	−1.000	−1.000	−1.006	−1.008
Sulfite	−2.000	−2.000	−1.825	−1.797
Sulfate	−2.000	−2.000	−1.269	−1.296
Thiosulfate	−2.000	−2.000	−1.592	−1.593
Phosphate	−2.000	−2.000	−1.365	−1.367
Thiocyanate	−1.000	−1.000	−0.944	−0.939
Acetate	−1.000	−1.000	−0.893	−0.923
Oxalate	−2.000	−2.000	−1.333	−1.365
Carbonate	−2.000	−2.000	−1.329	−1.363
System	—	—	−1.650	−1.641

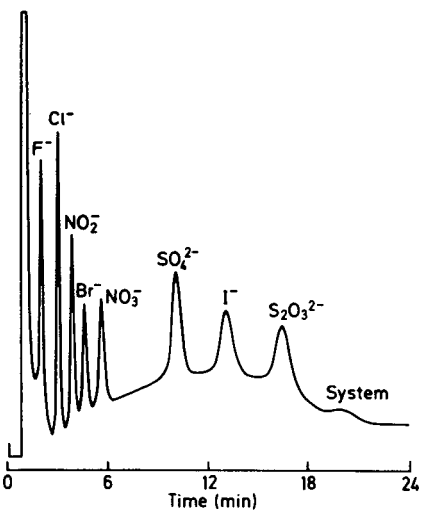

Fig. 1. Chromatogram obtained using the optimal mobile phase composition predicted by the end-points optimization strategy. Conditions: eluent, 1.74 m*M* phthalate at pH 5.0; column, Waters IC Pak A at 35°C: flow-rate, 1.0 ml/min; solute concentrations, Cl^-, Br^-, NO_2^-, NO_3^-, SO_4^{2-}, $S_2O_3^{2-}$ (all 10 ppm), F^- (20 ppm) and I^- (30 ppm); injection volume, 20 μl.

TABLE XIII

OBSERVED AND PREDICTED SLOPES OF LOG k' *VERSUS* LOG{PHOSPHATE} PLOTS FOR ANIONS ON TWO COLUMNS (HAMILTON PRP-X100 AND WATERS IC PAK A)

Model:	pH 5.0						pH 7.2	
	Dominant equilibrium	Effective charge	Hamilton		Waters		Dominant equilibrium	Effective charge
			Observed slope	End points	Observed slope	End points		
Fluoride	−0.495	−0.990	−2.547	−2.640	–	–	−0.500	−0.667
Chloride	−0.500	−1.000	−0.588	−0.518	−0.653	−0.662	−0.500	−0.667
Bromide	−0.500	−1.000	−0.583	−0.552	−0.674	−0.677	−0.500	−0.667
Iodide	−0.500	−1.000	−0.611	−0.700	−0.654	−0.664	−0.500	−0.667
Chlorate	−0.500	−1.000	−0.946	−1.011	−0.774	−0.840	−0.500	−0.667
Bromate	−0.500	−1.000	−0.564	−0.524	−0.684	−0.715	−0.500	−0.667
Iodate	−0.500	−1.000	−0.740	−0.733	−0.690	−0.714	−0.500	−0.667
Nitrite	−0.495	−0.990	−0.576	−0.553	−0.668	−0.704	−0.500	−0.667
Nitrate	−0.500	−1.000	−0.590	−0.585	−0.757	−0.757	−0.500	−0.667
Bisulfite	−0.505	−1.010	−0.625	−0.615	−0.677	−0.693	−0.500	−0.667
Sulfite	−1.000	−2.000	–	–	–	–	−1.000	−1.333
Thiosulfate	−1.000	−2.000	–	–	–	–	−1.000	−1.333
Thiocyanate	−0.500	−1.000	–	–	−0.576	−0.615	−0.500	−0.667
Acetate	−0.315	−0.630	−0.565	−0.540	−0.673	−0.673	−0.500	−0.667
Oxalate	−0.930	−1.860	−1.609	−1.565	–	–	−1.000	−1.333
System	–	–	−0.660	−0.618	−0.838	−0.923	–	–

concentrations over which the optimization process would operate. The retention times of the solute anions at eluent concentrations throughout the search area were predicted by assuming linearity between log k' and log{eluent} (an assumption which has been justified throughout this work). A suitable optimization criterion [1] was then used to predict the eluent concentration providing the best separation of the anion mixture. The chromatogram obtained with this predicted concentration (1.74 mM) is shown in Fig. 1, from which it can be seen that resolution of all eight anions present in the mixture, and the system peak, was achieved. Table XVII shows the observed retention times for this eluent composition, together with those predicted from the linear retention model. The differences between these retention times are also listed in Table XVII, from which the correlation between predicted and actual retention times can be seen to be good. This further indicates the validity of the linear retention model which permits successful one-factor optimization using the "end points" approach to be achieved.

CONCLUSION

Simple linear retention models are of limited suitability for optimization in IC. Extensive retention data for a range of analytes, eluents and stationary phases demonstrate that plots of $\log k'_A$ *versus* $\log\{E_m^{y-}\}$ show good linearity, but the slopes of these plots are not in accordance with theoretical predictions. Linear models are therefore unreliable for use in theoretical optimizations unless the slopes of the

				pH 10.0					
Hamilton		Waters		Dominant equilibrium	Effective charge	Hamilton		Waters	
Observed slope	End points	Observed slope	End points			Observed slope	End points	Observed slope	End points
−0.781	−0.795	−0.841	−0.849	−0.500	−0.500	−0.734	−0.713	−0.831	−0.831
−0.546	−0.562	−0.382	−0.375	−0.500	−0.500	−0.523	−0.513	−0.545	−0.569
−0.359	−0.348	−0.340	−0.352	−0.500	−0.500	−0.471	−0.462	−0.485	−0.519
−0.474	−0.490	−1.430	−1.685	−0.500	−0.500	−1.251	−1.251	−0.492	−0.549
−0.436	−0.372	−0.346	−0.348	−0.500	−0.500	−0.500	−0.492	−0.515	−0.551
−0.355	−0.350	−0.384	−0.401	−0.500	−0.500	−0.465	−0.453	−0.534	−0.565
−0.639	−0.625	−0.410	−0.459	−0.500	−0.500	−0.625	−0.616	−0.604	−0.616
−0.393	−0.376	−0.384	−0.397	−0.500	−0.500	−0.489	−0.481	−0.525	−0.565
−0.329	−0.331	−0.333	−0.338	−0.500	−0.500	−0.521	−0.512	−0.520	−0.565
−1.158	−1.161	−0.370	−0.383	−0.500	−0.500	−0.592	−0.581	−0.583	−0.617
−1.520	−1.546	−0.959	−0.944	−1.000	−1.000	–	–	−0.807	−0.807
−0.954	−0.930	−0.872	−0.854	−1.000	−1.000	−1.313	−1.340	−1.010	−1.080
–	–	−1.378	−1.378	−0.500	−0.500	–	–	−0.433	−0.481
−0.704	−0.561	−0.388	−0.418	−0.500	−0.500	−0.573	−0.561	−0.509	−0.494
−0.982	−0.982	–	–	−1.000	−1.000	−1.000	−0.994	−0.348	−0.353
−0.017	0.105	−0.428	−0.438	–	–	−0.663	−0.670	−1.001	−0.748

TABLE XIV

OBSERVED AND PREDICTED SLOPES OF LOG *k'* *VERSUS* LOG{PHTHALATE} PLOTS FOR ANIONS ON THREE COLUMNS (HAMILTON PRP-X100, VYDAC 302 IC 4.6 AND WATERS IC PAK A)

Model:	pH 4.0							
	Dominant equilibrium	Effective charge	Hamilton		Waters		Vydac	
			Observed slope	End points	Observed slope	End points	Observed slope	End points
Fluoride	−0.435	−0.935	−1.041	−1.042	−0.792	−0.792	–	–
Chloride	−0.500	−1.075	−1.049	−1.049	−0.725	−0.726	−0.924	−0.923
Bromide	−0.500	−1.075	−1.030	−1.031	−0.737	−0.737	−0.940	−0.940
Iodide	−0.500	−1.075	−1.008	−1.008	−0.751	−0.752	−0.985	−0.985
Chlorate	−0.500	−1.075	−1.060	−1.060	−0.762	−0.763	−0.922	−0.921
Bromate	−0.500	−1.075	−1.026	−1.026	−0.728	−0.730	−0.870	−0.869
Iodate	−0.500	−1.075	−1.087	−1.087	−0.498	−0.498	−0.866	−0.864
Nitrite	−0.440	−0.946	−0.976	−1.976	−0.751	−0.752	−0.892	−0.891
Nitrate	−0.500	−1.075	−1.042	−1.042	−0.731	−0.732	−0.928	−0.927
Sulfite	−1.000	−2.150	−1.727	−1.727	−1.248	−1.249	−0.653	−0.657
Sulfate	−1.000	−2.150	−1.735	−1.735	−1.242	−1.243	−0.659	−0.664
Thiosulfate	−1.000	−2.150	−1.798	−1.798	–	–	−0.961	−0.964
Phosphate	−0.495	−1.064	−1.135	−1.136	−0.265	−0.262	−0.876	−0.875
Acetate	−0.075	−0.161	−0.445	−0.446	−0.598	−0.600	−0.555	−0.554
Oxalate	−0.690	−1.483	−2.295	−2.295	−1.262	−1.264	−0.661	−0.659
System	–	–	−0.565	−0.566	−0.810	−0.811	−0.867	−0.864

(*Continued on p. 56*)

TABLE XIV (*continued*)

Model:	pH 5.0							
	Dominant equilibrium	Effective charge	Hamilton		Waters		Vydac	
			Observed slope	End points	Observed slope	End points	Observed slope	End points
Fluoride	−0.495	−0.779	−0.821	−0.828	−0.947	−0.946	–	–
Chloride	−0.500	−0.787	−1.021	−1.021	−0.937	−0.937	−0.968	−0.969
Bromide	−0.500	−0.787	−0.995	−0.995	−1.093	−1.092	−0.999	−1.000
Iodide	−0.500	−0.787	−0.924	−0.924	−1.050	−1.048	−1.053	−1.054
Chlorate	−0.500	−0.787	−0.982	−0.982	−0.876	−0.877	−0.955	−0.955
Bromate	−0.500	−0.787	−1.017	−1.018	−0.888	−0.889	−0.950	−0.951
Iodate	−0.500	−0.787	−1.035	−1.035	−0.942	−0.942	−0.761	−0.761
Nitrite	−0.495	−0.779	−1.004	−1.004	−0.887	−0.888	−0.981	−0.982
Nitrate	−0.500	−0.787	−0.953	−0.953	−0.954	−0.955	−1.002	−1.003
Sulfite	−1.000	−1.574	−1.522	−1.522	−1.370	−1.371	−1.415	−1.416
Sulfate	−1.000	−1.574	−1.525	−1.525	−1.431	−1.431	−1.410	−1.411
Thiosulfate	−1.000	−1.574	−1.528	−1.528	−1.444	−1.444	−1.578	−1.578
Phosphate	−0.500	−0.787	−1.042	−1.043	−1.030	−1.031	−0.537	−0.535
Acetate	−0.315	−0.496	−0.665	−0.665	−0.858	−0.859	−0.752	−0.754
Oxalate	−0.930	−1.464	−1.292	−1.291	−1.490	−1.491	−0.794	−0.797
System	–	–	−1.046	−1.045	−0.976	−0.977	−1.096	−1.096

Model:	pH 6.0							
	Dominant equilibrium	Effective charge	Hamilton		Waters		Vydac	
			Observed slope	End points	Observed slope	End points	Observed slope	End points
Fluoride	−0.500	−0.555	3.618	3.601	−0.500	−0.502	–	–
Chloride	−0.500	−0.555	−0.819	−0.819	−0.663	−0.664	−1.128	−1.129
Bromide	−0.500	−0.555	−0.746	−0.746	−0.694	−0.696	−1.205	−1.205
Iodide	−0.500	−0.555	−0.663	−0.663	−0.730	−0.732	−1.410	−1.410
Chlorate	−0.500	−0.555	−0.693	−0.693	−0.424	−0.426	−1.242	−1.242
Bromate	−0.500	−0.555	−0.778	−0.778	−0.414	−0.416	−1.084	−1.085
Iodate	−0.500	−0.555	−0.822	−0.822	−0.641	−0.645	−0.849	−0.851
Nitrite	−0.500	−0.555	−0.765	−0.765	−0.734	−0.736	−1.197	−1.198
Nitrate	−0.500	−0.555	−0.741	−0.741	−0.747	−0.749	−1.106	−1.107
Sulfite	−1.000	−1.111	−1.267	−1.267	−1.133	−1.136	−1.573	−1.574
Sulfate	−1.000	−1.111	−1.275	−1.275	−1.160	−1.164	−1.536	−1.537
Thiosulfate	−1.000	−1.111	−1.258	−1.258	−1.045	−1.047	−1.690	−1.690
Phosphate	−0.500	−0.588	−0.926	−0.927	−0.579	−0.582	−0.682	−0.684
Acetate	−0.475	−0.527	−0.753	−0.753	−0.448	−0.451	−0.721	−0.723
Oxalate	−0.990	−1.100	−0.957	−0.957	−1.273	−1.275	−1.301	−1.303

TABLE XV

OBSERVED AND PREDICTED SLOPES OF LOG *k'* *VERSUS* LOG{*p*-TOLUENESULFONATE} PLOTS FOR ANIONS ON THREE COLUMNS (HAMILTON PRP-X100, VYDAC 302 IC 4.6 AND WATERS IC PAK A) AT pH 4.0

Model:	Dominant equilibrium	Effective charge	Hamilton		Waters		Vydac	
			Observed slope	End points	Observed slope	End points	Observed slope	End points
Fluoride	−0.870	−0.870	−1.326	−1.375	−0.900	−0.897	–	–
Chloride	−1.000	−1.000	−1.368	−1.396	−1.041	−1.020	−1.300	−1.279
Bromide	−1.000	−1.000	−1.270	−1.309	−0.949	−0.949	−1.378	−1.370
Iodide	−1.000	−1.000	−1.093	−1.108	−0.973	−0.940	−1.511	−1.485
Chlorate	−1.000	−1.000	−1.255	−1.278	−0.945	−0.943	−1.377	−1.353
Bromate	−1.000	−1.000	−1.359	−1.389	−0.935	−0.929	−1.373	−1.361
Iodate	−1.000	−1.000	−1.210	−1.259	−0.918	−0.908	−1.364	−1.344
Nitrite	−0.880	−0.880	−1.198	−1.224	−0.913	−0.916	−1.477	−1.477
Nitrate	−1.000	−1.000	−1.267	−1.288	−0.961	−0.941	−1.404	−1.380
Sulfite	−2.000	−2.000	−1.073	−1.105	−1.947	−1.942	−2.329	−2.200
Sulfate	−2.000	−2.000	−1.046	−1.078	−1.929	−1.905	−2.382	−2.282
Thiosulfate	−2.000	−2.000	−1.251	−1.784	−1.981	−2.010	−2.536	−2.393
Phosphate	−0.990	−0.990	−1.209	−1.122	−0.940	−0.936	−1.585	−1.615
Acetate	−0.150	−0.150	−0.835	−0.887	−0.518	−0.515	−1.118	−1.178
Oxalate	−1.380	−1.380	−1.000	−1.037	−3.764	−3.759	−2.404	−2.404
System	–	–	−0.178	−0.159	−1.497	−1.414	−1.361	−1.341

TABLE XVI

SUMMARY OF *t*-TEST STATISTICS SHOWING PERCENTAGE SUCCESS OF PREDICTING RETENTION TIMES USING FOUR RETENTION MODELS

Column	Eluent	pH	Retention model			
			Dominant equilibrium	Effective charge	End points	Observed slope
Hamilton	Benzoate	6.4	93.3	93.3	100.0	100.0
	Gluconate/borate	8.5	35.7	35.7	100.0	100.0
	Phosphate	5.0	50.0	16.6	27.2	100.0
	Phosphate	7.2	53.8	53.8	80.0	100.0
	Phosphate	10.0	66.6	66.6	90.0	100.0
	Phthalate	4.0	78.6	92.8	–	100.0
	Phthalate	5.0	66.7	100.0	–	100.0
	Phthalate	6.0	73.3	73.3	–	100.0
	p-Toluenesulfonate	4.0	26.7	26.7	92.8	100.0
Vydac	Benzoate	4.0	42.8	7.1	91.6	100.0
	Phthalate	4.0	26.6	92.8	–	100.0
	Phthalate	5.0	92.8	100.0	–	100.0
	Phthalate	6.0	85.7	85.7	–	100.0
	p-Toluenesulfonate	4.0	30.7	30.7	85.7	100.0

(*Continued on p. 58*)

TABLE XVI (*continued*)

Column	Eluent	pH	Retention model			
			Dominant equilibrium	Effective charge	End points	Observed slope
Waters	Benzoate	6.4	100.0	100.0	100.0	100.0
	Carbonate/bicarbonate	8.5	18.7	25.0	93.7	100.0
	Carbonate/bicarbonate	10.3	68.7	6.2	93.7	100.0
	Gluconate/borate	8.5	6.6	6.6	13.3	100.0
	Hydroxide	11–12	66.6	66.6	94.1	100.0
	Phosphate	5.0	0.0	90.9	75.7	100.0
	Phosphate	7.2	38.4	15.4	64.3	100.0
	Phosphate	10.0	92.3	92.3	76.9	100.0
	Phthalate	4.0	100.0	85.7	--	100.0
	Phthalate	5.0	66.7	93.3	—	100.0
	Phthalate	6.0	100.0	100.0	—	100.0
	p-Toluenesulfonate	4.0	73.3	73.3	86.6	100.0
Times model was more than 90% successful			6/26	10/26	9/17	26/26

TABLE XVII

COMPARISON OF PREDICTED AND ACTUAL RETENTION TIMES OBTAINED FOR EIGHT ANIONS USING 1.74 m*M* PHTHALATE ELUENT AT pH 5.0 ON A WATERS IC PAK A COLUMN

Anions	Predicted retention time (min)	Actual retention time (min)	Difference (%)
F^-	1.78	1.80	1.12
Cl^-	2.77	2.81	1.44
Br^-	4.35	4.37	0.45
I^-	12.72	12.82	0.78
NO_2^-	3.60	3.62	0.55
NO_3^-	5.33	5.37	0.75
SO_4^{2-}	9.65	9.78	1.34
$S_2O_3^{2-}$	15.74	16.18	2.79

retention plots are determined by preliminary measurements of retention times at the extremes (end points) of the search area. Under these circumstances, successful optimization can be achieved.

Although the end points approach offers promise, it is limited in its utility since it can be applied to only one eluent parameter at a time. In order to optimize both the eluent concentration and pH, a more complex retention model is necessary. The multiple eluent species model [9] or its variants [10,11] may be suitable for this purpose, and we are currently undertaking a comprehensive evaluation of these models.

REFERENCES

1 P. R. Haddad and A. D. Sosimenko, *J. Chromatogr. Sci.*, 27 (1989) 456.
2 D. T. Gjerde, G. Schmuckler and J. S. Fritz, *J. Chromatogr.*, 187 (1980) 35.
3 P. R. Haddad and C. E. Cowie, *J. Chromatogr.*, 303 (1984) 321.
4 R. D. Rocklin, C. A. Pohl and J. A. Schibler, *J. Chromatogr.*, 411 (1987) 107.
5 R. C. L. Foley and P. R. Haddad, *J. Chromatogr.*, 366 (1986) 13.
6 D. R. Jenke and G. K. Pagenkopf, *Anal. Chem.*, 54 (1982) 2603.
7 R. J. Williams, *Anal. Chem.*, 55 (1983) 851.
8 D. R. Jenke, *Anal. Chem.*, 56 (1984) 2674.
9 T. B. Hoover, *Sep. Sci. Technol.*, 17 (1982) 295.
10 D. R. Jenke, *Ph.D. Thesis*, Montana State University, Montana, 1983.
11 M. Maruo, N. Hirayama and T. Kuwamoto, *J. Chromatogr.*, 481 (1989) 315.

Journal of Chromatography, 546 (1991) 61–71
Elsevier Science Publishers B.V., Amsterdam

CHROMSYMP. 2181

Sample preparation for ion chromatography by solid-phase extraction

INGA K. HENDERSON*, RAAIDAH SAARI-NORDHAUS and JAMES M. ANDERSON, Jr.
Alltech Associates Inc., 2051 Waukegan Road, Deerfield, IL 60015 (U.S.A.)

ABSTRACT

The most difficult part of many ion chromatographic (IC) applications is elimination of interfering components from the sample matrix. These interfering compounds may overload the column, contaminate or mask the peaks of interest or may be retained irreversibly on the packing. Some type of sample preparation is usually necessary to clean up samples prior to analysis. Sample preparation cartridges have been developed for IC using solid-phase extraction. These cartridges take part in specific, selective, solid-phase reactions with samples to eliminate interferences. Recovery of the ions after sample preparation was examined.

INTRODUCTION

Sample preparation in ion chromatography (IC) is often required to eliminate interfering components from samples before chromatographic analysis. Interferences may mask or co-elute with peaks of interest, overload the column or cause baseline disturbances, rendering analysis impossible. The column life can be reduced owing to sample components irreversibly binding to the packing. While many approaches to sample preparation exist, not all will solve the interference problems unique to IC. Two of the simplest and easiest to use sample preparation methods, dilution and filtration, are not suitable with some samples. If the analytes are present at trace levels, differ greatly in concentration or the interfering compound and the analytes are both soluble, neither method is satisfactory. Hydrophobic components in samples may be irreversibly retained on the column, thus shortening the column lifetime. Injection of samples with either a high or a low pH will often produce unacceptable chromatograms due to baseline disturbances. Naturally occurring anions such as chloride and sulfate can interfere with the determination of other ions in samples such as sea water and oil-field brine. These samples require selective removal of interfering matrix components.

Solid-phase extraction (SPE), introduced in the 1970s, is one of the fastest growing sample preparation techniques used in chromatography today [1]. SPE is frequently used to solve interference problems in high-performance liquid chromatography (HPLC) and thin-layer chromatography [1,2]. Solid-phase extraction cartridges can also be used to eliminate matrix interferences from samples prior to analy-

0021-9673/91/$03.50

sis by IC. Not all SPE devices are appropriate for IC applications. Conventional sample preparation devices were plagued with contaminants released from the cartridge or filter. Bagchi and Haddad [3] studied SPE devices packed with octadecylsilyl silica and discovered considerable amounts of extractable anions and cations. New SPE cartridges have been developed to alleviate the interference problem unique to IC without contaminating or altering the sample. Each cartridge consists of polystyrene-based packing material cleaned with ion-free water and molded into medical-grade polypropylene housing. These cartridges are available in five different chemistries to address a variety of IC sample pretreatment problems. This paper reports the recovery of ions using SPE for sample preparation before analysis by IC.

EXPERIMENTAL

Instrumentation

All chromatographic equipment, columns and reagents, unless stated otherwise, were obtained from Alltech (Deerfield, IL, U.S.A.). The ion chromatographic system, the ICM-300, includes a Rheodyne Model 9125 injection valve and a Model 315 conductivity detector with a Model 325 HPLC pump. Data collection was provided by a Spectra-Physics (Santa Clara, CA, U.S.A.) Chromjet integrator. A Model 204 UV detector (Linear Instrument, Reno, NV, U.S.A.) was used when UV detection was necessary. A 150 mm × 4.6 mm I.D. Alltech Universal Anion column, packed with hydroxyethyl methacrylate copolymer-based anion exchanger, was used to determine the recovery of anions. Cation applications were obtained using a sulfonated poly(styrene–divinylbenzene)-based Wescan Cation/R column (100 mm × 3.2 mm I.D.).

Eluents

The eluent used with the Alltech Universal Anion column was 5 m*M* *p*-hydroxybenzoic acid, adjusted to pH 7.9 with lithium hydroxide. To detect nitrite in the presence of sulfuric acid with UV detection, 15 m*M* sodium hydroxide was used with the Alltech Universal Anion column. The eluent used for cation determinations on the Cation/R column was 3.2 m*M* nitric acid. The *p*-hydroxybenzoic and nitric acid eluents were prepared using EZ-LUTE buffers from Alltech.

Reagents and chemicals

HPLC-grade water was used to prepare all standards and eluents. The standard mixtures were prepared using NBS or ACS materials. The anion mixture was prepared from the sodium or potassium salts of fluoride, chloride, nitrite, bromide, nitrate, phosphate and sulfate. The cation mixture was prepared from chloride or fluoride salts of lithium, ammonium, sodium and potassium. All other chemicals used for preparation of standards and eluents were of analytical reagent grade and were acquired from a variety of companies.

Sample pretreatment with solid-phase extraction cartridges

Each SPE cartridge (Maxi-Clean IC Cartridges; Alltech) consists of 0.5 ml of polystyrene-based packing material sandwiched between 20-μm polyethylene frits in a medical-grade polypropylene housing (Fig. 1). The chemical characteristics of the

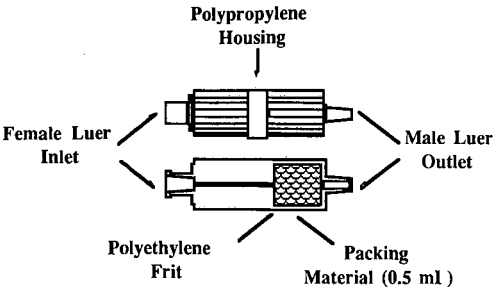

Fig. 1. Construction of the Alltech Maxi-Clean IC cartridge.

packing dictate which sample components are retained. The resin used in the SPE cartridges is polystyrene, which is free from ionic contaminants. The neutral form of the resin is used in the reversed-phase SPE cartridge. The sulfonated form of the resin is converted to the hydrogen, barium or silver form for selective retention of interfering components. The quaternary ammonium form of the resin in the hydroxide form was used in the SPE cartridge for retention of anions. Further information concerning the packing chemistries and the extraction procedure has been given previously [4].

Sample pretreatment with hollow-fiber material

An ion-exchange apparatus similar to that developed by Cox *et al.* [5] was prepared in-house to compare cation-exchange hollow-fiber material with cation-exchange resin. It consisted of a 1.5-m section of Nafion cation-exchange hollow-fiber material (Perma Pure Products, Toms River, NJ, U.S.A.) that was coiled and placed in a slurry of 100 g of Dowex AG 50W-X12 (H^+) analytical-reagent grade cation-exchange resin (50–100 mesh) (Bio-Rad Labs., Richmond, CA, U.S.A.) and 100 ml of IC-grade water. The slurry was stirred with a magnetic stirrer bar on a stir plate. One end of the Nafion tubing was connected with plastic tubing for sample collection and the other end was connected to a peristaltic pump. The anionic samples were passed through the hollow-fiber material at a rate of 1.32 ml/min. A commercially available hollow-fiber membrane-based sample preparation device (Millitrap H^+; Millipore, Milford, MA, U.S.A.) was also compared with the SPE cartridge packed with strong anion-exchange resin in the hydrogen form.

RESULTS AND DISCUSSION

Ion chromatography has been used for the determination of ions in water and in many other matrices. In most instances sample pretreatment other than filtration or dilution is not necessary. When sample matrices contain interfering components that cannot be removed by filtration or dilution, more extensive sample preparation may be required. Any handling of the sample may sometimes introduce imprecision greater than that found within the chromatographic process. The success of the analysis is often dependent on successful sample preparation. With SPE cartridges the sample is passed through the packing. Specific chemical interactions take place, which

TABLE I

CHARACTERISTICS OF SOLID-PHASE EXTRACTION CARTRIDGES (MAXI-CLEAN IC CARTRIDGES; ALLTECH)

Packing	Particle size (μm)	Retains	Capacity (mequiv.)	Applications
Polystyrene	~300	Hydrophobic components	Variable	Removal of surfactants, organic acids and other organic substances. Inorganic ions pass through
Strong anion exchanger in OH^- form	75	Anions	0.6	Exchanges anions for hydroxide. May be used to remove or concentrate anions from sample and to increase pH of acidic samples. Remove cations that form insoluble hydroxide salts
Strong cation exchanger in H^+ from	106	Cations	0.8	Exchanges cations for H^+. May be used to remove or concentrate cations from sample and to reduce pH of basic samples.
Strong cation exchanger in Ag^+ form	106	Chloride, iodide, bromide	0.8	Removes excess halides through formation of Ag halide salts
Strong cation exchanger in Ba^{+2} form	106	Sulfate	0.8	Removes excess sulfate through formation of $BaSO_4$

selectively retain certain components of the matrix in the cartridges, while the remaining components pass through unchanged. In most applications, SPE cartridges provide the means to analyze these samples without sacrificing the recovery of the analytes of interest. Table I summarizes the characteristics of these SPE cartridges.

Removal of hydrophobic compounds

The reversed-phase SPE cartridge provides a reliable method for the removal of surfactants, organic acids, proteins and other organic substances that would otherwise interfere with IC analysis or damage the column. Hydrophobic components of the sample are retained on the packing by reversed-phase mechanisms. Polar organic compounds and inorganic anions are not retained. The net result is removal of hydrophobic components from the matrix while polar components pass through intact.

Adjustment of sample pH

Samples that are strongly acidic or alkaline are difficult to analyze owing to the baseline disturbances that they create. With some IC eluents, system peaks result when the pH values of the sample and the eluent are different. The strong anion-exchange resin in the hydroxide form adjusts the pH of acidic samples prior to analysis of cations by IC. Hydroxide is weakly retained by the resin and is readily displaced by most other anions. The hydroxide contained on the packing reacts with hydronium from the sample to form water, thereby increasing the pH. In this process, anions from the sample displace the hydroxide on the resin, which is then consumed in a neutralization reaction. The net result is removal of hydronium and an equivalent amount of sample anions from the matrix.

The strong cation-exchange resin in the hydrogen form offers a reliable procedure to reduce the pH of alkaline samples prior to analysis. The hydronium contained on the packing reacts with hydroxide from the sample to form water, thereby reducing the pH. In this process, cations from the sample displace the hydronium on the resin, which is then consumed in the neutralization reaction. The net result is removal of hydroxide and the equivalent amount of sample cations from the matrix.

Selective removal of interferences by precipitation reaction

An SPE cartridge packed with strong cation-exchange resin in the barium or the silver form depends on selective precipitation reactions to remove or reduce the concentration of sulfate or halides, respectively. The barium or silver contained on the packing reacts with the sulfate or halides from the sample to form the insoluble barium sulfate or silver halide salt. In this process, cations from the sample displace the barium or silver from the resin, which is then consumed in the precipitation reaction. The net result is removal of sulfate or halides and an equivalent amount of sample cations from the matrix.

Recovery of ions with SPE

Often sample preparation results in the loss, dilution or alteration of components of interest. In most instances the SPE cartridges selectively eliminate matrix interferences without significant effects on the remaining ions. Recovery data were obtained by comparing standard solutions analyzed by IC before and after sample preparation with SPE cartridges. Table II exhibits the recovery data for these SPE cartridges. The reversed-phase SPE cartridge removes hydrophobic components without altering the anion or cation concentration in the sample. A seven-component anion standard and a four-component monovalent cation standard were passed through the reversed-phase SPE cartridge and analyzed by IC with quantitative recoveries.

The SPE cartridge packed with strong cation-exchange resin in the barium or the silver form selectively remove sulfate or halides with near perfect recovery of the remaining anions. Table III lists the solubilities of some of the silver and barium salts in aqueous solutions. As the removal of anions is dependent on the solubility of the salts in solution, fluoride, chloride, bromide, nitrite and nitrate pass through the barium SPE cartridge unchanged. Because of the limited solubility of barium phosphate, the recovery of the phosphate may be reduced by the SPE cartridges packed with strong cation-exchange resin in the barium form if phosphate is present in a high concentration. The insoluble silver halides are retained by the SPE cartridge in the silver form but fluoride, nitrite, nitrate, phosphate and sulfate ions are in mostly unaffected.

When high concentrations of halides or sulfates are present in a sample, low levels of other anions may be lost. This loss is probably due to the inclusion of the other ions in the precipitating barium sulfate or silver halides. A sample of low-level anions was passed through an SPE cartridge packed with strong cation-exchange resin in the barium form. As shown in Table IV, the recovery is good. However, when the same concentrations are present in a solution of 1000 ppm sulfate, the recovery from the barium-form cartridge ranges from 80 to 85%. Although the recovery is less than 100% under these conditions, the reproducibility of replicate injections is ac-

TABLE II

RECOVERY OF IONS WITH SPE CARTRIDGES

SPE cartridge	Concentration (ppm)	Average recovery (%)	S.D.[a] (%)	R.S.D.[a] (%)	No. of Measurements
Reversed-phase					
Fluoride	10	100.5	0.152	0.15	3
Chloride	20	100.9	0.45	0.45	3
Nitrite	20	99.1	0.65	0.65	3
Bromide	20	116.6	2.51	2.15	3
Nitrate	20	100.6	0.45	0.45	3
Phosphate	30	99.6	1.11	1.12	3
Sulfate	30	96.1	0.72	0.75	3
Litium	0.5	95.0	5.18	5.45	3
Sodium	3	97.2	6.56	6.75	3
Ammonium	3	95.8	5.75	6.00	3
Potassium	6	96.7	5.66	5.85	3
Strong cation-exchange resin in barium form					
Fluoride	10	101.7	–	–	1
Chloride	20	111.2	0.98	0.87	3
Nitrite	20	104.4	0.95	0.91	3
Bromide	20	99.3	–	–	1
Nitrate	20	101.1	0.77	0.77	3
Phosphate	30	96.5	–	–	1
Sulfate	30	0.0	–	–	1
Strong cation-exchange resin in silver form					
Fluoride	10	95.2	1.08	1.89	3
Chloride	20	0	0	0	3
Nitrite	20	90.6	15.9	17.6	3
Bromide	20	0.0	0.0	0.0	3
Nitrate	20	102.0	2.66	2.60	3
Phosphate	30	89.0	0.76	0.85	3
Sulfate	30	98.1	0.93	0.95	3
Strong anion-exchange resin in the hydroxide form					
Lithium	0.5	104.0	2.29	2.20	3
Lithium	0.05	96.0	5.30	5.53	3
Sodium	3	103.5	1.55	1.50	3
Sodium	0.3	100.1	0.56	0.60	3
Ammonium	3	103.0	0.36	0.35	3
Ammonium	0.3	100.5	2.31	2.30	3
Potassium	6	105.1	1.77	1.68	3
Potassium	0.6	98.3	2.73	2.78	3
Strong cation-exchange resin in the hydrogen form					
Fluoride	10	96.6	4.33	4.48	3
Chloride	20	102.3	2.57	2.52	2
Nitrite	20	79.1	3.71	4.70	3
Bromide	20	101.6	1.64	1.61	3
Nitrate	20	104.3	2.61	2.50	3
Phosphate	30	86.5	9.39	10.86	3
Sulfate	30	99.4	0.79	0.79	3

[a] S.D. = Standard deviation; R.S.D. = relative standard deviation

TABLE III

SOLUBILITIES OF SILVER AND BARIUM SALTS IN AQUEOUS SOLUTION [6]

Compound	Solubility (g per 100 ml)	Temperature (°C)
AgF	182	15.5
AgI	$2.8 \cdot 10^{-7}$	25
AgCl	$8.9 \cdot 10^{-5}$	10
$AgNO_2$	0.155	0
AgBr	$3.7 \cdot 10^{-4}$	100
$AgNO_3$	122	0
Ag_2SO_4	0.57	0
BaF_2	0.12	25
$BaCl_2$	37.5	26
$BA(NO_2)_2$	67.5	20
$Ba(NO_3)_2$	8.7	20
$BaHPO_4$	0.01–0.02	–
Ba_2SO_4	$2.2 \cdot 10^{-4}$	25

ceptable. Quantitative analysis should be possible by preparing standards in solutions containing the expected concentration of sulfate in actual samples and subjecting both standards and samples to the same SPE procedures. When the same experiments were repeated using the silver-form cartridge, the recovery is nearly perfect. With 1000 ppm chloride present, the recoveries of 1 ppm fluoride, nitrite, nitrate and sulfate were in the range 96–102%. The inclusion problems seem to occur only with the barium-form cartridge.

An SPE cartridge packed with strong anion-exchange resin in the hydroxide form adjusts the pH of acidic samples by neutralizing the hydronium ion. The concurrent removal of anions from the sample has little or no effect on the recovery of the cations in the sample even at low concentration levels. Some data reported in Table II shows a slight increase in the concentration of cations during sample pretreatment but it is well within the acceptable range for many applications. The reproducibility of

TABLE IV

RECOVERY OF LOW-LEVEL ANIONS WITH SPE BY PRECIPITATION REACTIONS

Strong cation-exchange resin in the barium form

	Concentration (ppm)	Average recovery (%)	S.D.[a] (%)	R.S.D.[a] (%)
Without sulfate present				
Chloride	1	102.8	0.98	0.87
Nitrite	1	104.4	0.95	0.91
With 1000 ppm of sulfate				
Chloride	1	85.3	3.46	4.06
Nitrite	1	81.4	3.71	4.56
Bromide	1	89.8	3.52	3.92

[a] $n = 3$.

the method will allow accurate quantification when the standards are pretreated similarly to the samples.

The SPE cartridge packed with strong cation-exchange resin in the hydrogen form adjusts the pH of caustic samples by neutralizing the hydroxide ion to water and removing cations in the process. As shown in Table II, the recovery of anions that are strongly ionized is nearly perfect. However, the recovery of weakly ionized anions such as nitrite and phosphate is poor after the sample treatment with this SPE cartridge.

Decrease of nitrite during sample pretreatment

The loss of of nitrite may take place through a number of different mechanisms, including evolution of nitrous oxide, oxidation to nitrate, adsorption in the resin or a combination of effects. When the nitrite ion in solution is passed through the cartridge, it is protonated to the volatile nitrous acid by the hydronium ion released from the resin. Nitrous acid is both volatile and easily oxidized to nitrate. Aqueous solutions of nitrous acid are unstable and can decompose to nitric acid, water and nitrous oxide [7]. The inconsistency of the recovery, apparent in Table II, may depend on the chemical instability and the extent of nitrite conversion to nitrous acid.

The ability of undissociated weak acids such as nitrous acid and carboxylic acid to penetrate past the functional group of the resin packing and be adsorbed in the resin is one reported explanation for the loss of nitrite [8–10]. The adsorption of the undissociated weak acid in the resin pores was examined. The nitrite ion was converted to nitrous acid using the SPE cartridge packed with strong cation-exchange resin in the hydrogen form and then passed through the neutral resin packing in the reversed-phase SPE cartridge. This sample was compared with the same nitrite sample which was passed through the reversed-phase SPE cartridge only. About 5–10% of the nitrite was lost when the sample converted to nitrous acid was passed through the reversed-phase SPE cartridge. The recovery of nitrite after passage through both SPE cartridges varied from 68 to 96%. The loss of nitrite in the nitrous acid sample after treatment with the reversed-phase SPE cartridge suggests that this undissociated weak acid is adsorbed in the resin. Although this experiment reveals some adsorption of nitrous acid in the resin it does not account for all of the nitrite lost in some replicate injections through the SPE cartridge packed with strong cation-exchange resin in the hydrogen form. Similar inconsistencies in the recovery of nitrite were also apparent when a hollow-fiber membrane was used in place of the strong cation-exchange resin in the hydrogen form. The nitrite loss was also studied using the cation-exchange hollow-fiber membrane devices described earlier. Table V compares the recoveries of anions with cation-exchange resin and hollow-fiber material. This data suggest that other mechanisms must also be active to account for the additional loss of nitrite.

Experiments were designed to observe how the recovery of nitrite ion is dependent on the conversion to nitrous acid. Increasing the total ionic concentration of the solution will increase the amount of hydronium available for conversion of nitrite salts to nitrous acid. Various concentration of sulfate were added to nitrite standards to increase the ionic strength of the solutions. After passage through the SPE packed with strong cation-exchange resin in the hydrogen form, the recoveries of nitrite in solutions containing both 10 and 50 ppm of sulfate were nearly perfect. At higher

TABLE V

RECOVERY OF ANIONS WITH CATION-EXCHANGE MATERIALS

	Concentration (ppm)	Average recovery (%)	S.D. (%)	R.S.D. (%)	No. of measurements
Strong cation-exchange resin in hydrogen form					
Fluoride	10	99.1	3.74	3.77	4
Chloride	20	102.8	2.12	2.06	4
Nitrite	20	58.3	15.3	28.24	12
Bromide	20	97.5	3.92	4.02	12
Nitrate	20	109.8	6.26	5.70	12
Phosphate	30	87.0	8.61	9.89	12
Sulfate	30	97.7	4.34	4.44	12
In-house cation-exchange membrane					
Fluoride	10	104.9	6.74	6.43	10
Chloride	20	106.6	3.05	2.86	10
Nitrite	20	49.1	13.54	27.58	11
Bromide	20	98.0	2.69	2.74	11
Nitrate	20	99.5	3.60	3.62	11
Phosphate	30	86.8	5.62	6.48	11
Sulfate	30	97.7	1.86	1.91	11
Commercial cation-exchange membrane					
Fluoride	10	79.8	10.47	13.11	9
Chloride	20	104.9	4.24	4.04	9
Nitrite	20	68.5	10.11	14.75	9
Bromide	20	108.8	6.42	5.91	9
Nitrate	20	106.4	6.68	6.38	9
Phosphate	30	94.2	6.30	6.69	9
Sulfate	30	102.1	7.09	6.95	9

sulfate concentrations the recovery of nitrite decreases. When 100 ppm of sulfate was present in the sample the nitrite recovery was in the range 74–84%, with 350 ppm of sulfate present, the recovery fell to 63% and with 1000 ppm of sulfate present the nitrite recovery was only 30–40%. Fig. 2 shows the chromatogram of nitrite in 1000 ppm sulfate before and after treatment with the SPE cartridge packed with strong cation-exchange resin in the hydrogen form. An increase in the total ionic strength of the solution reduces the recovery of nitrite. This effect can be explained by the increased concentration of hydronium available to drive the nitrite–nitrous acid reaction equilibrium to favor the formation of nitrous acid.

The ability of nitrous acid to oxidize to nitrate was examined as another mechanism for the loss of nitrite. The recovery of nitrate greater than 100% shown in Table II suggest that nitrite is being oxidized to nitrate during the cation-exchange process. To study the effect of an acidic solution on the loss of nitrite, the following experiment was performed. A 25-m*M* sulfuric acid solution was spiked with 30 ppm of nitrite. The Alltech Universal Anion column was used with 15 m*M* sodium hydroxide as eluent and UV detection to monitor the loss of nitrite with time. The nitrite was reduced from 92% to 75% over 2.5 h when compared with the nitrite standard in IC-grade water. After 4 days stored at 40°C the nitrite concentration was consid-

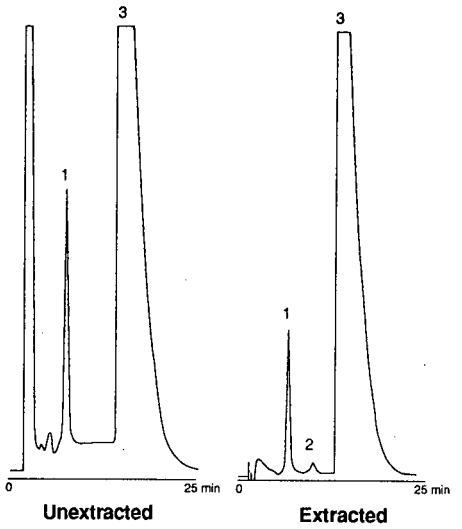

Fig. 2. Nitrite in the presence of 1000 ppm of sulfate, extracted with SPE cartridge packed with a strong cation-exchange resin in the hydrogen form. Column, 150 mm × 4.6 mm I.D.; packing, Universal Anion; eluent 5 m*M* *p*-hydroxybenzoic acid (pH 7.9); flow-rate, 1 ml/min; detector, conductivity. Peaks: 1 = nitrite (100 ppm); 2 = nitrate; 3 = sulfate (1000 ppm).

erably reduced and nitrate was present. The same nitrite concentration in water contained no nitrate after the same time period (see Fig. 3). This suggests that nitrite is oxidized to nitrate in acidic media. Nitrite samples in high concentrations of sulfate presented in Fig. 2 also show oxidation to nitrate when passed through these cartridges.

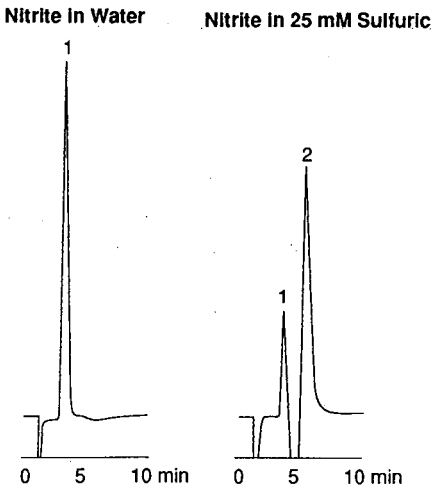

Fig. 3. Nitrite oxidation to nitrate in an acidic solution. Sample, 30 ppm nitrite stored for 4 days at 40°C. Conditions as in Fig. 2 except eluent, 15 m*M* sodium hydroxide solution, and detector, UV (214 nm). Peaks: 1 = nitrite; 2 = nitrate.

The above experiments showed that the poor recovery of nitrite after the sample pretreatment with the hydrogen-form cartridge is due to a combination of several effects which include adsorption in the resin, the formation and evolution of nitrous acid and oxidation to nitrate.

CONCLUSIONS

Solid-phase extraction cartridges provide sample preparation procedures that allow the IC analysis of complex samples. Sample matrix interferences such as acidic or alkaline solutions, interfering levels of halides or sulfate or hydrophobic components are eliminated. After sample pretreatment with SPE cartridges, recovery of all analytes (with the exception of nitrite with the SPE cartridge packed with strong cation-exchange resin in the hydrogen form) is well within the acceptable range for many applications. The exact mechanism of nitrite loss during the cation-exchange process, whether with resin or hollow-fiber, demands further investigation.

REFERENCES

1 R. E. Majors, *LC · GC*, 7 (1988) 99–100.
2 M. Zief and R. Kiser, *Am. Lab.*, January (1990) 70.
3 R. Bagchi and P. R. Haddad, *J. Chromatogr.*, 351 (1986) 541–547.
4 R. Saari-Nordhaus, J. M. Anderson, Jr., and I. K. Henderson, *Am. Lab.*, August (1990) 18.
5 J. A. Cox, E. Dabek-Zlotorzynska, R. Saari and N. Tanaka, *Analyst (London)*, 113 (1988) 1402.
6 R. C. Weast and M. J. Astle (Editors), *CRC Handbook of Chemistry and Physics*, CRC Press, Boca Raton, FL, 61st ed., 1980, pp. B81–B144.
7 A. Cotton and G. Willkinson, *Advanced Inorganic Chemistry*, Wiley, New York, 1980, pp. 426–431.
8 Y. Hanaoka, T. Murayama, S. Muramoto, T. Matsuura and A. Nanba, *J. Chromatogr.*, 239 (1982) 537–548.
9 T. S. Stevens and J. C. Davis, *Anal. Chem.*, 53 (1981) 1488–1492.
11 P. Jandik, P. R. Haddad and P. E. Sturrock, *CRC Crit. Rev. Anal. Chem.*, 20 (1988) 1–74.

Journal of Chromatography, 546 (1991) 73–88
Elsevier Science Publishers B.V., Amsterdam

CHROMSYMP. 2117

Review

Application of macrocyclic ligands to ion chromatography

JOHN D. LAMB* and ROBERT G. SMITH
Department of Chemistry, Brigham Young University, Provo, UT 84602 (U.S.A.)

ABSTRACT

Macrocyclic ligands such as crown ethers and cryptands are highly selective in binding metal and other cations and have been employed in a variety of separation technologies, including solvent extraction, membranes and chromatography. In recent years, groups have succeeded in applying these ligands to high-performance ion chromatography. Typically, crown ethers have been adsorbed, covalently bonded or polymerized on particulate substrates. In some instances, excellent separations among alkali and other metal ions have been achieved. As many macrocycles are uncharged and are insensitive to pH, cations, together with their accompanying anions, may be eluted using pure solvents such as water or methanol as eluents. Further, anions may be separated through the formation of ion pairs with the bound cations. The latter effect has been refined to make possible a unique form of gradient anion chromatography. When metal hydroxide eluents are used for anion chromatography, the capacity of a macrocycle column is determined by the stability constant of the metal ion complexation reaction. If the eluent cation is changed during the course of a single chromatogram so that the column capacity drops, a wide range of anions can be separated with excellent resolution. Little baseline perturbation is experienced since the eluent (OH^-) concentration remains constant throughout the gradient.

CONTENTS

0021-9673/91/$03.50

1. INTRODUCTION

Macrocyclic ligands have been studied for over two decades because of their unique cation-complexing characteristics [1]. A variety of macrocycles have been described, including crown ethers, cryptands, spherands, calixarenes and tetraaza ligands, with specific research emphasis on their potential for affecting a variety of separations. All are characterized by a cyclic carbon structure containing heteroatoms such as oxygen, nitrogen and sulfur, which provide an electron-rich environment for cations, some of which may fit into the central cavity of the molecule forming stable complexes. The best characterized synthetic macrocycle is 18-crown-6, a planar, cyclic polyether with an eighteen-membered ring containing six oxygen atoms (Fig. 1a). Another class of particular interest in this paper, the cryptands, provides a three-dimensional cavity for metal cation entrapment. The basic structure of cryptands is illustrated by the ligand 2.2.2 (Fig. 1b). The crown ethers, cryptands and other macrocycles have been used to separate both cations and anions by high-performance ion chromatographic and other methods [2–5].

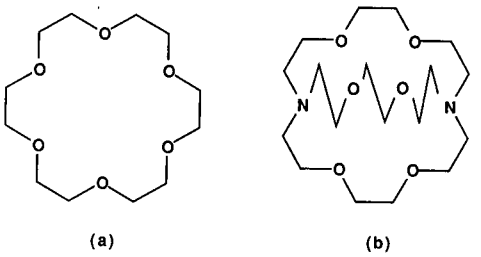

Fig. 1. Basic structures of typical macrocycles used in ion chromatography: (a) 18-crown-6; (b) cryptand 2.2.2.

The selectivity of macrocycles for cations is often determined by the ability of the cation to fit into the central cavity of the macrocycle. The dramatic variation of cryptand selectivities with the size of alkali metal cations is illustrated in Fig. 2. Because macrocycles are usually neutral molecules, an anion is often associated with the resulting cationic complex in order to maintain electrical neutrality, especially in low-dielectric media. As macrocycles are generally hydrophobic, they can be used to extract both cations and anions from aqueous into hydrophobic environments. Thus, macrocycle-based chromatographic columns can be used to separate not only cations with a common anion, but also anions with a common cation.

2. CHARACTERISTICS OF MACROCYCLE-BASED ION CHROMATOGRAPHY

Macrocycles were first used in chromatography by Cram and co-workers [6–8] to separate amino acid isomers. Since then, the use of macrocycles in chromatography to separate cations and anions has been an active area of research. Most applications of macrocycles to ion chromatography involve their incorporation into the stationary phase. The practical aspects of how this and other types of applications are

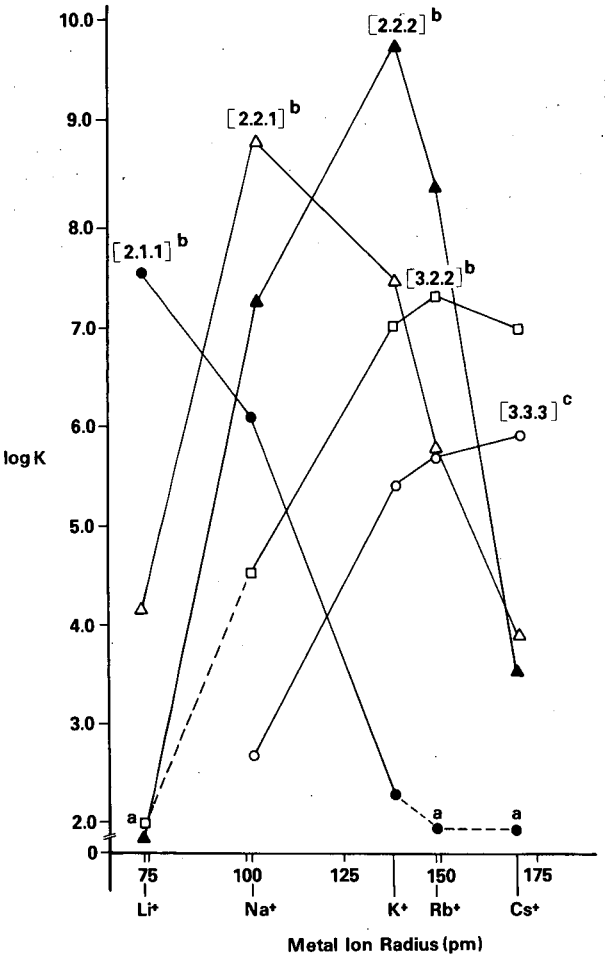

Fig. 2. Selectivities, given in terms of binding constant, K, of several cryptands among alkali metal cations. (a) Reported <2.0; (b) in 95% methanol; (c) in methanol.

accomplished is described in Section 3. The use of macrocycles as stationary phase exchange sites in ion chromatography offers several unique features. First, because macrocycles are commonly uncharged, cations can be eluted from the column without the addition of ionic eluents, making possible a very low background conductivity and concomitant increased sensitivity. Further, waste disposal is greatly simplified if the eluent consists only of solvents.

A second feature of macrocycle-based stationary phases is the variety of selectivities available. In ion chromatography with traditional fixed ionic exchange sites, cation selectivity is rather inflexible, although it may be influenced to some extent by altering the mobile phase conditions. With macrocycle-based stationary phases, on the other hand, the cation selectivity of the column differs from one macrocyclic ligand to another. By employing different macrocycles or combinations of macrocycles, the

selectivity can be varied over a wide range, allowing considerable flexibility in the types of separations that can be performed. Also, because cation affinities fall within a relatively narrow range, Group I and II and other metal cations may be separated isocratically, the preferred method for compatibility with conductivity detection.

A third characteristic of macrocycle-based stationary phases is their ability to separate both cations and anions. Cations are retained by complexation with the exchange site ligand. Anions are retained along with macrocycle-bound cations when the complex is positively charged, *i.e.*, when the unbound macrocycle is neutral.

Each of these features is treated in detail below.

2.1. Cation selectivity and retention

The retention of a cation by a macrocycle-based column depends on how strongly it is bound by the macrocycle and by the rate of ligand exchange. These factors, in turn, are determined by how well the cation's coordination requirements are met by the macrocycle relative to the solvent. One criterion that influences this featue is how well the cation fits into the central cavity of the macrocycle. Cations that are too small cannot interact with all of the heteroatoms in the ring without considerable ring distortion and are retained less strongly than those which fit better. Cations which are too large to fit in the cavity may form complexes by sitting on the ring, or by being sandwiched between two rings. The best fit, and hence the greatest degree of retention, is often exhibited by those cations which most closely approach an ionic radius/macrocyclic cavity radius ratio of 0.8 [2,9]. This size criterion is most significant among cations that have few geometric constraints in their coordination properties, such as the alkali and alkaline earth cations. For 18-crown-6, K^+ (ratio 0.9) fits most closely among the alkali metals, followed by Rb^+(1.02), Cs^+(1.20), Na^+(0.67) and Li^+(0.47). This order is reflected in the values of stability constants for complex formation [10,11].

Early work by Blasius and co-workers [2,12] showed that in macrocycle-based chromatography, cations elute in order of increasing binding constants. For example, the binding constants of dibenzo-18-crown-6 increase in the order $Li^+ < Na^+ < Cs^+ < Rb^+ < K^+$. This is also the experimentally observed elution order of the alkali metals. Among the alkaline earths the binding constants and elution order are $Mg^{2+} < Ca^{2+} < Sr^{2+} < Ba^{2+}$. These results illustrate that the mechanism of retention is based on ligand exchange rather than ion exchange. In fact, it is generally possible to predict the retention behaviour of cations with a particular macrocycle by referring to tabulated binding constants. The constants for a wide variety of macrocycles have been measured [10,11].

The retention of cations by one of the smallest macrocycles, 12-crown-4 and its derivatives, is of the order $Na^+ > K^+ > Rb^+ > Cs^+ > Li^+$ [9,13]. The selectivity for lithium, rubidium and cesium is very low, but a good separation of lithium, potassium and sodium is observed (Fig. 3a). Thus, the 12-crown-4 macrocycles show a higher affinity for sodium cations than for potassium cations, the opposite of the retention order in standard ion exchange.

Several derivatives of 15-crown-5 ethers have been applied to chromatography. While each has slightly differing properties, including cation retention times and resolutions, the retention order is generally $K^+ > Rb^+ > Cs^+ > Na^+ > Li^+$ (Fig. 3b). This ligand serves to illustrate the principle that when no one cation offers an ideal

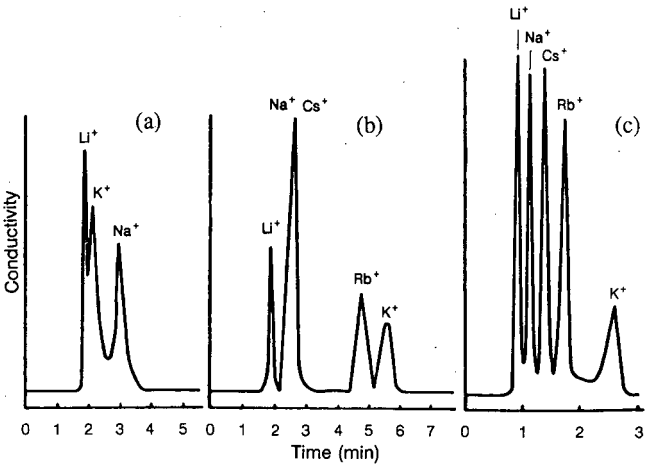

Fig. 3. Alkali metal cation separation (as iodides) on C_{18}-bonded silica dynamically coated with (a) dodecyl-12-crown-4, (b) dodecyl-15-crown-5 and (c) dodecyl-18-crown-6, using methanol–water (50:50) as eluent and conductivity detection (from ref. 9).

fit in the ligand cavity, other factors predominate in determining selectivity. Even Na^+ is slightly too large to fit ideally the 15-crown-5 cavity. In this instance, the desolvation energy of the cation couples with cation/ligand size considerations to determine the selectivity.

Among 18-crown-6 analogues, there is a deviation from the normal order $K^+ > Rb^+ > Cs^+ > Na^+ > Li^+$, shown in Fig. 3c [9,12,14,15], when bis- or polymeric crown ether stationary phases are used. Specifically, the latter retain Cs^+ longer than K^+. This result is probably due to the fact that the Cs^+ cation, being too large to fit into the macrocyclic cavity, commonly forms 2:1 macrocycle–cation complexes with this ligand which are more stable [16].

Blasius and Janzen [2] synthesized polymers of large macrocycles such as 21-crown-7 and 24-crown-8 for use in chromatography. Both of these macrocycles show the same elution order, $Cs^+ > Rb^+ > K^+ > Na^+ > Li^+$. These macrocycles exhibit high selectivity for the Cs^+ cation. The Cs^+: (21-crown-7 cavity) ratio is 0.89. This selectivity can be exploited to perform the separation of cesium from complex ionic solutions, a separation of interest in the nuclear industry [2].

Little work has been done on chromatographic cation separations using cryptands, which encapsulate the cation better than planar macrocycles. The measured binding constants for the cryptands are often several orders of magnitude higher than the constants for crown ethers, and the chromatographic retention of cations on cryptand-based columns is considerably longer and less efficient than for the corresponding crown ethers. For the cryptand 2.2.2 the selectivity is slightly different from that for the similar 18-crown-6 ligand, with the retention decreasing in the order $K^+ > Rb^+ > Na^+ > Cs^+ > Li^+$ [17].

2.2. Mobile phase options

One potential advantage of using macrocyclic sites in the stationary phase is that the addition of salts to the mobile phase is not necessary to elute analytes from the column. Thus, pure water or another pure solvent can be used as the mobile phase. It is generally true that the stability constants of cation–macrocycle complexes are higher in methanol and other organic solvents than in water [10]. Methanol and methanol-containing mobile phases reflect this higher stability, as the retention of cations and anions increases with increasing methanol content (Fig. 4) [9,14,16]. It is noteworthy that the addition of other organic solvents to the mobile phase may not have the same effect. Macrocycle–cation binding constants in acetonitrile and tetrahydrofuran are also higher than in pure water. However, it has been observed that retention decreases on addition of those solvents to the mobile phase in certain systems [14]. No explanation of this phenomenon was given, although these solvents may have affected the resin-based stationary phase used in these experiments.

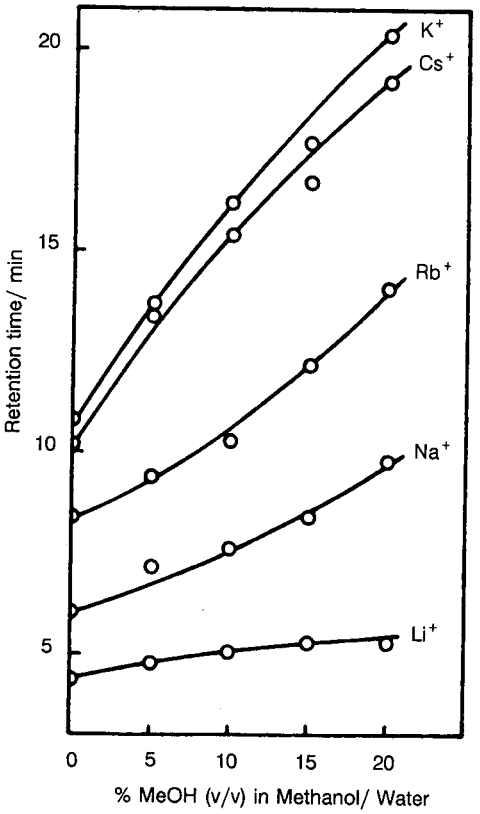

Fig. 4. Effect of methanol (MeOH) content in mobile phase on retention of alkali metal cations (as chlorides) on benzo-18-crown-6 covalently attached to silica. Analytes: 0.05 *M* metal chlorides. Flow-rate = 0.5 ml/min (from ref. 14).

2.3. Temperature effects

The complexation of cations with macrocycles is usually an exothermic process. The stability of the macrocycle–cation complex is lower at higher temperature in this instance. Increasing the temperature in chromatographic separations with macrocycles has two effects: the efficiency increases because the mobile phase become less viscous, allowing better diffusion, and Iwachido *et al.* [14] showed that the retention decreases as temperature increases, owing to the weaker cation–macrocycle interactions. However, resolution is not lost because of the increase in efficiency [16]. Another paper in this volume describes our own work on this topic [18].

2.4. Anion separations

In low-dielectric media, positively charged macrocyclic complexes exist in close associaton with anions to maintain electrical neutrality. Thus, in reversed-phase macrocycle chromatographic systems, the anion is included in the cation retention equilibrium. Those anions which facilitate extraction, such as iodide or thiocyanate, increase the retention of cations [12,16,19,20]. This anion dependence can lead to difficulties with cation peak identification if more than one anion is present in a sample.

The anion effect described above has been exploited to separate anions in the presence of a common cation. The retention order of anions is generally independent of macrocycle type, namely $SCN^- > I^- > NO_3^- > Br^- > Cl^- > F^- > SO_4^{2-}$. This selectivity is different from that of traditional ion exchange, in which divalent anions such as sulfate are more strongly retained. Cations which experience greater retention on a given macrocycle column increase the degree of retention of accompanying anions. For example, on 18-crown-6-based columns, mixtures of potassium salts show improved anion separations over mixtures of sodium salts [12,15] (Fig. 5). This effect is even more dramatically illustrated in Fig. 6, described below. Difficulties in separation arise if more than one type of cation is present, with multiple peaks possible for the same anion [20].

Macrocycles have been used to separate anions through an ion-exchange mechanism rather than a ligand-exchange mechanism [21,22]. This type of separation has been accomplished by the use of a mobile phase containing the hydroxide of a cation that is retained by the macrocycle. As mobile phase cations form complexes with the stationary phase macrocycle, anion-exchange sites are formed in equilibrium with free eluent cation in the mobile phase. Sample anions are eluted by hydroxide ion, which can in turn be chemically suppressed as in standard ion chromatography. The identity of the mobile phase cation greatly affects the column capacity under these conditions. Using a column loaded with decyl-2.2.2, little anion retention is observed with a lithium hydroxide eluent (Fig. 6a), whereas a sodium hydroxide eluent yields significant anion retention (Fig. 6b). The efficiencies observed with this system approach those of traditonal ion-exchange chromatography. Also, with the relatively high concentration of eluent cation in the mobile phase, the effects of analyte concentration and of sample counter ion are largely eliminated. A gradient in column capacity can be achieved by changing the eluent from sodium hydroxide to lithium hydroxide during the course of a chromatogram. Fig. 6c shows how such a gradient combines the desirable properties of each eluent used isocratically. During the course of the gradient, only the cation identity changes. As the eluent concentration does not

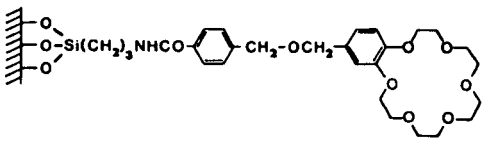

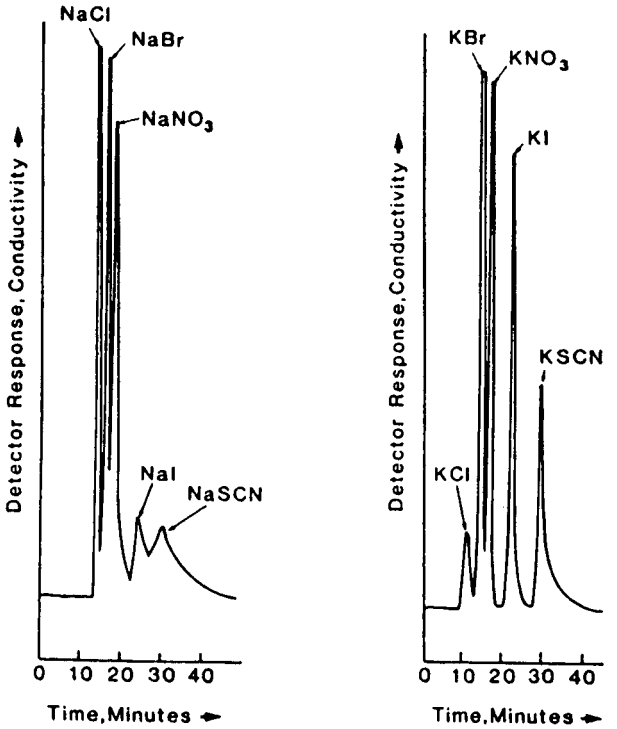

Fig. 5. Separations of anions in the presence of a common cation on silica-based benzo-18-crown-6 resin (top) using a water mobile phase and conductivity detection. Analytes: 0.1 *M*, 20 ml (from ref. 15).

change, little baseline distortion occurs, and system turnaround time is minimized. Such gradients can be used to perform efficient separations of a wide variety of anions.

3. METHODS OF APPLICATION

Macrocycles can be incorporated in the ion chromatographic system in the mobile phase or in the stationary phase. Incorporation in the stationary phase has been achieved in one of three ways: physical adsorption on a solid support; polymerization to form a stationary phase; or covalently bonding to either a polymeric or silica solid support.

3.1. Mobile phase applications

Crown ethers were first used as an additive to the mobile phase by Sousa *et al.* [6],

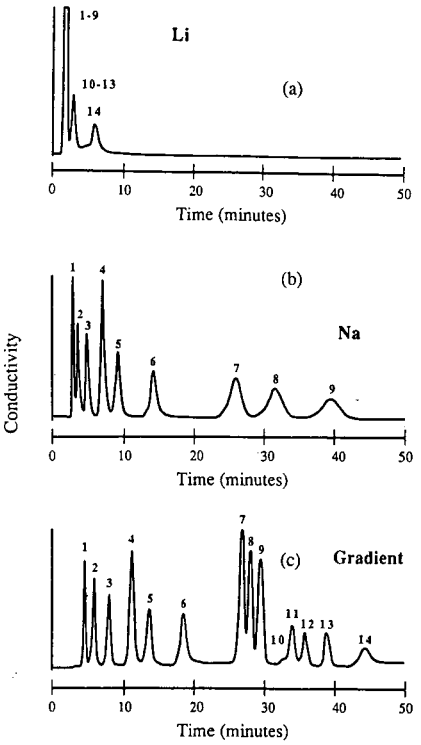

Fig. 6. Separation of fourteen common anions under three different chromatographic conditions: (a) with 20 m*M* LiOH as eluent (isocratic); (b) with 20 m*M* NaOH as eluent (isocratic); (c) with a 20 m*M* NaOH–20 m*M* LiOH gradient over 20 min. Chemically suppressed conductivity detection (from ref. 22).

who used a dinaphthal-18-crown-6 in the mobile phase to separate amino acid isomers. Common cations and anions can also be separated by this approach [21], in addition to protonated amine cations [23–25], amino acids and peptides [26] and β-lactam antibiotics [27]. Brugman and Kraak [28] used crown ether complexes of K^+ in the mobile phase to facilitate ion-pair retention of various sulfonic acids on reversed-phase columns. Similarly, Miyashita and Yamashita [24] used a crown ether complex of a protonated alkylamine as an ion-pairing agent for the retention of I^-. Separations of this type have been limited because of the need for soluble macrocycles, limiting the types that can be used and by the expense of using large amounts of these relatively costly reagents.

3.2. Physical adsorption on a solid support

Kimura's group pioneered the technique of macrocycle adsorption on silica-based C_{18} columns or polystyrene–divinylbenzene packings [9]. Appropriate macrocycles usually have a hydrophobic "tail" or other moiety that promotes strong adherence to the stationary phase. Specifically, Kimura and co-workers [9,17] adsorbed dodecyl-substituted 12-crown-4, 15-crown-5 and 18-crown-6 ligands on silica-based C_{18} columns, and also the cryptand decyl-2.2.2. Typical separations of

cations achieved using these modified stationary phases are shown in Fig. 3. Lamb and co-workers [21,22] used decyl-2.2.2 adsorbed on several types of reversed-phase columns for anion and cation separations.

The preparation of adsorbed macrocyclic stationary phases is straightforward and free from the difficulties involved in polymerization or covalent attachment. A water–methanol solution containing just enough methanol to dissolve the desired amount of the macrocycle is recycled through the column for several hours. The capacity of the column can be controlled by the amount of macrocycle loaded onto the column. A potential disadvantage to the adsorption method is the loss of the macrocycle from the stationary phase with time. Kimura *et al.* [9] showed that when a pure water eluent or eluents of low methanol concentration are used, the stationary phase is stable for long periods of time. We have observed that even with millimolar hydroxide eluents, the capacity of such columns remains unchanged after several weeks of use. However, if the methanol concentration is greater than 40%, the macrocycle is quickly eluted from the column. However, even after 50 h of continuous use at 80°C, no decrease in column capacity was detected in our laboratory [18].

Shinbo *et al.* [30] used a chiral crown ether dynamically coated on a reversed-phase packing to separate amino acid enantiomers. Racemic mixtures of almost all common amino acids were resolved using a dilute perchloric acid eluent. A typical chromatogram is shown in Fig. 7. Daicel Chemical Industries market analytical and preparative columns for amino acid enantiomer separations based on chiral crown ether exchange sites [31]. Joly and Gross [32] also reported the resolution of amino acid enantiomers on a C_{18}-bonded silica column containing an adsorbed optically active crown compound.

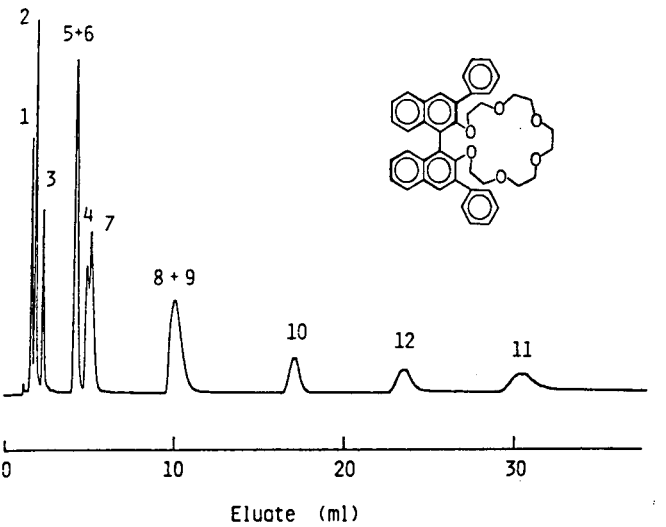

Fig. 7. Separation of six racemic amino acids at 2°C on a reversed-phase packing dynamically coated with the crown ether shown. Elution sequence: 1 = L-alanine; 2 = L-glutamic acid; 3 = D-alanine; 4 = D-glutamic acid; 5 = L-methionine; 6 = L-phenylglycine; 7 = L-leucine; 8 = D-methionine; 9 = D-leucine; 10 = L-phenylalanine; 11 = D-phenylglycine; 12 = D-phenylalanine. Eluent = 0.01 *M* perchloric acid. UV detection. Flow-rate = 0.5 ml/min (from ref. 30).

3.3. Polymeric macrocycle stationary phases

The development and use of polymeric crown ether stationary phases was pioneered by Blasius and co-workers [2,12,33–36]. These polymeric stationary phases have several advantages, *e.g.*, they are stable to a wide variety of solvents. For example, Blasius and co-workers used pure methanol as the mobile phase to perform separations of both cations and anions. As the stability constants of cation–macrocycle complexes can vary widely with the solvent, this stability provides another powerful variable that can be used to modify chromatographic performance.

Polymeric crown ether stationary phases can be formed in two different ways: formation of solid polymer particles or coating a macrocycle polymer on a solid support. Stationary phases were first formed by packing columns with particles of the polymeric resin generated by cross-linking benzo- or dibenzo-crown ethers in formic acid with formaldehyde, so that methylene bridges connected crown moieties [12]. Dibenzo-18-crown-has been the most common polymeric resin. This resin was used by Blasius and co-workers to perform a wide variety of separations, *e.g.*, HCl from NaCl, NaOH from KOH and Na_2SO_4 from NaCl. Separations of alkylammonium chlorides and of anions were also performed on this resin using methanol as the eluent (Fig. 8). Blasius and Janzen [2] also obtained a cesium-selective exchanger by forming a condensation polymer with dibenzo-24-crown-8, potentially useful for separating cesium from high-activity nuclear waste solutions. Polymeric polyamide-18-crown-6 was used by Igawa *et al.* [20] to perform separations. This resin was not successful in separating cations, and very little separation of anions was observed. Suh *et al.* [37] and Jung *et al.* [38] grafted nitrogen-containing crown ethers to styrene–divinylbenzene copolymer and demonstrated separations among lanthanides, Cu^{2+} and UO_2^{2+}.

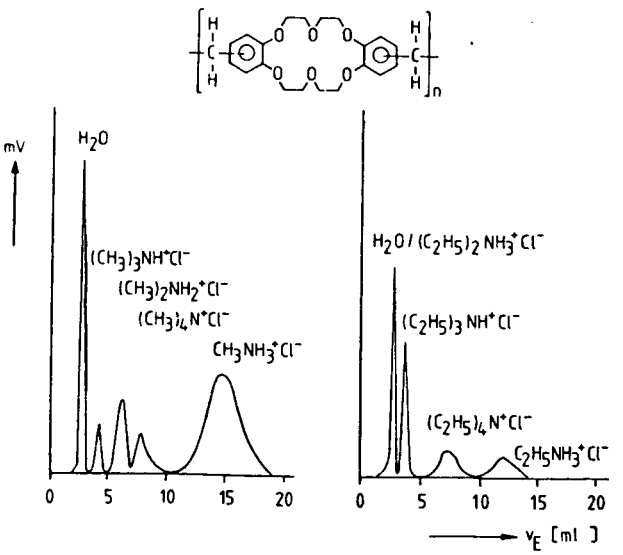

Fig. 8. Separation of alkylammonium chlorides on polymeric dibenzo-18-crown-6 (top) using methanol as eluent (from ref. 2).

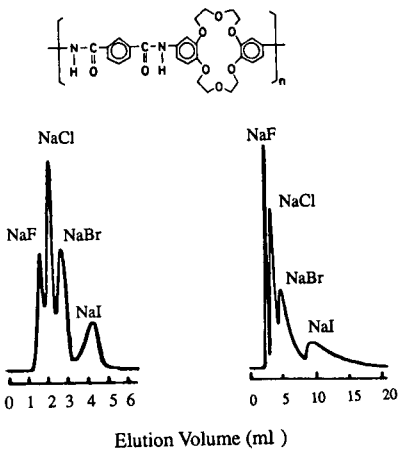

Fig. 9. Separation of sodium halides using the polyamide crown resin shown: (a) alone (flow-rate 0.15 ml/min) and (b) coated on silica particles (flow-rate 0.30 ml/min). Eluent: water. Conductivity detection (from ref. 20).

The polymeric crown ether resins are soft and unable to withstand the high pressures of typical high-performance liquid chromatographic (HPLC) environments. The separations performed with the resins were done at very low flow-rates of 0.05–0.1 ml/min to reduce compression. Hence, the separations are very long, requiring as much as 6 h. The efficiencies of the separations are also poor. To overcome this problem, the same polymeric crowns were coated on hard solid supports. Igawa *et al.* [20] coated polymeric polyamide-dibenzo-18-crown-6 on silica particles by dissolving the resin in N-methyl-2-pyrrolidone, adding silica particles and evaporating. This stationary phase showed superior separations over the polymeric resin alone (Fig. 9).

Blasius and co-workers also coated solid supports with polymeric resins either statically or by polymerization with functional groups on the solid support. The dibenzo-crown ether polymers were reacted with the silanol groups or with chloromethylated polystyrene to form an anchored polymeric resin [2,33–35]. Improved efficiencies at higher flow-rates were achieved over the polymer particles. In addition to separating inorganic anions, Blasius *et al.* [36] also showed that a series of short-chain carboxylic acids could be separated with these resins. Kimura *et al.* [39] were able to separate organic amines and phenols on a similar stationary phase.

3.4. Covalently bound macrocyles

Monomeric macrocycles have been covalently bonded to both silica and polymeric HPLC packings [12,15,16,19,40,41]. These stationary phases exhibit the higher efficiencies of adsorbed crowns and are easier to synthesize than the polymeric crowns. Much of the more recent research in macrocycle-based ion chromatography has been focused on the attachment of crown ethers to solid supports such as silica and polystyrene HPLC resins.

Blasius *et al.* [12] first bonded benzo-15-crown-5 to silica gel and used the resulting resin to separate alkali metals (Fig. 10a). The crown–silica linkage was

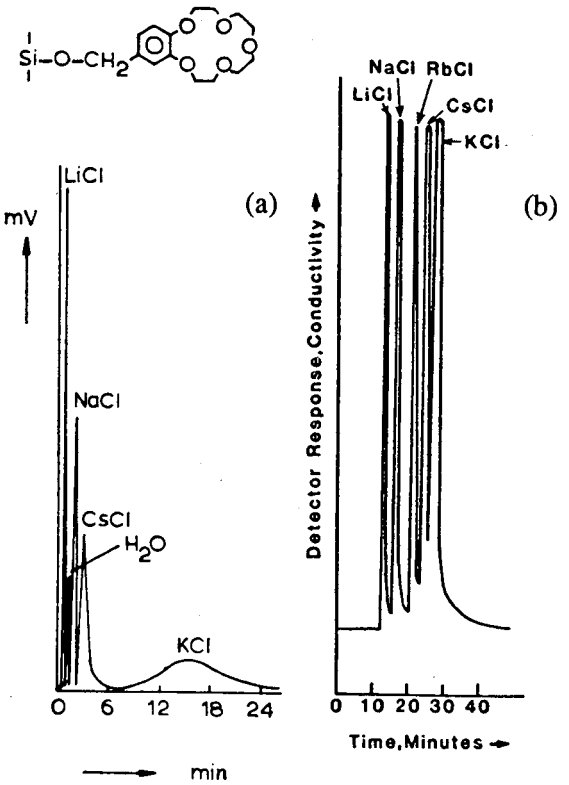

Fig. 10. Separation of alkali metal chlorides. (a) On benzo-15-crown-5 covalently bound to silica particles. Eluent: methanol. Conductivity detection. Flow-rate: 5 ml/min (from ref. 12). (b) On silica-based benzo-18-crown-6 resin, structure as shown in Fig. 5. Eluent: water. Conductivity detection. Flow-rate: 0.16–0.26 ml/min (from ref. 15).

Si–O–CH_2–, which is hydrolyzed by water. Hence methanol (containing less than 0.01% of water) was used as the mobile phase.

Several other types of bonded silica gel macrocycles were prepared by Kimura and co-workers [19,41,42]. The bis- and poly-crown-5 resins gave baseline separations of alkali metals using aqueous mobile phases. Nakajima *et al.* [16] also achieved the separation of a mixture of alkali metals and alkaline earths with these resins. The monomeric forms, while exhibiting some separating ability, provided less separation than the bis- and poly-crown resins. The 18-crown-6 resins showed better ability to separate cations than the 15-crown-5 derivatives [16].

Iwachido *et al.* [14] prepared silica-based resins with 15-crown-5, 18-crown-6 and 21-crown-7. The alkali and alkaline earth metal separations with the 15-crown-5 and 18-crown-6 resins were similar to those obtained by Kimura and co-workers. However, the 21-crown-7 resins showed selectivity toward Rb^+ and Cs^+.

Lauth and Gramain [15,43] also attached benzo-18-crown-6 to silica through a slightly different linkage (see Fig. 5). Anions and alkali and alkaline earth metal cations were separated. This resin showed a higher efficiency than that originally

obtained by Blasius and co-workers (see Fig. 10b). Szczepaniak and Szymanski [44] also used silica-bound macrocycles containing nitrogen to separate various phenolic compounds. Josic and Reutter [45] used nitrogen-containing crowns bound to silica to separate nucleic acids and proteins in the presence of K^+ ions.

Most of the above resins are based on benzo derivatives of crown ethers. These benzocrowns bind cations more weakly than the parent crown structures. Bradshaw *et al.* [46] prepared crown ether-modified silica resins that do not contain the aromatic ring in the crown structure. These resins show nearly the same cation-binding equilibrium constants as the unbound macrocycles, leading to the conclusion that cation complexation occurs in the aqueous phase. These resins have been applied with great efficacy to sample cation concentration and separation rather than to high-performance ion chromatographic separations. Samples are loaded onto packed columns, then stripped with EDTA, thiosulfate or some other appropriate complexer depending on the ion(s) to be recovered. A variety of macrocycles have been used in this fashion. Oxygen-only crowns have been used to concentrate alkali metal, alkaline earth metal, Pb^{2+} or Tl^+ cations according to size [46,47]. Nitrogen-containing macrocycles were used to concentrate Ag^+ and Hg^{2+} [47–49] and sulfur-containing macrocycles for gold(III), palladium(II), Ag^+ and Hg^{2+} [50]. Many of these separations were accomplished in the presence of very high concentrations of acid and/or completing cations. These phases are now available commercially through IBC (Provo, UT, U.S.A.). Separation of enantiomers has also been proposed for cationic organic amines using chiral crowns bound to silica in this way [51].

Diaza-crown ethers, in which two nitrogen atoms replace two crown oxygen atoms, have also been attached to silica [52]. These resins have been used in a preparative scale to separate transition metals, and show some promise for analytical separations. Recently two groups have reported the use of crown ethers loaded on solid supports for Cs^+, Sr^{2+} and Ba^{2+} separations of interest to the nuclear industry [53,54].

Very little work has been done to bond crown ethers to polymeric resins. Iwachido *et al.* [14] bonded a benzo-18-crown-6 to a –COOH-type gel through an amide linkage. The results were similar to those found for silica-based stationary phases, but with poorer resolution.

The covalent bonding of macrocycles to silica or other HPLC resins provides several advantages. The efficiencies are better than those observed for similar polymeric resins. They are easier to synthesize and show better mechanical stability. Most of the linkages are stable with respect to water and methanol, so mixed mobile phases that would elute adsorbed crowns from the column can be used. Lack of stability to basic solutions is a problem for silica-based resins.

4. ACKNOWLEDGEMENTS

The authors express appreciation to Dionex for a graduate fellowship to R.G.S.

REFERENCES

1 C. J. Pederson, *J. Am. Chem. Soc.*, 89 (1967) 7017–7036.
2 E. Blasius and K. P. Janzen, *Top. Curr. Chem.*, 98 (1981) 163–189.
3 K. Kimura and T. Shono, *J. Liq. Chromatogr.*, 5 (1982) 223–255.
4 T. Shono, *Jpn. Soc. Anal. Chem.*, 33 (1984) E449–E458.

5 M. Takagi and H. Nakamura, *J. Coord. Chem.*, 15 (1986) 53–82.
6 L. R. Sousa, D. H. Hoffman, L. Kaplan and D. J. Cram, *J. Am. Chem. Soc.*, 96 (1974) 7100–7101.
7 G. Dotsevi, Y. Sogah and D. J. Cram, *J. Am. Chem. Soc.*, 92 (1975) 1259–1261.
8 G. Dotsevi, Y. Sogah and D. J. Cram, *J. Am. Chem. Soc.*, 98 (1976) 3038–3041.
9 K. Kimura, H. Harino, E. Hayata and T. Shono, *Anal. Chem.*, 58 (1986) 2233–2237.
10 R. M. Izatt, J. S. Bradshaw, S. A. Nielsen, J. D. Lamb and J. J. Christensen, *Chem. Rev.*, 85 (1985) 271–339.
11 A. Bajaj and N. Poonia, *Coord. Chem. Rev.*, 87 (1988) 55–213.
12 E. Blasius, K. P. Janzen, W. Klein, H. Klotz, V. B. Nguyen, T. Nguyen-Tien, R. Pfeiffer, G. Scholten, H. Simon, H. Stockemer and A. Toussaint, *J. Chromatogr.*, 201 (1980) 147–166.
13 M. Nakajima, K. Kimura, E. Hayata and T. Shono, *J. Liq. Chromatogr.*, 7 (1984) 2115–2125.
14 T. Iwachido, H. Naito, F. Samukawa and K. Ishimaru, *Bull. Chem. Soc. Jpn.*, 59 (1986) 1475–1480.
15 M. Lauth and P. Gramain, *J. Chromatogr.*, 395 (1987) 153–158.
16 M. Nakajima, K. Kimura and T. Shono, *Bull. Chem. Soc. Jpn.*, 56 (1983) 3052–3056.
17 K. Kimura, H. Hayata and T. Shono, *J. Chem. Soc., Chem. Commun.*, (1984) 271–272.
18 R. G. Smith, P. A. Drake and J. D. Lamb, *J. Chromatogr.*, 546 (1991) 139–149.
19 K. Kimura, M. Nakajima and T. Shono, *Anal. Lett.*, 13(A9) (1980) 741–751.
20 M. Igawa, K. Saito, J. Tsukamoto and M. Tanaka, *Anal. Chem.*, 53 (1981) 1942–1944.
21 J. D. Lamb and P. A. Drake, *J. Chromatogr.*, 482 (1989) 367–380.
22 J. D. Lamb, P. A. Drake and K. E. Woolley, in P. Jandik and R. M. Cassidy (Editors), *Advances in Ion Chromatography*, Vol. 2, Century International, Franklin, MA, 1990, pp. 215–231.
23 M. Wiechmann, *J. Chromatogr.*, 235 (1982) 129–137.
24 T. Nakagawa, H. Murata, A. Shibukawa, K. Murakami and H. Tanaka, *J. Chromatogr.*, 330 (1985) 43–53.
25 S. Iwagami and T. Nakagawa, *J. Chromatogr.*, 369 (1986) 49–58.
26 T. Nakagawa, A. Shibukawa, A. Kaihara, T. Ita-Mochi and H. Tanaka, *J. Chromatogr.*, 353 (1986) 399–408.
27 T. Nakagawa, A. Shibukawa and T. Uno, *J. Chromatogr.*, 239 (1982) 695–706.
28 W. J. T. Brugman and J. C. Kraak, *J. Chromatogr.*, 205 (1981) 170–178.
29 M. Miyashita and S. Yamashita, *J. Liq. Chromatogr.*, 9 (1986) 2143–2151.
30 T. Shinbo, T. Yamaguchi, K. Nishimura and M. Sugiura, *J. Chromatogr.*, 305 (1987) 145–153.
31 *CROWNPAK, CHIRALPAK, CHIRALCEL: Chiral HPLC Columns for Optical Resolution*, Daicel Chemical Industries, Tokyo, 1989.
32 J. P. Joly and B. Gross, *Tetrahedron Lett.*, 26 (1989) 4231–4234.
33 E. Blasius and K. P. Janzen, *Isr. J. Chem.*, 26 (1985) 25–34.
34 E. Blasius, K. P. Janzen, H. Luxenburger, V. B. Nguyen, H. Klotz and J. Stockemer, *J. Chromatogr.*, 167 (1978) 307–320.
35 E. Blasius, K. P. Janzen, H. Simon and J. Zender, *Fresenius' Z. Anal. Chem.*, 320 (1985) 435–438.
36 E. Blasius, K. P. Janzen and J. Zender, *Fresenius' Z. Anal. Chem.*, 325 (1986) 126–128.
37 M. Suh, T. Eom and I. Suh, *Bull. Korean Chem. Soc.*, 8, No. 5 (1987) 2–8.
38 O. Jung, H. Jung and J. Kim, *J. Korean Chem. Soc.*, 32 (1988) 358–370.
39 K. Kimura, H. Harino and T. Shono, *Chem. Lett.*, (1985) 747–750.
40 T. G. Waddell and D. E. Leyden, *J. Org. Chem.*, 46 (1981) 2406–2407.
41 M. Nakajima, K. Kimura and T. Shono, *Anal. Chem.*, 55 (1983) 463–467.
42 K. Kimura, M. Nakajima and T. Shono, *J. Polym. Sci.*, 23 (1985) 2327–2331.
43 M. Lauth and P. Gramain, *J. Liq. Chromatogr.*, 8 (1985) 2403–2415.
44 W. Szczepaniak and A. Szymanski, *Chem. Anal. (Warsaw)*, 32 (1987) 273.
45 D. Josic and W. Reutter, *J. Chromatogr.*, 476 (1989) 309–318.
46 J. S. Bradshaw, R. L. Breuning, K. E. Krakowiak, J. B. Tarbet, M. L. Breuning, R. M. Izatt and J. J. Christensen, *J. Chem. Soc., Chem. Commum.*, (1988) 812–814.
47 R. M. Izatt, R. L. Bruening, M. L. Bruening, B. J. Tarbet, K. E. Krakowiak, J. S. Bradshaw and J. J. Christensen, *Anal. Chem.*, 60 (1988) 1825–1826.
48 J. S. Bradshaw, K. E. Krakowiak, B. J. Tarbet, R. L. Bruening, J. F. Biernat, M. Bochenska, R. M. Izatt and J. J. Christensen, *Pure Appl. Chem.*, 61 (1989) 1619–1624.
49 R. M. Izatt, R. L. Bruening, B. J. Tarbet, D. Griffin, M. L. Bruening, K. E. Krakowiak and J. S. Bradshaw, *Pure Appl. Chem.*, 62 (1990) 1115–1118.
50 J. S. Bradshaw, K. E. Krakowiak, R. M. Izatt, R. L. Bruening and B. J. Tarbet, *J. Heterocycl. Chem.*, 27 (1990) 347–349.

51 J. S. Bradshaw, R. M. Izatt, J. J. Christensen, K. E. Krakowiak, B. J. Tarbet, R. L. Bruening and S. Lifson, *J. Inclus. Phenom. Mol. Recog. Chem.*, 7 (1989) 127–136.
52 V. Dudler, L. F. Lindoy, D. Sallin and C. W. Schlaepfer, *Aust. J. Chem.*, 40 (1987) 1557–1563.
53 N. Y. Kremliakova, A. P. Novikov and B. F. Myasoedov, *J. Radioanal. Nucl. Chem. Lett.*, 145 (1990) 23–28.
54 E. Peimli, *J. Radioanal. Nucl. Chem. Lett.*, 144 (1990) 9–15.

Journal of Chromatography, 546 (1991) 89–99
Elsevier Science Publishers B.V., Amsterdam

CHROMSYMP. 2098

Universal stationary phase for the separation of anions on suppressor-based and single-column ion chromatographic systems

RAAIDAH SAARI-NORDHAUS*, INGA K. HENDERSON and JAMES M. ANDERSON, Jr.
Alltech Associates Inc., 2051 Waukegan Road,, Deerfield, IL 60015 (U.S.A.)

ABSTRACT

A stationary phase composed of a hydroxyethyl methacrylate-based macroporous copolymer with quaternary amine functional groups for the separation of anions was evaluated. The material is rigid, stable and compatible with a wide variety of eluents including *p*-hydroxybenzoic acid, phthalic acid, borate–gluconate, and carbonate–hydrogencarbonate. The column packed with this anion exchanger may be used with single-column ion chromatography in addition to suppressor-based ion chromatography. The hydrophilic nature of the methacrylate copolymer provides improved peak shapes for polarizable anions and eliminates system peaks typically encountered with poly(styrene–divinylbenzene) ion exchangers. The column performance with a wide variety of eluents is demonstrated with applications using both single-column and suppressor-based ion chromatography systems.

INTRODUCTION

Ion chromatography (IC) has become one of the most widely used techniques for the determination of inorganic anions. At present, two types of IC are in practical use. The first, the suppressor-based system, was developed by Small *et al.* [1]. In this system, a high-conductivity eluent is attenuated in the suppressor column prior to entering the detector by converting the highly conductive eluent to a low-conductivity form, and at the same time the anions are converted to highly conducting acids. The second type is single-column ion chromatography (SCIC), which was introduced by Gjerde *et al.* [2]. In this system, an eluent with low equivalent conductance is chosen so that the separator column can be coupled directly to the detector.

Since the introduction of IC, several stationary phases for the separation of anions have been developed. Some are microporous agglomerated pellicular anion exchangers [3] which were developed for suppressor-based IC, macroporous poly-(styrene–divinylbenzene) (PS–DVB) copolymer anion exchangers [4–6] developed for SCIC and silica-based anion exchangers [7,8], also developed for SCIC. The ultility of these anion exchangers is limited to a few specific eluents. For example, silica-based ion exchangers can only be used in the pH range 3–7. High-pH eluents such as hydroxide and carbonate–hydrogencarbonate will dissolve the silica-based packing.

0021-9673/91/$03.50

PS–DVB ion exchangers are pH stable, but work in our laboratory has demonstrated that they are not suitable for separating anions using carbonate–hydrogencarbonate or borate–gluconate eluents.

Recently, a new PS–DVB-based anion exchanger that can be used with both types of IC was developed [9]. This material may be used with carbonate–hydrogencarbonate eluent to separate the seven common inorganic anions by suppressor-based IC, and it may also be used with sodium hydroxide eluent for the analysis of weakly acidic anions by SCIC.

The stationary phase described here is compatible with both types of IC. It is demonstrated that this macroporous hydroxyethyl methacrylate-based (HEMA) anion exchanger is rigid, chemically stable and shows good ion-exchange kinetics with a wide variety of eluents including *p*-hydroxybenzoic acid, phthalic acid, borate–gluconate, hydroxide–benzoate and carbonate–hydrogencarbonate. The advantages of this HEMA anion exchanger over PS–DVB- and silica-based anion exchangers is discussed in terms of its universal characteristics, system peaks and peak shapes.

EXPERIMENTAL

Instrumentation

The system used was a Wescan ion chromatography system (Alltech, Deerfield, IL, U.S.A.). It consists of an Alltech Model 325 high-performance liquid chromatographic (HPLC) pump and a Wescan ICM-300 ion chromatography module equipped with a Model 315 conductivity detector, an active temperature control (ATC) module and a Rheodyne Model 9125 metal-free injection valve (100-μl sample loop). The temperature of the ICM-300 was maintained at 30°C. All data were recorded on a Spectra-Physics (Santa Clara, CA, U.S.A.) SP 4400 Chromjet integrator.

For suppressor-based IC, the above system was used with the addition of a suppressor built in-house using a 2 m × 0.61 mm I.D. × 0.84 mm O.D. Nafion 811X perfluorosulfonate tubular cation-exchange membrane (Perma Pure Products, Toms River, NJ, U.S.A.) as described by Dasgupta [10]. Sulfuric acid (12 m*M*) was used as a regenerant.

Columns

The universal stationary phase, a hydroxyethyl methacrylate-based anion exchanger with quaternary amine functional groups, was obtained from Tessek (Aarhus, Denmark). This material has a particle size of 10 μm and an ion-exchange capacity of 0.1 mmol/g. The material was slurry packed into 50 mm × 4.6 mm I.D., 100 mm × 4.6 mm I.D. and 150 mm × 4.6 mm I.D. columns (Alltech Universal Anion columns). A Wescan Anion/R (250 mm × 4.1 mm I.D.) column (Alltech) was used for comparison purposes.

Reagents

All eluents were prepared from EZ-LUTE buffer concentrate (Alltech), with the exception of borate–gluconate, for which analytical-reagent grade chemicals (Aldrich, Milwaukee, WI, U.S.A.) were used. The standards were prepared from Alltech certified IC standards. HPLC-grade water (Alltech) was used to prepare all eluents and standards solutions.

Eluents

Five eluents were tested with the HEMA column: *p*-hydroxybenzoic acid, phthalic acid, borate–gluconate, hydroxide–benzoate and carbonate-hydrogencarbonate. *p*-Hydroxybenzoic acid was 5 m*M*, and the pH was adjusted to 7.9 with lithium hydroxide. Phthalic acid was 4 m*M*, adjusted to pH 4.5 with lithium hydroxide. Two compositions of borate–gluconate eluents were tested. One (borate–gluconate 1) was prepared by diluting 40 ml of a concentrate containing 25.5 g/l boric acid, 13.2 ml/l gluconic acid (50%, w/w), 7.2 g/l lithium hydroxide monohydrate, and 94 ml/l glycerol with 120 ml of acetonitrile and 840 ml of water. The other (borate–gluconate 2) was prepared by diluting 40 ml of a concentrate containing 25.5 g/l boric acid, 13.2 ml/l gluconic acid (50%, w/w) and 7.2 g/l lithium hydroxide monohydrate with 960 ml of water; neither acetonitrile nor glycerol was used in borate–gluconate 2 eluent. Hydroxide–benzoate eluent was 2.5 m*M* in lithium hydroxide and 0.005 m*M* in sodium benzoate. Carbonate–hydrogencarbonate eluent contained 2.8 m*M* sodium hydrogencarbonate and 2.2 m*M* sodium carbonate. Table I summarizes the concentrations of the eluents used.

RESULTS AND DISCUSION

Chemical and physical properties

HEMA is a macroporous copolymer of 2-hydroxyethyl methacrylate and ethylene dimethacrylate. It is extensively cross-linked to produce a matrix with high chemical and physical stability. The maximum operating pressure is 2500 p.s.i. Fig. 1A shows the structure of HEMA. The tertiary α-carbonyl structure of pivalic acid is one of the most stable and least hydrolyzable esters known [11], which allows the HEMA stationary phase to be used with a variety of eluents in the pH range 2–12. The excess hydroxyl groups on the HEMA matrix also increase the hydrophilicity of this material, which will be shown later to result in improved peak shapes for polarizable anions. The strong-base anion exchanger of HEMA shown in Fig. 1B is prepared by treating the HEMA precursor with an aqueous solution of trimethylamine [12]. The preparation procedures and the influence of different functional groups on sorbent selectivity were discussed by Vlacil and Vins [12,13]. The sorbent contains *ca.* 0.1 mmol/g of quaternary amine ion-exchange functional groups. The particle size is 10 μm.

TABLE I

ELUENTS USED FOR EVALUATING THE UNIVERSAL ANION COLUMN

Eluent	Concentration and pH
p-Hydroxybenzoic acid	5 m*M*, adjusted to pH 7.9 with lithium hydroxide
Phthalic acid	4 m*M*, adjusted to pH 4.5 with lithium hydroxide
Borate–gluconate 1	40 ml of concentrate, 120 ml of acetonitrile and 840 ml of water. Concentrate contained 25.5 g/l boric acid, 13.2 ml/l gluconic acid (50%, w/w), 7.2 g/l lithium hydroxide monohydrate and 94 ml/l glycerol
Borate–gluconate 2	40 ml of concentrate and 960 ml of water. Concentrate contained 25.5 g/l boric acid, 13.2 ml/l gluconic acid (50%, w/w) and 7.2 g/l lithium hydrocide monohydrate
Hydroxide–benzoate	2.5 m*M* lithium hydroxide–0.05 m*M* sodium benzoate
Carbonate–hydrogencarbonate	2.2 m*M* sodium carbonate–2.8 m*M* sodium hydrogencarbonate

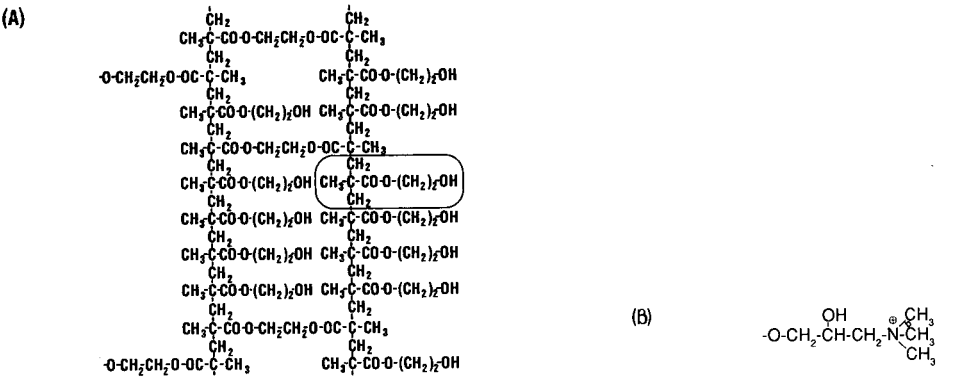

Fig. 1. Structures of (A) HEMA and (B) strong-base anion exchanger of HEMA.

Column performance with various eluents

The column performance with a wide variety of eluents was evaluated by injecting a standard mixture containing 10 ppm fluoride, 20 ppm each of chloride, nitrite, bromide, and nitrate and 30 ppm each of phosphate and sulfate. *p*-Hydroxybenzoic acid, phthalic acid, borate–gluconate and hydroxide–benzoate eluents were used in the SCIC mode and carbonate–hydrogencarbonate eluent was used with suppressor-based IC. The concentrations and pH of the eluents were optimized to give the optimum separation of the anions tested.

p-Hydroxybenzoic acid. *p*-Hydroxybenzoic acid (pHBA) is one of the most useful eluents in SCIC [14,15]. This large aromatic acid exhibits the characteristics desired for SCIC eluents. It has a lower equivalent conductance than most inorganic anions, and is capable of eluting both monovalent and divalent anions in one run. pHBA is used most commonly with PS–DVB-based anion exchangers in the pH range 8.0–8.6. The separation of fluoride, chloride, nitrite, bromide, nitrate, phosphate and sulfate on the HEMA column with pHBA is shown in Fig. 2. The seven anions were effectively separated within 20 min. The peak shapes for polarizable anions such as nitrate and bromide were sharper than those obtained with a PS–DVB ion-exchange column.

Phthalic acid. Phthalic acid is another useful eluent in SCIC [14]. It is useful in the pH range 4.0–7.0 and is used most commonly with silica-based ion-exchange columns. The chromatogram shown in Fig. 3 was obtained using 4 m*M* phthalic acid, adjusted to pH 4.5 with lithium hydroxide (LiHP). Under these conditions, a good separation of fluoride, chloride, nitrite, bromide, nitrate and sulfate was achieved. The phosphate peak was eluted in the column void volume with this eluent.

Borate–gluconate. A mixture of boric acid, sodium tetraborate and gluconic acid was introduced in 1986 as an eluent system for SCIC [16]. This eluent is popular because of its low background conductance and relatively strong eluting power. Borate–gluconate 1, which contained acetonitrile and glycerol, is the standard eluent composition used with most polyacrylate-based columns [16,17]. As can be seen in Fig. 4A, the efficiency of this eluent with HEMA column was poor. Borate–gluconate 2 was then prepared and tested with this column. As shown in Fig. 4B, a better

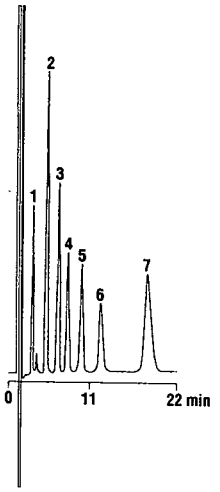

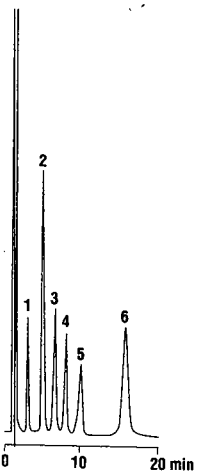

Fig. 2. Separation of the standard anion mixture using *p*-hydroxybenzoic acid eluent. Column, 150 mm × 4.6 mm I.D.; packing, Alltech Universal Anion; eluent, 5 m*M* *p*-hydroxybenzoic acid, pH 7.9 adjusted with lithium hydroxide; flow-rate, 1.0 ml/min; detection, conductivity. Peaks: 1 = fluoride (10 ppm); 2 = chloride (20 ppm); 3 = nitrite (20 ppm); 4 = bromide (20 ppm); 5 = nitrate (20 ppm); 6 = phosphate (30 ppm); 7 = sulfate (30 ppm).

Fig. 3. Separation of the standard anion mixture using phthalic acid eluent. Eluent, 4 m*M* phthalic acid, pH 4.5 adjusted with lithium hydroxide; other conditions as in Fig. 2. Peaks: 1 = fluoride (10 ppm); 2 = chloride (20 ppm); 3 = nitrite (20 ppm); 4 = bromide (20 ppm); 5 = nitrate (20 ppm); 6 = sulfate (30 ppm).

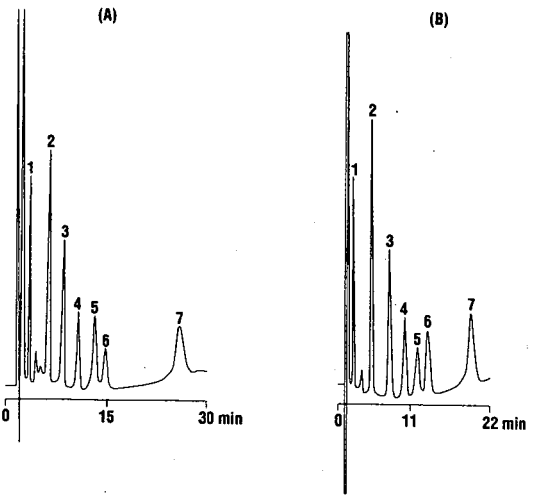

Fig. 4. Separation of the standard anion mixture using borate–gluconate eluent. (A) Eluent, borate–gluconate 1, prepared by diluting 40 ml of a concentrate containing 25.5 g/l boric acid, 13.2 ml/l gluconic acid (50%, w/w), 7.2 g/l lithium hydroxide monohydrate and 94 ml/l glycerol with 120 ml of acetonitrile and 840 ml of water; flow-rate, 1.5 ml/min; other conditions as in Fig. 2. (B) Eluent, borate–gluconate 2, prepared by diluting 40 ml of a concentrate containing 25.5 g/l boric acid, 13.2 ml/l gluconic acid (50%, w/w) and 7.2 g/l lithium hydroxide monohydrate with 960 ml of water; flow-rate, 1.5 ml/min; other conditions as in Fig. 2. Peaks: 1 = fluoride (10 ppm); 2 = chloride (20 ppm); 3 = nitrite (20 ppm); 4 = bromide (20 ppm); 5 = nitrate (20 ppm); 6 = phosphate (30 ppm); 7 = sulfate (30 ppm).

separation was obtained with this eluent. Some workers have suggested that the purpose of acetonitrile in a borate–gluconate eluent is to facilitate phase transfer and produce sharper peaks and shorter retention times [16]; however, the use of these additives with the HEMA column resulted in excessive retention of sulfate.

Lithium hydroxide–sodium benzoate. Hydroxide–benzoate eluent is used in SCIC for the analysis of weak acid anions such as borate, silicate, cyanide and sulfide [14]. As hydroxide has a higher equivalent conductance than most other anions, the peaks for the sample anions appear as negative peaks (decrease in conductance). Hydroxide ion is weakly held by the strong-base anion exchangers and it is not a good choice for separating the common inorganic anions. Fig. 5 shows a chromatogram of the standard anions using 2.5 m*M* lithium hydroxide–0.05 m*M* sodium benzoate eluent. This eluent is too weak to elute phosphate and sulfate.

Carbonate–hydrogencarbonate. This eluent is the most common eluent used in suppressor-based IC. As its equivalent conductance is very close to that of the common inorganic anions, it cannot be used in the SCIC mode. To evaluate the performance of the HEMA column with this eluent, a suppressor column was installed between the separator column and the conductivity detector. The chromatogram shown in Fig. 6A was obtained using 2.8 m*M* sodium hydrogencarbonate–2.2 m*M* sodium carbonate eluent on a 150 mm × 4.6 mm I.D. column. The resolution between the anions was good, but the retention times were too long. As shown in Fig. 6B, by modifiying the eluent concentration and using a shorter column, the retention times were reduced.

Selectivity and efficiency

The selectivity of the HEMA-based column with all the eluents tested is presented in Table II. The results indicate that this material has a "universal" character.

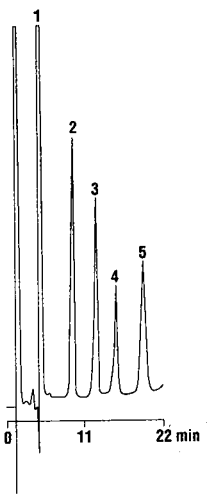

Fig. 5. Separation of the anion mixture using hydroxide eluent. Eluent, 2.5 m*M* lithium hydroxide–0.05 m*M* sodium benzoate; flow-rate, 1.5 ml/min; other conditions as in Fig. 2. Peaks: 1 = fluoride (10 ppm); 2 = chloride (20 ppm); 3 = nitrite (20 ppm); 4 = bromide (20 ppm); 5 = nitrate (20 ppm).

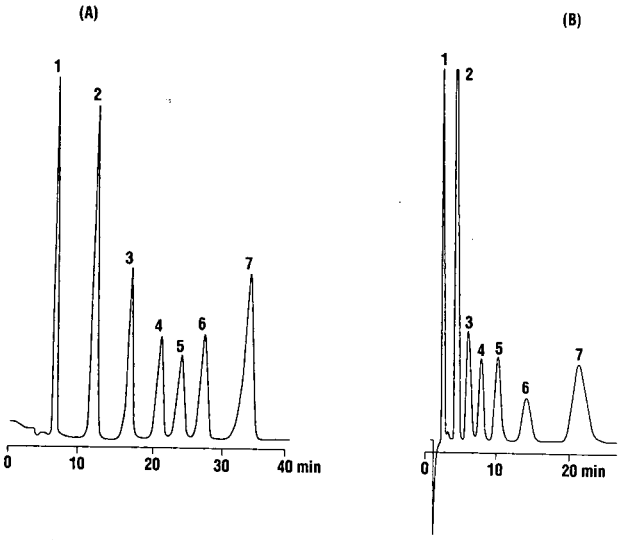

Fig. 6. Separation of the anion mixture using carbonate–hydrogencarbonate eluent. Packing, Alltech Universal Anion; suppressor, membrane, 12 m*M* sulfuric acid regenerant; detection, conductivity. Other conditions: (A) column, 150 mm × 4.6 mm I.D.; eluent, 2.2 m*M* Na_2CO_3–2.8 m*M* $NaHCO_3$; flow-rate, 0.7 ml/min; (B) column, 50 mm × 4.6 mm I.D.; eluent, 0.3 m*M* Na_2CO_3–5.7 m*M* $NaHCO_3$; flow-rate, 0.8 ml/min. Peaks: 1 = fluoride (10 ppm); 2 = chloride (20 ppm); 3 = nitrite (20 ppm); 4 = bromide (20 ppm); 5 = nitrate (20 ppm); 6 = phosphate (30 ppm); 7 = sulfate (30 ppm).

It gives good results with a wide variety of eluents and shows compatibility with both SCIC and suppressor-based IC.

The efficiency expressed as number of theoretical plates per meter with various eluents is shown in Table III. The results show good ion-exchange kinetics with a wide variety of eluents, and are comparable to those given by other commercially available columns [18].

TABLE II

ANION EXCHANGE CAPACITY FACTORS, k' ON THE UNIVERSAL ANION COLUMN

Anion	Eluent[a]				
	pHBA (pH 7.9)	LiHP (pH 4.5)	Borate–Gluconate 2	LiOH–benzoate	Na_2CO_3–$NaHCO_3$
Fluoride	1.5	1.7	1.4	1.7	0.6
Chloride	2.9	3.4	4.2	4.0	2.0
Nitrite	4.0	4.6	6.6	5.8	3.3
Bromide	4.9	5.9	8.6	7.2	4.3
Nitrate	6.2	7.6	10.5	9.3	5.0
Phosphate	8.0	–	11.9	–	5.8
Sulfate	12.6	12.5	18.1	–	7.4

[a] Concentrations of the eluents are given in Table I.

TABLE III

COLUMN EFFICIENCY WITH VARIOUS ELUENTS

Eluent	Efficiency[a] (plates/m)
5 m*M* *p*-hydroxybenzoic acid, pH 7.9 (lithium hydroxide)	21 573
4 m*M* phthalic acid, pH 4.5 (lithium hydroxide)	18 920
Borate–gluconate 2[b]	20 460
2.5 m*M* lithium hydroxide–0.05 m*M* sodium benzoate	25 813
2.2 m*M* sodium carbonate–2.8 m*M* sodium hydrogencarbonate	21 087

[a] Calculated at half-height using nitrate peak.

[b] The concentration of borate–gluconate 2 eluent is given in Table I.

Comparison between HEMA-, PS–DVB- and silica-based columns

The hydrophilic character of the HEMA-based anion exchanger offers several advantages over PS–DVB-based materials. System peaks typically encountered with PS-DVB anion exchangers when used with pHBA eluent [14] are not observed with the HEMA-based media. System peaks result from a change in equilibrium between the molecular form of the eluent and the resin matrix [14, 19, 20]. As HEMA is less hydrophobic than PS–DVB, the adsorbtion of the molecular form of pHBA by the resin is reduced. This may explain why the system peak is not observed. More research is required to determine the exact mechanism which causes system peaks.

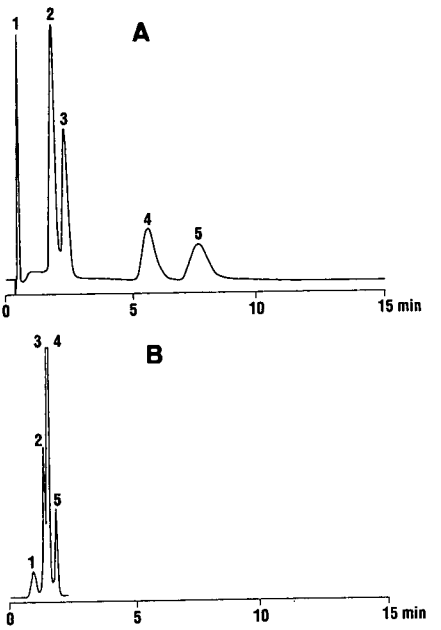

Fig. 7. Reversed-phase separation of five organic components on PS–DVB-based and HEMA-based columns. Column, 100 mm × 4.6 mm I.D.; eluent, acetonitrile–water (65:35); flow-rate, 1.0 ml/min; detection, UV at 254 nm. Packing: (A) PS–DVB (Wescan Anion/R); (B) Alltech Universal Anion. Peaks: 1 = uracil; 2 = phenol; 3 = benzaldehyde; 4 = N,N-diethyl-*m*-toluamide; 5 = toluene.

The peak shape for polarizable anions such as nitrate and bromide is improved with HEMA. PS–DVB-based anion exchangers have some hydrophobic or reversed-phase characteristics [6] and tend to cause peak tailing for polarizable anions. A Wescan Anion/R column (PS–DVB based) was used for a comparison study. The chromatograms in Fig. 7 show the hydrophilicity of HEMA as compared with PS–DVB. These chromatograms were obtained using reversed-phase conditions [acetonitrile–water (65:35) as the eluent with UV detection at 254 nm]. The five components were well resolved on the PS–DVB column (Fig. 7A) and were unretained on the HEMA column (Fig. 7B). Fig. 8 shows the peak shape of nitrate on both HEMA and PS–DVB columns. It is likely that the hydrophobic characteristics of PS–DVB cause peak tailing for nitrate owing to the retention of this polarizable anion on the packing by a "reversed-phase" mechanism.

Silica-based material provides excellent rigidity of the packing, but creates problems with eluent pH limitations and adsorption of fluoride ion, making it difficult to determine this ion. This HEMA-based sorbent may be used with phthalic acid eluent as a replacement for silica-based columns, with the additional advantage of allowing the determination of fluoride.

Applications

The physical, chemical and ion-exchange properties of HEMA allow a wide variety of separations. Fig. 9A shows the separation of chloride, chlorate and sulfate on a 100 mm × 4.6 mm I.D. HEMA column with pHBA eluent. The total analysis

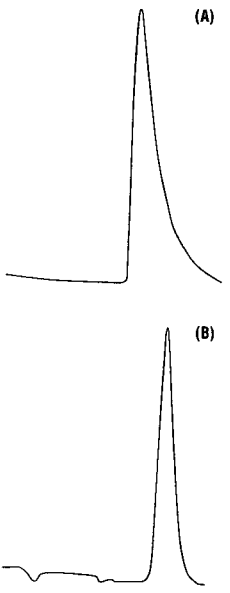

Fig. 8. Comparison of peak shape for nitrate ion on PS–DVB-based and HEMA-based columns. (A) Column, 250 mm × 4.1 mm I.D.; packing, PS–DVB (Wescan Anion/R); eluent, 5 m*M* pHBA, pH 8.5 adjusted with lithium hydroxide; flow-rate, 1.0 ml/min; detection, conductivity; sample size, 20 μl. (B) Column, 150 mm × 4.6 mm I.D.; packing, Alltech Universal Anion; eluent, 5 m*M* pHBA, pH 7.9 adjusted with lithium hydroxide; other conditions as in (A).

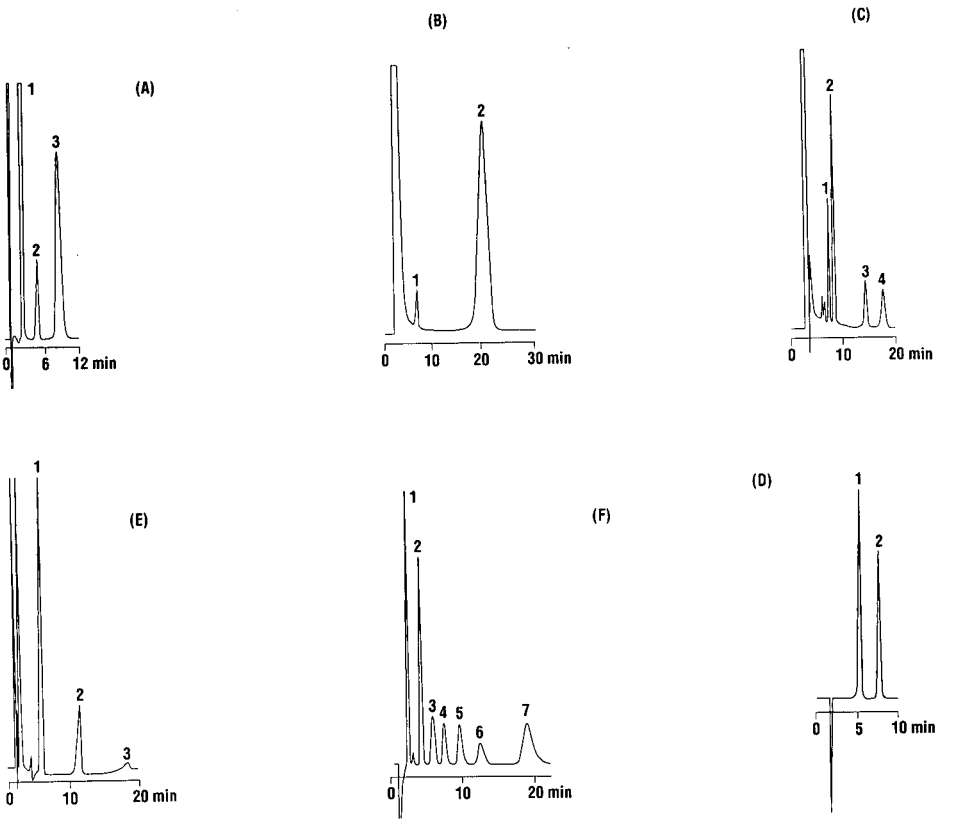

Fig. 9. Separation of various anions on HEMA (Alltech Universal Anion) column. (A) Separation of (1) chloride (100 ppm), (2) chlorate (40 ppm) and (3) sulfate (100 ppm): column, 100 mm × 4.6 mm I.D.; eluent, 4 m*M* pHBA, pH 7.9 adjusted with lithium hydroxide; flow-rate, 0.9 ml/min; detection, conductivity. (B) Separation of (1) chloride and (2) sulfate in surfactant: column, 150 mm × 4.6 mm I.D.; eluent, 4 m*M* LiHP in methanol–water (5:95), pH 4.5; flow-rate, 1.0 ml/min; detection, conductivity. (C) Separation of (1) chlorite, (2) chloride and (3) chlorate; peak 4 is a system peak: column, 300 mm × 4.6 mm I.D.; eluent, 10 m*M* sodium hydroxide; flow-rate, 1.0 ml/min; detection, conductivity. (D) Separation of (1) nitrite and (2) nitrate: column, 150 mm × 4.6 mm I.D.; eluent, 15 m*M* sodium hydroxide; flow-rate, 1.0 ml/min; detection, UV at 214 nm. (E) Separation of (1) chloride, (2) phosphate and (3) sulfate in plant food: column, 100 mm × 4.6 mm I.D.; eluent, borate–gluconate 2; flow-rate, 1.0 ml/min; detection, conductivity. (F) Separation of anions in antifreeze: column, 50 mm × 4.6 mm I.D.; eluent 0.3 m*M* Na_2CO_3–5.7 m*M* $NaHCO_3$; flow-rate, 0.8 ml/min; suppressor, membrane, 12 m*M* sulfuric acid regenerant; detection, conductivity; peaks: 1 = fluoride; 2 = chloride; 3 = nitrite; 4 = bromide; 5 = nitrate; 6 = phosphate; 7 = sulfate.

time is 13 min. The hydrophilic nature of HEMA allows direct injection of surfactant samples, as shown in Fig. 9B. Normally, the surfactant sample must be pretreated prior to injection, to remove any hydrophobic components in the sample that could irreversibly bind to the polystyrene-based packing. Fig. 9C shows the simultaneous separation of chlorite, chloride and chlorate using a 300 mm × 4.6 mm I.D. HEMA column with hydroxide eluent. A shorter column (150 mm × 4.6 mm I.D.) combined with a weaker eluent (2.8 m*M* sodium hydroxide) has also been successfully used for

this separation. Sodium hydroxide eluent may also be used for the determination of nitrite and nitrate in water with UV detection at 214 nm, as shown in Fig. 9D. Fig. 9E shows the separation of chloride, phosphate and sulfate in plant food with borate–gluconate eluent. Fig. 9F shows the separation of anions in antifreeze using carbonate–hydrogencarbonate eluent with suppressor-based IC.

The universal characteristics of HEMA allows a wide variety of separations. The methods that have been developed for other columns can be transferred directly to a HEMA column with minor modifications to the eluent concentration and pH. This column is compatible with most eluents commonly used in IC analysis of anions.

REFERENCES

1 H. Small, T. S. Stevens and W. S. Bauman, *Anal. Chem.*, 47 (1975) 1801.
2 D. J. Gjerde, J. S. Fritz and G. Schmuckler, *J. Chromatogr.*, 186 (1979) 509.
3 T. S. Stevens and M. A. Langhorst, *Anal. Chem.*, 54 (1982) 950.
4 R. M. Cassidy and S. Elchuck, *Anal. Chem.*, 54 (1982) 1558.
5 Z. Iskandarani and D. J. Pietrzyk, *Anal. Chem.*, 54 (1982) 2427.
6 D. P. Lee, *J. Chromatogr. Sci.*, 22 (1984) 327.
7 S. Matsushita, Y. Tada, N. Baba and K. Hosako, *J. Chromatogr.*, 259 (1983) 459.
8 *Vydac HPLC Columns and Separation Materials*, The Separations Groups, Hesperia, CA, 1990–91, pp. 20–23.
9 D. J. Gjerde, in P. Jandik and R. M. Cassidy (Editors), *Advances in Ion Chromatography*, Vol. 2, Century International, Franklin, MA, 1990, p. 169.
10 P. K. Dasgupta, *Anal. Chem.*, 56 (1984) 108.
11 F. A. Carey and R. J. Sundber, *Advanced Organic Chemistry, Part A*, Plenum Press, New York, 1977, Ch. 8, p. 335.
12 F. Vlacil and I. Vins, *J. Chromatogr.*, 391 (1987) 119.
13 F. Vlacil and I. Vins, *J. Chromatogr.*, 391 (1987) 133.
14 D. T. Gjerde and J. S. Fritz, *Ion Chromatography*, Hüthig, New York, 1987, Ch. 7, p. 133.
15 F. C. Smith, Jr., and R. C. Chang, *The Practice of Ion Chromatography*, Wiley, New York, 1983, Ch. 4, p. 83.
16 G. Schmuckler, A. L. Jagoe, J. E. Girard and P. E. Buell, *J. Chromatogr.*, 356 (1986) 413.
17 J. McClory and D. Warren, in P. Jandik and R. M. Cassidy (Editors) *Advances in Ion Chromatography*, Vol. 1, Century International, Franklin, MA, 1989, p. 261.
18 P. R. Haddad, P. E. Jackson and A. L. Heckenberg, *J. Chromatogr.*, 346 (1985) 139.
19 T. Okada and T. Kuwamoto, *Anal. Chem.*, 56 (1984) 2073.
20 S. Levin and E. Grushka, *Anal. Chem.*, 58 (1986) 1602.

Journal of Chromatography, 546 (1991) 101–110
Elsevier Science Publishers B.V., Amsterdam

CHROMSYMP. 2178

Anion–cation separations on a mixed-bed ion-exchange column with indirect photometric detection

DONALD J. PIETRZYK*, SCOTT M. SENNE[a] and DAVID M. BROWN[b]
Department of Chemistry, University of Iowa, Iowa City, IA 52242 (U.S.A.)

ABSTRACT

Inorganic cations and anions are separated simultaneously on a mixed bed of anion and cation exchangers. Columns studied are mixtures of polymer based and silica based anion and cation exchangers and stationary phases that contain both chemically bonded anion and cation ionogenic groups. The major parameters that influence retention and resolution are the mobile phase counterions, their concentration, and the ion-exchange capacities. Because electrolyte solutions are required for elution, detection by conductivity is limited. Using an electrolyte that is composed of a chromophoric cation and anion not only satisfies elution requirements but also premits analyte cations and anions to be detected by an indirect photometric detection strategy.

INTRODUCTION

Columns exhibiting a mixed mode of interactions are becoming increasingly more important in liquid chromatographic (LC) separations. Most are based on polymer matrix type low capacity ion exchangers where the combination of either anion exchange or cation exchange with reversed-phase properties are present [1–4]. Ion exchange of charged analytes occurs at the chemically attached ionogenic group and retention of uncharged molecules occurs at the polymer matrix. For analytes that contain both charged and hydrophobic centers both sites are capable of participating in retention with the analyte. Because of these characteristics retention order depending on the analytes can differ sharply between an ion-exchange column, a reversed-phase column, and one that contains both sites.

Columns containing a mixed bed of ion exchangers can also provide a mixed mode of interaction [5]. Thus, a mixed bed of anion and cation exchangers or a matrix containing both anion and cation exchange sites (both hereafter are referred to as MBIE columns) can be used for an efficient, simultaneous separation of anions and cations [5–7]. In this application a single MBIE column, a single injection, and a single eluent are used for the separation. Since retention of the cation and anion analytes is by ion exchange, their succesful elution must involve an eluent counter-

[a] Present address: Millipore-Waters, Waters Chromatography, Milford, MA 01757, U.S.A.
[b] Present address: Abbott Laboratories, North Chicago, IL 60064, U.S.A.

0021-9673/91/$03.50

cation and counteranion of appropriate ion-exchange selectivity and concentration. If conductance is used for detection, as was done previously [6,7], post column suppression cannot be used to alter background conductance due to the eluent since this will remove either anions or cations depending on the type of suppressor used. Thus, to monitor anion and cation analytes simultaneously as they appear in the column effluent from the MBIE column, an eluent electrolyte must be chosen that provides a cation and anion ionic equivalent conductance which differs sharply from the cations and anions that are being separated and detected. In previous studies using MBIE columns aqueous lithium acetate eluents were successfully used [6,7]. However, the use of conductance for detection limits the type of eluent that can be used since eluent strength cannot easily be altered based on principles of ion-exchange selectivity and mass action of eluent electrolyte without having a major influence on conductivity.

This report focuses on using chromophoric counterions as the eluent electrolyte and indirect photometric detection (IPD) to detect separated analyte anions and cations. Using IPD, which has been shown to be a useful detection strategy in ion chromatography [8–11], allows eluent strength to be adjusted through the use of different counterions and/or via altering counterion concentration. The only requirement is that the counterion must have a favorable absorptivity, if IPD is used.

EXPERIMENTAL

Reagents

Benzyltrimethyl ammonium chloride and *p*-toluenesulfonic acid were obtained from Aldrich while $Ce(NO_3)_3$ was purchased from Fisher Scientific. LC water was obtained by passing distilled water through a Millipore Milli-Q Plus water purification unit. Dionex HPIC-CS5 and HPIC-AS7 columns were purchased from Dionex. Polystyrene divinylbenzene polymer based cation ($PRP\text{-}SO_3^-$) and anion (PRP-X100) exchangers were obtained from Hamilton and/or prepared by sulfonation [3] and quaternization [2,4], respectively, of PRP-1 (Hamilton). Bulk particles of Zorbax SCX and SAX were obtained from Fisher Scientific.

Instrumentation

A Varian M2010 pump, Waters U6K injector, Beckman M160 (254 nm) or a Spectra Physics 770 variable-wavelength detector, and a Hewlett Packard M3390A integrator were used. Columns used and their properties are listed in Table I.

Procedures

Benzyltrimethyl ammonium ($BTMA^+$) chloride was converted to the hydroxide by anion exchange. Aliquots of standardized solutions of BTMAOH and *p*-toluene sulfonic acid (PTSH) were combined in aqueous solution to give the BTMA–PTS eluent. The aqueous $Ce(NO_3)_3$ eluent was prepared by dilution of a known weight of $Ce(NO_3)_3$. Sulfonated and quaternized PRP-1 particles were prepared and their exchange capacities were determined as described elsewhere [2–4]. Polyion MBIE columns (see Table I) were prepared by mixing quantities of the two exchangers in 20 ml of a solution consisting of 30 g NaCl and 100 ml glycerol per liter of LC water. The slurry of exchangers was packed upward in a column using a high flow-rate/high pressure procedure. The Zorbax MBIE column was packed similarly except the glyce-

rol was omitted. Dionex columns were obtained prepacked. Columns were conditioned with the mobile phase of interest and column efficiencies were determined using NaCl as the analyte (see Table I).

Analyte solutions were prepared by dissolving known weights of inorganic salts in LC water. Sample aliquots of 1 to 25 μl were delivered by a 25-μl syringe. A peak area method was used to determine calibration curves. Inlet column pressure at 1 ml/min was about 1000 p.s.i. while column void volume was 0.4 and 1.5 ml for 70 and 250 mm columns, respectively. IPD was at 254 nm for the BTMA–PTS eluent and 240 nm for the $Ce(NO_3)_3$ eluent.

RESULTS

When a mixed bed of cation and anion exchangers or a stationary phase containing both cation and anion ionogenic groups are packed into a column and a charged analyte is passed through the column using an aqueous salt solution as the eluent, both cation and anion exchange will occur in the column [6,7]. The parameters influencing analyte cation and anion retention are those that affect cation and anion exchange. These include: (1) anion and cation exchange capacity, (2) ratio of anion to cation exchange capacity, (3) analyte ion concentration, (4) concentration of the eluent electrolyte, (5) ion exchange selectivity of the eluent countercation and counteranion, and (6) pH if the analyte or eluent counterions have weak acidic/basic properties. Optimization of each parameter, which is discussed elsewhere [5–7,12],

TABLE I

MIXED-BED ION-EXCHANGE (MBIE) COLUMNS

Column	Packing, mixed-bed ratio, dimensions	Cation-exchange capacity (equiv./g)	Anion-exchange capacity (equiv./g)	Particle size (μm)	Sodium efficiency (plates/m)	Chloride efficiency (plates/m)
Dionex HPIC-CS5	[a] 250 × 4.6 mm I.D.	160	70	10	10 000[c]	18 000[c]
Dionex HPIC-AS7	[b] 250 × 4.6 mm I.D.	43	250	10		
Polyion-1	$PRP\text{-}SO_3^-$/PRP-X100 (1:1) 70 × 4.1 mm I.D.	48	50	10	2 000[c]	1 000[c]
Polyion 2	$PRP\text{-}SO_3^-$/PRP-X100 (1:1) 70 × 4.1 mm I.D.	58	29	10		
Zorbax	Zorbax SCX/Zorbax SAX (1:1) 70 × 4.1 mm I.D.	32	245	6	8 000[c]	7 000[c]

[a] A polystyrene divinylbenzene core containing quaternary ammonium groups coated with sulfonated latex.

[b] A polystyrene divinylbenzene core containing sulfonated groups coated with quaternary ammonium latex.

[c] A 1.00 m*M*, 0.10 m*M* and 1,61 m*M* BMTA–PTS eluent, respectively.

must be done while recognizing that both anion and cation exchange are occurring simultaneously.

If the analyte cation and anion ion exchange selectivities differ, each analyte will appear in the column effluent at different elution times. By using an electrolyte in the eluent that is significantly different in ionic equivalent conductance from the analyte cation and anion, the separated analyte cation and anions can be detected using a conductance detector [6,7]. The conductance detector, however, limits the type of electrolyte that can be used in the eluent because of the electrolyte's contribution to the background conductance.

In ion chromatography it has been shown that cations separated on a cation exchanger [8,10] can be detected by IPD if a chromophoric counter cation is used in the eluent. Similarly, anions can be separated and detected by IPD [8,9] by using a chromophoric counteranion. Inorganic anions and metals as anionic EDTA complexes were separated on an anion exchange column using IPD and an EDTA eluent [13]. For a MBIE column IPD should be possible if the eluent electrolyte used in the mobile phase is composed of a chromophoric countercation and chromophoric counteranion. When this chromophoric eluent electrolyte passes through the column the ion exchange process between the chromophoric countercation and counteranion, AB, and the analyte cation and anion, MX, takes place as shown in eqns. 1 and 2, respectively,

$$R^-M^+ + B^+ \rightleftharpoons R^-B^+ + M^+ \tag{1}$$

$$R^+X^- + A^- \rightleftharpoons R^+A^- + X^- \tag{2}$$

where R is the anionic or cationic ionogenic group on the stationary phase. If the effluent is monitored where both A and B absorb and the mobile phase background absorbance due to AB is electronically offset by the detector, the chromatographic peaks for M and X will appear as negative peaks (absorbance decrease) when each passes through the detector. In general, background absorbance should be less than 0.8 providing the absorbance detector used has a favorable offset capability [8,11,12].

In order to obtain a favorable simultaneous detection of analyte cations and anions using IPD and a MBIE column, eluent counterions must meet several requirements: (1) they must be chromophoric and both must have an appreciable absorptivity, (2) they must provide appropriate eluting power, and (3) they must have a reasonable solubility and dissociation at the mobile phase pH required for the separation. Two mobile phase eluent electrolytes that meet these requirements and were chosen to be used in this study were cerium nitrate and BTMA–PTS. Both of these electrolytes also have the property whereby both the eluent countercation and counteranion will absorb at the same wavelength, thus permitting the use of a single wavelength type absorbance detector.

For the case where both the eluent countercation and counteranion absorb at the same wavelength the total absorbance (A_t) indicated by the detector when set at the wavelength of absorbance is given by eqn. 3,

$$A_t = a_m^+ bc^+ + a_m^- bc^- \tag{3}$$

where a_m^+ and a_m^- are the molar absorptivities of the chromophoric countercation and counteranion, respectively, c^+ and c^- are the respective concentrations, and b is the detector cell path length. When an analyte cation and anion travel through the column the concentration of the chromophoric ion of the same charge decreases in the analyte peak as each emerges from the column (see eqns. 1 and 2). Because the analyte cation and anion displace an equivalent amount of chromophoric cation and anion in the mobile phase, respectively, negative peaks are obtained. For the case where an analyte cation displaces an equivalent amount of chromophoric cation in the mobile phase, the concentration of the chromophoric cation decreases while the concentration of the chromophoric anion and its contribution to absorbance is constant. For an analyte anion the concentration of the chromophoric anion would decrease causing an absorbance decrease while the concentration of the chromophoric cation and its contribution to absorbance is constant. In both cases, therefore, a linear relationship exists between the change in absorbance and the change in the concentration (of analyte cation and anion, respectively) according to Beer's law providing the ion-exchange processes are maintained well below a column overload condition. In all the experiments reported here the analyte ion sample sizes were always below 0.17 μequiv., which is well below the exchange capacity for each type of ion exchange site (see Table I), and in a region where capacity factor is independent of column loading.

Three kinds of MBIE columns were studied (see Table I). The Polyion and Zorbax columns are polymeric and silica based, respectively, and were packed as intimate mixtures of anion and cation exchangers. The polymer based exchangers have several unique features: (1) these exchangers can be prepared to vary widely in ion exchange capacity, and (2) if ion exchange capacity is low enough the low capacity exchanger can participate in reversed-phase interaction in addition to ion exchange at the polymeric matrix surface, thus providing an additional mode of interaction which is potentially useful when separating ionic and non-ionic samples and/or lipophilic type analytes [5]. The Polyion and Zorbax columns can be prepared by mixing anion and cation exchangers to obtain different anion–cation exchange ratios either by mixing different weights of the two exchangers or by mixing equal weights of the two exchangers that differ in exchange capacity. The Dionex MBIE columns are unique in that these stationary phases are not an intimate mixture of exchangers but rather are composed of a latex containing either sulfonated or quaternary ammonium groups that is deposited and held via electrostatic forces on a polystyrene–divinylbenzene core containing either quaternay ammonium or sulfonated groups, respectively. While the ionogenic group located on the latex layer will be the larger of the two ion exchange capacities (see Table I) both anion and cation exchange sites are available.

Fig. 1 shows that the retention of both analyte cations and anions on the two Dionex columns decreases as mobile phase BTMA–PTS concentration increases typical of mass action effects of eluent counterion on ion exchange. In all cases IPD at 254 nm, where both $BTMA^+$ and PTS^- absorb, was used to detect analyte cations and anions, respectively. In Fig. 1A where a Dionex HPIC-CS5 column was used, anions have lower retention than cations because the cation-exchange capacity is in excess (see Table I) and monovalent cations have lower retention than monovalent anions (see Fig. 1B). In these studies peak identification was confirmed by using different salts as analytes. For example, Na^+, K^+, Br^- and Cl^- peak assignments were based on the comparison of chromatograms obtained by using NaCl, NaBr,

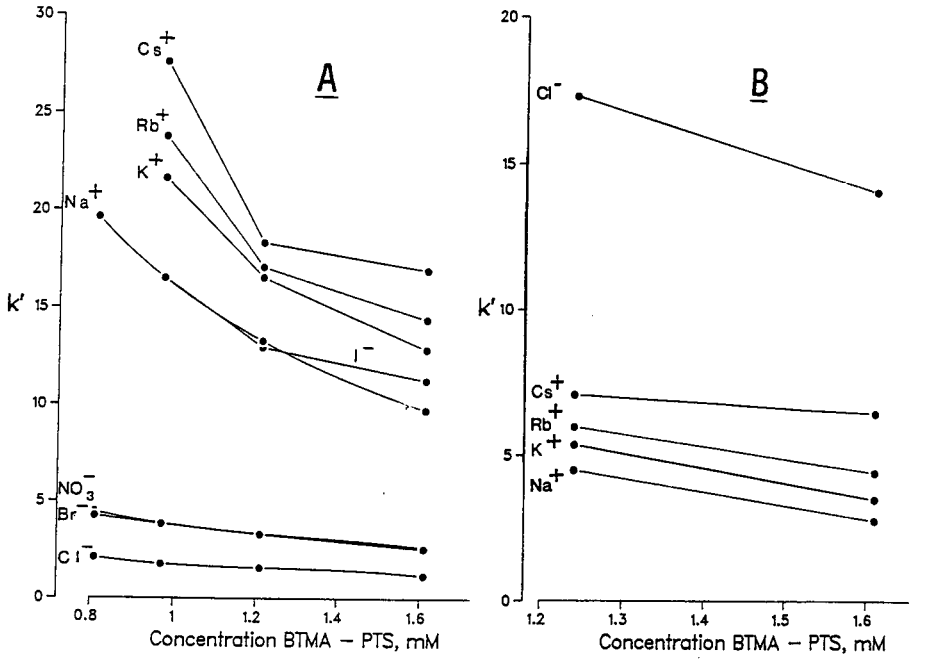

Fig. 1. Effect of BTMA-PTS concentration on the retention of analyte cations and anions on the Dionex columns. (A) Dionex HPIC-CS5 column and aqueous BTMA–PTS eluent at 1.0 ml/min with IPD at 254 nm, (B) Same as (A) except Dionex HPIC-AS7 column.

KCl and KBr as analytes. Other salts were also used to confirm peak assignment.

Fig. 2 shows a separation of anions and cations on the Dionex HPIC-CS5 column. BTMA–PTS mobile phase concentration can be reduced to improve anion resolution, however, if this is done elution time for cations is much longer. For a HPIC-AS7 column (see Fig. 1B) where anion exchange capacity is higher, analyte cations elute early and analyte anions are resolved at higher retention times depending on mobile phase BTMA–PTS concentration.

Calibration curves based on peak area were determined for both Na^+ and Cl^- on a Dionex HPIC-CS5 column using NaCl as an analyte. The range covered 29 to 3630 ng for Na^+ and 45 to 5620 ng for Cl^- in a 20-μl injection volume; no attempt was made to determine the upper limit of linearity. Detection limits for Na^+ and Cl^- using IPD and a Beckman M160 fixed-wavelength detector at 254 nm was about 31 and 3.0 ng, respectively, for a signal-to-noise ratio of 3:1. Correlation coefficients over the range studied exceeded 0.999 for both ions.

An eluent containing $Ce(NO_3)_3$ provides a countercation of high cation-exchange selectivity due to charge and a counteranion of modest anion-exchange selectivity. Both absorb at the same wavelength and IPD of separated analyte cations and anions is possible. Fig. 3 shows how mobile phase concentration of $Ce(NO_3)_3$ influences analyte cation and anion retention on a HPIC-CS5 column. Monovalent anions are more highly retained than the divalent cations because of the favorable cation-exchange selectivity exhibited by the trivalent cerium. Fig. 4 illustrates the separation

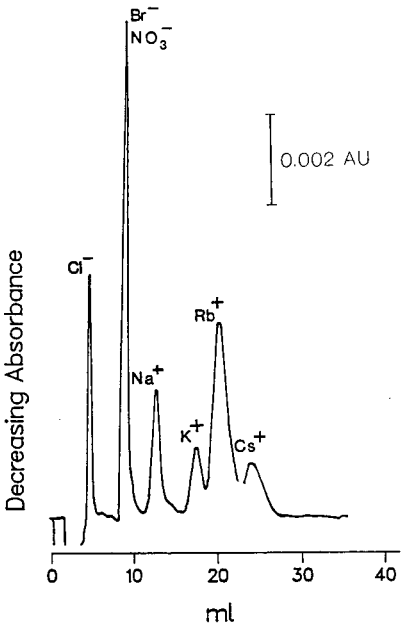

Fig. 2. Simultaneous separation and IPD of analyte cations and anions. Dionex HPIC-CS5 column and aqueous 1.31 m*M* BTMA–PTS eluent at 1.0 ml/min with IPD at 254 nm.

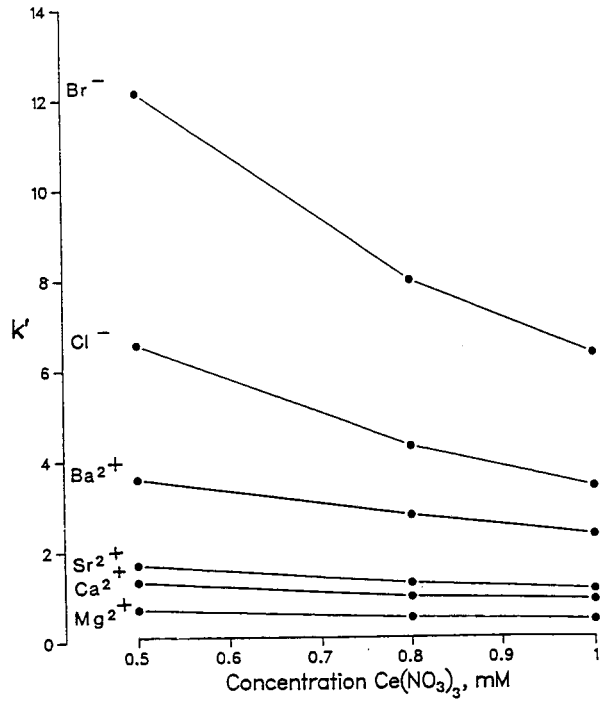

Fig. 3. Effect of $Ce(NO_3)_3$ on retention of analyte cations and anions on a Dionex column. Dionex HPIC-CS5 column and aqueous $Ce(NO_3)_3$ eluent at 1.0 ml/min with IPD at 240 nm.

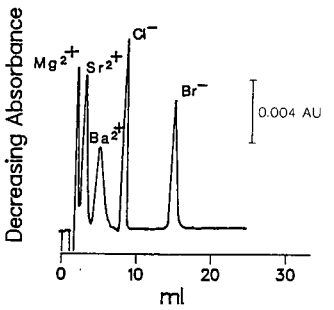

Fig. 4. Simultaneous separation of divalent cations and anions. Conditions are the same as in Fig. 3 except 0.50 m*M* $Ce(NO_3)_3$.

of alkaline earth and common halide ions on the HPIC-CS5 column using $Ce(NO_3)_3$ as the eluent and IPD at 240 nm.

When polymeric cation and anion exchangers (Polyion columns in Table I) and silica-based cation and anion exchangers (Zorbax column in Table I) were each mixed and packed into a column, analyte cations and anions could be separated on each of the columns. If cation-exchange capacity is in excess over anion-exchange capacity, retention of analyte cations is higher than analyte anions when compared to the reverse situation. In both columns BTMA–PTS and $Ce(NO_3)_3$ eluents could be used for the elution of cations and anions and for their indirect detection. Fig. 5, for example, shows how retention of analyte cations and anions decreases on a Polyion column where cation- and anion-exchange capacity are equal as mobile phase BTMA–PTS concentration increases. Since Polyion and Zorbax column efficiencies are lower than for the Dionex columns (see Table I) baseline separation of complex mixtures are more readily obtained on the Dionex columns.

Separations on the Polyion and Zorbax columns can also be improved by increasing column length [see Fig. 5 where capacity factors (k') for analyte cations and anions can be compared]. No attempt was made to optimize column length for the Polyion and Zorbax columns. The 7.0-cm length was chosen because of a limitation in the availability of the stationary phases and interest in studying the effects of exchange capacity on retention. This could only be easily done by preparing limited quantities of polymeric ion exchangers that differ in exchange capacities.

Fig. 6 illustrates two typical separations on the short 7.0-cm Polyion-2 (Fig. 6A) and Zorbax (Fig. 6B) column using a $Ce(NO_3)_3$ and a BTMA–PTS eluent. In Fig. 6A analyte cation retention is sharply reduced due to the $Ce(NO_3)_3$ eluent and analyte cations are eluted before analyte anions even though the cation-exchange capacity is twice the anion exchange capacity (see Table I). A Mg^{2+} and Ca^{2+} mixture would be separated similarly as Sr^{2+} and Ba^{2+} but at lower retention time. If all four cations are present only partial resolution is obtained because of the column efficiency and the short 7.0-cm column. For the Zorbax column (Fig. 6B) anion-exchange capacity is over seven times the cation-exchange capacity (see Table I) and analyte cations elute rapidly when the eluent BTMA–PTS concentration is increased in order to elute analyte anions at lower retention times. If BTMA–PTS mobile phase concentration is reduced resolution of the early eluted analytes is improved.

When the Polyion-2 column (see Table I) was used to prepare a peak area

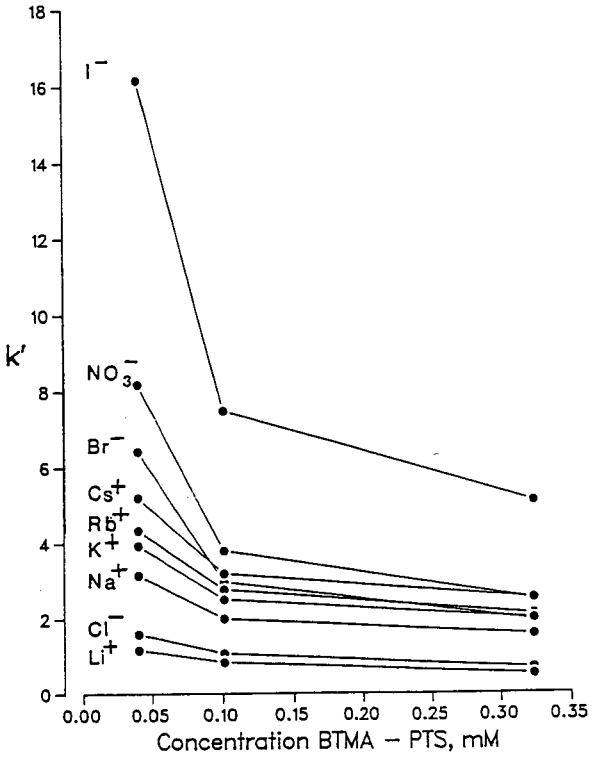

Fig. 5. Effect of BTMA–PTS concentration on the retention of analyte cations and anions on a Polyion column. Polyion-1 column and aqueous BTMA–PTS eluent at 1.0 ml/min with IPD at 254 nm.

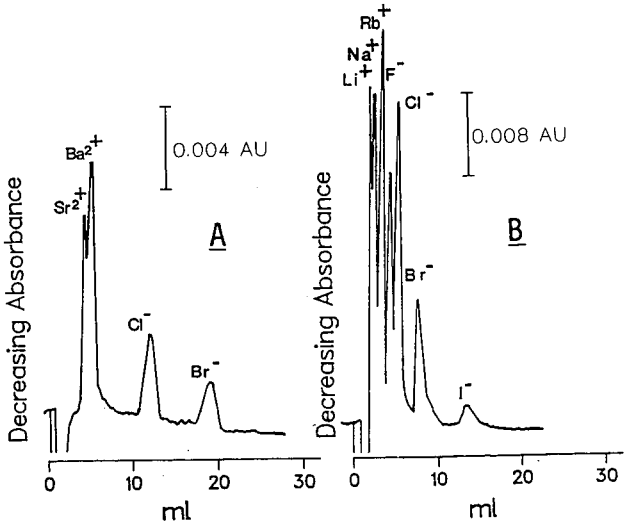

Fig. 6. Simultaneous separation of analyte cations and anions. (A) Polyion-2 column and aqueous 0.25 m*M* $Ce(NO_3)_3$ eluent at 1.0 ml/min with IPD at 240 nm. (B) Zorbax column and aqueous 1.61 m*M* BTMA–PTS eluent at 1.0 ml/min with IPD at 254 nm.

calibration curve for $CaCl_2$ as an analyte and aqueous 0.50 m*M* $Ce(NO_3)_3$ as an eluent, linear curves were obtained for both Ca^{2+} and Cl^- over the mass range studied (182 to 3630 ng for Ca^{2+} and 324 to 6460 ng for Cl^-) in a 20-μl injection volume. Correlation coefficients were greater than 0.998 for each. Detection limits for Ca^{2+} and Cl^{2-} using IPD at 240 nm and a Spectra Physics M770 absorbance detector was about 72 and 39 ng, respectively, for a signal-to-noise ratio of 3:1.

CONCLUSIONS

The experiments indicate that indirect photometric detection is feasible for the simultaneous separation of cations and anions using a mixed-bed ion-exchange column. Since analyte cations and anions can coelute, peak purity must be carefully established. Mobile phase chromophoric electrolyte eluent concentration can be altered within detector offset limits in order to affect analyte retention. If a detector capable of monitoring two different wavelengths is used then chromophoric electrolyte eluents composed of a cation and anion that absorb at different wavelengths can also be used. This provides additional flexibility in manipulating eluent strength for elution of cations and anions and their detection.

REFERENCES

1 F. F. Cantwell, in J. Marinsky (Editor), *Advances in Ion Exchange and Solvent Extraction*, Marcel Dekker, New York, 1985, p. 339–371.
2 S. Afrashtehfar and F. F. Cantwell, *Anal. Chem.*, 54 (1982) 2422–2427.
3 R. A. Hux and F. F. Cantwell, *Anal. Chem.*, 56 (1984) 1258–1263.
4 D. J. Pietrzyk, Z. Iskandarani and G. L. Schmitt, *J. Liq. Chromatogr.*, 9 (1986) 2633–2659.
5 D. M. Brown, *Ph. D. Thesis*, University of Iowa, December 1987.
6 D. J. Pietrzyk and D. M. Brown, *Anal. Chem.*, 58 (1986) 2554–2557.
7 D. M. Brown and D. J. Pietrzyk, *J. Chromatogr.*, 466 (1989) 291–300.
8 H. Small and T. E. Miller, Jr., *Anal. Chem.*, 54 (1982) 462–469.
9 A. Jardy, M. Caude, A. Diop, C. Curvale and R. Rosset, *J. Chromatogr.*, 439 (1988) 137–149.
10 J. H. Sherman and N. D. Danielson, *Anal. Chem.*, 59 (1987) 490–493.
11 E. S. Yeung, *Acc. Chem. Res.*, 22 (1989) 125–130.
12 S. M. Senne, *M. S. Thesis*, University of Iowa, Iowa City, IA, August 1988.
13 K. Hayakawa, T. Sawada, K. Shimbo and M. Miyazaki, *Anal. Chem.*, 59 (1987) 2241–2245.

Journal of Chromatography, 546 (1991) 111–118
Elsevier Science Publishers B.V., Amsterdam

CHROMSYMP. 2169

Review

Principles and applications of ion-exclusion chromatography

JAMES S. FRITZ
Ames Laboratory–U.S. Department of Energy, and Department of Chemistry, Iowa State University, Ames, IA 50011 (U.S.A.)

ABSTRACT

Ion-exclusion chromatography is a relatively old technique that has been attracting increased attention. It is particularly useful for separating hydrophilic molecular species from one another and from large amounts of ionic materials. The basic principles and methodology of ion-exclusion chromatography are presented and illustrated with typical examples. Several recent developments in ion-exclusion chromatography are discussed. These include methods for the enhancement of conductivity detection of weakly ionized substances and a new method for the chromatographic separation and detection of water.

CONTENTS

1. INTRODUCTION

Ion-exclusion chromatography actually involves the chromatographic separation of molecular species rather than ions. Of course, ions can often be readily converted into molecular species as is the case when anions of weak acids are acidified. Another possible reason for including ion-exclusion chromatography in a symposium devoted to ion chromatography is that an ion-exchange column is generally used for separations performed by ion-exclusion chromatography.

The most widely accepted explanation of ion-exclusion chromatography is that separation occurs because of differences in partition of molecular solutes between the

0021-9673/91/$03.50

eluent and eluent that is immobilized within the resin phase. Sample anions are excluded from the resin phase by the fixed charges of the sulfonate groups of the cation-exchange resin. If an anion-exchange column is used, sample cations are excluded by the fixed positive charges on the resin. Thus sample ions pass rapidly through the column and elute as a group. Molecular substances are free to partition into the occluded solvent within the resin and are therefore separated from the anions and from one another. The ability to separate molecular substances from much larger amounts of ions is one of the appealing advantages of ion-exclusion chromatography.

The mechanism of the separation process is undoubtedly more complex than the explanation that has just been given. Partly for this reason ion-exclusion chromatography has often been given other names such as Donnan exclusion ion-exclusion chromatography, ion-exclusion partition chromatography and ion-moderated partition chromatography.

Excellent and comprehensive reviews of ion-exclusion chromatography have been given by Gjerde and Mehra [1] and by Haddad and Jackson [2]. The goal of the present paper is to review the fundamental theory and typical applications in a concise manner and to focus on some selected recent developments.

2. METHODOLOGY AND THEORY

Separations by ion exclusion are carried out on a cation-exchange column, or occasionally on an anion-exchange column. The cation resin contains sulfonate groups ($-SO_3^-$) or mixed sulfonate and carboxylate groups [1]. The resin is most commonly used in the H^+ form, although another cation can serve as the counter ion. In fact, effective separation of sugars necessitates the use of a resin in the Ca^{2+} form. The introduction of ionic groups causes a microporous resin to take up water and become a gel. However, macroporous ionic resins have a large surface due to numerous pores and channels that can hold occluded water. In either case molecular solutes can partition between the mobile phase solvent and the occluded solvent within the resin phase. Assuming this is the only operative mechanism, the solute retention volume (V_R) is given by:

$$V_R = V_0 + DV_i$$

where V_0 is the interstitial volume of eluent (the eluent outside the resin beads), V_i is the internal volume of eluent (the occluded eluent within the resin beads), and D is the distribution ratio of a given solute. If a solute cannot enter the resin phase because of very large size (size exclusion) or because it is an ion (ion exclusion), the value of D is zero. If a solute is entirely molecular and entirely free to enter the resin phase, the value of D is 1. However, solutes may vary in their ability to enter the resin occluded phase and D can therefore be some value between zero and 1. This short range of D values provides only a narrow window for separations. For this reason, columns used in ion-exclusion chromatography frequently are fairly long and of large diameter in order to provide a good separation of samples containing several molecular compounds.

Acids are found to elute in the decreasing order of their acid dissociation constants, the stronger acids eluting first. Even fairly weak acids may be partially ionized and thereby exist as a mixture of the molecular acid and the acid anion. The

presence of more than one species results in broad peaks. It is common practice to avoid this complication by incorporating a low concentration (1 to 10 m*M*) of a strong acid (sulfuric acid for example) to the eluent. The H^+ from this acid represses the ionization of a weak acid solute (HA) and sharpens the chromatographic peak.

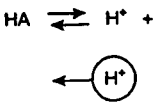

Factors other than partition between the mobile and occluded solvent phases are likely to affect the chromatographic behavior of molecular solutes. There may be a size effect in which molecules of larger size have greater difficulty in entering the resin. Older work [3] has indicated that the extent of resin cross-linking also plays a role. Finally, as the size of the molecule increase there is likely to be an increasing hydrophobic interaction between the molecule and the polymeric matrix. This interaction is especially strong when the molecule contains a benzene ring. Addition of an organic solvent modifier to the aqueous eluent will reduce hydrophobic interactions of organic solutes, sharpen the peaks, and reduce the retention time. However, an organic solvent can be added to the eluent to *increase* the retention of a polar solute such as ammonia [4].

2.1. Detectors

It is best to select a detector that responds well to the solutes to be determined but not to the eluent itself. A variable-wavelength UV detector, a refractive index detector, or some type of electro chemical detector will often meet these criteria. However, conductivity continues to be the most popular and widely used detector for ion-exclusion chromatography. As already discussed, it is often necessary to add a low concentration of a strong acid to the eluent to repress the ionization of weakly acidic sample constituents. This means that a relatively small increase in an already high background conductivity needs to be measured.

Two strategies have been used to remedy this situation. The first is to reduce the background conductance of the eluent.

(1) The oldest method is to place a Ag^+-form cation-exchange column between the separation column and the detector cell and to use hydrochloric acid as the strong acid added to the eluent. The hydrochloric acid is effectively removed by the ion-exchange suppressor:

$$H^+Cl^- + \text{resin-}Ag^+ \rightarrow \text{resin-}H^+ + AgCl(s)$$

The silver chloride stays in the suppressor column and gradually plugs it. One answer to this problem was to use a plastic tube as the suppressor and periodically cut off the plugged portions.

(2) A cation-exchange membrane can be used as the suppressor. This is kept in the tetrabutylammonium cationic form (TBA^+) by continuously circulating TBA^+Cl^- solution over the outside of the membrane. The H^+Cl^- of the eluent is thereby converted to TBA^+Cl^- which has a significantly lower conductance (Table I).

TABLE I

RELATIVE CONDUCTANCE OF 1 m*M* SOLUTIONS USED IN ION-EXCLUSION CHROMATOGRAPHY

TBA = Tributylamine; OSA = octanesulfonic acid; TDFHA = tridecafluoroheptanoic acid.

Ion pair	Conductance (μS)
H^+Cl^-	425
TBA^+Cl^-	100
TBA^+OSA^-	40
TBA^+TDFHA^-	30

A still lower conductance is obtained by using a strong acid in the eluent that has an anion that is larger and less conducting than chloride [5].

(3) Tanaka and Fritz [6] showed that addition of a somewhat weaker and less conducting acid to be the eluent will still repress the ionization of carboxylic acid solutes and given sharp chromatographic peaks. An eluent containing 5 m*M* benzoic acid has a background conductivity of only 5.6 μS cm^{-1} compared to 81.6 μS cm^{-1} for 5 m*M* sulfuric acid. The detector response for alkane carboxylic acids is higher for the benzoic acid eluent than for the eluent containing sulfuric acid. Later it was found that succinic acid worked as well as benzoic acid and required a much shorter time for initial equilibration of the column.

A second strategy for improving the sensitivity of conductivity detection in ion-exclusion chromatography is to enhance the conductivity of the sample solute(s).

(1) Carbon dioxide and carbonates can be determined by ion-exclusion chromatography on a H^+-cation-exchange column using pure water as the eluent. The conductivity detection signal is weak owing to the small degree of ionization of carbonic acid. Tanaka and Fritz [7] showed that the detection signal could be increased several fold by inserting ion-exchange "enhancement" columns between the separation column and the detector cell. The first enhancement column is a cation exchanger that converts carbonic acid into potassium bicarbonate, which is more completely ionized and therefore more conducting.

$$H_2CO_3 + \text{resin-}K^+ \rightarrow \text{resin-}H^+ + K^+HCO_3^-$$

This reaction appears to be quantitative, which might seem surprising because of the weakly acidic nature of carbonic acid. However, the concentration of K^+ in the resin phase is very high (*ca.* 4 *M*) and is therefore able to shift the equilibrium strongly to the right.

An anion-exchange column in the hydroxyl form serves as a second enhancement column. This converts potassium bicarbonate to potassium hydroxide and further increases the conductivity.

$$K^+HCO_3^- + 2\,\text{resin-}OH^- \rightarrow \text{resin}_2\text{-}CO_3^{2-} + K^+OH^- + H_2O$$

(2) A Japanese group [8] used this enhancement principle to improve the conductivity detection of carboxylic acids, dicarboxylic acids, and fluoride. A hollow-fiber, cation-exchange membrane was used as the enhancement unit, and an appropriate electrolyte flowed over the outside to provide continuous regeneration. They found sodium sulfate regenerant to give better chromatographic peaks than sodium hydroxide. The carboxylic acid solutes were converted to the highly ionized sodium salts

$$RCO_2H + \text{cation exchanger-}Na^+ \rightarrow \text{cation exchanger-}H^+ + Na^+RCO_2^-$$

Similarly, the sulfuric acid in the eluent was converted to the lower conducting sodium sulfate. A very large peak enhancement of approximately 34-fold was obtained using this system.

(3) Okada and Dasgupta [9] used a similar membrane system to convert nitric acid in the eluent to sodium nitrate and weakly acidic solutes (HA) to the sodium salt (Na^+A^-); sodium salts of weak acids are of course bases. The increase in pH is measured using 4-nitrophenol as indicator.

3. SELECTED APPLICATIONS

3.1. Inorganic acids and anions

Fluoride [10,11], phosphite and hypophosphite [12], arsenate [12] and nitrite [13–15] are readily determined by ion-exclusion chromatography. Bicarbonate [6,16] and sulfide [16] are anions of very weak acids and can be determined using only water as the eluent. Determination of sulfite in food [17–19] is now of considerable interest owing to a U.S. Federal regulation limiting the permissible amounts. A high-pH buffer is used to extract both "free" sulfite and sulfite that is bound to carbonyl compounds in food. Free sulfite only is determined after extraction with a pH 2.0 buffer.

Borate is separated by ion-exclusion chromatography as boric acid [20,21] but the ionization is so slight that sensitivity of conductivity detection is poor. Use of an aqueous eluent containing mannitol or fructose forms a complex that is more highly ionized and better detected by conductivity [22].

3.2. Organic acids

Determination of low-molecular-weight organic acids is probably the most common use of ion-exclusion chromatography. Acids such as formic, acetic, hydroxyacetic, citric, tartaric, oxalic, malonic and ascorbic acid have been determined in a large number of aqueous samples. Good compilations are available in recent books [1,2,4]. The eluent is always predominately aqueous and usually contains a low concentration of a strong acid to maintain the sample acids in the molecular form. A number of acids can often be separated with good resolution in a single run.

3.3. Sugars

Sugars can be separated by ion-exclusion chromatography on a cation-exchange column in the H^+ form [23]. However, better separations are obtained on a Ca^{2+}-form column where complexation probably plays a major role. Sucrose, a disaccharide, elutes before dextrose, fructose and other monosaccharides. Oligomers elute still earlier in order of decreasing molecular weight.

Detection of sugars presents a problem. A differential refractometer or a UV spectrophotometer at 195 nm can be used but the sensitivity is somewhat limited. Cowie *et al.* [24] were able to detect reducing carbohydrates potentiometrically using a metallic copper electrode.

3.4. Polar molecular compounds

Low-molecular-weight alcohols and glycols have been determined by ion-exclusion chromatography using conductivity [23,25] or refractive index [26] as the detector. Dimethylsulfoxide has been determined in sea water using a UV detector [27]. McClure [28] determined parts-per-billion (10^9) concentrations of formaldehyde in aqueous solution using post-column detection with acetylacetone and direct UV detection at 420 nm.

3.5. Determination of water

If an alcohol such as methanol can be separated by ion-exclusion chromatography using water as the eluent, why not do the reverse and separate water using a methanol eluent? Stevens *et al.* [29] did just this. They added a small amount of sulfuric acid to the eluent and detected the chromatographic water peak by a decrease in conductivity. The main drawback with this method was a non-linear calibration curve with very poor detection sensitivity in some concentration regions.

Fortier and Fritz [30] devised a unique equilibrium system for spectrophotometric detection of water after separation by ion-exclusion chromatography. This method has been studied and refined by continuing research of Chen and Fritz [31,32]. Water is separated chromatographically from the sample matrix on a short column packed with cation-exchange resin in the H^+ form using dry methanol as the eluent. Detection of the water peak is made possible by addition of a low concentration of cinnamaldehyde to the methanol eluent. In the presence of an acid catalyst, such as a H^+-cation exchanger, cinnamaldehyde reacts with methanol to form the dimethylacetal.

$$C_6H_5CH=CHCHO + 2\,CH_3OH \overset{H^+}{\rightleftarrows} C_6H_5CH=CHCH(OCH_3)_2 + H_2O$$

The UV spectra of cinnamaldehyde and the acetal are quite different; only the cinnamaldehyde absorbs strongly around 300 nm. Since most of the cinnamaldehyde has been converted to the acetal, the background absorbance at 300 nm is low. However, a water zone passing through the column will shift the equilibrium towards the formation of more cinnamaldehyde and the absorbance at 300 nm will increase.

$$H_2O + \text{acetal} \overset{H^+}{\rightleftarrows} \text{aldehyde} + 2CH_3OH$$

In methanol the equilibrium constant, K, has been measured [31].

$$K = \frac{[\text{aldehyde}]}{[\text{acetal}]\,[H_2O]} = 5.3 \cdot 10^{-4}$$

The detector signal (A_{det}), which is the change in absorbance when water passes through the detector cell is given by the following equation

$$A_{det} = kC_{ca}(C_{samp} - C_{blank})$$

where k is a proportionality constant related to the equilibrium constant K, C_{ca} is the total concentration of cinnamaldehyde added to the eluent, C_{samp} is the water concentration of sample, and C_{blank} is the water concentration in the eluent itself. As predicted by this equation, the detector signal has been shown experimentally to be a linear function of the total aldehyde and of the concentration of water present.

Typically, a sharp water peak is obtained in approximately 2 min. The water peak is always well separated from an earlier injection peak that is due to the sample matrix. Under favorable conditions a very short column (length 2.5 cm) can be used and a water peak obtained in as little as 20 s [32].

Samples that can react with methanol pose a special problem for water determination. For example, how can small amounts of water in acetone be determined when acetone can react with methanol to produce a much larger quantity of water?

$$CH_3COCH_3 + 2CH_3OH \overset{H^+}{\rightleftarrows} CH_3C(OCH_3)_2CH_3 + H_2O$$

The key to this problem is that the above reaction will not take place unless H^+ is present to catalyze the reaction. By using a cation-exchange column in the Li^+ form, water in the acetone can be separated chromatographically from the acetone. A H^+-form column placed in series then catalyzes the cinnamaldehyde–acetal equilibrium shift that is necessary for detection of the water. Reaction of acetone with methanol to form water is also catalyzed in this second column, but separation of the acetone and initial water has already taken place in the first column.

The detection limit of water is limited in part by the amount of water in the

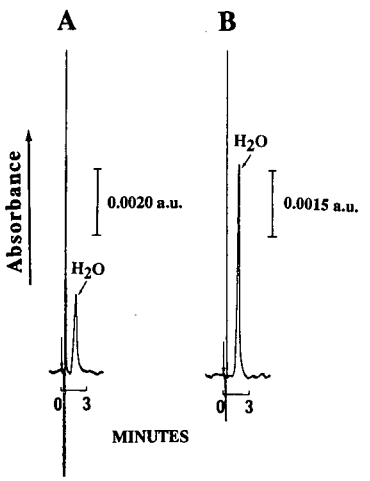

Fig. 1. Determination of water by ion-exclusion chromatography. For conditions, see text. (A) 26 ppm H_2O in anhydrous decahydronaphthalene; (B) 46 ppm H_2O in anhydrous acetonitrile.

methanol eluent. It is impossible to remove all of the water from methanol by conventional methods such as addition of molecular sieves or distillation after adding a reagent such as calcium hydride. We have recently found that addition of an *ortho* ester (plus an acid catalyst) to methanol will reduce the water content to an extremely low level [33]. Fig. 1 shows chromatograms for determination of only 26 ppm and 46 ppm of water, respectively in "anhydrous" samples of two organic liquids. These were run with a methanol eluent that had been dried by addition of trimethylorthoformate.

4. ACKNOWLEDGEMENTS

Ames Laboratory is operated for the U.S. Department of Energy under Contract W-7405-Eng-82. This work was supported by the Director of Energy Research, Office of Basic Energy Sciences.

The author wishes to thank P. R. Haddad and D. T. Gjerde for generously supplying many of the references used in preparing this manuscript.

REFERENCES

1 D. T. Gjerde and H. Mehra, in P. Jandik and R. M. Cassidy (Editors), *Advances in Ion Chromatography*, Vol. 1, Century International, Medfield, MA, 1989, p. 139.
2 P. R. Haddad and P. E. Jackson, *Ion Chromatography — Principles and Applications*, Elsevier, Amsterdam, 1991, p. 195.
3 G. A. Harlow and D. H. Morman, *Anal. Chem.*, 36 (1964) 2438.
4 K. Tanaka, T. Ishizuka and H. Sunahara, *J. Chromatogr.*, 177 (1979) 227.
5 D. T. Gjerde and J. S. Fritz, *Ion Chromatography*, Hüthig Verlag, Heidelberg, 2nd ed., 1987, p. 243.
6 K. Tanaka and J. S. Fritz, *J. Chromatogr.*, 361 (1986) 151.
7 K. Tanaka and J. S. Fritz, *Anal. Chem.*, 59 (1987) 708.
8 T. Murayama, T. Kubota, Y. Hanaoka, S. Rokushika, K. Kihara and H. Hatano, *J. Chromatogr.*, 435 (1988) 417.
9 T. Okada and P. K. Dasgupta, *Anal. Chem.*, 61 (1989) 548.
10 K. Tanaka, *Bunseki Kagaku*, 32 (1983) 439.
11 K. Tanaka and H. Sato, *Bunseki Kagaku*, 27 (1978) 95.
12 E. C. V. Butler, *J. Chromatogr.*, 450 (1988) 353.
13 K. Tanaka, *Bunseki Kagaku*, 31 (1982) T106.
14 K. Tanaka and Y. Ishihara, *Mizu Shori Gijutsu*, 23 (1982) 855.
15 H. J. Kim and Y. K. Kim, *Anal. Chem.*, 61 (1989) 1485.
16 D. T. Gjerde, in P. Jandik and R. M. Cassidy (Editors), *Advances in Ion Chromatography*, Vol. 1, Century International, Medfield, MA, 1989, p. 159.
17 D. T. Gjerde, in P. Jandik and R. M. Cassidy (Editors), *Advances in Ion Chromatography*, Vol. 1, Century International, Medfield, MA, 1989, p. 164.
18 H. J. Kim, *J. Assoc. Off. Anal. Chem.*, 72 (1989) 113, 266.
19 H. J. Kim and Y. K. Kim, *Food Technol.*, 41 (1987) 85.
20 W. R. Jones, A. L. Heckenberg and P. Jandik, *J. Chromatogr.*, 366 (1986) 225.
21 T. Okada and T. Kuwamoto, *Fresenius' Z. Anal. Chem.*, 325 (1986) 683.
22 J. P. Wilshire and W. A. Brown, *Anal. Chem.*, 54 (1982) 1647.
23 K. Tanaka and J. S. Fritz, *J. Chromatogr.*, 409 (1987) 271.
24 C. E. Cowie, P. R. Haddad and P. W. Alexander, *Chromatographia*, 21 (1986) 417.
25 T. Okada and T. Kuwamota, *Anal. Chem.*, 58 (1986) 1375.
26 *Application Note 25*, Dionex Corp., Sunnyvale, CA, Dec. 1984.
27 J. P. Ivey and P. R. Haddad, *J. Chromatogr.*, 391 (1987) 309.
28 J. E. McClure, *Anal. Lett.*, 21 (1988) 253.
29 T. S. Stevens, K. M. Chritz and H. Small, *Anal. Chem.*, 59 (1987) 1716.
30 N. E. Fortier and J. S. Fritz, *J. Chromatogr.*, 462 (1989) 323.
31 J. Chen and J. S. Fritz, *J. Chromatogr.*, 482 (1989) 279.
32 J. Chen and J. S. Fritz, in P. Jandik and R. M. Cassidy (Editors), *Advances in Ion Chromatography*, Century International, Medfield, MA, 1990, Vol. 2, p. 73.
33 J. Chen and J. S. Fritz, unpublished results, 1990.

Journal of Chromatography, 546 (1991) 119–124
Elsevier Science Publishers B.V., Amsterdam

CHROMSYMP. 2131

The use of pulsed amperometry combined with ion-exclusion chromatography for the simultaneous analysis of ascorbic acid and sulfite

HERBERT P. WAGNER* and MICHAEL J. McGARRITY
John Labatt Limited, Brewing Research Department, London, Ontario N6A 4M3 (Canada)

ABSTRACT

Initial attempts to monitor ascorbic acid and sulfite, in a beer matrix, by combining ion-exclusion chromatography with a pulsed amperometric detector using a single applied voltage to the platinum working electrode, were unsuccessful. Alternatively, good chromatograms for the separation of the two antioxidants were achieved utilizing a standard, amperometric cell. However, remarkably superior results were observed when this standard cell was operated in a pulsed mode and cleaning cycles were continually applied throughout the analysis. The working electrode stability and precision have been examined. Preliminary spike recovery data indicate acceptable accuracy for the method. Comparisons of this method to standard reference methods are currently ongoing.

INTRODUCTION

Several methods are available for detecting the presence of sulfite and ascorbic acid, two antioxidants commonly utilized by food and beverage industries [1–7]. Sulfiting agents, in particular, have received wide-spread attention, in recent years, as a result of their allergenic effect on those individuals who are hypersensitive.

To assay sulfite, the Monier–Williams reference method generally provides accurate results, in most matrices, above 10 mg SO_2/l [1,3]. However, the complexity, time requirements and susceptibility of the method to interferences stimulated the search for suitable alternative analytical methods. In addition, the simultaneous analysis of ascorbic acid has often been a parallel goal.

Amperometry is an extremely sensitive and selective detection method for analytes which are easily oxidized. In combination with ion-exclusion chromatography, this offers the potential of rapid, accurate assays for both ascorbic acid and sulfite [1,2,4–8]. However, normal amperometry is prone to errors resulting from the loss of detector sensitivity which occurs as the working electrode becomes contaminated. In order to minimize these errors, the calibration standards and sample solutions must be analysed sequentially [9]. Pulsed amperometry, which maintains the integrity of the working electrode, has successfully been employed as a means of overcoming these difficulties. Applications include the analysis of carbohydrates using a gold electrode

0021-9673/91/$03.50

[10,11] and the determination of alcohols, glycols, acetaldehyde and formic acid using a platinum electrode [10].

Satisfactory chromatograms for the separation of the two antioxidants in beer matrices were achieved utilizing a standard amperometric cell in combination with ion-exclusion chromatography. However, remarkably superior results were observed when this cell was operated in a pulsed mode and cleaning cycles were continually applied throughout the analysis.

The working electrode stability and precision have been examined. Preliminary standard addition recovery data indicate the method to be accurate. Comparisons of this method to standard reference methods are currently ongoing.

EXPERIMENTAL

Apparatus

A Dionex Model 4000i ion chromatograph, a pulsed amperometric detection (PAD) system and a PAD cell with platinum working electrode and a standard amperometric cell with platinum working electrode *vs.* Ag/AgCl reference electrode, autosampler, HPICE-AS1 column and Spectra-Physics Model 4270 integrator for data handling were employed throughout this study.

Ion-exclusion chromatography

The eluent, 10 m*M* H_2SO_4, prepared with deionized water, was prefiltered using a 0.45-μm membrane. The flow-rate was 1.0 ml/min. The standard amperometric cell was connected to a pulsed detector set at a range of 300 nA full-scale. A measuring potential (E_1) of +0.70 V for 240 ms and cleaning potentials (E_2) of +1.25 V for 60 ms and (E_3) −0.10 V for 240 ms were applied to the platinum working electrode. A 50-μl injection loop was employed and an attenuation of 1024 for the integrator.

Reagents, standards and samples

All reagents were either AnalaR or certified ACS grade. Individual 1000 mg/l standard solutions of both L-ascorbic acid (BDH) and sulfite (Na_2SO_3, Fisher Scientific) were prepared fresh daily in a 20 m*M* phosphate (Na_2HPO_4, BDH)–10 m*M* D-mannitol (BDH) buffer (pH 9). The phosphate was required for the determination of total sulfite in beer samples, whereas, the mannitol was utilized to stabilize the sulfite [1,4,9]. A combined standard solution was prepared for calibration of the instrument by diluting 150 μl and 80 μl of the above standard solutions respectively to 10 ml with pH 9 buffer. The calibration standard was diluted 1:20 with pH 9 buffer immediately prior to injection.

Beer samples were degassed by filtration (Whatman No. 4) and diluted 1:20 with pH 9 buffer immediately prior to injection.

RESULTS AND DISCUSSION

Initial attempts to assay ascorbic acid and sulfite in a beer matrix by ion-exclusion chromatography using a pulsed amperometric detector with a single applied voltage were unsuccessful. The loss of detector sensitivity was extremely rapid and presumably was the result of excessive contamination of the relatively small

surface area of the platinum electrode used. A standard amperometric detector cell employs an electrode with a much larger surface area than that of the pulsed detector. Consequently, a fifty-fold increase in sensitivity has been reported for the use of the standard cell in certain instances [8].

Satisfactory results were obtained for the two antioxidants contained in pH 9 buffer when the standard amperometric cell was combined with ion-exclusion chromatography. However, under the same conditions using beer, the co-elution of beer components was observed with both ascorbic acid and sulfite. The addition of 4% acetonitrile to the eluent combined with a reduced flow-rate eliminated the co-elution difficulties. A typical chromatogram is illustrated in Fig. 1.

This method, incorporating a single applied potential, was anticipated to be subject to errors resulting from the loss of electrode sensitivity observed when using a single applied potential. The introduction of these errors was reported in a collaborative study of sulfites in foods [9] and was attributable to detector sensitivity changes over time when using normal amperometry. This decrease in director sensitivity could be as much as 40% over an 8-hour period [9]. As discussed previously, the sequential analysis of standards and samples would be required to compensate for this loss of detector sensitivity associated with normal single applied potential electrochemical analyses [9]. Pulsing the cell was, therefore, investigated as a means of maintaining the stability of the working electrode.

When the standard amperometric cell was operated in a pulsed mode and cleaning cycles were continually applied, some very interesting effects were observed. Using the standard buffer solution, a noticeable change in the chromatogram was observed, particularly with increased sensitivity being noted, especially at the column void volume response. The co-elution of ascorbic acid with the column void volume

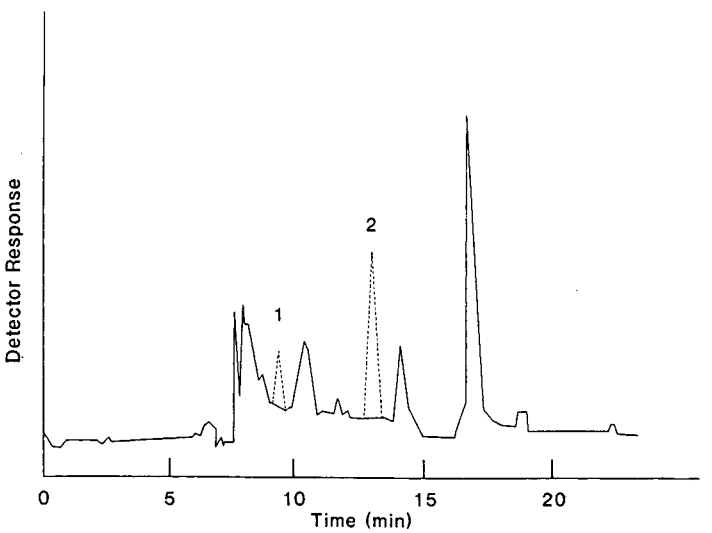

Fig. 1. Chromatogram obtained from a commercial beer (solid line), spiked with 15 mg/l ascorbic acid and sulfite (dotted line), diluted 1:10 with pH 9 buffer. Column, HPICE-AS1. Eluent 4% acetonitrile–10 m*M* H_2SO_4, Flow-rate 0.8 ml/min. PAD with standard amperometric cell and fixed potential of +0.70 V. Attenuation × 1024, range 1000 nA. Peaks: 1 = ascorbic acid; 2 = sulfite.

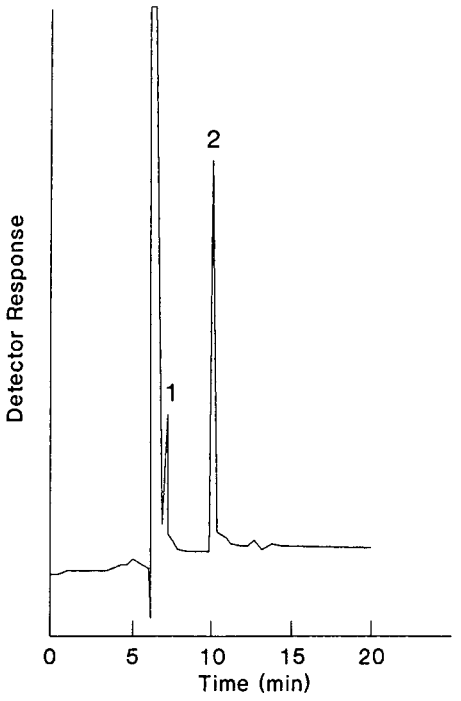

Fig. 2. Chromatogram obtained from 15 mg/l ascorbic acid and 8 mg/l sulfite, diluted 1:20 with pH 9 buffer. For conditions, see text. Attenuation × 1024, range 300 nA. Peaks: 1 = ascorbic acid; 2 = sulfite.

was, in this instance, overcome by eliminating the acetonitrile and marginally increasing the flow-rate. As indicated in Fig. 2, excellent separation of the two antioxidants in pH 9 buffer, was achieved.

To confirm the individual analytes identification, similar additions of 8 mg/l ascorbic acid and 2 mg/l sulfite were made to both the pH 9 buffer and a commercial beer. The spiked beers, when compared to the control beers (no addition) showed recoveries of 99–118% and 95–105% respectively, based on results for the same additions to pH 9 buffer. These recoveries indicated the method to be free of interferences.

A commercial beer, which is known to have added ascorbic acid, and to also contain approximately 2–3 mg/l sulfite (residual from fermentation), was similarly analysed. A typical chromatogram is illustrated in Fig. 3.

The precision of this method was anticipated to be highly dependant on the electrode stability. The susceptibility of sulfite to oxidation was also expected to have a significant effect on the precision of the method. Therefore, in this instance, the combined random and systematic errors were used to establish the precision of the method. Ten samples of the production beer, known to contain both analytes, were analysed consecutively. Individual bottles, from a single purchased lot, were analysed rather than a single bottle repeated ten times. Immediately prior to injection the samples were degassed by filtration and diluted with pH 9 buffer. The samples were

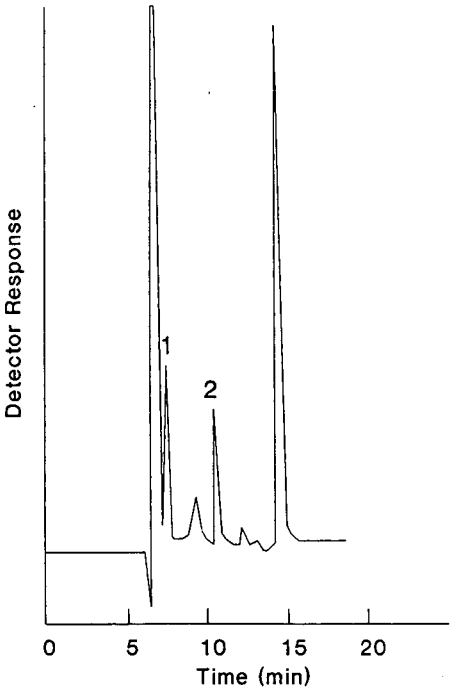

Fig. 3. Chromatogram obtained from a commercial beer known to contain ascorbic acid and sulfite, diluted 1:20 with pH 9 buffer. For conditions, see text. Attenuation × 1024, range 300 nA. Peaks: 1 = ascorbic acid (20.5 mg/l); 2 = sulfite (2.8 mg/l).

TABLE I

DETERMINATION OF METHOD PRECISION

Sample	Ascorbic acid (mg/l)	Sulfite (mg/l)
1	18.93	2.97
2	20.04	3.14
3	19.65	3.10
4	20.23	3.17
5	18.79	2.58
6	18.94	2.66
7	19.29	2.64
8	18.53	2.35
9	19.68	2.55
10	20.23	2.68
Range	18.53–20.23	2.35–3.17
Mean	19.43	2.78
Standard deviation	0.6229	0.2871
R.S.D. (%)	3.2	10.3

injected at exactly 20-min intervals. As illustrated in Table I, relative standard deviations (R.S.D.) of 3.2% for ascorbic acid and 10.3% for sulfite were achieved. Further studies of the accuracy of the method, by comparison to standard reference methods, are currently in progress.

CONCLUSIONS

A novel method for the simultaneous analysis of ascorbic acid and sulfite in beer has been developed and this method can have wide application. The electrode stability and hence the method precision appear acceptable. Excellent recoveries of ascorbic acid and sulfite added to beer were obtained, indicating the method to be free of interferences.

ACKNOWLEDGEMENTS

The authors are grateful to the management of John Labatt Ltd. for their support and permission to publish this paper. The support and guidance of Mr. Mike Callahan and Dionex Canada is also gratefully acknowledged.

REFERENCES

1 T. Wisk, T. Fazio, B. Bubnis, B. Frost, S. Zeller and V. Chu, *Brewers Digest*, 63 (1988) 14–27.
2 M. Moll, N. Moll and J. P. Joly, *J. Am. Soc. Brew. Chem.*, 48 (1990) 51–57.
3 S. L. Taylor, N. A. Highley and R. K. Bush, in C. O. Chichester, E. M. Mark and B. S. Schweigert (Editors), *Sulfites in Foods: Uses, Analytical Methods, Residues, Fate, Exposure Assessment, Metabolism, Toxicity and Hypersensitivity (Advances in Food Research, Vol. 30)*, Harcourt, Brace, Jovanovich, Academic Press, New York, 1986, pp. 1–76.
4 H.-J. Kim and Y.-K. Kim, *J. Food Sci.*, 51 (1986) 1360–1361.
5 H.-J. Kim and Y.-K. Kim, *J. Food Sci.*, 53 (1988) 1525–1527.
6 H.-J. Kim, *J. Assoc. Off. Anal. Chem.*, 72 (1989) 681–686.
7 H.-J. Kim and Y.-K. Kim, *U.S. Pat.*, 4 780 417 (1988).
8 *Dionex Application Note No. 034004 —Determination of Sulfite*, Dionex Corporation, Sunnyvale, CA, 1987.
9 H.-J. Kim, *J. Assoc. Off. Anal. Chem.*, 73 (2) (1990) 216–222.
10 *Dionex Technical Note No. 032284-03 —Determination of Electroactive Species by Ion Chromatography*, Dionex Corporation, Sunnyvale, CA, 1987.
11 R. D. Rocklin and C. A. Pohl, *J. Liq. Chromatogr.*, 6(9) (1983) 1577–1590.

Journal of Chromatography, 546 (1991) 125–137
Elsevier Science Publishers B.V., Amsterdam

CHROMSYMP. 2349

Comparison of gradient elution separations for organic and inorganic anions with chemically suppressed conductometric detection

SAM HARVEY

Houston Lighting and Power Company, South Texas Project, Electric Generating Station, Technical Services Department, P.O. Box 289, Wadsworth, TX 77483 (U.S.A.)

ABSTRACT

Gradient elution separations were developed for four pellicular and two macroporous resin based columns for the analysis of high-purity water. These elution techniques are applicable to both concentrator and loop injections and used sodium hydroxide and sodium tetraborate eluents with suppressed conductivity detection. The analytes of interest are fluoride, acetate, formate, pyruvate, chloride, nitrite, nitrate, bromide, sulfate and oxalate. These comparisons allow for the proper selection of column and eluent for part-per-billion (10^9) and sub-part-per-billion analysis of high purity water.

INTRODUCTION

As with all industry, managing escalating costs is of major concern. This is true as well for the power industry and especially true with nuclear power due to the size of the investment. With construction costs continuing to rise and increased regulatory requirements, power plants (fossil or nuclear fueled) now run into the billions (10^9) of U.S. dollars to construct. Because of these rising costs, emphasis is now being placed on increasing the life span of power plants through maintaining plant equipment integrity and material condition.

There are currently two major types of commercial nuclear reactors in the U.S.A.; boiling water reactors and pressurized water reactors. The boiling water reactor simply boils water in the reactor core to form steam to drive the turbine and electrical generator. As a result of this, non-volatile cationic and anionic impurities are concentrated in the reactor core and the recirculation piping causing stress corrosion and cracking. This is highly undesirable and must be minimized, due to the corrosive effect of these impurities.

The pressurized water reactor is different in that there are two separate systems or "loops" of water. The primary loop is pressurized to approximately 2250 p.s.i. which results in the heating of the reactor cooling water to 565°F without boiling. The secondary loop (low pressure) is where the steam is produced to drive the turbine and electrical generator. The interface between the primary and secondary loops is the

0021-9673/91/$03.50

steam generator. The secondary loop does not normally contain any radioactivity unless there is a material failure of the boundary. The steam generator functions solely as a heat exchanger through which the primary loop provides heat to the secondary loop to create steam and hence the term "steam generator".

Due to the function of the steam generator, an environment is created which promotes the concentration of impurities and the buildup of sludge, both of which have detrimental effects on system components and piping. These impurities initiate stress corrosion cracking and the buildup of sludge causing a loss of heat transfer efficiency and eventually causes a loss in generation capability.

If the sludge is not removed, the steam generators may degrade to the point where they need to be replaced at a cost of hundreds of millions of U.S. dollars, not to mention the costs associated with the loss of revenue due to the downtime required to replace the steam generators. This can be prevented by maintaining impurity levels as low as possible and by taking an active role in identifying the sources of impurities. Ion chromatography has become increasingly important by allowing for the detection and measurement of extremely low levels of impurities and determination of the type of impurity in the high purity water used by the power industry.

It was rapidly recognized in the initial developing stages of high-performance liquid chromatography (HPLC), that like gas chromatography, it was a powerful technique for the separation and determination of organic analytes. During this period few chromatographic studies were devoted to inorganic separations, and other methods (electrode, spectroscopic) remained the major choice when solving inorganic analytical problems. This changed in 1975 when Small *et al.* [1] published their classic paper on high-performance ion-exchange separation with post column suppression, generally referred to as modern day ion chromatography (IC). This technique allowed the separation and determination of common inorganic anions and cations at ppm levels under isocratic conditions.

Additional developments in IC have continued into other applications where IC plays a role, concurrently increasing sensitivity of analysis through the use of "stripping" (concentrator) columns. As this separation technology progressed through the use of new eluents and more efficient columns, it was recognized that other species were eluting and co-eluting with the primary species of interest. To determine what these species were another instrument had to be set up under different conditions to resolve the problem. An example of this in the power industry is the presence of organic anions (most notably acetate and formate) which caused elution problems with fluoride and chloride in the standard carbonate–bicarbonate eluent conditions often used with chemically suppressed conductometric detection.

A means of resolving these coelution problems presented itself in 1986 when the Dionex Corporation introduced a new pump to fill the perceived need for gradient IC. Gradient elution begins with an eluent of low ionic displacement capabilities and progresses either gradually or in a series of steps to an eluent of greater ionic displacement capabilities to cope with species of widely varying affinities (capacity factors, k') for the stationary phase. In these cases, eluent conditions that favor the resolution of the most weakly retained species are often unsuitable for the more strongly held ions in that they lead to frustratingly long elution times and poor efficiencies. The reverse is also true in that using a stronger eluent, while it may elute the strongly held ions in a reasonable time, typically compromises the resolution of

early eluting ions. In these cases gradient elution is the means for solving the problem.

Suppressed conductometric methods, since they reduce the background conductance of the eluent, are readily adapted to the use of gradient eluent methodology. With the advent of new high-capacity membrane suppression devices, gradient elution can be achieved in anion analyses. In this regard, sodium hydroxide as an eluent is becoming increasingly important in gradient analysis. From the suppression standpoint sodium hydroxide is the ideal eluent since its product is water, but its low ion-exchange affinity has limited its usefulness in the past [2].

While gradient elution is an effective way of handling ions of diverse affinities, it is not without its problems. The most noteworthy of these is the buildup of eluent impurities in the separator column and later release as the eluent concentration is increased. This problem has been examined by Rocklin *et al.* and measures have been suggested to alleviate it [3], such as the use of trap columns. It is therefore apparent that eluent preparation technique plays a vital role in gradient elution methodology. However, the purer the reagent the less this becomes a problem.

There has been some work in gradient IC that is useful for the power industry [4,5]. However, most of this work is based on a continuous gradient profile. Due to the continuously changing baseline, problems may be encountered with the reproducibility and resolution in the low ppb range that is normally required by the power industry. The work presented in this study focuses on the use of a single step gradient profile to minimize baseline changes thereby increasing reliability and reproducibility. This is also done so that laboratories without gradient eluent pumps may also benefit by the usefulness of gradient analysis and apply it without having to purchase additional equipment.

This study will concentrate on the determination of organic and inorganic anions in a single chromatographic run, utilizing pellicular and macroporous resin based columns in conjunction with hydroxide and tetraborate eluents, using suppressed conductivity detection. The methods presented here are applicable to loop injections in the ppm range also.

EXPERIMENTAL

Instrumentation

All chromatography in this study was performed using a Dionex (Sunnyvale, CA, U.S.A.) series 2020i ion chromatograph, except that a gradient pump was substituted for the analytical pump. The dual-channel ion chromatograph was interfaced with a multichannel data-and-control system consisting of a Autoion 450 Dionex computer interface, Dell (Austin, TX, U.S.A.) System 200 desk-top computer with a 40-megabyte hard drive, a 5.25-in. floppy drive, and a Epson FX850 printer (Seiko Epson, Japan). Sample delivery was accomplished with a Dionex ASM autosampler in all instances but two. In these two cases, a Dionex DQP pump was used due to the normal higher backpressure expected when using the AS5A and Omnipac PAX 500 column sets. Dionex AI450 software provided data acquisition, data reduction and control of the ion chromatograph. A diagram of the system is shown in Fig. 1.

Reagents and standard solutions

Gradient IC is still in its infancy. Consequently, eluent purity, analogous to

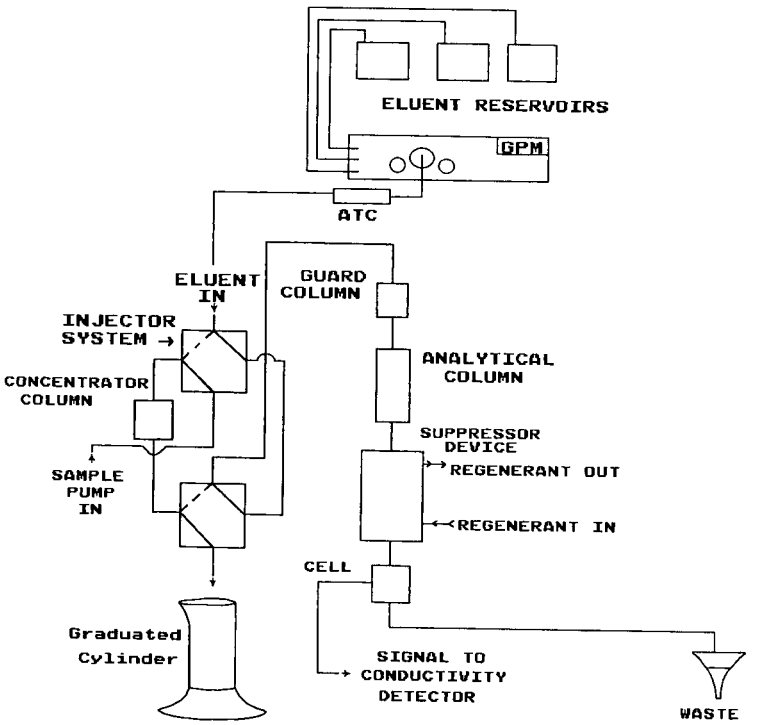

Fig. 1. Schematic of chromatographic system. ATC = Anion trap column.

HPLC-grade solvents, is an issue of vital importance. Reagent-grade chemicals were used throughout this study with the exception of the sodium hydroxide used for an eluent. Suprapure sodium hydroxide available from VWR (Houston, TX, U.S.A.) was used in hydroxide eluent preparation due to the minimal contaminant content. The water used was plant-prepared demineralized water passed through a Barnsted Nanopure (Barnsted/Thermolyne, Dubuque, IA, U.S.A.) water system to ensure 18-MΩ quality. Due to the rapid deterioration of the organic anion standards below 10 ppm, they were prepared from stock standards as needed. The stock 1000-ppm standards were kept refrigerated when not in use. The sodium hydroxide eluent concentrate was prepared by dissolving 4.00 grams in 600 ml of high-purity water, diluted to 1000 ml to yield a 0.1 *M* solution and degassed to minimize carbonate and sealed under a nitrogen overpressure blanket to prevent carbonate uptake. The sodium tetraborate eluent was prepared in the same fashion with 38.1 g of sodium borate decahydrate to yield a 0.1 *M* solution. Heat had to be applied to affect dissolution of the tetraborate.

Table I lists the standards and amount of reagent needed to make a 1 l of 1000-ppm stock standard [6] of each anion. The salts were dried at 105°C for 4 h prior to use with the exception of the organic anions which would break down under these conditions. Standard solutions were stored in dedicated and precleaned Pyrex lab-

TABLE I

1000 ppm STANDARD SOLUTIONS

Standard	Reagent	Amount required (g)
Fluoride	Sodium fluoride	2.2100
Acetate	Sodium acetate	1.6585
Formate	Sodium formate	1.5111
Pyruvate	Sodium pyruvate	1.2614
Chloride	Sodium chloride	1.6484
Nitrite	Sodium nitrite	1.4998
Bromide	Sodium bromide	1.2877
Nitrate	Sodium nitrate	1.3707
Sulfate	Sodium sulfate	1.4791
Oxalate	Sodium oxalate	1.5227

ware to minimize anion leaching. The organic standards were refrigerated when not in use to prevent deterioration.

Columns

To reduce eluent impurities, an anion trap column (ATC as shown in Fig. 1) was placed on the outlet of the eluent pump going to the chromatographic module and before the injection valve. The trap column function is to "smear out" eluent impurities by preventing the impurities from building up on the analytical column and eluting as a peak as the gradient program is run. The analytical column sets used in this study were all manufactured by Dionex and are presented in Table II. Table III lists the general column characteristics of the columns used in this study.

Procedures

In the secondary loop of power plants, cation additives such as ammonia, morpholine and hydrazine are added to control pH and oxygen. These cationic additives are removed by passing a sample through a cation-exchange column to remove them prior to the analysis of anions. This effectively returns the samples to a "high-purity" condition. The results presented below focus on the analysis of anions in

TABLE II

COLUMN SETS

Concentrator	Guard	Analytical
AG4A	AG4A	AS4A
AG5	AG5	AS5
AG5A	AG5A	AS5A
AG9	AG9	AS9
PAX 100 Guard	PAX 100 Guard	PAX 100 Analytical
PAX 500 Guard	PAX 500 Guard	PAX 500 Analytical

TABLE III

COLUMN CHARACTERISTICS

Analytical column[a]	Substrate (μM)	Latex X-link (%)	Capacity (μequiv./column)	Hydrophobic nature
AS4A	15	0.5	20	Medium–low
AS5	15	1.0	20	Low
AS5A	5	4.0	35	Low
AS9	15	[a]	35	Medium–low
PAX 100[b]	8.5	4.0	40	Hydrophilic
PAX 500[c]	8.5	4.0	40	Hydrophilic

[a] Contains a multiple functionality cross-linking which is different than other columns. This column is acrylic based.
[b] Latex diameter 60 nm, surface area < 1 m^2/g.
[c] Latex diameter 60 nm, surface area 300 m^2/g.

high-purity water without the additives. All anions were detected with a full scale of 30 μS output range. Volumes of 10 ml of the mixed standard were concentrated in all cases. Standards were analyzed singly under the conditions listed in Table IV to insure optimum resolution and to determine the corresponding retention times. The standards were then run all together by performing three sequential injections at the 5-, 25- and 50-ppb levels and averaging the values at each level for the calibration. All calibration data revealed linearity (r^2) values of at least 0.99. The precision of the analytical methods presented were determined by performing 25 replicate analysis at the 25-ppb level containing the ten anions of interest. These replicate analyses were used for the determination of relative standard deviations (R.S.D.) and ensured accurate reproducibility.

RESULTS AND DISCUSSION

The separation and quantification of organic and inorganic anions was

TABLE IV

GENERAL CONDITIONS

Concentrator column	Analytical column	Eluent type	Eluent flow (ml/min)	Gradient profile
AG4A	AS4A	NaOH	2.0	3.5 mM/35 mM
AG4A	AS4A	Tetraborate	2.0	5.0 mM/30 mM
AG5	AS5	NaOH	1.5	2.0 mM/25 mM
AG5	AS5	Tetraborate	1.5	3.0 mM/25 mM
AG5A	AS5A	NaOH	1.5	3.0 mM/60 mM
AG9	AS9	Tetraborate	2.0	1.0 mM/30 mM
PAX 100	PAX 100	NaOH–methanol	1.0	5 mM NaOH–5% methanol
Guard	Analytical	NaOH–methanol	1.0	80 mM NaOH–10% methanol
PAX 500	PAX 500	NaOH–methanol	1.0	1 mM NaOH–2.5% methanol
Guard	Analytical	NaOH–methanol	1.0	60 mM NaOH–2.5% methanol

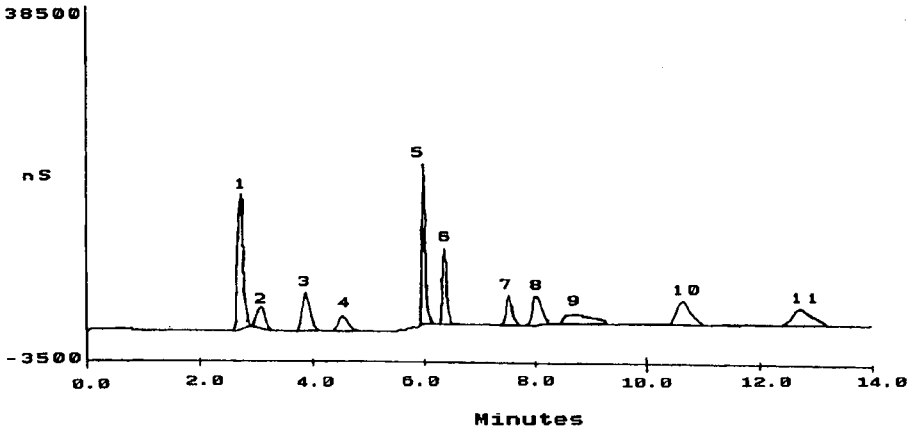

Fig. 2. AS4A separation using sodium hydroxide. Peaks: 1 = fluoride; 2 = acetate; 3 = formate; 4 = pyruvate; 5 = chloride; 6 = nitrite; 7 = bromide; 8 = nitrate; 9 = carbonate; 10 = sulfate; 11 = oxalate. Gradient program: 3.5 m*M* NaOH stepped to 35 m*M* NaOH 4 min after injection. Regenerant: 20 m*M* sulfuric acid at 5.0 ml/min.

achieved successfully on all the analytical columns with the exception of the AS9 column. The acetate peak coeluted with the fluoride peak and the formate and pyruvate peaks coeluted. This may be attributed to the fact that the AS9 column is the only acrylic based column tested and was designed to perform U.S. Environmental Protection Agency drinking water analyses. Example chromatograms are presented in Figs. 2–9 for each method developed.

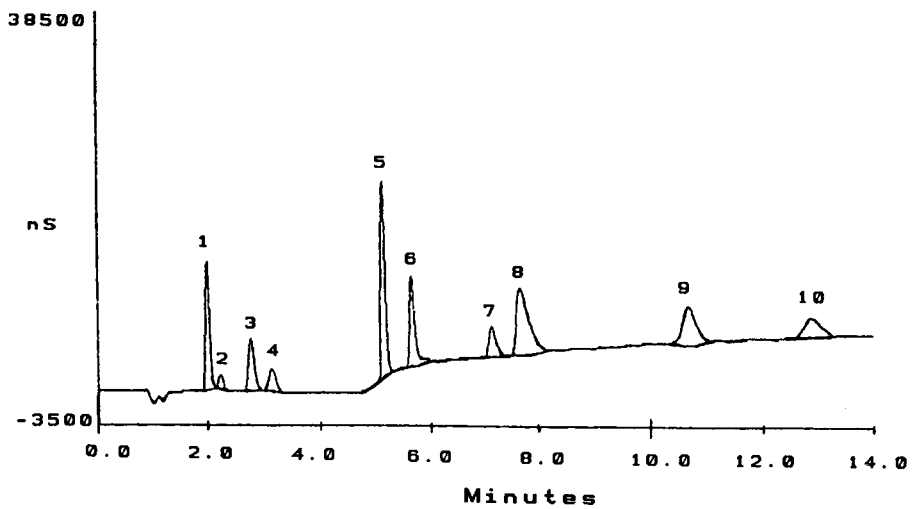

Fig. 3. AS4A separation using sodium tetraborate. Peaks: 1 = fluoride; 2 = acetate; 3 = formate; 4 = pyruvate; 5 = chloride; 6 = nitrite; 7 = bromide; 8 = nitrate; 9 = sulfate; 10 = oxalate. Gradient program: 5.0 m*M* tetraborate stepped to 30 m*M* tetraborate 4 min after injection. Regenerant: 20 m*M* sulfuric acid at 10.0 ml/min.

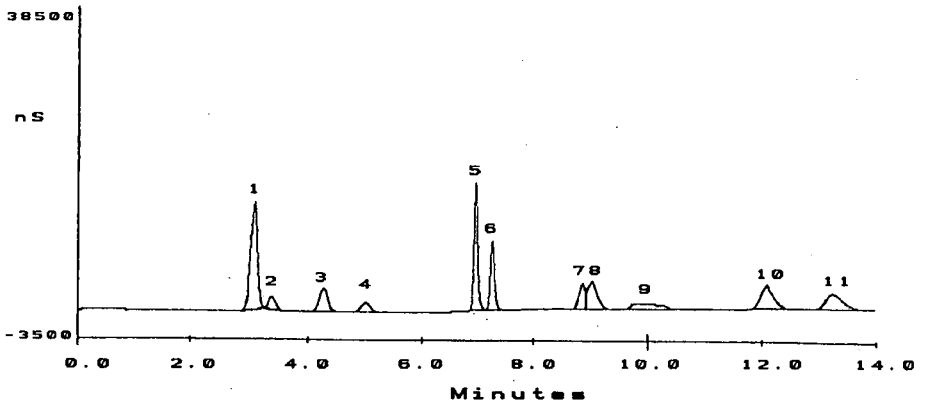

Fig. 4. AS5 separation using sodium hydroxide. Peaks as in Fig. 2. Gradient program: 2.0 m*M* NaOH stepped to 25 m*M* NaOH 4 min after injection. Regenerant: 20 m*M* sulfuric acid at 5.0 ml/min.

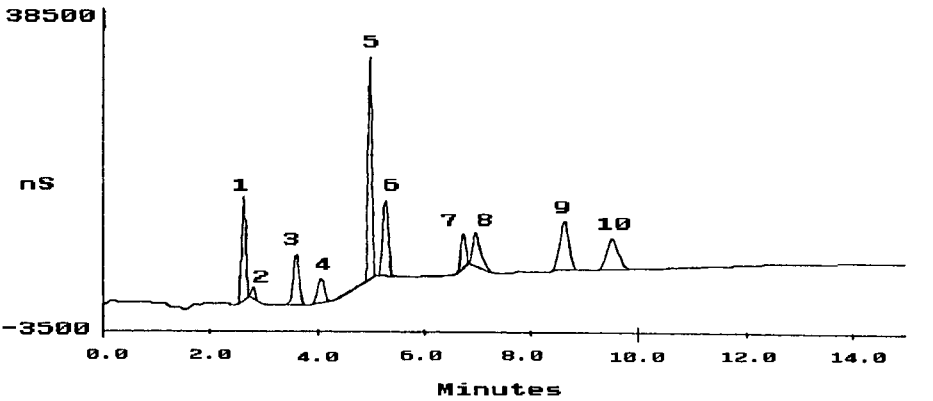

Fig. 5. AS5 separation using sodium tetraborate. Peaks as in Fig. 3. Gradient program: 3.0 m*M* tetraborate stepped to 25 m*M* tetraborate 3 min after injection. Regenerant: 20 m*M* sulfuric acid at 10.0 ml/min.

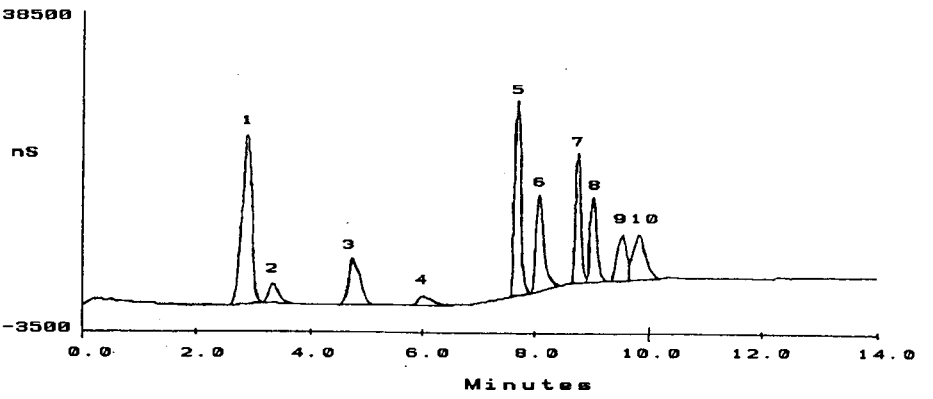

Fig. 6. AS5A separation using sodium hydroxide. Peaks: 1 = fluoride; 2 = acetate; 3 = formate; 4 = pyruvate; 5 = chloride; 6 = nitrite; 7 = sulfate; 8 = oxalate; 9 = bromide; 10 = nitrate. Gradient program: 3.0 m*M* NaOH stepped to 60 m*M* NaOH 5 min after injection. Regenerant: 20 m*M* sulfuric acid at 5.0 ml/min.

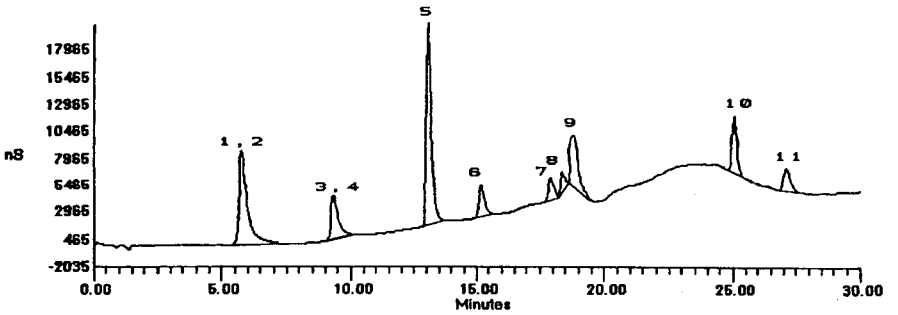

Fig. 7. AS9 separation using sodium tetraborate. Peaks: 1 = fluoride; 2 = acetate; 3 = formate; 4 = pyruvate; 5 = chloride; 6 = nitrite; 7 = bromide; 8 = unknown; 9 = nitrate; 10 = sulfate; 11 = oxalate. Gradient program: 1.0 m*M* tetraborate ramping to 30 m*M* tetraborate starting 5 min after injection and finishing 25 min after injection. Regenerant: 20 m*M* sulfuric acid at 10.0 ml/min.

To assist in column and method evaluation the capacity factors of each organic and inorganic anion were calculated using the equation [7]: $k' = (t_R - t_0)/t_0$, where t_R is the retention time and t_0 the retention of an unretained compound and are presented in Table V.

To further assist in column evaluation the theoretical plates (efficiency) were calculated for each anion using the equation [7]: $N = 16(t_R/w)^2$, where w is the peak width. The values obtained are presented in Table VI.

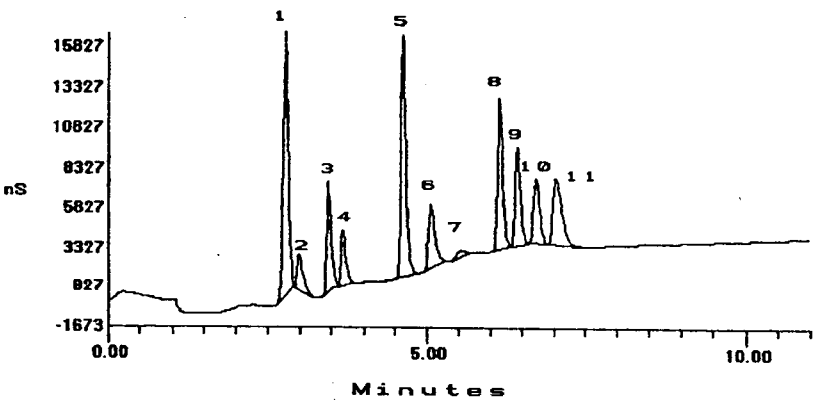

Fig. 8. Omnipac PAX 100 separation using sodium hydroxide. Peaks: 1 = fluoride; 2 = acetate; 3 = formate; 4 = pyruvate; 5 = chloride; 6 = nitrite; 7 = carbonate; 8 = sulfate; 9 = bromide; 10 = nitrate; 11 = oxalate. Gradient program: eluent 1: 100 m*M* NaOH; eluent 2: methanol–water (50:50); eluent 3: deionized water. Regenerant: 20 m*M* sulfuric acid at 5.0 ml/min.

Time (min)	Eluent 1 (%)	Eluent 2 (%)	Eluent 3 (%)	Comments
0.0	5.0	10.0	85.0	Equilibrate and load
4.0	5.0	10.0	85.0	Start gradient ramp
6.0	40.0	10.0	50.0	Inject sample
6.1	80.0	20.0	0.0	Step gradient
17.0	80.0	20.0	0.0	End run

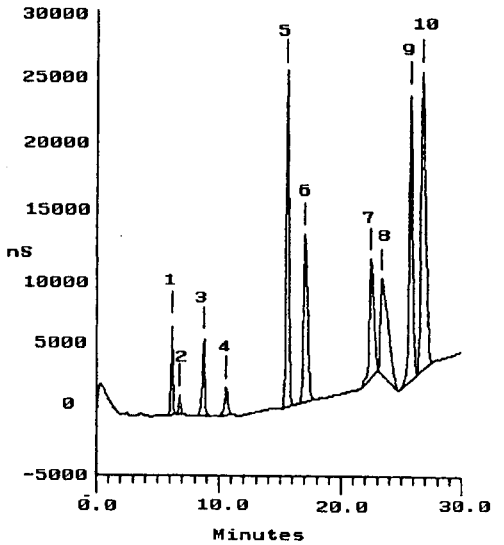

Fig. 9. Omnipac PAX 500 separation using sodium hydroxide. Peaks: 1 = fluoride; 2 = acetate; 3 = formate; 4 = pyruvate; 5 = chloride; 6 = nitrite; 7 = bromide; 8 = nitrate; 9 = sulfate; 10 = oxalate. Gradient program: eluent 1: 2 m*M* NaOH; eluent 2: methanol–water (50:50); eluent 3: 200 m*M* NaOH. Regenerant: 40 m*M* sulfuric acid at 5 ml/min.

Time	Eluent 1 (%)	Eluent 2 (%)	Eluent 3 (%)	Comments
0.0	95.0	5.0	0.0	Equilibrate and load
5.0	95.0	5.0	0.0	Inject
10.0	95.0	5.0	0.0	Start gradient ramp 1
22.0	80.0	5.0	15.0	Start gradient ramp 2
35.0	55.0	5.0	40.0	End run

As can be seen from Tables V and VI the most effective column for use in the power industry is the PAX 100 with the NaOH and methanol eluent due to its efficiency and the rapidity of the separations. Concerning the use of the Omnipac PAX 100, it was found to function better if it was only re-equilibrated for 4 min while the next sample was loading.

Using Figs. 2, 4, 6, 8 and 9 as guidelines, it can be seen that there is very little baseline disturbance. This fact is due to the use of NaOH as an eluent with the use of an anion trap column (ATC). During this study, a single ATC was used for the NaOH separations without having to be regenerated, and the baseline conductivities ranged from 1–3 μS. A new ATC was used for the tetraborate separations and had to be regenerated every 40–50 samples, with the baseline conductivities running 6–10 μS.

One other point that should be noted is the use of an autosampler. A Dionex ASM was used in all cases with the exception of the AS5A and PAX 500 column sets. The backpressure from these columns would not allow for the use of the autosampler. A new autosampler needs to be designed to allow for higher backpressures. The Dionex ASM autosampler is satisfactory if only 5 ml are being concentrated, but is unacceptably slow (1 ml/min). This makes for long analysis times, where it takes almost as long to concentrate 10 ml of sample as it takes for the analysis.

TABLE V

CAPACITY FACTORS (k')

Column/eluent	Fluoride	Acetate	Formate	Pyruvate	Chloride	Nitrite	Bromide	Nitrate	Sulfate	Oxalate
AS4A/NaOH	2.47	2.89	3.95	4.79	6.68	7.16	8.68	9.26	12.58	15.32
AS4A/tetraborate	0.81	1.52	2.14	2.57	4.95	5.57	9.24	9.90	11.33	13.90
AS5/NaOH	2.17	2.52	3.43	4.18	6.13	6.42	8.04	8.33	11.46	12.67
AS5/tetraborate	1.22	1.33	2.04	2.41	3.15	3.41	4.26	4.85	5.48	6.96
AS5A/NaOH	2.40	2.95	4.50	5.15	8.20	8.65	10.4	10.75	9.35	9.65
AS9/tetraborate	3.06	3.06	5.56	5.56	8.19	10.19	11.44	12.13	16.44	17.88
PAX 100/NaOH–methanol	1.52	1.75	2.13	2.35	3.23	3.62	4.85	5.12	4.60	5.42
PAX 500/NaOH–methanol	0.71	0.97	2.43	4.64	5.17	5.83	8.03	8.46	9.33	9.79

TABLE VI

THEORETICAL PLATES

Column/eluent	Fluoride	Acetate	Formate	Pyruvate	Chloride	Nitrite	Bromide	Nitrate	Sulfate	Oxalate	Mean
AS4A/NaOH	4600	1450	2300	2000	21 300	24 300	15 000	9600	10 800	6000	9750
AS4A/tetraborate	2300	2900	1900	2600	15 900	8500	7600	3900	5400	8100	5900
AS5/NaOH	2600	7100	4800	3700	28 200	31 000	11 400	11 900	13 600	11 400	12 500
AS5/tetraborate	3600	4100	3000	3800	13 000	6400	9000	6400	9600	7500	6650
AS5A/NaOH	1200	1600	3000	2900	15 400	9600	8500	8900	20 000	21 100	9200
AS9/tetraborate	N/A[a]	N/A	N/A	N/A	22 600	22 900	N/A	N/A	91 900	56 400	N/A
PAX 100/NaOH–methanol	6100	5300	8100	11 600	14 600	9800	28 200	17 300	32 600	11 100	14 500
PAX 500/NaOH–methanol	11 300	9700	9500	10 700	20 600	12 300	19 100	6800	47 600	21 900	16 950

[a] N/A = Not applicable.

TABLE VII

RELATIVE STANDARD DEVIATION AT 25 ppb

Column/eluent	R.S.D. (%)									
	Fluoride	Acetate	Formate	Pyruvate	Chloride	Nitrite	Bromide	Nitrate	Sulfate	Oxalate
AS4A/NaOH	3.2	3.9	2.2	4.8	1.9	2.1	3.3	3.4	4.6	5.4
AS4A/tetraborate	4.4	5.6	2.4	5.3	2.4	2.9	4.7	4.1	5.3	6.3
AS5/NaOH	2.2	3.1	2.4	5.1	1.8	2.5	4.8	5.1	4.3	4.9
AS5/tetraborate	4.1	4.3	2.3	3.9	1.9	2.8	4.3	5.1	4.6	5.4
AS5A/NaOH	3.1	3.8	2.9	6.4	3.4	3.6	6.6	6.9	5.3	5.8
AS9/tetraborate	N/A	N/A	N/A	N/A	4.6	3.8	7.9	8.4	4.2	4.6
PAX 100/NaOH–methanol	4.8	4.7	2.3	2.4	1.6	1.8	2.6	2.8	2.4	3.2
PAX 500/NaOH–methanol	3.4	4.1	2.4	2.5	1.8	2.1	3.8	4.1	2.5	3.1

The R.S.D. values for the methods developed are presented in Table VII. As listed in the table, better R.S.D. values were found for the NaOH eluents than with the tetraborate eluents. This is due to less baseline disturbance and lower eluent conductivities. This also plays a role in higher sensitivities. The less baseline disturbance and the lower the background conductivity, the higher the sensitivity will be for ions of interest. However, tetraborate eluent has been shown to be beneficial in reducing interferences for analysis of anions in matrices containing boric acid.

CONCLUSIONS

The need for gradient IC is obvious from the diversity of demands made on the power plant chromatographer. In particular, the ability to quickly screen a sample for organic and inorganic anions that cause performance losses can potentially save millions of dollars. Screening for a diverse range of ions in a single ion chromatographic run is a lofty goal. The methods presented here are also applicable to loop injections for the study of anions in the ppm range.

It is recommended that for analysis of organic and inorganic anions that the PAX 100 columns be used with the conditions listed with Fig. 9. It has also been seen that with the higher efficiency of the PAX 100 that lower limits of detection for on-line ion chromatographs may be achieved at the 5 part-per-trillion (10^{12}) level by concentrating only 30 ml of sample. For those chromatographers only interested in the separation of the common inorganic anions (F^-, Cl^-, SO_4^{2-}), the AS5 column with an 25 m*M* NaOH eluent will yield excellent results in only a four minute run. As a direct result of this study, the PAX 100 method developed has been adapted to the on-line ion chromatographs employed in monitoring the secondary loop at the South Texas Project.

The Omnipac PAX 500 column appears to have a lot of potential due to its ability to perform both anion-exchange and reversed-phase separations in a single injection. Future work with this column should prove very interesting. Other work also needs to be focused on an advanced design autosampler for use with large volumes (10–25 ml) of sample so that they may be concentrated at a faster rate (3–4 ml/min).

REFERENCES

1 H. Small, T. S. Stevens and W. C. Bauman, *Anal. Chem.*, 47 (1975) 1801–1809.
2 H. Small, *Ion Chromatography*, Plenum, New York, 1989, Ch. 7.
3 R. D. Rocklin, C. A. Pohl and J. A. Schibler, *J. Chromatogr.*, 411 (1987) 107–119.
4 *Application Note AN56: Determination of Trace Anions and Key Organic Acids in High Purity, Ammoniated, and Borated Waters Found in Steam Cycle Power Plants*, Dionex, Sunnyvale, CA, 1988.
5 *Technical Note TN19: Gradient Elution in Ion Chromatography —Anion Exchange with Conductivity Detection*, Dionex, Sunnyvale, CA, 1987.
6 R. E. Dickerson, H. B. Gray, M. Y. Darensbourg and D. J. Darensbourg, *Chemical Principals*, Benjamin/Cummings, Reading, MA, 4th ed., 1984, Ch. 5.
7 L. R. Snyder and J. J. Kirkland, *Introduction to Modern Liquid Chromatography*, Wiley, New York, 2nd ed., 1979, Ch. 2.

Journal of Chromatography, 546 (1991) 139–149
Elsevier Science Publishers B.V., Amsterdam

CHROMSYMP. 2227

Temperature programming in macrocycle-based ion chromatography

ROBERT G. SMITH, PHILLIP A. DRAKE and JOHN D. LAMB*
Department of Chemistry, Brigham Young University, Provo, UT 84602 (U.S.A.)

ABSTRACT

The well documented affinity of macrocyclic ligands for alkali and alkaline earth metal cations has been exploited in performing chromatographic separations of both cations and anions. It is shown that because the complexation reaction of metal ions with macrocycles is exothermic, the column capacity, and hence the retention of ions, is decreased as the column temperature is increased. While ion retention in classical ion exchange is also a function of temperature, the effect is less pronounced than in macrocycle-based systems. Temperature gradient elution of anions on macrocycle-based columns is performed based on the decrease of column capacity as the temperature is increased, showing improvements over separations performed under isothermal conditions.

INTRODUCTION

Since their discovery, macrocycles, such as crown ethers and cryptands, have been noted for their unique complexing abilities. This capability to selectively complex cations has led to their use in ion chromatography, as discussed in another paper by us at this symposium [1]. The selectivity of macrocycles for cations is mainly determined by the ability of the cation to fit into the central cavity of the macrocycle. Those cations that fit best into the cavity are often bound strongest, and can be separated from cations that are too small or too large to fit into the cavity.

Since most macrocycles are neutral molecules, the cations are complexed into the macrocycle in close association with an anion in order to maintain electrical neutrality. Since the macrocycle is generally hydrophobic in nature, the most hydrophobic anions allow greater interaction of the cation with the macrocycle in low dielectric media. Thus, not only cations with a common anion, but also anions with a common cation can be separated [2–6].

Gradient elution ion chromatography was generally considered incompatible with conductometric detection until recently. The changes in eluent composition or concentration resulted in significant baseline distortion, and impurities in eluents also resulted in baseline aberrations and spurious peaks. With improvements in column and suppressor technology, gradient separations of both anions and cations have become more feasible using salts of weak acids for anion separations and protonated cations of weak bases or amino acids as eluents for cation gradients [7,8]. Gradients in

0021-9673/91/$03.50

unsuppressed ion chromatography have been performed using a concentration gradient between two isoconductive eluents [9]. Anion gradients have also been performed by our group by altering the column capacity instead of the eluent ionic strength by using macrocyclic ligand–cation complexes as the exchange site. The column anion-exchange capacity is decreased during the course of the separation by switching from a mobile phase cation that is relatively strongly bound by the macrocycle to a cation with a lower affinity for the macrocycle, resulting in fewer macrocycle–cation complexes, and hence lower column anion exchange capacity [10,11].

While temperature gradient separation is a very common technique in gas chromatography, its use has been very limited in high-performance liquid chromatography (HPLC). It has been shown that increasing the column temperature causes the retention of some ions to increase, while decreasing the retention of others. Improved separations have been shown for specific analytes of interest by careful choice of operating temperature [12–15].

The dependence of cation retention on temperature with macrocycle-based systems was noted by Iwachido *et al.* [5], who described the changes in the retention of alkali metal cations between 15°C and 55°C. In our work the effect of temperature on the retention of both anions and cations on macrocycle-based stationary phases is more closely examined and compared to classical ion exchange. A novel gradient separation of anions is presented based on the decrease of column capacity with increasing temperature.

EXPERIMENTAL

Materials

Reagent grade cryptand *n*-decyl-2.2.2 (D-2.2.2), whose structure is shown in Fig. 1, was obtained from EM Science (Gibbstown, NJ, U.S.A.). All compounds used to make eluents and standards were reagent grade. Water used in making eluents was purified to 18 MΩ resistivity using a Milli-Q purification system (Millipore) and was degassed by sparging with helium.

Apparatus

A Dionex Series 4000i ion chromatograph was used in conjunction with Dionex anion micro membrane (AMMS) and cation micro membrane (CMMS) suppressors for eluent suppression prior to conductometric detection with a Dionex CDM-2 conductivity detector. The suppressant was 12.5 m*M* H_2SO_4 flowing at 3–5 ml/min for anion separations and 50 m*M* tetrabutylammonium hydroxide (TBAOH), flowing at

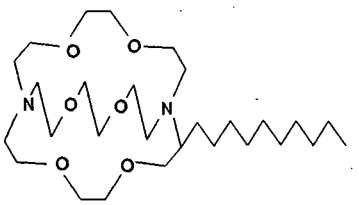

Fig. 1. Structure of cryptand *n*-decyl-2.2.2 (D-2.2.2).

3–5 ml/min for cation separations. Columns used were Dionex AG-4A and AS-4A anion separators, CG-3 and CS-3 cation separators, and NS-1 MPIC columns. Temperature was controlled either by coiling 1 m of tubing in a Dionex column heater just prior to the column or by placing the column and coiled tubing in a water jacket with a circulating water–ethylene glycol mixture from a constant temperature bath. The chromatograph was controlled and data captured with a personal computer using the Dionex AI400 software.

Column preparation

The macrocycle column was prepared as previously described by circulating a solution of the D-2.2.2 in a methanol–water (60:40) mixture through the MPIC column for 12 h [10].

RESULTS AND DISCUSSION

Macrocycle-based separation system

Macrocycles separate cations on the basis of a complexation–decomplexation reaction rather than an ion-exchange reaction. Thus separations with a pure water mobile phase are possible as no ionic species need to be added to the mobile phase in order to elute the cations from the column [2–6].

We have previously reported the use of macrocycles to separate anions through an ion-exchange mechanism rather than a ligand-exchange mechanism. This was accomplished by the addition to the mobile phase of the hydroxide of a cation that is known to bind to the macrocycle. The cation complexes with the macrocycle, forming an anion-exchange site on the stationary phase and anions are then eluted by the hydroxide eluent. The cation in the mobile phase has a large influence on the column capacity. With the cryptand D-2.2.2, lithium hydroxide eluent shows little retention of anions, while potassium hydroxide eluent of the same concentration shows a very high capacity. This effect of the mobile phase cation on column capacity has been exploited to perform gradient separations of anions by switching from a mobile phase cation that is strongly bound by the macrocycle to one that has a lower affinity for the macrocycle during the course of the separation [10,11].

Temperature effects

In ion chromatography of both cations and anions, the exchange reaction for an analyte ion, A, of charge y, and eluent ion, E, with charge x, can be written as:

$$yE^xR_x + xA^y \rightleftharpoons xA^yR_y + yE^x \quad (1)$$

where R_x and R_y represent the resin exchange sites occupied by E and A ions respectively. The exchange reaction can be either exothermic or endothermic, depending on the ions involved. The ion-exchange equilibrium can thus be shifted in either direction as the temperature is increased. This results in either a positive or negative change in the capacity factor, k', for the analyte ion.

The complexation of cations with macrocycles can be written as:

$$M^+ + L \rightleftharpoons ML^+ \quad (2)$$

where M^+ is the metal cation, L is the free macrocyclic ligand, and ML^+ is the cation–macrocycle complex. This is most often an exothermic reaction, favoring a lower amount of complexation as the temperature is increased. Thus the capacity factor for cations would be expected to decrease as the temperature is increased for this reason.

Our results illustrating the effect of temperature on retention for both cations and anions in classical ion-exchange and macrocycle-based systems are shown in Figs. 2–4. The retention of anions and cations, by both ion-exchange and ligand-exchange mechanisms, was measured as a function of temperature by placing the appropriate column in a jacket with circulating water controlled by a constant temperature bath around the column in order to control the temperature.

The cation exchange of alkali metal cations was measured using a Dionex CS-3 column with a 10 m*M* HCl eluent at 1.0 ml/min. The retention of alkali metal cations on the macrocycle-based column was measured using a Dionex MPIC NS-1 column, loaded with D-2.2.2 as described above, with a pure water eluent at 1.0 ml/min. Fig. 2a, plotting ln k' (capacity factor) *versus* $1/T$ (where T = temperature), shows that for the ion exchange of alkali metal cations the capacity factors of lithium and sodium increase slightly, while those of potassium, rubidium, and cesium decrease as the temperature is increased. These changes in retention are relatively small. On the other

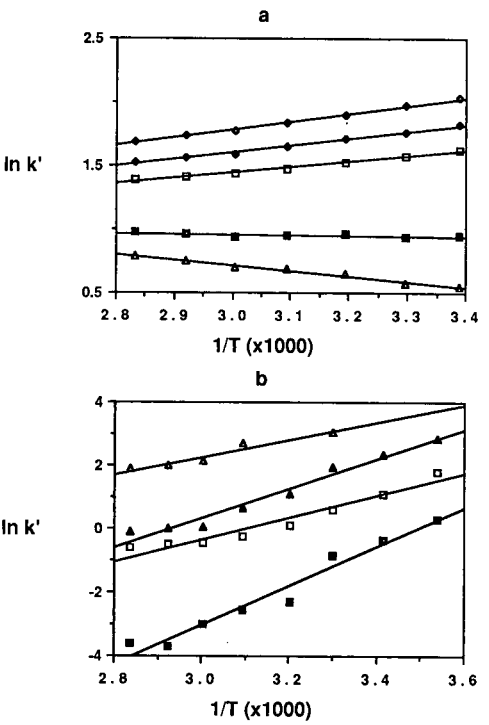

Fig. 2. (a) Variation in ln k' *versus* $1/T$ for alkali metal cations on ion-exchange column, Dionex CS-3 column, 10 m*M* HCl eluent. ◇ = Cs^+; ◆ = Rb^+; □ = K^+; ■ = Na^+; △ = Li^+. (b) Variation in ln k' *versus* $1/T$ for alkali metal cations on macrocycle-based column, pure water eluent. △ = K^+; ▲ = Rb^+; □ = Na^+; ■ = Li^+.

hand, for the macrocycle-based system (Fig. 2b), the capacity factors of all of the alkali metals decrease with increasing temperature. The magnitude of the change in retention with temperature is also much greater than that observed in ion exchange (Fig. 2a).

Similar experiments, using the same temperature controlling apparatus with the same columns, were performed to measure the retention of the alkaline earth cations. The experimental conditions were the same as those for the alkali metals, except that the eluent was 50 m*M* HCl–3.75 m*M* histidine–3.75 m*M* diaminoproprionic acid for the cation-exchange measurements. We observe that the behavior of the alkaline earth metal cations is similar to that of the alkali metals, with retention increasing for all of the cations in ion exchange (Fig. 3a), but decreasing in the macrocycle column (Fig. 3b).

The retention of anions on the ion-exchange and macrocycle columns is compared in Fig. 4a and b, respectively. The anion-exchange column was a Dionex AS-4A column and the eluent was 15 m*M* NaOH eluent flowing at 1.0 ml/min. The macrocycle-based separation was done using the MPIC column loaded with D-2.2.2 with a 20 m*M* NaOH eluent at 1.0 ml/min. Again the columns were placed in a water jacket, with the temperature controlled with a constant temperature bath. As with the cations, in classical ion exchange (Fig. 4a) the trend in capacity factors as a function of

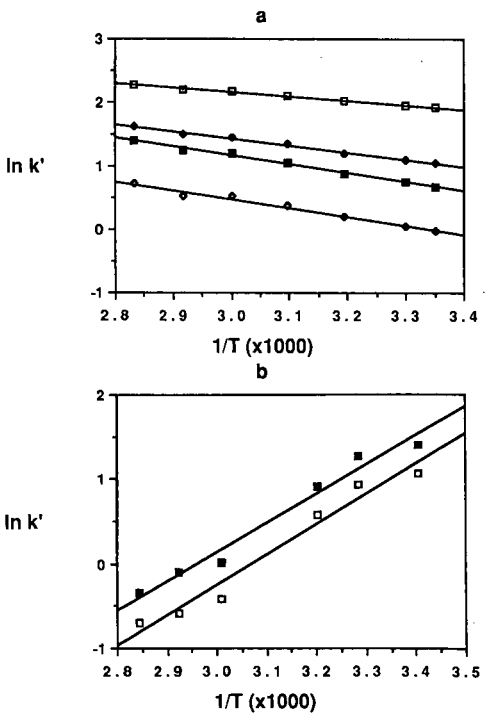

Fig. 3. (a) Variation in ln *k' versus* 1/*T* for alkaline earth cations on ion-exchange column, CS-3 column, 50 m*M* HCl–3.75 m*M* histidine–3.75 m*M* diaminopropionic acid eluent: □ = Ba^{2+}; ◆ = Sr^{2+}; ◘ = Ca^{2+}; ◇ = Mg^{2+}. (b) Variation in ln *k' versus* 1/*T* for alkaline earth cations on macrocycle-based column, pure water eluent: □ = Mg; ◘ = Ca.

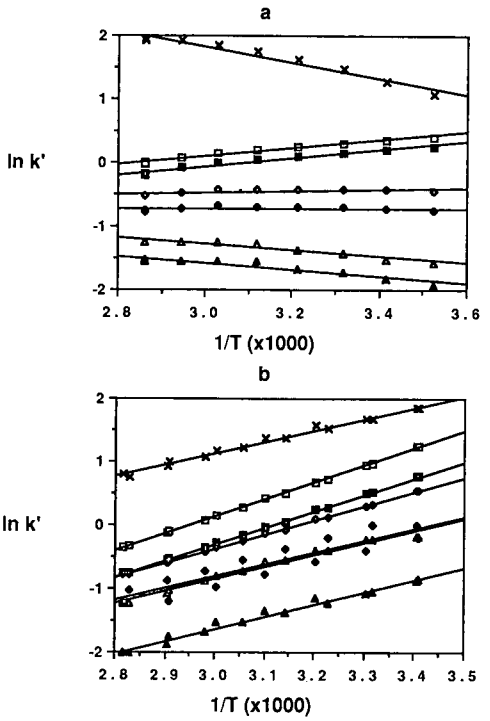

Fig. 4. (a) Variation in ln k' *versus* $1/T$ for seven common anions on anion-exchange column, Dionex AS-4A column, 15 mM NaOH eluent. (b) Variation in ln k' *versus* $1/T$ for same anions on macrocycle-based column, 20 mM NaOH eluent. Anions for (a) and (b): ▲ = fluoride; △ = acetate; ◆ = chloride; ◇ = nitrite; ◘ = bromide; □ = nitrate; × = sulfate.

temperature varies from ion to ion. The capacity factors of chloride, nitrite, bromide, and nitrate decrease, while those of fluoride, acetate, and sulfate increase with temperature. Except for sulfate, the changes are relatively small. However, with the macrocycle column (Fig. 4b), the capacity factors of all of the anions decrease significantly as the temperature is raised.

The variation of the capacity factor as a function of temperature is described by the equation:

$$\ln k' = \frac{-\Delta H}{RT} + \frac{\Delta S}{R} + \ln \varphi \tag{3}$$

where φ is the phase ratio for the column, a constant for a given column [12] and ΔS is the entropy change. Plots of ln k' *versus* $1/T$ for the separations in Figs. 2–4 generate straight lines with a slope equal to $-\Delta H/R$ where ΔH is the enthalpy change for the retention reaction and R is the molar gas constant. The ΔH for the exchange (anion) or complexation (cation) retention reactions can thus be calculated. A comparison of the values thus obtained for the ΔH values for the exchange and complexation reactions is shown in Table I. The ΔH values for the complexation reactions are larger than those

TABLE I

MEASURED ΔH VALUES FOR BOTH ION-EXCHANGE AND MACROCYCLE-BASED COLUMNS FOR VARIOUS CATIONS AND ANIONS

Ion	Ion exchange ΔH (kcal/mol)[a]	Macrocycle ΔH (kcal/mol)[b]	Literature ΔH[c]
Li^+	0.837	−12.145	−1.401
Na^+	0.0066	−6.861	−7.620
K^+	−0.833	−5.423	−11.57
Rb^+	−1.081	−9.211	−11.77
Cs^+	−1.218	–	–
Mg^{2+}	2.774	−6.805	–
Ca^{2+}	2.742	−7.118	−0.800
Sr^{2+}	2.227	–	–
Ba^{2+}	1.363	–	–
F^-	1.073	−3.811	
Acetate	0.966	−3.750	
Cl^-	−0.017	−3.734	
NO_2^-	−0.256	−4.451	
Br^-	−1.328	−5.163	
NO_3^-	−1.251	−5.391	
SO_4^{2-}	2.548	−3.594	

[a] The ΔH for the ion-exchange reaction.

[b] For cations the ΔH for the cation–macrocycle complexation on the stationary phase. For anions the ΔH of the exchange reaction between analyte anions and hydroxide ions.

[c] The ΔH for the homogeneous solution cation–macrocycle complexation in water (from ref. 16).

for the exchange reaction, reflecting a much larger dependence on temperature than the ion-exchange reactions.

Column capacity as a function of temperature

The retention of anions on the macrocycle column is affected by two different factors with respect to temperature. The separation takes place mainly by an ion-exchange mechanism, with the cation–macrocycle complex acting as the ion-exchange site. If this mechanism were the only factor, as the temperature is raised, the behavior should resemble that of a classical ion-exchange column. However, Fig. 4b shows that the anion capacity factors decrease with a slope that is greater than that ascribed to the effect of temperature on the ion-exchange reaction (Fig. 4a). Indeed, there is decreased retention even for anions like sulfate that show increased retention with increasing temperature under classical ion-exchange conditions.

In order to better understand this phenomenon, we measured the column capacity at different temperatures by measuring the uptake of the sodium counterion on the column. The column was placed in the jacket connected to the constant temperature bath to carefully control the temperature. The 20 mM NaOH eluent was run through the column to reach equilibrium between the mobile phase and the stationary phase. The column was switched out of line and all of the connecting tubing was rinsed free of eluent by pure water. The column was then switched back on line and the sodium was eluted from the column by 0.1 M HNO_3 and the column effluent was

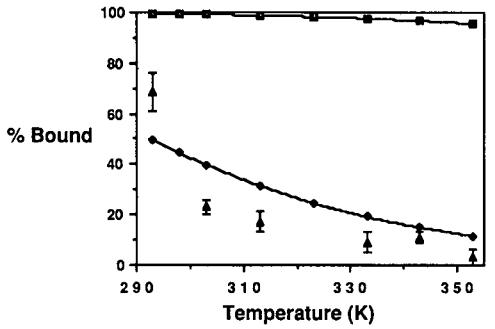

Fig. 5. Comparison of experimental *versus* calculated column anion-exchange capacity of macrocycle column expressed as the percent of macrocycle sites binding sodium cations. ■ = Theory, $K = 8000$; ◆ = theory, $K = 40$; ▲ = experimental.

collected. The sodium concentration in the effluent was measured, and by taking into account the column dead volume and the eluent sodium concentration, the amount of sodium uptake of the column was determined. Fig. 5 describes the drop of column capacity, shown as the percent of macrocyclic sites containing sodium ions.

The Van 't Hoff equation

$$\ln \frac{K_2}{K_1} = \frac{\Delta H}{R}\left(\frac{1}{T_2} - \frac{1}{T_1}\right) \tag{4}$$

relates the change in equilibrium constant (K) with temperature. Thus, the amount of macrocycle sites containing metal ions ($[ML^+]$) at any temperature can be calculated if the complexation constant at a given temperature, the ΔH for the complexation reaction, the total amount of ligand on the column, and the free metal ion concentration are known. In Fig. 5, the experimentally observed values for the percent of the macrocycle sites binding sodium ions are compared to the calculated values using two different possible complexation reaction mechanisms, each with its own values for the binding constant and the ΔH for the reaction. The first theoretical curve is generated using the literature value for the binding constant ($\log K = 3.9$ at 25°C) and the ΔH (-7.62 kcal/mol) for the homogeneous complexation reaction [16] in aqueous solution. This curve is much higher than the observed values, implying that under these conditions complexation does not occur in the aqueous phase. Indeed, in previous work we have directly measured the apparent binding constant ($K = 40$) for sodium with the macrocycle D-2.2.2 under the same chromatographic conditions [10]. This result agrees with those of Bourgoin *et al.* [17], who demonstrated that ion-pair formation leads to binding constants 300 or 400 times lower than for free cations. Using this value for the binding constant and the corresponding ΔH determined from the slope of the Na^+ line in Fig. 2b (using eqn. 3), the second theoretical curve in Fig. 5 was generated. This curve corresponds to a heterogeneous extraction complexation mechanism in which the sodium ion, together with its anion, leaves the aqueous environment upon complexation. The fact that the experimental curve lies close to this second theoretical curve implies that the heterogeneous rather than the homogeneous

mechanism is prevalent. This result, in turn, implies that as anions are separated on this column, they undergo an extraction into the hydrophobic stationary phase environment. This conclusion reinforces our interpretation of previous results [10] and is the subject of ongoing investigation. The fact that the complexation constant is of moderate strength makes possible the large changes in column capacity necessary to achieve capacity gradients.

Temperature gradient separation of anions

According to theory, the retention of anions is directly proportional to the column ion-exchange capacity and inversely proportional to the eluent concentration. Most gradients are performed by increasing the eluent strength. However, the retention can also be modified by changing the column capacity. As seen previously, macrocycle-based columns display lowered anion capacity as the temperature is increased. Thus column capacity can be changed throughout the course of a separation by increasing the column temperature during the separation.

The capability to do temperature gradient separations is illustrated by Fig. 6. The column was heated by placing 1 m of tubing immediately preceding the column in a Dionex column heater. The temperature was controlled by the Dionex AI400 software. The eluent was 20 m*M* NaOH flowing at 1.0 ml/min. The separation of an

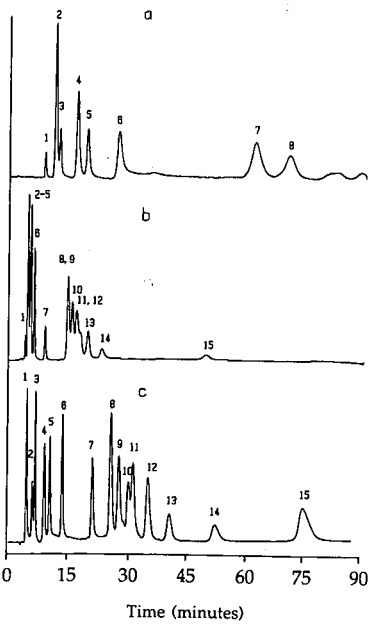

Fig. 6. Separation of 15 common anions: 1 = F^-, 1.5 ppm; 2 = acetate, 10 ppm; 3 = Cl^-, 2.5 ppm; 4 = NO_2^-, 10 ppm; 5 = Br^-, 10 ppm; 6 = NO_3^-, 10 ppm; 7 = I^-, 10 ppm; 8 = SO_4^{2-}, 10 ppm; 9 = oxalate, 10 ppm; 10 = CrO_4^{2-}, 10 ppm; 11 = MoO_4^-, 10 ppm; 12 = fumarate, 10 ppm; 13 = ClO_4^-, 10 ppm; 14 = PO_4^{3-}, 10 ppm; 15 = phthalate, 10 ppm; under three different chromatographic conditions: (a) at 30°C; (b) at 80°C; and (c) temperature gradient with program starting at 30°C and increasing to reach 80°C beginning at 5 min and ending at 30 min.

anion standard clearly shows the change in column capacity at different temperatures. In Fig. 6a, at 30°C, the first peaks are well resolved, but stronger retained anions do not elute from the column. In Fig. 6b, at 80°C, the stronger retained species elute, but resolution of the earlier peaks is lost. It should also be noted that the selectivity is different at higher temperatures, with iodide eluting before sulfate at 80°C. Fig. 6c displays the ability to perform temperature gradient separations on macrocycle-based columns. The temperature begins to increase at 5 min from 30°C to reach 80°C at 30 min. The resulting chromatogram shows good resolution of the earlier eluting peaks, while the stronger retained peaks elute much sooner than at ambient temperature, due to the decrease in column anion-exchange capacity at elevated temperatures.

To ensure that the loss of capacity is not due to loss of the adsorbed cryptand from the column, the column stability at elevated temperatures was explored on a freshly prepared column. Repeated injections of anions were made while the column was maintained at 80°C. Fig. 7 shows that the column showed a decrease in retention in the first three hours, probably due to the time required to fully reach thermal equilibrium. After equilibrium was reached, the retention showed no change over the duration of the experiment (50 h). Thus, it can be concluded that gradient retention is due to changes in the column capacity because of the decrease in the population of macrocycle–cation complexes, not from the loss of cryptand from the column.

One important consideration in gradient ion chromatography with conductometric detection is the stability of the baseline. With concentration gradients, baseline drift is caused by incomplete suppression of eluent ions, decreasing the quality of the chromatogram. In temperature programming, the baseline may be affected by the increase in temperature of the mobile phase during the chromatogram. Conductivity is a strong function of temperature, with the background conductivity increasing with increasing temperature. In order to maintain a stable baseline, the temperature of the eluent entering the detection cell was kept constant. With suppressed conductivity detection, temperature reequilibration with the room was accomplished in the suppressor. The heated eluent stream was cooled in the suppressor by the room temperature regenerant, which is flowing generally 3–5 times faster than the eluent stream, and which is separated from the eluent by only a thin membrane. This is sufficient to cool the eluent stream to near room temperature before entering the

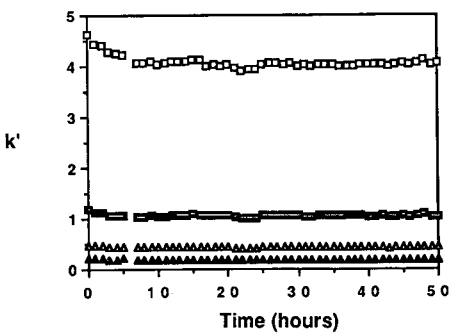

Fig. 7. Macrocycle column stability over time at elevated temperatures (80°C). □ = Sulfate; ■ = nitrate, △ = chloride; ▲ = fluoride.

detection cell, decreasing the amount of baseline perturbation that might otherwise be observed.

Temperature programming with macrocycle-based separation systems shows several possible advantages over other gradient techniques. The vaseline drift and other aberrations caused by increasing the eluent concentration and by eluent impurities are reduced, resulting in a stable baseline. Also, gradient elution can be performed with a single eluent reservoir, eliminating the need for expensive pumps and mixing systems.

ACKNOWLEDGEMENTS

Funding for this research was provided by a graduate fellowship from Dionex Corporation.

REFERENCES

1 J. D. Lamb and R. G. Smith, *J. Chromatogr.*, 546 (1991) 73.
2 E. Blasius, K. P. Janzen, W. Klein, H. Klotz, V. B. Nguyen, T. Nguyen-Tien, R. Pfeiffer, G. Scholten, H. Simon, H. Stockemer and A. Toussaint, *J. Chromatogr.*, 201 (1980) 147.
3 M. Nakajima, K. Kimura and T. Shono, *Bull. Chem. Soc. Jpn.*, 56 (1983) 3052.
4 M. Takagi and H. Nakamura, *J. Coord. Chem.*, 15 (1986) 53.
5 T. Iwachido, H. Naito, F. Samukawa, K. Ishimaru and K. Toei, *Bull. Chem. Soc. Jpn.*, 59 (1986) 1475.
6 M. Lauth and P. Gramain, *J. Chromatogr.*, 395 (1987) 153.
7 R. Rocklin, C. Pohl and J. Schibler, *J. Chromatogr.*, 411 (1987) 107.
8 R. Rocklin, M. Rey, J. Stillian and D. Campbell, *J. Chromatogr. Sci.*, 27 (1989) 474.
9 W. Jones, P. Jandik and A. Heckenburg, *Anal. Chem.*, 60 (1988) 1977.
10 J. D. Lamb and P. A. Drake, *J. Chromatogr.*, 482 (1989) 367.
11 J. D. Lamb, P. A. Drake and K. Woolley, in P. Jandik and R. M. Cassidy (Editors), *Advances in Ion Chromatography, Vol. 2*, Century International, Medfield, MA, 1990, p. 215.
12 G. Bonn and P. Jandik, in P. Jandik and R. M. Cassidy (Editors), *Advances in Ion Chromatography, Vol. 2*, Century International, Medfield, MA, 1990, p. 197.
13 N. Fortier and J. Fritz, *Talanta*, 34 (1987) 415.
14 R. Dybczynski, H. Polkowska-Motrenko and R. M. Shabana, *J. Chromatogr.*, 134 (1977) 285.
15 R. Dybczynski, *J. Chromatogr.*, 31 (1967) 155.
16 R. M. Izatt, J. S. Bradshaw, S. Nielsen, J. D. Lamb and J. J. Christensen, *Chem. Rev.*, 85 (1985) 271.
17 M. Bourgoin, K. H. Wong, J. Y. Hui and J. Smid, *J. Am. Chem. Soc.*, 97 (1975) 3462.

Journal of Chromatography, 546 (1991) 151–158
Elsevier Science Publishers B.V., Amsterdam

CHROMSYMP. 2120

Determination of analytes at extreme concentration ratios by gradient ion chromatography with solid-phase reaction detection

D. T. GJERDE*
Sarasep, Inc., 1600 Wyatt Drive, Suite 10, Santa Clara, CA 95054 (U.S.A.)
D. J. COX
Cox Consulting, 3073 Wagner Street, Waterloo, NY 13165 (U.S.A.)
and
P. JANDIK and J. B. LI
Waters Chromatography Division of Millipore, 34 Maple Street, Milford, MA 01757 (U.S.A.)

ABSTRACT

Conditions for separating anions by gradient ion chromatography are explored where detection is performed with the post-column addition of a solid-phase reagent (SPR). Gradient ion chromatography can be useful when analyzing samples containing trace analytes in the presence of large amounts of a particular anion. However, loss of peak height and area of early eluting anions can occur when there is an extremely high concentration of a second later eluting anion. The distortion appears to result from a moving zone overloading of the separation column. Only early eluting anions are affected. The concentration dependence of the excess anion is studied and various approaches to mitigate the peak distortion are discussed.

INTRODUCTION

Gradient elution ion chromatography is still a new field. Some early limited gradient work was performed [1–4], but the first modern, practical gradient ion chromatography work using membrane suppression and conductivity detection was published by Rocklin and co-workers in 1987 [5].

Gjerde and Benson have recently introduced a new method for conductivity detection in ion chromatography. The method is called suspension detection method or solid-phase reagent (SPR) detection method [6,7]. A colloidal suspension of SPR is added to the eluent stream prior to conductivity detection to produce a low background eluent signal (see experimental section). Jandik and co-workers [8,9] adapted the SPR detection method for gradient ion chromatography. Their work showed that the method works well with a variety of eluents for ion-exchange and ion-interaction chromatography. These include eluents based on borate, hydroxide, and carbonate counter ions.

In this work, gradient ion chromatography and SPR detection is used to exam-

0021-9673/91/$03.50

ine the determination of minor amounts of analytes in the presence of excess concentration of anions. Conditions are described needed to adjust peak windows for the IC-Pak Anion column. Large amounts of chloride in the sample may cause overloading of the column for early eluting peaks. Although the chromatogram may look normal, the overloading can cause a reduction of certain sample peak heights from what they would be without the presence of extreme analyte concentrations.

EXPERIMENTAL

Chemicals for the preparation of standard solutions and eluents were laboratory grade as obtained from a range of suppliers. All chromatographic mobile phases were filtered with a Millipore Solvent Purification Kit prior to use. Only 18 MΩ water obtained from a Milli-Q Laboratory Water System (Millipore, U.S.A.) was utilized in the experiments.

Two versions of polymethacrylate-based anion-exchange columns were used. IC Pak A Anion column (50 × 4.6 mm I.D.) contains a 10-μm packing material. The second column, IC Pak A HR Anion, has the dimensions of 75 × 4.6 mm I.D. and contains 6 μm diameter material. The exchange capacity for both of these columns is 30 μequiv./g. Sarasep AN1, a polystyrene-based anion exchanger, was used for some experiments. This column has dimensions of 250 × 4.6 mm I.D.

The SPR is manufactured by Sarasep, and distributed exclusively by Waters (patents pending). The SPR is obtained as a concentrate (Part No 36546) containing about 12% solids with a cation-exchange capacity not less than 500 milliequivalents per liter of suspension. The SPR concentrate was diluted about tenfold with deionized water prior to use. The diluted suspension did not show any appreciable sedimentation as determined in a 100-ml graduated cylinder filled with 100 ml of SPR over a period of time lasting 8 hours. The conductivity of the SPR suspension (1.2%) did not exceed 10 μS/cm. To eliminate any effects of contaminants introduced by handling or during prolonged storage of SPR suspensions, the manufacturer recommends use of an inline polishing column (SPR-H^+ Polishing column kit, Waters, U.S.A., Part No. 36547.) The column contains a high-capactiy anion exchanger in the OH-form. The polishing column was regenerated every 50 hours with 10 ml of 100 m*M* KOH followed by a rinsing with a least 15 ml of deionized water.

Basic eluents such as sodium carbonate are highly conductive. SPR reacts with the eluent stream to produce low-conducting carbonic acid. At the same time, Na^+ or any other eluent counter ion is taken up by the SPR. Also, sample anions are converted to high-conducting strong acids.

A Water M600 MS and a Waters Action Analyzer IC were used in the work. The pump flow-rate was set at 1 ml/min for all chromatograms. All injections were 100 μl. The eluents were prepared using degassed water and degassed during use by continuous sparging with He. This treatment prevented CO_2 from being absorbed by the basic eluents. Carbonate absorbed in the eluent may contribute to gradient 'ghost' peaks.

Fig. 1 gives details of the instrumental configuration for post-column addition of SPR suspensions. The flow-rate of SPR (0.4 ml/min) is determined by adjustments of pressure from the air supply (12). The reagent flows from the pressurized PTFE vessel (13) through the SPR polishing column (10) and through a check valve (8) to a

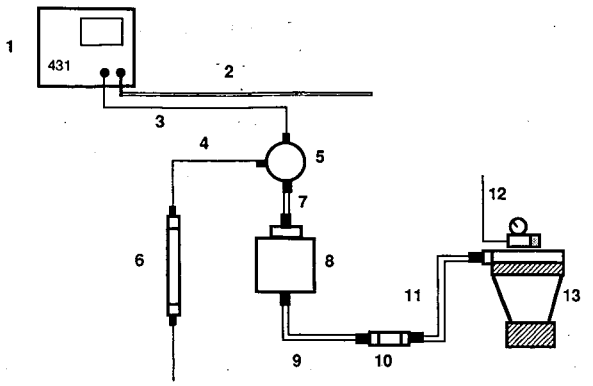

Fig. 1. Detailed diagram of hardware configuration for post-column addition of SPR. 1 = Conductivity detector: Waters 431 detector, four electrode cell design; 2 = waste line: 4 × 0.009 in. stainless connected to 431 + 24 × 1/16 × 0.060 in. PTFE tubing; 3 = tee to 431: 15 × 1/16 × 0.010 in. PTFE to 431 inlet; 4 = column to tee: shortest 1/16 × 0.010 in. PTFE from column to tee; 5 = tee: Unmount tee from check valve block for shortest path length; 6 = analytical column: Waters IC PAK A or IC PAK A HR; 7 = check valve to tee: 2 × 1/8 in. O.D. PTFE; 8 = check valve; 9 = polisher column to check valve; 3 × 1/8 in. O.D. PTFE; 10 = polisher column: 8 × 25 mm containing AG1 × 8, 200 mesh; 11 = reservoir to polisher column: 12 × 1/8 in. O.D. PTFE; 12 = air supply: minimum of 90 p.s.i. compressed air supply; 13 = reservoir for SPR: reconfigure with outlet on left side.

mixing tee (5), where it blends into the eluate from the chromatographic column (6). The check valve prevents any accidental addition of chromatographic phase to the SPR supply inside the vessel. The instrumentation shown in Fig. 2 should be used with SPR within the prescribed range of 0.5–1.5% solids suspension concentration. During more than a 12-month period of evaluation, the authors did not experience any sedimentation or plugging problems.

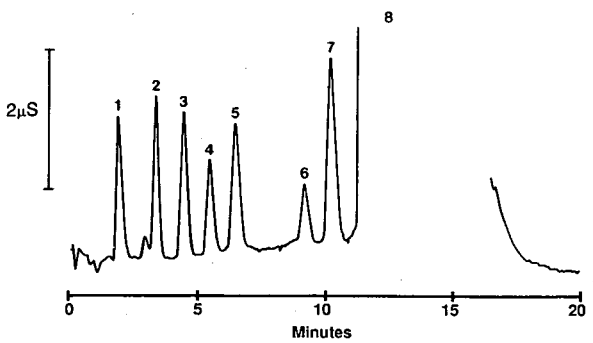

Fig. 2. Separation of traces of inorganic anions in a sample matrix containing high levels of chromate. Column: IC Pak Anion; Eluent: 1 ml/min. A = water, B = 100 m*M* boric acid adjusted to pH 8.3 with sodium hydroxide. Gradient: 0 to 5 min, 25 to 50% B, and then hold 50% B 5 to 20 min. Peaks: 1 = fluoride (0.5 ppm); 2 = chloride (1 ppm); 3 = nitrite (2 ppm); 4 = bromide (2 ppm); 5 = nitrate (2 ppm); 6 = phosphate (3 ppm); 7 = sulfate (2 ppm); 8 = chromate (500 ppm).

RESULTS AND DISCUSSION

Gradient ion chromatography can be used to analyze samples containing extreme ratios of analyte concentrations. In these samples, gradients may be used to modify the spacing between the peaks in the critical regions of the chromatogram. Generally, it is possible to design separations with maximized peak to peak resolution in those regions where the highly concentrated analytes are expected to elute. In some instances, in order to reduce the total run time, it may be desirable to compress the remaining regions of a chromatogram after the separation of the critical peaks has been achieved.

Equations have been derived that describe the effect of different gradient profiles on sample anion retention [5]. However, there are no set rules for developing the gradients needed in ion chromatography. The gradient used, depends on the column and the desired sample resolution. Method development for gradient ion chromatography is still largely a trial and error method. Dilute monovalent eluents are used to resolve early eluting monovalent sample species. Then, the eluent concentration is increased to elute strongly retained anions. A steeper eluent concentration increase will shift multivalent sample species to shorter retention times faster than monovalent sample species. The eluent pH shift with gradient can also be an important factor in gradient separations. For example a pH change in the gradient can change phosphate from a divalent to a trivalent anion resulting in longer retention.

Samples containing high levels of chromate are common in the electroplating industry as well as in environmental contracting laboratories. Fig. 2 shows an example of a gradient separation of a sample with concentration ratios of the analyte peaks ranging from 1:1000 to 1:166. All peaks between fluoride and sulfate are well resolved. The peak due to an elevated level of chromate elutes within a reasonable time. Under otherwise identical conditions, an isocratic separation require an analysis time in excess of 60 minutes to accomplish a similar resolution of the seven inorganic anions in the presence of the high chromate concentrations. The unidentified peak eluting shortly before chloride is due to carbonate which entered the sample by absorption from the atmosphere.

The chromatogram in Fig. 3 shows the separation of trace amounts of anions in the presence of high levels of phosphate. The phosphate was added to the standard

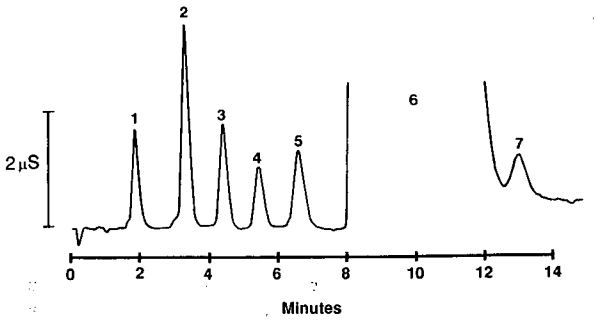

Fig. 3. Chromatographic analysis of low concentrations of anions in the presence of high concentration of phosphate. Conditions are the same as in Fig. 2. Gradient: 0 to 7 min, 50% B, 7 to 20 min 100% B. Peaks 1–7 and concentration as in Fig. 2. except for phosphate (peak 6) which is 500 ppm.

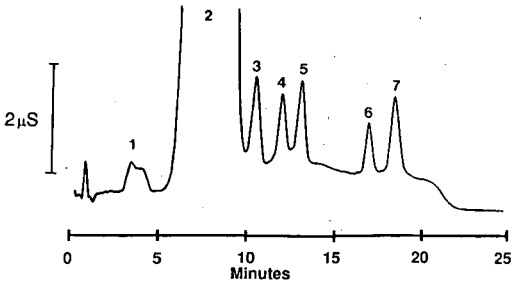

Fig. 4. Separation of low levels of anions in the presence of high concentration of chloride. Column: IC Pak Anion; Eluent: 1 ml/min. A = water, B = 50 m*M* boric acid, pH 8.3. Gradient: 0 to 8 min, 20% B; 8 to 12.5 min, 20 to 100% B; 12.5 ot 20 min, 100% B. Peaks 1–7 and concentrations as in Fig. 2, except for chloride (peak 2) which is 500 ppm.

mixture as dibasic anion. An advantage of the borate mobile phase is its relatively high buffering capacity toward alkaline samples. At pH 8.3, only about 10% of the boric acid is converted to borate. The remaining 90% is available as a buffer preventing large changes of pH due to alkaline samples matrices. Carbonate elutes with chloride under the conditions listed in Fig. 3. To prevent this, eluent A can be changed to either 7.28 m*M* or 10.68 m*M* boric acid adjusted to pH 8.6 with KOH (ref. 8).

Optimization of separation conditions for samples containing elevated levels of chloride was studied next. The chromatogram shown in Fig. 4 shows traces of nitrite, bromide, nitrate, phosphate, and sulfate relatively well resolved from the chloride matrix peak. However, the distorted shape of the fluoride peak is an indication of a strong interference that would be typical for a sample of this type.

The distortion of the fluoride peak was investigated with a series of standard mixtures containing 1 ppm fluoride in the presence of several different levels of chloride. As shown in Fig. 5, the size of the peak for constant levels of fluoride decreases with increasing amounts of chloride. Between 2 and 100 ppm of chloride, the fluoride peak was not yet visibly distorted. Consequently, the interference of chloride at con-

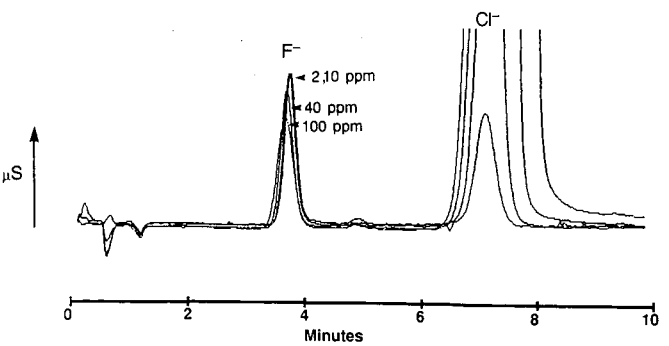

Fig. 5. Decreasing peak heights of 1 ppm fluoride peak with increasing concentrations of chloride (2 to 100 ppm). Column: IC Pak Anion. Isocratic elution with 10 m*M* boric acid, pH 8.3.

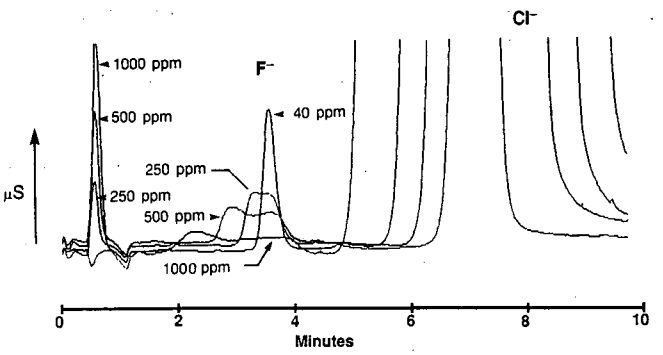

Fig. 6. Distortion of peak shapes for 1 ppm fluoride at elevated levels of chloride (40 to 1000 ppm). Conditions are the same as in Fig. 6.

centrations about 20–100 ppm with the quantitative determination of fluoride could be easily overlooked. At a higher range of chloride concentrations, 250–1000 ppm, the fluoride peak showed distortion that increased with increasing chloride concentration (Fig. 6). At the same time, the peak at the void (retention time = 0.2 min) increased in peak height with increasing chloride concentration. Normally the void peak is negative and is called a water dip. It is highly unusual for this peak to be positive. In an experiment with 2.8 m*M* $NaHCO_3$ and 2.2 m*M* Na_2CO_3 eluent and two IC Pak A columns in series, the void was collected and reinjected onto the ion chromatograph. It was found that virtually all of the lost fluoride and some excess chloride was in the void peak. The peak heights of the other anions —nitrite, bromide, nitrate, phosphate, and sulfate— were not affected. The peak height of fluoride was affected by the presence of up to 2000 ppm of chromate, nitrate, or phosphate. Experiments performed with membrane suppression detection showed the same behavior.

Table I shows that the counter ion of the sample has no effect of the fluoride peak reduction. The rate of peak height reduction with increasing chloride concentra-

TABLE I

PEAK HEIGHT OF FLUORIDE IN THE PRESENCE OF EXCESS KCl, LiCl, AND HCl SAMPLE

5.6 m*M* $NaHCO_3$, 4.4 m*M* Na_2CO_3 isocratic eluent, 1 ml/min with 2 IC Pak A columns in series. All chromatograms and data are from 100-μl injections.

ppm Cl	Peak height (cm)		
	KCl	LiCl	HCl
2	3.55	3.50	3.50
40	3.35	3.40	3.40
100	3.35	3.40	3.35
250	3.35	3.25	3.25
500	2.60	2.70	2.70
1000	2.30	2.30	2.30

tion was the same in all three cases. Therefore, it is unlikely that loss of fluoride is due to protonation of fluoride by the sample matrix.

Next, other early eluting anions were investigated. Fig. 7 shows a plot of normalized peak height of fluoride, propionate, and iodate. The results show that iodate is affected the greatest, then fluoride, and finally propionate. The relative loss of each anion is related to the affinity of the anion for the anion-exchange resin. Anions with the lowest selectivity for the anion-exchange column have the greatest loss of peak height. The elution order of these anions is iodate, fluoride, and propionate. In separate experiments, acetate and formate also showed reduced peak height.

Early eluting peaks by nature compete poorly for the ion-exchange sites. When an injection is made, three different anions are in competition: the early eluting anion, chloride, and the eluent anion. Presumably, changing the eluent type might help. Three different eluents were tried in these experiments: borate, carbonate/bicarbonate, and hydroxide. But when the eluent concentration for each eluent is adjusted so that sample peak elutes at roughly the same time, the peak reduction behaviour is similar for eluent types tested.

Increasing the column capacity may help. In fact, better results by a factor of 2 were obtained when two columns were connected in series. However, it should be

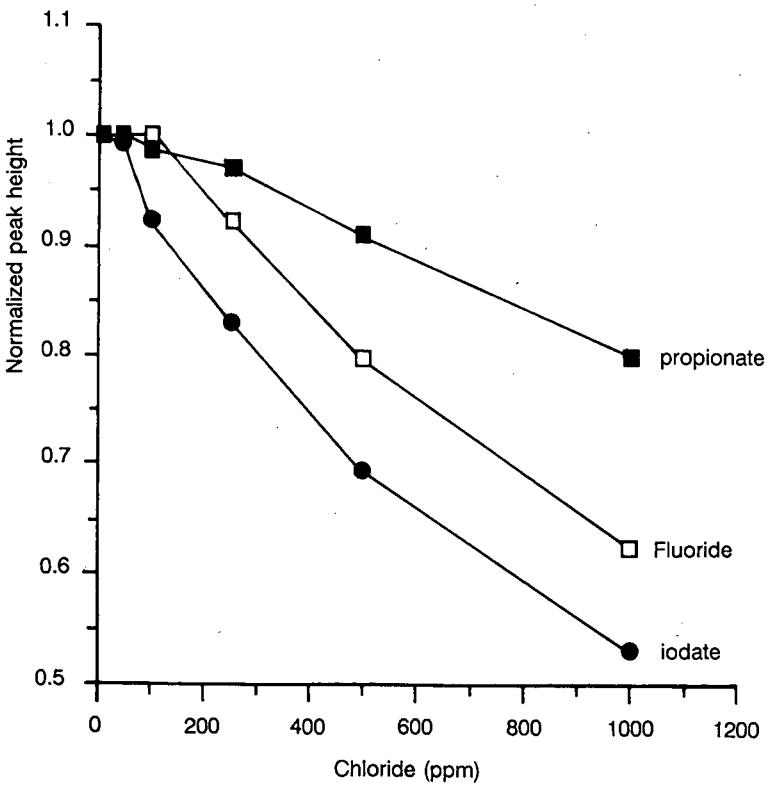

Fig. 7. Plots of normalized peak heights of 30 ppm propionate, 5 ppm fluoride, and 30 ppm iodate as a function of chloride concentration. Column: 2 × IC Pak Anion column in series. Eluent: 2.8 m*M* $NaHCO_3$, 2.2 m*M* Na_2CO_3.

noted that simply increasing the capacity may not be enough. Some commercial columns may have higher capacity, but have poorer selectivity for early eluting anions (indicated by whether these anion elute near the void).

Another method is to use ion-exclusion chromatography to determine anions of weak acids [10]. Trace amounts of these acids can be determined in the presence of large amounts of anions of strong acids. Of course, anions of strong acids cannot be determined unless a coupled system (ion exclusion and ion exchange) is used. Then both types of anions can be determined simultaneously.

An eluent gradient may be used to adjust eluent conditions so that the early eluting anions are better retained by the column. Thus, the early eluting anions do not have to compete with the eluent anions to be retained by the anion-exchange sites. This increases the peak window between chloride and the void peak. Under some experiments performed with a Sarasep AN1 column, a 10-min gradient of 0 to 10 m*M* KOH gradient produced no loss of 2 ppm fluoride in the presence of 500 ppm of chloride. However, it's impossible to be more than qualitative with recommending gradient conditions. Whether a gradient works depends on the type selectivity, and condition of the anion-exchange column. It may be better to remove chloride with a sample preparation column prior to analysis. In any case, method calibration should be performed with standard solutions that are similar to the sample matrix.

REFERENCES

1 D. T. Gjerde and J. S. Fritz, *J. Chromatogr.*, 188 (1980) 391.
2 R. M. Cassidy, *Chem. Geol.*, 67 (1988) 185.
3 P. K. Dasgupta, *Anal. Chem.*, 56 (1984) 769.
4 T. Sunden, M. Lindgren, A. Cedergren and D. D. Siemer, *Anal. Chem.*, 55 (1983) 1357.
5 R. D. Rocklin, C. A. Pohl and J. A. Schibler, *J. Chromatogr.*, 411 (1987) 107.
6 D. T. Gjerde and J. V. Benson, *Anal. Chem.*, 62 (1990) 612.
7 D. T. Gjerde, in P. Jandik and R. M. Cassidy (Editors), *Advances in Ion Chromatography*, Vol. 2, Century International, Medfield, MA, 1990, pp. 1–19.
8 P. Jandik, J. B. Li, W. R. Jones and D. T. Gjerde, *Chromatographia*, 30 (1990) 509.
9 J. Li and P. Jandik, *J. Chromatogr.*, 546 (1991) 395.
10 D. T. Gjerde and H. Mehra, in P. Jandik, and R. M. Cassidy (Editors), *Advances in Ion Chromatography*, Vol. 1, Century International, Medfield, MA, 1989, pp. 139–178.

Journal of Chromatography, 546 (1991) 159–173
Elsevier Science Publishers B.V., Amsterdam

CHROMSYMP. 2205

Electrodialytic eluent generation and suppression

Ultralow background conductance suppressed anion chromatography

DOUGLAS L. STRONG, CHANG UNG JOUNG[a] and PURNENDU K. DASGUPTA*
Department of Chemistry and Biochemistry, Texas Tech University, Lubbock, TX 79409-1061 (U.S.A.)

ABSTRACT

An electrodialytic generator has been linked to a newly designed electrodialytic suppressor. This combination greatly reduces suppressed conductivity due to residual acids originating from the anionic impurities in the eluent sodium hydroxide and completely eliminates the conductivity contribution from chemical regenerant penetration in the suppressor. The system provides reproducible sodium hydroxide gradients obtained by current programming the generator and is able to operate typically with a suppressed conductivity of 300–400 nS/cm providing commensurate performance with respect to detection limits and response linearity.

INTRODUCTION

In the realm of suppressed anion chromatography the two most commonly used eluents, carbonate and hydroxide, exhibit suppressed conductivities of 12–15 and 2–5 μS/cm, respectively, at typical eluent strengths. For carbonate eluents it is well recognized that the residual conductivity after suppression is largely due to dissociation of the carbonic acid formed in the suppressor. Actually, carbonic acid is also the principal contributor to the suppressed conductance of an hydroxide eluent because carbonate is by far the principal impurity typically present in the stock hydroxide solutions used for dilution. In our experience, the carbonate content of commercial 50% sodium hydroxide solutions ranges from 0.06 to 0.17 mol%. With both eluents, there are also contributions from impurity anions such as Cl^- and SO_4^{2-} which form the corresponding strong acids in the suppressor. Presently, an acid-regenerated membrane device, is most commonly used for the continuous ion-exchange process referred to as suppression. With such devices, the penetration of the acid regenerant anion, *e.g.* sulfate, into the suppressor effluent also contributes to the background conductance. A suppressor column packed with ion-exchange resin does

[a] Permanent address: Department of Chemistry, Soonchunhyang University, Onyang, Chungnam 336-600, South Korea.

0021-9673/91/$03.50

not suffer from regenerant penetration but has myriad other, unattractive, characteristics [1] such that its resurrection is hardly likely.

As in most detection systems, it is logical to seek the lowest detector background (which in the present case is the suppressed conductance of the eluent) because a low background is conducive to low noise and hence better limits of detection. In ion chromatography (IC), particularly strong incentives exist to produce essentially a pure solvent background to carry out the ion replacement detection technique [2–7] which can, in principle, be exquisitely sensitive. Further, coupling the column effluent to a mass spectrometer [8] is facilitated when the effluent is free of dissolved solids. For an acid-regenerated membrane suppressor, regenerant penetration can be reduced by using an acid with a large and preferably multiply charged counterion, the bulk and the charge of this Donnan-forbidden ion deters transmembrane transport due to a lower diffusion coefficient and better electrostatic exclusion. Thus, the use of acids such as poly(styrenesulfonic), naphthalenetrisulfonic, dodecylbenzenesulfonic acid, etc. has been advocated for this purpose [9–13]. It is possible to avoid renegerant penetration altogether by electrodialytically removing the eluent cation. The necessary H^+ ions are generated by the electrolysis of water. Although a number of papers and patents exist on the electrodialytic scheme [14–17], all but one [17] use acid electrolytes and it is questionable with the others as to how much of the suppression process is actually accomplished electrodialytically. It has in fact been shown that applying an electric field in an otherwise functional acid-regenerated membrane suppressor is not necessarily beneficial [17].

With an electrodialytic suppressor (EDS) that can function adequately without any acid electrolyte, the only remaining obstacle to the attainment of a detector background approaching that of pure water with a suppressed hydroxide eluent is anionic impurities in the eluent. We have previously reported on the construction and characteristics of a series of on-line electrodialytic sodium hydroxide generators (EDGs) based on perfluorosulfonate cation exchange (catex) membranes [18,19]. These generators produce ultrapure sodium hydroxide on-line and afford the added versatility of gradient elution with isocratic pumps because the output concentration from the generator varies directly with the current input which can be programmed.

The full advantage of the purity of an electrodialytically generated eluent can only be realized when it is used in conjunction with an EDS. The characteristics of such a system are reported here.

EXPERIMENTAL

Materials

Stock sodium hydroxide solution was 50% sodium hydroxide (J. T. Baker). House-distilled water fed a Barnstead Nanopure unit, the output of this was used as the feed for a continuously recirculating water polisher (Dionex). The eluent generators were supplied off a tee in the recirculating loop.

Chromatographic system

EDGs. Two different styles of EDG devices were used in this work. The operating principles of these are illustrated in Fig. 1. In one (Fig. 1a), a single tubular Nafion membrane (811x, Perma-pure Products, Toms River, NJ, U.S.A.) containing

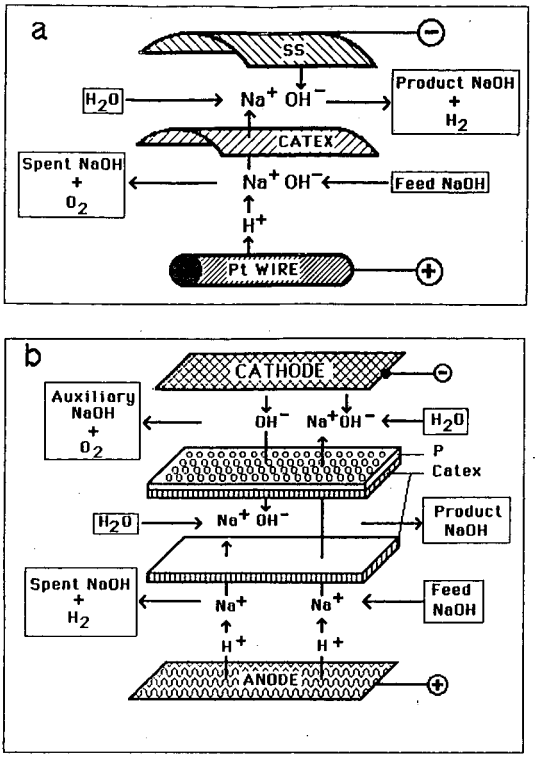

Fig. 1. Principles of operation for (a) a single membrane tubular and (b) a double membrane/perforated plate (P) planar electrodialytic sodium hydroxide generator.

an inserted platinum wire and surrounded by a stainless steel jacket (17 cm × 1 mm I.D.) is fed with ordinary sodium hydroxide in the lumen and sodium hydroxide and hydrogen are produced in the outer channel (type 1 device) [18]. The second device is based on electrodialytic transport through one catex membrane (Nafion 117, Aldrich) and Donnan breakdown of a second similar catex membrane [19] (Fig. 1b). Briefly, the device is built inside a micromembrane suppressor shell (MMS, Dionex). The feed sodium hydroxide flows below one catex membrane and this bottom flow channel contains 50 cm of 0.25 mm diameter platinum wire woven as an electrode on a coarse weave cation-exchange screen (Dionex). Another catex membrane lies atop the first one and the intervening space constitutes the product channel; water is fed from one end and the gas-free product sodium hydroxide flows out of the other end. Atop the top catex membrane is placed a perforated plate P of FEP-Teflon (0.5 mm thick, 4 rows of evenly spaced 1.55 mm holes, 72/row) and water flows over this; atop the plate is placed a stainless-steel screen to function as the cathode. Accumulation of significant concentrations of sodium hydroxide take place in the wells of the plate and causes Donnan breakdown of the top membrane, permitting OH^- transport through it. This (type 2) device generates a gas-free product. Complete construction details of the above devices have been given previously [18,19].

The type 1 EDG output was fed to a degasser made by machining shallow channels into two aligned blocks of nylon separated by a hydrophobic gas-permeable membrane sandwiched in-between. The flow channels were accessed by appropriately drilled holes in the blocks. Microporous Teflon (Gore-Tex, W. L. Gore, Elkton, MD, U.S.A.) or polypropylene (Celgard, Hoechst–Celanese, Charlotte, NC, U.S.A.) are both suitable membrane materials, with the latter being more resistant to stretch induced by the sudden nature of the pump intake strokes. Also, because of the short duration of the intake strokes of a typical piston pump, movement of fluid through the generator product channel is intermittent while the electrical current is constant. A gradient mixer cartridge is therefore placed after the degasser to ameliorate any temporal imhomogeneities in the sodium hydroxide concentration. The degassed output was fed via a tee into the dual inputs of a Dionex Model 4000i pump directly into the pump head. The EDG was under the control of a constant current source, temporally programmable by an AT-class computer. The overall experimental arrangement is depicted in Fig. 2. The type 2 EDG was controlled by a manually adjustable constant current source and its output was fed to a Beckman 110A pump equipped with a pulse dampener. Common to both systems were an injection volume of 50 μl, an AS-5A column, an EDS described below, a CDM-II conductivity detector (Dionex) and a generator product flow of 1 ml/min as controlled by the chromatographic pump. Chromatographic results were acquired on a disk-based C-R3A integrator system (Shimadzu Scientific).

EDS. The EDS used in these experiments is a planar device constructed within a Dionex MMS body. This new design is simpler to fabricate than the previously reported tubular EDS [17] and does not require any carbon packing. The operating principle is illustrated in Fig. 3. An understanding of the fabrication details of the current EDS given below is facilitated by familiarity with the design of the standard MMS devices as described by Stillian [20]. The MMS shell consists of two blocks, one with four external connections (A) and another with no external connections (B). There are three flow channels in the assembled MMS, a central eluent channel flanked by a renegerant channel on each side. In the commercial device, the two flanking channels are connected in parallel and are fed from a common regenerant source. In

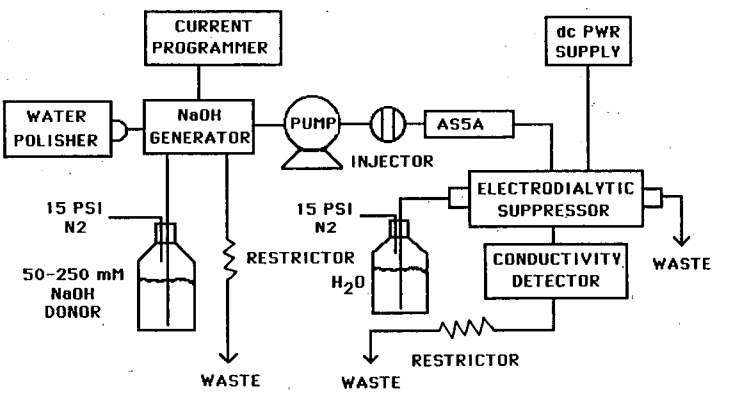

Fig. 2. Complete experimental arrangement including the electrodialytic generator and suppressor.

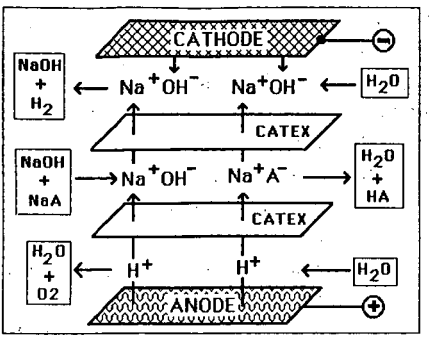

Fig. 3. Principle of operation of the electrodialytic suppressor.

the present device, these flanking channels must be separated for use as the cathode and anode flows of the EDS. This is done by plugging the inter-block connections in the MMS shell and by drilling appropriately placed holes in the side of block B and press-fitting stainless-steel tubing in these holes to access the flow channel in the block. The original regenerant flow connections in block A now access only the flow channel in this block. It is important that block B be selected as the anode channel because the flow path is longer and the effective membrane area greater than in the cathode compartment. Referring to Fig. 3, it can be seen that the anode and the cathode membrane remain respectively in the H^+- and Na^+-form. It is advantageous to have the membrane with the greater length as the H^+-form anode membrane; this diminishes the opportunity for the suppressor effluent to contact a Na^+-laden membrane as it exits.

For the anode, 50 cm of 250 μm diameter platinum wire was woven onto one of the original MMS coarse catex screens and a short length of thick stainless steel wire pressed through a hole drilled through the bottom of block B to contact the platinum wire. For the cathode, a 200 mesh stainless steel screen was cut to fit the well in block A and a parafilm sheet pressed into the screen with a hydraulic press at *ca.* 0.26 ton/in.^{2} to form a gasket on the screen; this closely resembles the parafilm gasket on the ion-exchange screen from this channel in the original MMS device. Like the MMS, the eluent flow channel is accessed through holes in the cathode membrane. Holes are punched in the cathode screen at these locations to keep the cathode out of the eluent flow where it may introduce gas during operation. A polypropylene mesh (250 μm opening, D-CMP-250, Small Parts, Miami, FL, U.S..) separates the cathode from the cathode membrane while a coarse catex screen separates the anode from the anode membrane. Without these, gas appears in the suppressed eluent. Electrical contact to the cathode is established in a fashion similar to that with the anode by a push-fitted stainless-steel rod through a hole in the top of block A. A fine mesh ion-exchange screen is present in the eluent channel of the MMS, a similar catex screen occupies the eluent channel of the present EDS as well. Water flow through the flanking channels and eluent flow through the central channel were all maintained at 1 ml/min.

Measurement of the permeation of carbon dioxide through polymeric tubing

The intrusion of carbon dioxide through polymeric components is a major concern in maintaining the purity of an ultrapure sodium hydroxide eluent. The permeation rate of carbon dioxide through Tefzel tubing was studied in the following manner. The pure water output from the water polisher was first directly connected to the injection port of the chromatographic system with the minimum tubing necessary (4 cm) and a "blank" obtained by allowing the sample loop to flush for 30 s, then injecting. A 2.1-m length of Tefzel tubing (0.5 mm wall, 0.5 mm I.D.) was then inserted between the water polisher and injection port. The valve was next put in the load mode and water flowed through the Tefzel tubing and the sample loop of the valve for $\geqslant$ 1 min. The residence time of the water in the Tefzel conduit was 0.42 min. The sample was then injected and after 9.5 min the analysis cycle was completed, the valve was put in the load mode again for 20 s to analyze the water that remained stationary in the Tefzel conduit during the preceding analytical cycle.

Conductance measurement of sodium hydroxide solutions

The specific conductances of standard sodium hydroxide solutions were measured as a function of concentration (0–100 m*M*) and temperature (15–40°C). A home-made flow-through thermostating device was used for temperature adjustment of the sodium hydroxide solution. Sodium hydroxide solutions of known concentration were pumped at 1 ml/min through *ca.* 35 cm of coiled stainless steel tubing embedded in silver epoxy atop two Peltier heat pumps (30 × 30 × 4 mm, Melcor, Trenton, NJ, U.S.A.) stacked serially above each other. The bottom of the stack was mounted on a fan-cooled finned heat sink with silicone heat sink compound. The temperature of the assembly was measured by a reference current source that produces an output of 1 μA/K (AD-540, Analog Devices, Norwood, MA, U.S.A.) which is used in turn by appropriate control electronics to maintain the temperature within 0.1°C of set temperature. After exiting the thermostating coil the liquid passed sequentially through a Dionex CDM-II detector cell D1 and a home-made detector cell D2 (see below). Minimum lengths of polymeric connecting tubing were used to connect the cells to each other and to the thermostating cell and the whole assembly above the bottom plate of the Peltier stack was insulated with styrofoam.

Cell D2 was constructed to have a significantly larger cell constant than D1. This was necessary to measure the conductivity of sodium hydroxide solutions $\geqslant$ 5 m*M* in concentration because the detector electronics is incapable of measuring conductance values above 1.3 mS. The cell constant of D1 is 1.0 cm^{-1}. Increasing the cell constant proportionately increases the applicable range of measurement. Cell D2 was constructed by securing two 3 cm long × 1/16 in. O.D. thin wall stainless steel tubing segments to each side of a 10–32 poly(etheretherketone) (PEEK) female compression coupling. The steel tubes serve both as the flow conduit and the measuring electrodes. Both cells are connected to the Dionex CDM-II electronics module through a switchbox which allows either cell to be read. The cell constant of D2 was measured to be *ca.* 14 cm^{-1} at 25°C. During conductivity calibrations of sodium hydroxide solutions, the temperature compensation feature of the detector electronics was disabled. During chromatographic use, however, the conductance measured with D2 is temperature-compensated by the thermistor located in the serially connected D1 cell. It is possible to modify the electrode connections to cell D1 itself to greatly increase the

effective cell constant. Using the two original electrodes in common as one electrode and the cell grounding block as the other electrode results in a cell with an effective cell constant of *ca.* 320 cm^{-1}. Cell D2, however, has a very low flow resistance and, when terminated with the proper fittings, it can be used between the pump and the injector at eluent pressures commonly encountered in IC.

Corrections to the CDM readouts are necessary at high conductance values. Made for use in suppressed IC, the detector is optimized for the 0–200 μS range. The necessary correction is very significant at conductance levels above 1 mS. Note that this correction pertains to the apparent conductance values and not to the specific conductance values. Thus with two cells of different cell constants connected in series, it is possible to evaluate the necessary correction factors by noting the ratio of the apparent conductance values read by D1 and D2 under the following conditions: (a) when both read < 200 μS and (b) when the concentration is increased further to explore the full range of the detector readout with cell D1 without exceeding a reading of 200 μS with cell D2. Assuming that the ratio of the cell constants is independent of the measured conductance it is now possible to arrive at the correction factors necessary to correct the detector reading at high conductance readouts. Interpolation through a second degree polynomial fit was used in this work to arrive at the correction factors.

RESULTS AND DISCUSSION

Concentrations of sodium hydroxide by conductance measurements

Should the present method of electrochemical eluent generation eventually enjoy widespread use, it may not be necessary to specify eluent concentrations *per se* to describe a given chromatographic condition. For a faradaically efficient generator, specification of the product flow-rate and current automatically specifies the generated concentration. To characterize generators with less than faradaic efficiency, the actual concentration generated at a given current must be known. An on-line measurement of the generated eluent concentration is also a good diagnostic tool for overall system behavior and is most easily accomplished in the present case with conductance measurements. Measuring such high specific conductance values does not require particularly sophisticated electronics and a dedicated detector can be provided. In general, however, it is not necessary to continuously monitor the eluent concentration during chromatography. The detector cell of a large cell constant to measure the eluent concentration can be simply switch-multiplexed to the chromatographic detector electronics. The results of the conductivity calibrations are shown in Fig. 4a as linear and in Fig. 4b as log–log plots. These data show that a significant deviation from linearity is observed at higher concentrations. Insofar as the temperature dependence is concerned, a comparison of Fig. 4a and b shows that although on an absolute scale the conductivities increasingly diverge from each other at higher concentrations, on a relative scale the conductivities maintain essentially the same relationship as a function of temperature, regardless of the concentration. The nonlinear dependence of the conductance on concentration at any given temperature is satisfactorily represented at each temperature by a quadratic equation and these are presented in Table I. It should be noted that the specific conductance values as reported in this work and as represented by the equations in Table I differ significantly,

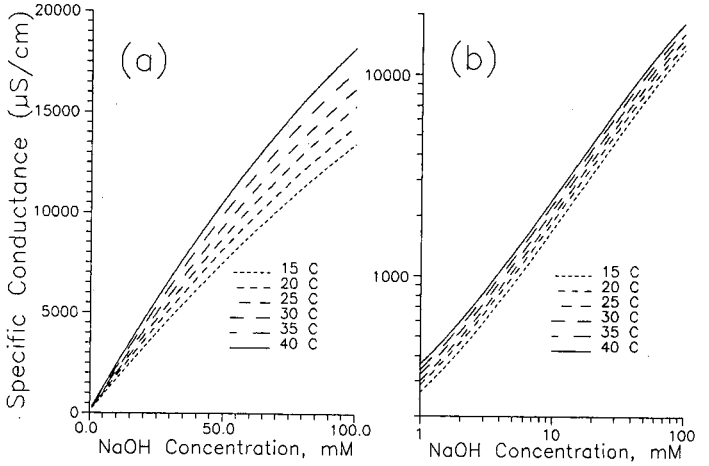

Fig. 4. Specific conductance of sodium hydroxide solutions as a function of temperature and concentration shown in (a) linear and (b) logarithmic plots.

especially at higher concentrations, from conductance values calculable from equivalent conductance data reported for sodium hydroxide solutions at 18°C in standard compilations [21]. Whether this is due to intrinsic differences between conductance measurements in static and flowing situations [22], the presence of impurities or the failure in our case to fully correct for the error in the readout at high conductance values could not be established with certainty. Realistically, a user interested in the absolute accuracy of such calibrations and wishing to use a different conductance detector for this purpose will likely need to perform his own calibrations, given the general inability of chromatographic conductivity detectors to produce reliable values with high conductance solutions. Nevertheless, the temperature-dependence data represent a relative measurement and are expected to be valid, regardless of the absolute accuracy. Fig. 5 shows the specific conductance of sodium hydroxide solutions of different concentrations as a function of temperature. As may be evident, the

TABLE I

COEFFICIENTS OF QUADRATIC EQUATION DESCRIBING SPECIFIC CONDUCTANCE OF NaOH

Specific conductance = $A_0 + A_1$[NaOH, mM] + A_2[NaOH, mM]^2.

Temperature (°C)	Coefficient		
	Zero degree, A_0	First degree, A_1	Second degree, A_2
15	99.4	164.3	−0.3090
20	106.1	181.6	−0.3936
25	106.9	193.9	−0.4179
30	116.8	207.5	−0.4679
35	118.5	222.4	−0.5244
40	126.1	236.3	−0.5533

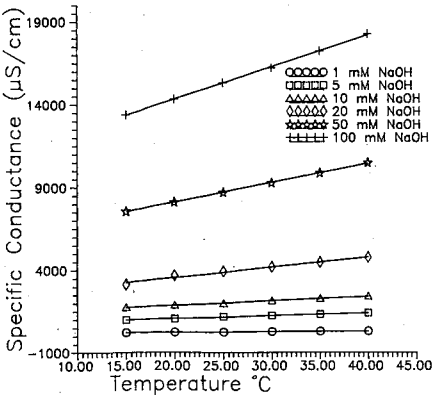

Fig. 5. Specific conductance of sodium hydroxide solutions of individual concentrations as a function of temperature.

data indicate a linear dependence on temperature. Temperature dependence is often expressed as a percent dependence per °C, although such results are clearly dependent on the reference temperature. Referred to 25°C, the data in Fig. 5 represent a temperature dependence of 1.34 ± 0.12%/°C.

The EDGs and EDS: operation and performance. Fig. 6 shows the generated product concentrations and the suppressed product conductances as a function of the generator current. All data were obtained with a feed of 250 m*M* sodium hydroxide flowing at 2 ml/min. The suppressor current was optimized for each generator current, typically requiring 110–120% of the faradaic transport current. For reasons not fully understood, a large excess of suppressor current not only leads to greater baseline noise but the background conductance actually increases as well. Otherwise, as Fig. 6 shows, the background conductance remains 300–400 nS/cm, regardless of the generated eluent concentration. Even when pure water is input to the EDS in place of

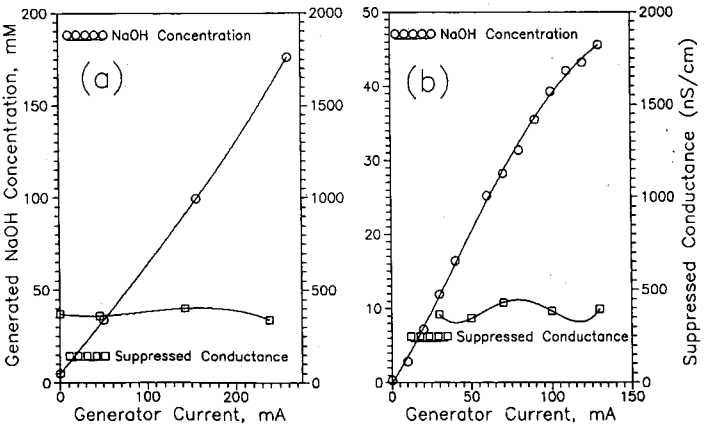

Fig. 6. Generated product concentration as a function of current and the corresponding EDS suppressed conductance for (a) type 1 and (b) type 2 generator. The circles and squares pertain in each case to the left and right ordinate, respectively.

sodium hydroxide, the specific conductance measured by the detector in the presence of a finite amount of current flow (*ca.* 35 mA) is 150–200 nS/cm. Whether this elevation over the theoretical specific conductance of water (*ca.* 60 nS/cm) arises within the suppressor due to electrochemical degradation of some wetted part or results from the permeation of carbon dioxide into the water as it is pumped and transferred to the EDS through Tefzel tubing (see below), is not clear; however, even without any current, the background conductance can not be reduced below *ca.* 100 nS/cm.

The current efficiency of the type 1 generator is excellent; the results shown in Fig. 6a correspond to a linear relationship ($r = 0.999$) with a slope of 0.657 ± 0.024 mM/mA, essentially indistinguishable from the faradaic value of 0.625 mM/mA (at the operative flow-rate of 1 ml/min). With the specific donor concentration used, this device will easily generate 250 mM sodium hydroxide at 1 ml/min. In contrast, the maximum current efficiency of the type 2 device, 0.419 mM/mA, is reached around a current of 60 mA and decreases thereafter. At currents above 100 mA, the product concentration begins to level off. Currents above 130 mA are not practical as gas appears in the product. The 0–260 mA current range in the type 1 device is attained with an applied voltage $\leqslant 3.55$ V while it requires up to 11 V to pass 130 mA through the type 2 device.

The most critical requirement of the overall system appears to be the purity of the water fed to the EDG since, after addition of sodium hydroxide in the generator and its removal in the suppressor, the conductivity of the original water (plus whatever adventitious impurity manages to find its way in) is registered by the detector. The purity of the water which flows as anolyte and catholyte through the EDS is not as critical. Water, originally of resistivity 12 M$\Omega \cdot$ cm, kept in a 4-l polyethylene bottle is adequate even after standing for 2–3 days. The specific recirculating water polisher used exhibits significant pump pulsations and if this is directly connected to the EDS, a baseline noise of related frequency is observed; a pneumatically pressurized water source was therefore preferred. Regarding the feed sodium hydroxide, the donor concentration can be the same as the maximum concentration the generator is expected to deliver but delivered at twice the generated eluent flow-rate. The feed reservoir used in this work was a heavy wall polyethylene container and it was necessary to replace the feed solution every 3–4 days for optimum performance. Apparently within such a period, sufficient carbon dioxide is absorbed through the polyethylene walls to cause an observable rise in the suppressed conductance due to the less than perfect anion rejection by the generator anode membrane. In a similar vein, a donor concentration greater than that necessary compromises the suppressed conductance due to the higher concentration of impurity anions in the donor. Also, with greater donor concentration there is greater zero current penetration of sodium hydroxide through the generator membrane. This means a higher minimum eluent strength with no current applied to the generator. When the donor concentration is reduced to 75 mM, the zero current eluent concentration is *ca.* 0.1 mM sodium hydroxide. All the above factors suggest that the minimum donor concentration be used.

Chromatography

Enhanced sensitivity to carbonate. the first striking feature of this system is its sensitivity for carbonate. Conventional suppressed IC displays relatively poor sensitivity for carbonate; innovative post-column measures were taken by Tanaka and

Fritz [23] to improve the detectability of eluite carbon dioxide in a water eluent ion-exclusion chromatography system. It may be calculated that pure water in equilibrium with atmospheric carbon dioxide contains *ca.* 13 μM total dissolved carbon dioxide. Due to the ubiquity of atmospheric ammonia, the total dissolved carbon dioxide in a water sample exposed to the atmosphere may be somewhat higher. Indeed, even if an aqueous sample is strongly acidic, *ca.* 11 μM carbon dioxide will be dissolved in it at equilibrium. In pure water, a solution of carbon dioxide is *ca.* 11 μM carbon dioxide (aq.) and *ca.* 2 μM each H^+ and HCO_3^-. In suppressed IC many other samples are detectable at these concentrations. Carbonate, however, is normally invisible. With a carbonate eluent, the suppressed product already has *ca.* 5 mM total carbon dioxide species and the addition of 13 μM more to this system has little effect on the equilibrium which is already shifted greatly toward the associated and non-conductive carbon dioxide (aq.). With a 30-mM hydroxide eluent prepared from 50% sodium hydroxide stock containing 0.17 mol% carbon dioxide, there is minimally 50 μM carbonate, not counting the carbon dioxide contribution of the diluent water. The dissociation of the carbonic acid produced from this source seriously masks the response to any carbon dioxide present in the sample. In the present system, the carbon dioxide content of the eluent is minimally 30-fold lower than that of a typical hydroxide eluent system [18] and small amounts of carbonate/dissolved carbon dioxide in a sample should be much more easily detected.

The great sensitivity of the system to carbon dioxide is a mixed blessing. In ultratrace analysis, carbon dioxide will invariably show up as a major peak. This is illustrated in the chromatogram of Fig. 7. At concentrations of analyte ions of interest below *ca.* 1 μM, unless chromatographic conditions are carefully chosen, a large carbonate peak can significantly overlap the nitrate peak.

Permeation of carbon dioxide through tubing. The permeation of carbon dioxide through Tefzel tubing into water was measured as a function of residence time of the water in the tubing as described in the experimental section. Some results are shown in Fig. 8. The dissolved total carbon dioxide in the tubing was found to be 2.8 and 7.6 μM for 9.5 and 60 min residence times respectively. Assuming the equilibrium sat-

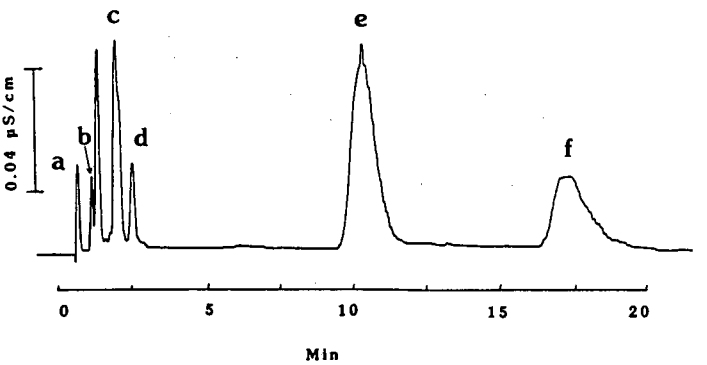

Fig. 7. Low level isocratic chromatogram obtained on the type 2 system. Eluent 39 mM NaOH. a = 1 μM F^-; b = 1 μM NO_2^-; c = 3.5 μM N_3^- + 5 μM SO_4^{2-}; d = 1 μM $C_2O_4^{2-}$; e = 20 μM PO_4^{3-}; and f = 12 μM I^-. The unmarked peak is from CO_2.

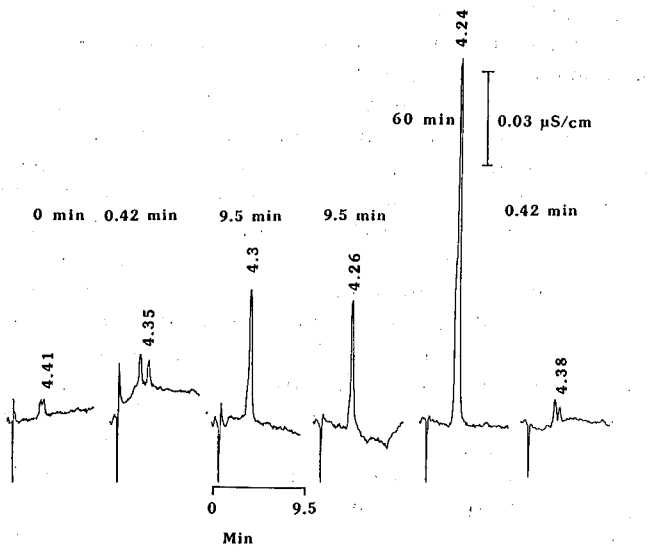

Fig. 8. Chromatograms illustrating the permeation of CO_2 through polymeric tubing with a wall thickness of 0.5 mm. Residence times are indicated.

uration value, C_s of carbon dioxide (aq.) to be 11 μM, the permeation rate of carbon dioxide through the tubing can be modelled as:

$$dC/dt = k(C_s - C') \tag{1}$$

where C', the undissociated carbon dioxide (aq.) in the tubing contents is related to the total dissolved carbon dioxide C, by:

$$C' = C - [-K + (K^2 + 4KC)^{0.5}]/2 \tag{2}$$

where K is the effective dissociation constant of "carbonic acid", $4.4 \cdot 10^{-7}$. Eqns. 1 and 2 were numerically evaluated to obtain the best fit value of the rate constant k to be $4.3 \cdot 10^{-4}$ s^{-1}. Considering that this pertains to a tube of 0.5 mm wall thickness and 0.5 mm internal diameter, the rate of carbon dioxide accumulation for short exposure times, *ca.* 0.3 μM/min, is remarkably large and emphasizes the need for the careful selection of the container and conduit material and minimizing residence times wherever possible if freedom from carbon dioxide contamination is to be maintained.

Strong acid anions —Response linearity and retention reproducibility. Linearity of response in suppressed IC at low concentrations is of considerable interest. This was determined for Cl^-, NO_3^- and SO_4^{2-} in the 0.03–100 μM concentration range. The linear coefficients of determination, r, were 0.998, 0.999 and 0.999, respectively. The slightly worse result for chloride indicates the difficulty of preparing this standard at low concentrations without contamination rather than any intrinsic non-linearity. The respective relative standard deviation of the slopes of the calibration lines were

1.4, 1.1 and 0.4%. The absolute retention times for the test ions are quite reproducible; mean absolute retention times (± S.D.) were: 2 (0.01), 6.01 (0.14) and 7.61 (0.06), respectively. The retention of nitrate is known to be partially controlled by hydrophobic interactions and as such is more susceptible to thermal effects; this is atypical.

Miscellaneous chromatographic applications. The excellent overall sensitivity of the system and facile gradient analysis led us to explore some unusual samples. Fig. 9 shows a series of gradient chromatograms. From bottom up, we progress through a system blank (which identifies the carbon dioxide still present in the system), an injection of water (residual chloride in this water is just visible), a dilute carbonate standard and the breath of a pipe smoker (one tidal volume exhaled through *ca.* 2 ml water). A comparison of these with a standard containing chloride and sulfate and a similar standard "spiked" with the exhaled air clearly shows that precursors to chloride and sulfate are present in the breath sample. The presence of metabolic hydrochloric acid is logical but whether the agent responsible for the sulfate peak is aerosol sulfate or gaseous sulfur dioxide is uncertain. At the levels involved, sulfite originally formed from dissolved sulfur dioxide is expected to be rapidly oxidized to sulfate, before or during chromatography.

Because the residual acidity in the EDG/EDS system is so low it seems likely that a variety of weak acid anions will give better conductometric response because of their greater dissociation at the detector compared to that in a carbonate or conventional sodium hydroxide system. This hypothesis was tested in a general way by

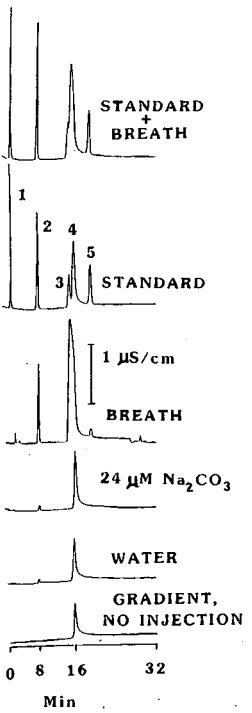

Fig. 9. Breath analysis. 1 = F^-; 2 = Cl^-; 3 = NO_3^-; and 4 = SO_4^{2-}; 30 μM each in the standard.

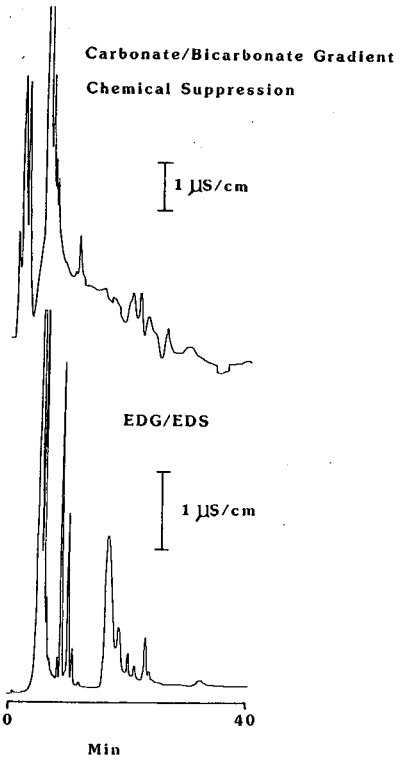

Fig. 10. Pipe smoke extract chromatograms. See text for details.

exhaling one tidal volume of pipe tobacco smoke through water as above and the resultant solution analyzed by IC, both with gradient EDG/EDS and gradient carbonate systems. The respective gradients were formulated to have very similar temporal elution strengths as judged by the retention times of the ions in a standard containing F^-, Cl^-, NO_3^- and SO_4^{2-}. Due to the considerable baseline rise involved in the carbonate gradient run, a blank baseline subtraction technique [24] was performed with this eluent. The results are shown in Fig. 10. Peaks eluting after *ca.* 15 min are difficult to demarcate in the carbonate run. These peaks are less numerous and of lower height even when the unsubtracted chromatogram is carefully examined, compared to the EDG/EDS run. The integrator identified 33% more peaks in the EDG/EDS run compared to the carbonate run.

CONCLUSION

An ultrapure sodium hydroxide generation system coupled with electrodialytic suppression affords an ion chromatographic system of unusual purity with respect to contamination by carbonate and ions derived from penetration of a chemical regenerant into the suppressed eluent. Freedom from carbonate results in much greater sensitivity for this ion while the general rejection of anions in the generator and lack

of acid regenerant bleed into the suppressed eluent (*ca.* 1.5 μM H^+ with 12.5 mM sulfuric acid) apparently allow for greater dissociation of and sensitivity for weak acids with pK_a values in the range 5–7.

The system was operated both in isocratic and gradient modes for several months. After stabilizing a new generator membrane by operating at various currents for *ca.* 3 h, the generated eluent concentration and resulting analyte retention times are repeatable on a day-to-day basis to better than *ca.* 3%. If the actual eluent concentration is conductometrically monitored, even better performance can be obtained.

ACKNOWLEDGEMENTS

We thank E. L. Loree (Bern Tech-Lite) for the design and fabrication of the flow-through thermostatic device, J. L. Lopez for the design, fabrication and programming of the programmable current generator and K. Friedman (Dionex) for helpful discussion. This research was supported by the US Department of Energy, through DE-FG05-84-ER13281 and by the Dionex Corporation. However, this manuscript was not subjected to review by the above agencies and no endorsements should be inferred. C.U.J. also thanks Soonchunhyang University for financial support.

REFERENCES

1 H. Small, *Ion Chromatography*, Plenum, New York, 1989, p. 170.
2 S. W. Downey and G. M. Hieftje, *Anal. Chim. Acta*, 153 (1983) 1.
3 L. J. Galante and G. M. Hieftje, *Anal. Chem.*, 59 (1987) 2293.
4 H. Shintani and P. K. Dasgupta, *Anal. Chem.*, 59 (1987) 1963.
5 L. J. Galante and G. M. Hieftje, *Anal. Chem.*, 60 (1988) 995.
6 T. Takeuchi, E. Suzuki and D. Ishii, *Chromatographia* 25 (1988) 582.
7 P. K. Dasgupta, *J. Chromatogr. Sci.*, 27 (1989) 422.
8 J. J. Conboy, D. J. Henion, M. W. Martin and J. A. Zweigenbaum, *Anal. Chem.*, 62 (1990) 800.
9 Y. Hanaoka, M. Takeshi, S. Muramoto, M. Tamizo and A. Nanba, *J. Chromatogr.*, 239 (1982) 537.
10 S. Rokushika, Z. L. Sun and H. Hatano, *J. Chromatogr.*, 253 (1982) 87.
11 S. Rokushika, Z. Y. Qiu and H. Hatano, *J. Chromatogr.*, 260 (1983) 81.
12 P. K. Dasgupta, R. Q. Bligh, V. D'Agostino and J. Lee, *Anal. Chem.*, 57 (1985) 253.
13 S. Gupta and P. K. Dasgupta, *J. Chromatogr. Sci.*, 26 (1988) 34.
14 T. Ban, T. Murayama, S. Muramoto and Y. Hanaoka, Yokagawa Electric Works, *U.S. Pat.*, 4 403 039 (1983).
15 K. H. Jansen, K. H. Fischer and B. Wolf, Biotronik Wissenschaftliche Geraete, *U.S. Pat.*, 4 459 357 (1984).
16 Z. W. Tian, R. Z. Hu, H. S. Lin and J. T. Wu, *J. Chromatogr.*, 439 (1988) 159.
17 D. L. Strong and P. K. Dasgupta, *Anal. Chem.*, 61 (1989) 939.
18 D. L. Strong, P. K. Dasgupta, K. Friedman and J. R. Stillian, *Anal. Chem.* 63 (1991) 480.
19 D. L. Strong and P. K. Dasgupta, *J. Membr. Sci.*, 57 (1991) 321.
20 J. R. Stillian, *LC Mag.*, 3 (1985) 802.
21 J. A. Dean (Editor), *Lange's Handbook of Chemistry*, McGraw-Hill, New York, 13th ed., 1969, pp. 6–42.
22 S. R. Palit, *Proc. Ist Australian Conference on Electrochemistry, Sydney 1963*, Hobart, Tasmania, 1965, p. 711.
23 K. Tanaka and J. S. Fritz, *Anal. Chem.*, 59 (1987) 708.
24 H. Shintani and P. K. Dasgupta, *Anal. Chem.*, 59 (1987) 802.

Journal of Chromatography, 546 (1991) 175–187
Elsevier Science Publishers B.V., Amsterdam

CHROMSYMP. 2092

Review

Detection in ion chromatography

ROY D. ROCKLIN
Dionex Corporation, 1228 Titan Way, Sunnyvale, CA 94088-3603 (U.S.A.)

ABSTRACT

Species determined by ion chromatography are nearly all ionic, so that conductivity detection has become the workhorse detector. However, there are several other important types of detectors which offer major advantages for determining many species by ion chromatography. These include other forms of electrochemical detection, specifically d.c. and pulsed amperometry, as well as optical methods of absorbance and fluorescence. Using these forms of detection, nearly all forms of ionic species can be detected, ranging from inorganic ions to carbohydrates and peptides. In this paper, the factors to be considered when selecting a detection method are reviewed, for example, the properties of different classes of ions which make them amenable to a specific form of detection.

CONTENTS

1. INTRODUCTION

Ion chromatography is a form of high-performance liquid chromatography (HPLC). Its true definition is a matter of debate. A good definition is that ion chromatography is simply the liquid chromatography of ions, implying that any HPLC separation and detection method can be used and still be called ion chromatography. Regardless of which definition one accepts, ion chromatography is

0021-9673/91/$03.50

clearly more than just ion-exchange chromatography with conductimetric detection. All the detectors commonly used in HPLC are now used in ion chromatography. Although the conductivity detector is probably the most popular, other forms of detection each have specific advantages for different types of analytes.

The main detection methods which have proven to be useful can be classified as either electrochemical or optical. They include the following: *Electrochemical*: conductimetric, d.c. amperometric, pulsed and integrated amperometric, and potentiometric. *Optical*: photometric (UV–visible absorbance), photometric following post-column derivatization, indirect photometric, fluorescence, and refractive index. In addition to the expansion of the separation and detection methods considered part of ion chromatography, the original application (the determination of inorganic ions) has expanded to include organic ions as well. Not only are strong acid inorganic anions, such as chloride and sulfate, determined by ion chromatography, but nowadays organic ions such as sulfonates and carboxylic acids are also included. Even carbohydrates (which are only ionic above pH 12) are determined by ion chromatography, although the detection method is pulsed amperometric instead of conductimetric. The increase in the number and types of ions determined has highlighted the need for many detection methods.

This article reviews the advantages of each detection method when applied to the detecton of ionic species.

2. ELECTROCHEMICAL DETECTION METHODS

Of the four types of electrochemical detection listed above, conductimetric detection and the forms of amperometric detection have in common the fact that voltage (or a voltage waveform) is applied to electrodes in a low-volume flow-through cell and that the current is measured. Potentiometric detection is different in that the potential of an ion-specific electrode is measured.

2.1. Conductimetric detection

This detection method is based on the application of an alternating voltage, E, to the cell electrodes and the measurement of the cell current, i, which is directly proportional to the conductance, G, of the solution between the electrodes by Ohm's law:

$$G = \frac{1}{R} = \frac{i}{E}$$

The solution conductivity, κ, is the conductance which would be measured in a cell with 1 cm^2 electrodes placed 1 cm apart and is easily calculated from the cell constant.

The measured conductivity is the sum of the individual contributions to the total conductivity of all the ions in solution. This is called Kohlraush's law of independent migration. It can be stated as:

$$\kappa = \frac{\Sigma_i \lambda_i^0 c_i}{1000}$$

where c_i is the concentration of each ion. λ_i^0 is the limiting equivalent conductivity, which is the contribution of an ion to the total conductivity divided by its concentration, extrapolated to infinite dilution. Kohlraush's law is only valid in dilute solutions, generally 1 m*M* or below. However, the concentrations commonly used in ion chromatography are generally dilute enough for the equation to be valid. For example, the equivalent conductivity of 1 m*M* potassium chloride is 146.9. Extrapolated to infinite dilution, the limiting equivalent conductivity is 149.9, a difference of only 2%.

Limiting equivalent conductivities for common ions are listed in Table I. The value of λ_i^0 is dependent on several atomic and molecular parameters. λ_i^0 increases as the charge on the ion increases, and as the ionic mobility increases. Mobility is largely dependent on the size of the ion, with small ions being more mobile than large ions. Therefore, the magnitude of the signal from a conductivity detector will be greatest for small, high-mobility ions with multiple charges, such as sulfate. Mobility, and therefore sensitivity, can be an order of magnitude less for large ions such as long-chain sulfonic acids. The size of the ion includes not only the atomic or molecular diameter, but also the hydration sphere. This explains why fluoride, which has a larger hydration sphere than chloride, also has a lower equivalent conductivity.

A second factor affecting detector response is the extent of the dissociation of the ion. Protonation of a weak acid has the effect of lowering the net ionic charge. If a monoprotic weak acid is 50% protonated (*i.e.* the eluent pH is the same as the acid's pK_a), then the effective charge on the ion will be one-half, and the conductivity will be about one-half that of the fully dissociated ion. In addition to strong acid inorganic anions such as chloride and sulfate, all sulfonic, phosphonic, and carboxylic acids are sufficiently strong acids to be largely dissociated when they enter the detector cell, making conductivity an excellent choice as a detector for these species. A more extensive presentation of the principles of conductivity can be found in Ch. 4 of ref. 1.

During ion-exchange chromatography, the ionic strength of the column effluent is constant after the column void volume has eluted. In an eluting volume containing analyte ions, there must be an equivalent decrease in the eluent concentration. The

TABLE I

LIMITING EQUIVALENT CONDUCTIVITIES IN AQUEOUS SOLUTIONS AT 25°C

In units of S · cm²/equiv. From ref. 3, p. 19.

Anions	λ_i^0	Cations	λ_i^0
OH^-	198	H^+	350
F^-	54	Li^+	39
Cl^-	76	Na^+	50
Br^-	78	K^+	74
I^-	77	NH_4^+	73
NO_3^-	71	Mg^{2+}	53
HCO_3^-	45	Ca^{2+}	60
SO_4^{2-}	80	Sr^{2+}	59
Acetate	41	$CH_3NH_3^+$	58
Benzoate	32	$N(CH_3CH_2)_4^+$	33

analyte ions can be thought of as displacing an equivalent amount of eluent ions. All ions in the solution contribute to conductivity regardless of whether they are analyte ions or part of the eluent. Therefore, maximum sensitivity is produced by maximizing the difference in equivalent conductivity between the analyte and eluent ions. In chemically suppressed ion chromatography [2], this is accomplished by reducing the eluent conductivity to a very low value, either by removing it completely or by neutralizing it. All analytes then produce conductivities greater than the eluent ions displaced, so sensitivity is directly proportional to the conductivity of the ion.

In non-suppressed ion chromatography [3], sensitivity is directly proportional to the difference in equivalent conductivity between the analyte and the eluent ions. If the eluent contains low-conductivity ions such as benzoate and/or phthalate, then sensitivity will increase as the analyte ion's equivalent conductivity is increased. If the eluent contains a high-conductivity ion such as a hydrogen ion (cation exchange), then sensitivity will be greatest for ions of the lowest conductivity. In this case, the detector response is a decrease in measured conductivity, producing a dip instead of a peak. Although there is no fundamental difference between this form of detection and non-suppressed ion chromatography with the eluent conductivity lower than the analyte, it is commonly referred to as *indirect conductimetric detection.*

Taking the factors discussed above into account, conductivity detection has been found to be the optimum detection method for many small inorganic and organic ions, especially those which do not absorb UV light and are difficult to detect by optical means. This includes all strong acid anions such as chloride, nitrate, sulfate and trifluoroacetate; organic sulfates, sulfonates, phosphates and phosphonates. Carboxylates are also strong enough acids to be detected by conductivity following ion-exchange separation [4]. Using indirect detection or ion-exclusion chromatography with suppression, weaker acids such as silicic, carbonic and boric acids may be detected.

Cations detected by conductivity [5] include the strong base inorganic cations: alkali metals and alkaline earths. Nearly all the other inorganic ions commonly considered to be cations are amphoteric, hydrolyzing water to form oxyanions except in highly acidic conditions. Most transition metals fall into this category. Another reason why conductivity detection is not used for transition metals is that selectivity is poor without the addition of chelating agents to the eluent. These are highly conductive and can not be suppressed to adequately low conductivities, so the addition of chelating agents makes conductimetric detection impractical due to poor signal-to-noise ratios. Organic cations are nearly all amines. Quaternary amines are very strong base cations. Aliphatic primary, secondary and tertiary amines are all sufficiently strong bases to be protonated cations under normal separation and detection conditions. Aromatic and heterocyclic amines (analine, pyridine) are weak bases. They can be detected by indirect conductimetric detection, but not by suppressed conductivity. However, since they absorb UV light, direct UV photometric detection avoids a problem common to indirect detection methods: that of high background noise caused by high baseline levels (see ref. 2, section 7.5 for a discussion of the effect of high baselines on background noise).

Conductimetric detection is one of the most useful forms of detection in ion chromatography, being applicable to a wide variety of small organic and inorganic ions. An example of both organic and inorganic ions detected by conductivity is shown in Fig. 1.

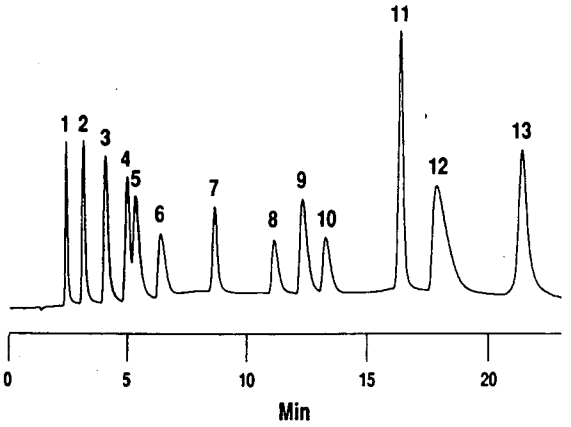

Fig. 1. Alkali metals, alkaline earths and organic amines using gradient elution with suppressed conductivity detection. Peaks: 1 = Li^+; 2 = Na^+; 3 = NH_4^+; 4 = methylammonium$^+$; 5 = K^+; 6 = trimethylammonium$^+$; 7 = diethylammonium$^+$; 8 = triethylammonium$^+$; 9 = piperidinium$^+$; 10 = tetraethylammonium$^+$; 11 = cyclohexylammonium$^+$; 12 = Mg^{2+}; 13 = Ca^{2+}. Column: Dionex IonPac CS-10, 250 × 4 mm cation-exchange column. Eluent: gradient of HCl, 2,3-diaminopropionic acid and CH_3CN at 1 ml/min.

2.2. d.c. Amperometric detection

This detection method is based on the oxidation or reduction (electrolysis) of analyte molecules at the surface of the working electrode in a flow-through cell. A single constant potential is applied to the electrode, and the current is measured directly and reported to the data recording device.

Under the right conditions, any molecule can be oxidized or reduced. However, to be detected by d.c. amperometry, it must be electrolyzed at a lower potential than the components of the mobile phase. If the electrolysis is an oxidation, it must also occur at a lower potential than the oxidation of the working electrode itself. There are several major classes of analytes that fit into this category. The most important are molecules containing aromatic rings substituted with amine or hydroxyl (phenol and catechol) functional groups. Aromatic amines, phenols and catechols have in common the presence of pairs of non-bonding electrons on the nitrogen and oxygen atoms. These are able to shift toward the aromatic ring and stabilize the positive charge resulting from oxidation, making the reaction favorable at a relatively low potential.

The major application of d.c. amperometry is the determination of catecholamine and other biogenic amine neurotransmitters [6–8]. These molecules are cations at both physiological and commonly used mobile phase pH values and are separated by either reversed-phase ion pair or by cation exchange. The amino acid tyrosine is a phenol and can be detected by d.c. amperometry. Also, peptides [9] containing either tyrosine or phenylalanine can be detected. The neurotransmitter serotonin is based on the tyrosine structure and can also be detected. There are other oxidizable organic species. Aromatic amines are easily oxidized [10]. Thiols can be oxidized to disulfides [6]. Examples are glutathione and peptides containing cystein. Ascorbate (vitamin C) [11] and fumarate can also be oxidized. Aromatic nitro compounds [12] are detected by reduction. The electron-withdrawing nitro group stabilizes the negative charge on the aromatic ring.

The mechanism of oxidation for organic molecules is simply the transfer of electrons from the molecules to the electrode. The electrode is otherwise not involved in the reaction and acts as an inert electron sink. Although metal electrodes such as platinum can be used, carbon electrodes have been found to provide the greatest freedom from fouling and the largest resistance to electrode oxidation; *i.e.* the positive potential limit is greatest on carbon. In contrast, most oxidizable inorganic species require more direct involvement of the electrode either as a catalyst or as part of the reaction mechanism. For example, sulfite is oxidized to sulfate at a platinum electrode [13]. The platinum oxide surface of the electrode acts as a catalyst, providing a mechanism for the transfer of an oxygen atom to the sulfite. An example of the electrode being involved in the reaction is the oxidation of iodide at a platinum electrode [14]. The electrode is first dipped into an iodide solution before placing it inside the cell. Iodide becomes adsorbed onto the surface, and is available to form iodine or triiodide during the oxidation of analyte iodide ions.

An important use of an electrode involved in the oxidation reaction is the detection of cyanide [15,16], sulfide [16] and the halides [16] at a silver electrode. In this reaction, it is the electrode itself which is actually oxidized in the presence of these complex or precipitate forming anions, as shown in the reactions below.

$$\begin{aligned} Ag + 2CN^- &\rightarrow Ag(CN)_2^- + e^- \\ 2Ag + S^{2-} &\rightarrow Ag_2S + 2e^- \\ Ag + X^- &\rightarrow AgX + e^- \end{aligned}$$

The chromatogram shown in Fig. 2 was produced using an amperometric detector with a silver working electrode.

Because of the excellent sensitivity and selectivity of d.c. amperometric detection, it is usually the optimum detection method for the analytes discussed above.

Fig. 2. Sulfide (peak 1, 50 ng/ml) and cyanide (peak 2, 100 ng/ml) separated on a Dionex IonPac AS4A 250 × 4 mm anion-exchange column using d.c. amperometric detection at a silver working electrode, E_{app} = 0 V *vs.* Ag/AgCl. (Reprinted with permission from Dionex).

2.3. Pulsed and integrated amperometric detection

These detection methods are similar to d.c. amperometric detection in that current resulting from the electrolysis of analyte molecules is measured. They are different from d.c. amperometry in that a repeating sequence of potentials is applied to the working electrode and the current is only measured during a portion of the potential *vs.* time waveform (for a recent discussion of the difference between pulsed and integrated amperometry, see ref. 17). The purpose of using a repeating potential waveform is to clean the surface of the working electrode electrochemically, thereby providing a reproducible surface for the detection of analytes. This is only necessary for those analytes whose oxidation products coat and poison the surface of the electrode, preventing further detection. These analytes are carbohydrates [18–21], alcohols [22], glycols and aldehydes [23]; amines (primary, secondary and tertiary) [17]; and most sulfur species [17] such as thiols, the exception being fully oxidized sulfur species such as sulfate, organic sulfates, sulfonates, and sulfones.

It is interesting that carbohydrates, which are not usually considered ionic species, are anionic at the high pH used for detection, while amines, which are cations at neutral pH, must be deprotonated, neutral molecules to be detected. However, all of the species detected by pulsed and integrated amperometry are separated using ion-exchange resins, so this detection method should be considered an ion chromatographic method.

The major purpose of pulsed and integrated amperometry is to provide a sensitive and selective detection method for certain aliphatic organic molecules which do not absorb UV light and are therefore difficult to detect by other means. Aliphatic amines can also be detected by conductivity, with comparable sensitivity. However, the only other direct detection methods for carbohydrates are refractive index and low-wavelength UV absorbance. Both methods are very non-selective and have only moderate sensitivity. With pulsed amperometric detection, sensitivity and selectivity are excellent, as seen in the chromatogram shown in Fig. 3.

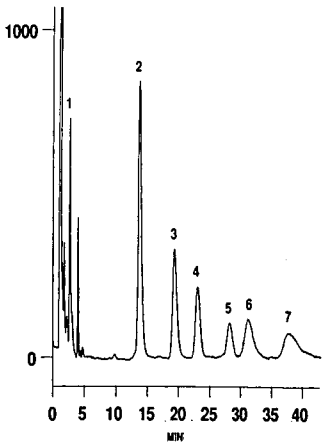

Fig. 3. Carbohydrates in instant coffee with pulsed amperometric detection at a gold working electrode. Peaks and concentrations in ppm: 1 = mannitol 21; 2 = arabinose 140; 3 = galactose 76; 4 = glucose 44; 5 = xylose 26; 6 = mannose 51; 7 = fructose 93. The eluent was 15 m*M* NaOH from 0–1 min, deionized water after that, flowing at 1 ml/min. Post-column addition of NaOH to 0.15 *M* enabled detection. The column was a Dionex CarboPac PA1 250 × 4 mm anion-exchange column.

2.4. Potentiometric detection

This detection method is based on the measurement of the concentration dependent potential which develops at a metal or ion-selective electrode. When ion-selective electrodes are used without chromatography to measure concentration, the highest degree of ion specificity is desired. When the detection is preceded by chromatography, the separation provides selectivity and a more general degree of detector specificity is useful. A potentiometric detector with wide applicability is that based on a metallic copper electrode [23]. For this detector, the measured electrode potential is dependent on the concentration of cuprous and cupric ions in the solution immediately next to the electrode surface; the dependence being described by the Nernst equation. These concentrations are affected by analytes in solution by several mechanisms:

(1) Complexing agents will consume copper ions. These include amines, the halides, cyanide, and many sulfur species.

(2) Analytes can be reduced at the copper electrode, causing copper itself to be oxidized, increasing the concentration of copper ions in the solution. Reducible ions include iodate, bromate, and chlorate. For these ions, the detector response will be opposite to that of the copper ion-consuming analytes.

(3) If a dilute copper-complexing agent (such as tartrate) is added to the eluent, eluting non-complexing analytes will displace the complexing agent. Non-complexing analytes include nitrate and sulfate. These analytes will also produce inverse peaks.

In addition to the metallic copper electrode, a silver electrode has also been used [24]. The principles of the two electrodes are the same.

Although there has been research published on potentiometric detection in ion chromatography, it has generally not been used as a routine analytical method. Potentiometric detection has the disadvantages of having a somewhat lower sensitivity than conductimetric detection, a slower response time, and a less stable baseline. Perhaps the major reasons why potentiometric detection is not used more commonly is that it possesses no major advantages over other forms of detection, and that there are also no commercial detectors available.

3. OPTICAL DETECTION METHODS

3.1. Photometric detection

This detection method is based on direct measurement of the visible or ultra-violet light absorbance by the analytes (photometric detection following post-column derivatization will be discussed separately). Although all ions absorb light at some wavelength, photometric detection is only useful for those ions with appreciable absorbance above the solvent cutoff wavelength, approximately 200 nm. Although "appreciable absorbance" is a relative term, ions with an extinction coefficient above 1000 can be detected with good or excellent sensitivity. Not all ions fit into this category. In fact, the important ions chloride, sulfate, and the alkali metals and alkaline earths can not be detected by direct absorbance. This was of course the driving force for the development of conductimetric detection. However, many other important ions such as nitrate, iodide, and sulfide can be detected by direct UV absorbance.

The major category of UV-light absorbing ions are aromatic and heterocyclic

acids and amines. These include benzoic acid, benzenesulfonic acid, analine, pyridine, pyrrole, and the numerous *o*-, *m*-, and *p*-substituted derivatives of these molecules. Most have one or more wavelengths of maximum absorbance in the ultraviolet with extinction coefficients between 1000 and 10 000. An example of the use of direct UV absorbance detection for aromatic anions is shown in Fig. 4. UV-light-absorbing inorganic anions and the best wavelengths for detecting them are listed in Table II.

For analytes with strong UV absorbance, direct UV photometric detection provides several advantages compared to conductivity detection. High concentrations of salts from either the sample matrix or the eluent do not interfere with detection. Highly conductive eluents can be used, expanding the list of permissible eluents and thereby increasing the control the user has over the chromatography. Also, a suppressor is not needed.

An example of the use of UV-absorbance detection is the determination of nitrite and nitrate in potassium chloride soil extracts (Fig. 5) [25]. The diluted extracts contain 1% potassium chloride, which greatly overloads both the column and the detector when standard carbonate–bicarbonate eluent is used with conductivity detection. Using UV-absorbance detection allows potassium chloride to be used as the eluent. This matching of the eluent to the sample matrix greatly increases the amount of potassium chloride which may be loaded onto the column, since the form of the resin (chloride) does not need to be converted back to carbonate from the eluent. The same technique can also be used to determine UV-light-absorbing anions in seawater, using sodium chloride as the eluent. Another example is the detection of precious metal cyanides, usually contained in high ionic-strength sample matricies such as mining leachates (Fig. 6).

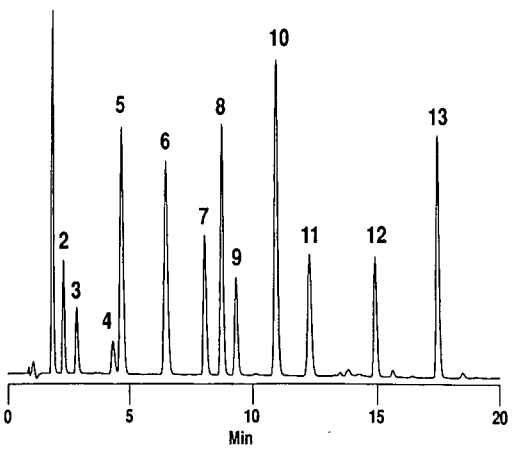

Fig. 4. Anion exchange separation of aromatic anions with direct UV detection at 254 nm. Peaks and concentrations in ppm: 1 = benzoate 40; 2 = benzenesulfonate 40; 3 = *p*-toluenesulfonate 40; 4 = *p*-chlorobenzenesulfonate 40; 5 = *p*-bromobenzoate 20; 6 = 3,4-dinitrobenzoate 10; 7 = phthalate 20; 8 = terephthalate 6; 9 = *p*-hydroxybenzoate 2; 10 = *p*-hydroxybenzenesulfonate 2; 11 = gentisate 10; 12 = trimesate 20; 13 pyromellitate 10 ppm. Column: Dionex OmniPac PAX-100, 250 × 4 mm. Eluent: constant 20% CH_3CN, 1 m*M* NaOH, 0.05–0.4 *M* NaCl gradient in 20 min; 1 ml/min flow-rate. (From ref. 36).

TABLE II

IONS DETECTED BY ABSORBANCE

Wavelengths of maximum absorbance (λ_{max}, nm) and extinction coefficients, ε, for UV-light-absorbing inorganic anions with extinction coefficients greater than 1000. For each anion, approximately 0.1 m*M* of the sodium salt was dissolved in deionized water. For some anions, λ_{max} is below 200 nm. Detection below that wavelength is impractical because of the absorbance of the eluent. However, absorbance above 200 nm is substantial for many of these anions, although absorbance decreases rapidly as wavelength increases. For these anions the optimum detection wavelength is determined by measuring both signal and noise. Extinction coefficients at 200 and 210 nm are listed for those ions with substantial absorbances at those wavelengths. For anions with multiple peaks in the absorbance spectrum, maximum sensitivity is obtained at the wavelength with the greatest extinction coefficient. However, freedom from interferences may be better using a longer wavelength.

Ion	$\varepsilon \times 10^3$ (200 nm)	$\varepsilon \times 10^3$ (210 nm)	$\lambda_{max\ 1}$	$\varepsilon \times 10^3$ ($\lambda_{max\ 1}$)	$\lambda_{max\ 2}$	$\varepsilon \times 10^3$ ($\lambda_{max\ 2}$)	$\lambda_{max\ 3}$	$\varepsilon \times 10^3$ ($\lambda_{max\ 3}$)
AsO_2^-	9.5	5.0						
$AuCl_4^-$ [a]			227	38	313	5.5		
Br^-	8.9	1.9						
BrO_3^-	2.0	1.1						
CrO_4^{2-}			273	3.6	372	4.7		
$Fe(CN)_6^{3-}$	12.3	10.0	260	1.0	303	1.6	420	1.0
I^-			226	12.1				
IO_3^-	17	3.9						
MoO_4^{2-}			207	10.0	227[c]	5.1		
N_3^-	6.0	1.7						
NO_2^-		5.2	209	5.2				
NO_3^-	9.3	7.8						
HS^- [b]			230	8.0				
SCN^-	5.1	3.2	215	3.1				
$S_2O_3^{2-}$	2.8	3.5	215	3.8				
SeO_3^{2-}	5.1	2.3						
VO_3^-	6.6	4.3	266	3.4				
WO_4^{2-}	6.7	2.7						

[a] In 100 m*M* HCl.
[b] In 1 m*M* NaOH.
[c] Shoulder.

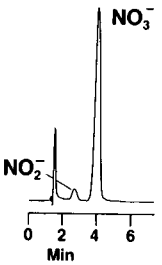

Fig. 5. Determination of 2 ppm nitrite and 38 ppm nitrate in a 10% KCl soil extract using direct UV-absorbance detection at 215 nm. Sample was diluted 1:10, filtered, and injected. Column: Dionex IonPac CS5, 250 × 4 mm. Eluent: 35 m*M* KCl at 1 ml/min. (Reprinted with permission from ref. 25, © 1987, Dionex, Sunnyvale, CA.)

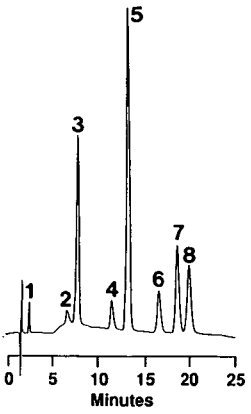

Fig. 6. Separation of metal cyanide complexes with direct UV detection at 215 nm. Peaks (10 ppm each): 1 = Ag(I); 2 = Au(I); 3 = Cu(I); 4 = Ni(II); 5 = Fe(II); 6 = Pd(II); 7 = Co(III); 8 = Pt(II). Gradient of 30–135 m*M* $NaClO_4$ in 18 min with constant 20 m*M* NaCN and 20 m*M* NaOH at 1 ml/min. Column is an IonPac AS5 250 × 4 mm anion-exchange column.

3.2. Photometric detection following post-column derivatization

The most common application of photometric detection following post-column derivatization is the detection of metal ions derivatized with 4-(2-pyridylazo)resorcinol (PAR) [26,27]. The post-column reagent usually contains less than 1 m*M* PAR dissolved in a high pH buffer, such as ammonia–ammonium acetate. The PAR forms a visible-light-absorbing complex with most transition metals with a λ_{max} at 520 nm. This method also works for the detection of lanthanides [28]. Other ions which may be detected in this manner and the post-column reagents used include aluminum derivatized by 4,5-dihydroxy-*m*-benzyenedisulfonic acid (Tiron) [29], Cr(VI) (chromate/dichromate) derivatized by 1,5-diphenylcarbohydrazide [30], and silicate and phosphate derivatized by molybdate [31]. Another application is the detection of polyphosphonate-based sequestering agents using post-column addition of ferric ion [32].

The major advantage of post-column derivatization is that ions may be detected which cannot be detected by any other means. This far outweighs the disadvantages of requiring the addition of a post-column pump and the minor difficulty of ensuring the correct operation of the post-column system.

3.3. Indirect photometric detection

This detection method is based on the decrease in absorbance of eluent ions during elution of analyte ions in ion-exchange chromatography [33]. Any ions which *do not* absorb UV light at the detection wavelength may be detected. As described earlier in regards to inverse conductimetric chromatography, the ionic strength of the column effluent is constant following elution of the column void volume. Therefore, the eluent concentration must decrease in an amount equivalent to the eluting analyte concentration, so eluting analytes cause a decrease in the absorbance background and are recorded as dips instead of peaks. This technique is called *indirect photometric chromatography*. It is nearly as sensitive as conductimetric detection. The major disadvantage is that detection is accomplished against a high background. Any factors

affecting the background absorbance, such as pump pulsations and temperature fluctuations, will produce noise at the detector. Another disadvantage, common to non-suppressed conductimetric detection, is the presence of system peaks (see ref. 2, section 4.4.5).

For anion exchange, useful UV-light-absorbing eluents include low millimolar concentrations of nitrate, benzoate and phthalate. For cation exchange, cupric ion may be used.

3.4. Fluorescence detection

In ion chromatography, fluorescence detection is rarely used as a direct detection method since very few ions fluoresce (exceptions include Ce^{IV} and U^{VI}). If one stretches the definition of ion chromatography, then the fluorescence detection of proteins separated on ion-exchange columns could be considered. However, for small ions, fluorescence detection is only used following post-column derivatization. The major application is the detection of primary amines following derivatization with *o*-phthalaldehyde and 2-mercaptoethanol. This is an extremely sensitive method, and has been used for many years to detect amino acids [34]. Since the reaction is specific to primary amines, selectivity is exceptional. Although it is not commonly used for other primary amines, there is no reason why it should not be. There are many other organic molecules containing primary amines that are difficult to detect by other means, such as direct UV absorbance. These include numerous pharmaceutical compounds such as aminoglycoside antibiotics.

3.5. Refractive index detection

A general, non-selective detection method commonly used in HPLC is refractive index detection. Because of its only moderate sensitivity, poor selectivity, and sensitivity to baseline fluctuations, it is rarely used in ion chromatography. Also, nearly all ions can be detected by one or more of the methods discussed above. One report in the literature of refractive index (RI) detection used in ion chromatography is the detection of polyphosphonate sequestering agents [35].

4. CONCLUSIONS

Of the many forms of detection used in ion chromatography, conductimetric detection is still the most useful. However, all of the detection methods commonly used in HPLC are also applicable to ion chromatography. In particular, amperometric and photometric detection methods are especially important. New detection methods, some first developed for HPLC, are being used in ion chromatography. For example, a powerful method now being developed is ion chromatography–mass spectroscopy. Ion chromatographic separation may also be coupled with atomic spectroscopy, providing exceptional selectivity for metals. Detection methods used in ion chromatography have come a long way since the days of the first publications.

REFERENCES

1 J. A. Plambeck, *Electroanalytical Chemistry: Basic Principles and Applications*, Wiley, New York, 1982.
2 H. Small, *Ion Chromatography*, Plenum, New York, 1989.

3 D. T. Gjerde and J. S. Fritz, *Ion Chromatography*, Hüthig, Heidelberg, Basel, New York, 2nd ed., 1987.
4 R. D. Rocklin, R. W. Slingsby and C. A. Pohl, *J. Liq. Chromatogr.*, 9 (1986) 757.
5 R. D. Rocklin, M. A. Rey, J. R. Stillian and D. L. Campbell, *J. Chromatogr. Sci.*, 27 (1989) 474.
6 D. Radzik and S. M. Lunte, *CRC Crit. Rev. Anal. Chem.*, 20 (1989) 317.
7 P. T. Kissinger, *J. Chromatogr.*, 488 (1989) 31.
8 H. Parvez, M. Bastart-Malsot, S. Parvez, T. Nagutsu and G. Carpentier (Editors), *Progress in HPLC, Vol. 2, Electrochemical Detection in Medicine and Chemistry*, VNU Science Press, Utrecht, 1987.
9 J. T. Bretz and P. R. Brown, *J. Chromatogr. Sci.*, 26 (1988) 310.
10 D. M. Radzik, Ph.D. Thesis, Purdue University, West Lafayette, IN, 1984.
11 H. Kim, *J. Assoc. Off. Anal. Chem.*, 72 (1989) 681.
12 W. A. Jacobs and P. T. Kissinger, *J. Liq. Chromatogr.*, 5 (1982) 881.
13 H. Kim, *J. Assoc. Off. Anal. Chem.*, 73 (1990) 216.
14 K. Han, W. F. Koch and K. W. Pratt, *Anal. Chem.*, 59 (1987) 731.
15 Y. Liu, R. D. Rocklin, R. J. Joyce and M. J. Doyle, *Anal. Chem.*, 62 (1990) 766.
16 R. D. Rocklin and E. L. Johnson, *Anal. Chem.*, 55 (1983) 4.
17 D. C. Johnson and W. R. LaCourse, *Anal. Chem.*, 62 (1990) 589A.
18 M. R. Hardy and R. R. Townsend, *Proc. Natl. Acd. Sci.*, 85 (1988) 3289.
19 M. R. Hardy, R. R. Townsend and Y. C. Lee, *Anal. Biochem.*, 170 (1988) 54.
20 J. D. Olechno, S. R. Carter, W. T. Edwards and D. G. Gillen, *Anal. Biotechnol. Lab.*, 5 (1987) 38.
21 S. Hughes, P. L. Meschi and D. C. Johnson, *Anal. Chim. Acta*, 132 (1981) 1.
22 R. D. Rocklin, in V. Turoski (Editor), *Formaldehyde: Analytical Chemistry and Toxicology*, (*Adv. Chem. Ser.*, No. 210), American Chemical Society, Washington, D.C., 1985, Ch. 2, p. 13.
23 P. R. Haddad, P. W. Alexander and M. Trojanowicz, *J. Chromatogr.*, 321 (1985) 363.
24 J. Lockridge, N. Fortier, G. Schmuckler and J. S. Fritz, *Anal. Chim. Acta*, 192 (1987) 41.
25 *Determination of Nitrite, Nitrate, and Ammonia in KCl Soil Extracts, Application Update No. 118*, Dionex, Sunnyvale, CA, Nov. 1987.
26 R. B. Rubin and S. S. Heberling, *Am. Lab. (Fairfield, Conn.)*, May (1987) p. 46.
27 A. Siriraks, H. M. Kingston and J. M. Riviello, *Anal. Chem.*, 62 (1990) 1185.
28 S. S. Heberling, J. M. Riviello, S. Mou and A. W. Ip, *R&D*, Sept. (1987), p. 74.
29 P. M. Bertsch and M. A. Anderson, *Anal. Chem.*, 61 (1989) 535.
30 *Determination of Cr(VI) in Water, Wastewater, and Solid Waste Extracts, Technical Note 26*, Dionex, Sunnyvale, CA, May 1990.
31 M. E. Potts, E. J. Gavin, L. O. Angers and E. L. Johnson, *LC·GC*, 4 (1986) 912.
32 A. W. Fitchett and A. Woodruff, *LC Mag.*, 1 (1983) 48.
33 H. Small and T. E. Miller, *Anal. Chem.*, 54 (1982) 462.
34 M. Roth, *Anal. Chem.*, 43 (1971) 880.
35 D. Wong, P. Jandik, W. R. Jones and A. Haganaars, *J. Chromatogr.*, 389 (1987) 279.
36 J. R. Stillian and C. A. Pohl, *J. Chromatogr.*, 499 (1990) 249.

Journal of Chromatography, 546 (1991) 189–198
Elsevier Science Publishers B.V., Amsterdam

CHROMSYMP. 2218

Practical applications of solid-phase reagent conductivity detection in ion chromatography

PETER E. JACKSON, PETR JANDIK*, JEANNE LI and JIM KROL
Waters Chromatography Division of Millipore, 34 Maple Street, Milford, MA 01757 (U.S.A.)
GERARD BONDOUX
Millipore S.A., B.P. 307, 78054 St. Quentin en Yvelines Cedex (France)
and
DOUGLAS T. GJERDE
Sarasep, Inc., 1600 Wyatt Drive, Santa Clara, CA 95054 (U.S.A.)

ABSTRACT

The post-column addition of a solid-phase reagent (SPR) is a new detection technique which permits enhanced conductivity detection in ion chromatography. The SPR for anion analysis is a high-capacity, hydrogen-form cation-exchange resin which is added as a suspension to the column effluent. This results in reducing the background conductivity of the eluent while producing an enhanced analyte signal. SPR conductivity detection has the advantages of linear calibration curves, is relatively matrix-independent and, most importantly, it enables conductivity detection to be used in conjunction with relatively broad ionic strength gradients. The parameters which influence SPR detection are discussed and a variety of eluents were investigated for gradient use. The practical utility of gradient separations with SPR conductivity detection is demonstrated for a number of complex anion analyses.

INTRODUCTION

The technique of ion chromatography (IC) has broadened significantly to encompass many separation and detection modes since its introduction in 1975 [1]. Of the detection modes available, conductivity is the most universal and still most widely used [2]. One disadvantage of conductivity detection is that it has historically been difficult to use in conjunction with gradient separations. Gradient IC separations offer the potential to give good resolution of short-chain carboxylic acids from weakly retained anions such as fluoride and chloride, while maintaining reasonable chromatographic run times and peak shapes for later-eluting anions such as sulfate, thiosulfate and chromate. Varying approaches which enable the use of gradient separation and conductivity detection in IC have been reported. Micromembrane suppressor devices permit the use of ionic strength gradients with conductivity detection by minimizing the background conductivity of the eluent before it reaches the detector [3]. Alternatively, isoconductive gradients use two counter cations of different conductivity to balance the conductance of two solutions of different eluting

0021-9673/91/$03.50

strength [4]. Isoconductive gradients are somewhat limited as they can only be operated over a relatively narrow ionic strength range and membrane devices have also been shown to have eluent ionic strength restrictions [5].

It has recently been demonstrated that the post-column addition of a solid-phase reagent (SPR) permits sensitive conductivity detection in IC [6]. The SPR is typically a high-capacity cation-exchange resin in the hydrogen form which is added as a colloidal suspension to the column effluent prior to the conductivity detector. The SPR reacts with the eluent and solute anions producing an eluent stream of low background conductivity and an enhanced analyte response. The SPR itself is minimally conductive and only slightly contributes to the background signal. This technique has the advantages that it allows gradient separations to be used with conductivity detection and it also offers a relatively high degree of matrix independence making it ideal for the analysis of 'difficult' samples. In this paper the parameters which influence SPR detection are discussed and the practical utility of gradient separations with SPR conductivity detection is demonstrated for a number of complex anion analyses.

EXPERIMENTAL

Instrumentation

The liquid chromatograph consisted of a Waters Chromatography Division of Millipore (Milford, MA, U.S.A.) gradient 600 Series pump, a Model 431 conductivity detector, a Model 441 fixed-wavelength UV detector, a pneumatic reagent delivery module (RDM), a Rheodyne 7010 injector and either a Waters 820 or a Waters 840 data station. The analytical column used was either a Waters IC-Pak Anion HR (75 × 4.6 mm I.D.) or a Waters IC-Pak Anion (50 × 4.6 mm I.D.) methacrylate-based anion exchanger.

Reagents

Water (18 MΩ) purified using a Millipore Milli-Q water-purification system (Bedford, MA, U.S.A) was used for all solutions. Analytical-grade boric acid and potassium hydroxide were obtained from Sigma and analytical-grade sodium hydrogencarbonate and sodium carbonate were obtained from Aldrich. Acetonitrile (HPLC grade) was obtained from J. T. Baker, as were the analytical-grade sodium salts used for the preparation of all the anion standards. Eluents were prepared daily, filtered and degassed with a Waters solvent clarification kit.

Solid-phase reagent

The SPR is manufactured by Sarasep (Santa Clara, CA, U.S.A.) and distributed by Waters. The SPR is obtained as a concentrate of about 12% solids with a cation-exchange capacity of not less than 500 mequiv./l. Typically, the concentrate is diluted 1:8 for post-column use with gradients. The conductivity of the diluted suspension ideally should not exceed 20 μS/cm. To eliminate any contaminants, a Waters SPR polisher column is inserted between the RDM and the mixing tee. The SPR polisher column is a strong anion exchanger in the hydroxide form which requires regeneration after about 50 h of continuous use. Regeneration is simply a matter of flushing the column with 10 ml of 100 m*M* potassium hydroxide, then 15 ml of deionized water.

Instrumental configuration for SPR

A basic instrumental configuration for gradient separations with SPR conductivity detection was as previously described [7,8]. The RDM is a standard pneumatic post-column delivery device. The flow-rate of SPR into the eluent stream is determined by the pressure from the air supply to the pneumatic delivery module: typically a flow-rate of 0.5 ml/min is used for SPR addition. The RDM contains a check-valve to prevent accidental introduction of mobile phase into the SPR supply in the pressurized vessel. Careful attention was paid to minimizing tubing lengths in the set-up of the delivery module in order to prevent unnecessary band broadening. Concerns about pumping a 1% solid suspension of submicron particles through the RDM and conductivity detector proved unfounded as no blockage problems occurred provided that the RDM and detector were briefly flushed out with water at the conclusion of each days work.

RESULTS AND DISCUSSION

Eluents for use with gradient SPR conductivity detection

The eluents most commonly used for gradient separations with conductivity detection are carbonate–bicarbonate, hydroxide and borate buffers. Two reactions occur on contact of the SPR with the eluent stream. Considering the case of a bicarbonate eluent, firstly, the eluent co-cations (usually sodium) are exchanged for H^+ from the SPR forming the protonated acid of the eluent anion, *i.e.* H_2CO_3. Secondly, the analyte co-cations are exchanged for H^+ from the SPR producing an enhanced analyte signal. The more basic the eluent anion, the less conductive is the background after reacting with the SPR, *e.g.* the reaction product from SPR with hydroxide is water which has the lowest conductivity, borate is converted to H_3BO_3 while carbonate–bicarbonate is converted to H_2CO_3 as discussed above. This is illustrated in Fig. 1 which shows the effect of the rate of post-column addition of SPR on the peak height of chloride using hydroxide, borate and carbonate–bicarbonate eluents of similar eluting strength. The flow-rate of the eluent was kept constant at 1.0 ml/min. Hydroxide produces the greatest signal, followed by borate, then carbonate as would be expected from the pK_a values of water, H_3BO_3 and H_2CO_3. Fig. 1 also shows that the optimal rate of addition of SPR is between 0.4 and 0.7 ml/min. The net peak height obtained is the sum of three contributions: the total cation-exchange capacity of the SPR added, the dilution of the column effluent resulting from the addition of the SPR and the fact that peak heights are reduced as a result of increasing total flow through the detector.

The three eluents listed above were investigated for use with gradient separations and SPR conductivity detection. Each of the three eluents proved to have their relative advantages and disadvantages. Carbonate–bicarbonate is a mobile phase with good eluting strength which allowed the separation of a wide range of anions. The major drawback was that the SPR reaction product, H_2CO_3, is too strong an acid, therefore a significant baseline shift occured during the course of a gradient run. This behavior has been noted previously and for this reason, carbonate–bicarbonate eluents are not generally favored for use with gradients in IC [2]. A very interesting feature of SPR conductivity detection with carbonate–bicarbonate eluents was the fact that linear calibration curves were obtained for both strong and weak acid

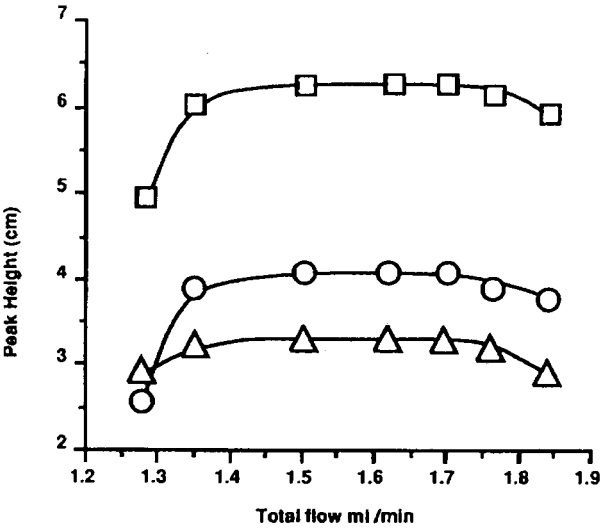

Fig. 1. Dependency of chloride peak height upon the rate of post-column addition of SPR with hydroxide, borate and carbonate–bicarbonate eluents. The ion-exchange capacity of the SPR was constant at 70 mequiv./l. The eluent flow-rate was constant at 1.0 ml/min and the SPR flow-rate was varied between 0.25 and 0.85 ml/min. □ = 15 m*M* KOH; ○ = 50 m*M* H_3BO_4, pH 8.35; △ = 2.8 m*M* $NaHCO_3$–2.2 m*M* Na_2CO_3.

anions. The non-linearity of calibration curves with carbonate–bicarbonate eluents and conventional chemically suppressed conductivity detection has been well documented and it is generally agreed that the non-linearity occurs as a results of variations in the extent of ionization of the suppressed eluent acid, *e.g.* H_2CO_3 [9,10].

Linearity of calibration using SPR conductivity detection was subjected to a test described by Scott [11]. According to that procedure, calibration curves can be considered as linear, if the value of the slope of a logarithmic plot (*i.e.* log peak area *versus* log concentration) remains within the range 0.98–1.02. Chloride and formate were chosen for the linearity evaluation to represent both, weakly and strongly acidic analyte anions. For eight evenly spaced concentrations between 0.05 and 50 ppm the respective slopes of logarithmic plots (logarithmic response factors) for formate and chloride were found to be 0.99394 and 0.99320, respectively. This result, indicating linearity over three orders of magnitude, was somewhat unexpected, and further investigations into the linearity of SPR conductivity detection are currently underway in our laboratory.

Hydroxide is a weak ion-exchange eluent and is particularly suited to the separation of weakly retained anions, however, this requires high eluent concentrations to elute strongly retained anions such as citrate and thiocyanate. This fact has led to problems in the past when using hydroxide gradients with chemically suppressed conductivity detection as suppressor breakthrough may occur before the peaks of interest elute from the column, although the addition of modifiers such as *p*-cyanophenol can reduce the required hydroxide concentration in the eluent [5]. As the ion-exchange reaction for the SPR enhancement is carried out directly in the bulk

liquid phase rather than across a membrane as is the case with suppressor devices, higher ion-exchange capacities can be applied by simply increasing the rate of addition of the SPR or increasing the concentration of the applied post-column reagent. Other problems with hydroxide gradients are that the eluent will readily absorb CO_2 from the atmosphere resulting in baseline drift unless precautions such as helium sparging and the use of ascarite tubes are taken; and very-high-purity hydroxide must be used to minimize accumulation of anionic impurities on the column when operating low-ionic-strength steps in the gradient [2]. Despite the difficulties involved with hydroxide gradients, they permit the most sensitive detection in SPR conductivity, have a rapid re-equilibration time and, as will be shown later, give useful separations, particularly for oxyhalide speciation.

Of the three eluents investigated for use with gradient separations and SPR conductivity detection, borate proved to be the most versatile. It has intermediate eluting strength with a high buffering capacity and can be used for the separation of a wide range of anions. As the SPR reaction product is a weak acid with a pK_a of 9.24, only a relatively small baseline rise is observed during the course of a gradient run. Its use does not require any special precautions and it also has a rapid re-equilibration time between successive gradient runs. Examples of SPR gradient chromatograms are given in the next section of the paper.

Practical applications of gradient SPR conductivity detection

Fig. 2 shows a chromatogram of fluoride through to citrate using a borate gradient with SPR conductivity detection. The early-eluting peaks (fluoride, acetate, formate and chloride) are well resolved with this eluent while strongly retained analytes such as chromate and citrate are eluted within 25 min. The gradient program for this separation is given in Table I. Considering that the gradient is from 10 to 150 m*M* borate, pH 8.3, the baseline rise with this eluent is quite insignificant. Fig. 3 shows a chromatogram of anionic impurities in a diluted synthetic peptide obtained using the same conditions as for Fig. 2. The separation of acetate, chloride and trifluoroacetate is a difficult isocratic separation and the quantitation of these impurities (especially trifluoroacetate) is of importance in the pharmaceutical use of synthetic peptides.

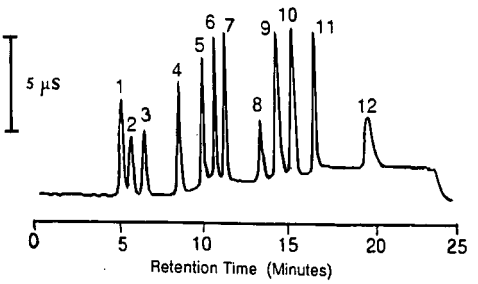

Fig. 2. Gradient separation of anions with borate eluent and SPR conductivity detection. Conditions: column, Waters IC-Pak Anion HR; eluent, 10–150 m*M* borate gradient, pH 8.3 (see Table I for gradient profile); flow-rates, eluent 1.0 ml/min and SPR 0.7 ml/min; injection, 100 μl. Peaks: 1 = fluoride (1 ppm); 2 = acetate (4 ppm); 3 = formate (2 ppm); 4 = chloride (2 ppm); 5 = nitrite (3 ppm); 6 = bromide (4 ppm) 7 = nitrate (4 ppm); 8 = phosphate (6 ppm); 9 = sulfate (4 ppm); 10 = oxalate (10 ppm); 11 = chromate (10 ppm); 12 = citrate (20 ppm).

TABLE I

PROGRAM (WATERS 600 SERIES PUMP) FOR BORATE GRADIENT SEPARATION

Gradient: A = Milli-Q water; B = 200 m*M* sodium borate, pH 8.3.

Time (min)	A (%)	B (%)	Curve[a]
Initial	95	5	–
3.00	95	5	9
9.00	70	30	9
15.00	25	75	10
22.00	95	5	11

[a] Curves 9 and 10 are non-linear (convex) gradient profiles, while curve 11 is a step gradient to return to initial conditions.

Fig. 4A shows a fifteen-anion standard run using a borate gradient with SPR conductivity detection, while Fig. 4B shows the same standard but with UV detection at 214 nm. The UV detector must be placed before the mixing tee when using SPR detection. Such an instrumental configuration is a useful tool, both qualitative and quantitative, for the analysis of samples which contain many analyte peaks at dissimilar levels. This approach was used for the analysis of anions in post-ignition residue from low explosive/pyrotechnic materials. The anion profile in the residue is of interest as it allows different pyrotechnic materials to be distinguished [12]. Fig. 5A shows a chromatogram of a 1:5 dilution of burned Pyrodex Powder with SPR conductivity detection using the same conditions as for Fig. 4, while Fig. 5B shows a chromatogram of a sample with UV detection at 214 nm. The use of a borate gradient in conjunction with a UV and SPR conductivity detection enables the total anion profile of this very complex sample to be characterized in one chromatographic run in under 30 min. Chromatograms obtained for a similar sample, a 1:5 dilution of burned Gopher Gasser, are shown in Fig. 6A and B for SPR conductivity and UV detection,

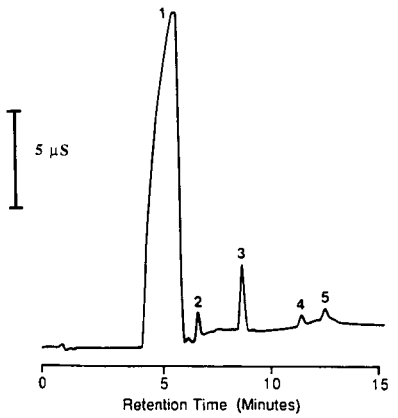

Fig. 3. Gradient separation of anionic impurities in synthetic peptide. Conditions as for Fig. 2. Peaks: 1 = acetate; 2 = chloride; 3 = trifluoroacetate; 4 = phosphate; 5 = sulfate.

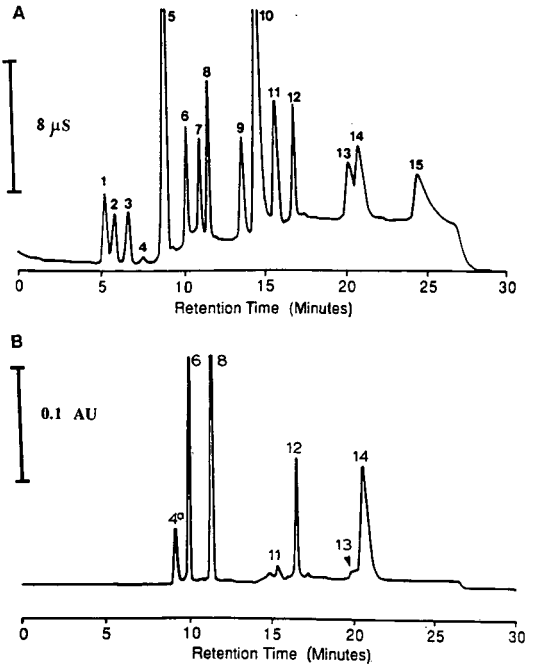

Fig. 4. Gradient separation of a fifteen-anion standard with borate eluent and dual SPR conductivity and UV detection. Conditions as for Fig. 2 except (A) SPR conductivity detection and (B) UV detection at 214 nm. Peaks: 1 = fluoride (1 ppm); 2 = acetate (4 ppm); 3 = formate (2 ppm); 4 = chlorite (4 ppm); 4a = sulfide (4 ppm); 5 = chloride (2 ppm); 6 = nitrite (3 ppm); 7 = chlorate (4 ppm); 8 = nitrate (4 ppm); 9 = phosphate (10 ppm); 10 = sulfate (4 ppm); 11 = oxalate (10 ppm); 12 = thiosulfate (10 ppm); 13 = citrate (20 ppm); 14 = thiocyanate (10 ppm); 15 = perchlorate.

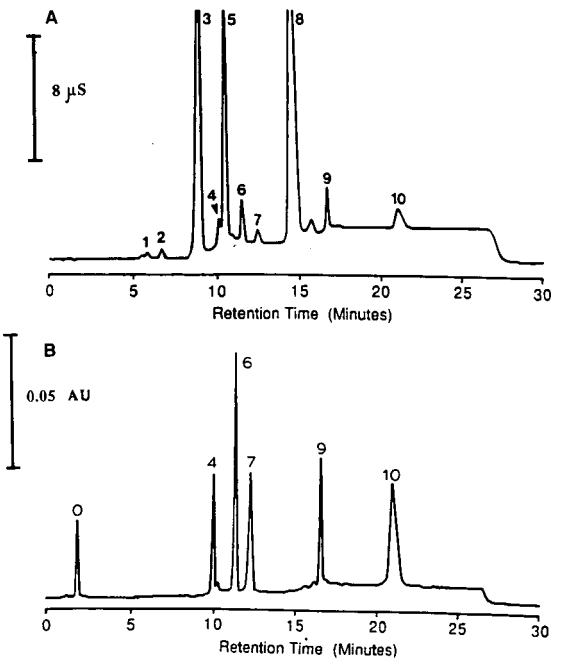

Fig. 5. Determination of anions in burned Pyrodex Powder. Conditions as for Fig. 4 [(A) SPR conductivity detection and (B) UV detection at 214 nm] except sample: 100 μl of a 1:5 dilution of burned Pyrodex Powder. Peaks: 0 = unknown; 1 = acetate; 2 = formate; 3 = chloride; 4 = nitrite; 5 = unknown; 6 = nitrate; 7 = unknown; 8 = sulfate; 9 = thiosulfate; 10 = thiocyanate.

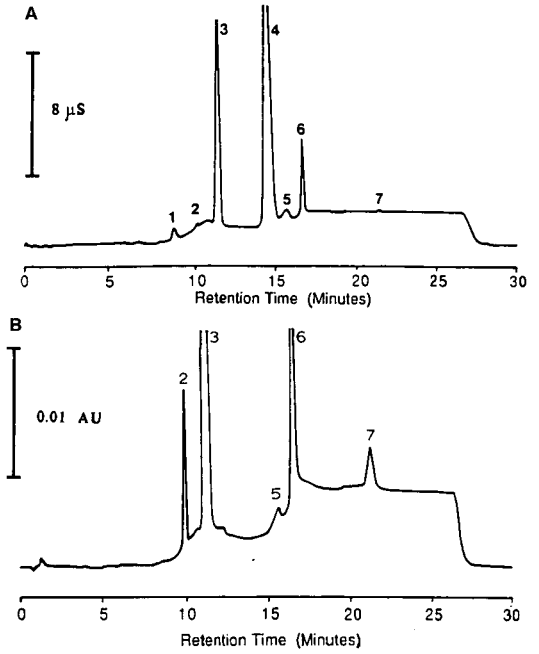

Fig. 6. Determination of anions in burned Gopher Gasser. Conditions as for Fig. 4 [(A) SPR conductivity detection and (B) UV detection at 214 nm] except sample: 100 μl of a 1:5 dilution of burned Gopher Gasser. Peaks: 1 = chloride; 2 = nitrite; 3 = nitrate; 4 = sulfate; 5 = oxalate; 6 = thiosulfate; 7 = thiocyanate.

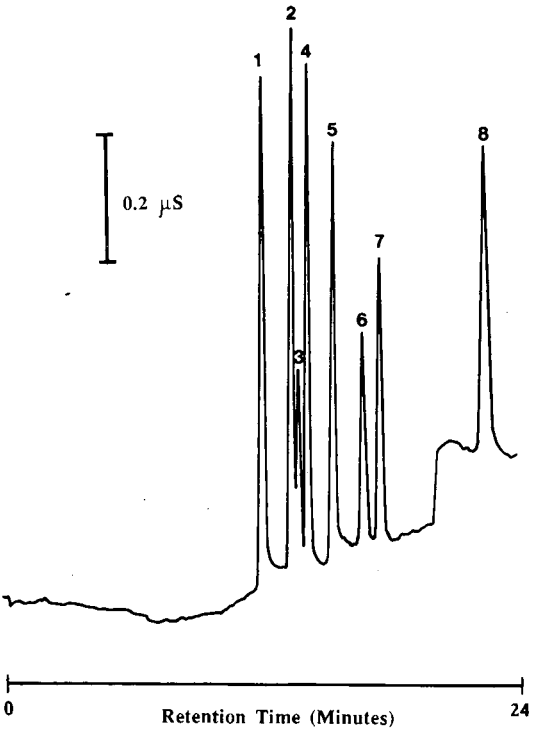

Fig. 7. Gradient separation of oxyhalides and other common anions with hydroxide eluent and SPR conductivity detection. Conditions: column, Waters IC-Pak Anion HR; eluent, 0.5–15 m*M* potassium hydroxide gradient (5% acetonitrile); flow-rates, eluent 1.0 ml/min and SPR 0.4 ml/min; injection, 100 μl Peaks: 1 = fluoride (2.5 ppm); 2 = chlorite (10 ppm); 3 = bromate (5 ppm); 4 = chloride (2.5 ppm); 5 = nitrite (5 ppm); 6 = chlorate (5 ppm); 7 = nitrate (5 ppm); 8 = sulfate (5 ppm).

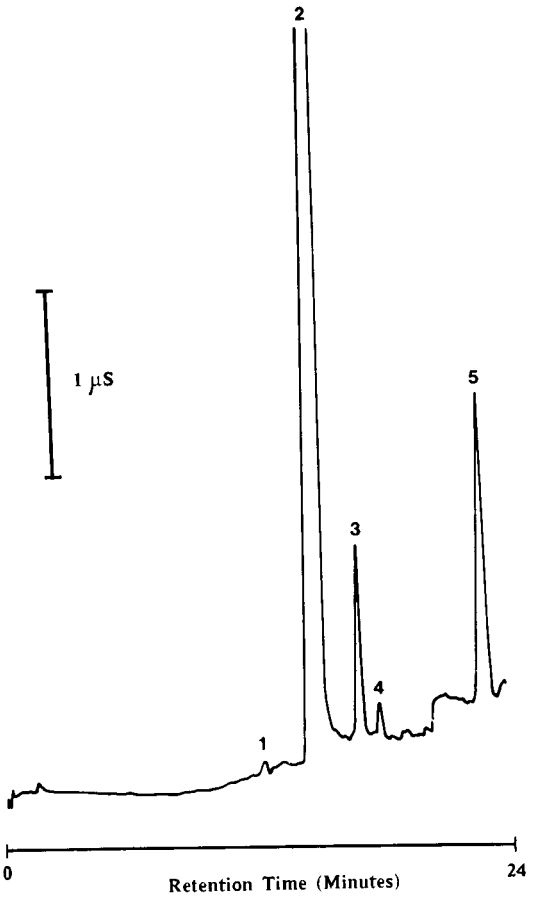

Fig. 8. Determination of disinfection by-products in swimming pool water. Conditions as for Fig. 7 except sample: 100 μl of swimming pool water. Peaks: 1 = fluoride (0.2 ppm); 2 = chloride (>50 ppm); 3 = chlorate (11.3 ppm); 4 = nitrate (1.4 ppm); 5 = sulfate (12.5 ppm).

respectively. This amount of peak information could not be attained using isocratic IC, as was also the case with the previous sample.

Another important application of gradient SPR detection is the analysis of anions formed as by-products from the disinfection of water by chlorination. The levels of these anions, *i.e.* chlorite, bromate, chloride, chlorate, are soon to be regulated by the US Environmental Protection Agency [13]. Fig. 7 shows a chromatogram of some oxyhalides and other common anions using a hydroxide gradient with SPR conductivity detection. Both of the eluents for the gradient were sparged with helium during the chromatographic run. Fig. 8 shows the analysis of chloride and chlorate in swimming pool water chromatographed using the same conditions as for Fig. 7.

REFERENCES

1 H. Small, T. Stevens and W. Bauman, *Anal. Chem.*, 47 (1975) 1801.
2 P. R. Haddad and P. E. Jackson, *Ion Chromatography: Principles and Applications* (*Journal of Chromatography Library*, Vol. 46), Elsevier, Amsterdam, 1990.
3 R. D. Rocklin, C. A. Pohl and J. A. Schilber, *J. Chromatogr.*, 411 (1987) 107.
4 W. R. Jones, P. Jandik and A. Heckenberg, *Anal. Chem.*, 60 (1988) 1977.
5 M. W. Martin and R. A. Giacofei, in P. Jandik and R. M. Cassidy (Editors), *Advances in Ion Chromatograhpy*, Vol. I, Century International, Franklin, MA, 1989, p. 119.
6 D. T. Gjerde and J. V. Benson, *Anal. Chem.*, 62 (1990) 612.
7 P. Jandik, J. B. Li, W. R. Jones and D. T. Gjerde, *Chromatographia*, 30 (1990) 509.
8 D. T. Gjerde, D. J. Cox, P. Jandik and J. B. Li, *J. Chromatogr.*, 546 (1991) 151.
9 M. J. Van Os, J. Slanina, C. L. DeLigny and J. Agterdenbos, *Anal. Chim. Acta*, 156 (1984) 169.
10 M. Doury-Berthod, P. Giampaoli, H. Pitsch, C. Sella and C. Pointrenaud, *Anal. Chem.*, 57 (1985) 2257.
11 R. P. W. Scott, *Liquid Chromatography Detectors* (*Journal of Chromatography Library*, Vol. 33), Elsevier, Amsterdam,, 2nd ed., 1986, p. 13.
12 E. C. Bender, *Crime Lab. Digest*, 16 (1989) 78.
13 J. D. Pfaff and C. A. Brockhoff, *Res. Tech.*, April (1990) 192.

Journal of Chromatography, 546 (1991) 199–208
Elsevier Science Publishers B.V., Amsterdam

CHROMSYMP. 2116

Separation of inorganic analyte anions on dye-coated stationary phases

THOMAS A. WALKER
Technical Development, Marion Merrell Dow Inc., P.O. 9627, Kansas City, MO 64134 (U.S.A.)

ABSTRACT

The separation of inorganic analyte anions on a dye-coated stationary phase was studied. The dye employed in this study is typically used for pH titrations and is composed of hydrophobic groups and a fixed charge site. The mobile phase variables that affect analyte anion retention were studied and include: concentration of dye, type and concentration of organic modifier, mobile phase pH, type and concentration of counter anion, and ionic strength. Different stationary phases were studied including a polymer-based packing and a silica-based ODS packing. Linear regression studies were done on the polymer column using conductivity detection. Correlation coefficients were found to be greater than 0.999 over a range of 1 to 1000 ppm, with detection limits between 0.5 and 1.0 ppm.

INTRODUCTION

In ion-interaction chromatography, the hydrophobic counter ion is sorbed onto the stationary phase and forms a charged double layer. The analyte ions of interest are then separated in the diffuse secondary layer. The ion-interaction retention model has been studied and theoretical interpretations have been developed [1–11].

An area of ion-interaction chromatography that has not received as much attention is the addition of dyes to the mobile phase. DiNunzio and Freiser [12] reported on the separation of aliphatic acids on a chemically bonded ODS column that was coated with brilliant green. The separation was described as true ion-pair chromatography since the mobile phase was composed of only organic solvents. One study described the separation of organic and inorganic anions using methylene blue as the counter ion [13], while Golombek and Schwedt [14] used a methyl green coated column for the separation of inorganic anions. The separation of metal ions was described by Jones and Schwedt [15] where several different dyes were studied.

In the studies where a dye was used as an ion-interaction reagent (IIR), detection was usually done using a conductivity detector or by indirect UV detection where the counter anion was UV-active. In this study, however, the dye is used as both the IIR and for indirect visible detection. This paper describes the mobile and stationary phase variables that affect the separation of inorganic and organic analyte anions on dye-coated stationary phases. The analyte anions were detected either by conductivity or indirect visible detection. The results that were obtained will be discussed.

0021-9673/91/$03.50

EXPERIMENTAL

Chemicals

HPLC-grace acetonitrile was obtained from Baxter Scientific Products (McGaw Park, IL, U.S.A.). HPLC-grade water was obtained by passing deionized water through a Nanopure water purification unit. Ethyl violet, citric acid, potassium hydrogen phthalate (KHP), salicyclic acid, sodium benzoate, succinic acid, *p*-hydroxybenzoic acid, inorganic salts and metal salts were obtained from Aldrich (Milwaukee, WI, U.S.A.). All chemicals were reagent grade.

Apparatus

The liquid chromatographic apparatus used in this study consisted of a Spectra-Physics Model 8800 high-performance liquid chromatography (HPLC) pump, Spectra-Physics Model 8875 full loop autosampler, Spectra-Physics Model SC101-100 variable-wavelength UV–visible detector, and Spectra-Physics ChromJet integrator. The columns used in this study were: a 150 × 4.1. mm Hamilton PRP-1 column (Hamilton, Reno, NV, U.S.A.), a 150 × 4.6 mm PLRP-S column (Polymer Labs., Amherst, MA, U.S.A.) and a 5-μm, 150 mm × 4.6 B&J ODS column (Baxter Healthcare Corp., McGaw Park, IL, U.S.A.). The PRP-1 column is a spherical, 10-μm poly(styrene–divinylbenzene) packing. The PLRP-5 column is composed of a spherical 5-μm poly(styrenedivinylbenzene) packing. Flow-rates of 1.0 ml/min were used, unless noted. Aqueous analyte samples of approximately 500 μg/ml were used. Sample aliquots of 10 μl were used, except for the calibration curves where 20-μl injections were used. Inlet pressures of 500–1000 p.s.i. were observed. A wavelength of 620 nm was used for the indirect visible detection.

Ethyl violet was purchased as a chloride salt and was converted to a fluoride salt by passing the dye through an Amberlite IRA-400 anion-exchange column (Aldrich) that was charged in the F^- form.

Mobile phase preparation

The ethyl violet dye was quantitatively transferred (appriopriate volume of a 0.01 *M* ethyl violet solution) to a beaker that contained the aqueous buffer solution. The desired pH was achieved by adding acid or base. The aqueous solution was diluted to the appropriate volume and the organic modifier was then added. The solution was mixed and then filtered through a 0.45-μm PTFE membrane.

Column loading

Column loading was determined by running the mobile phase through the column and UV–visible detector until the breakthrough occurred. The number of μmoles of ethyl violet adsorbed onto the stationary phase was calculated from the breakthrough volume [3]. The column was then allowed to equilibrate for an additional 30–60 min.

RESULTS AND DISCUSSION

Retention of inorganic and organic analyte ions on reversed stationary phases using a mobile phase containing a hydrophobic ion of opposite charge is determined

by two major equilibria [3,4,8–11]. The first equilibria describes the interaction that takes place between the stationary phase and the hydrophobic ion (eqn. 1), while the second equilibria describes the ionic interaction that takes places between the analyte ion and the counterion associated with the retained hydrophobic ion (eqn. 2). The second equilibria takes place in what has been termed the diffuse secondary layer. These equilibria are shown by eqns. 1 and 2, respectively:

$$A + EV^+ + C^- + M^+ \rightleftarrows A \cdots EV^{+-}C + M^+ \quad (1)$$

$$A \cdots EV^{+-}C + X^- + M^+ \rightleftarrows A \cdots EV^{+-}X + C^- + M^+ \quad (2)$$

where A represents the stationary phase, EV^+ represents an ion-interaction reagent (UV-active counter cation) in the mobile phase, C^- is the counter anion associated with the ion-interaction reagent, the buffer and/or added inert electrolyte, M^+ is a cation associated with the counter anion and/or the analyte anion, and X^- is the analyte anion. The variables that will affect the separation are; the reversed stationary phase, the type and mobile phase concentration of the IIR, the mobile phase concentration of organic modifier, the type and mobile phase concentration of counter anion in the mobile phase, and mobile phase pH. It should be noted that the inorganic analyte anions studied in this paper had no retention on the stationary phases in the absence of the IIR whereas organic analyte anions have some retention depending on the hydrophobicity of the organic analyte anion.

The IIR used in this study has the added feature of being chromophoric which allows for the indirect visible detection of the analyte anions. Both conductivity and indirect detection were used in this study. When using indirect visible detection, the absorbance of the UV–visible detector should not exceed its linear working range (usually an absorbance range of 0.8 or less). As an analyte anion travels down the column (eqns. 1 and 2) the concentration of the UV-active IIR band changes relative to the background absorbance. The IIR in the band either increases do to removal from the column and provides a positive chromatographic peak, or decreases due to its uptake onto the column and produces a negative chromatographic peak. The IIR in the mobile phase is responsible for the retention and resolution of the analyte anions and in their indirect visible detection.

Effect of ethyl violet concentration

The first mobile phase parameter that was studied was the concentration of ethyl violet. The retention of the ethyl violet onto the stationary phase was high and required either a long breakthrough time (> 12 h) or a high mobile phase concentration of organic modifier (> 20% acetonitrile). The amount of ethyl violet retained on the column was calculated from the breakthrough volumes [3]. It was found that as the mobile phase concentration of ethyl violet was increasd, the amount of ethyl violet adsorbed onto the stationary phase increased. Since ethyl violet is quite hydrophobic, it produces a significant amount of surface anion-exchange sites on the column. At a concentration of $2.0 \cdot 10^{-4}$ *M* of ethyl violet, there are 145 μequiv./column of anion-exchanges sites. This concentration compares with that found for mobile phases using tetraalkylammonium salts [4] and low-capacity anion exchangers [16].

Fig. 1. compares the separation of several inorganic anions at two different

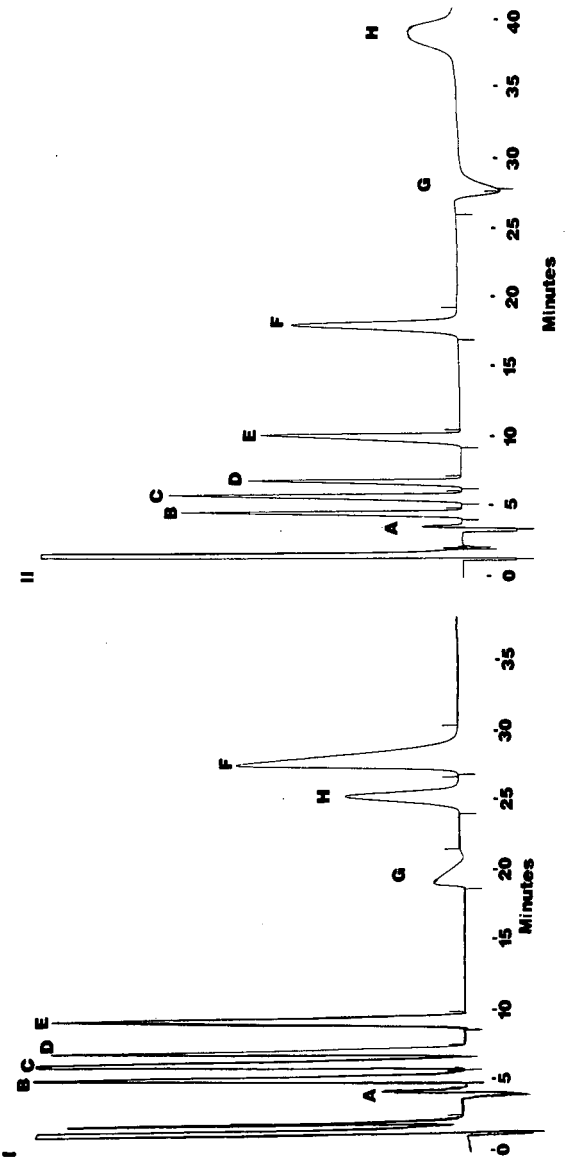

Fig. 1. The separation of several inorganic anions at different mobile phase concentrations of ethyl violet. Mobile phase: (I) 0.1 m*M* ethyl violet, 2.0 m*M* KHP, pH 4.0, acetonitrile–water (20:80), (II) same as I except 0.3 m*M* ethyl violet. Peaks: A = F^-; B = Cl^-; C = NO_2^-; D = Br^-; E = NO_3^-, F = SO_4^{2-}; G = system peak; H = I^-.

mobile phase concentrations of ethyl violet. Chromatogram I shows the separation where 0.1 m*M* ethyl violet was used while chromatogram II shows the separation where the ethyl violet concentration was increased to 0.3 m*M*. The analyte anions were baseline resolved using 0.3 m*M* ethyl violet, however the separation took longer than when the 0.1 m*M* ethyl violet mobile phase was used. It is interesting to note that almost all of the analyte anions had lower retention times when the mobile phase concentration of ethyl violet was increased, except for I^- which increased in retention.

Mobile phase variables —effect on ethyl violet adsorption

The concentration of organic modifier also had an effect on the amount of ethyl violet adsorbed onto the stationary phase. As the mobile phase concentration of organic modifier was increased, the amount of ethyl violet adsorbed onto the stationary phase decreased. This decrease in the amount of adsorbed ethyl violet produced a corresponding decrease in the number of anion-exchange sites present on the stationary phase.

The mobile phase ionic strength was found to affect the amount of ethyl violet adsorbed onto the stationary phase. The amount of ethyl violet adsorbed onto the stationary phase was found to increase with increasing ionic strength. The increase in the amount of ethyl violet adsorbed led to an increase in the apparent number of anion-exchange sites present. Although more anion-exchange sites were present at a higher mobile phase ionic strength, retention of the analyte anions decreased due to increased competition for the anion-exchange sites from the higher concentration of counter anions (see eqn. 2).

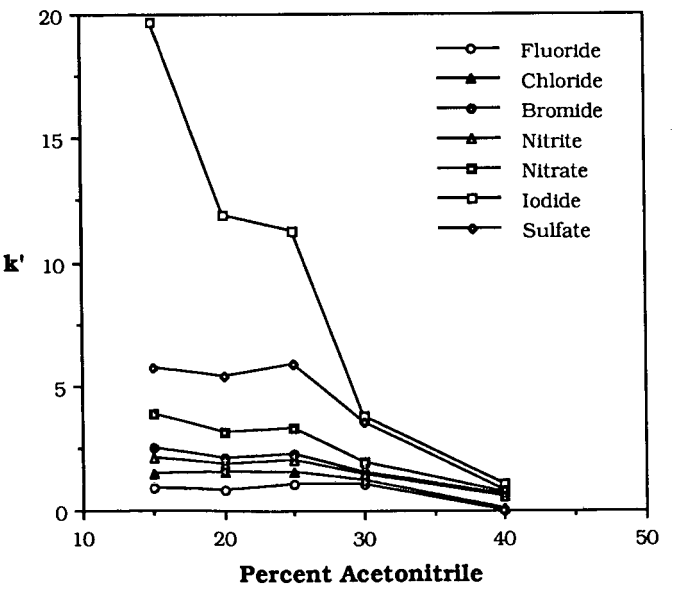

Fig. 2. The effect of acetonitrile concentration on analyte anion retention. Mobile phase conditions: 0.1 m*M* ethyl violet, 1.0 m*M* KHP, pH 4.5, acetonitrile–water. k' = Capacitiy factor.

Effect of organic modifier on anion retention

Fig. 2 shows how retention of the analyte anions were affected by the concentration of acetonitrile that covered a range of 15% to 40%. Retention of the anions is dependent on the number of anion-exchange sites provided by the adsorbed ethyl violet. As the concentration of acetonitrile was increased, the amount of adsorbed ethyl violet decreased which led to a lower number of anion-exchange sites present. Resolution of the anions was found to be better at lower concentrations of acetonitrile due to the higher number of anion-exchange sites present on the stationary phase.

Effect of pH

The effect that the mobile phase pH had on analyte retention is shown in Fig. 3. Retention times did not change for most of the anions over the pH range of 4 to 10 (ionic strength held constant). Three anions, however, were affected by pH; sulfate which decreased in retention, and phosphate and iodide which increased in retention. The increase in retention for phosphate is attributed to the change in ionization over the pH range studied. The mobile phase pH appears to have had an effect on the polarizability of sulfate and iodide which in turn affected their retention [17]. Fig. 4 shows the separation of Cl^-, NO_2^-, Br^-, NO_3^-, I^-, SO_4^{2-} at pH 6.0. Several differences are readily apparent when comparing Fig. 1 (I) with a mobile phase pH of 4.0, to Fig. 4 with a pH of 6.0. At pH 4.0, all of the anions were baseline resolved and the system peak did not interfere with the separation. At pH 6.0, the retention times for I^- and SO_4^{2-} were significantly different when compared to pH 4.0. SO_4^{2-} had a much lower retention time whereas I^- had an increase in retention. Also at pH 6.0, the system peak interfered with the Cl^- peak and NO_3^- and SO_4^{2-} were not baseline

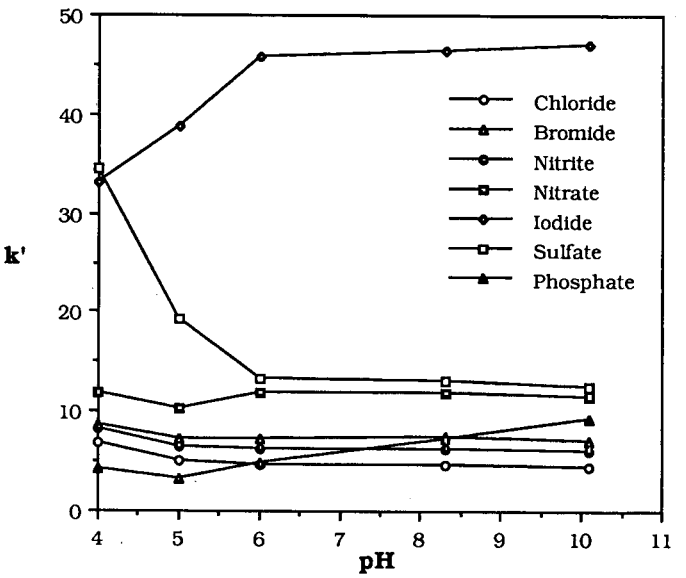

Fig. 3. The effect of mobile phase pH on analyte anion retention. Mobile phase conditions: 0.1 m*M* ethyl violet, 1.0 m*M* KHP, acetonitrile–water (20:80).

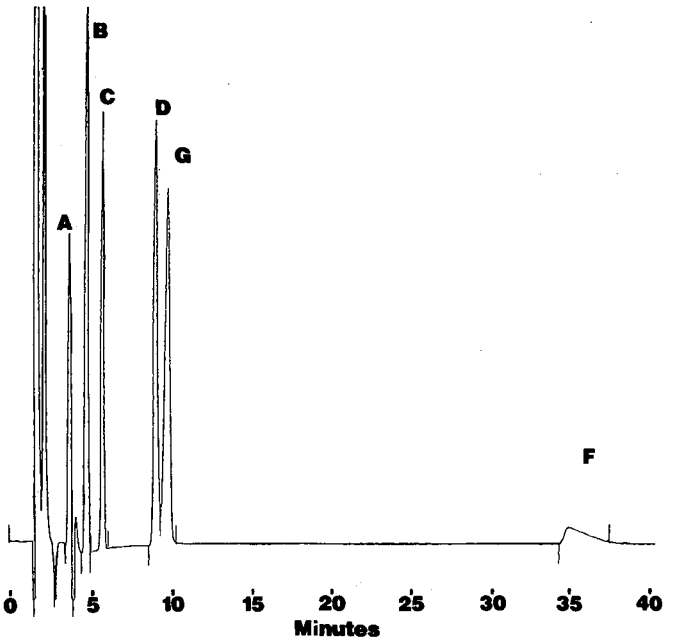

Fig. 4. The separation of several inorganic analyte anions at pH 6.0. Mobile phase conditions: 0.1 m*M* ethyl violet, 2.0 m*M* KHP, pH 6.0, acetonitrile–water (20:80). Peaks: A = Cl^-; B = NO_2^-; C = Br^-; D = NO_3^-; E = system peak; F = I^-; G = SO_4^{2-}.

resolved. This study indicated that a lower mobile phase pH would provide a better separation without any interference from the system peak.

Effect of ionic strength

The concentration of counter-anion (KHP) in the mobile phase was increased in order to determine what effect ionic strength would have on anion retention. All of the anions studied decreased in retention as the concentration of KHP was increased. This is due to increased competition for the anion-exchange sites (eqn. 2). Increasing the mobile phase concentration of KHP increases the amount of IIR adsorbed onto the stationary phase and leads to an increase in the number of anion-exchange sites. This did not, however, lead to an increase in anion retention since competition was increased for the anion-exchange sites due to the higher concentration of counter-anions present.

Comparison of conductivity and indirect visible detection

Detection of the inorganic anions was done by using conductivity and indirect visible detection. The conductivity of the mobile phase was low enough so that sensitive detection (< 1 ppm) of the anions could be done. Indirect visible detection at a wavelength of 620 nm provided for the analysis of phosphate which was poorly detected when using conductivity. Fig. 5 shows the separation of Cl^-, NO_2^-, Br^-, NO_3^-, SO_4^{2-}, I^-, and $H_2PO_4^-$ on a PLRP-S column using conductivity (I) and indirect visible detection (II).

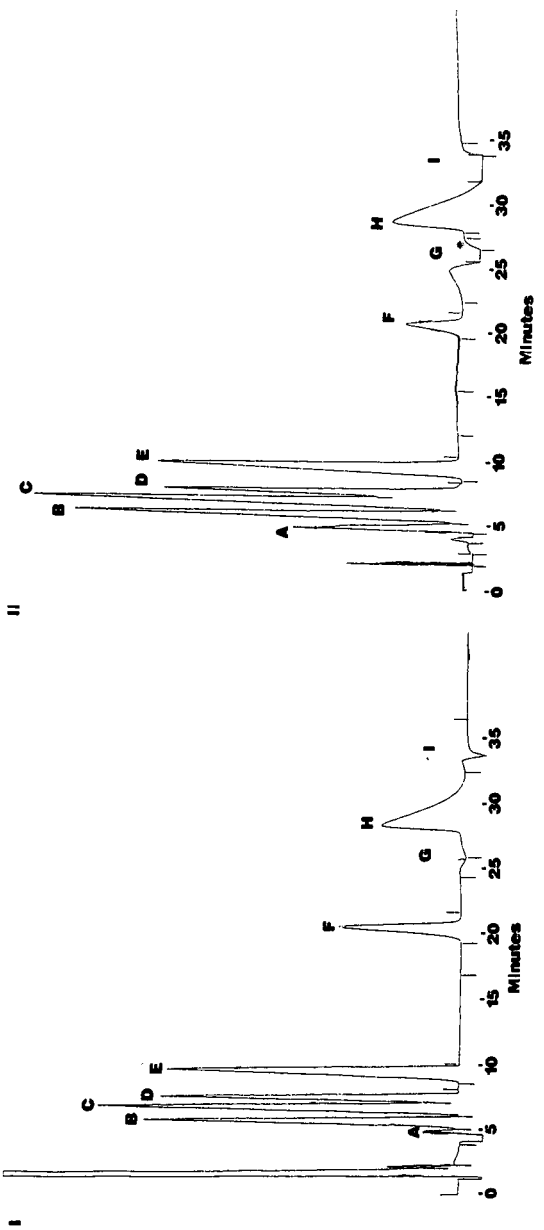

Fig. 5. The separation of several inorganic anions using (I) conductivity and (II) indirect visible detection. Mobile phase conditions: 0.1 m*M* ethyl violet, 1.0 m*M* KHP, pH 4.5, acetonitrile–water (25:75). Peaks: A = $H_2PO_4^-$; B = Cl^-; C = NO_2^-; D = Br^-; E = NO_3^-; F = I^-; G = system peak; H = SO_4^{2-}; I = system peak.

Other counter anions studied

Different counter anions were also used for the separation of inorganic anions. The counter anions that were studied and found to be acceptable were sodium benzoate, *p*-hydroxybenzoic acid (pHBA), salicylic acid, succinic acid and citric acid. The counter anions that provided the best separations were KHP, pHBA and sodium benzoate. A higher concentration of sodium benzoate was required when compared to KHP since sodium benzoate is a weaker eluant. pHBA was found to be a stronger counter anion than either KHP or sodium benzoate.

Separation on an ODS column

A silica-based ODS column was also coated with the dye and used for the separation of the inorganic analyte anions. The peaks obtained on the ODS column were broad and resolution was poor. Several disadvantages were apparent with the silica-based column when compared to the polymer-based column. First, it took a significant amount of acetonitrile–water to strip the IIR off the ODS column. The ethyl violet was found to adsorb very strongly onto the stationary phase. The polymer column, however, could easily be cleaned by passing 100 ml of an acetonitrile–water (80:20) eluent through it. Secondly, the results were not as reproducible as the polymer-based column. This may be due to ethyl violet that remained adsorbed on the column, as well as degradation of the silica-based packing. Studies have indicated that free silanol sites within the silica backbone can participate in cation exchange. Some of the cationic ethyl violet is retained as a cation and thereby eliminating it as a source for anion exchange [18]. Thirdly, the polymer column is stable throughout the pH range of 1 to 13, whereas the silica based column is not.

Calibration curve

Calibration curves using a 20-μl sample loop were made covering the range of 1 to 1000 ppm for Cl^-, Br^-, and NO_3^-, as well as 5 to 1000 ppm for SO_4^{2-}. The mobile phase consisted of 0.1 m*M* ethyl violet, 1.0 m*M* KHP, pH 4.5, acetonitrile–water (20:80). Correlation coefficients of 0.999, 1.00, 1.00 and 1.00 were obtained for Cl^-, Br^-, NO_3^-, and SO_4^{2-}, respectively. The limit of detection for each anion was found to be 0.5 ppm, except for SO_4^{2-} which was found to be 1.0 ppm.

CONCLUSIONS

It was found that an ethyl violet-coated stationary phase provided acceptable separations of the inorganic anions studied. The mobile phase variables that affect anion retention were identified and studied. Both conductivity and indirect visible detection could be used for the analysis of the anions. Correlation coefficients were better than 0.999 with detection limits of 1.0 ppm or less were found.

REFERENCES

1 R. M. Cassidy and S. Elchuk, *Anal. Chem.*, 54 (1982) 1558.
2 R. M. Cassidy and S. Elchuck, *J. Chromatogr. Sci.*, 21 (1983) 454.
3 Z. Iskandarani and D. J. Pietrzyk, *Anal. Chem.*, 54 (1982) 1065.
4 Z. Iskandarani and D. J. Pietrzyk, *Anal. Chem.*, 54 (1982) 2427.
5 G. Schmuckler, B. Rossner and G. Schwedt, *J. Chromatogr.*, 302 (1984) 15.

6 Q. Zianren and W. Baeyens, *J. Chromatogr.*, 456 (1988) 267.
7 P. Haddad and R. C. Foley, *J. Chromatogr.*, 500 (1990) 301.
8 F. F. Cantwell, in J. A. Marinsky and Y. Marcus (Editors), *Ion Exchange and Solvent Extraction*, Vol. 9, Marcel Dekker, New York, 1985, p. 339.
9 R. A. Hux and F. F. Cantwell, *Anal. Chem.*, 56 (1984) 1258.
10 S. Afrashtefar and F. F. Cantwell, *Anal. Chem.*, 54 (1982) 2422.
11 F. F. Cantwell and S. Puon, *Anal. Chem.*, 51 (1979) 623.
12 J. DiNunzio and H. Freiser, *Talanta*, 26 (1979) 587.
13 S. W. Kang, *Taehan Hwahakhoe Chi*, 29 (1985) 365.
14 R. Golombek and G. Schwedt, *J. Chromatogr.*, 452 (1988) 283.
15 P. Jones and G. Schwedt, *J. Chromatogr.*, 482 (1989) 325.
16 T. A. Walker, T. V. Ho and N. Akbari, *J. Liq. Chromatogr.*, 12 (1989) 1213.
17 L. G. Daignault, D. P. Rillema and D. C. Jackman, *J. High Resolut. Chromatogr.*, 13 (1990) 293.
18 R. L. Smith, Z. Iskandarani and D. J. Pietrzyk, *J. Liq. Chromatogr.*, 7 (1984) 1935.

Journal of Chromatography, 546 (1991) 209–220
Elsevier Science Publishers B.V., Amsterdam

CHROMSYMP. 2199

Recent advances in the simultaneous determination of anions and silica in high-purity water

SAM HARVEY
Houston Lighting and Power Co., South Texas Project Electric Generating Station, Technical Services Department, P.O. Box 289, Wadsworth, TX 77483 (U.S.A.)

ABSTRACT

It is possible to determine anions and silica in a single injection. However, there are interactions that occur between the anions and silica that are not completely understood. This work provides the data for the hypothesis that the hydronium ion occurring at a suppressor promotes a catalytic formation of silica complexes. Silica forms halogen complexes and uses sulfur as a bridge to form other compounds thereby reducing the amount of free silica, fluoride, chloride and sulfate. This in turn is reflected in the response at the conductivity and visible detectors. This work also provides the data that even when the system is not coupled there still are anion–silica complexes being formed which inhibit complete detection of either the anions or silica separately. The interactions between silica and the anions occur either precolumn or oncolumn with the possible exception of fluoride which coelutes with silica.

INTRODUCTION

Monitoring water in power plants for anion and silica impurities allows the detection of breakthrough of polishers before changes in conductivity are noticed, thus preventing deposition of these impurities on turbines and steam generators. This deposition "buildup" of impurities can result in decreased heat transfer efficiency and the initiation of stress corrosion cracking in plant equipment. Component failures of this nature will lead to repairs and power plant shutdowns resulting in millions of dollars of repair costs and millions more in loss of generation revenue.

Ion chromatography (IC) as originally designed and reported by Small *et al.* [1] was a technique for the rapid, sensitive determination of multiple inorganic cations or multiple inorganic anions in one injection. This original work revolutionized the determination of inorganic ions, especially the anions, and opened up many new application areas.

IC has been described as a branch of ion exchange chromatography in which two columns are used. The second column is a suppressor which removes from the eluent all non-analyte ions. Having done this a simple conductivity meter can be used for detection. This allows for use of a precise, rapid analytical technique to determine such common anions as fluoride, chloride and sulfate [2]. This technique used in

0021-9673/91/$03.50

conjunction with the development of the concentrator (stripping) column now allows for the detection of impurities in the sub-ppb[a] range.

Photometrically silica is determined routinely and accurately with the silicomolybdate–heteropolyblue method. Silica in a sample reacts with ammonium molybdate in an acidic medium to form yellow α and β forms of molybdosilicic acid [3]. The molybdosilicic acid is reduced by stannous chloride to the molybdenum blue color, and the absorbance of the solution is measured at 820 nm. Oxalic acid, tartaric acid or citric acid is added to eliminate the interferences caused by any phosphate in the sample reacting to form the blue color [4]. This interference is already eliminated as ion chromatography readily resolves the phosphate and silica.

A logical extension of the work by Small *et al.* is the combination of two different approaches (conductometric and visible detection), producing a technique which performs anion and silica analysis, thus providing greater flexibility and information per injection. Although the coupling of detection systems is not new, the coupling for detection of silica and anions is.

The purpose of this work is to study and define the interactions between silica and anions previously reported [5]. The ion chromatograph coupled system led to the discovery of these interactions. These interactions are important to the power industry to ensure proper quantification of the anions so that cation conductivity and anion–cation balances may be achieved to maintain steam generator integrity.

EXPERIMENTAL

Instrumentation

All chromatography in this study was performed on a Dionex Series 2020i ion chromatograph. The dual-channel ion chromatograph was interfaced with a multichannel data-and-control system consisting of an AI450 (Dionex) interface, Dell System 200 desk-top computer (Dell Computer Corp., Austin, TX, U.S.A.) with a 40-megabyte hard drive and 5.25 in. floppy drive, and an Epson FX850 (Seiko Epson, Japan) printer. This in turn was interfaced with a Dionex reagent delivery module and a Dionex variable-wavelength detector (VDM-II) equipped with a 1500-μl beaded reaction coil. The software (Dionex) provided data acquisition, data reduction and control of the ion chromatograph.

Reagents and standard solutions

Reagent-grade chemicals were used in the majority of the work with two exceptions. Suprapure sodium hydroxide available from VWR (VWR, Houston, TX, U.S.A.) was used as an eluent, and puriss-grade sodium molybdate from Fluka Chemical (Fluka, New York, NY, U.S.A.) was used as part of the postcolumn reagent. The water used was plant-produced demineralized water passed through a Barnsted Nanopure (Barnsted/Thermolyne, Dubuque, IA, U.S.A.) water system. Stock silica solution was prepared by dissolving 0.473 g sodium metasilicate ($Na_2SiO_3 \cdot 9H_2O$) in high-purity water and diluting to 100 ml. Two eluents were used in these experiments. The first eluent was 30 m*M* sodium tetraborate and was prepared by dissolving 22.86 g sodium borate decahydrate in 2 l of high-purity water.

---

[a] Throughout the article, the American billion (10^9) is meant.

The second eluent used was 30 m*M* sodium hydroxide and was prepared by dissolving 2.40 g of NaOH in 2 l of high-purity water and degassed to eliminate carbonate and sealed under a nitrogen overpressure blanket to prevent the uptake of carbonate. The silica postcolumn reagent was prepared by dissolving 9.68 g of sodium molybdate ($Na_2MoO_4 \cdot 2H_2O$) in 800 ml of high-purity water slowly adding 25.0 ml of concentrated HNO_3 (15.9 *M*) and mixing thoroughly. To this solution 2.39 g of sodium lauryl sulfate was added and the solution was diluted to a final volume of 1000 ml. The eluent and postcolumn reagent were mixed using a membrane reactor and a 1500-μl beaded reaction coil.

Nalgene plastic labware (Nalge, Rochester, New York, NY, U.S.A.) was used throughout the study to minimize silica contamination. Standard solutions were stored in Teflon fluorinated ethylene propylene (FEP) labware to minimize anion and silica leaching.

Columns

The columns used in this study were a Dionex AS4A analytical column, an AG4A guard column and an AG5 guard column as the concentrator. These columns were packed with a pellicular anion exchange resin. A standard Dionex membrane suppressor (AMMS-I) and a prototype AMMS-II Dionex membrane suppressor were used to lower the eluent background conductivity and enhance sensitivity.

Procedures

Standards and samples were analyzed by ion chromatography under the operating conditions listed in Table I. The calibration standards were prepared from separate stock ppm standard solutions. The precision of the analytical method was

TABLE I

OPERATING CONDITIONS

Item	Condition 1	Condition 2
Eluent	30 m*M* Tetraborate	30 m*M* NaOH
Eluent flow-rate	1.5 ml/min	1.5 ml/min
Concentrator	AG5	AG5
Guard column	AG4A	AG4A
Separator column	AS4A	AS4A
Detection		
Anions	Conductivity with AMMS suppressor	Conductivity with AMMS suppressor
Silica	Visible detection at 410 nm	Visible detection at 410 nm
Full-scale sensitivity		
Conductivity	30 μS	30 μS
Visible	0.005 a.u.f.s.	0.005 a.u.f.s.
Suppressor	AMMS-1	AMMS-1
Regenerant	20 m*M* H_2SO_4	20 m*M* H_2SO_4
Regenerant flow-rate	10 ml/min	5 ml/min
Postcolumn reagent	40 m*M* Sodium molybdate	40 m*M* Sodium molybdate
	0.4 *M* Nitric acid	0.4 *M* Nitric acid
	6 m*M* Sodium lauryl sulfate	6 m*M* Sodium lauryl sulfate
Postcolumn flow-rate	0.5 ml/min	0.5 ml/min

determined by replicate analysis of water samples containing varying ratios of F^-, Cl^-, SO_4^{2-} and SiO_3^{2-}.

The determination of silica and anions separately is a well-known process [6,7]. The determination of anions and silica simultaneously has received some attention in the past, but was essentially a method for splitting a process sample into two different analyzers so the separations could run concurrently [8].

Silica can be concentrated as the silicate ion on a strong-base anion-exchange resin and eluted with a base in a more concentrated condition [3]. This is also the method of choice for anions which are water soluble and ionic. Based on this and previous work [7,8] the concentrator selected was a Dionex AG5 due to higher capacity and stronger base form resin as contrasted with the trace anion concentrator (TAC) or AG4A columns. The analytical and guard column selection were also based on previous work [8] and the AS4A and AG4A columns were used.

The eluent described in refs. 7 and 8 (15 m*M* NaOH–15 m*M* boric acid) was determined to be satisfactory for the determination of silica, fluoride and chloride; however, this eluent is not strong enough to elute sulfate efficiently. A 30-m*M* tetraborate eluent is ideal for separation of these species.

The chromatograph was then set up with a 30-m*M* tetraborate eluent and 20 m*M* H_2SO_4 was used as regenerant. This is coupled to a reagent-delivery module (RDM) and a variable-wavelength detector (VDM-II) as shown in Fig. 1. Introduction of the postcolumn reagent was accomplished with a Dionex DQP pump and a membrane reactor. To increase reaction time with the postcolumn reagent before detection a 1500-μl beaded reaction coil was added between the RDM and VDM-II.

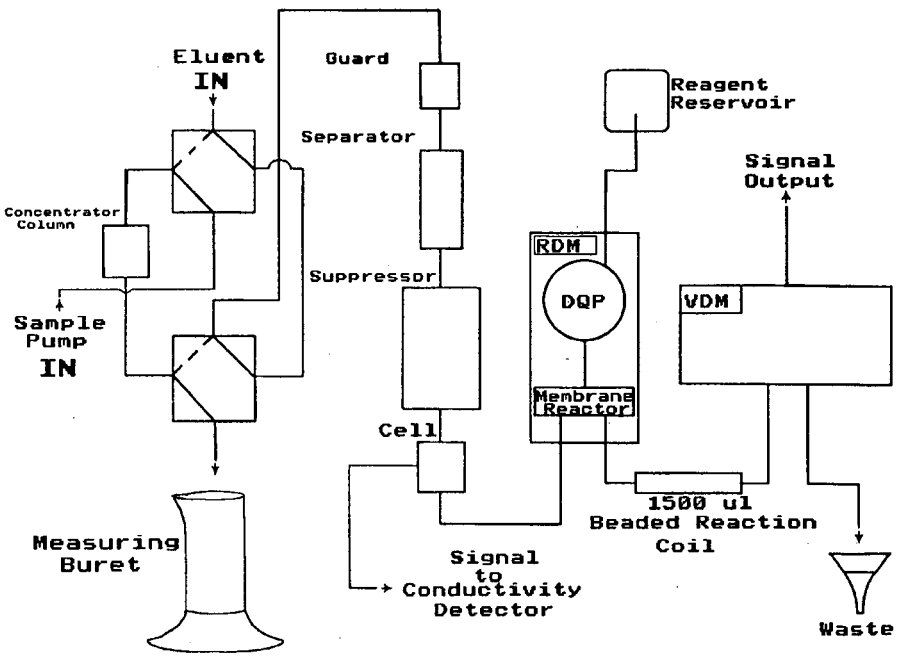

Fig. 1. Scheme of the chromatographic system used in this study.

In all experiments, 18 ml of sample was concentrated for this study. The methodology used was to inject 25 replicates of sample containing known concentrations of F^-, Cl^-, SO_4^{2-} and SiO_3^{2-} to insure reproducibility. The separations containing only 25 ppb of each anion yielded 100% resolution of all peaks in under 6 min with less than 3% relative standard deviation (R.S.D.). This step was then repeated with a 25-ppb standard containing only silica. Again the R.S.D. was less than 3% with silica eluting at 1.9 min. Silica was observed to tail slightly with the tetraborate eluent, but this was considered negligible. It was also observed by measuring the volume between the conductivity cell and the VDM-II and the flow-rate that fluoride and silica were coeluting.

RESULTS AND DISCUSSION

A mixed standard containing 25 ppb of the anions and silica was prepared and 25 injections were made. The resultant chromatograms had a high degree of resolution between all species with less than 5% R.S.D. It is noted that fluoride and silica coelute, but are detected independently by separate detectors. There was also a decrease of approximately 15% in the peak heights of all species when silica was present with the anions. This decrease was not observed when the silica was removed from the samples. To further evaluate this phenomenon, both the peak heights and peak areas were investigated. The evaluation indicated that while peak areas were more stable, the apparent decrease in sensitivity was still present. Injections of steam generator samples at this time indicated fairly good agreement with separate laboratory analysis; however, this might be due to no measurable presence of fluoride or sulfate in the samples. The steam generator values for anions by IC were: $F^- < 1$ ppb, Cl^- 1.4 ppb, $SO_4^{2-} < 1$ ppb and silica results by spectrophotometer were 115 ppb. The corresponding values by coupled IC were: $F^- < 1$ ppb, $Cl^- < 1$ ppb, $SO_4^{2-} < 1$ ppb and silica 95 ppb. This lead to the hypothesis that the silica chemistry is interacting at the suppressor and some secondary reactions were occurring. These secondary reactions could interfere with the postcolumn reaction for silica determination. It was also hypothesized that interactions between anions and silica occur oncolumn or precolumn to the suppressor.

Investigation into this behavior revealed that there is a catalytic effect of hydronium ions in the pH range of 0–2 with fluoride ions that affect the state of silica at low pH. It is believed that it converts silica to SiF_4, SiF_5^- and SiF_6^{2-} [3]. This behavior has been reported in the presence of chloride and other halogens [9]. This information tends to confirm that secondary reactions are occurring at the suppressor and further study was indicated into the suppressor chemistry. Further investigation was called for to explain why the sulfate was affected and it was found that silica may use sulfur as a bridge to form binary compounds [9]. Similar interaction has been reported between silica with cations such as sodium, magnesium and calcium [10–12].

To evaluate the hydronium–silica interactions at the suppressor, a series of experiments was conducted varying the strength of the regenerant to ensure that regenerant strength did not affect the results. A 5-l combined standard at the 25-ppb levels were used to insure uniform standard consistency and were used throughout this experiment. The regenerant flow-rate was maintained at 10 ml/min.

The regenerant varied from 2.5 m*M* H_2SO_4 and increased in steps of 2.5 m*M* to

a final concentration of 25 m*M*. For each concentration of regenerant, 25 injections of the mixed standard were performed. The peak heights and areas remained constant with an overall R.S.D. of 6.4% which indicate the conditions in the suppressor interface are constant, regardless of regenerant strength.

With this information it was decided to check the lower limits of detection. It was determined that by concentrating 18 ml of sample the lowest reliable values (R.S.D. values < 10%) obtained were 5 ppb for fluoride and chloride and 20 ppb for sulfate and silica. It was decided to try sodium hydroxide as an alternate eluent to try and improve sensitivity. The sodium hydroxide was also chosen to study the interactions with a stronger base eluent.

The sodium hydroxide eluent did improve the sensitivity of the ions of interest with no noticeable tailing of the silica peak, as shown in Fig. 2. This is due to changes in selectivity and also the possibility that some of the silica may be inhibited from the formation of SiF_4, SiF_5^-, SiF_6^{2-}, $SiCl_4$ and other halogen complexes. This is due to the pH of the eluent being higher and inhibiting the formation of these complexes [10]. The silica reaction may also be increased due to the formation of monomeric silicic acid [$Si(OH)_4$] [3,10]. From this point on, all experiments were performed with the NaOH eluent at a flow-rate of 1.5 ml/min and a postcolumn flow-rate of 0.5 ml/min. The linearity response data for these ions is presented in Table II. The lower limit of reliable detection (R.S.D. values < 10%) was then determined to be 1 ppb for fluoride and chloride, 5 ppb for sulfate and 10 ppb for silica. The suppressor experiment previously described using varying strengths of regenerant from 2.5 to 25 m*M* H_2SO_4 was again performed with the sodium hydroxide eluent. The results for the peak heights and areas also remained constant with an overall R.S.D. of 5.2%. This confirms that conditions in the suppressor interface are constant even with the stronger base sodium hydroxide eluent.

To verify that the peak maximum for silica was detected a spectral array detector (Linear Instruments, Reno, NV, U.S.A.) was installed in the place of the VDM-II

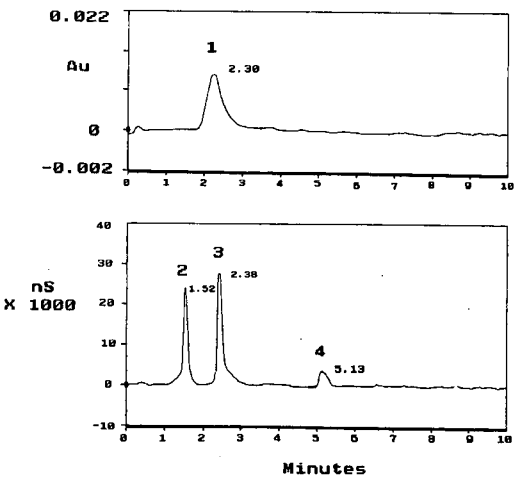

Fig. 2. Separation of anions and silica using NaOH. Peaks: 1 = silica, 10 ppb; 2 = fluoride, 5 ppb; 3 = chloride, 5 ppb; 4 = sulfate, 10 ppb. Au = Absorbance units.

TABLE II

LINEARITY RESPONSE (R^2)

Ion	Range (ppb)	R^2
Fluoride	1–10	0.9996
Chloride	1–10	0.9996
Sulfate	5–25	0.9968
Silica	10–30	0.9994

and five injections performed of the mixed 25-ppb level standard. Scans were performed in both the ultraviolet and visible regions and the peak maximum for silica was observed to be 410 nm (Fig. 3).

After the peak maximum for silica was verified, the system was returned to its original configuration using the VDM-II and another set of experiments was performed to check the suppressor interaction of the hydronium ion and silica in both the AMMS-I and prototype AMMS-II suppressors. The two different suppressors were evaluated at the request of a Dionex research chemist. It was postulated that neutral compounds such as SiF_4 and $SiCl_4$ may be forming and migrating across the suppressor membrane in the AMMS-I, thereby decreasing the silica and anion response. The theory was that the AMMS-II suppressor had a thicker membrane which would inhibit a migration of neutral compounds across the membrane. This would result in an increase in silica response if this was the case. The experimental conditions are listed in Table III and the results are depicted in Tables IV–VII. As shown in Tables IV–VII, a decreased response is still reported with both the AMMS-I and the prototype AMMS-II suppressor. However, the decrease is not as significant as with the AMMS-I. This provided some evidence for the formation of neutral species, but is not conclusive. Also of interest at this point is that with the system uncoupled there still are interactions occurring between silica and the anions. To further support this hypothesis the AMMS-I was reinstalled and the instrument was recalibrated using peak heights. The anion calibration was carried out in a 3 × 3 mode at the 5-, 25- and 50-ppb level in silica-free water. Likewise, the silica calibration was performed in a 3 × 3 calibration mode in anion-free water at the 25-, 50- and 100-ppb level. A 2-l standard containing 25 ppb of F^-, Cl^- and SO_4^{2-} was prepared to insure uniform standard concentration. This standard was split into eight separate 200-ml volu-

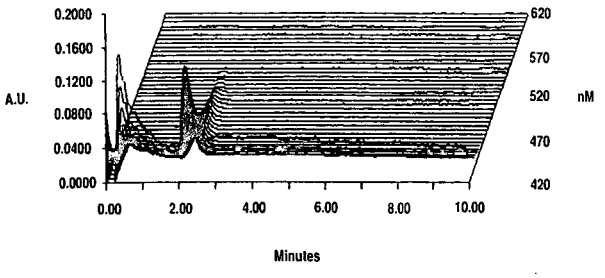

Fig. 3. Visible spectrum of silica. A.U. = absorbance units.

TABLE III

SUPPRESSOR COMPARISON

Experiment	Amount concentrated	100 ppb Standard solution	Conditions
1	18 ml	anions only	AMMS-1, postcolumn on
2	18 ml	anions only	Postcolumn bypassed
3	18 ml	anions only	Prototype suppressor, postcolumn bypassed
4	18 ml	silica only	Prototype suppressor, postcolumn on
5	18 ml	silica only	Suppressor bypassed
6	18 ml	silica only	AMMS-1, postcolumn on
7	18 ml	combined	AMMS-1, postcolumn on
8	18 ml	combined	Prototype suppressor, postcolumn on

TABLE IV

COMPARISON OF ANION RESPONSE WITH AMMS-I *VS.* AMMS-II[a]

All anion concentrations are at the 100-ppb level. Postcolumn system "bypassed" for the study.

Anion	AMMS-I	AMMS-II	Δ (%)
Fluoride			
height	$1.573 \cdot 10^8$	$1.588 \cdot 10^8$	+ 0.9
area	$1.065 \cdot 10^9$	$8.203 \cdot 10^8$	−23
Chloride			
height	$1.201 \cdot 10^8$	$1.263 \cdot 10^8$	+ 5.0
area	$9.423 \cdot 10^8$	$7.905 \cdot 10^8$	−16
Sulfate			
height	$1.376 \cdot 10^7$	$1.209 \cdot 10^7$	−12
area	$5.317 \cdot 10^8$	$4.272 \cdot 10^8$	−19.6

[a] Prototype —regenerant not optimized for application.

TABLE V

COMPARISON OF ANION RESPONSE WITH AND WITHOUT SILICA PRESENT USING AMMS-I

All anion and silica concentrations were at the 100-ppb level. Postcolumn system "on" for both studies.

Anion	Without silica	With silica	Δ (%)
Fluoride			
height	$1.468 \cdot 10^8$	$1.293 \cdot 10^8$	−11.9
area	$1.199 \cdot 10^9$	$1.069 \cdot 10^9$	−10.8
Chloride			
height	$1.111 \cdot 10^8$	$9.831 \cdot 10^7$	−11.5
area	$1.010 \cdot 10^9$	$8.915 \cdot 10^8$	−11.2
Sulfate			
height	$1.535 \cdot 10^7$	$1.147 \cdot 10^7$	−25.2
area	$6.298 \cdot 10^8$	$4.850 \cdot 10^8$	−22.9

TABLE VI

COMPARISON OF ANION RESPONSE WITH POSTCOLUMN SYSTEM "ON" *VS.* POST-COLUMN "BYPASSED" USING AMMS-I

All anion concentrations are at the 100-ppb level. No silica present in samples.

Anion	On	Bypassed	Δ (%)
Fluoride			
height	$1.468 \cdot 10^8$	$1.573 \cdot 10^8$	+ 7.1
area	$1.199 \cdot 10^9$	$1.065 \cdot 10^9$	−11.1
Chloride			
height	$1.111 \cdot 10^8$	$1.201 \cdot 10^8$	+ 8.1
area	$1.010 \cdot 10^9$	$9.423 \cdot 10^8$	− 6.7
Sulfate			
height	$1.535 \cdot 10^7$	$1.376 \cdot 10^7$	−10.3
area	$6.298 \cdot 10^8$	$5.317 \cdot 10^8$	−15.6

metrics to which varying amounts of silica were added. The silica concentration for each sample was as follows: (1) 10 ppb, (2) 20 ppb, (3) 30 ppb, (4) 40 ppb, (5) 50 ppb, (6) 100 ppb, (7) 150 ppb and (8) 200 ppb. For each combined sample, ten injections were performed to ensure reproducibility and the results were averaged. The results obtained are presented in Figs. 4–7, and the R.S.D values for each sample set were: (1) 4.8, (2) 5.4, (3) 6.2, (4) 4.9, (5) 5.4, (6) 3.8, (7) 3.6 and (8) 2.4%.

As the graphs indicate, there is an interaction of the anions with silica due to the formation of silica–halogen and silica–sulfur compounds. This is further documented in that the silica recovery in the presence of the anions is roughly 50% the calibration value as depicted in Fig. 7.

TABLE VII

COMPARISON OF SILICA RESPONSE WITH AND WITHOUT SUPPRESSORS

Silica concentration: 100 ppb. No anions present.

	AMMS-I	AMMS-II	No suppressor	Δ (%)
Silica				
height	1026	1236		+20.5
area	14 087	15 114		+ 7.29
Silica				
height	1026		1698	+65.5
area	14 087		18 383	+30.5
Silica				
height		1236	1698	+37.4
area		15 114	18 383	+21.6

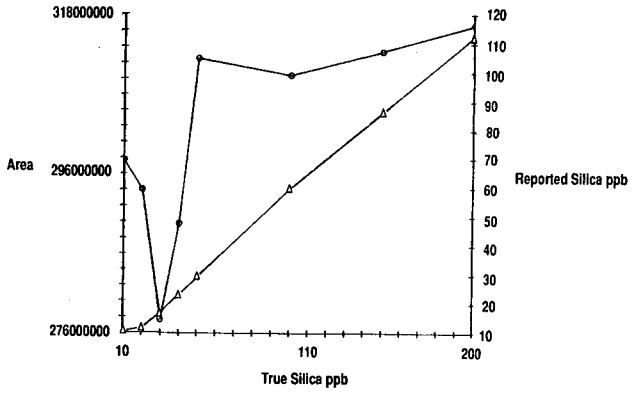

Fig. 4. Peak-height areas of fluoride *versus* silica. ○ = Fluoride; △ = silica.

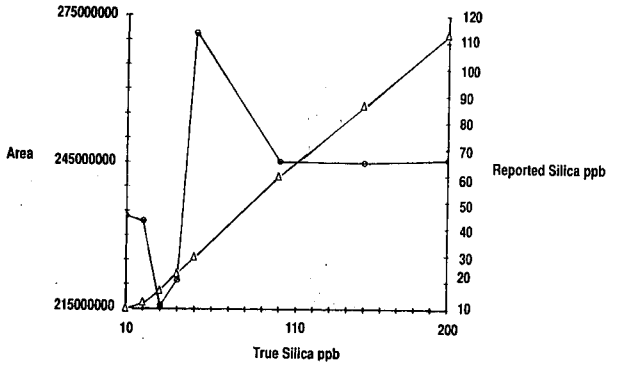

Fig. 5. Peak-height areas of chloride *versus* silica. ○ = Chloride; △ = silica.

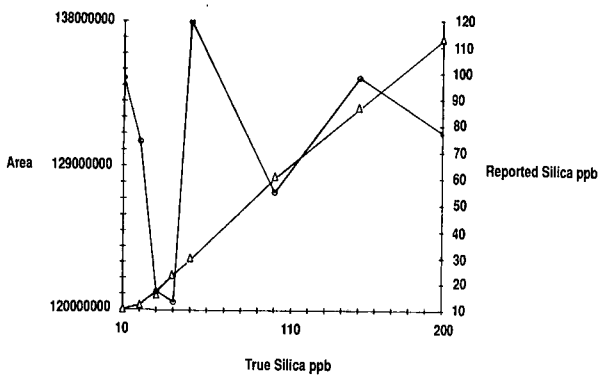

Fig. 6. Peak-height areas of sulfate *versus* silica. ○ = Sulfate; △ = silica.

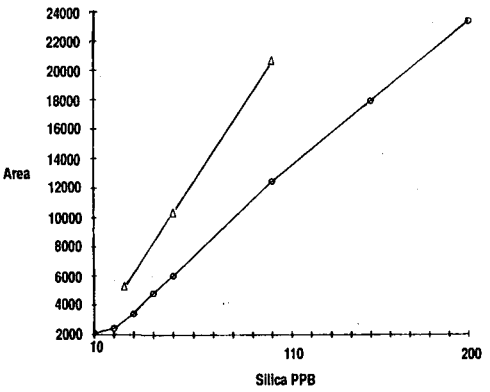

Fig. 7. Silica response with and without anions present. ○ = With anions present; △ = without anions present.

CONCLUSIONS

It is possible to determine anions and silica simultaneously using a single chromatograph with dual detectors. However, much work still needs to be done to verify that the reactions for silica are occurring at the suppressor and to verify the chemistry involved. It becomes necessary to determine where in the system (precolumn or oncolumn) the interactions between the anions and silica occur. The verification of complexes that are being formed between the anions and silica still needs to be performed. Models will have to be developed to explain the interaction between anions and silica. This will provide information for improved quantification of anions and silica in power-plant waters. This study is also useful in that it helps explain why we in the power industry are not able to achieve a cation conductivity balance with the reported anions in the system. The versatility of IC has been demonstrated in this study and holds promise for future developments in the area of coupled detection. Further work on this separation will be forthcoming, including the use of a single-column chromatography.

ACKNOWLEDGEMENTS

The author expresses his gratitude for the efforts of F. W. Williams of the Manville Corp. in Denver, CO, U.S.A., for verifying this effect in loop injections and the preliminary work performed with sodium carbonate/sodium bicarbonate eluents. The author also deeply appreciates the support and encouragement of Dan Campbell of the Dionex Corp. for this project as well as verifying the experiments conducted with the AMMS-I suppressor and the prototype AMMS-II suppressor.

REFERENCES

1 H. Small, T. S. Stevens and W. C. Bauman, *Anal. Chem.*, 47 (1975) 1801.
2 C. D. West, *Essentials of Quantitative Analysis*, McGraw-Hill, New York, 1987, p. 354.
3 K. Iler, *The Chemistry of Silica*, Wiley, New York, 1979, pp. 95–104, 137, 177, 250–268.

4 *Standard Methods for the Examination of Water and Wastewater*, American Public Health Association, Washington, DC, 17th ed., 1989, pp. 4–184 and 4-189.
5 S. Harvey, presented at the *Dionex Ion Chromatography Power Symposium, Atlanta, GA, 1990.*
6 *Dionex Application Update AU102*, Dionex, Sunnyvale, CA, 1985.
7 *Dionex Application Update AU113*, Dionex, Sunnyvale, CA, 1989.
8 M. E. Potts, E. J. Gavin, L. O. Angers and E. L. Johnson, *LC·GC*, 4 (9) (1986) 914.
9 F. A. Cotton and G. Wilkinson, *Advanced Inorganic Chemistry*, Wiley, New York, 1988, Ch. 9, 13 and 14.
10 R. H. Busey and R. E. Mesmer, *Inorg. Chem.*, 16 (1977) 2444.
11 J. W. Cobble, R. C. Murray, Jr., P. J. Turner and K. Chen, *High-Temperature Thermodynamic Data for Species in Aqueous Solution*, Electric Power Research Institute, Palo Alto, CA, Report NP-2400.
12 J. H. Alexander and L. Luu, *MULTEQ: Equilibrium of an Electrolytic Solution with Vapor-Liquid Partitioning and Precipitation, Vol. II, The Database*, Electric Power Research Institute, Palo Alto, CA, Report NP-5561.

Journal of Chromatography, 546 (1991) 221–228
Elsevier Science Publishers B.V., Amsterdam

CHROMSYMP. 2247

On-column matrix elimination of high levels of chloride and sulfate in non-suppressed ion chromatography

MARHENI, PAUL R. HADDAD* and ANDREW R. McTAGGART
Department of Analytical Chemistry, University of New South Wales, P.O. Box 1, Kensington, N.S.W. 2033 (Australia)

ABSTRACT

On-column matrix elimination, in which samples containing a very high level of a matrix anion are chromatographed using the same matrix anion as eluent, is evaluated for samples containing chloride or sulfate. The detection method employed must be selective, and direct UV absorbance at 210 nm is utilized. A mixture of ten UV-absorbing anions (iodate, bromate, nitrite, bromide, nitrate, molybdate, chromate, vanadate, iodide and thiocyanate) is separated on a Waters IC Pak A column using 15 m*M* sodium chloride containing 5 m*M* phosphate buffer at pH 6.5 as eluent. The chromatographic performance of this separation was virtually unaltered for sample chloride concentrations in the range 0–20 000 ppm. Detection limits are in the sub-ppm range for a 10-μl injection, but can be reduced substantially through the use of larger injection volumes. The same approach was applied to samples containing elevated levels of sulphate, and a mixture of eight anions (as above, except for molybdate and chromate) could be separated using 10 m*M* sodium sulphate containing 5 m*M* phosphate buffer at pH 6.5 as eluent. Again, chromatographic performance was maintained in samples containing up to 20 000 ppm sulphate.

INTRODUCTION

The determination of a trace component in the presence of very high levels of potentially interfering sample matrix components is a common problem in many areas of analytical chemistry. In ion chromatography (IC), this problem becomes particularly severe when the sample contains high levels of ionic species, as typified by the determination of trace ionic components in brine samples. Although it may be possible to separate chromatographically the ionic matrix components from the analyte ion(s), this separation becomes difficult to achieve when the concentrations of the matrix ions are high and they are eluted as very large peaks which may obscure the analyte peaks. Even when a selective detection method is employed with which the matrix ions give little or no detector signal, the matrix ions can still exert a major influence on the final chromatogram by inducing variable retention times and loss of chromatographic efficiency. For example, the peaks for 5 ppm nitrite and nitrate have been shown to be broadened by the presence of chloride at levels above 300 ppm [1]. These effects are the direct result of the presence of a high ionic concentration in the sample, leading to either self-elution by the sample itself, or to loss of the band-

0021-9673/91/$03.50

compression effect which occurs normally when a dilute sample is injected onto an ion-exchange IC column.

Several approaches have been suggested to overcome these adverse effects of matrix ions. First, the concentration of the matrix ion(s) in the sample can be reduced prior to the analysis, usually with the aid of a suitable pre-column. For example, chloride levels can be lowered by passage of the sample through a cation-exchange pre-column in the silver form [2–4]. However, this approach must be applied selectively because of the danger that some analyte ions may also be lost [5]. The same process of removal of an interfering matrix ion can also be accomplished using dialysis through membranes, rather than pre-columns [6–8]. A second general approach to the problem of matrix ions is the selective removal of the analyte ion(s) from the matrix, again using pre-columns [9] or membranes [10,11]. In all of these methods, sample contamination arising from the clean-up steps must be considered [12].

A third general approach, which may be described as on-column matrix elimination, has been suggested by Ito and Sunahara [13] and involves the use of the major matrix ion as the eluent. When this is done, the column is in the form of the major matrix ion before injection of the sample, so that the matrix ion shows little or no retention. Provided that the detection method used can discriminate against the matrix ion, a workable IC procedure results. As an example, the determination of anions in brine solutions can be considered. Here, an anion-exchange column can be used with a sodium chloride eluent and direct UV absorbance detection at 210 nm. At this wavelength, chloride does not absorb appreciably [14] and because chloride is present in the eluent, the method should also be resistant to high levels of chloride in the sample. This approach has been utilized for the determination of iodide and thiocyanate in concentrated salt solutions using UV absorbance and amperometric detection [15], and for iodide in sea water using amperometric detection [13].

In this paper, we investigate the use of on-column matrix elimination with UV absorbance when chloride or sulphate is the major matrix anion. The utility of sodium chloride or sodium sulfate eluents for these situations is assessed.

EXPERIMENTAL

Instrumentation

The IC system consisted of a Millipore Waters (Milford, MA, U.S.A.) Model M 6000A pump and U6K injector, a Shimadzu (Kyoto, Japan) Model SPD-6AV UV–visible spectrophotometric detector operated at 210 nm and a Houston Instruments (Austin, TX, U.S.A.) Omniscribe recorder. The column used was a Waters IC Pak A, 50 × 4.6 mm I.D., packed with methacrylate-based anion exchanger of capacity 30 ± 3 μequiv./ml.

Reagents

All reagents were of analytical-reagent grade. Water used in this study was purified on a Millipore (Bedford, MA, U.S.A.) Milli-Q system and was filtered through a 0.45-μm membrane filter and degassed in an ultrasonic bath before use.

Stock solutions (1000 ppm) of the standard anions were prepared by dissolving appropriate amounts of sodium or potassium salts in purified water and were stored in glass containers. Working mixtures of these anions were prepared at the concentra-

tions specified in the figure captions by dilution of the stock solutions. Sodium chloride eluents containing 5 m*M* phosphate buffer (pH 6.5) were prepared from stock solutions of 2 *M* analytical-reagent grade sodium chloride (Ajax, Sydney, Australia), 0.25 *M* disodium hydrogenphosphate and 0.25 *M* sodium dihydrogenphosphate. Sodium sulphate eluents containing 5 m*M* phosphate buffer (pH 6.5) were prepared in a similar manner. All eluents were operated at a flow-rate of 1.2 ml/min and separations were carried out at room temperature.

RESULTS AND DISCUSSION

Selection of chromatographic conditions

One of the first aims of this work was to investigate the utility of sodium chloride and sodium sulphate as eluents for the separation of anions. Since the ultimate purpose of these studies was to find chromatographic conditions which were tolerant towards very high levels of chloride and sulphate as matrix ion, it was necessary to employ a detection method which shows little response to these species.

Two suitable detection approaches are UV absorbance (at wavelengths greater than 200 nm) and amperometry at a suitable electrode surface. Of these two methods, we selected the former because of its more widespread applicability. Numerous common anions show substantial absorptivities in the wavelength range 200–220 nm, and Williams [14] has listed the wavelengths of maximum absorption for many of these species. In this study, we have considered only bromide, bromate, iodide, iodate, nitrite, nitrate, chromate, vanadate, molybdate and thiocyanate as solute anions.

Optimal eluent compositions were sought for the separation of the above anions. A buffered eluent was considered preferable because of the weakly acidic nature of some of the solute anions, especially nitrite. For this reason, a 5-m*M* phosphate buffer at pH 6.5 was included in each eluent. When the concentration of chloride ion in the eluent was increased, the capacity factors (k') for solute anions decreased in the manner shown in Fig. 1. The linear relationship observed between log [NaCl] and log k' is in accordance with theoretical predictions for ion-exchange separations [16] and the observed slopes of these plots are in the range -0.68 to -0.97 for the singly charged solutes and -1.25 to -1.53 for the doubly charged solutes. These values are less than the theoretical slopes and indicate that the phosphate ions present in the eluent make some contribution to the elution of solute anions. Retention plots were also prepared for sodium sulphate eluents, and similar results were obtained. These plots were then used for an empirical optimization of the separation of the test solutes. The optimal eluents were 15 m*M* sodium chloride and 10 m*M* sodium sulphate, both containing 5 m*M* phosphate buffer at pH 6.5. The chromatograms obtained with these eluents are shown in Figs. 2a and 3a. It is noteworthy that only eight of the ten anions in the sample mixture could be resolved with the sulphate eluent (chromate and molybdate could not be separated from the other ions), whereas all ten anions were resolvable with the chloride eluent.

Performance characteristics and interference effects

Detection limits (for a 10-μl injection volume) obtainable in both eluents are listed in Table I, from which it can be seen that most of the test anions were detectable in the sub-ppm range. Peak height precision values for ten replicate injections of a

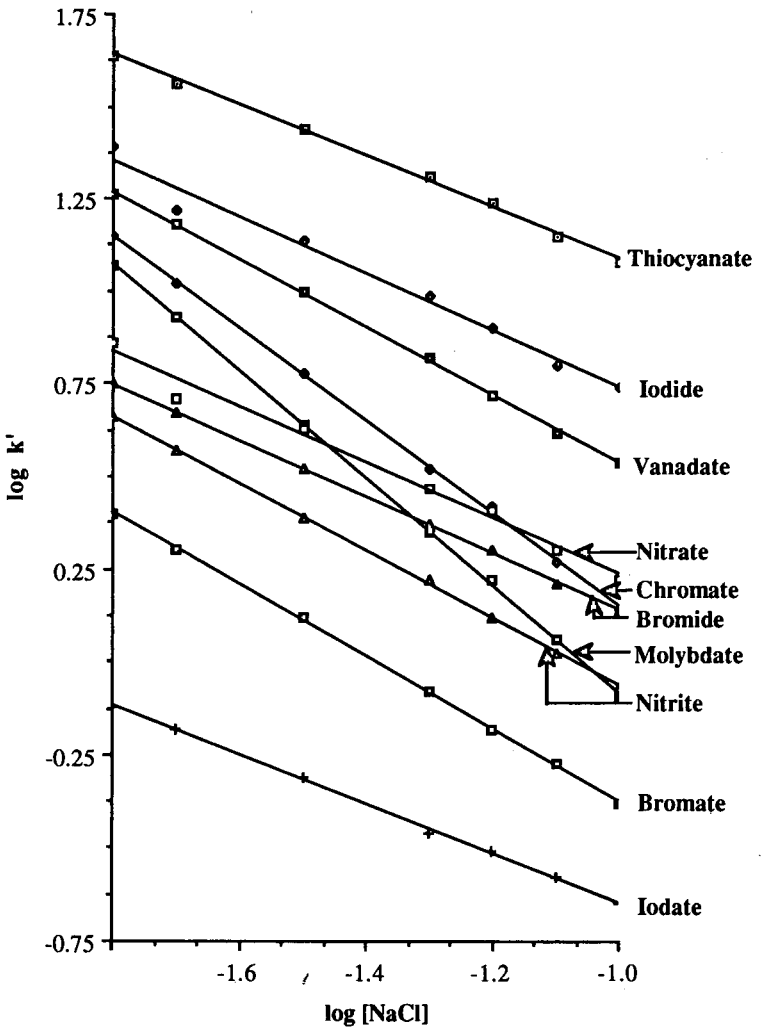

Fig. 1. Variation of solute retention with the concentration of chloride in the eluent.

standard mixture of anions were in the range 0.2–1.2% relative standard deviation (R.S.D.) for the chloride eluent and 1.6–3.1% R.S.D. for the sulphate eluent.

The tolerance of the separation shown in Fig. 2a to high levels of chloride present in the sample was studied using standards containing chloride in the range 0–30 000 ppm. The peak heights, detection limits, peak shapes and resolution of adjacent peaks were noted for each injection. Virtually no changes were observed up to 20 000 ppm, as evidenced by comparison of the chromatograms shown in Fig. 2a and b. The only exception to this was that the peak heights for some solutes (especially bromate) showed decreases; however, the areas of these peaks were not altered significantly. For samples containing more than 20 000 ppm of chloride, the negative peak which was eluted prior to nitrite became slightly more pronounced and some

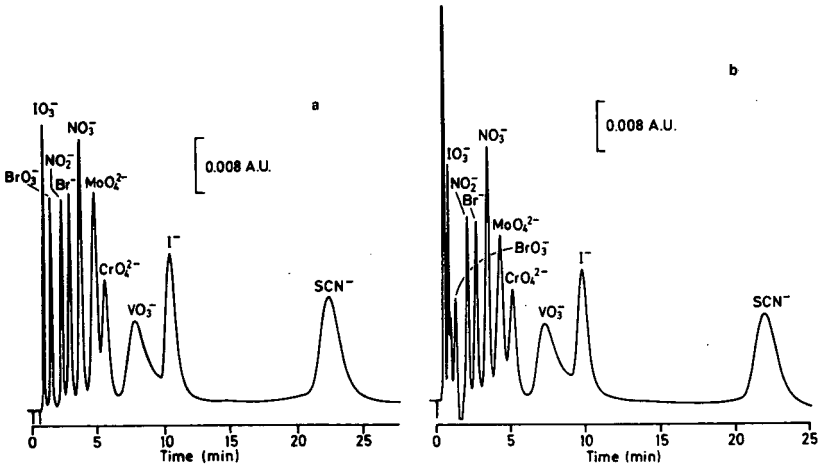

Fig. 2. Separation of ten anions in (a) water and (b) 20 000 ppm chloride. A Waters IC Pak A column was used and the eluent was 15 m*M* sodium chloride containing 5 m*M* phosphate buffer at pH 6.5, operated at a flow-rate of 1.2 ml/min. Detection was by UV absorbance at 210 nm. Solute concentrations are 5 ppm for nitrite, 10 ppm for nitrate and iodide, 25 ppm for iodate, bromide and molybdate, and 50 ppm for the remainder. The injection volume was 10 μl.

band broadening was observed. The identity of this negative peak is unknown. These effects are summarized in Table II, which shows the effect of chloride levels in the sample on some indicative performance characteristics. Data given in Table I show that there was a moderate increase in detection limits with increased chloride content in the sample. These results suggest that the chromatographic performance of the method is constant up to the approximate levels of chloride present in sea water, and

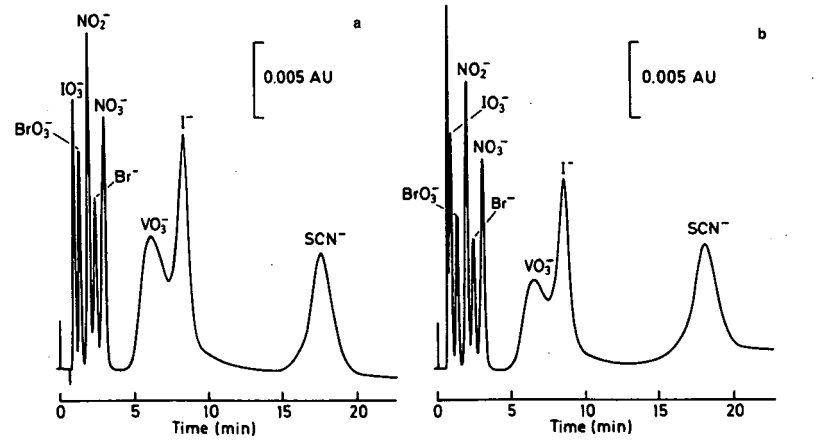

Fig. 3. Separation of eight anions in (a) water and (b) 20 000 ppm sulphate. A Waters IC Pak A column was used and the eluent was 10 m*M* sodium sulphate containing 5 m*M* phosphate buffer at pH 6.5, operated at a flow-rate of 1.2 ml/min. All other conditions as in Fig. 2.

TABLE I

DETECTION LIMITS (ppm) FOR THE PROPOSED METHODS, USING A 10-μl INJECTION VOLUME

Anion	Eluent 15 m*M* NaCl		Eluent 10 m*M* Na_2SO_4	
	Sample in H_2O	Sample in 20 000 ppm Cl^-	Sample in H_2O	Sample in 20 000 ppm SO_4^{2-}
IO_3^-	0.12	0.26	0.56	0.63
BrO_3^-	0.32	1.2	1.36	1.94
NO_2^-	0.03	0.06	0.07	0.08
Br^-	0.16	0.29	1.75	2.3
NO_3^-	0.08	0.12	0.17	0.21
MoO_4^{2-}	0.18	0.40	–	–
CrO_4^{2-}	0.70	1.32	–	–
VO_3^-	1.70	2.6	1.9	3.4
I^-	0.57	0.82	0.25	0.3
SCN^-	0.60	1.0	1.2	1.3

this behaviour is in marked contrast to previously reported results with a tetraborate–carbonate eluent, wherein a maximum of 300 ppm of chloride could be tolerated [1].

A similar study was conducted by determining the tolerance of buffered sodium sulphate eluents towards concentrations of sulphate in the sample within the range

TABLE II

PERFORMANCE PARAMETERS FOR THE DEVELOPED SEPARATIONS IN THE PRESENCE OF HIGH LEVELS OF MATRIX ANIONS

The values shown for each parameter are percentages normalized to the value of that parameter for samples containing no matrix anion.

Performance parameter	Eluent 15 m*M* NaCl			Eluent 10 m*M* Na_2SO_4		
	ppm Cl^- in sample			ppm SO_4^{2-} in sample		
	10 000	20 000	30 000	10 000	20 000	30 000
Peak height BrO_3^-	92	65	38	83	79	75
Peak height IO_3^-	94	88	76	99	96	94
Peak height NO_2^-	96	95	88	97	92	71
Peak height Br^-	91	85	84	88	84	81
Peak height NO_3^-	97	95	95	99	98	94
Peak height MoO_4^{2-}	86	80	70	–	–	–
Peak height CrO_4^{2-}	89	83	75	–	–	–
Peak height VO_3^-	99	96	95	92	87	82
Peak height I^-	92	86	86	98	95	95
Peak height SCN^-	90	85	85	99	96	95
R_s IO_3^-/BrO_3^-	100	100	98	100	98	96
R_s NO_2^-/Br^-	100	98	97	100	99	99
R_s Br^-/NO_3^-	100	99	95	99	97	95
R_s VO_3^-/I^-	100	97	96	100	98	95
N for NO_3^-	100	96	96	100	99	97
N for SCN^-	99	99	98	100	98	98

0–30 000 ppm. Again, indicative performance characteristics are summarized in Table II, which shows that the presence of 20 000 ppm of sulfate produced little effect. Above this level, some changes in performance (especially on peak heights) were observed, but these were relatively slight. Comparison of Fig. 3a and b illustrates these effects. Again, detection limits increased slightly as sulphate was added to the sample (Table I), but the changes were relatively small.

Determination of trace levels of iodide

In view of the apparent ruggedness of the methods when used for samples containing ppm levels of solute anions, the application of the technique to trace level determinations was also studied. In particular, we wished to investigate the effects produced by varying the ratio of the matrix ion concentration in the sample to that in the eluent. These effects could be most clearly demonstrated using a solute anion with strong retention, since high eluent concentrations could be employed. For this reason, the determination of iodide in high-chloride matrices was selected as a model system.

Fig. 4 shows chromatograms obtained for 100-μl injections of 100 ppb (10^9) of iodide in a matrix of 20 000 ppm of chloride, using eluents containing 15, 50 and 100 mM of sodium chloride. As expected, the retention time of iodide decreased with increasing eluent concentration, leading to sharper peaks, but the chromatographic efficiency (as determined by calculation of the number of theoretical plates for each peak) was approximately constant for all injections. This suggests that the concentration ratio of the matrix anion in the sample and the eluent does not play a significant effect in the matrix elimination technique. That is, provided the eluent contains sufficient concentration of the matrix anion to saturate all of the ion-exchange sites on the stationary phase, then effective on-column matrix elimination will occur.

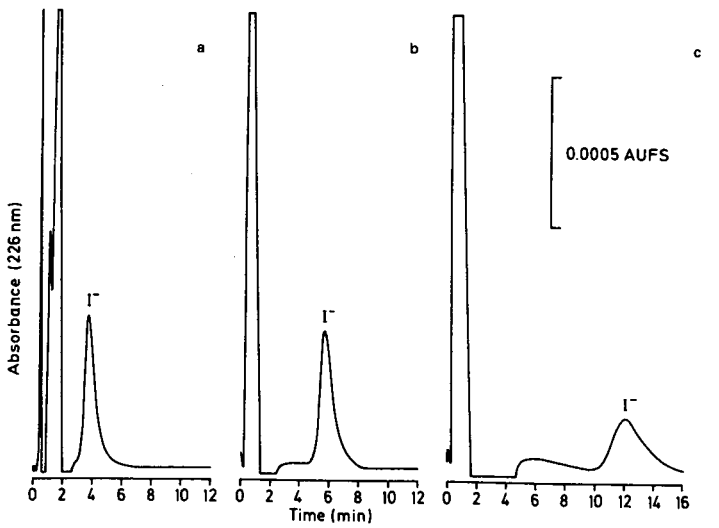

Fig. 4. Elution of trace iodide with eluents comprising (a) 100, (b) 50 and (c) 15 mM sodium chloride with 5 mM phosphate buffer at pH 6.7. The sample was 100 μl of 100 ppb (10^9) iodide in 20 000 ppm chloride. A Waters IC Pak A column was used, but the particular column employed was a different one than that used for Fig. 2.

CONCLUSIONS

On-column matrix elimination, wherein the major matrix anion is utilized as the eluent anion, has been shown to be an effective method for dealing with samples containing very high levels of chloride and sulphate. Under the conditions described, the method is restricted to the separation and detection of UV-absorbing anions, but would be equally applicable to other selective detection methods, such as amperometry and potentiometry. The method provides a viable approach to the ubiquitous problem of determining anionic species in saline samples.

REFERENCES

1 H. Saitoh and K. Oikawa, *Bunseki Kagaku*, 33 (1984) E441.
2 K. Oikawa, H. Sato, S. Sakazume and M. Fujii, *Bunseki Kagaku*, 31 (1982) E251.
3 F. A. Buytenhuys, *J. Chromatogr.*, 218 (1981) 57.
4 R. Bagchi and P. R. Haddad, *Proc. 9th Aust. Symp. Anal. Chem., Sydney, May, 1987*, Royal Australian Chemical Institute, Analytical Chemistry Division, Sydney, 1987, p. 147.
5 P. R. Haddad, *J. Chromatogr.*, 482 (1989) 267.
6 J. A. Cox and N. Tanaka, *Anal. Chem.*, 57 (1985) 385.
7 W. R. Jones and P. Jandik, *J. Chromatogr. Sci.*, 27 (1989) 449.
8 J. M. Pettersen, H. G. Johnsen and W. Lund, *Talanta*, 35 (1988) 245.
9 W. Buchberger and K. Winsauer, *J. Chromatogr.*, 482 (1989) 401.
10 J. A. Cox, E. Dabek-Zlotorzynskaya, R. Saari and N. Tanaka, *Analyst (London)*, 113 (1988) 1401.
11 F.R. Nordmeyer and L. D. Hansen, *Anal. Chem.*, 54 (1982) 2605.
12 P. R. Haddad and P. E. Jackson, *Ion Chromatography –Principles and Applications*, Elsevier, Amsterdam, 1990, p. 435.
13 K. Ito and H. Sunahara, *Bunseki Kagaku*, 37 (1988) 292.
14 R. J. Williams, *Anal. Chem.*, 55 (1983) 851.
15 K. Ito and H. Sunahara, *J. Chromatogr.*, 502 (1990) 121.
16 P. R. Haddad and C. E. Cowie, *J. Chromatogr.*, 303 (1984) 321.

Journal of Chromatography, 546 (1991) 229–242
Elsevier Science Publishers B.V., Amsterdam

CHROMSYMP. 2099

Separation and detection of group I and II cations by ion chromatography

DANIEL L. CAMPBELL*, JOHN STILLIAN, STEVE CARSON, ROBERT JOYCE and SHAWN HEBERLING
Dionex Corporation, 1228 Titan Way, Sunnyvale, CA 94086 (U.S.A.)

ABSTRACT

Lithium, sodium, magnesium and calcium are routinely monitored in environmental samples and in analysis of ultrapure water for semiconductor and power generation facilities. The use of graphite furnace, atomic absorption and ICP have long been recognized as the analytical instruments of science for the detection and quantization of these cations. These spectral detectors have been the detection method of choice because of their inherent speed, sensitivity, and lack of interferences.

This paper will present results of a recent advance using ion chromatography with chemical suppression and conductivity detection for group I and group II cations. The method allows the separation and detection of lithium, sodium, ammonium, potassium, magnesium, calcium and morpholine at the sub-μg/l levels in ultrapure water and common power plant waters.

INTRODUCTION

This paper discusses many new applications of cation-exchange ion chromatography to the analyses of power plant and semiconductor water chemistries. With the continued development of ion chromatography during the past few years, the full capabilities and potential of modern ion chromatographs are only now being exploited. With these improvements in the ability to analyze high purity water, it is expected that more power plants and semiconductor manufacturing facilities will employ ion chromatography for solving their water chemistry problems than ever before.

High-performance ion chromatography (HPIC) techniques have long been employed in power plant laboratories for recognition, qualitative identification, and quantitative analysis of ionic impurities and various additives, both inorganic and organic. In this paper, the most recent cation developments and applications to analysis of ultrapure water samples and steam generator water samples will be presented.

Monitoring the presence and movement of impurities in feed waters, boiler waters, steam, and cooling waters at all power plants, fossil-fired and nuclear, is increasingly important. This is because submicrogram/liter (ppb) concentrations of these impurities, through concentration mechanisms, can accumulate in kilogram quantities in steam generators and turbines. Buildup of deposits can result in decreased heat transfer efficiency and, more seriously, in initiation and propagation of stress

0021-9673/91/$03.50

corrosion cracking and in other corrosion mechanisms in steam generator tubing, turbines, recirculation piping and other "balance-of-plant", water cycle components. Corrosion problems of this type lead to component failures and power plant shutdowns, costing the affected utility up to a million dollars a day for replacement power [1] and millions more for repairs.

Considerable research has been conducted showing increased evidence that it is the low ppb levels of chloride, sulfate, and organic acids, amongst other ionic contaminants, that are harmful to steam generators over the expected plant life of 30 years [2]. By minimizing the concentration of corrosive ions in boiler feedwater and effluent from condensate polishers, corrosion damage to turbines and nuclear power plant steam generators can be minimized. Minimizing the concentrations of the trace counter ions, sodium and potassium, is equally important for controlling condensate polisher slippage and for controlling crevice build-up in steam generators. Measurements of ionic contamination throughout the system can provide corrosion engineers and water chemistry personnel with valuable information regarding the source of the contamination, the likely rates of contaminant build-up, and the probable rates of corrosion, as well as extremely useful and timely data during the start-up and shutdown of power plants. Continuous monitoring of these ions in condensate polishing systems also indicates when an ion exchange demineralizer requires regeneration.

Recent developments in ion chromatography instrumentation have resolved a number of practical difficulties in high purity samples, and ion chromatography is now finding increased application in the direct quantitative analysis of trace cation and neutralizing amines in many power plant matrices. In the remainder of this paper, we shall consider a number of these important cation analyses both qualitative and quantitative analyses, that have been recently developed.

EXPERIMENTAL

Equipment

All chromatography in these studies was performed on a Dionex Series 4500i ion chromatograph, as shown in Fig. 1.

The entire flow path of the chromatograph is constructed from polymeric and other non-metallic materials in order to eliminate corrosion from the acidic eluents used. All eluents were mixtures of dilute hydrochloric acid (HCl) and/or 2,3-diaminopropionic acid monohydrochloride (DAP), (Fluka, Ronkonkima, NY, U.S.A.). A cation trap column (CTC) filled with high-capacity, low-efficiency cation-exchange resin in the hydrogen form was placed between the pump and the injection valve. This column removed metals and other cation contaminants from the eluent, thus protecting the analytical column from unnecessary capacity losses and retention time shifts.

Concentrator columns. The analysis of ultra-trace quantities of anions in the ppb range was first described by Wetzel *et al.* [3]. The injection loop was replaced with a short guard column containing ion-exchange material similar to that of the analytical column to strip, *i.e.* "concentrate," ions from measured volumes of relatively clean aqueous samples. This process concentrates the desired species leading to a lowering of detection limits by orders of magnitude. The unique advantage of their use to the

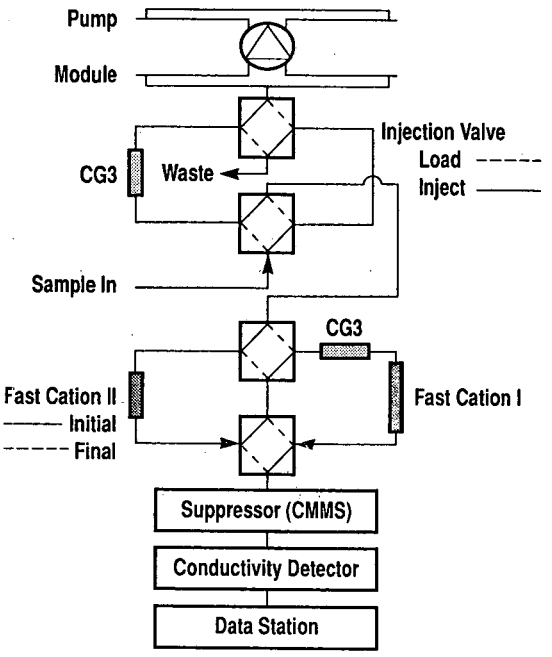

Fig. 1. Fast cation configuration for determining ppb levels of monovalent and divalent cations.

analyst is the capability of routine analysis of ions at sub-ppb (μg/l) levels, without extensive and laborious sample pretreatment.

The principal function of any concentrator is to strip ions from a sample matrix, without compromising the integrity of the analysis. For cation determinations, any cation-exchange column can function as a concentrator, assuming that it has adequate capacity and that the resin is compatible with the eluent. Short columns containing the same resin (guard columns) or columns with higher-capacity resins have both shown excellent performance characteristics for sample concentration. Commonly, to prevent overloading the concentrator column and/or loss of sample ions, a higher-capacity concentrator resin is used.

Sample loading is performed via a separate positive-displacement pump. Kinetics of mass transfer on pellicular ion-exchange resins is fast. This allows sample loading pump flow-rates of approximately 3–5 ml/min to be used, and sample concentration efficiencies high enough to assure good quantization [4]. Flow direction during concentration is also critical. The sample is loaded in one direction and then "backflushed" for injection with eluent flow in the opposite direction.

This configuration concentrates the cations in a compact band at the bottom of the column. When injected, all of the ions are rapidly eluted off the concentrator onto the guard, if present, and analytical columns, a desired effect. If instead, the sample is loaded in the same flow direction as the eluent flow, the cations are concentrated at the head of the column rather than at the bottom. When injected, the cations begin chromatographic separation in the concentrator before reaching the analytical columns. This is only useful when increased capacity is needed for better resolution of

the ions. However, for the column switching techniques described in this paper and for ions with large differences in capacity factor (k'), sample loading in the same direction as the eluent flow can severely reduce analytical performance. Almost always the function of the concentrator is to strip the ions of interest and not act as an analytical column. In order to ensure this, it is recommended that concentration be performed in a backflush manner routinely. A CG3 column is used as the concentrator for all applications in this paper.

Analytical columns. The analytical columns used in this study are the Dionex Fast Cation I, the CG3 and the Fast Cation II columns. These columns are packed with a pellicular cation-exchange resin. The resin is made from 13-μm diameter substrate made of styrene–divinylbenzene polymer resin and coated with cation-exchange latex particles. The Fast Cation I is a 250 × 4 mm column with 4% cross-linked latex, and the Fast Cation II is a 50 × 3 mm column with 2% cross-linked latex. All columns were used for the column-switching method. Use of a CG3 column with the Fast Cation I column improves resolution of the monovalents, and this was found in this study to improve quantization of samples containing ppm (mg/l) levels of ammonium or morpholine.

Column switching. Traditionally mono- and divalent cations have been difficult to analyze in the same injection because of large k' differences on cation-exchange materials. Column-switching procedures have been applied widely in gas chromatography during the past 20 years to deal with similar problems. In general, switching allows diversion of different sample components to different columns for maximum resolution with minimum time [5].

In this application for trace level analysis of cations, column switching has the effect of eluting the two groups of cations (mono- and divalents) through separate columns optimized for the chromatography of the respective groups. The monovalent cations elute through the Fast Cation I/CG3 combination. The divalent cations elute through a shorter column, the Fast Cation II. (The monovalent cations elute through both column sets, but their retention on the short Fast Cation II column is negligible.) The columns are different in two characteristics. First, the Fast Cation I/CG3 has the much higher capacity necessary to retain the monovalent cations. Second, the lower crosslinked latex used in the short Fast Cation II is designed to decrease retention of divalent cations without decreasing efficiency [6].

At injection, the Fast Cation II is placed in front of the Fast Cation I/CG3. Following injection, all the cations begin eluting through the Fast Cation II. The position of the two columns is reversed 1.25 min after injection with the use of the column switching valve.

This 1.25-min time period allows for all the cations to be removed from the concentrator and for the monovalent cations to have been eluted onto the Fast Cation I/CG3, but before the divalent cations have been eluted off of the Fast Cation II. This technique keeps the more strongly-retained divalent cations from reaching the higher-capacity Fast Cation I/CG3 columns. After the monovalent cations elute through the Fast Cation I/CG3, they then pass through the Fast Cation II again, actually passing through the divalent cations. All the cations then elute from the Fast Cation II to the suppressor and detector, with the monovalent cations eluting first, followed by the divalent cations.

Conductivity detection. A Dionex cation micromembrane suppressor (CMMS) is

used as part of the conductivity detector. It minimizes background conductivity from the eluent and enhances detector response. Regenerant is 100 m*M* tetrabutylammonium hydroxide (TBAOH). The hydroxide ions in the regenerant migrate across the anion-exchange membrane in the suppressor and react with hydronium ions in the eluent, producing water. At the same time, the anions (chloride) in the eluent cross into the regenerant and are replaced by the hydroxide ion. The suppression reaction has two effects: one, it decreases the conductivity of the acidic eluent by converting it to water, and two, it pairs the analytes with hydroxide counter ions. The combination of the two effects is a significant increase in the signal-to-noise ratio, which lowers the detection limit and widens the operating range.

The regenerant solution is continuously recycled by a Dionex AutoRegen Accessory. This device recirculates the regenerant solution through a high-capacity anion-exchange column in the hydroxide form. In this manner, anions in the suppressor regenerant effluent are removed and replaced by the hydroxide ions necessary for continuous eluent suppression.

Regenerant flow-rate in the AutoRegen Accessory was 5 ml/min. Higher and lower regenerant flow-rates produced minor changes in background conductivity without affecting performance. As the separate cation groups in the stream pass through the conductivity cell, they produce a peak-shaped trace on a recording chart. The heights or areas of the peaks are proportional to the specific cation concentrations, and quantization is achieved by comparing peak heights or areas to the same peak heights or areas for a calibration standard with known concentration.

Data station. Ion identity, analysis time, peak retention time, ion concentration, number of injections per standard, total number of standards, and type of calibration methods (area, height, linear, quadratic, etc.) were collected using a Dionex AI-450 computer data station. In these studies, multilevel calibration was used with linear least-squares best fit regression analysis, and peak heights were found, in general, to have better linearities and better reproducibilities. Unless otherwise noted, all calculations are based on comparison of peak height measurements and not peak areas.

Reagents

One cannot emphasize the need for high-quality deionized water too strongly. Blanks are as important for accurate trace level analysis as properly prepared standards and, in some ways, more important. Blanks establish the baseline reference for analysis. If a working detection limit of 50 parts-per-trillion (ppt, ng/l) is to be achieved, then the blank must be at least 10–20 ppt lower.

Water used in the preparation of the standards should be 18 MΩ · cm deionized water. The quality of the dilution water for standards must be determined by ion chromatography, since even 18 MΩ · cm water may contain several ppb of the ions of interest. To do this, analyze your dilution water in exactly the same manner as you would your sample.

At ppb levels, changes of contamination during collection or storage are high. Every container and every procedural step constitute a potential source of contamination. Polystyrene containers with leak-tight caps can be used to store 1 to 5 ppb levels of inorganic cations for up to 8 days [7]. Reagent-grade or better chemicals should be used in all tests. Unless otherwise indicated, all reagents should conform to the

specifications of the Committee on Analytical Reagents of the American Chemical Society. Other grades may be used, provided it is ascertained that the reagent is of sufficiently high purity to permit its use without lessening the accuracy of the determination.

RESULTS AND DISCUSSION

Methods

The goal of this project was to identify and develop as few analytical methods as possible for the broadest range of cationic chemical species found in power plant waters. The Fast Cation column-switching method proved very promising. One method was optimized for: (1) samples of ultrapure water, (2) water containing up to 1 ppm ammonium, (3) water containing up to 20 ppm morpholine and (4) water containing up to 1.2% boric acid. In each of the different power plant waters, both linearity and reproducibility studies were conducted.

Power plant water containing 1.2% boric acid and 1 ppm lithium hydroxide required alternate methods to achieve acceptable resolution of the lithium from other cations in the samples. Two existing isocratic, non-column-switching methods, were used: one for the determination of monovalent cations only, and one for the determination of divalent cations only.

Each sample was concentrated at different volumes ranging from 3.3 to 50 ml. Overloading effects, linearity, sensitivity and reproducibility were evaluated to determine a single concentrator volume useful for all water samples. This volume was experimentally found to be approximately 10 ml. All the data presented here is based on a 10-ml volume concentration. By modification of eluent and sample volumes, individual sample matrices can be optimized for increased sensitivity and reproducibility.

Trace cations in ultra-pure water

The method employed for trace cations in ultrapure water uses the column-switching method with the Fast Cation I/CG3 columns and the Fast Cation II column (see Table I). Fig. 2 represents a standard chromatogram for cations in ultra-pure

TABLE I

FAST CATION COLUMN-SWITCHING METHOD

Optimized for all Matrices except 1.2% boric acid and 1 ppm lithium.

Analytical columns	Dionex Fast Cation I, CG3 and Fast Cation II
Concentrator	CG3
Eluent	13.5 m*M* HCl, 0.23 m*M* DAP
Backpressure	1500–2000 p.s.i.
Flow-rate	2 ml/min
Column switch	1.25 min
Suppressor	Dionex CMMS
Regenerant	100 m*M* TBAOH, 5 ml/min with AutoRegen
Background conductivity	2–10 μS
By-pass loop	20 μl

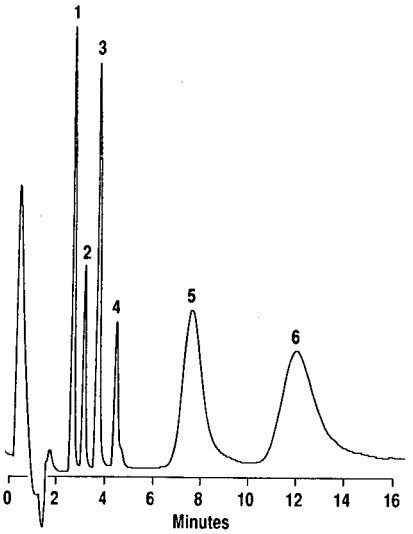

Fig. 2. Trace cations in ultrapure water. Column: Fast Cation I/CG3, Fast Cation II. Concentrator: CG3. Eluent: 13.5 m*M* HCl, 0.23 m*M* DAP. Flow-rate: 2 ml/min. Column switch: 1.25 min. Detector: conductivity, 3 μS. Suppressor: CMMS. Regenerant: 100 m*M* TBAOH. Volume concentrated: 10 ml. Peaks 1 = Li^+ (1 ppb); 2 = Na^+ (1 ppb); 3 = NH_4^+ (3 ppb); 4 = K^+ (3 ppb); 5 = Mg^{2+} (5 ppb); 6 = Ca^{2+} (10 ppb).

water. Six mixed multi-element standards ranging from 0.5, 1, 3, 5, 10 and 15 ppb of lithium, sodium, ammonium, potassium, magnesium and calcium were prepared. Sample volumes of 3.3, 9.9, 19.9, 39.9 and 49.9 ml were used. Three to five replicate measurements were made for each sample. Linearities of the cations for all volumes concentrated were found to have correlation coefficients (r) greater than 0.9960. No overloading of the concentrator or the analytical columns was observed over this analytical range.

The correlation coefficient for sodium over the range of 0.5 to 10 ppb using 10 ml concentrated was determined to be 0.9992. The relative standard deviation (R.S.D.) for 26 replicated analyses of a sodium standard at the 0.5-ppb level was 1.6%. Magnesium also showed a high degree of linearity over the range of 1 to 15 ppb with a correlation coefficient of 0.9989 using 10 ml concentrated. The R.S.D. for 24 replicate analyses of a magnesium standard at the 5-ppb level was 4.8%. All other monovalent and divalent cations showed similar performance capabilities as shown in Table II.

Power plant waters containing ammonium

The method employed for trace cations in water containing ammonium uses the column-switching method with the Fast Cation I/CG3 columns and the Fast Cation II column (see Table I). Fig. 3 represents a standard chromatogram for cations in 1 ppm ammonium. Six mixed multi-element standards ranging from 0.5, 1, 3, 5, 10 and 15 ppb of lithium, sodium, potassium, magnesium and calcium were prepared. Ammonium was varied from 200–1000 ppb in each of the mixed standards. Sample volumes of 3.3,

TABLE II

ANALYTICAL PERFORMANCE CAPABILITY

	Cations (ppb)						
	Li^+	Na^+	NH_4^+	K^+	Mg^{2+}	Ca^{2+}	Morpholine
In ultra pure water							
Level	0.5	0.5	1.0	1.0	5.0	5.0	
n	26	26	24	26	24	23	
R.S.D. (%)	2.8	1.6	5.9	2.6	4.8	5.8	
In 5 ppm morpholine							
Level	0.5	0.5	1.0	1.0	5.0	5.0	5000
n	20	20	20	20	20	21	20
R.S.D. (%)	4.5	5.0	4.2	6.1	6.5	11.7	2.7
In 1 ppm ammonium							
Level	0.5	0.5	1000	1.0	5.0	5.0	
n	24	23	24	24	23	22	
R.S.D. (%)	3.5	3.6	0.36	6.4	3.8	15	
In 1.2% boric acid							
Range	0.5–10	0.5–10	1–15	1–15			
Recovery (%)	97.4	98.3	98.2	106			

5.0, 9.9 and 19.9 ml were used. Three to five replicate measurements were made for each sample. Linearities of the cations for all volumes concentrated were found to have correlation coefficients (r) greater than 0.9900. Volumes greater than 10 ml with 1-ppm

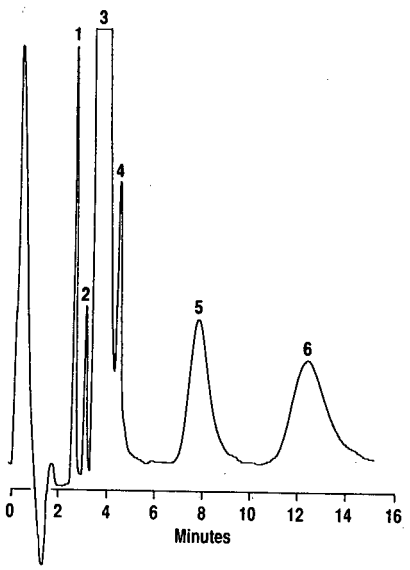

Fig. 3. Trace level cations in power plant waters containing 1 ppm ammonium. Conditions as in Fig. 2. Peaks: 1 = Li^+ (1 ppb); 2 = Na^+ (1 ppb); 3 = NH_4^+ (1 ppm); 4 = K^+ (3 ppb); 5 = Mg^{2+} (5 ppb); 6 = Ca^{2+} (10 ppb).

levels of ammonium began to compromise the reproducibility and linearity of sodium and potassium. The reproducibilities of calcium and magnesium were also affected by sample volumes greater than 10 ml with 1 ppm ammonium.

The correlation coefficient for sodium over the range of 0.5 to 10 ppb using 10 ml concentrated in water containing 200 to 1000 ppb ammonium remained greater than 0.9990. The R.S.D. for 23 replicate analyses of a sodium standard at the 0.5-ppb level was 3.6%. Magnesium's linearity over the range of 1 to 15 ppb in 200 to 1000 ppb ammonium exhibited a correlation coefficient of 0.9910 using 10 ml concentrated. The R.S.D. for a magnesium standard at the 5-ppb level was 3.8%. Calcium was the only cation which had a R.S.D. greater than 10%. All other cations showed similar performance capabilities over the analytical range as shown in Table II.

The reproducibility of ammonium from the concentrator was 0.36% R.S.D. at the 1-ppm concentration and 10 ml concentrated for 24 replicate analyses, as shown in Table II. Linearity of ammonium from the concentrator column over the range of 200–500 ppb revealed a correlation coefficient of 0.9990. Concentrations higher than 500 ppb were non-linear for both peak height and peak areas. Current development work is being conducted on improving quantization and the linear working range of ammonium.

A recently invented technique has shown promising results for quantitating ppm levels of ammonium and trace level cations in the same injection. A standard slider valve for concentrator work is comprised of a concentrator side and a by-pass loop side. In the inject position, the by-pass loop is flushed with the next sample to be concentrated. This purges the previous sample from the system tubing. When the valve is switched to load, the small volume in the by-pass loop (10 to 100 μl) is injected into the ion chromatograph. This volume behaves as a normal-loop sample injected through the column and the conductivity detector. For ultrapure water no peaks are detectable from the ions in the loop injection because of their low level. When samples of water containing ppm levels of cation additives are flushed through this loop and injected, measurable peaks for the additives can be detected and are capable of being quantified. This procedure can often be optimized for monitoring a major additive and for measuring trace level components in the same run.

By adjusting when the concentrator is injected and when data sampling begins, the peak due to the by-pass loop can be accurately detected or eliminated from a chromatographic run. This technique shows strong promise for waters containing ammonium or lithium. An example of this effect is shown in Fig. 4 where the ammonium (peak 3) appears twice.

The first peak labeled 3 is caused by the by-pass loop and the second, larger peak labeled 3 is due to the ammonium from the concentrator column. Linearity of the ammonium from the by-pass loop measured from 250 ppb to 2500 ppb showed a correlation coefficient of 0.9980.

Power plant waters containing morpholine

Diethylenimide oxide or tetrahydro-1,4-isoxazine, commonly known as morpholine, is becoming popular as a corrosion inhibitor. Morpholine, with a pK_a of 8.3 [8], exists as a weak base in normal power waters.

The method employed for trace cations in water containing morpholine uses the column-switching method with the Fast Cation I/CG3 columns and the Fast Cation II

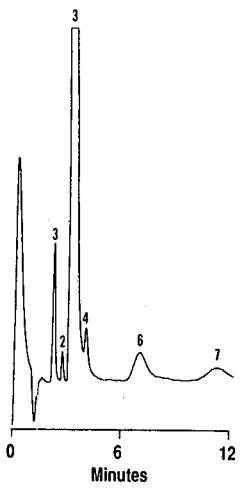

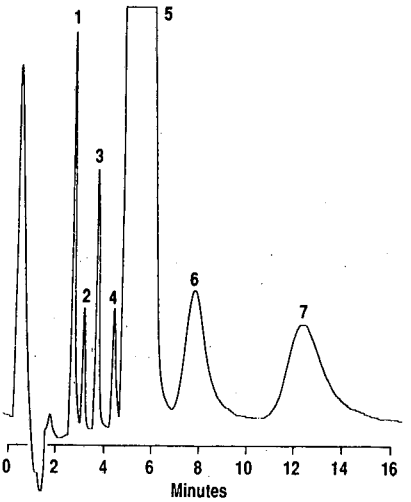

Fig. 4. Trace level cations in power plant waters containig 1 ppm ammonium. Column: Fast Cation I and II. Concentrator: CG3. Volume concentrated: 10 ml. Eluent: 13.5 m*M* HCl, 0.229 m*M* DAP. Flow-rate: 2 ml/min. Range: 3 μS. Column switch: 1.25 min. Suppressor: CMMS. Regenerant: 100 m*M* TBAOH, 3–5 ml with AutoRegen. Peaks: 2 = Na^+ (1 ppb); 3 = NH_4^+ (1 ppm); 4 = K^+ (3 ppb); 6 = Mg^{2+} (5 ppb); 7 = Ca^{2+} (5 ppb).

Fig. 5. Trace level cations in power plant waters containing morpholine. Conditions as in Fig. 2. Peaks: 1 = Li^+ (1 ppb); 2 = Na^+ (1 ppb); 3 = NH_4^+ (3 ppb); 4 = K^+ (3 ppb); 5 = morpholine$^+$ (5 ppm); 6 = Mg^{2+} (5 ppb); 7 = Ca^{2+} (10 ppb).

column (see Table I). Fig. 5 represents a standard chromatogram for cations in 5 ppm morpholine. Six mixed multi-element standards ranging from 0.5, 1, 3, 5, 10 and 15 ppb of lithium, sodium, ammonium, potassium, magnesium and calcium were prepared. Morpholine was varied from 1 to 20 ppm in each of the different samples. Sample volumes of 3.3, 5.0, 9.9 and 19.9 ml were used. Three to five replicate measurements were made for each sample. Linearities of the cations for all volumes concentrated were found to have correlation coefficients (r) greater than 0.9900. Volumes greater than 10 ml with ppm levels of morpholine exhibited overloading of the analytical columns and shifting retention times of the cations.

The correlation coefficient for sodium over the range of 0.5 to 5 ppb using 10 ml concentrated in water containing 1 to 20 ppm morpholine was 0.9989. The R.S.D. for 20 replicate analyses of a sodium standard at the 0.5-ppb level was 5.0%. Magnesium linearity over the range of 1 to 15 ppb in 1 to 20 ppm morpholine exhibited a correlation coefficient of 0.9993 using 10 ml concentrated. The R.S.D. for 20 replicate analyses of a magnesium standard at the 5-ppb level was 6.5%. Calcium was the only cation which had a R.S.D. greater than 10%. All other cations performance capabilities were similar over the analytical range as shown in Table II.

The reproducibility of the morpholine from the concentrator demonstrated a R.S.D. of 2.7% at the 5-ppm concentration and 10 ml concentrated for 20 replicate analyses, as shown in Table II. Linearity of morpholine from the concentrator column over the range of 1 to 20 ppm morpholine by peak area was 0.9970, as shown in Fig. 6.

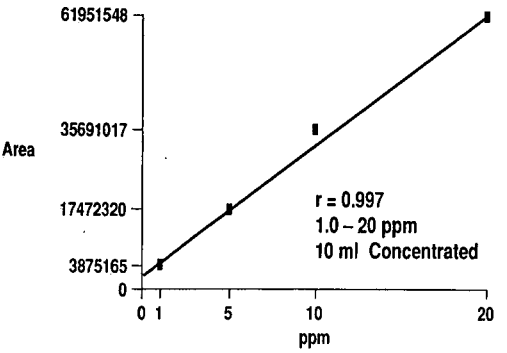

Fig. 6. Linearity of morpholine in power plant waters by area. Range: 10 μS. Other conditions as in Fig. 4.

Trace cations in the presence of 1.2% boric acid

The method employed for trace cations in water containing boric acid also uses the column-switching method with the Fast Cation I/CG3 columns and the Fast Cation II column (see Table I).

In dealing with this matrix the most noticeable problem is the difficulty in preparing sample standards. After adding sufficient quantity of boric acid for a 1.2% solution, blanks of the cations can be as high as 20 ppb!

In this study, the solution of 1.2% boric acid was pumped through a cation trap column (CTC) in the hydrogen form to reduce the cation contamination. This procedure produced ultrapure boric acid solutions, but the procedure was time consuming and tedious. Because of the limited volume of boric acid solution produced, limited experiments were performed.

Recovery experiments were performed on the monovalent cations (see Table II). All cations were shown to have recoveries better than 97%. The recovery value was determined by the ratio of the peak height of a standard 50-μl loop injection of a known mass concentration to the peak height of a 10-ml concentrated sample with the same theoretical mass concentration. This data indicates that the boric acid solution should have an analytical performance similar to other power plant waters.

Trace cations in the presence of 1.2% boric acid and lithium hydroxide

The column-switching method with the Fast Cation I/CG3 column and Fast Cation II column did not have the resolution necessary to quantitate 1 ppb sodium in the presence of 1 ppm lithium, regardless of the boric acid concentration. Two isocratic methods were used to detect and quantitate the cations: a method for the determination of the monovalent cations and a separate method for the determination of the divalent cations.

The monovalent cations were separated using an isocratic eluent of 10 m*M* hydrochloric acid, the Fast Cation II column as a guard, and the Fast Cation I column as the analytical column. The flow-rate of the eluent is 2 ml/min. A solution of 100 m*M* TBAOH was used as the regenerant with the Dionex CMMS. This combination allows for the maximum resolution of 1 ppm lithium and 1 ppb sodium (Fig. 7).

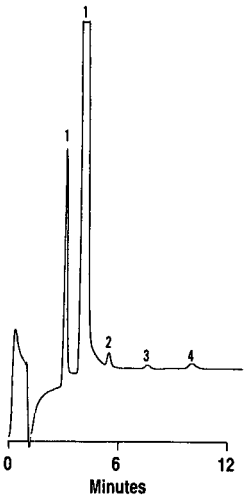

Fig. 7. Trace level monovalent cations in power plant waters containing 1.2% boric acid and 1 ppm lithium hydroxide. Column: Fast Cation II. Analytical column: Fast Cation I. Concentrator: CG3. Volume concentrated: 2 ml. Eluent: 10 m*M* HCl. Flow-rate: 2 ml/min. Range: 10 μS. Suppressor: CMMS. Regenerant: 100 m*M* TBAOH, 3–5 ml with AutoRegen. Peaks: 1 = Li^+ (1000 ppb); 2 = Na^+ (3 ppb); 3 = NH_4^+ (4 ppb); 5 = K^+ (6 ppb).

The divalent cation determination uses only the Fast Cation I column for the separation. The monovalent cations elute in the void volume. The divalent cations can be determined in under 6 minutes with an isocratic eluent of 34 m*M* hydrochloric acid, 9 m*M* 2,3-diaminopropionic acid monohydrochloride at a flow-rate of 2 ml/min. Again 100 m*M* TBAOH was used with the Dionex CMMS.

ADVANCED CATION SEPARATIONS

Dionex recently introduce a new column, the Ion Pac CS-10, specifically for the analysis of alkaline metals and alkaline earth metals. It is 250 mm × 4 mm cation-exchange column with an approximate capacity of 30 μequiv./column.

The pellicular particles used in the CS-10 column consist of a latex coating on a non-porous core. The non-porous core consists of an 8.5-μm diameter 50% cross-link ethylvinylaromatic polymer bead. The high cross-link of the core assures virtually no swelling of the core occurs if organic solvents are used. The core particles are synthesized so as to obtain directly a spherical particle with negative surface charge. While pellicular anion-exchange can be made via electrostatic attachment of the anion-exchange particles to this surface, the preparation of cation-exchange materials from this same core particle requires a double layer attachment process. The primary pellicle consists of an anion-exchange latex coating. The size and composition of this anion-exchange latex was chosen so that the magnitude of anion-exchange retention is relatively minor. The secondary pellicle is a 175-nm cation-exchange latex coating. This layer comprises the analytical ion-exchange layer with a nominal efficiency for magnesium using standard operating conditions of 24 000 plates/m [9].

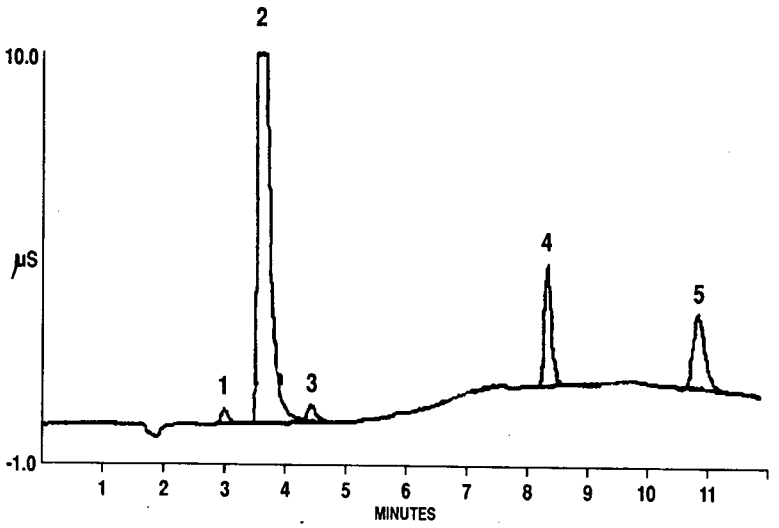

Fig. 8. Calibration standard for cations in high-purity water, Virginia Power Company, Surrey Power Station. Column: CG-10, CS-10. Concentrator: CG-10. Trap column: CTC. Eluents: (EI) 30 m*M* HCl, 0.5 m*M* DAP and (E2) 50 m*M* HCl, 12 m*M* DAP. Eluent switch: 2.0 min. Flow-rate: 1 ml/min. Volume concentrated: 30 ml. Suppressor: CMMS-II. Regenerant: 50 m*M* TBAOH. Peaks: 1 = Na^+ (0.2 ppb); 2 = NH_4^+ (2.0 ppb) ;3 = K^+ (0.5 ppb); 4 = Mg^{2+} (1.0 ppb); 5 = Ca^{2+} (2.0 ppb).

This column used with an eluent step change has shown high resolution and sensitivity for the monovalent cations, even with high ratios of ammonium to sodium, and improved efficiencies and sensitivities for the divalent cations. These improvements for the divalent cations have lowered their detection limits by at least an order of magnitude compared to the column switching technique presented in this paper. This CS-10 has developed the ability to monitor, for the first time, sub-ppb levels of divalent cations in ultrapure and power plant waters.

Fig. 8, developed by Dennis Bostics, Senior Chemist of Virginia Power Company, shows an example of the capability of the CS-10 column for the separation of cations at low and sub-ppb levels. Note the resolution of the monovalents and efficiency for the divalents using an eluent step change. The eluent for this separation begins with a weak 30 m*M* hydrochloric acid–0.5 m*M* 2,3-diaminopropionic acid monohydrochloride eluent; 2 min after injection the eluent is step changed to a stronger eluent, 50 m*M* hydrochloric acid–12 m*M* 2,3-diaminopropionic acid monohydrochloride, for eluting the divalent cations. After the calcium is eluted from the column, the eluent is switched back to the weak eluent for reequilibration of the column. During the reequilibration of 5 to 10 min, the next sample can be concentrated for analysis.

Fig. 9 is an actual sample of Virginia Power's unit one feedwater. For this chromatogram, 60 ml of sample were concentrated. Again, notice the resolution of the low sodium, sub-ppb, in the presence of the higher ppb levels of ammonium. Under these conditions it has been discovered that hydrazine is also retained on this column. The peak labeled potassium in this chromatogram is actually a coelution of potassium

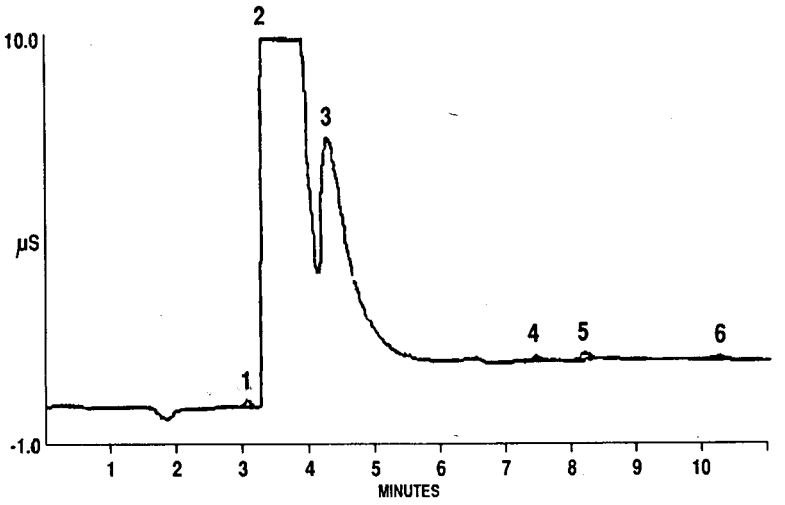

Fig. 9. Unit 1 feedwater, Virginia Power Company, Surrey Power Station. Volume concentrated: 60 ml. Other conditions as in Fig. 8. Peaks: 1 = Na^+ (0.017 ppb); 2 = NH_4^+ (36 ppb); 3 = K^+ (0.94 ppb); 4 = Mg^{2+} (0.008 ppb); 5 = Mn^{4+}; 6 = Ca^{2+} (0.018 ppb).

and the hydrazine present in the feedwater. Finally, it has been discovered that manganese is detected very well using this technique and can be accurately determined to low ppt levels. In conclusion, the use of the new CS-10 column holds strong promise for the rapid determination of both monovalent and divalent cations to low ppt levels in ultrapure and power plant waters.

REFERENCES

1 D. Dutina, M. N. Robles and T. O. Passell, *In-Plant System for Continuous Low Level Ion Measurement in Steam Producing Water, Research Project 1447-1, Final Report*, EPRI, Palo Alto, CA, Sept. 1987.
2 J. Noyes, *Experience with the Dionex 8000 Inline Ion Chromatograph*, presented at the *9th Annual EPRI Plant Chemists Meeting, Lake Buena Vista, FL, June 1987.*
3 R. A. Wetzel, C. L. Anderson, H. Schleicher and G. D. Crook, *Anal. Chem.*, 51 (1979) 1532.
4 *Technical Note 8R*, Dionex, Sunnyvale, CA, May, 1985.
5 L. R. Snyder and J. J. Kirkland, *Introduction to Modern Liquid Chromatography*, Wiley, New York, 2nd ed., 1979.
6 R. D. Rocklin, M. A. Rey, J. R. Stillian and D. L. Campbell, *J. Chromatogr. Sci.*, 27 (1989) 474–478.
7 D. F. Pensenstadler, S. H. Person, J. C. Bellows and W. M. Hickum, *Program for Steam Purity Monitoring, Number 1, Instrumentation and Sampling, Proceedings ASTM D-19, Milwaukee, WI, June, 1980.*
8 R. C. Weast (Editor), *Handbook of Chemistry and Physics*, CRC Press, Boca Raton, FL, 56th ed., 1975–1976.
9 J. Stillian, C. Pohl, A. Woodruff and C. R. Devasa, presented at the *Pittsburgh Conference, New York, 1990*, paper No. 628.

Journal of Chromatography, 546 (1991) 243–249
Elsevier Science Publishers B.V., Amsterdam

CHROMSYMP. 2263

Progress in optimization of transition metal cation chromatography and its application to analysis of silicon wafer contamination

KENNETH A. RUTH* and ROGER W. SHAW
MEMC Electronic Materials Co., P.O. Box 8, St. Peters, MO 63376 (U.S.A.)

ABSTRACT

Methods are reported which yield sensitive semi-quantitative analysis of transition metal contaminants on silicon wafers. An effective extracting solution is proposed together with compatible concentrators and two eluent (column and post-column) chemistry combinations to measure ppt (10^{12}) concentrations and surface densities extending into the 10^{10} atoms per cm^2 range. Possible applications include numerous steps in wafer and integrated circuit manufacture as well as other solid-surface analysis.

INTRODUCTION

Silicon wafers are the building blocks upon which integrated circuits are formed. The production of these wafers involves poly-crystal silicon manufacture, single crystal growth, slicing, lapping, edge grinding, heat treatment, polishing, final cleaning and packaging. At every step, purity is a key issue, since the intentional dopants which govern the semiconducting properties are typically present in the ppb[a] range. Other impurities must generally be controlled at still lower levels. Certain metals such as Cu, Fe and Ni are of particular concern because of the speed with which they enter and move through silicon during heat treatments and their detrimental effects on electrical and defect properties once there. We have utilized a number of sensitive techniques for the study of these contaminants including total reflection X-ray fluorescence (TXRF), secondary-ion mass spectroscopy (SIMS) and ion chromatography (IC). Among these options, IC offers a cost-effective method for rapid, in-house testing and process control. It also is complementary to the other methods in that it samples all surface and edges of the wafers rather than localized, generally front-side-only areas.

This paper will present improvements over prior transition metal methods [1–6] for this type of work. The process development has necessarily been done simultaneously with regular analytical work so that the final solutions are probably not fully optimized.

[a] Throughout this article, the American billion (10^9) is meant.

0021-9673/91/$03.50

EXPERIMENTAL

Auxiliary equipment

Silicon, in the presence of air and moisture, rapidly forms a native oxide layer of approximately 1 nm thickness. Indeed, the traditional cleaning processes [7] incorporate oxidative baths prior to the final rinse and spin dry in order to yield a stable surface. Any foreign elements incorporated into this oxide are potential contaminants of the silicon or the silicon dioxide layers formed in later processing. Thus an effective method for studying the wafer surface must include a means of digesting this SiO_2 layer. HF is the traditional solvent in this case and the one used here. Additional additives to this digestion–extraction solution have been investigated and are reported below.

Cells for the wafer extraction process have been fabricated from PTFE polymer sheets backed by stainless steel as shown in Fig. 1. The requirements were (1) chemical inertness and purity, (2) a maximum wafer surface to liquid volume ratio consistent with (a) ready access of the liquid to all surfaces and (b) the machinability of PTFE, (3) approximately 60 ml liquid volume and (4) a design which accepts whole wafers. Each of the standard wafer diameters, 100, 125, 150 and 200 mm, therefore has its own cell designed to accept four, three, two and one wafer, respectively. The edges of the multiple-wafer cells are grooved to maintain separation of the wafers while several raised points formed in the sidewalls serve this purpose for the single-wafer, 200-mm cell. Fig. 1 illustrates the four wafer, 100-mm cells. Drain and fill ports are machined into the bottom and top of each cell. The top includes an O-ring seal (not shown) so that the liquid can be forced out and through the concentrator column by gas pressure rather than pumping at this critical point. Conversion from impurity concentration in the liquid to surface concentration on the wafers is a geometrical calculation; 1 ppb corresponds to roughly $1 \cdot 10^{12}$ atoms per cm^2.

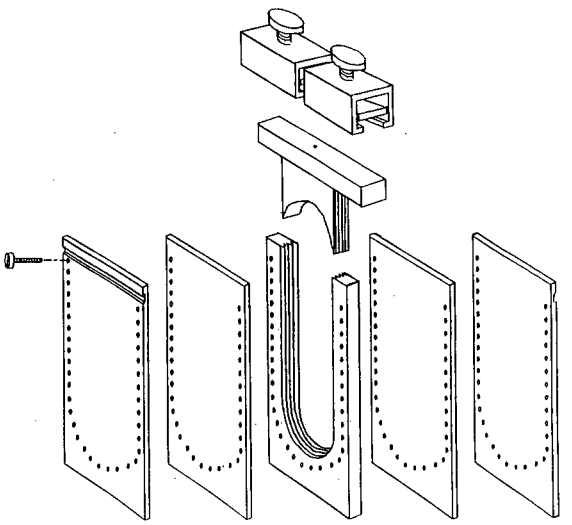

Fig. 1. Exploded view of cell for extraction of contaminants from wafer surfaces. The U-shaped piece, its cap and neighboring plates are PTFE and form the cell walls. The outer plates are stainless steel and the cap clamps are aluminum and stainless.

Water purity

The water supply to our laboratory utilizes reverse osmosis/deionization treatment which produces 18 MΩ water with less than 15 ppb total organic carbon. Nevertheless, column lifetimes on the order of weeks have been common using this water. Tests using water from sources with point-of-use final purification systems have indicated that water was a major factor in the problem. In an effort to improve the water a four-bowl Milli-Q point-of-use purification system was first tested. This yielded improved but still limited lifetimes. A Milli-Q UV Plus system was then installed and, with the other changes described below, has led to very satisfactory column lifetimes and background levels.

Progress toward a stable method

All of this work has involved the use of a concentrator cartridge to enhance sensitivity. This concentrator must be stable and non-contaminating in the presence of the extracting acid. This has necessitated the use of a polymer-based packing material and the avoidance of all metal parts such as the frits which are frequently used in concentrators. Both Waters and Dionex cation concentrator packings have been used successfully in this function.

Following excellent initial results with the Waters TSK column and ethylenediamine plus citric acid eluent, water-related column degradation soon became evident. Tailing of the Cu peak was the initial symptom followed by disappearance of this peak and tailing of other peaks. A number of packings and guard column arrangements were tried, always with more or less limited success until the water supply was improved with the installation of the Milli-Q UV Plus system. With this system the degradation of a Spherisorb ODS-5 column then in use was slowed but not stopped. The Dionex HPIC-CS5 polymer-based column has now given seven months of service without problems. The Waters TSK column has not been tested with this water supply.

The present system

The current system starts with the PTFE extraction cells. These are filled with a solution of 18.9 m*M* HF, 50 m*M* HCl and 4.9 m*M* H_2O_2 (see discussion below). The entire cell assembly is subjected to ultrasonic excitation and two 11-ml samples are taken to provide background data. The wafers are then added and the cell refilled from the same reservoir. The Si native oxide is dissolved within approximately 15 min with further ultrasonic agitation, and two more samples are taken. Concentration is accomplished by forcing these samples through a Dionex TCC-1 trace cation concentrator using approximately 45 p.s.i. nitrogen pressure on the cell. Flow switching at this point is handled by a Rheodyne inert switching valve (Model 90910).

Separation occurs on a Dionex HPIC-CS5 column with eluent composition of 3 m*M* pyridine-2,6-dicarboxylic acid (PDCA), 4.3 m*M* LiOH, 2 m*M* Na_2SO_4 and 25 m*M* NaCl [8]. The eluent is driven by a Wescan inert pump and membrane pulsation suppressor operating at 1 ml/min. Post-column derivatization utilizes a solution of 1 m*M* 4-(2-pyridylazo)resorcinol (PAR) and 3 *M* NH_4OH, (adjusted to pH 11 with acetic acid) flowing at 0.6 ml/min from a Waters reagent delivery module. Detection is via a Waters 484 UV–VIS detector operating at 520 nm. This method is referred to elsewhere in this paper as method 1. Data handling and valve switching are under the

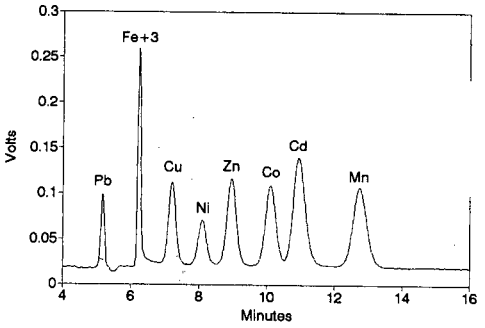

Fig. 2. Chromatogram for a 5-ppb multiple standard (except Cd and Pb at 20 ppb) using method 1.

control of Waters Maxima software and an NEC Powermate computer. A typical chromatogram using this system is shown in Fig. 2.

RESULTS AND DISCUSSION

Improvements to standard methods

The paper of Yan and Schwedt [9] suggested several means of increasing the sensitivity above that of the standard methods. These have been investigated and the positive results incorporated into the methods discussed. Data are presented here supporting their efficacy.

Increasing the PAR concentration to 1 m*M* from the recommended 0.2 m*M* yields the results shown in Fig. 3 for the present system. A pH near 11 is needed to stabilize the PAR at this concentration. This solution can be held for a week under a nitrogen atmosphere. The operating point of 1 m*M* was chosen in order to maximize the Ni response with little loss elsewhere.

The following improvements were found to be effective for a modified Waters Method SMTE-708 [10] (Nova-Pak C_{18} column with 100 m*M* tartaric acid, 2 m*M* octanesulfonate and 10% acetonitrile adjusted to pH of 3.05 with NaOH). First, the addition of 10 ft. of 1/16 in. diameter PTFE tubing held at 60°C following introduction of the post-column reagents increases the sensitivity of most of the detectable elements, Fe^{2+}, in particular, yields a factor of 10 larger signal. Other elements show fractional improvements. Second, Zn-EDTA (the $ZnNa_2$ salt of ethylenediaminetetraacetic acid) at 0.13 m*M* concentration in the post-column reaction solution enables the alkaline earth ions Ca and Mg to be detected. It also increases the sensitivity for Pb by a factor of 2. The optimum wavelength for detection in this case is 490 nm. In this method Fe^{3+} elutes in the void volume and is not quantitatively detected. This method is referred to here as method 2. A 10-ppb chromatogram is shown in Fig. 4. We have not yet returned to this method following the water improvement in order to test its stability.

Only the PAR increase is effective for method 1. Increased post-column temperature reduces sensitivity in this case while Ca and Fe^{3+} elute simultaneously.

Optimization of the digestion–extraction solution

The minimum HF concentration in the solution used to sample contaminants

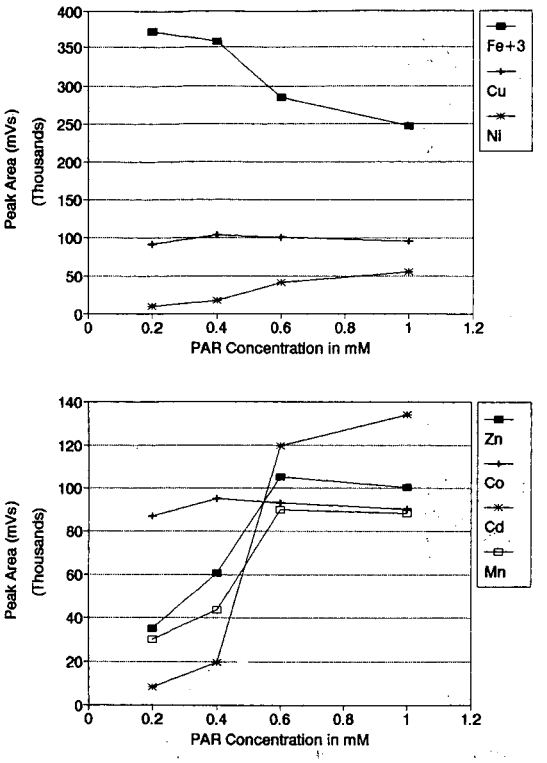

Fig. 3. Effect of PAR concentration on peak area response to a 1.5-ppb multiple standard.

from the wafers is limited by the need for a reasonable time to dissolve the native oxide. This solution does not yield high recovery and detection of the elements on those surfaces. In addition, the iron on the surface may be divided between valence 2 and 3 states, with quite different sensitivities to the two states. Since this valence information is secondary for the present purpose, Fe is converted entirely to the more sensitive 3+ state by the addition of H_2O_2 at the 4.9 mM level for method 1.

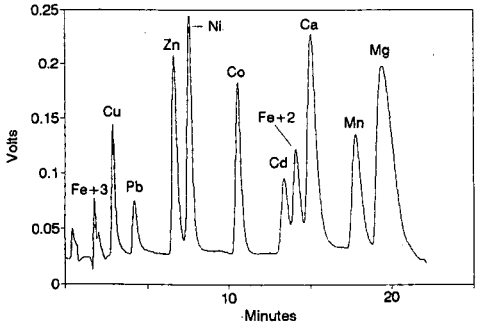

Fig. 4. Chromatogram for a 10-ppb multiple standard using method 2.

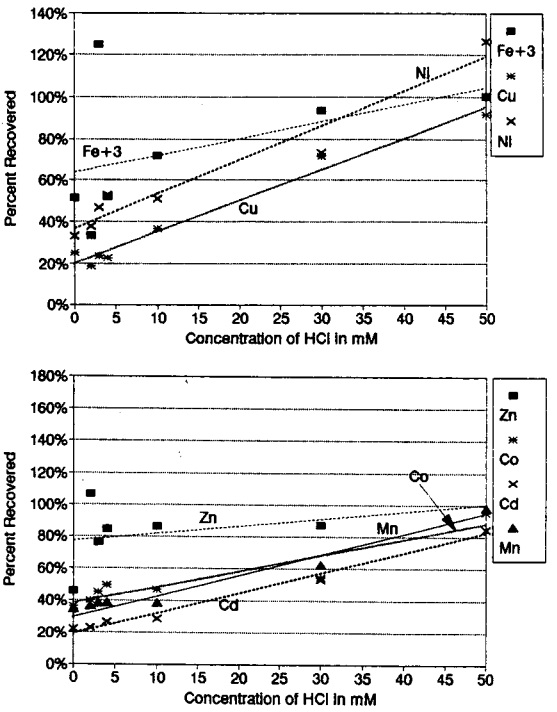

Fig. 5. Percentage recovery of intentional contamination at the 1.5-ppb level on a 100-mm wafer using method 1. In each case the system background reading measured prior to the introduction of the wafer has been subtracted. The straight lines are linear regressions to each set of data.

TABLE I

DETECTION LIMITS MEASURED FOR THE TWO COLUMNS AND CHEMISTRIES DISCUSSED

Signal-to-noise ratio = 3.

Ion	Method 1[a]		Method 2[b]		System background	
	ppb	$1 \cdot 10^{10}$ atoms/cm^2	ppb	$1 \cdot 10^{10}$ atoms/cm^2	ppb	$1 \cdot 10^{10}$ atoms/cm^2
Pb	0.30	7	0.20	5		
Fe^{3+}	0.02	2			3.20	300
Fe^{2+}	—[c]	—[c]	0.11	10		
Cu	0.06	5	0.08	6		
Ni	0.12	10	0.05	4		
Zn	0.06	5	0.05	4	0.43	35
Co	0.07	6	0.06	5		
Cd	0.20	17	0.15	13		
Mn	0.07	6	0.10	9		
Ca			0.05	6		
Mg			0.06	13		

[a] PAR concentration, 1 m*M*; Zn-EDTA concentration, 0 m*M*; no reaction coil used.
[b] PAR concentration, 1 m*M*; Zn-EDTA concentration, 0.13 m*M*; reaction coil used at 60°C.
[c] Can be detected but is converted to Fe^{3+} with H_2O_2.

In order to improve the recovery and detection of the surface impurities, HCl has been added as mentioned earlier. The effect of this addition is shown in Fig. 5. Here the proper amount of dilute multiple standard to yield a 1.5-ppb solution of each of the elements in the cell has been placed on a wafer surface and allowed to dry. Such wafers were then placed in the cell containing the extraction solution with variable HCl concentration, and the resulting solution was analyzed. Zinc was approximately fully recovered in all cases but all of the other elements studied benefitted from the HCl addition. At higher levels of the metals the recovery was more complete even at low HCl concentration. For the cell without wafers, recovery was also complete except for Fe and Cd at approximately 65%. Thus the retained amounts are primarily associated with sites on the silicon wafers themselves.

Detection limits and background levels

Table I illustrates typical detection limits for the methods discussed above together with the surface concentration equivalents. The system backgrounds shown limit the practical detection limits for Fe and Zn to three times their standard deviation or approximately 3 and 0.4 ppb, respectively.

REFERENCES

1 R. M. Cassidy, S. Elchuk and J. O. McHugh, *Anal. Chem.*, 54 (1982) 727.
2 I. M. Hwang, F. C. Chang and Y. C. Yeh, *J. Chin. Chem. Soc.*, 30 (1983) 167.
3 W. N. Wang, Y. J. Chen and M. T. Mu, *Analyst*, 109 (1984) 281.
4 G. I. Schmidt and P. P. W. Scott, *Analyst*, 109 (1984) 997.
5 P. Jones, K. Barron and L. Ebdon, *J. Chromatogr.*, 354 (1986) 407.
6 D. R. Yan and G. Schwedt, *Fresenius' Z. Anal. Chem.*, 320 (1985) 325.
7 W. Kern and D. A. Puotinen, *RCA Rev.*, 31 (1970) 187.
8 *Dionex Technical Note TN 10*, Dionex, Sunnyvale, CA, December, 1987.
9 D. Yan and G. Schwedt, *Fresenius' Z. Anal. Chem.*, 327 (1987) 503.
10 R. M. Cassidy and S. Elchuck, *Anal. Chem.*, 54 (1982) 1558.

Journal of Chromatography, 546 (1991) 251–257
Elsevier Science Publishers B.V., Amsterdam

CHROMSYMP. 2095

Cation analysis of fermentation broth by high-performance liquid chromatography utilizing ion interaction

ROBERT G. BELL
A. L. Laboratories, Inc., 400 State Street, Chicago Heights, IL 60411 (U.S.A.)

ABSTRACT

Nutrient information concerning the specific needs of microorganisms in fermentation broth is crucial to the potency and production of an antibiotic. Nutrient analysis is hindered by an array of fermentation broth matrix interferences. These matrix interferences can be effectively removed by ashing the sample, although most of the major interferences can be removed by solid-phase extraction. The ashed sample was extracted using 10^{-3} *M* nitric acid and filtered through a 0.45-μm filter. The sample extract was chromatographed on an Adsorbosphere HS C_{18} column with conductivity detection. The mobile phase consisted of 40 m*M* tartaric acid, 2 m*M* sodium octanesulfonate in 5% methanol adjusted to pH 4.0 with sodium hydroxide. The flow-rate was 0.8 ml/min. Under these conditions, calcium, copper, lead, zinc, nickel, cobalt, cadmium, iron(III), magnesium and manganese are separated in less than 35 min. All analytes, with the exception of calcium and iron, are baseline-resolved. The response is linear for the range 1–1000 ppm. This method is able to monitor the microorganisms' cation consumption from the starting raw materials such as the flours and water used in producing a suitable starting culture to the final fermentation products. The use of post-column derivatization using ultraviolet detection allows for greater minimum detectable quantities (approximately 10^{-9} g) with a larger linear dynamic range.

INTRODUCTION

Information concerning the nutritional requirements of a microorganism in fermentation broth is crucial to the potency and production of an antibiotic. Their shifting nutrient consumption of carbohydrates, amino acids, vitamins, minerals and medium additives need to be monitored in order to promote optimal growth of the microorganism. All nutrients can limit the antibiotic production rate by being present in concentrations that imbalance the microorganisms' metabolic processes. The concentration ranges which enhance or inhibit fermentation activity vary with each microorganism, chemical species and growth conditions. The conditions and medium required for the optimal growth phase may differ somewhat from the conditions required for the production phase.

Concentrations of specific elements are vital as co-factors to the optimal metabolism of commercially important compounds. Optimal bacitracin production requires manganese at 0.7 μM but is inhibited by a manganese concentration of 40 μM [1]. *Streptomyces griseus* requires five times as much iron to produce streptomycin as

0021-9673/91/$03.50

it does for growth [2]. *Corynebacterium diphtheriae* only produces its toxin when iron levels are below 0.8 ppm [2].

Analysis of the trace elements is hindered by an array of fermentation broth matrix interferences. Industrial fermentation broth contains a host of natural ingredients, such as soy and cottonseed flours, peanut and corn meals, molasses, starch, beef extract and lard oil, as well as the starting culture. Through aerobic respiration, these starting materials undergo enzymatic and chemical degradation which result in numerous metabolic by-products which can interfere with chromatographic analysis. These matrix interferences can be effectively removed by ashing the fermentation broth sample, although most of the major interferences can be removed by solid-phase extraction, enabling trace mineral measurement by high-performance liquid chromatography (HPLC) utilizing an ion-interaction or ion-pairing reagent (IC).

HPLC–IC is a version of ion-exchange chromatography where ionizable solutes can be separated by differences in the electrostatic interaction with an ionizable stationary phase. The conductivity of the mobile phase has to be low in order to attain instrumental sensitivity if conductivity detection is used. This is usually attained by either suppressed conductivity or with the use of low-conductivity eluents.

An alternative to ion-exchange and ion-suppression analysis of ionic samples is the technique referred to as ion-pair chromatography. The pH of the eluent is adjusted to optimize ionization of the sample. The chromatographic retention is altered by including a counter ion in the mobile phase. This technique has the ability to separate both ionic and neutral materials. The detection of the separated species can be done with conductivity detection unless post-column derivitization is performed to enable UV–visible or fluorescence detection. In this paper, techniques for sample preparation and HPLC–IC analysis for several trace metals in fermentation broth are described.

EXPERIMENTAL

Materials

The mobile phase components were prepared with HPLC-grade methanol and water (Burdick and Jackson, Muskegon, MI, U.S.A.), sodium octanesulfonate and tartaric acid (Sigma, St. Louis, MO, U.S.A.). A system suitability solution containing calcium, cadmium, cobalt, copper, iron, lead, maganese, magnesium, nickel and zinc as the chloride salts was prepared. The system suitability solution provides a measure of performance of the chromatographic systems' ability to reproducibly resolve the ions of interest.

Chromatographic system

A chromatograph equipped with a constant-flow pump (Wescan 2815, Alltech Assoc., Deerfield, IL, U.S.A.) was used with a conductivity detector (Wescan 215), a variable-wavelength UV–visible detector (Shimadzu SPD-6AV, Kyoto, Japan), an autosampler (Shimadzu SIL-9A) and integrator (Shimadzu CR-501). The separations were performed on an Adsorbosphere HS C_{18} column (250 mm × 4.6 mm, 7 μm particle size, Alltech Assoc.). The mobile phase consisted of 40 m*M* tartaric acid and 2 m*M* sodium octanesulfonate in 5% methanol. The pH of the mobile phase was adjusted to 4.0 with sodium hydroxide. The mobile phase was filtered and degassed.

The flow-rate was 0.8 ml/min. The system temperature was maintained at 30°C. Injection volume was 50 μl.

Sample preparation

Approximately 10–20 g of fermentation broth were placed in a porcelain ashing crucible and placed in an ashing oven (Neytech 85P, Ney Corp., Yucaipa, CA, U.S.A.). The oven was programmed to heat to 160°C for 1 h, then increased at 10°C/min to 600°C and hold at that temperature for 3 h. After ashing was complete, the sample was dissolved in 100 ml of $1.0 \cdot 10^{-3}$ *M* nitric acid, shaken, then stirred for 30 min. The extract was filtered and prepared for HPLC–IC analysis by filtering an aliquot through a 0.45-μm Nalgene syringe filter (Nalge, Rochester, NY, U.S.A.). An alternative to ashing would be solid-phase sample preparation which was used for the post-column reaction. This involves a 1:1 (v/v) dilution of the broth sample with a 1:1 (v/v) methanol–water mixture. The sample was centrifuged and filtered. Approximately 5–10 ml of the sample were passed through a Maxi-Clean IC-RP (Alltech Assoc.) cartridge (previously conditioned with methanol) using a luer-lok syringe at a flow-rate of approximately 1 ml/min. The first 1 ml of solution was discarded. The remaining eluent was collected for analysis.

The solid-phase sample preparation method was more reproducible and less time-consuming than ashing. Fermentation media for erythromycin (starch, soybean meal and lard oil) and cephalosporin C (cottonseed flour, peanut meal, lactose and methionine) were spiked with zinc chloride. Six samples of each fermentation media were ashed or solid phase-extracted. The ashing technique had a 95% recovery (94.87 ppm ± 2.11% Zn). The solid-phase extraction had greater than 99% recovery (99.58 ppm ± 0.917% Zn) with better reproducibility. The choice of sample preparation technique depends on the concentration of analyte to be determined and the type of detection [3]. In many instances in fermentation, a large amount of broth (20–100 ml) would have to be extracted in order to attain analyte concentrations needed for conductivity detections, making ashing the preferred choice. If a post-column reactor is available, solid-phase extraction is the preferred method.

Standard and system suitability preparation

Standards were prepared from the individual chloride salts by dissolving an accurately weighed amount in a 100-ml volumetric flask and diluting with $1.0 \cdot 10^{-3}$ *M* nitric acid. The concentrations of the stock solutions were 1000 ppm of the aforementioned ions. Dilutions were made accordingly. The system suitability solution contained calcium, cadmium, cobalt, copper, iron(III), lead, manganese, magnesium, nickel and zinc. The concentration of these salts were approximately 100 ppm.

RESULTS AND DISCUSSION

Fig. 1 illustrates the ability of the chromatographic system to separate the cations present in the system suitability mixture. There is excellent resolution for all the cations except for calcium and iron(III). The chromatrographic system was specific for the ions examined. There were no interfering fermentation components after ashing or solid-phase extraction. Monovalent cations in this system elute at the void. A linearity test for zinc, cobalt and maganese was conducted (Fig. 2). There was

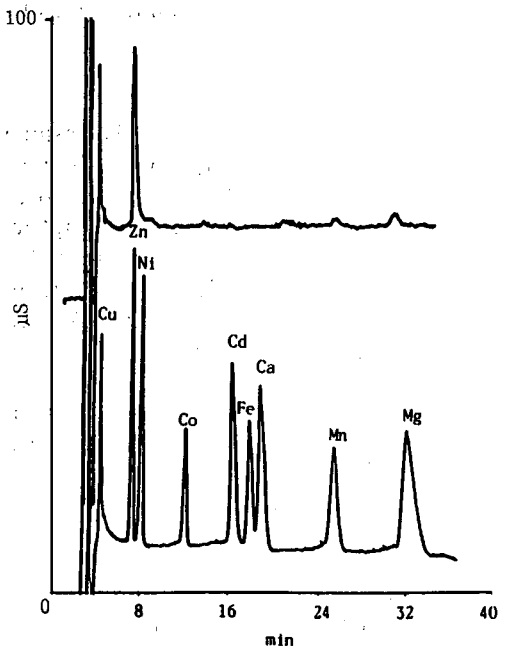

Fig. 1. Chromatogram of system suitability cations using conductivity detection. Chromatogram inset of 23-h fermentation broth sample.

excellent linear correlation (r = 0.999) for these cations in the concentration range 1–1000 ppm. The chromatographic method and system were precise and accurate (within 2%, n = 6) for repeated analysis of samples and standards.

The purpose of ion pairing is to add a second ion to the eluent which will combine with the sample ions, effectively binding them to create a neutral ion pair which then will undergo the normal partitioning or other distribution process between the stationary and mobile phase. From this point on, changes in retention time are accomplished by using standard reversed-phase techniques such as adjusting the pH, organic/inorganic solvent ratio or buffer concentrations. If the pH of the mobile

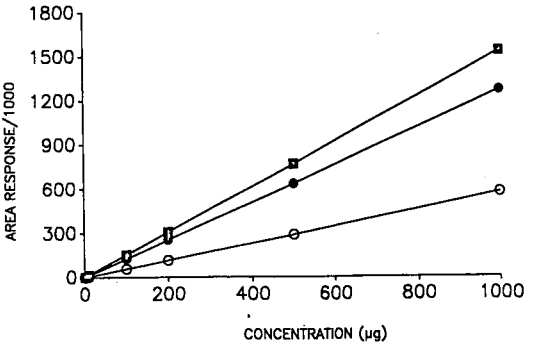

Fig. 2. Calibration curves of peak areas *versus* concentrations of zinc (□), manganese (●) and cobalt (○).

phase is changed from 4.0 to 3.5, the retention time for the cations examined doubled. The conditions used in this analysis can separate and elute the above cations in approximately 35 min. The inset in Fig. 1 represents a chromatogram of a 23-h fermentation broth sample. Zinc is the most abundant cation present (55 ppm ± 1.84%) with smaller amounts (less than 20 ppm) of copper, iron and magnesium. These chromatograms illustrate that these cations can be monitored in fermentation broth for the lifetime of the microorganism, which is approximately 24 h. This method is applicable to other forms of fermentation media such as beverage production [4]. Chromatographic monitoring of these elements can also reflect the varying seasonal composition of starting materials as well as elucidate incidental metal contaminants from the metal-based fermentation tanks or other contact materials which can lead to low antibiotic titer production.

This procedure provides valuable information for fermentation monitoring. It, however, has several limitations. A large amount of sample is needed in order to obtain sufficient quantities of the trace elements. Conventional ashing requires 4–6 h, thus increasing the time requirement for this analysis. If ashing is the preferred method of sample preparation, one might consider microwave ashing to reduce the sample ashing time. Solid-phase sample preparation is a viable alternative to ashing,

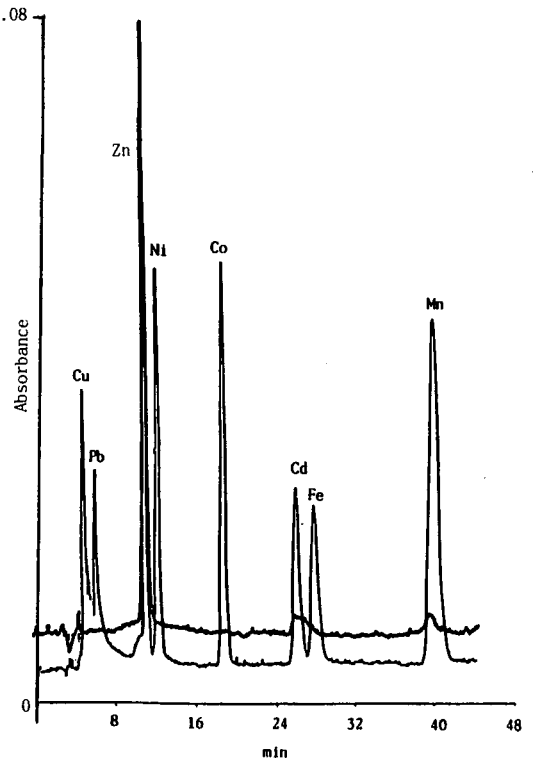

Fig. 3. Chromatogram of system suitability cations using post-column derivatization with UV–visible detection. Chromatogram inset of fermentation broth sample at 1 h using post-column derivatization with UV–visible detection.

although a large amount (20–100 ml) of fermentation broth needs to be eluted through the cartridge in order to obtain the amounts needed for conductivity detection. Conductivity detection is usually limited to approximately 1 ppm of analyte. Many elements can inhibit antibiotic metabolic pathways at concentrations well below 1 ppm [1].

A modification of this procedure can be accomplished by using a post-column derivitization technique. The sensitivity of the trace metal analysis can be increased dramatically by using a post-column reaction combined with a UV–visible detection. The sample preparation would involve dilutions, filtrations and solid-phase extraction (as describe in Experimental) to reduce the hydrophobic components that exist in the sample matrix.

The separation conditions are the same except for the addition of a post-column reactor. Although commercial units are available, the equipment needed to perform post-column reactions is relatively simple. A low dead volume tee for adding the post-column reagent to the column effluent is connected to a single-bead string reactor (Supelco, Bellefonte, PA, U.S.A.) and a 3-m delay tube. The apparatus is temperature-controlled by either a water jacket or a column heating box. The post-column reactant, 0.2 m*M* 4-(2-pyridylazo)resorcinol (PAR) (Sigma) in 3 *M* ammonium hydroxide and 1 *M* acetic acid was used to derivatize the cations. Detection was by visible at 520 nm [5]. Fig. 3 depicts the system suitability solution at a concentration of approximately 1 ppm. The response and baseline stability are improved considerably in comparison to the non-derivatized conductivity detected cations. Although calcium and magnesium are retained on the column, they do not react with PAR, and are not detected. The inset of Fig. 3 is a fermentation broth sample at 1 h. Comparisons of Figs. 1 and 3 illustrate the sensitivity enhancement of the post-column technique over conductivity detection. The post-column technique is 10–500 times more sensitive in detecting inorganic ions than conventional conductivity detectors.

CONCLUSIONS

HPLC–IC provides a means in which to analyze multiple trace elements in fermentation media with a single analysis. Ashing of the sample will eliminate many of the matrix interferences although a large amount of sample is needed in order to concentrate the trace elements and conventional ashing is rather time-consuming. Solid-phase sample preparation is a viable method for sample preparation and clean up, although a large amount of sample needs to be eluted through the cartridge in order to obtain the amounts needed for conductivity detection. The chromatographic system is capable of separating and detecting calcium, cadmium, cobalt, copper, iron(III), lead, manganese, magnesium, nickel and zinc at levels close to 1 ppm using conductivity detection. Sensitivity can be increased at least 100 fold over conventional conductivity detection by the use of a post-column derivitization reaction, enabling visible detection of metal complex formed. HPLC–IC is capable of monitoring the ions present in the starting raw materials, such as the flours and water used for the production of a suitable starting culture or trouble shooting media contamination by metal fermentation tanks or incidental additives.

ACKNOWLEDGEMENTS

Technical assistance and expertise was provided by R. Saari-Nordhaus, J. M. Anderson, Jr. and I. K. Henderson of Alltech Assoc. (Deerfield, IL, U.S.A.), Chem-Sultants (Steger, IL, U.S.A.), Quantitative Technologies (Bound Brook, NJ, U.S.A.) and M. K. Peterson.

REFERENCES

1 E. D. Weinberg, in A. H. Rose and J. F. Wilkinson (Editors), *Advances in Microbial Physiology*, Vol. 4, Academic Press, New York, 1970, pp. 26–28.
2 J. Riviere, *Industrial Applications of Microbiology*, Masson, Paris, 1977, p. 81.
3 R. Saari-Nordhaus, J. M. Anderson, Jr. and I. K. Henderson, *Am. Lab.*, August (1990) 18.
4 R. Youngstrom, Resolution, Inc., Overland Park, KS, personal communiication.
5 R. M. Cassidy and S. Elchuck, *Anal. Chem.*, 54 (1982) 1558.

Journal of Chromatography, 546 (1991) 259–271
Elsevier Science Publishers B.V., Amsterdam

CHROMSYMP. 2359

Optimization of the procedure for the determination of alkali and alkaline-earth elements in sea water by suppressed ion chromatography

M. BETTI, G. GIOVANNONI, M. ONOR and P. PAPOFF*
Institute of Instrumental Analytical Chemistry, CNR, Department of Chemistry, University of Pisa, Via Risorgimento 35, 56126 Pisa (Italy)

ABSTRACT

An ion chromatographic procedure is described for the determination of alkali and alkaline-earth metal ions in sea water the molar ratios of which, referred to lithium, are: $2.5 \cdot 10^4$ for sodium, $5 \cdot 10^2$ for potassium and calcium, and $3.5 \cdot 10^3$ for magnesium.

Lithium, potassium, magnesium and calcium are simultaneously analyzed after a 50-fold dilution, sodium is determined separately after a 2000-fold dilution. For all these elements, a dynamic range of several orders of magnitude and a R.S.D. varying from 0.2–2.2%, though typically lower than 1%, were found.

INTRODUCTION

The main aim of this research was to set up a procedure for measuring the concentrations of some alkali and alkaline-earth metal ions, namely lithium, sodium, potassium, calcium and magnesium, in sea-water samples where alkali and alkaline-earth metal ions are present at high molar concentrations: 0.5 for sodium, 0.02 for potassium and calcium, and 0.07 for magnesium (which are macro elements); $2 \cdot 10^{-5}$ for lithium (which is a microelement) [1]. The molar ratios, referred to lithium, are $2.5 \cdot 10^4$ for sodium, $5.0 \cdot 10^2$ for potassium and calcium and $3.5 \cdot 10^3$ for magnesium.

Ion-exchange chromatography was chosen for its inherent potential to obtain, under suitable experimental conditions, a good individual determination and high sensitivity for all the elements under investigation, by a restricted number of sequential chromatographic runs.

The main difficulty which had to be overcome was the vastly different selectivity of the ion-exchange resins, normally used to separate the monovalent and divalent cations, respectively [2]. These resins have a much higher selectivity for divalent cations than for monovalent cations, thus divalent cations have greater retention times than monovalent cations. Column switching, in addition to eluent-step change have been proposed to solve this problem [2,3]. In both procedures described, alkali and

0021-9673/91/$03.50

alkaline-earth metal ions are efficiently separated, provided that all the concentrations are of the same order of magnitude.

In this paper the use of eluent step-change and column-switching techniques for the simultaneous determination of lithium (at ppb[a] levels) and potassium, magnesium and calcium (at ppm levels) in the presence of high concentrations of sodium are discussed.

Because of the very large dilution required, sodium was determined in sea-water samples separately, with just a slight change in the procedure used for the other elements.

EXPERIMENTAL

Instrumentation

A Dionex Model 4500i ionic chromatograph (Dionex, Sunnyvale, CA, U.S.A.) equipped with a conductivity detector was used along with an Autolon 450 system for data acquisition and processing.

In order to minimize background conductivity and enhance the analytical response, a Dionex micro membrane suppressor (CMMS) was employed.

A cation-trap column filled with high-capacity, low-efficiency cation-exchange resin was placed between the pump and the injection valve to remove cation impurities from the eluent. The separations were carried out on CS3 and CS10 cation-exchange columns (250 mm × 4.6 mm I.D.), used in conjunction with CG3 and CG10 guard columns (50 mm × 4.6 mm I.D.), respectively.

A 50-μl loop was used for the injection of the samples. All the samples have been analyzed five times each, if not otherwise specified.

Reagents

Hydrochloric acid (Merck), 2,3-diaminopropionic monohydrochloride acid (DAP–HCl, Nova Chimica), 55% aqueous solution of tetrabutylammonium hydroxide (TBAOH, Nova Chimica) and methanol Chromosol V (Riedel de Haen) for high-performance liquid chromatography (HPLC) were supra-pure reagent-grade materials. Ultra-pure water (18 MΩ/cm resistivity at 25°C) obtained by treating double-distilled water (Carlo Erba) in a UHQ system (Elga, U.K.), was used throughout. Stock solutions (1000 mg/l) of sodium, lithium, potassium, calcium and magnesium were prepared in 0.1 *M* HCl from Tritisol (Merck) ampoules. Working standard diluted solutions were prepared daily. All standards, samples and reagents were prepared and stored in polyethylene containers, previously cleaned and conditioned following a procedure for trace element determination [4].

Eluent solution

The eluents consisted of mixtures of dilute HCl, DAP and 10% methanol, as reported in Table I, where the working conditions for the different columns are reported.

---

[a] Throughout this article, the American billion (10^9) is meant.

TABLE I

WORKING CONDITIONS FOR THE DIFFERENT COLUMNS TESTED

Eluent solution composition: A = 0.25 m*M* DAP, 6 m*M* HCl, 10% methanol; B = 6 m*M* DAP, 30 m*M* HCl, 10% methanol; C = H_2O, 10% methanol; D = 100 m*M* HCl, 10% methanol.

Column	Elution program			Retention time of the last analyte, calcium (min)	Reequilibration time (min)	Total time (min)
	Time (min)	Flow-rate (ml/min)	Eluent composition			
CS3	0.0	0.5	100% A			
	10.0	1.0	100% B			
	15.0	1.5	100% C	31	15	50
CS10	0.0	2.0	5%B, 85% C, 10% D			
	7.0	2.0	50% B, 40% C, 10% D	25	20	50
CS10/CG3	0.0	2.0	5% B, 85% C, 10% D			
	4.0	2.0	5% B, 85% C, 10% D (column switching)			
	5.0	2.0	20% B, 70% C, 10% D	18	5	25

Regenerant solution for the CMMS

The CMMS was continuously regenerated with a solution of 100 m*M* TBAOH at a flow-rate of 5 ml/min. The CMMS regenerant solution was continuously recycled using a Dionex AutoRegen accessory.

RESULTS AND DISCUSSION

Optimization of the determination of lithium, potassium, magnesium and calcium

In addition to a good peak separation, two other conditions must be fulfilled in the optimization of a chromatographic procedure: firstly, all the analytes should be eluted in a moderate eluent volume; and secondly, the time for the reequilibration of the columns between runs should be as short as possible.

Different procedures were tested: (a) the use of the Ion Pac CS3 or CS10 column separately; and (b) the use of the Ion Pac CG3 column coupled with the CS10 column using the column-switching technique. The results are reported below.

Ion Pac CS3 separator. The elution of alkali and alkaline-earth metal ions on a low-capacity cation-exchange sulphonated divinylbenzene–styrene copolymer column, such as CS3, is well documented. When their concentrations are of the same order of magnitude, the use of the DAP–HCl solutions in the concentration step mode has been suggested [5]. It is reported that calcium elutes after 18 min and a further 10 min is required for column reequilibration.

With respect to lithium–sodium (and sodium–potassium) resolution, at a lithium–sodium molar ratio of 1:300, the procedure summarized in Table I has led to the best results (see Fig. 1). Methanol (10%) was added to the eluent solutions because in a preliminary investigation it was found that this organic reagent shortens both the magnesium and calcium retention times by about 5 min.

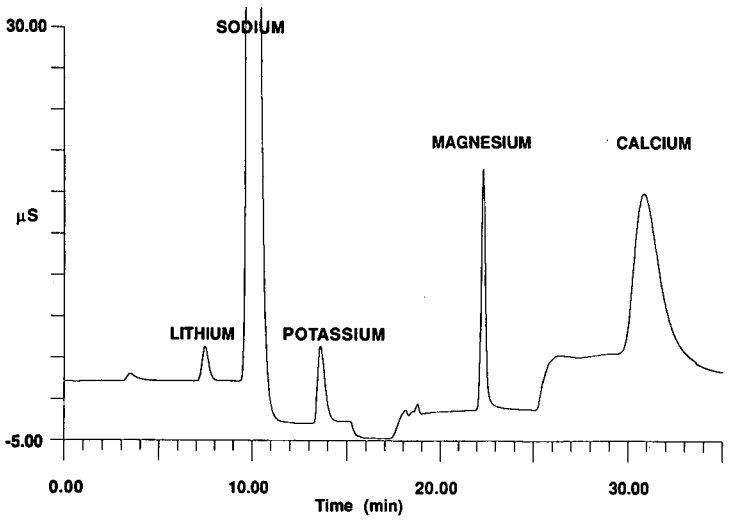

Fig. 1. Chromatogram obtained on the CS3 column by injecting 50 µl of a standard solution containing: lithium (0.5 mg/l), sodium (150 mg/l), potassium (10 mg/l), magnesium (10 mg/l) and calcium (20 mg/l). (For elution conditions see Table I.)

However, the analysis time is unacceptably long: 35 min for the analysis and 15 min for column reequilibration.

Ion Pac CS10 separator. For this column, which is also a low-capacity cation-exchange sulphonated divinylbenzene–styrene copolymer separator but with a higher efficiency than the CS3 column, it has been reported that it is possible to carry out an isocratic elution of both alkali and alkaline-earth cations, when their concentrations are of the same order of magnitude, and to separate small amounts of ammonium in the presence of a large excess of sodium as well [6].

Eluent solutions consisting of DAP and HCl mixed in different concentration ratios were tested. The chromatogram obtained by isocratic elution, with a mixture of 11.5 m*M* HCl, 0.3 m*M* DAP and 10% methanol at a flow-rate of 2 ml/min, is shown in Fig. 2. The separation between lithium and sodium is more efficient than the one obtained by the procedure described above using CS3. The so-called system peak, appearing at the void volume, is due to the high chloride concentration in this sample. In order to elute magnesium and calcium in a reasonably short time, a step to 25 m*M* HCl and 3 m*M* DAP was performed after 7 min. Even in this way, the analysis time was still unacceptably long. In fact, the ill-defined calcium peak was eluted after 25 min and the column reequilibration took 15 min. A further increase in the eluent flow-rate or the eluent concentration would sharply affect the efficiency of the suppressor column or increase the reequilibration time.

Ion Pac CG3 and CS10 —column-switching technique. Following the scheme reported in Fig. 3a, the sample, collected in the loop by a DQP pump, was injected onto the CG3 column where alkaline-earth metal cations are retained. Alkali metal ions, which are rapidly eluted from the CG3 column, are separated on the CS10 column. Four minutes after the start of the chromatographic run, the position of the

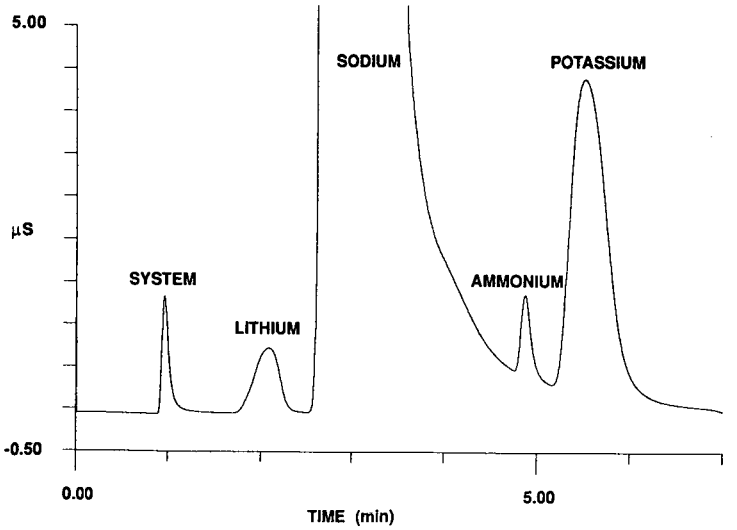

Fig. 2. Chromatogram obtained on the CS10 column by injecting 50 µl of a standard solution containing: lithium (0.1 mg/l), sodium (2000 mg/l), ammonium (8 mg/l) and potassium (2 mg/l). (For elution conditions see Table I.)

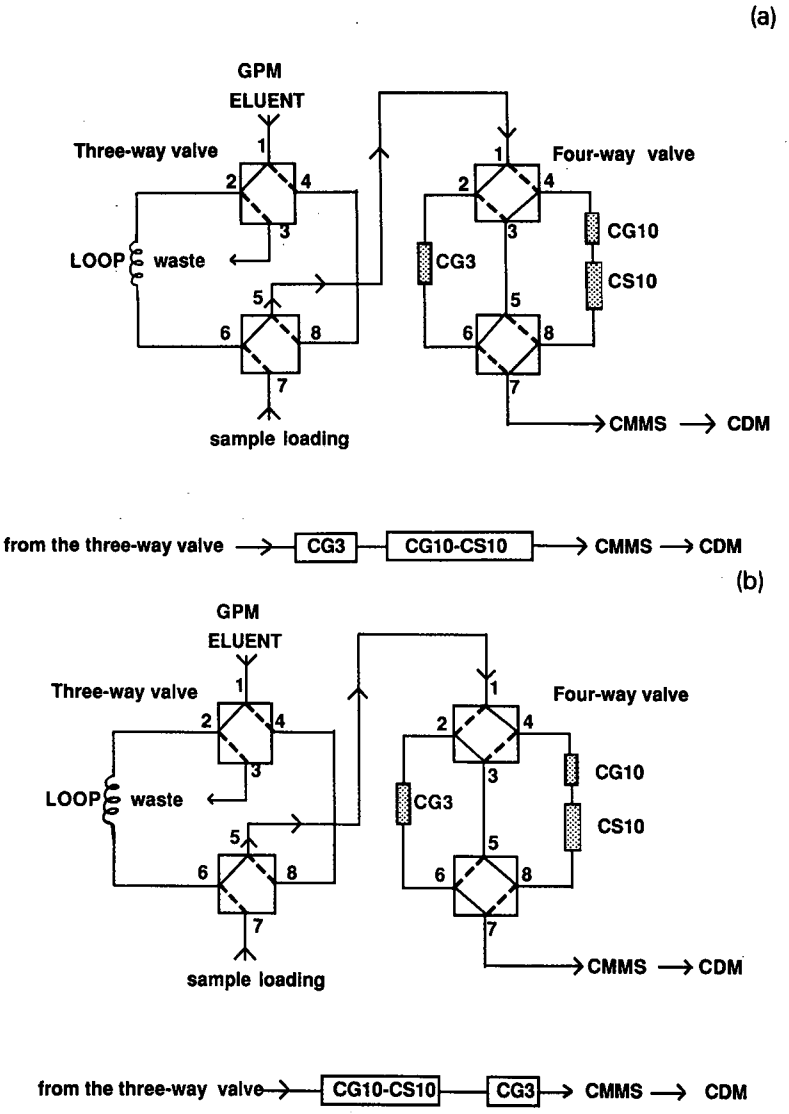

Fig. 3. Valve configuration used for the column-switching technique. The pathway of the eluent solution is represented by the solid line. (a) Before switching; (b) after switching. CDM = Conductivity detector; GPM = gradient pump.

four-way valve was changed (Fig. 3b) and the eluite from CS10 passed again onto CG3 where the separation and elution of magnesium and calcium were accomplished. In order to shorten the analysis, an eluent step was also performed after 5 min. As reported in Table I, during the first 5 min the elution was carried out with 11.5 m*M* HCl, 0.3 m*M* DAP and 10% methanol. Then the eluent was changed to 16 m*M* HCl and 1.5 m*M* DAP. Twenty minutes after the start of the chromatographic run the system was reset to the initial conditions for column reequilibration.

In Fig. 4 the chromatogram obtained for a 50-fold diluted sea-water sample is shown. The lithium peak, located at 2.46 min, refers to a concentration in the injected sample of 3 μg/l. The peaks of potassium, magnesium and calcium refer to a concentration of 6, 28 and 8 mg/l, respectively. Sodium can be measured in the same run provided that its concentration is lower than 50 mg/l.

In conclusion, by column switching coupled with the eluent step change, lithium, potassium, magnesium and calcium, in the presence of a very large excess of sodium were determined in a reasonably short time during the same chromatographic run. The calcium peak eluted at 18 min and because the change of the eluent composition was not very large, column reequilibration takes only a few minutes, leading to a total time between consecutive runs of 25 min.

Determination of sodium

When the sodium concentration in the sample is higher than 50 mg/l, as in sea-water samples, it must be analyzed separately from the other elements. In order to use the same set-up used for the other analytes with minimum modifications, the CG10–CS10 columns were eliminated and only one position for the four-way valve was used (Fig. 5). Sodium was analyzed by an isocratic elution of CG3 at a flow-rate of 2 ml/min with the eluent used in the early step of the procedure for lithium, potassium, magnesium and calcium. Thus the sodium peak eluted after 0.73 min (Fig. 6). At this dilution the other analytes are not detected as far as sea-water is concerned.

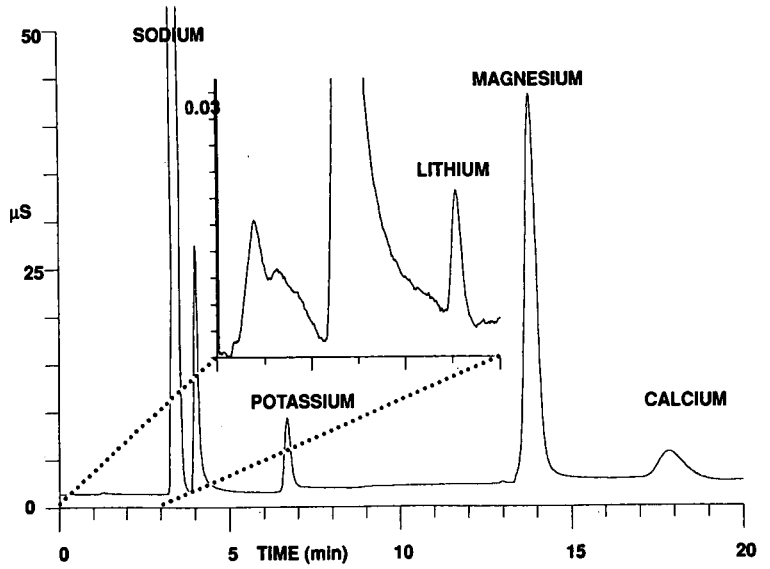

Fig. 4. Chromatogram obtained by injecting 50 μl of a 50-fold diluted sea-water sample using the column-switching technique (for elution conditions see Table I). Analyte concentrations after dilution: lithium, 3 μg/l; sodium, 200 mg/l; potassium, 6 mg/l; magnesium, 28 mg/l; and calcium, 8 mg/l.

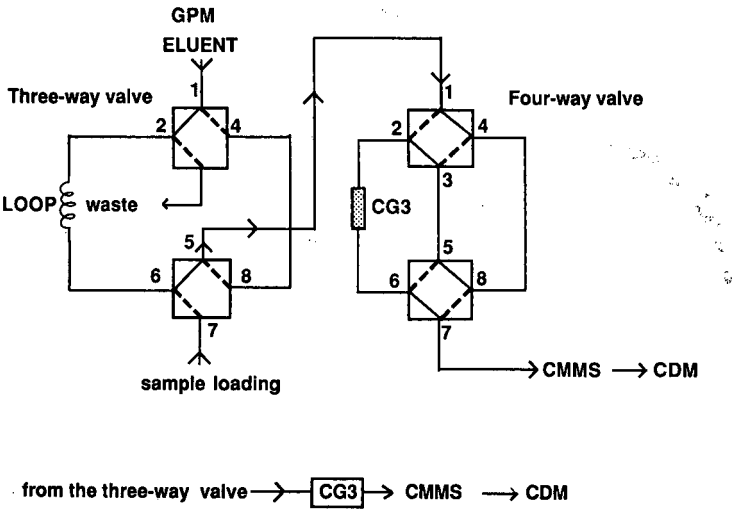

Fig. 5. Valve configuration for sodium analysis. The pathway of the eluent solution is represented by the solid line.

Range of concentrations tested, retention times, and relevant relative standard deviations (R.S.D.)

For each element the sensitivity S, *i.e.* the ratio of the peak area and concentration, has been found to be an unambiguous value in the range of concentration tested (several orders of magnitude). The range of these concentrations with the retention times and relevant R.S.D. values are shown in Table II. The R.S.D. was found to be

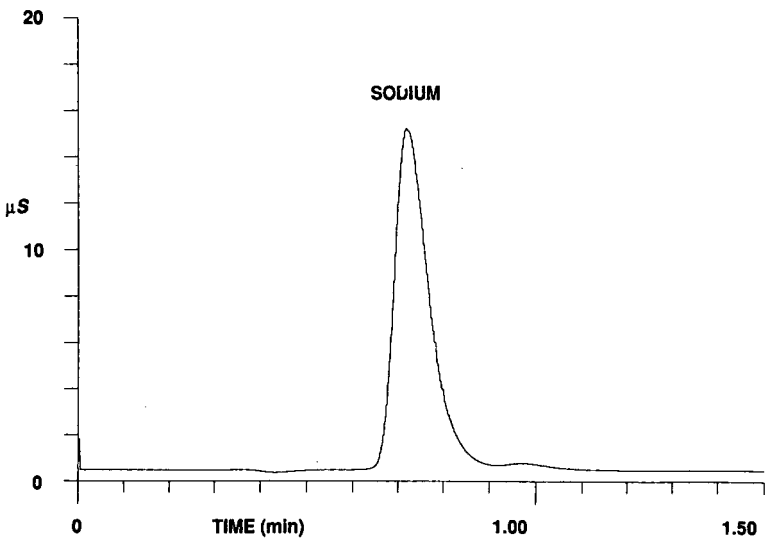

Fig. 6. Chromatogram obtained by injecting 50 μl of a 2000-fold diluted sea-water sample. Sodium concentration after dilution: 5 mg/l. Isocratic elution performed on a CG3 with 11.5 mM HCl, 0.3 mM DAP and 10% methanol.

TABLE II

RANGE OF CONCENTRATIONS TESTED, RETENTION TIMES AND RELEVANT R.S.D.

Elements	Range of concentrations tested	R.S.D.[a] (%)	Retention time (min)	R.S.D.[a] (%)
Lithium	5.0 μg/l– 10 mg/l	0.3–2.9	2.46	0.5
Sodium	0.1 mg/l–100 mg/l	0.1–0.8	0.73	0.1
Potassium	0.1 mg/l–100 mg/l	0.1–0.7	6.05	0.7
Magnesium	0.1 mg/l– 30 mg/l	0.2–1.8	13.82	0.3
Calcium	0.1 mg/l–200 mg/l	0.1–1.5	17.84	0.4

[a] R.S.D. relevant to 5 replicates for each concentration tested (10 replicates for lithium).

independent of concentration both for area and retention time. The area R.S.D. was lower than 1% for sodium and potassium, 2% for calcium and magnesium, and 3% for lithium. These differences, which can be considered effective and not casual, can be attributed to the exchange-mechanism differences of the individual ions on the suppressor membrane.

As observed for anions [7–10], calibration graphs are non-linear. In the present case the curves are precisely described by an empirical equation of the form: $Y = c + bC + aC^2$ (eqn. 1), where Y is the peak area, and C the analyte concentration. Lithium, for instance was measured systematically for eleven concentrations in the range $5 \cdot 10^{-3} - 10$ mg/l: ten replicates were performed for each sample. Depending on whether the data were on all or only on the seven highest concentrations tested, the value of c was negative and went from -0.10 to -0.84 while the relative standard error of estimate (R.S.E.), *i.e.* the R.S.D. about the regression line, goes from 1.9 to 0.9. Furthermore, when the highest concentrations values are disregarded, depending on whether the first five or the first nine lowest concentration values are considered, c, b, a, and R.S.E. remain quite stable: c ranges between -0.08–-0.09, b between 0.154–0.152, a between $4.6 \cdot 10^{-6}$ to $4.0 \cdot 10^{-6}$ and the R.S.E. between 1.4 and 1.8%.

From the above findings and by considering that even at the lowest concentrations of lithium, it has been proved that the solutions do not exchange with the container walls and are stable for months, it is possible to assess that the negative value of the intercept is not assignable to experimental effects, such as an incorrect instrumental baseline subtraction (in the integration step) nor to a loss of lithium in the chromatographic set-up at the lowest concentrations. While it is outside the scope of the present paper to ascertain the physical meaning of this behaviour, possible reasons are (a) the non-linear relationship of the conductivity of salts with concentration [11]; (b) systematic errors due to the conductivity cell design and conductivity measurements, and (c) changes in the background conductivity of the eluent, with or without the analyte, due to variations in the membrane exchange mechanisms or to a rearrangement of the equilibria in the solutions.

In Fig. 7 the contribution of the terms c, $c+bC$ and aC^2 respectively, to Y are shown *vs.* concentration, for lithium. The intercept term c is significant ($>0.5\%$) up to 200 ppb, while the quadratic term aC^2 is significant for concentrations higher than 500 ppb. These findings must be considered whenever a standard addition procedure is used. In this case systematic errors are introduced whenever S is not constant with the concentration. The size of error depends both on the original analyte concentra-

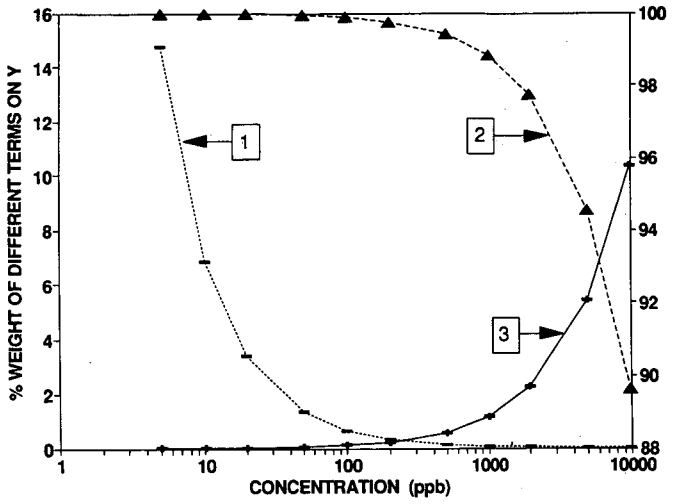

Fig. 7. Contribution of the different terms of eqn. 1 (see text) on the calculated area Y, for lithium. Curves: 1 = percentage c/Y; 2 = percentage $(c+bC)/Y$; 3 = percentage aC^2/Y. Curves 1 and 3: left scale; curve 2: right scale.

tion and on the amount of analyte added to the solution in the standard addition step. In Fig. 8 errors are shown *vs.* the apparent concentration found, as was calculated simulating for several concentrations of lithium, in the range $5\text{–}4 \cdot 10^3$ ppb, two standard additions which lead, respectively, to a double- and three-fold increase in the original concentration.

The values of the parameters in eqn. 1 and in general the values of $S(Y,C)$ for all

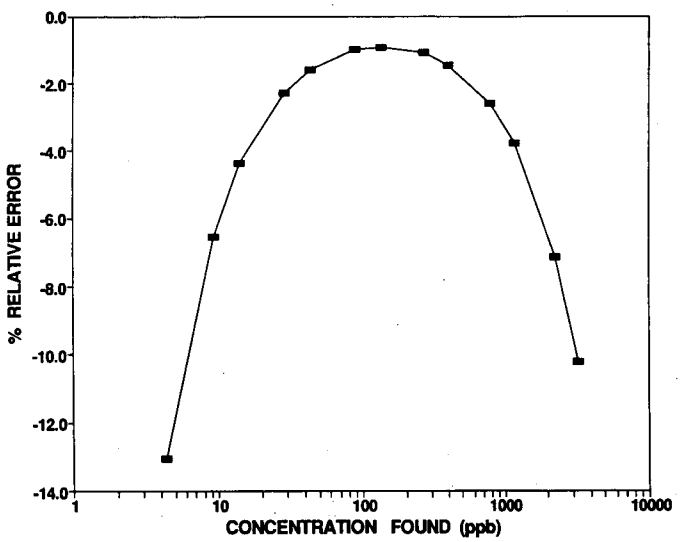

Fig. 8. Relative error *vs.* apparent concentration for lithium as calculated by simulating two points standard additions.

TABLE III

EFFECTS OF STORAGE TIME AND DIFFERENT ANALYTICAL PROCEDURES SAMPLE STATISTICS

Data refer to the 1988–1989 Italian Antarctica expedition (Ross Sea). All the mean concentration values ($\bar{x}$) are expressed in mM units with the exception of lithium whose values are in μM units. $R = \bar{x}_n/\bar{x}_1$ (n = second or third line data for each station). R.S.D. relevant to 5 replicates.

Station	Date	Element														
		Lithium			Sodium			Potassium			Magnesium			Calcium		
		$\bar{x}$	R	R.S.D. (%)	$\bar{x}$	R	R.S.D. (%)	$\bar{x}$	R	R.S.D. (%)	$\bar{x}$	R	R.S.D. (%)	$\bar{x}$	R	R.S.D. (%)
1	29.05.90	26.27		0.92	450.7		0.25	5.86		1.71	55.2		0.53	14.70		0.95
	10.01.91				455.0	0.990	0.38	5.98	1.020	1.53	55.7	1.009	0.76	15.00	1.020	1.09
	15.01.91	26.10	0.994	1.09	454.2	0.992	0.29	5.93	1.012	1.35	56.0	1.014	0.65	14.80	1.007	0.87
2	29.05.90	23.18		0.70	438.2		0.39	7.09		1.41	52.9		1.32	11.20		0.42
	11.01.91				440.0	0.996	0.46	7.06	0.996	1.09	53.3	1.008	0.97	10.80	0.964	0.65
	16.01.91	23.00	0.992	0.83	439.2	0.998	0.42	7.03	0.991	1.23	53.7	1.015	1.22	11.00	0.982	0.56
3	29.05.90	24.56		0.85	453.5		0.33	7.57		0.53	54.8		1.22	8.50		1.09
	10.01.91				450.0	0.992	0.53	7.61	1.005	0.96	54.4	0.993	1.14	8.67	1.020	0.97
	16.01.91	25.00	0.982	1.03	451.0	0.994	0.45	7.60	1.004	0.76	54.0	0.985	1.07	8.70	1.023	1.06
4	29.05.90	24.10		1.40	447.5		0.62	7.50		0.40	53.5		0.59	10.70		0.84
	11.01.91				451.0	1.008	0.57	7.43	0.991	0.65	54.0	1.009	0.63	10.50	0.980	0.56
	16.01.91	24.00	0.996	0.99	449.7	1.005	0.95	7.50	1.000	0.74	54.0	1.009	0.67	10.20	0.953	0.72
5	29.05.90	23.80		1.34	443.7		0.92	6.34		0.32	56.2		0.30	12.80		1.29
	15.01.91	24.00	1.008	1.25	444.0	1.007	0.67	6.30	0.994	0.46	56.0	0.996	0.28	13.00	1.016	1.14
6	29.05.90	23.50		1.32	441.7		1.12	7.47		0.27	57.8		0.27	13.20		1.09
	15.01.91	23.50	1.000	1.09	440.0	0.996	1.04	7.50	1.004	0.33	58.0	1.003	0.31	13.00	0.985	1.95

the elements considered, are reproducible for 1 month with an R.S.D. of 2%. Refreshing of the equation parameters can be performed by replicating the measures, say nine times, for three significant concentration values, covering the range of interest. In the case of lithium these concentrations are: 5 ppb for a good estimate of the intercept c; 100 ppb for a good estimate of b; and 4000 ppb for a good estimate of a.

Analysis of sea-water samples

All the sea-water samples were filtered through a 0.45-μm membrane filter by means of a closed system pressurized with nitrogen, acidified at about pH 2 (2 ml of 10 *M* HCl per liter) and stored at 4°C in 1-l high-density linear polyethylene containers which had previously been cleaned and conditioned [4] in our laboratory. Two 1-l containers were filled for each sampling station.

Before the injection, the samples were passed through a Dionex OnGuard-RP cartridge to remove humic substances. There was a 100% recovery concentration from this cartridge for all the analytes considered in this investigation. Lithium, potassium, magnesium and calcium were measured after a 50-fold dilution of the sea-water samples. For sodium a 2000-fold dilution was necessary.

The cumulative effect due to the storage time of the samples and to the different procedures of analysis on the scattering of the mean value $\bar{x}$, are shown in Table III. Six sampling stations, relevant to the 1988–1989 Italian expedition in the Ross Sea (Antarctica) are considered. For each station the first horizontal line refers to samples analyzed according to the first procedure used, the other two lines refer to the second procedure. The percentage variation of the ratio $\bar{x}_n/\bar{x}_1$ (n = second or third line) was higher than 1%: (i) practically every time for calcium (maximum variation: 4.7%); (ii) three times for magnesium (maximum variation: 1.5%); and (iii) once for lithium and potassium (maximum variation: 1.6 and 2.0%, respectively) and never for sodium (maximum variation: 0.8%).

Comparison of the sea-water composition between stations and between two consecutive expeditions is in progress.

CONCLUSIONS

Chemically suppressed ion-exchange chromatography, using the column switching technique coupled with an eluent step change, is very effective for the simultaneous determination of lithium at μg/l levels, potassium, magnesium and calcium at mg/l levels, and sodium up to 50 mg/l. For higher concentrations, sodium is analyzed separately in a second run after a proper dilution.

The procedure was successfully applied for the analysis of sea-water samples.

The variation within months (7 months) between mean values was lower than: 1% for sodium, 2% for lithium, potassium and magnesium, and 4% for calcium.

ACKNOWLEDGEMENTS

P.P. and M.B. wish to thank MURST and CNR (Progetto Finalizzato Chimica Fine II) for their financial support.

REFERENCES

1 R. Bond and C. Straub (Editors), *Handbook of Environmental Control*, CRC Press, Cleveland, OH, 1973, pp. 109, 110.
2 H. Small, *Ion Chromatography*, Plenum, New York, 1990.
3 R. D. Rocklin, M. A. Rey, J. R. Stillian and D. L. Campbell, *J. Chromatogr. Sci.*, 27 (1989) 474.
4 M. Betti, M. P. Colombini, R. Fuoco and P. Papoff, *Mar. Chem.*, 17 (1985) 313.
5 *Doc. No. 032 654* Dionex, Sunnyvale, CA, 27 Nov., 1987.
6 *Doc. No. 034 341* Dionex, Sunnyvale, CA, 1 Jan., 1990.
7 J. Slanina, F. P. Bakker, P. A. C. Jongejan, L. van Lamoen and J. J. Mols, *Anal. Chim. Acta*, 130 (1981) 1.
8 M. J. Van Os, J. Slanina, C. L. De Ligny, W. E. Hammers and J. Agterdendos, *Anal. Chim. Acta*, 114 (1982) 73.
9 M. Doury-Berthod, P. Giampaoli, H. Pitsch, C. Sella and C. Poitrenaud, *Anal. Chem.*, 57 (1985) 2257.
10 D. Midgley and R. L. Parker, *Talanta*, 12 (1990) 1283.
11 H. S. Harned and B. B. Owen, *The Physical Chemistry of Electrolytic Solutions*, Reinhold, New York, 1958.

Journal of Chromatography, 546 (1991) 273–287
Elsevier Science Publishers B.V., Amsterdam

CHROMSYMP. 2153

Ion chromatographic methods for the detection of starch hydrolysis products in ruminal digesta

KAREN BARSUHN* and SUSAN F. KOTARSKI

Performance Enhancement Research, 7921-190-MR, The Upjohn Company, 7000 Portage Road, Kalamazoo, MI 49001 (U.S.A.)

ABSTRACT

Dionex high-performance ion chromatographic methods were evaluated for separation and quantitation of plant sugars and starch digestion products in the ruminal digesta of cattle. Mono- and disaccharides were eluted from a Dionex CarboPac PA1 column with sodium hydroxide used isocratically or as a pH gradient. Maltooligosaccharides which had a degree of polymerization (DP) less than 30 glucose residues were eluted in 60 min by a sodium hydroxide eluent containing a sodium acetate gradient. Carbohydrates were detected amperometrically. Responses were linear ($r^2 > 0.99$) for glucose, disaccharides and maltooligosaccharides (DP < 8). Precipitation and solid-phase extraction methods were evaluated for clean-up of samples of feedstuffs, ruminal contents, and bacterial culture fluids. Perchloric acid precipitation hydrolyzed sucrose but did not affect recoveries of cellobiose, isomaltose or maltose. Ethanol in concentrations of 79 and 86% precipitated maltooligosaccharides having chain lengths larger than 14 and 9 glucose residues, respectively. Maltooligosaccharide recoveries from solid-phase extraction columns varied with maltooligosaccharide size and column packing. Recoveries were > 94% for short chains (DP < 6) eluted from phenyl-substituted columns and variable for all oligosaccharides eluted from C_{18} columns. Applications of these methods are presented and include: (1) detection of sugars in ruminant feed, (2) monitoring changes in ruminal sugars after feeding and (3) monitoring changes in extracellular sugars and oligosaccharides in the culture fluids of the ruminal bacterium, *Bacteroides ruminicola*.

INTRODUCTION

Starch is a major component of the diets of commercially raised beef and dairy cattle in the U.S.A. The initial digestion of starch occurs in the rumen where the indigenous microbial community hydrolyzes and ferments starch to volatile fatty acids (VFA). These acids are used by the animal for its metabolism and growth [1]. Our laboratory is examining starch digestion in cattle, monitoring the changes in low-molecular-weight carbohydrates and maltooligosaccharides resulting from starch hydrolysis in the rumen. The ruminal digesta samples in our studies are complex, containing bacteria, protozoa, fungi, plant materials, inorganic ions, short chain carboxylic acids and protein. High-performance ion chromatography (HPIC) with pulsed amperometric detection (PAD) affords us a convenient means of monitoring ruminal carbohydrates with minimal sample processing. It specifically detects both reducing and non-reducing sugars without chemical derivatization and its sensitivity is as low as 50 n*M* [2]. Moreover, carboxylic acids and most inorganic ions do not cause interference with saccharide detection [2]. The chemical and electrochemical

0021-9673/91/$03.50

details of this methodology and its advantages over other methods for the analysis of saccharides in soil and other complex samples have been discussed previously in detail [3–6].

This report describes some minor modifications of existing HPIC methods [2] for the separation and quantitation of various sugars and maltooligosaccharides resulting from starch hydrolysis. Sample clean-up procedures are evaluated for recovery of glucose and maltooligosaccharides. Finally, these methods are applied for analysis of the carbohydrate content of complex biological samples, including feedstuffs, ruminal fluid and ruminal bacterial culture fluids.

EXPERIMENTAL

Instrumentation

A Dionex 4000i ion chromatograph system (Dionex, Sunnyvale, CA, U.S.A.) was used and equipped with a pulsed amperometric detector, autosampler and either a 4270 integrator or Auto Ion 450 data system. The PAD consisted of a gold working electrode and a silver–silver chloride reference electrode. The applied potentials were $E_1 = 0.10$ V, $E_2 = 0.6$ V and $E_3 = -0.80$ V with pulse durations of 300, 120 and 300 ms, respectively. Carbohydrates were separated on a Dionex HPIC-AS6 anion-exchange column (10 μm; 250 × 2 mm I.D.) with a HPIC-AG6 guard column (50 × 2 mm I.D.) unless otherwise indicated. Eluents were sparged continuously with helium and passed through an ATC-1 ion trap at a flow-rate of 1 ml/min. Prior to injection, the 25- and 50-μl sample loops were flushed with 500 μl of sample prefiltered through the 20-μm frit of the autosampler vial cap.

Materials

Perchloric acid, sodium hydroxide, potassium hydroxide, acetic acid and sodium acetate were analytical grade of Mallinckrodt (Paris, KY, U.S.A.). Ethanol was obtained from Aaper (Shelbyville, KY, U.S.A.) and acetonitrile was the B and J Brand from Baxter, Burdick and Jackson (Muskegon, MI, U.S.A.). The C_{18} solid-phase extraction (SPE) columns (3 ml column volume) were obtained from Analytichem (Harbor City, CA, U.S.A.). The C_2 and phenyl SPE columns (3 ml) were from J. T. Baker (Phillipsburg, NJ, U.S.A.). Filtered, 18 MΩ deionized water (NanoPure II, Barnstead, Boston, MA, U.S.A.) was used for all eluent and reagent preparations.

Carbohydrate standards and their preparation

Carbohydrate standards were purchased from the following suppliers: Mallinckrodt, (glucose, sucrose); Sigma (St. Louis, MO, U.S.A.) (cellobiose, 2-deoxyribose, fucose, fructose, isomaltose, maltooligosaccharide G4-G10, sorbitol, xylose); Fisher Scientific (Fair Lawn, NJ, U.S.A.) (maltose); Calbiochem (San Diego, CA, U.S.A.) (maltotriose); Boehringer Mannheim, (Germany) (malto-tetraose, -pentaose, -hexaose, -heptaose); Difco Labs. (Detroit, MI, U.S.A.) (soluble starch).

All mono-, di- and oligosaccharides were prepared as aqueous stocks and stored at −15°C. Working stocks, diluted in deionized water, were stored at 4°C. Standard solutions used for calibration were prepared to represent the concentration ranges expected to be found in the samples to be analyzed. Soluble starch (0.5 mg/ml) was prepared in deionized water daily by boiling for less than 1 min in a capped tube.

Elution of mono- and disaccharides

Glucose, fructose, sucrose, isomaltose, cellobiose and maltose were separated isocratically with a 150 m*M* sodium hydroxide eluent on a CarboPac PA 1 (250 × 4 mm I.D.) column and CarboPac PA guard column (25 × 3 mm I.D.). A more complex mixture of sorbitol, fucose, 2-deoxyribose, sucrose, glucose, xylose, mannose, fructose, isomaltose and maltose was separated by a pH gradient on the AS6 column. Sodium hydroxide and acetic acid concentrations were changed linearly from 0 to 100 and 1.5 m*M*, respectively, over 40 min and then maintained for 20 min (flow-rate, 1 ml/min). Sodium hydroxide (500 m*M*) was delivered (1 ml/min) into the postcolumn eluent stream prior to the detector cell.

Elution of maltooligosaccharides

Glucose, maltose and the maltooligosaccharide standards [degree of polymerization (DP) < 8] were eluted in 18 min by a 125 to 300 m*M* sodium acetate linear gradient in 150 m*M* sodium hydroxide (flow-rate, 1 ml/min). Maltooligosaccharides (DP < 30) in soluble starch were eluted within 60 min by a 125 to 375 m*M* sodium acetate gradient. Column equilibration required 2 and 5 min for the 18- and 60-min gradients, respectively.

Ethanol precipitation

Ethanol (95%) was added to soluble starch solutions (final concentrations, 48, 79 and 86%) and held overnight at room temperature. Ethanol insoluble components were removed from solution by centrifugation (12 000 *g*, 15 min, 20°C) and were redissolved in deionized water. The ethanol soluble carbohydrates were recovered from the supernatant by rotary evaporation and redissolved in deionized water for analysis. Concentrations of oligosaccharides in these redissolved fractions were compared to those measured in the original soluble starch solution.

Perchloric acid precipitation

Ruminal fluid samples (1 ml) were added to prechilled tubes containing 48 μl of 70% (v/v) perchloric acid and held on ice for 30 min. The tubes were centrifuged (12 000 *g*, 15 min, 4°C) and stored at 4°C for a minimum of 3 days. Just prior to HPIC analysis, 48 μl of a 45% (w/v) potassium hydroxide solution was added to the samples for removal of excess perchloric acid. The resulting precipitate was removed by centrifugation (12 000 *g*, 15 min, 25°C) and the supernatant was assayed for sugar content by the isocratic HPIC method.

To test whether disaccharides commonly found in ruminal digesta were hydrolyzed during this procedure, we made a comparison of disaccharide recoveries before and after potassium hydroxide addition. Sucrose, isomaltose, cellobiose and maltose were diluted 1:10 in supernatants of ruminal fluid samples (previously shown to contain no detectable sugar) following the samples' precipitation with perchloric acid. Final concentrations of the added sugar solutions were 20 m*M* for each disaccharide except cellobiose (10 m*M*). Potassium hydroxide was added to the control tubes prior to the addition of the sugar. For tests of the effects of storage in perchloric acid, potassium hydroxide was added 24 and 120 h after the addition of the sugar. Recoveries of the sugars in rumen fluid were compared to those of sugars diluted similarly in water, without added perchloric acid or potassium hydroxide. All treatments were run in triplicate.

Solid-phase extraction

The disposable C_2-, C_{18}- and phenyl-SPE columns were conditioned with 2.5 ml acetonitrile followed by 5 ml deionized water. A mixture of glucose, isomaltose, maltose and seven other monosaccharides (2 ml of 672 μM total sugar concentration) was eluted with 3 ml of water. The soluble starch solutions (0.5 ml of a 5 mg/ml sample) were eluted with 5 ml of water.

RESULTS AND DISCUSSION

Separation of mono- and disaccharides

Glucose, fructose and four disaccharides (sucrose, isomaltose, cellobiose and maltose) were well separated by a 150 mM sodium hydroxide eluent (Fig. 1). The detector response was linear for 1.5–50 μM for glucose, fructose and cellobiose, 3–100 μM for sucrose and isomaltose, and 6–100 μM for maltose. When a detector setting of 3 mA was used, and 5 concentrations of each sugar were tested, the calculated slopes of the standard curves ranged from 1.01 to 1.03 area counts ($\cdot 10^{-5}$)/μM and the y-intercepts ranged from -0.48 to -0.04 area counts ($\cdot 10^{-5}$). The r^2 values were all greater than 0.99.

Although the isocratic separation method was appropriate for eluting the carbohydrates in feedstuffs and ruminal fluid (see Applications 1 and 2), it did not adequately resolve glucose, maltose, isomaltose and cellobiose from the more complex mixture of sugars found in cultures of ruminal bacteria (see Application 3).

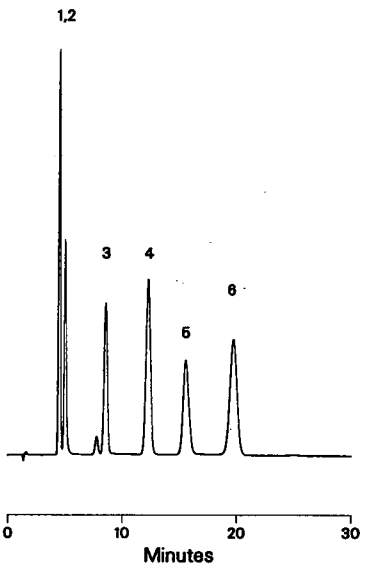

Fig. 1. Isocratic elution of 50 μl of a mixture of mono- and disaccharides by sodium hydroxide. The sugars (and concentrations) in the mix, in order of their elution, were: 1 = glucose (4.6 μM); 2 = fructose (4.2 μM); 3 = sucrose (4.2 μM); 4 = isomaltose (9.3 μM); 5 = cellobiose (4.6 μM); 6 = maltose (5.6 μM). Peaks 4, 5 and 6 are disaccharides which differ only in their respective α-1,6, β-1,4 and α-1,4 glucose linkages.

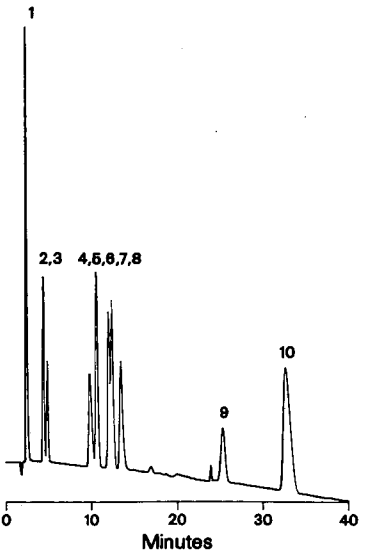

Fig. 2. pH gradient elution of 25 μl of a complex mixture of mono- and disaccharides. The sugars (and concentrations) in the mixture, in order of their elution, were: 1 = sorbitol (500 μM); 2 = 2-deoxyribose (500 μM); 3 = fucose (500 μM); 4 = sucrose (500 μM); 5 = glucose (500 μM); 6 = xylose (500 μM); 7 = fructose (500 μM); 8 = isomaltose (292 μM); 9 = cellobiose (500 μM); 10 = maltose (500 μM).

Accordingly, we adapted a gradient method [2] for the separation of a complex mixture of bacterial and plant sugars likely to be found in these samples [7].

In our hands, the gradient described by Dionex (3.5 mM sodium hydroxide–0.1 M acetic acid for 15 min, increasing to 50 mM sodium hydroxide–1.5 mM acetic acid over the next 10 min [2]) did not resolve our mixture of 10 mono- and disaccharides. Resolution was achieved (Fig. 2) when the elutions conditions were changed to a simple 40 min linear gradient of 0 to 100 mM sodium hydroxide–1.5 mM acetic acid. The elution order was sugar alcohols, deoxy sugars, mono- and disaccharides except for sucrose which preceded glucose. The pH gradient required post-column delivery of sodium hydroxide to eliminate the pH effect on the detector. The lowest detector setting providing maximum sensitivity was 10 mA under these conditions. Thus, this method resolved more sugars than the isocratic method at the expense of sensitivity. Glucose sensitivity was 10-fold lower than that of the isocratic method. The linear detection range of both glucose and isomaltose was 14–1100 μM. The ranges for cellobiose and maltose were, respectively, 15 to 580 μM and 7 to 550 μM. The slopes of the standard curves estimated for 5 different concentrations of standards of all four sugars ranged from 0.5 to 0.65 area counts $(\cdot 10^{-5})/\mu M$. The y-intercepts ranged from 5.0 to 11.1 area counts $(\cdot 10^{-5})$ and the r^2 values were greater than 0.99.

Separation of maltooligosaccharides

A gradient of increasing sodium acetate concentration at constant pH eluted and separated glucose, maltose and the maltooligosaccharides in order of increasing glucose polymerization. The gradient conditions specified by Dionex [2] (250 mM acetate for 1 min, increasing to 500 mM acetate in 8 min and then maintaining for 7

more minutes) did not provide adequate resolution of the soluble starch oligomers in our samples. We adjusted both the initial and final eluent concentrations and the gradient slope to reproduce the resolution demonstrated by Dionex. By extending the gradient run time to 60 minutes, we were able to increase the resolution of larger oligomers from 22 glucose residues [2] to 30 residues (Fig. 3). This elution method required a 10 mA detector setting for minimal baseline drift due to the gradient. Standard curves were linear (r^2 values > 0.99) for glucose (2.5 to 25 μg/ml) for maltose and maltotriose (2.5 to 100 μg/ml) and for the maltooligosaccharide standards (DP = 3–7; 2.5 to 200 μg/ml). Calculated slopes of standard curves were 0.10, 0.10, 0.11, 0.13, 0.15, 0.17 and 0.19 area counts ($\cdot 10^{-5}$)/μM for glucose, maltose, maltotriose, maltotetraose, maltopantaose, maltohexaose and maltoheptaose, respectively, while intercepts were 0.54, 1.3, 0.77, 0.43, 0.49, 0.35 and 0.40 area counts ($\cdot 10^{-5}$), respectively.

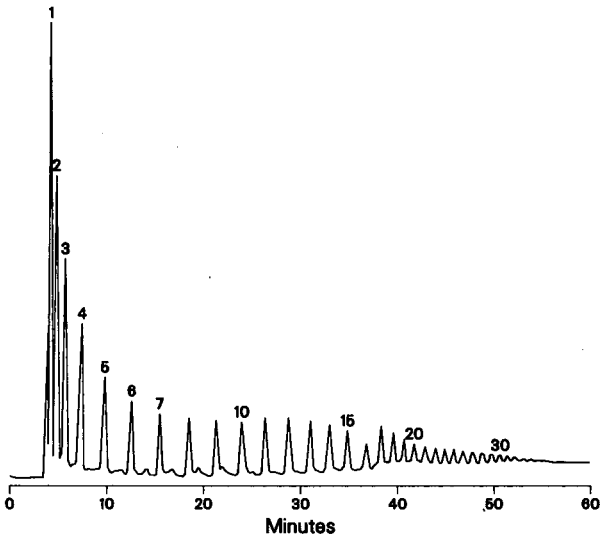

Fig. 3. Sodium acetate gradient elution of 50 μl of soluble starch oligosaccharides (0.5 mg/ml). Peak number represents the DP of α-1,4 linked glucose. Minor peaks between the major peaks are maltooligosaccharides having α-1,6 linkages [8]. The sample load was 250 μg soluble starch.

Sample clean-up by ethanol precipitation

Ethanol is used commonly to fractionate soluble sugars and polysaccharides from complex mixtures [9–11], but the solubility of the intermediate maltooligosaccharides have not been reported. Since individual standards (DP > 7) were not commercially available and the soluble starch prepared by Difco Manufacturers contained a wide range of maltooligosaccharides (Fig. 3), we used this soluble starch preparation to evaluate the solubility of these oligosaccharides in 48, 79 and 86% ethanol.

When the supernatant fractions were evaporated, the residues, like the air-dried precipitates, were readily dissolved in water. However, the sum of the maltooligo-

saccharides measured in these fractions were 0–30% less than their amounts measured in the untreated soluble starch sample (Table I). This did not appear to be due to a systematic recovery error since recovery was: (1) highly variable within a treated soluble starch sample and (2) independent of oligomer size and alcohol concentration.

In general, the solubility of the starch oligosaccharides decreased with increasing chain length and increasing alcohol concentration. Oligosaccharides with less than 28, 15 and 10 glucose residues were detected solely in the supernatant fraction obtained from the 48, 79 and 86% ethanol treatments, respectively (Table I). Larger oligosaccharides ($14 < DP < 23$ for 79% ethanol treatment and $9 < DP < 19$ for 86%

TABLE I

PEAK AREA COUNTS OF MALTOOLIGOSACCHARIDES DETECTED IN SUPERNATANT AND PRECIPITATE FRACTIONS OBTAINED AFTER TREATMENT OF SOLUBLE STARCH WITH DIFFERENT CONCENTRATIONS OF ETHANOL

Oligosaccharide (DP)	Area counts ($\cdot 10^{-5}$) of oligomers after treatment[a]						
	Untreated	48% Ethanol		79% Ethanol		86% Ethanol	
		Super	Precip	Super	Precip	Super	Precip
1	218±3[b]	184	5.4	189	0	223	0
2	187±8	172	1.6	123	0	197	0
3	146±8	128	0	99	0	152	0
4	96±4	97	0	63	0	93	0
5	67±6	62	0	42	0	64	0
6	54±3	49	0	37	0	52	0
7	45±2	41	0	30	0	39	0
8	47±9	38	0	27	0	35	0
9	46±1	45	0	30	0	38	0
10	49±2	40	0	30	0	37	6.1
11	49±2	44	0	30	0	35	8.3
12	49±3	44	0	31	0	32	13
13	47±2	42	0	28	0	26	16
14	45±2	41	0	28	0	20	15
15	40±2	36	0	22	3.0	14	15
16	28±2	26	0	17	4.9	8.8	16
17	28±5	20	0	14	4.1	6.9	13
18	21±4	16	0	10	4.0	3.6	16
19	13±0.2	13	0	6.1	5.4	0	10
20	11±0.1	10	0	3.7	6.0	0	8.9
21	11±0.4	10	0	2.9	5.9	0	9.4
22	11±0.1	10	0	3.3	6.5	0	9.8
23	11±0.1	10	0	0	7.3	0	9.1
24	11±0.5	9.7	0	0	7.8	0	8.8
25	9.7±0.6	7.8	0	0	7.5	0	0
26	8.8±0.4	7.6	0	0	7.0	0	0
27	8.8±0	7.5	0	0	6.5	0	0

[a] Area counts of oligosaccharides detected in supernatant (super) and precipitate (precip) fractions recovered from 48, 79 or 86% ethanol treatment. See text for details.

[b] Mean of two determinations ± standard deviation.

ethanol treatment) were detected in both precipitate and supernatant fractions. The largest oligosaccharides 23 $\leqslant$ DP $\leqslant$ 27 and 19 $\leqslant$ DP $\leqslant$ 24) were detected only in the precipitate fractions of the 79 and 86% ethanol treatments, respectively. Thus, ethanol precipitation provided a selective means of retaining or removing oligomers of various lengths.

Sample clean-up by perchloric acid

Since our laboratory uses perchloric acid to deproteinate ruminal fluid samples for assays of bacterial fermentation acids, we tested the suitability of using this acid treatment for the analysis of small molecular weight plant carbohydrates. In preliminary analysis of perchlorate treated samples, we observed decreased retention times of the sugars and loss of column resolution. This was prevented by the removal of excess perchlorate by potassium hydroxide precipitation (Dionex, personal communication).

We tested the stability of disaccharide standards added to perchloric acid-treated ruminal fluid previously shown to contain no detectable sugars. When maltose, isomaltose and cellobiose standards were added to this acid-precipitated sample and stored at 4°C for 120 h, their measured concentrations upon potassium hydroxide addition (22.7 ± 2.2 m*M*, 21.9 ± 2.3 m*M* and 10.6 ± 1.5 m*M*, respectively) were comparable to measured concentrations of standards (27.5 ± 0.33 m*M*, 21.3 ± 0.7 m*M* and 10.9 ± 0.8 m*M*, respectively) stored in water at 4°C for 120 h. Continued storage of these potassium hydroxide-treated samples yielded significant glucose concentrations (8.6 ± 0.4) and lower concentrations of maltose (11.4 ± 0.5). No sugars appeared in ruminal fluid controls (no added sugars) following the same perchlorate–potassium hydroxide treatment. Thus, maltose was stable in acid but not in base while isomaltose and cellobiose were stable regardless of the storage conditions. No glucose or maltose was detected in acid-precipitated ruminal fluid to which a mixture of maltooligosaccharides (DP 4–10; 1 mg/ml total) was added after 7 days storage at 4°C. Although these data were supportive that hydrolysis of maltooligosaccharides to glucose did not occur, we have not confirmed that partial hydrolysis did not occur.

When sucrose was stored in acid-precipitated ruminal fluid at 4°C, both glucose and fructose were measurable (3.6 ± 0.3 m*M* and 2.0 ± 0.2 m*M*, respectively) after 24 h storage and increased to 15.2 ± 1.1 m*M* and 11.0 ± 0.7 m*M*, respectively, after 120 h storage. Sucrose concentrations concomitantly declined with storage in acid-precipitated ruminal fluid, dropping from 26.6 ± 0.8 m*M* immediately after its addition to rumen fluid to 17.3 ± 0.7 m*M* and 10.1 ± 0.7 m*M* when held for 24 h and 120 h at 4°C, respectively. Sucrose was stable in water at 4°C, measuring 21.2 ± 0.7 m*M* throughout the storage period. Thus, sucrose was not stable under these acid storage conditions.

Sample clean-up by solid-phase extraction

Solid-phase extraction is recommended for protein and organic compound removal from complex biological samples [2]. Recoveries of individual sugars (glucose, isomaltose, cellobiose and maltose) from C_{18} SPE cartridges were comparable, averaging 86 ± 3% and 96 ± 2% for two different column batches. This variability between batches may have been due to column aging [12] and should be monitored. The recoveries of the oligosaccharide standards also varied considerably between

TABLE II

PERCENTAGE OF SOLUBLE STARCH OLIGOSACCHARIDES ELUTED FROM SOLID-PHASE EXTRACTION COLUMNS

Oligosaccharide (DP)	Recovery from column packings[a]		
	C_{18}	C_2	Phenyl
1	91.98[b]	100	99.96[b]
2	75.96	96	95.96
3	74.98	99	95.98
4	73.98	99	98.99
5	70.99	98	94.98
6	62.94	99	64.92
7	60.90	116	61.98
8	42.72	91	90
9	39.51	120	101
10	30.60	103	102
11	24.42	97	98
12	17.0	96	98
13	10.0	104	99
14	0.0	86	99

[a] Expressed as a percent of the amount of the same oligosaccharide measured in the soluble starch sample before application on the SPE column.
[b] Duplicate determinations.

column batches and, to a lesser extent, with the hydrophobicity of the packing material (Table II). Recoveries of the soluble starch oligosaccharides having more than 8 glucose residues decreased with increasing chain length. The limited recoveries of the longer oligosaccharides could have been due to the interaction of these longer carbohydrate chains with the column bed or with each other [13]. Although organic solvents might increase recoveries of the oligomers from the SPE packing, they were not used since they interfered with detection of the carbohydrates. We were also concerned about the solubility of the longer oligomers in even low concentrations of organic solvent. Thus, the utility of solid-phase extraction for the quantitation of oligosaccharides was limited by saccharide size and column batch variability.

APPLICATIONS

The following shows our applications of the HPIC methods described above in our *in vitro* and *in vivo* studies of the effects of small molecular weight carbohydrates on bacterial digestion and fermentation of ruminal carbohydrates. Summaries of our methods and results are presented below.

(1) Carbohydrate profiles of feedstuffs

We have compared ground corn against a ground corn–molasses mixture (90:10) to determine the impact of molasses on ruminal sugar concentrations and other ruminal fermentation variables in cattle. The feedstuffs were first analyzed for sugar content. Triplicate 3-g samples of the two feedstuffs were extracted in alcohol

by the AOAC method [14]. The alcohol solution was removed by evaporation under a stream of nitrogen. The residue was resuspended in water and particulate was removed by centrifugation (12 000 *g*, 5 min, 25°C). The supernatant solution was diluted 200-fold and analyzed (25 μl) by the isocratic elution HPIC method (Fig. 4).

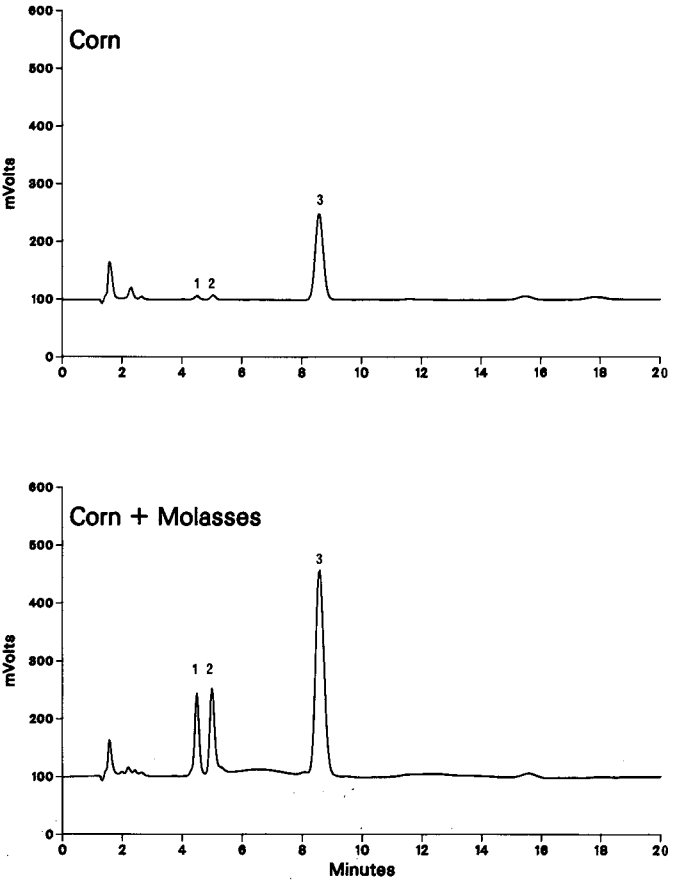

Fig. 4. Chromatograms of alcohol-soluble mono- and disaccharides in feedstuffs. Glucose (peak 1), fructose (peak 2) and sucrose (peak 3) were extracted in ethanol from either ground corn or a mixture of ground corn–molasses (90:10) and were eluted isocratically with sodium hydroxide.

Fig. 4 shows chromatograms of the alcohol-soluble carbohydrates detected in the feeds. Ground corn contained (on a dry weight basis) 1.3 ± 0.01% sucrose and equal amounts (0.03 ± 0.01%) of glucose and fructose. The corn–molasses mixture contained 3.2 ± 0.4% sucrose, 0.8 ± 0.03% glucose and 0.4 ± 0.03% fructose. Molasses contains roughly 30% sucrose [14]. The measured sugar concentration of the 10% molasses-ground corn mixture was 4.4% as expected since the measured concentrations of sugars in the ground corn were 1.3% and the molasses would have contributed an additional 3% sugar.

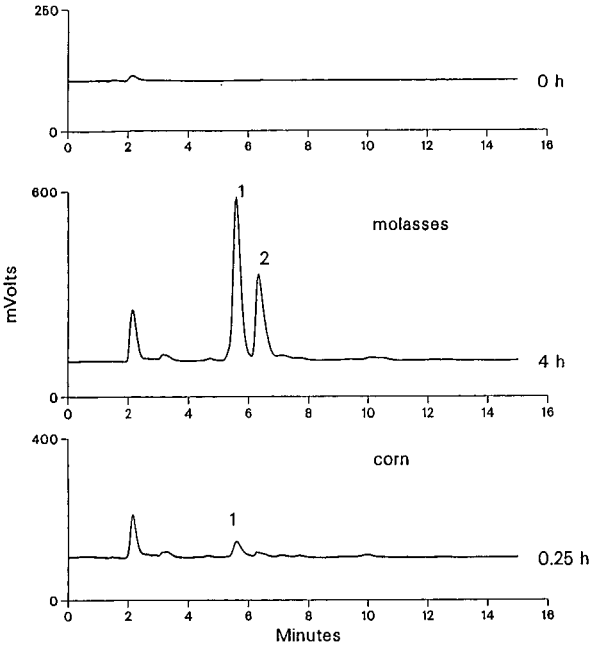

Fig. 5. Typical chromatograms of sugars in ruminal fluid. Glucose (peak 1) and fructose (peak 2) were eluted isocratically. Plots shown are from 50 μl of a 1:20 dilution of perchloric acid, potassium hydroxide-treated ruminal fluid sample collected prior to dosing (0 h) with a feedstuff; 4 h after dosing animals with a ground corn–molasses mixture (4 h, molasses) and 0.25 h after dosing with ground corn (0.25 h, corn).

(2) Ruminal carbohydrate profiles

The feedstuffs described above were delivered into the rumen in four equal doses (1.6 kg/dose/cow) at hourly intervals. Ruminal fluid samples were collected hourly, frozen immediately in a dry ice-aceton bath and stored at −20°C. The samples were prepared for analysis by centrifugation (2000 *g*, 4°C, 30 min), deproteinated with perchloric acid and stored at 4°C. Immediately prior to analysis potassium hydroxide was added as described above. Samples were diluted 20-fold and analyzed by the HPIC isocratic method.

Typical chromatograms and changes in total ruminal sugar concentrations (glucose and fructose) are shown in Figs. 5 and 6. Carbohydrates were not detected in the samples collected before feeding (Fig. 5, 0 h). Carbohydrates were barely detectable in the ruminal fluid of the animals fed the ground corn diet (low sugar content; Fig. 5, 0.25 h and Fig. 6, closed bars) compared to those observed in the ruminal fluids of the animals fed molasses-ground corn mixture (high sugar content; Fig. 5, 4 h and Fig. 6, open bars). One hour after the last portion of feed was introduced into the rumen, the average concentration of ruminal sugar (glucose and fructose) was 44 m*M*. This value is comparable to a 46 m*M* theoretical value based on the amount of sugars detected in the molasses–ground corn mixture (see Application 1), the average amount of total feed given to induce acidosis (5.7 kg/animal, $n = 4$ cattle) and an estimated ruminal volume of 30 liters [16]. The sugars that were measured were glucose and fructose which may have been present in the ruminal fluid as sucrose

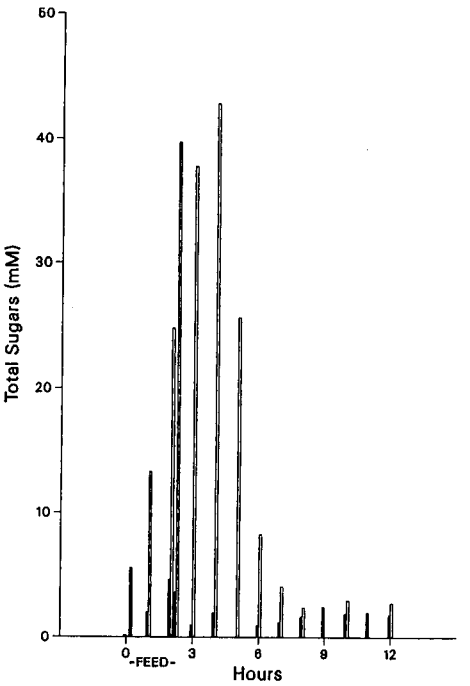

Fig. 6. Postprandial changes in dietary carbohydrates in the rumen. Equal doses of a feedstuff were delivered through a fistula into the rumen at 0, 1, 2 and 3 h. Sugars in perchloric acid, potassium hydroxide-treated ruminal fluid samples were separated by the HPIC isocratic method. A bar graph representing the sums of ruminal glucose and fructose concentrations measured at each sampling time in animals dosed with either ground corn (closed bars) or a 90:10 mixture of ground corn–molasses (open bars) is shown.

before perchloric acid precipitation. It is likely that complete hydrolysis of sucrose occurred during the lengthy storage time (up to 3 months for these samples) in acid.

Extracellular carbohydrates in culture supernatant

The purpose of this experiment was to measure the extracellular appearance of the hydrolysis products of amylopectin during growth of one of the more prominent species of amylolytic bacteria in the rumen, *Bacteroides ruminicola. B. ruminicola* strain 118B was grown at 37°C under strictly anaerobic conditions (100% CO_2) in batch cultures containing 0.2% amylopectin. Extracellular fluids were collected by centrifugation (12 000 *g*; 10 min; 4°C) at selected times during the growth cycle. Following alcohol precipitation and C_{18} SPE clean-up, the supernatant fluid was assayed by the acetate gradient method to characterize the appearance of maltooligosaccharides. Supernatants were also assayed by the pH gradient method for characterization of small molecular weight carbohydrates formed during growth.

Recoveries of maltooligosaccharide standards (G3–G7) in the extracellular fluid were 90 to 100% (data not shown). However, the identification of these carbohydrates was difficult due to variation of their retention times between chromatographic elutions. Retention times for the standards suspended in water were repro-

Fig. 7. Chromatograms of standards and sugars in the extracellular fluids of cultures of *Bacteroides ruminicola*. Glucose (peak 1), isomaltose (peak 2), cellobiose (peak 3) and maltose (peak 4) were separated by the pH gradient elution method and had elution times of 15.5, 24.5, 31.9 and 39.3 min, respectively. (A) Sugar standards prepared in water; (B) sugar standards added to extracellular fluids; (C) sugars in extracellular fluids without added standards.

ducible. Two oligosaccharides with retention times comparable to maltotetraose and maltohexaose were detected at low levels (2–42 μM) (data not shown) compared to glucose levels (50–300 μM, see below). The variability in retention times may have been due to the effects of the culture fluid components in the samples on the elution characteristics of the starch hydrolysis products. We have not identified what these factors are.

Fig. 7C illustrates the numerous peaks which were observed in chromatography of the amylopectin medium and shows why we needed the better resolving power of the gradient method. In contrast to the maltooligomers, the elution times of mono- and disaccharide standards in extracellular fluids were reproducible and recovery was 100% (Fig. 7A and B). Peaks having retention times identical to glucose, isomaltose and maltose showed the most dramatic concentration changes during the growth cycle of *Bacteroides ruminicola* and are shown in Fig. 8.

CONCLUSIONS

The isocratic HPIC method worked well for the analysis of mono- and disaccharides in feedstuffs and ruminal fluid samples. The saccharides of interest were in sufficient concentrations (mM) in our samples (Applications 1 and 2) so that interfering substances were diluted out. This was not the case for bacterial culture supernatants (Application 3) where saccharides in the bacterial medium were in concentrations (μM) equivalent to the saccharides of interest. Therefore, we adapted a gradient method to assure that glucose, isomaltose and maltose were well resolved from these other mono- and disaccharides. This pH gradient provided greater resolution than the isocratic method at the expense of sensitivity and total run time. An

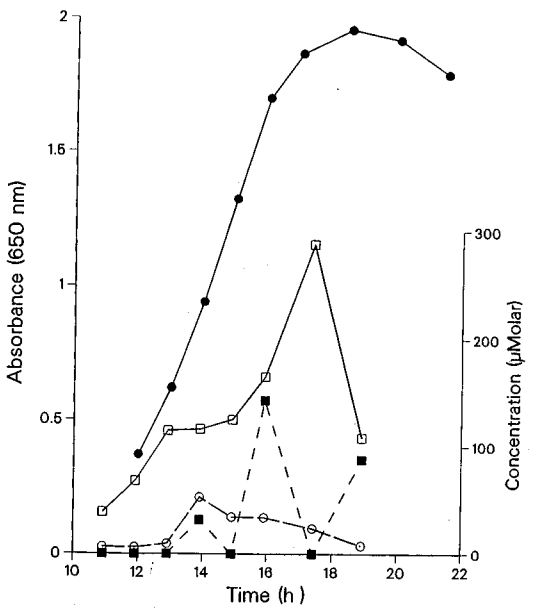

Fig. 8. Changes in concentrations of extracellular sugars during the growth of *Bacteroides ruminicola* in batch cultures containing amylopectin, a starch polysaccharide. Sugars were detected by the pH gradient method. A typical chromatogram is shown in Fig. 7C. Bacterial growth was monitored as the change in culture absorbance (650 nm). ● = Absorbance; □ = glucose; ■ = maltose; ○ = isomaltose.

acetate gradient method was used to monitor the appearance of maltooligosaccharide products of amylopectin hydrolysis. The retention times of the maltooligomer products of amylopectin in culture fluids were not as consistent as those of standards ($2 < DP < 7$) or soluble starch oligomers in spite of the clean-up procedures used (see below). However, we were able to follow the appearance of maltotetraose and -hexaose. Since both gradient methods required adjustments in eluent strength and gradient slope to obtain the same resolution as the published method, we suspect that differences in laboratory conditions and individual columns may have been the cause.

Three sample clean-up methods were examined. Ethanol provided a selective means for solubilizing mono-, di- and small maltooligosaccharides ($DP < 10$) and precipitating the large ($DP > 19$) maltooligomers. However, the alcohol needed to be removed from the sample before analysis because it was detected by the PAD and interfered with saccharide detection. Perchloric acid successfully deproteinated ruminal fluid samples, but it was necessary to remove excess acid by potassium hydroxide precipitation to maintain column integrity. Although perchloric acid did not affect the recoveries of cellobiose, maltose or isomaltose, it did hydrolyze sucrose. Maltose appeared to be hydrolyzed after potassium hydroxide addition. The solid-phase extraction columns gave the highest recoveries of the smaller maltooligosaccharides. Retention times of the maltooligosaccharides in bacterial culture fluids varied despite clean-up by a C_{18} solid phase extraction.

HPIC with pulsed amperometric detection offers both isocratic and gradient capabilities. In combination with its selectivity and sensitivity it is a powerful tool for the separation of a variety of mono-, di- and large maltooligosaccharides ($DP < 30$) in complex samples.

ACKNOWLEDGEMENTS

The authors thank R. L. Bell and K. K. Thurn for providing ruminal fluids and bacterial extracellular fluid samples for analysis, M. M. Johnson for technical assistance and M. S. McBride and K. H. Wagner for secretarial assistance.

REFERENCES

1 R. E. Hungate, *The Rumen and its Microbes*, Academic Press, New York, 1966, p. 532.
2 Dionex LPN 032861, *Ion Chromatography Cookbook*, Dionex, Sunnyvale, CA, 1987, p. II-34.
3 R. D. Rocklin and C. A. Pohl, *J. Liq. Chromatogr.*, 6 (1983) 1577.
4 J. Weiss, *Handbook of Ion Chromatography*, Dionex, Sunnyvale, CA, 1986, pp. 65, 150.
5 D. A. Martens and W. T. Frankenberger, Jr., *Chromatographia*, 29 (1990) 7.
6 S. C. Churms, *J. Chromatogr.*, 500 (1990) 555.
7 G. H. M. Counotte, A. Lankhorst and R. A. Prins, *J. Anim. Sci.*, 56 (1983) 1222.
8 Dionex, *IC Exchange*, 5, No. 2 (1987) 3.
9 J. A. Z. Leedle, K. Barsuhn and R. B. Hespell, *J. Anim. Sci.*, 62 (1986) 789.
10 D. A. T. Southgate, *Determination of Food Carbohydrates*, Applied Science Publishers, London, 1976, p. 32.
11 J. H. Pazur, in M. F. Chaplin and J. F. Kennedy (Editors), *Carbohydrate Analysis. A Practical Approach*, IRL Press, Oxford, 1986, p. 58.
12 W. J. Hurst, *LC·GC*, 6 (1988) 216.
13 N. W. H. Cheetham, P. Sirimanne and W. R. Day, *J. Chromatogr.*, 207 (1981) 439.
14 W. Horwitz (Editor), *Official Methods of Analysis*, AOAC, Washington, DC, 1980, p. 135.
15 S. Budavari (Editor), *The Merck Index*, Merck, Rahway, NJ, 1989, p. 1324.
16 J. P. Peters, J. B. Paulissen and J. A. Robinson, *J. Anim. Sci.*, 68 (1990) 1711.

Journal of Chromatography, 546 (1991) 289–295
Elsevier Science Publishers B.V., Amsterdam

CHROMSYMP. 2139

Determination of xylose oligomers and monosaccharides by anion-exchange chromatography with pulsed amperometric detection

SHIFEN MOU*, QUN SUN and DEPEI LU
Research Centre for Eco-Environmental Sciences, Academia Sinica, P.O. Box 934, Beijing 100083 (China)

ABSTRACT

Anion-exchange chromatography followed by pulsed amperometric detection (AE–PAD) was applied to the determination of xylose oligomers and some monosaccharides. Under alkaline conditions, underivatized xylose oligomers (DP1–DP7; DP = degree of polymerization) were readily separated within 12 min. Underivatized monosaccharides (fucose, galactose, glucose, mannose, arabinose, xylose, galactosamine and glucosamine) were separated within 30 min at an eluent flow-rate of 1 ml min^{-1}. The limits of determination of xylose oligomers were from 0.08 to 0.01 nmol. Results for both xylose oligomers and monosaccharide determination by AE–PAD were more sensitive than those obtained by conventional high-performance liquid chromatography. This method was also employed to determine the monosaccharides in pretreated peat samples.

INTRODUCTION

Compared with thin-layer chromatography [1–3], liquid chromatographic methods [4–10] for the determination of carbohydrates are faster and give higher resolution capacities, but they have often suffered from both poor column performance with respect to selectivity and efficiency and detector insensitivity. Gradient incompatibility is also a problem associated with refractive index (RI) (and occasionally UV) detectors. Rocklin and Pohl [11] first applied high-performance anion-exchange chromatography with pulsed amperometric detection (AE–PAD) to the determination of carbohydrates. Not only does this method provide more efficient separation and detection than high-performance liquid chromatography (HPLC), it also minimizes sample preparation. Larew and Johnson [12] used AE–PAD to separate and determine maltooligosaccharides found in corn syrup. Chatterton and Harrison [13] determined the kestose in plants. Hardy and Townsend [14–17] studied the determination of mono- and oligosaccharides in glycoconjugates extracted from biological samples.

This paper reports the separation and detection of eight monosaccharides (fucose, galactosamine, arabinose, glucosamine, galactose, glucose, xylose and mannose) and a series of β-1–4-linked xylose oligomers (from xylose to xyloheptaose) using AE–PAD.

0021-9673/91/$03.50

EXPERIMENTAL

Materials

Xylose oligomers were kindly provide by C. C. Tu [18]. They were obtained through partial acid hydrolysis of the xylan from corncob holocellulose.

L-Fucose and D-mannose were purchased form Serva, D-galactosamine and D-glucosamine from Sigma, L-arabinose and D-xylose from Shanghai Chemical Factory and D-galactose, D-glucose, sodium hydroxide and sodium acetate from Beijing Chemical Factory. All the reagents were of analytical-reagent grade.

Sodium hydroxide solution (50% w/w) was prepared uing 10 MΩ deionized water and handled according to ref. 19.

Chromatographic apparatus

All chromatography was performed on a Dionex Series 4500i IC system at 25°C. A Dionex GPM pump and a Model PAD II pulsed amperometric detector with a gold working electrode were used. The potentials and durations used for detecting xylose oligomers were as follows: $E_1 = 0.08$ V, $t_1 = 300$ ms; $E_2 = 0.6$ V, $t_2 = 120$ ms; $E_3 = -0.8$ V, $t_3 = 300$ ms. For monosaccharides, the detection conditions by PAD were as follows: $E_1 = 0.1$ V, $t_1 = 480$ ms; $E_2 = 0.6$ V, $t_2 = 120$ ms; $E_3 = -0.8$ V, $t_3 = 60$ ms.

The carbohydrates were separated on a column (250 × 4 mm I.D.) of Dionex CarboPac PA1 pellicular anion-exchange resin coupled with a Dionex CarboPac guard column. A Dionex post-column reactor was used to provide a flow-rate of 0.300 *M* sodium hydroxide solution of 0.8 ml min^{-1}. The chromatographic data were collected and plotted by using a Spectra-Physics Model SP4270 integrator.

Four eluents were used: (1) 0.100 *M* sodium hydroxide solution, (2) deionized water, (3) 0.150 *M* sodium hydroxide solution and (4) 0.150 *M* sodium hydroxide–0.500 *M* sodium acetate. In order to remove dissolved carbon dioxide from the eluents, they were degassed by a sonicator coupled with a vacuum aspirator pump for 30 min prior to use.

Procedure

Fig. 1 shows the chromatographic configuration for detecting carbohydrates. The gradient programme used to elute xylose oligomers was 4 min of isocratic elution

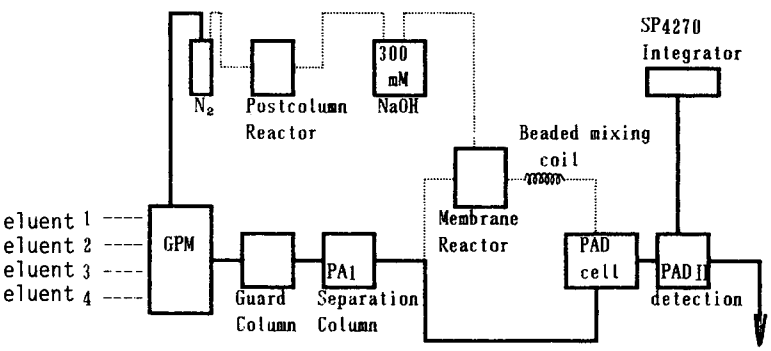

Fig. 1. Chromatographic configuration for analysis of carbohydrates by AE–PAD.

with a mixture of eluents 3 and 4 (85:15), followed by a linear increase to 20% eluent 4 from 4 to 6 min.

For the separation of monosaccharides, two gradient programmes were used. In programme A, the sample was introduced into the system equilibrated with a mixture of eluents 1 and 2 (10:90) and the proportion of eluent 2 was increased linearly to 100% from 0 to 2.5 min, the latter condition being maintained until the end of the analysis. Programme B stated with a mixture of eluents 1 and 2 (7:93) with a linear increase to 100% eluent 2 from 0 to 2.5 min. In order to optimize the PAD sensitivity and minimize baseline drift, post-column addition of 0.300 *M* sodium hydroxide solution was required. As shown by the dotted line in Fig. 1, a post-column reactor, instead of a DQP-1 pump, was used to provide a flow-rate of 0.8 ml min^{-1} of 0.300 *M* sodium hydroxide solution; the eluent and 0.300 *M* sodium hydroxide solution were mixed in a membrane reactor and a beaded mixing coil 80 cm long, then passed to the PAD cell.

In order to remove carbonate and other strongly retained contaminants, 0.200 *M* sodium hydroxide solution should be run for 15 min between injections, thus ensuring reproducibility. The peak heights of the sugars have a tendency to vary with time. Frequent calibration could minimize the errors in concentration measurements.

RESULTS AND DISCUSSION

Optimum conditions for detection of xylose oligomers (X_1–X_7)

In general, the observed anion-exchange affinity follows the trend [11] sugar alcohols < monosaccharides < disaccharides < oligosaccharides. Hence the eluent for the separation of xylose oligomers should be strong enough to push the retained components out of the column. With 0.150 *M* sodium hydroxide solution as the eluent, the retention times of X_4, X_5, X_6 and X_7 were more than 50 min, the peaks were tailed and the detection sensitivity was very low. With 0.075 *M* sodium acetate

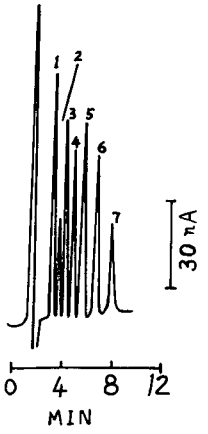

Fig. 2. Chromatogram of β-1-4-linked xylose oligomers. Peaks: 1 = 0.2 ppm xylose; 2 = 4.0 ppm xylotriose; 3 = 1.0 ppm xylobiose; 4 = 4.0 ppm xylotetraose; 5 = 5.0 ppm xylopentaose; 6 = 5.0 ppm xylohexaose; 7 = 5.0 ppm xyloheptaose.

TABLE I

LINEARITY, RELATIVE STANDARD DEVIATION (R.S.D.) AND DETECTION LIMITS FOR XYLOSE OLIGOMERS

Compound[a]	Linearity correlation coefficient	R.S.D. (%) (n = 5)	Detection limit (mg l^{-1})
X_1	0.9997 (range 0.01–0.24 ppm)	4.47 (at 0.08 ppm level)	0.01
X_2	0.9980 (range 0.06–1.20 ppm)	3.72 (at 0.40 ppm level)	0.06
X_3	0.9985 (range 0.40–5.00 ppm)	4.51 (at 1.60 ppm level)	0.40
X_4	0.9997 (range 0.30–5.00 ppm)	3.72 (at 1.60 ppm level)	0.30
X_5	0.9981 (range 0.30–6.00 ppm)	4.60 (at 2.00 ppm level)	0.30
X_6	0.9986 (range 0.30–6.00 ppm)	3.82 (at 2.00 ppm level)	0.30
X_7	0.9992 (range 0.50–6.00 ppm)	2.89 (at 2.00 ppm level)	0.50

[a] X_1–X_7 are xylose oligomers DP1–DP7.

as the eluent for the xylose oligomers in a gradient programme, a good separation and detection within 12 min were achieved (see Fig. 2).

From Fig. 2, the retention time of xylobiose was longer than that of xylotriose. This phenomenon has often been observed in the separation of oligosaccharides by HPAE–PAD [11,15–17].

Hardy and Townsend [15] deduced that the retention time of oligosaccharides was related to the accessibility of oxyanions in the latter to the functional groups on the stationary phase of the HPAE column. Hence the retention time of oligosaccharides is not proportional to the degree of polymerization (DP).

The detection limits for xylose oligomers ranged from 0.01 to 0.08 nmol (see Table I); however, the detection limits of xylose oligomers by HPLC with RI detection was only 4.0 nmol [10].

The results also showed good linearity and reproducibility (see Table I). All the linearity correlation coefficients for the xylose oligomers were between 0.9998 and 0.9980, the R.S.D.s were less than 4.6%.

Optimum conditions for detection of monosaccharides

Fucose, galactosamine, glucosamine, galactose, glucose, mannose, xylose and arabinose are common monosaccharides in glycoconjugates of biological samples. The determination of these sugars is of fundamental importance in nutrition, medical

TABLE II

DISSOCIATION CONSTANTS OF MONOSACCHARIDES (IN WATER AT 25°C)[a]

Sugar	pK_a
Arabinose	12.34
Galactose	12.35
Glucose	12.28
Xylose	12.15
Mannose	12.08

[a] From *Lange's Handbook of Chemistry*, 13th ed.

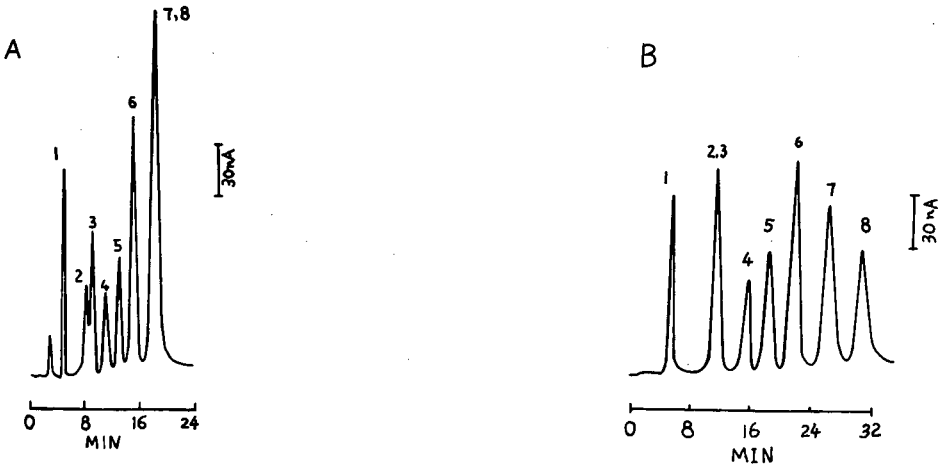

Fig. 3. Chromatogram of the monosaccharides. Peaks: 1 = 0.3 ppm fucose 2 = 0.9 ppm galactosamine; 3 = 1.2 ppm arabinose; 4 = 1.2 ppm glucosamine; 5 = 1.2 ppm galactose; 6 = 3.0 ppm glucose; 7 = 3.0 ppm xylose; 8 = 3.0 ppm mannose. (A) Gradient programme A; (B) gradient programme B.

cell biology and biotechnology research. These sugars have similar structures, some of which are epimers. It has been difficult to separate them by conventional HPLC.

The hydroxyl groups of the monosaccharides have pK_a values in the range 12–14 [19], allowing ionization at alkaline pH and potential separation by anion-exchange chromatography (see Table II). The experiments showed that, with gradient programme A, the sugars were well resolved except mannose, which overlapped with xylose (see Fig. 3A). With gradient programme B, mannose was well separated from xylose, but galactosamine overlapped with arabinose (see Fig. 3B).

Fig. 3 and Table II show that the retention times of the separated monosaccharides increase as their pK_a values decrease. This suggests that the pK_a values have a high potential for chromatographic selectivity. Galactosamine and glucosamine are amino sugars, and the different functional groups between galN and galactose gave a good resolution. Glucosamine and glucose were of the same character.

TABLE III

LINEARITY, RELATIVE STANDARD DEVIATION AND DETECTION LIMITS FOR MONOSACCHARIDES

Compound	Linearity correlation coefficient	R.S.D. (%) (n = 5)	Detection limit (mg l^{-1})
Fucose	0.9998 (range 0.05–0.6 ppm)	2.22 (at 0.1 ppm level)	0.01
Galactosamine	0.9966 (range 0.06–1.0 ppm)	4.89 (at 0.3 ppm level)	0.06
Arabinose	0.9990 (range 0.02–0.8 ppm)	4.67 (at 0.4 ppm level)	0.05
Glucosamine	0.9958 (range 0.06–0.8 ppm)	4.00 (at 0.4 ppm level)	0.06
Galactose	0.9995 (range 0.03–1.2 ppm)	2.36 (at 0.4 ppm level)	0.05
Glucose	0.9993 (range 0.08–2.2 ppm)	4.48 (at 1.0 ppm level)	0.10
Xylose	0.9989 (range 0.08–2.5 ppm)	4.49 (at 1.0 ppm level)	0.15
Mannose	0.9998 (range 0.10–2.5 ppm)	4.00 (at 1.0 ppm level)	0.20

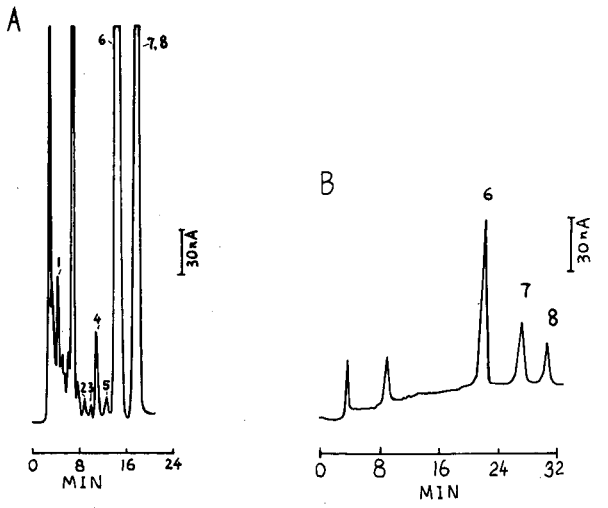

Fig. 4. Chromatogram for the analysis of a peat sample. Peaks: 1 = fucose; 2 = galactosamine; 3 = arabinose; 4 = glucosamine; 5 = galactose; 6 = glucose; 7 = xylose; 8 = mannose. (A) Gradient programme A; (B) gradient programme B.

Arabinose and galactose have the same pK_a values, but the ionic radius of arabinose is smaller that that of galactose. Is is clear that the latter has a greater affinity tot the resin than arabinose, so that its retention time was longer.

This experiment for detecting the sugars improved the detection limits by one to two orders of magnitude compared with HPLC [9], and ranged from 0.01 to 0.20 mg l^{-1} (see Table III). Table III also shows good linearity and reproducibility for the determination of the sugars.

Sample analysis

Peat is a new culture medium for cultivating bacteria, and measuring the sugar content of peat is important. Fig. 4 shows the chromatogram of the pretreated peat sample. Table IV gives the detection results. The sugars in the peat sample were numerous with large amounts of glucose, xylose and mannose.

TABLE IV

RESULTS FOR ANALYSIS OF PRETREATED PEAT SAMPLE

Compound	Concentration (mg l^{-1})	Compound	Concentration (mg l^{-1})
Fucose	0.36	Galactose	0.19
Galactosamine	0.20	Glucose	36.67
Arabinose	0.13	Xylose	34.00
Glucosamine	1.73	Mannose	38.57

ACKNOWLEDGEMENTS

The authors thank the National Natural Science Foundation of China and Dionex for offering a grant.The authors also thank Dr. C. C. Tu of Hawaii University for the gift of xylose oligomers and Shanxi Chemistry of Coal Institute of Academia Sinica for kindly providing the pretreated peat sample.

REFERENCES

1 L. L. Larson and O. Samuelson, *Acta Chem. Scand.*, 19 (1965) 1357.
2 B. G. Chan and J. C. Cain, *J. Chromatogr.*, 127 (1976) 133.
3 M. Ghebregzabher, *J. Chromatogr.*, 127 (1976) 133.
4 H. D. Scobell, K. M. Brobst and E. M. Steel, *Cereal Chem.*, 54 (1977) 905.
5 R. T. Yang, L. P. Milligan and G. W. Mathison, *J. Chromatogr.*, 209 (1981) 316.
6 K. J. Aitztmueller, *J. Chromatogr.*, 156 (1978) 354.
7 J. Sinner and J. Pauls, *J. Chromatogr.*, 156 (1978) 197.
8 L. A. Verhaar, *Carbohydr. Res.*, 53 (1977) 247.
9 D. P. Lu, K. W. Huang and R. C. Li, *Acta Biochem., Biophys. Sin.*, 14 (1982) 501.
10 K. W. Huang, R. C. Li and D. L. Lu, *Acta Biochem. Biophys. Sin.*, 14 (1982) 507.
11 R. D. Rocklin and C. A. Pohl, *J. Liq. Chromatogr.*, 6 (1983) 1577.
12 L. A. Larew and D. C. Johnson. *Anal. Chem.*, 60 (1988) 1867.
13 N. J. Chatterton and P. A. Harrison, *Plant Physiol. Biochem.*, 27 (1989) 289.
14 M. R. Hardy and R. R. Townsend, *Anal. Biochem.*, 170 (1988) 54.
15 M. R. Hardy and R. R. Townsend, *Proc. Natl. Acad. Sci. U.S.A.* 85 (1988) 3289.
16 M. R. Hardy and R. R. Townsend, *Carbohydr. Res.*, 188 (1989) 1.
17 R. R. Townsend and M. R. Hardy, *Nature (London)*, 335 (1988) 379.
18 R. L. Whistler and C. C. Tu, *J. Am. Chem. Soc.*, 74 (1952) 3609.
19 *Dionex Technical Note, No. 20*, Dionex, Sunnyvale, CA, March 1989.

Journal of Chromatography, 546 (1991) 297–309
Elsevier Science Publishers B.V., Amsterdam

CHROMSYMP. 2162

Determination of saccharides in biological materials by high-performance anion-exchange chromatography with pulsed amperometric detection

D. A. MARTENS and W. T. FRANKENBERGER, Jr.*
Department of Soil and Environmental Sciences, University of California, Riverside, CA 92521 (U.S.A.)

ABSTRACT

High-performance anion-exchange chromatography (HPAEC) coupled with pulsed amperometric detection (PAD) under alkaline conditions (pH 9–13) separates aminosaccharides, neutral saccharides and glycuronic acids based upon their molecular size, saccharide composition and glycosidic linkages. Carbohydrates were extracted by utilizing 0.5 *M* H_2SO_4 (neutral monosaccharides), 0.25 *M* H_2SO_4 coupled with enzyme catalysis (glycuronic acids) and 3 *M* H_2SO_4 (aminosaccharides). Solid-phase extraction with strong cation and strong anion resins was used to partition the cationic aminosaccharides and anionic glycuronic acids and to deionize acid extracts for neutral saccharides. Separation was conducted on a medium-capacity anion-exchange column (36 mequiv.) utilizing sodium hydroxide (5–200 m*M* and sodium acetate (0–250 m*M*) as the mobile phase. The saccharides were detected by oxidation at a gold working electrode with triple-pulsed amperometry. HPAEC–PAD was found superior to high-performance liquid chromatography with refractive index (RI) detection for neutral monosaccharides and aminosaccharides and to low-wavelength UV detection for glycuronic acids in terms of resolution and sensitivity. HPAEC–PAD was not subject to interferences as was the case for low UV detection (210 nm) or RI analyses and was highly selective for mono- and aminosaccharides and glycuronic acids. The use of HPAEC–PAD was applied for the determination of the saccharide composition of organic materials (plant residues, animal wastes and sewage sludge), microbial polymers and soil.

INTRODUCTION

Saccharides play a major role as structural (*e.g.*, cellulose and hemicellulose) components of plants and provide a major source of energy for microbial processes when cycled in soil. Aminosaccharides have been reported in plants [1], microorganisms [2], crustaceae and insects [3] and an important source of organic nitrogen in soil [4]. Uronic acids occur in animal tissue [5], microbes [6] and plant [7] structures. In addition to energy and structural roles in animals, insects, microbes and plants, some of the more important microbial ecological functions of saccharides include conferring virulence of pathogenic bacteria, protecting organisms from dessication, regulating ionic traffic at the cell surface, concentrating nutrients, protecting microbes from toxic heavy metals or antibacterial agents and attachment to solid surfaces [8].

Detection of a wide diversity of monosaccharides, aminosaccharides and glycuronic acids in nature has lead to the development of many analytical techniques.

0021-9673/91/$03.50

Current methods for quantification of polysaccharides in biological materials include colorimetric assays [9–13], planar chromatography [14], gas chromatography (GC) [1,15,16] and high-performance liquid chromatography (HPLC) [18,19]. Colorimetric assays do not provide information on the composition of saccharides in biological materials and are often subject to many interferences. Planar chromatography has limitations in separation of similar saccharides. GC analyses involve the necessity of making derivatives. The most common method for quantification of saccharides with HPLC analysis is refractive index (RI) detection, which has several drawbacks. RI detection monitors the bulk property of the LC eluent, thus is non-selective, and cannot easily be used with gradient elution. It also lacks high sensitivity. Uronic acids can be analyzed by UV detection, although the use of low UV wavelengths (210 nm) is subject to interference from other low UV absorbing compounds. The use of high-performance anion-exchange chromatography (HPAEC) coupled with pulsed amperometric detection (PAD) has several advantages over RI and low-UV detection. PAD equipped with a gold electrode is selective only to compounds containing oxidizable functional groups including hydroxyl, amine and sulfide groups. Carboxylic acids and inorganic species do not interfere with detection by PAD. Glycosidic monomers derived from polysaccharides are weak acids with pK_a values in the range 9–13.5 and thus can be separated as anions by controlling the pH of the mobile phase.

Analysis of glycosidic units comprising polysaccharides presents many problems. The susceptibility of the glycosidic linkage to acid hydrolysis varies greatly along with the stability of the resulting monosaccharide unit in the acid solution. Pyranose forms of neutral monosaccharides exhibit the greatest stability to acid conditions, while the furanoses are more susceptible [20]. Polysaccharides containing aminosaccharides or uronic acid units are resistant to mild acid hydrolysis because of the amino and carboxylic moieties.

The objective of this study was to evaluate saccharide extraction, purification and detection of aminosaccharides, neutral saccharides and glycuronic acids present in various biological materials. HPAEC–PAD was used to detect the saccharide composition of various organic materials including plant residues, animal wastes, sewage sludge and soil extracts.

EXPERIMENTAL

Reagents

All neutral monosaccharide and aminosaccharide standards were obtained from Supelco (Bellefonte, PA, U.S.A.). D-Glucuronic acid, D-galacturonic acid and the enzymes, pectolyase from *Aspergillus japonicus* [reported to contain both endopolygalacturonase (EC 3.2.1.15) and endopectin lyase (EC 4.2.2.10)] and β-D-glucuronidase (EC 3.2.1.31) were obtained from Sigma (St. Louis, MO, U.S.A.).

Chromatographic instrumentation

HPAEC–PAD. The HPAEC–PAD analysis was performed on a Dionex (Sunnyvale, CA, U.S.A.) LC gradient pump module and a Model PAD2 detector. Sample injection was via a Dionex autosampler equipped with a 200-μl sample loop. Neutral monosaccharides, aminosaccharides and glycuronic acids were separated on a CarboPac PA1 pellicular anion-exchange resin (250 × 4 mm I.D.) and a CarboPac PA

guard column (25 × 3 mm I.D.) at a flow-rate of 0.8 ml min^{-1} at ambient temperature. Neutral monosaccharides were separated with the following gradient [21]:

Eluent A: 18 MΩ 0.22-μm filtered water; Eluent B: 50 m*M* sodium hydroxide containing 1.5 m*M* sodium acetate

	Eluent	
Time (min)	A (%)	B (%)
0	93	7
15	93	7
25	0	100
30	93	7

Aminosaccharides were separated with the following gradient [22]:

Eluent A: 18 MΩ 0.22-μm filtered water; Eluent B: 100 m*M* sodium hydroxide; Eluent C: 200 m*M* sodium hydroxide

	Eluent		
Time (min)	A (%)	B (%)	C (%)
0	95	5	0
15	95	5	0
20	0	0	100
25	0	0	100
30	95	5	0

Sodium hydroxide (200 m*M*) was used to elute interfering species that may act as displacing ions and shorten the retention times of subsequent runs. Uronic acids were separated with the following gradient [23]:

Eluent A: 18 MΩ 0.22-μm filtered water; Eluent B: 200 m*M* sodium hydroxide; Eluent C: 100 m*M* sodium hydroxide containing 250 m*M* sodium acetate

	Eluent		
Time (min)	A (%)	B (%)	C (%)
0	25	25	50
10	25	25	50
25	8	8	84
30	25	25	50

All mobile phases were degassed to prevent absorption of carbon dioxide producing carbonate. Carbonate will act as a displacing ion and shorten retention times. Detection was by triple-pulsed amperometry with a gold working electrode [24]. The following working pulse potentials (E) and durations (t) were used for the detection of saccharides: $E_1 = 0.10$ V ($t_1 = 300$ ms); $E_2 = 0.60$ V ($t_2 = 120$ ms); $E_3 = -0.60$ V ($t_3 = 60$ ms). The CHOH groups are oxidized at E_1, E_2 removes the reaction prod-

ucts, while E_3 cleans the electrode at a negative potential. Cyclic voltammetry was used to choose the three potentials. The PAD response time was set to 1 s. Chromatographic data were collected and plotted using the Dionex AutoIon 300 software. HPLC-RI and UV determinations were described in previous studies for aminosaccharides [22], neutral monosaccharides [21] and glycuronic acids [23].

Saccharide extraction

Neutral monosaccharides and glycuronic acids were extracted by the methods described by Martens and Frankenberger [21,23]. Briefly, the samples were pretreated with 0.4 ml 6 *M* H_2SO_4 for 2 h at room temperature and then refluxed with 0.5 *M* H_2SO_4 for 16 h at 80°C. Neutral saccharides in poultry manure and sewage sludge were extracted as described above and, in addition, refluxed with 3 *M* H_2SO_4 for 5 h at 80°C. Aminosaccharides were extracted by the method of Martens and Frankenberger [22] with a 6 *M* H_2SO_4 pretreatment and a 3 *M* H_2SO_4 reflux for 16 h at 90°C. The neutral monosaccharides, aminosaccharides and glycuronic acid samples were then treated with 1 ml 0.1 *M* EDTA, titrated to pH 4 with 5 *M* KOH and centrifuged at 10 000 rpm (RCF = 12 062).

Purification of acidic extracts

*Neutral monosaccharides.*The colored materials present in the refluxed organic materials (poultry manure, sewage sludge, straw and alfalfa) and soil extracts were removed by filtration through a Supelco solid-phase extraction column system composed of a 3-ml strong cation (SCX, 3-propylsulfonic acid, H^+) and a 3-ml strong anion (SAX, 3-quaternary propylammonium, Cl^-) column [21].

Aminosaccharides. A 1-ml aliquot of the refluxed organic amendments, microbial polymers, or soil extracts was diluted to 5 ml with water and passed through a Supelco 3-ml SCX solid-phase extraction column. The SCX column was then rinsed with 3 ml of water to elute all non-retained compounds. The aminosaccharides were eluted with 5 ml of 0.3 *M* HCl [22].

Glycuronic acids. A 1-ml aliquot of the acid-hydrolyzed sample was diluted to 5 ml and passed through a SCX column (Supelco). Pectolyase (3 units ml^{-1}; pH 5.5) or β-D-glucuronidase (30 units ml^{-1}; pH 6.8) were added to the SCX eluent and the mixture was incubated at ambient temperatures overnight (16 h). The enzyme–extract mixture was passed through a SAX column (Supelco) and rinsed with several ml of water. The glycuronic acids were then eluted with 0.1 *M* NaCl (pH 8.0) [23].

All samples were filtered before analysis through a Millipore type GS 0.22-μm filters (Bedford, MA, U.S.A.).

RESULTS AND DISCUSSION

Extraction

The following solvents have been reported for extraction of saccharides in biological materials: water, aqueous buffers, complexing reagents, mineral acids (0.25–12 *M*), organic reagents, alkali and combinations of the above [25]. The association between saccharides and soil constituents is believed to involve hydrogen and covalent bonds [26]. Sulfuric acid is often used as the extracting reagent to break these bonds.

Several reports have shown that aminosaccharides can be extracted from biological materials by treatment with hot mineral acids [1,27,28]. Isolation of uronic acids from polysaccharides, however, is very difficult because their glycosidic linkages are more stable than that of the neutral saccharides. Higher concentrations of mineral acids (3–6 M H^+) have been employed to release glycuronic acids [16,29,30], but these concentrations can also decarboxylate the free glycuronic residues [31] and convert them into lactones which are difficult to separate from the neutral saccharides [17].

Various extraction procedures have been used for quantifying saccharides in soils and organic amendments with different degrees of effectiveness. Seven monosaccharides in soil were detected by GC [15]. Angers *et al.* [19], using a lead-loaded cation-exchange column with HPLC–RI, detected five monosaccharides in soil. They recognized problems with coelution of certain monosaccharides with their technique. Coelution of saccharides with HPLC-RI is a common problem as illustrated in Fig. 1. A sample of barley straw was separated on a calcium-based resin column [21]. The solutes were collected with a fraction collector and analyzed with HPAEC–PAD. This work clearly shows that glucose and galactose coelute during the analysis. Retention times of standards analyzed by HPLC–RI indicated that complex materials may be prone to coelution of xylose, mannose and rhamnose with galactose and fucose with arabinose [21]. These saccharides must be resolved because they are important constituents of soils. HPAEC–PAD analyses indicated that in addition to these saccharides, inositol, mannitol and/or ribitol are also present in soils, plant residues, animal wastes and sewage sludge. A HPAEC–PAD chromatogram of ten saccharide standards shows the potential of ion-exchange chromatography for the analysis of saccharides with high resolution (Fig. 2).

Recent reports have suggested that saccharides determined in hot water extracts of soil samples by the anthrone–sulfuric acid analysis were significantly correlated

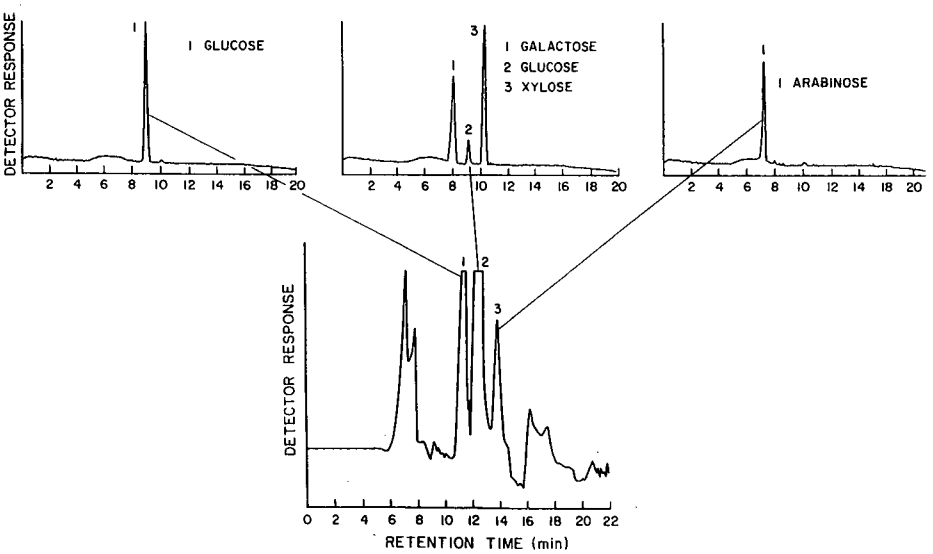

Fig. 1. Chromatogram of an acidic extract of barley straw detected by HPLC–RI. Insets are HPLC–RI fractions collected and then analyzed by HPAEC–PAD.

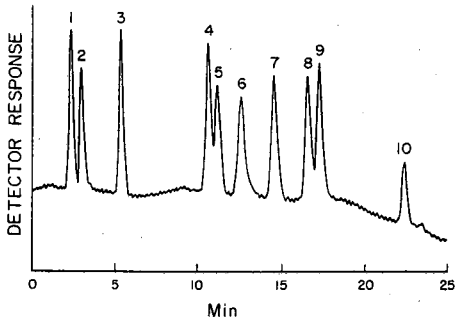

Fig. 2. Chromatogram of saccharides detected by HPAEC–PAD. Peaks: 1 = inositol; 2 = ribitol; 3 = fucose; 4 = arabinose; 5 = rhamnose; 6 = galactose; 7 = glucose; 8 = xylose; 9 = mannose; 10 = lactose (internal standard).

with the structural improvement in soil [32–33]. Martens and Frankenberger [34] found that little or no saccharides were extracted from organic-amended soil with hot (80°C) or cold (25°C) water and that the anthrone–sulfuric acid analysis of these extracts was prone to many interferences. However, the combination of heat (80°C) with H_2SO_4 concentrations as low as 0.13 *M* was effective in extracting saccharides (Fig. 3). The optimum concentration of H_2SO_4 for extraction of saccharides in soils and plant materials was determined to be 0.5 *M* (Table I). However, this $[H^+]$ is not

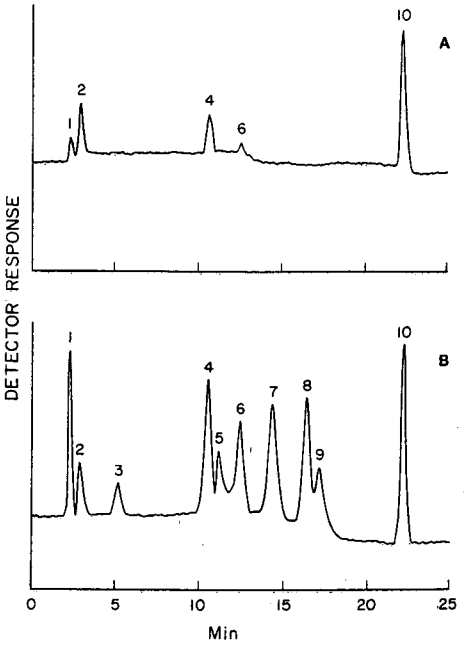

Fig. 3. HPAEC–PAD chromatograms of the acidic extracts of (A) straw-amended soil extracted with 2.5 *M* H_2SO_4 (25°C) and (B) straw-amended soil extracted with 0.13 *M* H_2SO_4 (80°C). Peaks as in Fig. 2.

TABLE I

COMPARISON OF H_2SO_4 CONCENTRATIONS AND HEAT ON EXTRACTION OF SACCHARIDES FROM BIOLOGICAL SAMPLES DETECTED BY HPAEC–PAD

Treatment	Saccharides extracted (mg kg^{-1})									
	Inositol	Ribitol	Fucose	Arabinose	Rhamnose	Galactose	Glucose	Xylose	Mannose	Total
Soil										
0.13 *M* H_2SO_4 (80°C)	35	53	20	279	48	265	192	242	62	1196
0.5 *M* H_2SO_4 (80°C)	38	46	30	303	45	365	423	208	157	1616
2.5 *M* H_2SO_4 (25°C)	13	25	ND[a]	133	ND	Trace	ND	ND	ND	172
Poultry manure										
0.5 *M* H_2SO_4 (80°C)	213	232	160	2313	ND	ND	172	ND	ND	3090
3.0 *M* H_2SO_4 (80 °C)	300	104	231	2889	349	2055	2906	6425	488	15644
Earthworm casts										
0.5 *M* H_2SO_4 (80°C)	38	39	288	2210	396	1736	1099	2951	658	9518
3.0 *M* H_2SO_4 (80°C)	59	32	ND	318	ND	189	1196	320	462	2547

[a] ND = not determined.

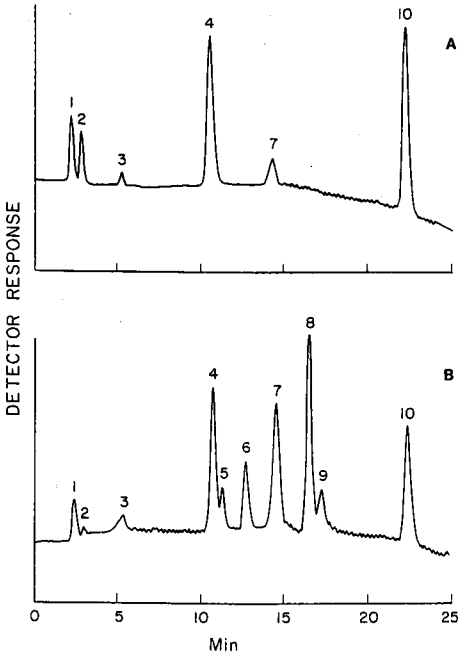

Fig. 4. HPAEC–PAD chromatograms of the acidic extracts of (A) poultry manure extracted with 0.5 *M* H_2SO_4 (80°C) and (B) poultry manure extracted with 3.0 *M* H_2SO_4 (80°C). Peaks as in Fig. 2.

effective for extracting saccharides in sewage sludge or poultry manure. Fig. 4 indicates that low levels of saccharides were extracted by 0.5 *M* H_2SO_4 from poultry manure and that much higher H_2SO_4 concentrations were required. The optimum H_2SO_4 concentration for saccharide determination in animal waste and sludge was 3.0 *M* H_2SO_4.

Research has shown that earthworm (*Lumbricus terrestris*) activity can have a beneficial effect on soil. Part of this benefit may be due to the breakdown of organic residues and deposition of saccharide-rich worm casts on the soil surface (Fig. 5).

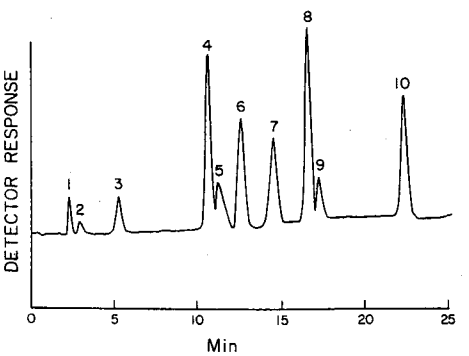

Fig. 5. HPAEC–PAD chromatogram of the acidic extract of worm casts (0.5 *M* H_2SO_4; 80°C). Peaks as in Fig. 2.

These casts were found to be 7.5 × richer in saccharide content than the surrounding soil (Table I). The optimum H_2SO_4 concentration for saccharide extraction from earthworm casts was determined to be 1 *M*.

Saccharide analysis of acid extracts of various biological materials by HPAEC–PAD has revealed new information on the composition of these materials. The saccharide composition of plant residues appears to be composed mainly of arabinose, galactose, glucose and xylose (Table II). The composition of poultry manure, sewage sludge and soil, in addition to the above four listed saccharides, included fucose, rhamnose and mannose units (Tables II and III). The analysis of worm casts showed the same trend as soil and animal wastes but tended to be richer in the saccharides arabinose, galactose, glucose and xylose, reflecting the decomposition of plant residues (Table I).

TABLE II

COMPOSITION AND QUANTITY OF AMINO-, MONOSACCHARIDE AND URONIC ACIDS EXTRACTED FROM ORGANIC AMENDMENTS

Polysaccharide material	Organic amendment (mg kg^{-1})			
	Poultry manure	Sewage sludge	Straw	Alfalfa
Monosaccharides				
Inositol	514	556	1042	11842
Ribitol	ND[b]	196	271	ND
Mannitol	337	ND	490	ND
Fucose	391	1320	ND	ND
Arabinose	5203	10503	26407	40961
Rhamnose	350	1846	ND	46
Galactose	2296	4409	8754	20222
Glucose	3079	3338	12457	31337
Xylose	6575	2599	154035	58045
Mannose	734	2930	ND	373
Total	19479	27697	203456	162826
Aminosaccharides				
Galactosamine	49	188	1405	1825
Mannosamine	39	90	230	685
Glucosamine	38	115	905	1212
N,N′-Diacetylchitobiose	187	84	13140	6040
Acetylgalactosamine	18	35	149	245
Acetylmannosamine	67	73	390	1565
Acetylglucosamine	60	59	968	1950
Total	450	643	17195	13533
Glycuronic acids				
Galacturonic acid	212	740	39790	34900
Glucuronic acid	195	987	58890	43880
Total	407	1787	98680	78780
Total[a]	20336	30127	319331	255139

[a] Sum of monosaccharides + aminosaccharides + glycuronic acids.
[b] ND = Not determined.

TABLE III

COMPOSITION AND QUANTITY OF AMINO-, MONOSACCHARIDE AND URONIC ACIDS EXTRACTED FROM ORGANIC AMENDED AND UNAMENDED SOIL

Polysaccharide material	Organic-amended soil (mg kg^{-1})				
	Poultry manure	Sewage sludge	Straw	Alfalfa	Check (unamended)
Monosaccharides					
Inositol	189	212	238	232	187
Ribitol	64	65	97	61	49
Fucose	91	88	88	94	82
Arabinose	421	386	419	404	288
Rhamnose	120	169	109	128	89
Galactose	407	413	391	332	292
Glucose	282	307	308	237	201
Xylose	708	342	497	335	252
Mannose	62	67	74	78	55
Total	2344	2049	2221	1901	1495
Aminosaccharides					
Galactosamine	4	5	5	13	1
Mannosamine	3	3	3	2	<1
Glucosamine	4	5	5	34	2
N,N′-diacetylchitobiose	6	3	4	5	1
Acetylgalactosamine	<1	1	13	1	1
Acetylmannosamine	2	3	3	0	1
Acetylglucosamine	3	2	3	1	<1
Total	24	23	36	56	7
Glycuronic acids					
Galacturonic acid	94	20	2	7	2
Glucuronic acid	28	132	16	42	11
Total	122	170	218	49	13
Total[a]	2490	2242	2275	2006	1515

[a] Sum of monosaccharides + aminosaccharides + glycuronic acids.

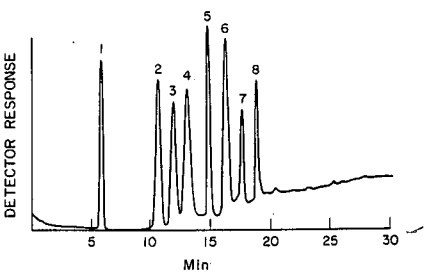

Fig. 6. Chromatogram of aminosaccharides detected by HPAEC–PAD. Peaks: 1 = 2-deoxyribose (internal standard); 2 = galactosamine; 3 = mannosamine; 4 = glucosamine; 5 = N,N′-diacetylchitobiose; 6 = acetylgalactosamine; 7 = acetylmannosamine; 8 = acetylglucosamine.

Many of the oligosaccharides found in plant, microbial and animal tissues consist of various combinations of neutral monosaccharides, aminosaccharides and uronic acids [20]. Fig. 6 shows the separation of seven aminosaccharides by HPAEC–PAD. Cation-exchange chromatography (SXC) [22] separates the aminosaccharides from the neutral monosaccharides and glycuronic acids released by the hydrolysis process. Aminosaccharides, principally chitin (acetyl-D-glucosamine repeating units), have been reported to be present in the cell walls of algae and fungi but have not been found as a component in higher plants [35]. Both straw (Fig. 7) and alfalfa were found to contain large amounts of aminosaccharides (Table II), with the majority of aminosaccharides present in straw as chitobiose (N,N′-diacetylchitobiose) [22]. In lower plants, chitin frequently replaces cellulose as the structural entity in cell walls and may have the same role in maintaining the structural integrity of straw and alfalfa. The aminosaccharide-N fraction in straw was found to account for about 20% of the total N content [22]. Aminosaccharides were also found to compose about 8% of a bacterial polymer produced by *Chromobacterium violaceum* [22] (Fig. 7). Incorporation of straw and alfalfa residues into soil and incubation for eight months resulted in decomposition of nearly all of the added aminosaccharides (Table III).

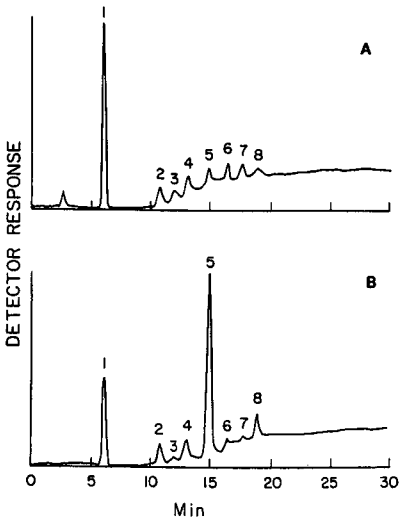

Fig. 7. HPAEC–PAD chromatograms of the acidic extracts (3.0 *M* H_2SO_4; 90°C) of (A) a bacterial polymer produced by *Chromobacterium violaceum* and (B) barley straw. Peaks as in Fig. 6.

The use of pectolyase and β-D-glucuronidase enzymes can be a powerful tool in the preparative separation and elucidation of the structure of polysaccharides. The use of mild acid hydrolysis (0.25 *M* H_2SO_4) to fragment the saccharide polymers coupled with enzyme catalysis released large amounts of uronic acids from the plant materials but released less from the animal waste or sewage sludge and only trace amounts from the organic-amended soil (Tables II and III). Fig. 8 shows a chromatogram of galacturonic acid and glucuronic acid as detected by HPAEC–PAD. Structural analysis of a hemicellulose fraction of barley straw indicated that uronic acids

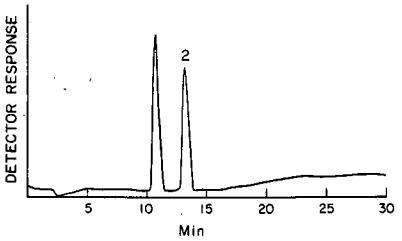

Fig. 8. Chromatogram of glycuronic acids detected by HPAEC–PAD. Peaks: 1 = galacturonic acid; 2 = glucuronic acid.

and L-arabinose monomers link the xylose chains to form the structural polymers [36]. Treatment of the barley straw extract with pectolyase resulted in the release of low levels of uronic acids but use of β-D-glucuronidase with the same extract resulted in a 10× increase in the release of uronic acids (Fig. 9). Incorporation of the straw residue into soil resulted in a rapid decomposition of added uronic acids and after eight months, only trace amounts were present (Table III).

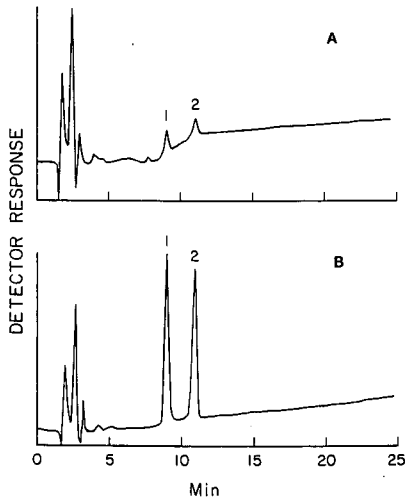

Fig. 9. HPAEC–PAD chromatograms of the acidic-enzyme extracts of (A) barley straw treated with pectolyase and (B) barley straw treated with β-D-glucuronidase. Peaks as in Fig. 8.

CONCLUSIONS

The work presented here showed that plant materials, animal waste, sewage sludge and soil contain neutral monosaccharides, aminosaccharides and glycuronic acids. The saccharide composition of each of these materials was quantified by optimizing the conditions for extraction, purification and chromatography. The use of HPAEC–PAD for separation of saccharides in these complex materials was superior to HPLC–RI and HPLC–UV in terms of sample preparation, resolution and sensitiv-

REFERENCES

1 L. Benzing-Purdie, *Soil Sci. Soc. Am. J.*, 48 (1984) 219.
2 H. R. Perkins, *Bact. Rev.*, 27 (1963) 18.
3 G. Ledderhose, *Berichte*, 9 (1876) 1200.
4 J. M. Bremner and K. Shaw, *J. Agr. Sci.*, 44 (1954) 152.
5 M. Stacey and S. A. Barker, *Carbohydrates of Living Tissues*, Van Nostrand, London, 1962, p. 1.
6 M. Stacey and S. A. Barker, *Polysaccharides of Microorganisms*, Oxford University Press, London, 1960, p. 8.
7 G. O. Aspinall, *Adv. Carbohyd. Chem. Biochem.*, 24 (1969) 333.
8 W. F. Dudman, in I. W. Sutherland (Editor), *Surface Carbohydrates of the Prokaryotic Cell*, Academic Press, New York, 1977, p. 357.
9 R. H. Brink, Jr., P. Dubach and D. L. Lynch, *Soil Sci.*, 89 (1960) 157.
10 M. Dubois, K. A. Gilles, J. K. Hamilton, P. A. Rebers and F. Smith, *Anal. Chem.*, 28 (1956) 350.
11 L. A. Elson and W. T. J. Morgan, *Biochem. J.*, 27 (1933) 1824.
12 A. H. Brown, *Arch. Biochem.*, 11 (1946) 269.
13 Z. Dische, *J. Biol. Chem.*, 167 (1947) 189.
14 M. V. Cheshire, C. M. Mundie and H. Shepherd, *Soil Biol. Biochem.*, 1 (1969) 117.
15 J. M. Oades, M. A. Kirkman and G. H. Wagner, *Soil Sci. Soc. Amer. Proc.*, 34 (1970) 230.
16 L. Benzing-Purdie and J. H. Nikiforuk, *Soil Sci.*, 145 (1988) 264.
17 S. A. Fazio, D. J. Uhlinger, J. H. Parker and D. C. White, *Appl. Environ. Microbiol.*, 43 (1982) 1151.
18 A. G. J. Voragen, H. A. Schols, J. A. DeVries and W. Pelnik, *J. Chromatogr.*, 244 (1982) 327.
19 P. A. Angers, P. Nadeau and G. R. Mehuys, *J. Chromatogr.*, 454 (1988) 444.
20 J. H. Pahur, in W. Pigman and D. Horton (Editors), *The Carbohydrates*, Vol. IIA, Academic Press, New York, 1970, p. 78.
21 D. A. Martens and W. T. Frankenberger, Jr., *Chromatographia*, 29 (1990) 7.
22 D. A. Martens and W. T. Frankenberger, Jr., *Talanta*, in press.
23 D. A. Martens and W. T. Frankenberger, Jr., *Chromatographia*, 30 (1990) 651.
24 S. Hughes and D. C. Johnson, *Anal. Chim. Acta*, 132 (1983) 11.
25 G. D. Swincer, J. M. Oades and D. J. Greenland, *Aust. J. Soil Res.*, 6 (1969) 211.
26 J. W. Parson and J. Tinsley, *Soil Sci.*, 92 (1961) 46.
27 L. Benzing-Purdie, *Soil Sci. Soc. Am. J.*, 45 (1981) 66.
28 J. M. Bremner, *J. Sci. Food Agr.*, 9 (1958) 528.
29 N. Blumenkrantz and G. Asboe-Hansen, *Anal. Biochem.*, 54 (1973) 484.
30 O. Raunhardt, *Dissertation*, ETH Zürich, Zürich, No. 4161, 1968.
31 O. Theander, in W. Pigman and D. Horton (Editors), *The Carbohydrates*, Vol. IB, Academic Press, New York, 1980, p. 1032.
32 R. J. Haynes and R. S. Swift, *J. Soil Sci.*, 41 (1990) 73.
33 R. S. Kinsbursky, D. Levanon and B. Yaron, *Soil Sci. Soc. Am. J.*, 53 (1989) 1086.
34 D. A. Martens and W. T. Frankenberger, Jr., *Soil Biol. Biochem.*, 22 (1990) 1173.
35 K. Ward, Jr. and P. A. Seib, in W. Pigman and D. Horton (Editors), *The Carbohydrates*, Vol. IIA, Academic Press, New York, 1970, p. 435.
36 R. L. Whistler and E. L. Richards, in W. Pigman and D. Horton (Editors), *The Carbohydrates*, Vol. IIA, Academic Press, New York, 1970, p. 447.

Journal of Chromatography, 546 (1991) 311–315
Elsevier Science Publishers B.V., Amsterdam

CHROMSYMP. 2147

Determination of free nitrilotriacetic acid in environmental water samples by ion chromatography with potentiometric and amperometric detection with a copper electrode

W. BUCHBERGER, P. R. HADDAD* and P. W. ALEXANDER
Department of Analytical Chemistry, University of New South Wales, Kensington, NSW 2033 (Australia)

ABSTRACT

An ion-chromatographic method is described for the analysis of free nitrilotriacetic acid in water samples. Separations are achieved on a polymer-based anion-exchange column with 6 m*M* nitric acid as eluent. Both potentiometric and amperometric detection have been applied using metallic copper as the indicator electrode. Detection limits are at about 500 ng injected in the potentiometric mode and 100 ng in the amperometric mode. On-line sample preconcentration is possible for volumes up to 2 ml of river water samples. The response of the detector to other aminopolycarboxylic and aminopolyphosphonic acids has been investigated.

INTRODUCTION

To an increasing degree, nitrilotriacetic acid (NTA) is used in industry and as a substitute for phosphates in detergents. After release to the environment it may affect the distribution of metals within aquatic ecosystems. Therefore, efficient analytical methods are necessary for monitoring NTA, both in its free form and in the form of complexes with metals.

Several analytical techniques exist for the determination of NTA, among them gas chromatography [1–4] after derivatisation of the carboxylic groups, polarography [5,6] and ion-interaction high-performance liquid chromatography following formation of the Cu(II)–NTA complex [7,8]. Unfortunately, these methods do not meet all the requirements of differentiation between free and complexed NTA. More recently, ion chromatography has been used to separate free NTA and other complexing agents [9,10]. Detection is generally by UV-absorbance after post-column reaction with Fe(III) ions; furthermore, the applicability of amperometric detection at carbon paste electrodes has been reported [11].

In this paper the combination of ion chromatography with an electrochemical detector containing a copper wire electrode is described. The detector can be used in the potentiometric mode [12–14] as well as in the amperometric mode [15,16] and should exhibit high selectivity for strong chelating compounds such as NTA. As a consequence, extensive clean-up of environmental samples might be avoided.

0021-9673/91/$03.50

EXPERIMENTAL

The ion-chromatographic instrumentation consisted of a Waters (Milford, MA, U.S.A.) M510 pump, a Rheodyne (Berkeley, CA, U.S.A.) 7010 injection valve with a 20 μl loop or a Waters IC Pak A Guard-Pak precolumn (5.0 × 6.0 mm I.D.), a Waters IC Pak A separation column (50 × 4.1 mm I.D.) and a Waters NRC-1094 mixing device for post-column mixing of the eluent with buffer delivered by a Waters M45 pump.

The electrochemical cell fitted with a copper wire electrode has been described previously [13] and was used in the potentiometric mode with a Beckman (Fullerton, CA, U.S.A.) Φ34 pH-meter or in the amperometric mode with a Bioanalytical Systems (West Lafayette, IN, U.S.A.) LC4A amperometric detector. Chromatograms were recorded using a home-made analog-to-digital converter, interfaced with an Apple IIe computer. Nitric acid (6 m*M*) was used as mobile phase and 100 m*M* phosphate buffer at pH 7 was employed for post-column pH adjustment. The flow-rates of the mobile phase and of the post-column buffer were each 1 ml/min.

River water samples were passed through a Millipore (Bedford, MA, U.S.A.) 0.45 μm Millex filter and then through a Waters C18 SepPak cartridge before injection. Spiked river water samples were prepared by the addition of 500 μl of an NTA stock solution in Milli-Q water to 100 ml of sample. NTA standard solutions were prepared in Milli-Q water by appropriate dilution of a stock solution.

Flow-injection analysis experiments were performed with a home-made metal-free instrument fitted with a wall-jet type electrochemical cell (Ag/AgCl/3 *M* KCl as reference electrode, gold as auxiliary electrode) in combination with a Metrohm (Herisau, Switzerland) E510 pH-meter or a Metrohm E612 potentiostat.

RESULTS AND DISCUSSION

In the potentiometric mode, the potential of the copper electrode is governed by the concentration of free copper ions existing at the electrode surface. This concentration depends on, among other things, the oxygen content and the complexation properties of the eluent. When the electrode is conditioned with an eluent of constant composition at a steady flow-rate, a stable background potential results. Eluted solutes which form very stable complexes with copper ions, such as NTA, will cause a change in the level of copper ions at the electrode surface, thereby producing a decrease in the electrode potential (potential values given in Fig. 2 indicate relative mV changes only and the peak shown for NTA represents a *decrease* in potential).

In the amperometric oxidative mode, a potential of about +100 mV *versus* Ag/AgCl is applied to the electrode. Under these conditions metallic copper becomes oxidised but the oxidative current will be limited due to the formation of passivating layers if the pH is kept in the neutral range [17]. NTA will dissolve these passivating films and increase the current.

In order to develop a chromatographic separation which was compatible with the copper electrode detector both in the potentiometric and in the amperometric mode, we first examined the use of neutral mobile phases. Unfortunately even very strong eluents, such as 1 *M* sodium sulphate, failed to elute NTA in a reasonable time. Under these conditions, NTA carries a double negative charge and is retained strongly.

Therefore an acidic mobile phase such as 6 m*M* nitric acid was employed in order to partially protonate the NTA and thereby reduce the effective charge. Under these chromatographic conditions, NTA was eluted at a retention time of approximately 8 min. These conditions also necessitated a post-column pH adjustment to permit the use of the copper electrode detector, since high background potentials resulted when the nitric acid eluent was passed directly to the detector. Post-column pH adjustment was accomplished by mixing the eluent with 100 m*M* phosphate buffer at pH 7, prior to passage to the detector. Detection limits (measured for a signal-to-noise ratio of 3) were about 500 ng injected in the potentiometric mode and 100 ng injected in the amperometric mode. The linearity of the response, determined for peak heights in a range up to 12 μg injected, was good for the amperometric mode (Fig. 1) with $r = 0.9995$. On the other hand, potentiometric detection showed a non-linear response, as could be expected from the Nernst equation, but within a small concentration range linearity can be assumed.

For application to environmental water samples, on-line sample preconcentration was employed by replacing the injection loop with a small precolumn. Sample volumes of several millilitres were loaded, and the bound NTA was then backflushed onto the analytical column by the eluent. With standard solutions, 20 ml of sample (higher volumes were not tried) could be preconcentrated without loss. In river water samples, the recovery of the preconcentration step was affected mainly by the amount of sulphate present, since sulphate competes with NTA for ion-exchange sites on the concentrator column. Up to 2 ml of samples containing up to 25 μg/ml sulphate could be preconcentrated with quantitative recovery. In such cases, it proved to be advantageous to wash the precolumn with 1 ml of 2 m*M* sodium nitrate after loading the sample in order to strip-off ions, such as chloride, which could give a response at the electrode. The recovery was not affected by this washing step as long as the wash volume did not exceed 1 ml.

In Fig. 2 chromatograms of NTA standards and river water samples (Lane Cove River, Sydney) are shown for the potentiometric and amperometric mode. The performance of the method (expressed as the percentage recovery ± the standard deviation for five replicates) when applied to a 2-ml injection of spiked river water was

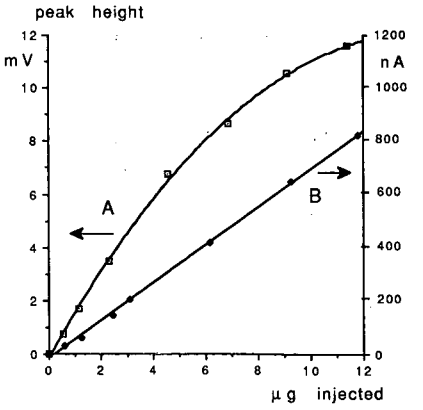

Fig. 1. Calibration plots for NTA obtained with a copper electrode in (A) the potentiometric mode and (B) the amperometric mode. Injection volume: 20 μl.

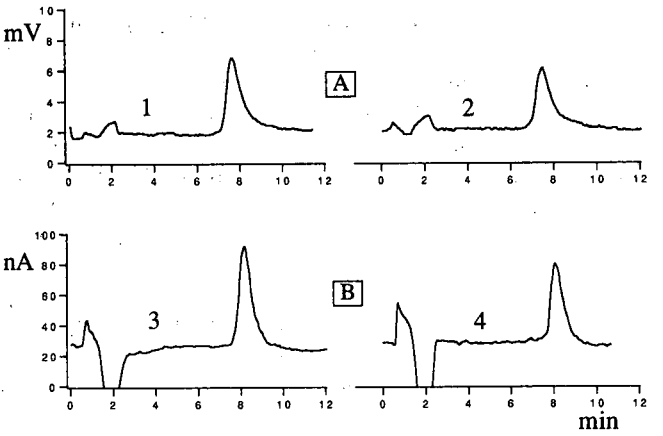

Fig. 2. Chromatograms of (1) standard containing 3.1 ppm NTA, (2) river water spiked with 2.2 ppm NTA, (3) standard containing 0.62 ppm NTA, (4) river water spiked with 0.49 ppm NTA, using (A) potentiometric detection and (B) amperometric detection. On-line preconcentration of 2 ml of sample was used.

97.2 ± 3.8% at a 2.46 μg/ml level for the potentiometric mode, and 95.6 ± 3.1% at a 430 ng/ml level for the amperometric mode. Whilst it is possible that poor recoveries might be encountered in samples of low pH, the results of the above spiking experiments suggest that it is not necessary to adjust the pH of the sample prior to preconcentration.

Similar chromatographic conditions can be used for the separation of other aminopolycarboxylic acids as well as organophosphonic acids, which may be present in detergents [9,10]. We therefore investigated the response of such compounds at a copper electrode by flow-injection analysis. The responses relative to NTA obtained by injecting 100 ng of each compound in 10 m*M* phosphate buffer pH 7 are listed in

TABLE 1

RESPONSE OF DIFFERENT AMINOPOLYCARBOXYLIC ACIDS AND ORGANOPHOSPHONIC ACIDS RELATIVE TO NTA (DETERMINED BY FLOW INJECTION ANALYSIS OF 100 ng)

Compound	Relative response	
	Amperometry	Potentiometry
NTA	1	1
EDTA	0.71	1.20
Dequest 2060 (Diethylenetrinitrilopentamethylenephosphonic acid)	1.52	2.33
Dequest 2041 (Ethylenedinitrilotetramethylenephosphonic acid)	1.55	2.49
2-Phosphonobutane-1,2,4-tricarboxylic acid	1.07	1.11
Dequest 2010 (1-Hydroxyethane-1,1-diphosphonic acid)	2.57	2.14
Dequest 2000 Aminotris(methylenephosphonic acid)	1.26	2.10

Table I. Since all compounds tested gave similar response, we tried in a series of experiments to analyse both NTA and EDTA using ion chromatography with potentiometric or amperometric detection. Unfortunately, some of the injected EDTA becomes lost when the amounts injected are less than 15 μg. The most probable cause of this behaviour is the complexation of EDTA with Fe(III) ions arising either as a contaminant of the nitric acid eluent or from stainless-steel parts of the chromatographic system. Similar problems occurred in the analysis of organophosphonic acids, but were not observed with NTA, presumably because of the lower formation constant for the complex of Fe(III) with NTA. A metal-free instrumentation might help to overcome the difficulties encountered with EDTA and organophosphonic acids.

REFERENCES

1 W. A. Aue, C. R. Hastings, K. O. Gerhardt, J. O. Pierce, H. H. Hill and R. F. Moseman, *J. Chromatogr.*, 72 (1972) 259.
2 D. T. Williams, F. Benoit, K. Muzika and R. O'Grady, *J. Chromatogr.*, 136 (1977) 423.
3 R. J. Stolzberg and D. N. Hume, *Anal. Chem.*, 49 (1977) 374.
4 C. Schaffner and W. Giger, *J. Chromatogr.*, 312 (1984) 413.
5 B. J. A. Haring and W. van Delft, *Anal. Chim. Acta*, 94 (1977) 201.
6 A. Voulgaropoulos, P. Valenta and H. W. Nürnberg, *Fresenius' Z. Anal. Chem.*, 317 (1984) 367.
7 D. G. Parkes, M. G. Caruso and J. E. Spradling, *Anal. Chem.*, 53 (1981) 2154.
8 C. C. T. Chinnick, *Analyst (London)*, 106 (1981) 1203.
9 J. Weiss and G. Hägele, *Fresenius' Z. Anal. Chem.*, 328 (1987) 46.
10 G. Tschäbunin, P. Fischer and G. Schwedt, *Fresenius' Z. Anal. Chem.*, 333 (1989) 111.
11 J. Dai and G. R. Helz, *Anal. Chem.*, 60 (1988) 301.
12 P. W. Alexander, P. R. Haddad and M. Trojanowicz, *Anal. Chem.*, 56 (1984) 2417.
13 P. W. Alexander, P. R. Haddad and M. Trojanowicz, *Anal. Chim. Acta*, 171 (1985) 151.
14 P. W. Alexander, P. R. Haddad and M. Trojanowicz, *Chromatographia*, 20 (1985) 179.
15 W. Th. Kok, U. A. Th. Brinkman and R. W. Frei, *J. Chromatogr.*, 256 (1983) 17.
16 W. Th. Kok, G. Groenendijk, U. A. Th. Brinkman and R. W. Frei, *J. Chromatogr.*, 315 (1984) 271.
17 W. Th. Kok, H. B. Hanekamp, P. Bos and R. W. Frei, *Anal. Chim. Acta*, 142 (1982) 31.

Journal of Chromatography, 546 (1991) 317–324
Elsevier Science Publishers B.V., Amsterdam

CHROMSYMP. 2296

Environmental applications of ion chromatography in China

SHIFEN MOU
Research Centre for Eco-Environmental Sciences, Academia Sinica, P.O. Box 934, Beijing 100083 (China)

ABSTRACT

A survey of environmental applications of ion chromatography (IC) in China is presented, including air, water and soil pollution. The chromatographic conditions for the analysis of environmentally common and critical compounds are discussed.

INTRODUCTION

Environmental chemists are often required to analyse many samples taken throughout regularly spaced areas in the environment. This enables them to perform a rapid survey of the environment for pollutant sources. However, the problems are compounded by the requirement for multi-component determinations on each sample. Several characteristics of ion chromatography make it attractive for environmental sample analysis, including its speed, simple operation and easily obtainable reagents, together with its versatility and high sensitivity. It can generate an ion profile for each sample and the presence or absence of a wide variety of ions can be ascertained in a single injection. Another feature is the clear separation of many chemically similar species. More recent innovations such as chelation IC, multi-phase separation columns, gradient IC and low-pressure IC offer expanded environmental capabilities. So far, IC has been applied successfully to the determination of ions in diverse types of environmental samples. This paper discusses the applications of IC in air, water and soil pollution studies and special attention is given to acid rain and sample pretreatment.

AIR POLLUTION

The first area in which IC found widespread acceptance was in air pollution analysis. The major areas where IC are used are atmospheric particulates, aerosols, acid rain, sulphur dioxide flue gas and automobile exhaust analysis. Coal combustion is a major source of air pollution in China, especially in cities. Particulates and sulphur dioxide are the two most significant pollutants. Energy consumption in China has increased more than 10-fold over about 30 years [1]. In 1987, about 859 million

0021-9673/91/$03.50

TABLE I

CONTENTS OF MAJOR WATER-SOLUBLE CHEMICAL CONSTITUENT OF AIRBORNE PARTICLES IN DIFFERENT SIZE RANGES (0.1 $\mu g/m^3$)

Area	Size range (μm)	Spring 1985				Autumn 1985			
		SO_4^{2-}	NO_3^-	NH_4^+	Ca^{2+}	SO_4^{2-}	NO_3^-	NH_4^+	Ca^{2+}
Guiyang	>7	46.9	5.15	11.7	19.0	20.1	2.68	5.53	7.84
(urban)	7–3.3	27.8	5.88	8.28	8.83	14.9	1.56	4.83	3.18
	3.3–2	31.6	4.04	9.06	6.40	18.5	1.34	5.73	2.43
	2–1.1	59.5	4.04	15.1	3.36	34.7	1.79	13.8	2.84
	<1.1	184	8.09	27.4	4.05	115	4.46	27.6	3.54
Guiyang	>7	48.6	5.88	12.6	18.3	18.8	4.46	4.06	9.64
(suburban)	7–3.3	20.2	5.88	7.35	5.40	15.2	3.13	4.90	4.98
	3.3–2	21.9	3.86	8.44	3.09	21.2	2.24	7.60	3.45
	2–1.1	37.2	2.75	10.9	3.18	46.3	2.24	15.4	3.00
	<1.1	129	5.14	21.6	22.0	105	3.56	30.3	5.95
Beijing	>7	15.1	6.7	5.55	31.6	44.5	24.7	8.83	39.4
(suburban)	7–3.3	8.88	4.46	4.49	15.7	28.7	22.6	10.6	21.5
	3.3–2	8.24	4.01	6.01	9.48	24.9	19.5	11.0	8.25
	2–1.1	9.15	3.58	7.18	5.03	45.8	44.5	16.2	9.19
	<1.1	47.5	21.5	18.8	18.6	107	106	26.5	7.01

tons of coal equivalent were consumed for energy production in the country, coal accounting for 76% of the total. Table I gives the contents of major water-soluble chemical constituents of airborne particles collected in Guiyang and Beijing. Acid rain and acidification of the environment have emerged as an environmental issue of increasing concern in China. Although the precipitation samples have been collected and analysed for acidity and chemical composition since the late 1970s, in some cities such as Beijing, Shanghai, Chongqing and Guiyang, extensive research and sample monitoring only began after IC had become more popular. The monitoring data gathered so far demonstrate that acid precipitation does occur in some parts of China. Approximately 90% of the sampling sites with mean precipitation pH values lower than 5.6 are situated to the south of the Yangtze River, especially in Sichuan, Guizhou and Jiangxi provinces. Areas with the most serious acid rain problem are in the southwestern region; Chongqing and Guiyang have annual mean pH values of 4.14 and 4.07, respectively. Table II shows the rainwater composition in different areas. Sample preservation is significant in rainwater analysis [2]. The monitoring of sulphite and sulphate is important for the mechanism of the formation of acid rain. Fig. 1 shows the concentrations of SO_3^{2-} and SO_4^{2-} in a typical acid rain sample collected in Guang Zhou; 0.2 ml of formaldehyde and 0.1 ml of 0.2 *M* Na_2CO_3–0.3 *M* NaOH were added to 10 ml of sample to prevent sulphite oxidation when the sample was collected. In addition to inorganic ions, some organic acids have been monitored. $AgNO_3$ was added to the rain sample to prevent formic and acetic acids from being decomposed by microorganisms in the water. Figs. 2–4 show ion chromatograms of some typical acid rain samples in Sichuan province which were obtained by low-pressure IC [3,4].

TABLE II

CONCENTRATION OF MAJOR IONS IN RAINWATER SAMPLES (μequiv./l)

Ion	North China			South China			
	Beijing (suburban) 1984	Tianjing (urban) 1981	Beijing (urban) 1981	Guiyang (urban) 1982–84	Guiyang (rural) 1982–84	Chongqing (urban) 1982–84	Chongqing (rural) 1982–84
pH	6.06	6.3	6.8	4.07	4.58	4.14	4.44
SO_4^{2-}	106	317.7	273.1	411	167	307	165
NO_3^-	27.7	29.4	50.2	21	15.9	31.6	18.0
Cl^-	66.2	183.1	157.4	8.2	21.1	15.0	23.9
NH_4^+	127.8	125.6	141.1	78.9	50.6	106	64.1
Ca^{2+}	78	278	184.0	231.2	87.8	110	42
Na^+	13.9	175.2	140.9	10.1	5.9	51.4	45.34
K^+	18.2	59.2	40.2	26.4	7	7.4	23.4
Mg^{2+}	15.6			56.5	29.4	48.3	18.3

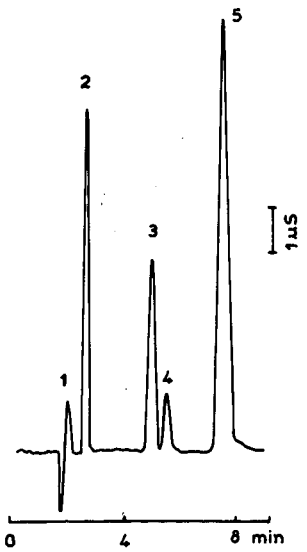

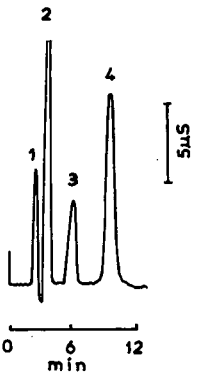

Fig. 1. Chromatogram of anions in acid rain collected in Guang Zhou. Column Dionex HPIC-AS4A; eluent, 2 m*M* Na_2CO_3–3 m*M* NaOH. Peaks (ppm): (1) F^-, 0.23; (2) Cl^-, 1.40; (3) NO_3^-, 6.87; (4) SO_3^{2-}, 1.98; (5) SO_4^{2-}, 14.6.

Fig. 2. Chromatogram of anions in acid rain obtained by low-pressure IC. Column, low-pressure YI; pressure, 43 p.s.i.; eluent, 1.4 m*M* Na_2CO_3; flow-rate, 1.0 ml/min. Peaks (ppm): (1) F^-, 0.30; (2) Cl^-, 1.04; (3) NO_3^-, 2.0; (4) SO_4^{2-}, 3.2.

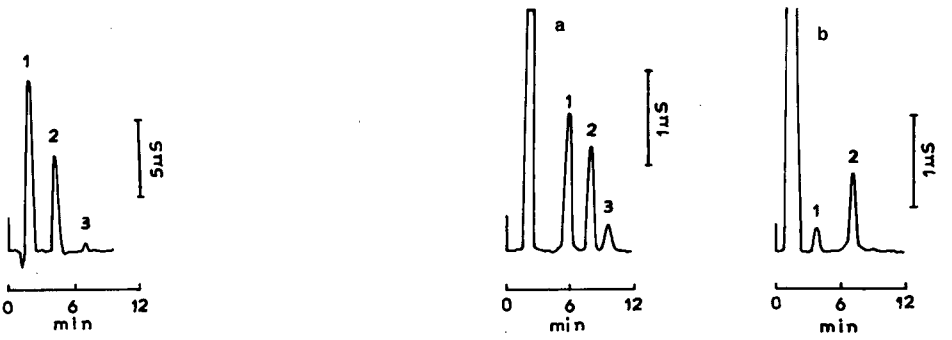

Fig. 3. Chromatogram of organic acids in acid rain obtained by low-pressure IC. Column, low-pressure ICE; pressure, 30 p.s.i.; eluent, 1 m*M* HNO_3; flow-rate, 0.6 ml/min. Peaks: (1) inorganic acid; (2) formic acid; (3) acetic acd.

Fig. 4. (a) Chromatogram of alkali metals in acid rain obtained by low-pressure IC. Column, low-pressure CI; pressure, 30 p.s.i.; eluent, 0.75 m*M* HNO_3; flow-rate, 0.7 ml/min. Peaks (ppm): (1) Na^+, 0.24; (2) NH_4^+, 0.63; (3) K^+, 0.10. (b) Chromatogram of alkaline earth metals in acid rain obtained by low-pressure IC. Column, pressure and flow-rate as in (a); eluent, 1 m*M* ethylenediamine–2.2 m*M* HNO_3. Peaks: (1) Mg^{2+}; (2) Ca^{2+}.

WATER POLLUTION

Drinking water

Water quality assessment and water pollution analysis are natural applications of IC. The general use of IC in these areas has been limited to some extent by the lack of equivalence with published methods of the Environmental Protection Agency and other guidelines. It is necessary when working under the guidelines and regulations of these agencies to use equivalent methods; once approval of IC has been achieved, its widespread acceptance for these types of analyses can be expected. IC has been used for routine water analysis for the determination of anions and cations in drinking water in some Chinese cities [5]. Because of the deleterious effects of nitrite on humans, there is great interest in the control of its concentration in drinking water. Drinking water from various cities has been analysed for some harmful agents, such as chromium(VI), cyanide, arsenic and halogenated organic acids. Using a new column from Dionex, chlorite, chlorate and bromate can be measured down to the low ppb level while other common anions are being simultaneously measured.

Industrial waste water

The next area of interest is industrial waste water. Using IC, an industrial waste water laboratory can not only measure the ions of interest more economically, but can also monitor the other ions which are present. Often this added information can help in solving pollution problems by providing a complete ion characterization of the waste stream. In addition to the classical use of IC for commonly occurring anions and cations in industrial waste water, IC can also be used for some of the less common but very toxic chemicals such as chromate and arsenite. Chromium, arsenic and selenium are elements with variable oxidation states, which influence their chemical properties and toxicities. Environmentally, chromate and arsenite are of primary

concern because of their greater toxicity than chromium(III) and arsenate, respectively. The determination of different oxidation states is of great interest. With IC, chromium(III) and chromium(VI) can be separated and detected with a single injection. Arsenate, selenate, selenite and seven common anions were separated by anion exchange and detected by conductivity detection with a single injection. Arsenite was separated on an ion-exclusion column and detected with amperometric detector [6]. The selectivity and sensitivity are satisfactory.

The results for the determination of chromium, arsenic and selenium are illustrated in Table III. The relative standard deviations are in the range 0.4%–4.4% and the detection limits are in the range 0.5–40 ppb.

Fig. 5 shows the detection of arsenate in semiconductor waste water. Most analytical procedures such as atomic absorption spectrometric, photometric and electrochemical methods are based on either total measurement or on preliminary chemical separation. IC can separate and determine different oxidation states simultaneously. If the oxidation states of a compound are stable in aqueous solution, it is possible to determine them by IC.

The determination of cyanide in various samples is very important environmentally because of its large-scale industrial uses and its extreme toxicity. In all the analytical methods developed so far for cyanide and sulphide, removal of interferences is a necessary first step when analysing most samples. In the IC method, cyanide and sulphide are separated and thus are determined simultaneously [7]. IC with an electrochemical detector has been used to determine free cyanide in ground water and waste water. When large amounts of chloride are present in the sample, ion-exclusion separation is a good choice.

Soil

Environmental studies usually overlap with agricultural studies in the fields of soil, plant and ground water analysis. The ions of particular interest here are those which strongly influence the plant growth process.

TABLE III

LINEARITY, RELATIVE STANDARD DEVIATIONS (R.S.D) AND DETECTION LIMITS (D.L.) FOR DIFFERENT ELEMENTS

Species	Linearity correlation coefficient	Range (ppm)	R.S.D. (%)	Level (ppm)	D.L. (ppb)
Cr(III)	0.9990	0.04–0.8	0.4	0.1	40
	0.9994	0.80–12.0	1.0	5.0	
Cr(VI)	0.9993	0.0003–0.05	4.4	0.005	0.5
	0.9996	0.05–5.00	1.1	0.2	
As(III)	0.9993	0.002–0.150	3.1	0.1	2
	0.9988	0.15–3.00	2.5	1.5	
As(V)	0.9989	0.008–0.250			8
	0.9995	0.25–10.00	1.5	5.0	
Se(IV)	0.9992	0.008–0.250			8
	0.9993	0.25–10.00	0.65	5.0	
Se(VI)	0.9987	0.008–0.250			8
	0.9995	0.25–10.00	0.97	5.0	

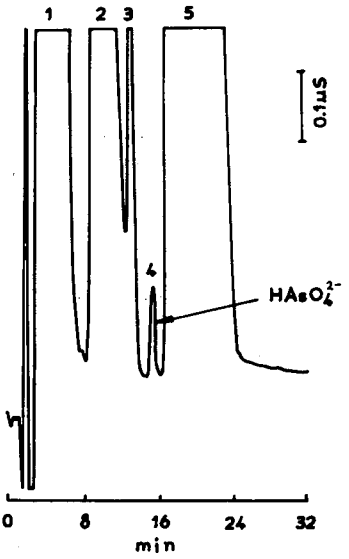

Fig. 5. Chromatogram for detection of $HAsO_4^{2-}$ in semiconductor waste water. Column, Dionex HPIC-AS4A; eluent, 7.5 m*M* $NaHCO_3$–1.2 m*M* Na_2CO_3. Peaks: (1) Cl^-; (2) NO_3^-; (3) HPO_4^{2-}; (4) $HAsO_4^{2-}$; (5) SO_4^{2-}.

Sample pretreatment is an important problem in soil analysis using IC. Extending IC to the analysis of soil has been hindered by the sample preparation problems associated with soil samples. Chromatographic procedures require that a sample to be analysed is in solution, and preferably in aqueous form in the case of IC. Dis-

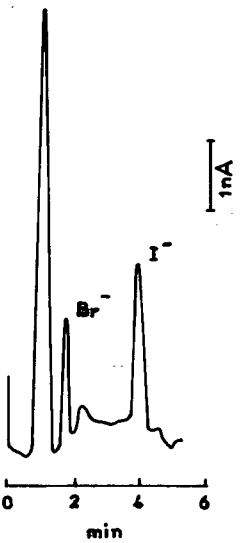

Fig. 6. Chromatogram of Br^- and I^- in soil. Column, Dionex HPIC-AS5; eluent, 0.015 *M* $NaNO_3$; detector, electrochemical with silver electrode, 0.26 V. Peaks: Br^-, 34.5 ppb; I^-, 15.7 ppb.

TABLE IV

EXTRACTANTS AND MONITORED IONS

Extractant	Ions
H_2O	F^-, Cl^-, NO_3^-
2 m*M* Na_2CO_3–2 m*M* NaOH	
3 m*M* $NaHCO_3$–2.4 m*M* Na_2CO_3	
5 m*M* $NaHCO_3$–5 m*M* K_3PO_4	
10 m*M* LiCl	NO_3^-, SO_4^{2-}
10 m*M* KCl	
3.2 m*M* $Ca(H_2PO_4)_2$	
10 m*M* $Ca(C_2H_3O_2)$	
0.1 m*M* $NaHCO_3$	F^-, Cl^-, NO_3^-, SO_4^{2-}
0.5 m*M* $NaHCO_3$	PO_4^{3-}
30 m*M* NH_4F–17 m*M* HCl	NO_3^-, SO_4^-, PO_4^{3-}
1 *M* $NH_4(C_2H_3O_2)$	Na^+, K^+, Mg^{2+}, CA^{2+}

solution of the sample in acids should be avoided when determining anions, unless a subsequent large dilution with water is possible, because the acid anions that are added could result in overloading of the analytical column.

Two procedures have been used in soil sample pretreatment. One is extraction [8], and Table IV gives a list of the extraction reagents that have been used for monitoring anions and cations. The method used to prepare the extract must give quantitative extraction of these ions in soils. Sometimes, these extraction procedures were repeated several times.

The other procedure is fusion–ion exchange [9]. Soil samples were weighed as air-dried powders into a ceramic crucible and an excess amount of NA_2CO_3 and ZnO was added. The flux and sample were mixed in the crucible and the covered crucible was heated for 30 min at 700°C. An excess amount of deionized water was added to the cooled crucible to dissolve partially the fused material, the solution was transferred to a volumetric flask and an excess amount of a strongly acidic cation-ex-

TABLE V

COMPARISION OF THE RESULTS OBTAINED BY IC AND CERTIFIED VALUES (CV) OF SOIL STANDARD SAMPLES

Samples[a]	Br^- (μg/g)		I^- (μg/g)		F^- (μg/g)		Cl^- (μg/g)	
	CV	IC	CV	IC	CV	IC	CV	IC
GSS1	2.9	2.6	2.0	1.9				
GSS2	4.5	4.5	1.8	1.9	220	213		
GSS3	4.3	4.2	1.4	1.4				
GSS4	4.0	4.0	9.0	10.0				
GSS5	1.8	1.6	3.8	3.9	50.0	48.7		
GSS6			19.4	19.8			98.0	92.0

[a] Certified soils reference materials from the Institute of Rock and Mineral Analysis, Ministry of Geology and Mineral Resources, Beijing, China.

change resin was added to remove the metal ions and CO_2. Fig. 6 shows the determination of Br^- and I^- in soil. Table V compares the results obtained by IC and the certified values for standard samples. The values obtained by the IC method were in close agreement with the published values for geological standards. The high precision of the procedure for the analysis of soil is also illustrated.

REFERENCES

1 D. W. Zhao, J. L. Xiong, Y. Xu and W. H. Chan, *Atmos. Environ.*, 22 (1988) 349.
2 X. Li, R. K. Yao and H. J. Guo, presented at the *Second Symposium on Ion Chromatography in China, Beijing, October 1989.*
3 X. S. Zhang, *Chin. Pat.*, 88218755.4, 1988.
4 X. S. Zhang, *Chinese Journal of Chromatography*, 2 (1990) 128.
5 Z. L. Zhang, presented at the *Second Symposium on Ion Chromatography in China, Beijing, October 1989*, paper No. 16.
6 S. F. Mou and Q. Sun, paper presented at the *10th Australian Symposium on Analytical Chemistry, August, 1989,* Abstract No. 152.
7 S. F. Mou, K. Han, Y. Z. Lou and X. P. Hou, *Fenxi Huaxue (Chinese)*, 13 (1985) 457.
8 L. T. Chen, S. F. Mou and K. N. Liu, *Fenxi Huaxue (Chinese)*, 11 (1983) 1988.
9 Z. H. Zhong and R. Fang, presented at the *Second Symposium on Ion Chromatography in China, Beijing, October 1989,* paper No. 3.

Journal of Chromatography, 546 (1991) 325–334
Elsevier Science Publishers B.V., Amsterdam

CHROMSYMP. 2111

Azide determination in protein samples by ion chromatography

PAUL L. ANNABLE* and LAURIE A. SLY
Marion Merrell Dow Inc., Marion Research and Development, Kansas City, MO (U.S.A.)

ABSTRACT

Sodium azide is used as an anti-fungal agent in protein samples in the health related scientific community. Due to its toxic nature, monitoring of the azide level in proteins used in scientific research is necessary. Ion-exchange chromatography has been used to quantitate azide levels in protein samples. Anion-exchange methodology is described which allows for the separation of azide from various common anions found in analytical grade protein sample matrices. The analytical system described utilizes a polymer [poly(styrene–divinylbenzene)] stationary phase which has been surface sulfonated followed by the binding of the aminated latex bead active ion-exchange sites (Dionex, AS4A column). Sodium tetraborate is used as the weak anion-exchange mobile phase. A vendor ion-exchange column comparison is made along with eluent composition and selection studies. Method validation data are presented including: calibration plots for external standardization, limit of detection and method recovery. Various types of proteins are assayed using the described method.

INTRODUCTION

Azide is typically used as an anti-fungal agent in protein samples prepared for scientific research. Due to the toxic nature of azide, its concentration must be accurately monitored in protein samples used in pharmaceutical research. Numerous methods for determining azide in various sample matrices can be found in the literature. Methods include: electrochemical [1], spectrometric [2–5], gas chromatography [6], volumetric [7], liquid chromatography [8] and ion-exchange chromatography [9,10]. Of these techniques, only reversed-phase liquid chromatography and ion-exchange chromatography offer a straight-forward, interference-free approach to quantitating azide in complex matrices such as proteins.

Having a pK_a of 4.8, azide is an excellent candidate for anion exchange with mobile phases having relatively high pH values. The net charge on the azide molecule would be -1 under typical alkaline mobile phase conditions. The primary challenge in developing an ion-exchange method for quantitating azide in proteins would be to completely resolve azide from the similarly sized monovalent common anions (nitrite, bromide and nitrate).

It has been shown that azide can be separated and detected using either single-column or dual-column ion chromatography. By single column, azide has been quan-

0021-9673/91/$03.50

titated on a Wescan anion-exchange column (269-0310) using a nicotinic acid eluent combined with non-suppressed conductivity detection. Azide has also been quantitated using chemically suppressed conductivity detection on a Dionex anion-exchange column with a carbonate–bicarbonate eluent.

The above ion-exchange methods are generally adequate but, they did not completely meet the needs of our laboratory. Using the described carbonate system as a starting point, the authors attempted to quantify low levels of azide in various protein matrices. Incomplete resolution of azide from the common anions (bromide and nitrate) was found. This paper presents an alternative ion-exchange eluent system combined with suppressed conductivity detection which was found to be capable of quantifying azide in various protein samples.

EXPERIMENTAL

Reagents

Sodium tetraborate was obtained from Fluka. Collagen was obtained from Sigma and the bovine serum albumin (BSA) was obtained from both Pierce and Sigma. Sulfuric acid was obtained from Baker. Sodium azide was obtained from Sigma. The sodium salts of the common anions (fluoride, chloride, bromate, bromide, nitrite, nitrate, phosphate and sulfate) were obtained from Fluka. The sodium salts of carbonate and bicarbonate were also obtained from Fluka. Both the metallo enzyme and the growth factor were acquired in-house. All reagents were analytical grade unless otherwise noted.

Stock solutions (100 ppm) of the common anions were prepared from their sodium salts in 18+ MΩ deionized water and were stored in Nalgene volumetric flasks. Working standards of the common anions were serially diluted from the prepared stock using freshly prepared mobile phase. Azide standards were similarly prepared from a 100 ppm azide stock solution and all resulting solutions were stored in Nalgene volumetric flasks. Eluents were prepared from their sodium salts and filtered through a 0.45-μm filter disk. All eluents were thoroughly degassed with helium prior to system start-up. Degassing was found to be especially important with the tetraborate eluents. Shifts in analyte retention times could be seen if eluents were not throughly degassed. This was attributed to carbon dioxide absorption into the tetraborate eluents. Adequate mobile phase degassing with helium eliminated the retention time shifts.

Instrumentation

Instrumentation used was a Dionex 4000i ion chromatograph with gradient pump capabilities and a Dionex conductivity detector. The following different anion-exchange columns were used to perfom a column comparison, Hamilton PRP-X100 [spherical, poly(styrene–divinylbenzene) trimethylammonium exchanger], Waters IC-PAK [poly(methacrylate) resin with a quaternary ammonium exchanger], and a Dionex AS4A [surface-sulfonated poly(styrene–divinylbenzene) with bonded aminated latex beads exchanger]. All azide detection was performed using chemically suppressed conductivity with the Dionex Anion Micromembrane Suppressor.

Sample preparation

The types of proteins assayed were either soluble or insoluble in the eluent system. BSA, zinc metallo enzyme and a growth factor were all soluble in the eluent. Therefore, sample preparation consisted of dissolving the protein then filtering the sample prior to injecting the sample. Collagen protein was not soluble in the eluent. Azide determination in collagen was accomplished by first performing a solid–liquid extraction of the azide from the parent protein. The extraction step consisted of weighing approximately 250 mg of protein into a centrifuge tube and adding 10 ml of eluent. After sealing the centrifuge tube was placed onto a wrist-action shaker for 15 min. The sample was then filtered and injected.

DISCUSSION

Early efforts to fully resolve azide from bromide and nitrate using the typical anion eluent (carbonate–bicarbonate) on a Dionex ion-exchange column (AS4A) were less than rewarding. In an effort to keep the eluent system simple, an isocratic chromatographic system was sought.

A tetraborate eluent system offers very weak elution strength (greater resolving power) while its background conductivity is also capable of being chemically suppressed under normal suppressor conditions. The weak elution strength of the tetraborate is more likely to separate the early eluting anions such as chloride, nitrite, bromide, azide and nitrate. The suppressor reactions for the tetraborate eluent can be seen in Fig. 1. The tetraborate anion is divalently charged in solution with a relatively high background conductance. Within the suppressor it is converted to the less conductive boric acid.

A comparison of columns from different manufacturers was made in an effort to identify the most appropriate column for the required separation. A standard solution was constructed with approximately 10 ppm of each of the following anions: fluoride, bromate, chloride, nitrite, bromide, azide, nitrate and phosphate. Under typical anion-exchange conditions bromide, azide and nitrate can coelute. The above described test solution was used to compare the following columns: Hamilton PRP-X100, Waters IC-PAK and Dionex AS4A. Column capacities for these columns range from 16–250 μequiv./g [11]. The wide variance of column type and capacity encompassed most of the ion-exchange column technology available.

In an effort to maintain a consistency in azide detection only anion-exchange eluents capable of being chemically suppressed were considered. The previously unsuccessful attempts to resolve bromide and nitrate from azide with dilute carbonate–bicarbonate eluents on the Dionex AS4A column led to the use of the previously

Eluent	Eluting Ion	Suppressor Reaction Product	Elution Strength
$Na_2B_4O_7$	$B_4O_7^{2-}$	H_3BO_3	Very Weak

Suppressor Reaction:

$$B_4O_7^{2-} + 8H^+ \rightarrow H_3BO_3 + 4H_2O$$

Fig. 1. Tetraborate eluent system and chemical suppressor reactions.

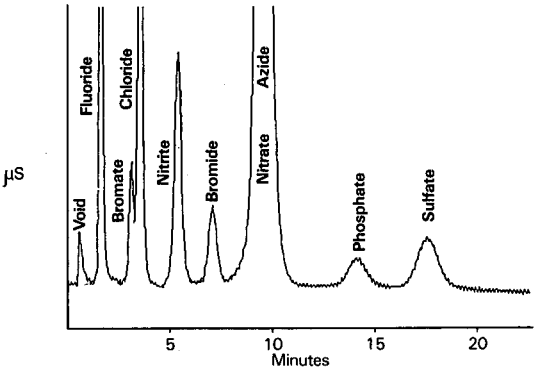

Fig. 2. Ten ppm common anions with azide. Chromatographic conditions: column, Waters IC-PAK A, polymethacrylate resin with quaternary ammonium functional groups; capacity, 30 μequiv./ml; particle size 10 μm; eluent, 0.85 m*M* $NaHCO_3$ and 0.90 m*M* Na_2CO_3; flow, 1.2 ml/min; detection: chemically suppressed conductivity.

described tetraborate eluent with all the above columns. This eluent choice did not improve the separation on either the Waters or Hamilton columns. Therefore, variations of the carbonate–bicarbonate eluent system were developed for the Waters and Hamilton columns. The resulting chromatograms are illustrated in Figs. 2 and 3.

It is quite obvious that the best separation on the Waters column using a carbonate–bicarbonate eluent still did not resolve azide from nitrate. Likewise on the Hamilton column the best separation achieved still did not result in baseline-to-baseline resolution between bromide, azide and nitrate. The authors realize that this comparison was not an all-inclusive investigation into optimum mobile phase conditions with these two columns. But as seen in Fig. 4, complete resolution of bromide,

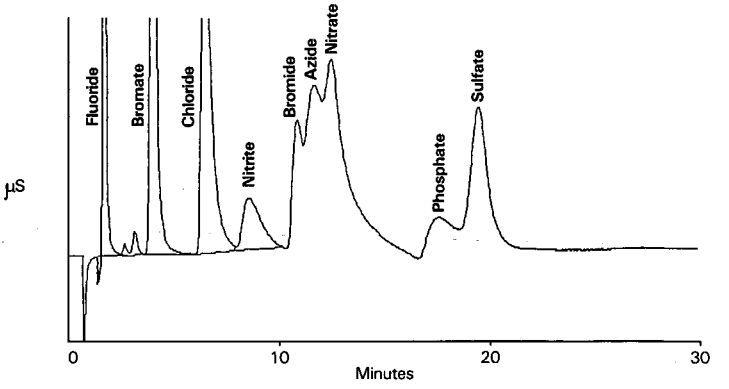

Fig. 3. Ten ppm common anions with azide. Chromatographic conditions: column, Hamilton PRP-X100, poly(styrene–divinylbenzene) resin with surface quarterized (trimethylamine) functional groups; capacity, 200 μequiv./g; particle size 10 μm; eluent, 2.55 m*M* $NaHCO_3$ and 2.70 m*M* Na_2CO_3; flow, 2.0 ml/min; detection: chemically suppressed conductivity.

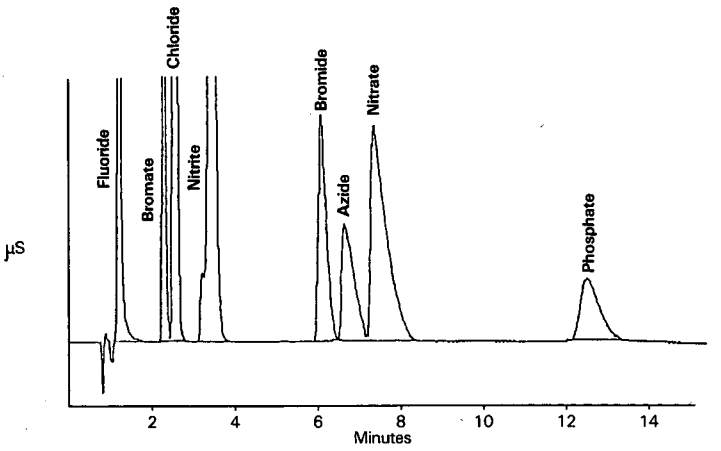

Fig. 4. Ten ppm common anions with azide. Chromatographic conditions: column, Dionex, poly(styrene–divinylbenzene) resin surface sulfonated with aminated latex bead functional groups, AS4A/AG4A; capacity, relatively high loadin capacity; particle size 10 μm; eluent, 16 mM $Na_2B_4O_7$; flow, 2.0 ml/min; detection: chemically suppressed conductivity.

azide and nitrate was obtained on the Dionex column using a tetraborate eluent system. At this point the decision was made to further define the azide chromatography on the Dionex AS4A column using a tetraborate eluent system.

Although sulfate is retained strongly under the tetraborate eluent system it was never a problem throughout these protein investigations. One should consider the effect of sulfate levels in each individual sample. The late eluetion of sulfate or other divalent anions could pose a problem for multi-sample automated analyses. This problem can be solved by establishing the required elution volume for sulfate and including a sufficient delay in the automation schedule. This would allow sulfate to elute between sample injections and eliminate sample carry-over related interferences. Fig. 5 is a typical 10 ppm (in solution) azide standard using the AS4A (Dionex)

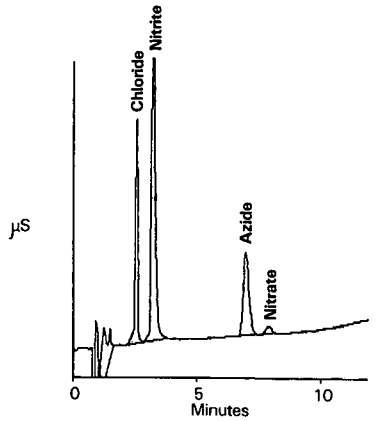

Fig. 5. Ten ppm (in solution) azide standard. Chromatographic conditions: column, Dionex, AS4A/AG4A; eluent, 17 mM $Na_2B_4O_7$; flow, 2.0 ml/min; detection, chemically suppressed conductivity.

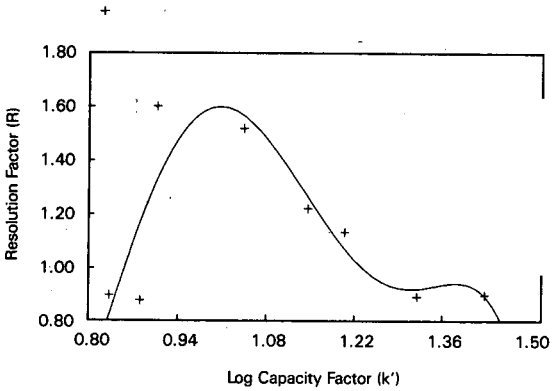

Fig. 6. Bromide and azide resolution map. Tetraborate eluent, AS4A anion column (Dionex). Flow: 2 ml/min, chemically suppressed conductivity detection.

column with a tetraborate eluent. With a flow-rate of 2 ml/min and a tetraborate concentration range of 12–18 mM one can expect retention times of 8–12 min for the azide peak.

A study of capacity factor, k', for azide *versus* resolution factors (azide/bromide and azide/nitrate) was made using the tetraborate eluent system on the AS4A (Dionex) column. The goal of the study was to determine the most optimum eluent concentration for the resolution of azide from the primary potential interferences bromide and nitrate. Figs. 6 and 7 are the resulting resolution maps of the log of the capacity factor *versus* resolution factors for bromide and nitrate respectively. In this study k' for azide was increased beyond the optimum range ($1 \leqslant k' \leqslant 10$) [12] to illustrate that typically little is gained in resolution beyond a k' value of 10. This is quite evident in the nitrate/azide plot (Fig. 7).

The maximum resolution obtained for bromide and azide occurs at an azide log k' between 0.95 and 0.98 ($8.9 \leqslant k' \leqslant 9.5$) which corresponds to an eluent concentration of 14–16 mM tetraborate. As illustrated in Fig. 6, the resolution map for bromide

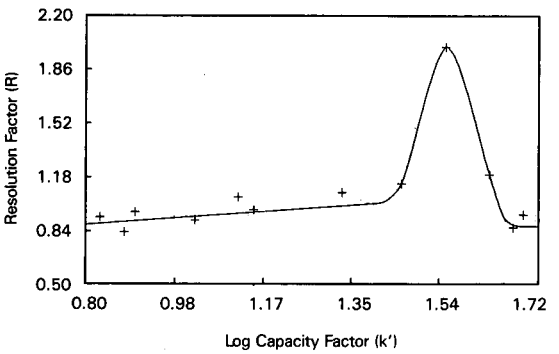

Fig. 7. Azide and nitrate resolution map. Tetraborate eluent, AS4A anion column (Dionex). Flow: 2 ml/min; chemically suppressed conductivity detection.

and azide is quite complex. It was found that if one alters the mobile phase within the above given concentration range then resolving bromide from azide in a given protein sample matrix is possible.

As illustrated in Fig. 7, between an azide k' of 6–20 there is little change in the resolution of azide and nitrate. Considering the fact that the majority of protein matrices will contain some level of nitrate this situation is helpful to the chromatographer. With a larger suitable k' range available to resolve azide from nitrate, method development is not as critical with respect to eluent concentration requirements. Therefore, one has the extended ability to address the bromide–azide interference issue without losing resolution of nitrate and azide. From this resolution map for azide and nitrate it can be concluded that a mobile phase concentration range of 10–18 mM tetraborate will provide adequate separation of azide from nitrate on the AS4A (Dionex) column.

Peak height response for azide using conductivity detection was found to be linear over the typical working range (0–15 ppm azide in solution). A comparison of calibration slopes at varying k' values for azide was made. While optimizing the chromatography for azide with a k' of 10–15, increased sensitivity for azide at the lower k' values was found. The detection limit for azide using the AS4A column and the tetraborate eluent system is estimated to be 30 ppb (in solution). Depending on the sample concentration this detection limit provides quite adequate assurance that this method can be used for trace level azide determination. The concentration range investigated for azide response linearity encompasses the levels that were expected in the protein samples studied.

The proteins used in this study consisted of BSA, zinc metallo enzyme, collagen and a growth factor. From a sample preparation viewpoint all but the collagen protein were soluble in the tetraborate mobile phase system. Azide determination in collegen was accomplished by first performing a solid–liquid extraction of the azide from the parent protein. Figs. 8 through 11 are the resulting chromatograms of the various proteins which were assayed for azide content.

It was assumed that the soluble proteins (BSA, metallo enzyme and growth

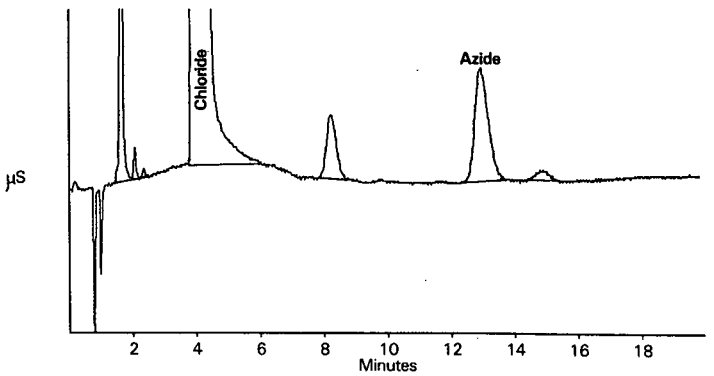

Fig. 8. BSA from Sigma (1000 ppm); 51 ppm chloride and 3.2 ppm azide. Chromatographic conditions: column, Dionex, AS4A/AG4A; eluent, 15 mM $Na_2B_4O_7$; flow, 2.0 ml/min; detection, chemically suppressed conductivity.

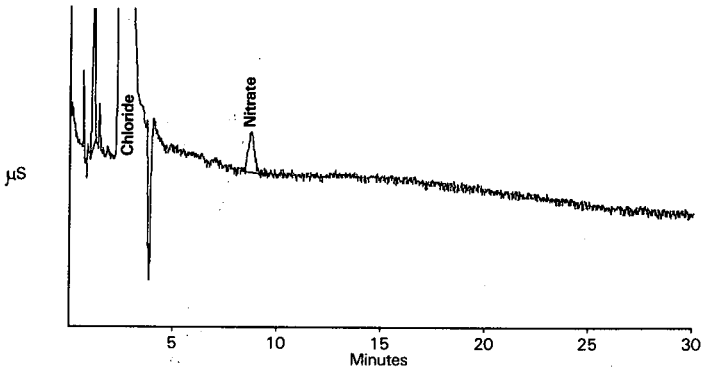

Fig. 9. Zinc metallo enzyme (0.5 ml in 5 ml of eluent). Chromatographic conditions: column, Dionex, AS4A/AG4A; eluent, 15 m*M* $Na_2B_4O_7$; flow, 2.0 ml/min; detection, chemically suppressed conductivity.

factor) were either removed by the sample pretreatment filter (0.45 μm) or were hung-up on the analytical guard column (AG4A, Dionex) or were washed completely through the entire system. If the proteins were absorbed onto either the guard or analytical columns during an assay one would expect column pressures to increase dramatically throughout the study. There was no significant change in the column backpressure from the start through to the end of the study. Approximately 50 protein injections were made through the course of the study. In agreement with the manufacture's literature, final column clean-up with a strong (0.1 *M*) sodium hydroxide column wash is advised. Although, if the tetraborate eluent system is to be used on the column at a later date, consideration for an extended initial equilibration time must be allowed.

BSA samples obtained from two different manufacturers (Sigma and Pierce) were assayed for azide. Fig. 8 is a representative chromatogram for the Sigma sample.

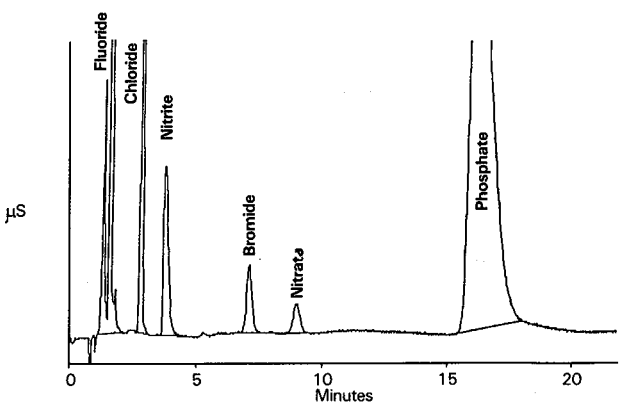

Fig. 10. Collagen (24 mg/ml, insoluble, Bovine Achilles Tendon, Sigma). Chromatographic conditions: column, Dionex, AS4A/AG4A; eluent, 16 m*M* $Na_2B_4O_7$; flow, 2.0 ml/min; detection, chemically suppressed conductivity.

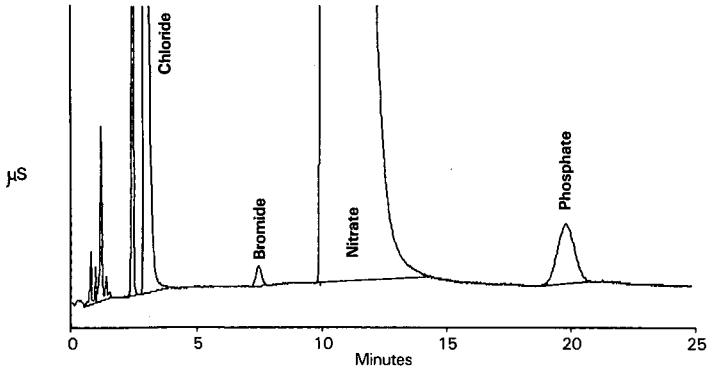

Fig. 11. Growth Factor (4 mg/ml, in solution). Chromatographic conditions: column, Dionex, AS4A/AG4A; eluent, 16 m*M* $Na_2B_4O_7$; flow, 2.0 ml/min; detection, chemically suppressed conductivity.

At a sample concentration of 1 mg/ml, the Sigma BSA was found to contain 0.3% azide while the Pierce BSA at a sample concentration of 0.02 mg/ml contained 16% azide. This level of azide in the Pierce BSA seems to be high and the authors do not have an explanation at this time.

A metallo enzyme (zinc, non-azide binding) was also assayed for azide. The resulting chromatogram of the solubilized protein can be seen in Fig. 9. Obtained from an "in-house" source, the original enzyme samples contained azide and this method was used to prove that azide was no longer present in a new sample lot. As an azide monitoring system, this separation works quite well.

Fig. 10 is the resulting chromatogram for a collagen sample extracted with mobile phase. No azide was detected in this sample and had it been present it would have eluted between the bromide and nitrate peaks. Due to the insolubility of collagen in the mobile phase, sample preparation consisted of a solid–liquid extraction. The extraction as performed at a sample concentration of approximately 25 mg/ml collagen in mobile phase. A wrist-action shaker was used for the azide extraction. Standard addition recoveries were performed with this sample and the results are in Table I.

The final protein assayed for azide was another "in-house" obtained growth factor. As illustrated in Fig. 11, no azide was detected in this sample. Confirmation of

TABLE I

METHOD RECOVERY SOLUBLE *VERSUS* INSOLUBLE PROTEIN SAMPLES

Protein sample	Sample preparation	Standard addition level (ppm in sample)	Recovery (%) (peak area)
Collagen	Solid–liquid extraction: sample is insoluble in the mobile phase	10	97
Albumin bovine serum	Sample is soluble in the mobile phase	100	92

this result was made by spiking azide directly into the sample prior to injection. Azide if present elutes just before the high levels of nitrate found in this sample. Limited available sample minimized further work with this particular protein. It has been proven that this system is capable of quantitating low levels of azide in this type of growth factor.

Method recoveries for azide were determined with two different proteins. The first protein being BSA which is soluble in the mobile phase and the second protein being collagen which is insoluble in the mobile phase. By determining azide recovery with these proteins the sample preparation of insoluble *versus* soluble proteins can be evaluated. The results are summarized in Table I.

Quite good recoveries for azide were obtained from both proteins. The authors found that using a wrist-action shaker provided the best wetting of the insoluble collagen with the tetraborate mobile phase. This, as expected, improved the recoveries of azide to greater than 90%.

CONCLUSIONS

The method described is selective and sensitive for the determination of azide in various types of proteins. In general, both soluble and insoluble proteins assayed for azide resulted in excellent analyte recoveries. The simplicity of the technique enables it to be used as a diagnostic tool in many pharmaceutical quality assurance laboratories.

The authors did not investigate any "azide binding" type proteins (hemoglobin, iron containing) and future work is planned to address this issue. The goal would be to break the bond between the active site (Fe^{3+}) and azide ion, allowing for the quantitation of the free azide ion.

REFERENCES

1 *Application Note H-1*, EG&G Princeton Applied Research, Princeton, NJ, 1980.
2 E. Terpinski, *Analyst (London)*, 110 (1985) 1403.
3 C. Roberson and C. Austin, *Anal. Chem.*, 29 (1957) 854.
4 L. Pepkowitz, *Anal. Chem.*, 24 (1952) 400.
5 J. Sutherland and H. Kramer, *J. Phys. Chem.*, 71 (1967) 4161.
6 M. Blais, *Microchem. J.*, 7 (1963) 464.
7 I. Kolthoff, R. Belcher, V. Stenger and G. Matsuyama, *Volumetric Analysis*, Vol. III, Interscience, New York, NY, 1957.
8 J. Vacha, M. Tkaczykova and M. Rejholcova, *J. Chromatogr.*, 488 (1989) 506.
9 L. Westwood and E. Stokes, *Ion Chromatographic Analysis of Environmental Pollutants*, Vol. II, Ann Arbor Science, Ann Arbor, MI, 1979.
10 D. Gjerde and J. Fritz, *Ion Chromatography*, Hüthig, Heidelberg, 2nd ed., 1987.
11 J. Stillian and C. Pohl, *J. Chromatogr.*, 499 (1990) 249.
12 L. Snyder and J. Kirkland, *Introduction to Modern Liquid Chromatography*, Wiley-Interscience, New York, 2nd ed., 1979.

Journal of Chromatography, 546 (1991) 335–340
Elsevier Science Publishers B.V., Amsterdam

CHROMSYMP. 2143

Determination of dissolved hexavalent chromium in industrial wastewater effluents by ion chromatography and post-column derivatization with diphenylcarbazide

ELIZABETH J. ARAR*
Technology Applications, Inc., 26 West Martin Luther King Drive, Cincinnati, OH 45219 (U.S.A.)
and
JOHN D. PFAFF
U.S. Environmental Protection Agency, 26 West Martin Luther King Drive, Cincinnati, OH 45268 (U.S.A.)

ABSTRACT

A proposed EPA method for the determination of dissolved hexavalent chromium in drinking water, groundwater and industrial wastewater effluents was developed using existing ion chromatographic techniques. Two solid waste matrices were briefly investigated. Aqueous samples were passed through a 0.45-μm filter and the filtrate was either (1) left unadjusted, (2) adjusted to pH 8 or (3) adjusted to pH 10 prior to analysis by ion chromatography. The method detection limits were 0.3–0.4 μg/l. When analyzed within 24 h, the two pH levels and the unadjusted sample yielded *ca.* 100% recovery of spikes. No oxidation of trivalent chromium to hexavalent chromium was observed at pH 7, 8 or 10 when aqueous samples were spiked with 50 mg/l Cr(III).

INTRODUCTION

Current U.S. Environmental Protection Agency (EPA) methods for dissolved hexavalent chromium are Methods 218.4 and 218.5 [1]. Method 218.4 is based on the chelation of hexavalent chromium with ammonium pyrrolidine dithiocarbamate (APDC) and extraction with methyl isobutyl ketone (MIBK) followed by flame atomic absorption spectrometry. Method 218.5 is based on coprecipitation of lead chromate with lead sulphate, which is resolubilized as Cr(III) prior to analysis by furnace atomic absorption spectrometry. Ion chromatography (IC) has proved to be a useful technique for the determination of hexavalent and trivalent chromium in various aqueous matrices [2–5]. Recent developments in IC have resulted in the coupling of anion exchange IC with post-column derivatization of Cr(VI) with diphenylcarbazide and detection of the colored complex at 520 nm [6]. This techniques does not suffer from the interferences common to the diphenylcarbazide spectrophotometric method when other potentially reactive metals are present in the sample because the Cr(VI) is separated from the matrix prior to color development. The primary focus of this work was to apply this existing ion chromatographic method to

0021-9673/91/$03.50

wastewater and to determine a sample preparation and preservation step that would work well for most types of wastewater effluents regulated by the Environmental Protection Agency.

EXPERIMENTAL

The most challenging problem in the determination of Cr(VI) is the preservation of its oxidation state. Cr(VI) exists predominantly as $HCrO_4^-$ in acidic solution and is a strong oxidizer. It is reduced to Cr(III) in the presence of organics or the oxides of nitrogen and sulfur. Conversely, Cr(III) in an alkaline medium will oxidize to Cr(VI) in the presence of oxidants such as Fe(III), oxidized Mn or dissolved oxygen [7,8]. At pH $\geqslant$ 6.5 Cr(VI) exists predominantly as CrO_4^{2-}, which is less reactive than $HCrO_4^-$. For this reason, two pH values (8 and 10) were chosen at which the samples were stabilized after filtration through a 0.45-μm filter. A 1.0 *M* sodium hydroxide solution (ultrapure grade; Aesar, Seabrook, NH, U.S.A.) was used to adjust the pH of the samples. Five types of water (ASTM Type I water, drinking water, groundwater, primary municipal wastewater effluent and electroplating wastewater effluent) were spiked at 0.1 and 1.0 mg/l. Additionally, two solid waste samples (treated municipal sludge and electroplating waste) were spiked with Cr(VI), extracted at various pH valves, filtered and adjusted to the same pH values as aqueous samples. Solid samples were extracted and analyzed on the day of collection. Aqueous samples were analyzed on the day of collection and the day after. Some of the aqueous samples were analyzed again 4–15 days after collection. All sample solutions were stored at 4°C and allowed to equilibrate to ambient temperature prior to analysis by IC.

Verification of ion chromatographic method

The instrumental operating conditions were as follows: instrument, Dionex 4506i ion chromatograph, AI450 software and Dionex VDM-2 detector; guard column, Dionex IonPac NG1; separation column, Dionex IonPac AS7; eluent, 250 m*M* ammonium sulfate–100 m*M* ammonium hydroxide solution at a flow-rate of 1.5 ml/min; Post-column reagent, 2 m*M* diphenylcarbazide–10% (v/v) methanol–1 *N* sulfuric acid at a flow-rate of 0.5 ml/min; Detector, visible (530 nm).

The IC method, which was developed by Dionex, was not altered in any way [6]. The linear range, precision, accuracy and detection limit were initially investigated by fortifying ASTM Type I water with Cr(VI) as CrO_4^{2-}. The linear range was tested by preparing eight standards covering the estimated linear range (0.5 μg/l–10.0 mg/l). A single injection was made of each standard and the peak height used in preparing a calibration graph. A log–log plot of peak height *vs.* analyte concentration was constructed and the correlation coefficient used to determine the working linear range.

The analytical precision for a single calibration was determined by the reproducibility of the measured peak height for eight consecutive injections of a low standard (0.5 μg/l) and a high standard (1.0 mg/l) and reported as relative standard deviation (R.S.D.). Accuracy was determined by the analysis of high- and low-concentration quality control samples and blinds obtained from another laboratory. Results within 10% of the true values were accepted. The method detection limit (MDL) of Cr(VI) in the various matrices was determined by taking seven replicate

aliquots of a single sample that did not contain a level of Cr(VI) exceeding five times the estimated MDL in ASTM Type I water. The MDL for each matrix is defined as the standard deviation (s) of the seven replicate analyses multiplied by the Student's t value for a 99% confidence level [9].

RESULTS

Verification of ion chromatographic method

The correlation coefficient for a log–log plot of peak height *vs.* concentration was 0.99988 for a concentration range covering four orders of magnitude. The analytical precision as determined by the R.S.D. of the peak height of eight consecutive injections of a low and a high standard was 4.9% for a 0.5 μg/l standard and 0.57% for a 1.0 mg/l standard. Two Cr(VI) standards of known concentrations were obtained from another laboratory together with two samples of unknown concentration. The low standard (4.0 μg/l) and the low unknown (2.0 μg/l) were both found to be within 10% of their nominal concentrations. The high standard (1.0 ml/l) and the high unknown (0.5 mg/l) were both found to be within 3% of their nominal concentrations.

Aqueous sample analysis

MDLs for each water matrix are listed in Table I. MDLs were determined using a 250-μl sample loop with a detector setting of 0.002 a.u.f.s. The instrumental detection limit, which was determined based on a chromatographic method by Knoll [10], was 0.15 μg/l in ASTM type I water.

TABLE I

METHOD DETECTION LIMITS FOR Cr(VI) IN WATER AND WASTEWATER

Matrix type	Retention time (min)	Method detection limit[a] (μg/l)
Reagent water	3.80	0.4
Drinking water	3.80	0.3
Groundwater	3.80	0.3
Primary sewage wastewater	3.80	0.3
Electroplating wastewater	3.80	0.3

[a] MDL concentrations are calculated for final analysis solution.

Sample collection sites were all within a 1-h drive of the laboratory, making it possible to filter, preserve and analyze the samples within 4 h of collection. Samples were stored on ice from the time of collection until received in the laboratory, at which time they were filtered, adjusted to pH 8 or 10 and left without pH adjustment. For each pH value spikes of 100 and 1000 μg/l were made. Each sample was analyzed immediately and on the next day. Recoveries for the same-day analysis and at a later date if performed are given in Table II. Native Cr(VI) was not found in any of the water sample at any of the pH values.

TABLE II

RECOVERIES OF Cr(VI) IN WATER AND WASTEWATER

Matrix type	pH	Spike level (μg/l)	Recovery (%)		
			Day 0	Day 1	Day n^a
Reagent water	7	100	100	98	98
		1000	100	95	94
	8	100	102	96	100
		1000	96	98	94
	10	100	100	94	98
		1000	100	94	97
Drinking water	7	100	105	105	108
		1000	98	95	93
	8	100	103	100	101
		1000	100	104	103
	10	100	99	100	98
		1000	99	99	97
Groundwater	7	100	94	94	No data
		1000	99	97	No data
	8	100	105	101	No data
		1000	90	95	No data
	10	100	98	98	No data
		1000	96	99	No data
Primary municipal wastewater effluent	7	100	96	96	81
		1000	101	102	99
	8	100	100	100	90
		1000	83	83	86
	10	100	100	100	100
		1000	104	104	111
Electroplating wastewater	7	100	102	99	No data
		1000	97	92	No data
	8	100	102	100	No data
		1000	98	95	No data
	10	100	99	103	No data
		1000	101	103	No data

[a] The reagent water and drinking water were re-analyzed on the fifteenth day after collection. The primary municipal wastewater effluent was re-analyzed on the fifth day after collection.

Solid waste samples

Solid waste samples were obtained from a municipal wastewater treatment plant and an electroplating plant. Solid samples were treated with the same timeliness as aqueous samples. A 10-ml volume of the moist sample was placed in a 50-ml metal-free centrifuge tube. ASTM Type I water (25 ml was added prior to the addition of the Cr(VI). The tube was capped, shaken thoroughly, placed in an ultrasonic water-bath for 15 min and centrifuged for 20–30 min at 2000 rpm (675 *g*). A 10-ml volume was filtered for each pH value to be investigated. The pH of the extraction solution was checked and in both solid waste extract samples had remained at 7. Recoveries of Cr(VI) at various spike levels and at various pH values are given in Table III for the municipal sludge cake. As a neutral extraction yielded nearly zero

TABLE III

RECOVERIES OF Cr(VI) FROM MUNICIPAL SLUDGE CAKE

Spike level (mg/l)	pH of extraction solution	Recovery (%)	Blank concentration (μg/l)
0.2	7	< 10	<MDL
2.0	7	< 10	<MDL
0.2	8	< 10	<MDL
4.0	9.5	76.5	No data
4.0	13	76.5	7.9

TABLE IV

RECOVERIES OF Cr(VI) FROM ELECTROPLATING SOLID WASTE

Spike level (mg/l)	pH of extraction solution	Recovery (%)	Blank concentration (μg/l)
1.0	8	61.9	No data
1.0	9	56.4	20.3

recoveries even when the pH of the filtrate was adjusted to 8 or 10, an extraction at pH 8 was attempted for the sludge cake. An extraction with the eluent (pH 9.7) and an extraction with 0.1 *M* sodium hydroxide solution (pH 13) were also attempted. The recoveries were improved but were still considered poor.

Only two pH values were examined for the electroplating waste, distilled, deionized water at pH 8 and 9 being used as the extracting solution. Recoveries of a 1.0 mg/l spike are given in Table IV together with the Cr(VI) concentration found in a blank. At this point it was decided that solid waste would require more method development than was planned in this assignment and it was excluded from the final proposed method. It should be noted, however, that the analytical technique using IC would remain the same.

DISCUSSION

As a pH of 7, 8 or 10 had little effect on the recovery of spikes in wastewaters when analyzed within 24 h of collection, the final proposed method recommends an adjustment to pH 9–9.5 using a concentrated buffer solution. The buffer is a 10-fold more concentrated form of the IC eluent. The buffer works well on samples at high or low pH and requires less precise addition than the 1.0 *M* sodium hydroxide solution.

As solid waste samples present special problems, they are not included in the method. The presence of Cr(VI) in the unspiked sludge cake found when the pH of the extraction solution was 13 but not at pH 8 raises the issue of a possible change in the oxidation state of chromium. Extraction solutions of higher pH may either solubilize otherwise insoluble chromates or they may oxidize available Cr(III) in a reactive matrix such as sludge waste.

It is recommended that all samples be analyzed within 24 h of collection, although drinking water samples have a longer holding time. As wastewater matrices will vary, it is the responsibility of the monitoring laboratory to show that the specific matrix type under study is stable for longer than the recommended 24 h.

ACKNOWLEDGEMENTS

The authors gratefully thank Theodore M. Martin, U.S. EPA, Cincinnati, OH, Stephen E. Long, Technology Applications, Cincinnati, OH, and Robert Joyce, Dionex, Sunnyvale, CA, for their many contributions to this work. This work was funded by the United States Environmental Protection Agency under Contract No. 68-03-3352 to Technology Applications.

REFERENCES

1 *Methods for Chemical Analysis of Water and Wastes*, EPA-600/4-79-020, Environmental Monitoring and Support Laboratory, Cincinnati, OH, 1983.
2 S. Ahmed, R. C. Murthy and S. V. Chandra, *Analyst (London)*, 115 (1990) 287.
3 H. C. Mehra and W. T. Frankenberger, Jr., *Talanta*, 36 (1989) 889.
4 D. Molina and M. T. Abell, *Am. Ind. Hyg. Assoc. J.*, 48 (1987) 830.
5 T. Williams, P. Jones and L. Ebdon, *J. Chromatogr.*, 482 (1989) 361.
6 *Dionex Technical Note*, No. 26, Dionex, Sunnyvale, CA, 1990.
7 R. Bartlett and B. James, *J. Environ. Qual.*, 8 (1979) 31.
8 V. J. Zatka, *Am. Ind. Hyg. Assoc. J.*, 46 (1985) 327.
9 J. A. Glaser, D. L. Foerst, G. D. McKee, S. A. Quave and W. L. Budde, *Environ. Sci. Technol.*, 15 (1981) 1426.
10 J. E. Knoll, *J. Chromatogr. Sci.*, 23 (1985) 422.

Journal of Chromatography, 546 (1991) 341–346
Elsevier Science Publishers B.V., Amsterdam

CHROMSYMP. 2136

Determination by ion chromatography and spectrophotometry of the effects of preservation on nitrite and nitrate

MIRIAM ROMAN*, ROBERT DOVI, RHONDA YODER, FRANK DIAS and BRUCE WARDEN
Waste Management Environmental Monitoring Laboratory, Geneva, IL 60134 (U.S.A.)

ABSTRACT

EPA method states that unpreserved samples analyzed for nitrite and nitrate must be analyzed within 48 h. If samples are preserved with sulfuric acid at pH < 2, then nitrite and nitrate are allowed a 28-day holding time. Early indications suggested that nitrite was not stable under acidic solutions and was in fact converted to nitrate within the holding time set by the methodology. Owing to this discrepency, an investigation was made of the effects of preservation on the stability and equilibrium of nitrite and nitrate in reagent-grade water, groundwater, leachate and surface-type waters. The results showed that when reagent-grade water is spiked with nitrite and nitrate, both anions are stable for > 30 days if simply kept refrigerated at 4°C, but when acidified to pH < 2 with sulfuric acid nitrite is rapidly converted to nitrate. When nitrite and nitrate were added to the matrices found in the environmental samples and held at 4°C, conversion of nitrite to nitrate only occurred in the surface water sample. This conversion is believed to have been caused by the presence of nitrogen-fixing bacteria. As it was believed that acid preservation would oxidize nitrite to nitrate, and bacteria could also cause conversion of nitrite and nitrate, we spiked these samples under highly basic conditions (preservation with sodium hydroxide at pH 12). It was hoped that these basic conditions would destroy the nitrogen-fixing bacteria and stabilize nitrite. The results indicated no conversion of nitrite during the 37-day test period in any of the test matrices when samples were preserved in base.

INTRODUCTION

Nitrite and nitrate are important parameters in ground water analysis [1]. Excessive amounts of nitrites have been shown to increase the methemoglobin in the blood of infants. A 35–50% increase causes headaches and a 70% increase is lethal. Nitrite in acidic solutions forms nitrous acid, which can react with secondary amines to form nitrosamines, many of which are carcinogenic [2].

U.S. Environmental Protection Agency (EPA) methodology states that unpreserved reagent-grade water and environmetal-type waters when analyzed for nitrite and nitrate are to be kept at 4°C and analyzed within 48 h. However, if samples are tested after 48 h, the procedure requires that samples need to be preserved with sulfuric acid at pH < 2 and stored at 4°C. Under these conditions, the samples are allowed a holding time of 28 days [3]. Early indications suggested that nitrite was not

0021-9673/91/$03.50

stable under acidic solutions and was in fact converted to nitrate within the holding time set by the methodology. Owing to this discrepency, an investigation was made of the effects of preservation on the stability and equilibrium of nitrite and nitrate in reagent-grade water, groundwater, leachate and surface-type waters.

The stabilities of nitrite and nitrate in acidic, basic and neutral waters were determined using a spectrophotometric method as stated in EPA Method 353.2 and by ion-exchange chromatography (IC) which is described in EPA Proposed Method B1011 [4,5]. The spectrophotometric method first measures nitrite, after reaction to form a colored complex, at a wavelength of 520 nm. Nitrate is reduced to nitrite and the combined nitrate plus nitrite is measured. The concentration of nitrate is determined by difference. In the chromatographic method, nitrite and nitrate are separated on an ion-exchange column with borate–gluconate as the eluent. The separated ions are measured by UV detection at 214 nm.

EXPERIMENTAL

This study was carried out in two parts. The first part focused on establishing the stability of nitrite and nitrate in neutral and acidic reagent-grade water. Four aliquots of reagent-grade water (obtained from a Milli-Q water purification system) were spiked with nitrite and nitrate at 0.5, 1.0, 2.0 and 5.0 mg/l. Four more aliquots were acidified to pH < 2 with sulfuric acid and spiked at the same levels with nitrite and nitrate.

The second part of the study focused on the stability of nitrite and nitrate in ground water, surface water and leachate samples, both unpreserved and preserved (basic). These field samples were collected from a local landfill in 5-gallon polyethylene containers and stored at 4°C. Each 5-gallon sample was split in order to obtain enough sample to test both preserved and unpreserved (samples were preserved with reagent-grade sodium hydroxide to pH 12). The three types of environmental samples, both unpreserved and preserved, were spiked with nitrite at levels of 0.5 and 1.0 mg/l for analysis on a TRAACS 800 AutoAnalyzer and 10.0 and 50.0 mg/l nitrite for analysis using a Waters ion chromatograph. Prior to analysis, samples tested by IC were diluted ten-fold and filtered through a 0.45-μm filter. Samples tested by the spectrophotometric method were filtered through a 0.45-μm filter prior to analysis. Once the initial samples had been prepared they remained in storage at 4°C except when sampled and analyzed at various intervals during the 37-day period.

Ion chromatographic method

The instrumentation used was a Waters single column ion chromatographic system (Millipore–Waters Chromatography Division, Milford, MA, U.S.A.). The system consisted of a high-performance liquid chromatographic pump delivering borate–gluconate eluent at 1.2 ml/min, an autosampler with a 100-μl injection loop, a high-capacity anion-exchange column with in-line precolumn filter and a UV–VIS detector set at 214 nm. Intergration was performed with a DEC Pro380 PC data station. The eluent consisted of a mixture of lithium gluconate and borate which forms a gluconate–borate anion complex. Sample anions pass into solution by exchange with eluent anions and ultimately are eluted from the column. The increase in absorbance was measured at 214 nm.

Spectrophotometric method

The spectrophotometric instrumentation used was a Bran and Luebbe TRAACS 800 AutoAnalyzer segmented-flow system consisting of a random-access autosampler sampling at 120 samples per hour, a multi-test cartridge for nitrite, a multi-test cartridge for nitrate + nitrite, a reagent sequencer, an IBM PC PS/2 30 data system and a UV–VIS detector set at 520 nm.

In the colorimetric reaction, nitrate is reduced by hydrazine solution to nitrite, which, together with the nitrite originally present, reacts with sulfanilamide to form a diazonium salt. This couples with N-(1-naphthyl)ethylenediamine dihydrochloride to form a highly colored azo dye which is measured at 520 nm. Nitrite and nitrate concentrations are determined by the difference in concentration before and after reduction.

Reagents and chemicals

Ion chromatographic method. Borate–gluconate concentrate contains 7.2 g of reagent-grade lithium hydroxide, 25.5 g of boric acid, 13.2 g of D-gluconic acid and 94 ml of glycerin diluted to 1 with water. The eluent is then prepared by diluting 20 ml of the concentrate and 120 ml of acetonitrile to 1 l with water. Purified (18 MΩ) water was obtained from a Milli-Q water purification system (Millipore-Waters). The eluent was then filtered through a 0.45-μm filter and degassed by suction. Analytical standards for nitrite and nitrate (200 ppm) were purchased from Wescan Instruments.

Spectrophotometric method. Copper(II) sulfate, Brij-35, hydrazine sulfate, hydrochloric acid, N-(1-naphthyl)ethylenediamine dihydrochloride, phosphoric acid, potassium nitrate, sodium hydroxide, sodium nitrite and sulfanilamide were used, with 18 MΩ water as above.

RESULTS AND DISCUSSION

Spiked reagent-grade water preserved at 4°C showed no deterioration of nitrite or nitrate during the 37-day test period. The nitrite levels in the unpreserved ground and leachate waters also remained stable up to 37 days. However, the surface water samples indicated some deterioration of nitrite after 14 days and it was totally converted to nitrate after 37 days (Fig. 1). This conversion of nitrite to nitrate is thought to be caused by nitrogen-fixing bacteria present in the surface water [6]. Reagent-grade water spiked with nitrite and nitrate and acidified with sulfuric acid to pH < 2 showed immediate deterioration of nitrite to nitrate. This would explain the poor nitrite spike recoveries experienced in our laboratory during routine analysis. Total conversion of nitrite to nitrate was observed within 14 days (Fig. 2).

The field water samples referred to above stored at 4°C and preserved with sodium hydroxide to a pH 12 showed excellent stability of nitrite up to 37 days (Fig. 3). The samples for IC were spiked with 50 and 10 mg/l nitrite and diluted 10-fold. The results obtained represent 116% and 111% recoveries, respectively. The slight increase in nitrite concentration is within the analytical error. No conversion of nitrite to nitrate was observed during this test period. It is believed that at this high pH, bacteria, which effect nitrite conversion, were not present. Nitrate was stable under both acidic and alkaline conditions.

In conclusion, base preservation seems to be the method of choice to obtain

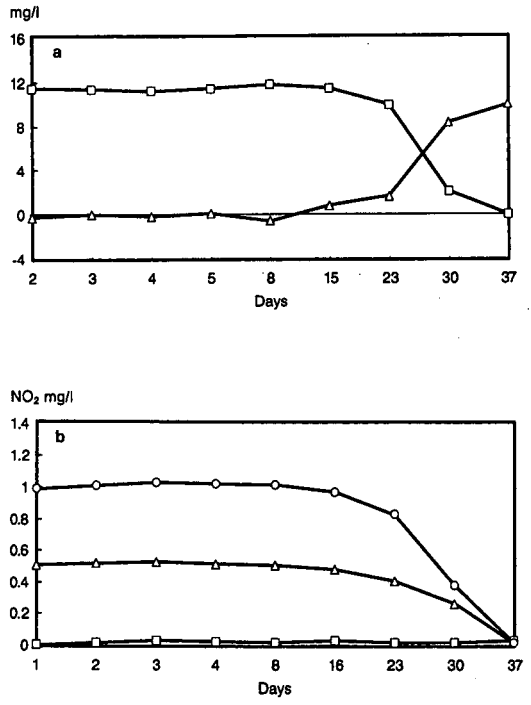

Fig. 1. (a) Results for unpreserved surface water: △ = nitrate; □ = nitrite. (b) Results for unpreserved surface water: ○ = 1.0 mg/l nitrite spike; △ = 0.5 mg/l nitrite spike; □ = unspiked.

accurate determinations of individual levels of nitrite and nitrate in environmental samples while maintaining a holding time of more than 28 days. Acid preservation of samples is not recommended if one wishes to determine individual nitrite and/or nitrate levels in environmental samples.

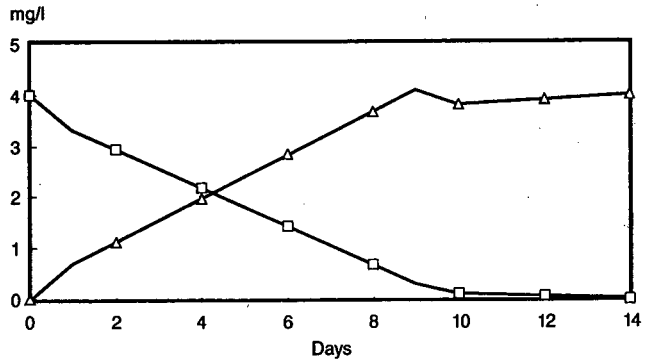

Fig. 2. Results for nitrite-spiked water acidified to pH < 2. △ = Nitrate; □ = nitrite spike.

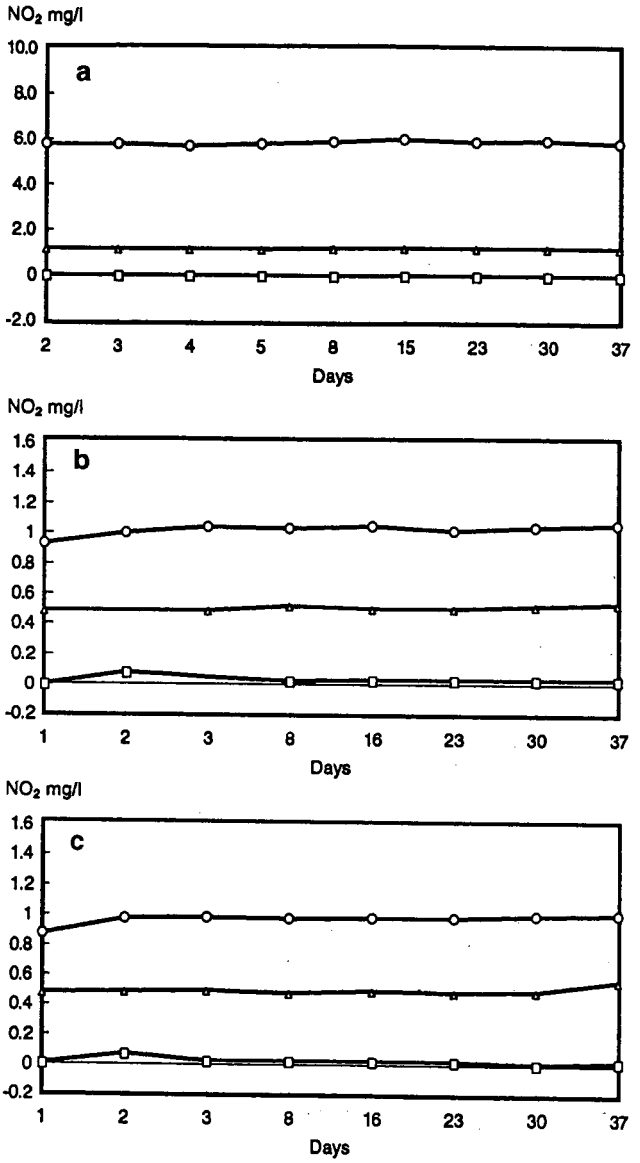

Fig. 3. (a) Results for preserved groundwater (pH 12): ○ = 5.0 mg/l nitrite spike; △ = 1.0 mg/l nitrite spike; □ = unspiked. (b) Results for preserved surface water (pH 12): ○ = 1.0 mg/l nitrite spike; △ = 0.5 mg/l nitrite spike; □ = unspiked. (c) Results for preserved leachate water (pH 12): ○ = 1.0 mg/l nitrite spike; △ = 0.5 mg/l nitrite spike; □ = unspiked.

ACKNOWLEDGEMENT

The authors thank Debbie Connet for providing technical assistance.

REFERENCES

1 H. J. Kim and Y. K. Kim, *Anal. Chem.*, 61 (1989) 1489–1493.
2 L. C. Green, D. Ralt and S. R. Tannenbaum, in A. Neuberger and T. H. Jukes (Editors), *Human Nutrition*, Jack K. Burgess, Englewood, NJ, 1982, p. 87.
3 *EPA Test Method 300.0, The Determination of Inorganic Anions in Water by Ion Chromatography*, U.S. Environmental Protection Agency, Cincinnati, OH, 1989.
4 *EPA Proposed Method B1011, Waters Test Method for the Determination of Nitrite/Nitrate in Water Using Single Column Ion Chromatography*, Millipore, Waters Chromatography Division, Milford, MA, 1990.
5 *EPA Method 353.2, Methods for Chemical Analysis of Water and Wastewater*, Technicon TRAACS 800 Method 782-86T, U.S. Environmental Protection Agency, Cincinnati, OH, 1986.
6 K. M. Pedersen, M. Kümmel and H. Soeberg, presented at the *International Association on Water Polution Research and Control (IAWPRC) Biennial, Kyoto, Japan, July 29–August 3, 1990.*

Journal of Chromatography, 546 (1991) 347–350
Elsevier Science Publishers B.V., Amsterdam

CHROMSYMP. 2303

Application of ion chromatography to failure analysis of electronics packaging

MARINA PLAT* and JUDY DE LEO

IBM Corporation, Product Quality Assurance, East Fishkill, Road 52, Hopewell Junction, NY 12533 (U.S.A.)

ABSTRACT

Ionic contamination is a frequent cause of corrosion failures in electronics packaging. Ionic Cl^-, SO_4^{2-}, Na^+ and K^+ are the species most frequently associated with corrosion and are easily detected by ion chromatography (IC) or other surface analysis techniques (XRF, EDX, etc). This paper will describe a corrosion problem, involving gold-plated copper wires and an automated wire bonding operation, and its solution using IC and Fourier transform infrared (FT–IR) analysis, which showed that the corrosion was caused by ionic NO_2^- and NO_3^-, species which are not easily detected by other surface analysis techniques.

INTRODUCTION

Ionic contamination is a frequent cause of corrosion failures in electronics packaging. Ionic Cl^-, SO_4^{2-}, Na^+ and K^+ are the species most frequently associated with corrosion [1,2].

Corrosion product was found on electronic modules after wire bonding operations, and ion chromatographic (IC) analyses of the modules showed the presence of ionic nitrite and nitrate. The wire bonding operation consists of two steps: stripping of the wire insulation using a direct current (d.c.) arc and ultrasonic bonding of the wire. Using IC analyses the contamination source was traced to the wire stripping operation, which produced NO_2^- and NO_3^- from the NO_2 and water in the air during arcing [3,4]. The wire insulation did not contribute greatly to the formation of these corrosive species.

This paper will show that formation of nitrogen species is directly proportional to the relative humidity and number of arcs. The contamination problem due to wire stripping was solved by installation of a vacuum tube next to the arc to evacuate the corrosive species formed by arcing. The vacuum effectiveness was monitored by collecting the sample in deionized (DI) water and analyzing it using IC.

This paper will also show correlation of IC analyses with micro Fourier transform infrared (FT-IR) analyses of the corrosion/arcing products.

0021-9673/91/$03.50

EXPERIMENTAL

Ion chromatography

The ionic contaminants were extracted from the surface of the package by covering it with DI water. The DI water was allowed to remain on the sample for 60 min with periodic agitation. An aliquot was collected and analyzed using Dionex ion-exchange chromatography. Chromatographic conditions used were: sample volume, 50 μl; separator column, HPIC-AS4A; guard column, AG4A; eluent, 1.8 m*M* Na_2CO_3–1.8 m*M* $NaHCO_3$; flow-rate, 2 ml/min; suppressor, AMMS; regenerant, 25 m*M* H_2SO_4 at 3 ml/min; conductivity detector.

IR spectrometry

IR spectra were acquired using an IR-PLAN (TM, Spectra-Tech) microscope coupled to a Nicolet 740 spectrometer. The corrosion product was removed from the wires and analyzed in transmission mode; material on gold pads was analyzed in reflectance mode. The IR spectra were acquired at 8 cm^{-1} resolution using either 128 or 256 scans.

RESULTS AND DISCUSSION

A corrosion product was found on the tips of wires after the wire bonding operation on an automatic wire bonding tool. The process consisted of two steps: stripping the wire insulation using a d.c. arc and ultrasonic bonding of the wires to a gold pad. The corrosion product appeared green and fuzzy and was found primarily on the tips and exposed areas of the wire. The wire was made of gold-plated copper with polyimide insulation. CI analyses showed that the parts with corroded wires had unusually high amounts of ionic nitrite and nitrate. Micro-FT-IR analyses identified the corrosion product as $CuNO_3$. To locate the source of contamination, the parts were analyzed sequentially using IC before and after the bonding process. There were no contaminants found prior to the wire bonding operation or after a manual wire bonding operation. However, after wire bonding on an automated bonder the parts were found to be contaminated with ionic nitrite and nitrate. Optical inspection revealed that areas surrounded by many bonded wires contained more corrosion than those near fewer wires. In addition, some areas of the part were found to have small droplets of an unknown liquid on their surfaces. The liquid droplets were identified using FT-IR as nitric acid.

Based on the experimental data, the parts were contaminated/corroded at some point during the wire bonding process on the auto-tool. The wire bonding operation on both manual and auto-tools consists of two steps: stripping of the wire insulation using a d.c. arc and ultrasonic bonding of the wire to the pad. The stripping on the manual tool is performed a few feet away from the part, whereas the stripping on the auto-tool is performed directly over the surface of the part being bonded. It was clear that the wire stripping process was the cause of the ionic contamination.

To understand the effect of the wire stripping process, the following experiments were conducted: A small petri dish containing 10 ml of DI water was placed under the wire stripping arc. The wire then was stripped 200 times using standard wire stripping parametes. Simultaneously, another petri dish with DI water (blank) was

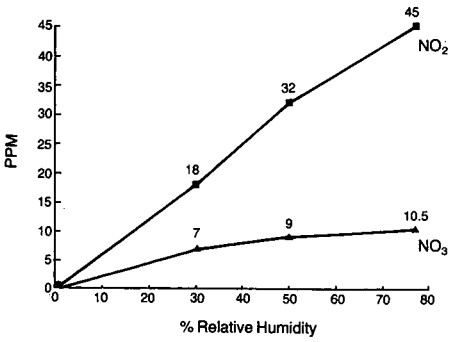

Fig. 1. Concentration of nitrates and nitrites formed during arcing *vs.* relative humidity in the room.

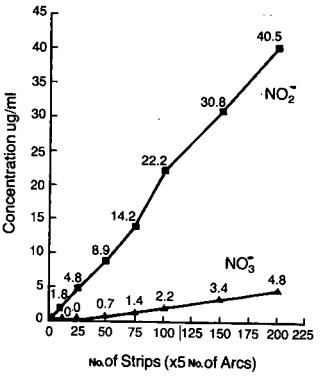

Fig. 2. Concentration of nitrates and nitrites formed during arcing *vs.* number of arcs.

placed a few feet away from the arcing operation. The water from both dishes was collected and analyzed via ion-exchange chromatography. High amounts of ionic nitrate and nitrite were detected in all samples placed under the arc, whereas none were detected in either blank. These experiments were then repeated with arcing only no wire was stripped. The results were interesting: the wire insulation itself did not contribute to the formation of nitrogen species. Rather, these species were being formed from NO_2 and moisture in the air (acid rain). The formation of nitrate and nitrite ions was found to be proportional to the number of arcs (Fig. 1) and relative humidity. Ionic nitrite could be detected in the water samples using the above techniques after only ten arcs and ionic nitrate after a minimum of 50 arcs. The arcing-over-water experiments were performed on the automated tools, varying the relative humidity in the room from 70 to 35%. The results showed that higher relative humidity produced higher concentrations of nitrite and nitrate (Fig. 2). It has been shown [5] that Cu will corrode [form blue $CuNO_3$–$Cu(OH)_2$ by-product] when exposed to an atmosphere polluted with oxides of nitrogen. With an NO_2 concentration of 8 ppm and a relative humidity of 15%, corrosion can be appreciable and increases with relative humidity. It is also known [6] that positive-polarity d.c. arc at atmospheric pressure yields predominantly a hydrated proton $H^+(H_2O)n$ and some other species, like O^-, NO_2^-, O_3^-, O_3, NO_2^+ and NO^+. Combining with water, nitrogen dioxide forms highly corrosive acids that precipitate on the part, causing exposed Cu to corrode.

An attempt to remove the contaminant introduced during wire bonding on the auto-tool using DI water and IPA rinse was unsuccessful. All engineering efforts were then directed toward eliminating or minimizing the source of the contamination. A successful solution to the problem was the installation of a small vacuum tube next to the arc to evacuate by-products away from the part surface. The effectiveness of the vacuum was tested by placing the petri dish with DI water on the automated tool under the arc, performing 200 wire strips with vacuum on, and analyzing the water sample using IC chromatography. No ionic nitrite or nitrate was detected in the samples collected on the auto-tool with vacuum of 15 p.s.i. or higher. The parts wired

on the automated tool with vacuum on had no visible corrosion or droplets of nitric acid.

IC analysis proved to be an indispensable tool for subsequently monitoring the automated operation. Misalignment of the vacuum tube or vacuum pressure lower than 15 p.s.i. lead to insufficient evacuation of the corrosive species, which were easily detected by IC analyses.

REFERENCES

1 W. Wargotz, *Proceedings from the International Symposium on Contamination Control, Denver, CO*, 1988, pp. 51, 836.
2 E. Sasher, *IEEE Trans Electr. Insul.*, 18 (1983) p. 369.
3 M. Malejczyk, *Ph.D. Thesis*, University of Dortmund, Dortmund, 1987.
4 M. J. van Os, Nederlands Energy Research Foundation ECN, *Pat.* PB89-227706/XAD, 1988.
5 R. W. Bigelow, *Appl. Surf. Sci.*, 32 (1988) 122–140.
6 H. W. Mackinney, *Technical Report E1142, Des*, IBM Technical Bulletin, 1964.

Journal of Chromatography, 546 (1991) 351–367
Elsevier Science Publishers B.V., Amsterdam

CHROMSYMP. 2115

Ion chromatography for the analysis of household consumer products

DAVID MURAWSKI
Church & Dwight Co., Inc., 469 North Harrison Street, Princeton, NJ 08543-5297 (U.S.A.)

ABSTRACT

Ion chromatography (IC) is an indispensable tool for the analysis of household consumer products. Items such as baking soda, laundry detergent, dental care products, mouthwash, etc., can be analyzed quickly and accurately using chemically suppressed IC, single-column ion chromatography (SCIC) or a combination of the two technologies.

In USP baking soda, trace anions can be determined at ppm levels to ensure product quality and conformance to FDA regulations.

In dental care products, the determination and speciation of soluble fluoride compounds will be shown, as well as the determination of the tartar control agent, pyrophosphate. The non-chromophoric sweetener, sodium cyclamate, will be determined in foreign dental care products.

In liquid laundry detergents, chloride is added for viscosity control; silicate, mono-, di- and triethanolamines are added for buffering. Formate is present as an enzyme stabilizer. Citrate and laurate are added for hardness control.

These species can be determined effectively in SCIC systems, as well as chemically suppressed systems. For some applications, the use of traditional SCIC columns along with chemical suppression improves detectability and simplifies sample preparation. The MilliTrap-H^+ membrane cartridge will be evaluated as an aid to sample preparation.

INTRODUCTION

Ion chromatography (IC) has been found to be extremely useful for the analysis of household consumer products. Most of these products contain compounds amenable to IC analysis, whether active ingredients or impurities, the levels of which must be monitored. Church & Dwight, makers of Arm & Hammer brand products, manufactures a variety of consumer products. Analysis of these products is necessary to ensure product quality. Testing of competitive brands is necessary to keep current with emerging trends in the industry, as well as monitor products for patent infringement.

The matrices of these products are as diverse as the species to be determined. Matrices containing largely or solely bicarbonate or carbonate present a challenge to the ion chromatographer. Anion analyses of products with these matrices have traditionally been performed using chemically suppressed IC. Indeed, the rationale behind this is, in many cases, quite valid. At times, sample preparation is simplified due to a compatibility of the sample and eluent. Enhancement of the analyte signal allows for

0021-9673/91/$03.50

greater sensitivity permitting the analyst to sometimes dilute away matrix interference. This is not always necessary, however, since the severity of the bicarbonate/carbonate matrix interference in single-column ion chromatography (SCIC) or non-suppressed IC, is determined by eluent strength, analyte retention, analyte detectability, and the relative concentrations of analyte and bicarbonate–carbonate in the sample.

In some cases, examples will be given of separations performed using both the suppressed and non-suppressed modes of IC. This is to demonstrate the flexibility of IC and not to imply a superiority of one technique over the other.

Many illustrations will be shown using the Hamilton PRP-X100 column with a bicarbonate–carbonate eluent. Although previously shown to produce less than ideal chromatography for bromide and nitrate [1], other anions elute with good peak symmetry. The compatibility of this column with organic solvents is advantageous. With matrices containing a variety of organic compounds including surfactants, rinsing the column with methanol can aid in removing potentially fouling compounds and increase column lifetime.

Ion-pairing and ion-exclusion techniques will be shown as appropriate for larger organic ions and neutral compounds, respectively.

Finally, a separation of two similar compounds —one anionic, one neutral— will be shown on a low-capacity resin-based anion exchanger. This will illustrate a previously reported observation concerning the retention of compounds with a hydrophobic center on a resin-based anion exchanger [2].

INSTRUMENTATION

Several different systems were used in this work. Solvent delivery systems included: Perkin-Elmer Series 10 (Perkin-Elmer, Norwalk, CT, U.S.A.), Altex 110A (Beckman Instruments, San Ramon, CA, U.S.A.), and the Waters 501 (Waters Chromatography Division, Milford, MA, U.S.A.). Conductivity detectors used for SCIC systems were the Perkin-Elmer LC-21 or the Waters 431. For UV absorbance, the Waters 480 variable-wavelength detector was used. Data handling was done by the Spectra-Physics 4270 computing integrator (Spectra-Physics, San Jose, CA, U.S.A.). Where suppressed conductivity was necessary, the Dionex series 4000i (Dionex, Sunnyvale, CA, U.S.A.) was used with the Dionex anion micromembrane suppressor (AMMS).

Analytical columns used were the Hamilton (Reno, NV, U.S.A.) PRP-X100 (250 × 4.1 mm), Wescan (Deerfield, IL, U.S.A.) ion exclusion 269006 (300 × 7.8 mm), Wescan Anion/R guard cartridge 269030, Wescan Cation S (50 × 4.6 mm), Vydac (The Separations Group, Hesperia, CA, U.S.A.) 302IC4.6 (250 × 4.6 mm), Dionex AG4A (50 mm × 4 mm) and AS4A (250 × 4 mm), Supelco (Bellefonte, PA, U.S.A.) LC-8 (150 × 4.6 mm) and LC-CN (150 × 4.6 mm). The MilliTrap-H^+ cartridge (Waters) was also used.

All eluents, standard and sample solutions were prepared using water pretreated via distillation and reverse osmosis, then passed through a Milli-Q Plus (Millipore, Bedford, MA, U.S.A.) water-purification system.

CHLORIDE AND SULFATE IN SODIUM BICARBONATE

Sodium bicarbonate, $NaHCO_3$, or more commonly, baking soda, is one of the most widely used consumer products. For the product to meet USP specifications, it must meet strict requirements for purity. Additionally, trace levels of certain impurities must be determined, as mandated by the USP monograph [3]. Two impurities that must be measured are chloride and sulfate. The USP limit for each of these is 150 ppm as the anion.

This is a particularly difficult situation for the ion chromatographer. First, trace levels of ions are to be measured, requiring maximum sensitivity. Second, the entire matrix is a completely soluble inorganic salt, allowing for potential interferences and severe baseline disturbances. In this particular case, chemically suppressed conductivity is clearly indicated. Conveniently, the Dionex eluent for anion analysis is typically a bicarbonate–carbonate solution chosen for its ability to be chemically suppressed. This eluent closely matches the sample matrix, which will be partially suppressed as well, resulting in a relatively small solvent peak. This is necessary for determination of the early eluting chloride peak. This method is a modification of that for trace anions in sodium carbonate (soda ash). In the latter case, sample preparation consists of a 0.4% (w/v) solution in deionized water. For $NaHCO_3$, a specific amount of NaOH must be added to a 0.32% (w/v) solution to essentially titrate the bicarbonate solution to carbonate. This is necessary to prevent a baseline disturbance that would obscure the chloride peak. A 1*M* NaOH solution is prepared from a 50% (w/w) NaOH solution ("Baker Analyzed" Reagent, J. T. Baker, Phillipsburg, NJ, U.S.A.) and is used to titrate the $NaHCO_3$ sample solution. The levels of chloride and sulfate in the 50% (w/w) NaOH solution are typically less than 10 ppm and can also be determined by ion chromatography. After the addition of NaOH, the concentration of chloride and sulfate in $NaHCO_3$ can easily be determined (see Fig. 1). The method is simple and rapid; the run time is less than 10 min. The minimum detectable limits for chloride and sulfate in sodium bicarbonate are approximately 15 ppm and 30 ppm, respectively.

FLUORIDE AND MONOFLUOROPHOSPHATE IN DENTAL CARE PRODUCTS

Fluoride and monofluorophosphate are active ingredients in dental care products. They function as anti-caries agents. The concentration of fluoride in these products is generally around 1000 ppm.

For dental care products without sodium bicarbonate, many columns and eluents will permit the rapid determination of fluoride. The Hamilton PRP-X100 column was selected for its favorable retention of the fluoride anion. A rather unique eluent consisting of 1.75 m*M* HNO_3 and 1.3 m*M* $Mg(NO_3)_2$ was found to work well. The eluent utilizes nitrate as the driving ion. An eluent consisting solely of dilute HNO_3 (*ca.* 3 m*M*) can be used but the background conductivity is rather high, approximately 1000–1100 μS. The eluent strength is maintained while the conductivity is reduced by *ca.* 30% if $Mg(NO_3)_2$ is substituted in part for the HNO_3. This results in reduced baseline noise [4] and a faster return to baseline prior to fluoride elution. Sample preparation is minimal. A 2% (w/v) slurry of the product is made in deionized water, then filtered. An example of a typical commercial toothpaste analyzed in this way is shown in Fig. 2.

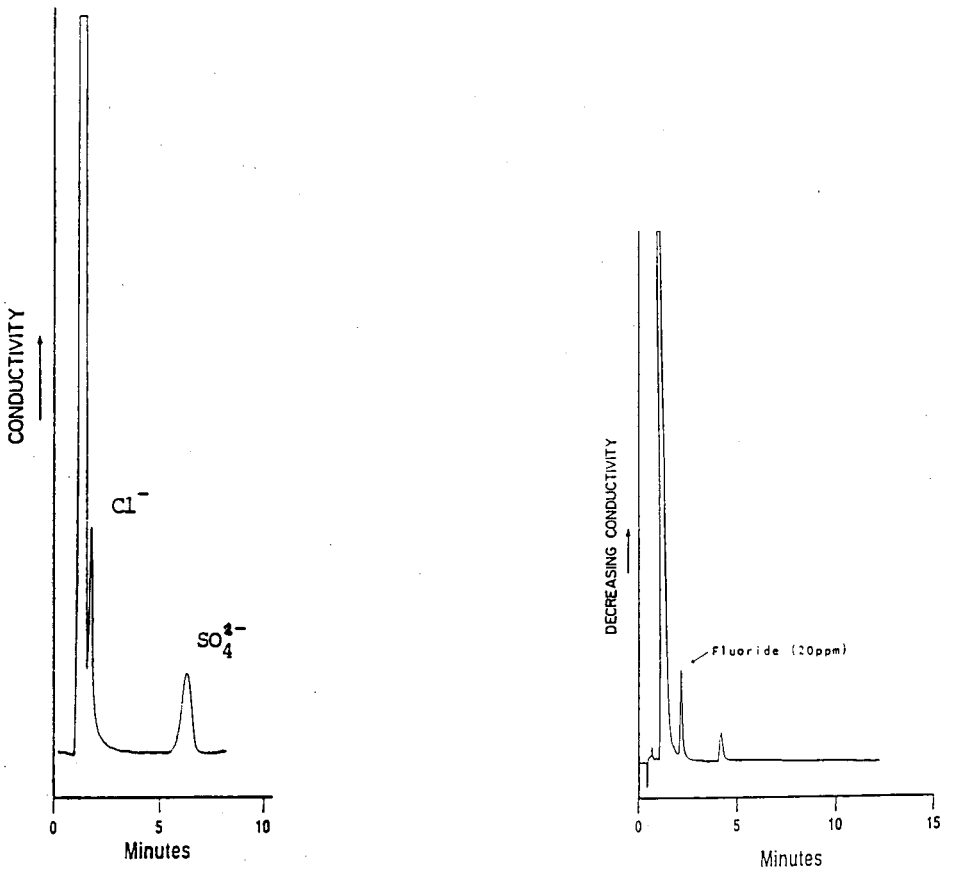

Fig. 1. Determination of trace levels of chloride and sulfate in sodium bicarbonate. Dionex AG4A/AS4A columns are used with a 0.75 m*M* $NaHCO_3$–2.2 m*M* Na_2CO_3 eluent. Flow is 2 ml/min. Range is 3 μS f.s. Regenerant is 6.25 m*M* H_2SO_4 at 3–4 ml/min.

Fig. 2. Fluoride in a commercially available toothpaste. PRP-X100 column is used with an eluent of 1.75 m*M* HNO_3 and 1.3 m*M* $Mg(NO_3)_2$. Flow is 2.5 ml/min. Indirect conductivity detection at 10 μS f.s. is used.

For bicarbonate-based dentifrices with fluoride as the active ingredient, sample preparation to remove the bicarbonate is necessary if SCIC is to be used. This is due to the weak retention of fluoride, the low level of fluoride (*ca.* 0.1%, w/w) in the product and the comparatively large amount of bicarbonate. Sample preparation consists of removing the bicarbonate from an aqueous solution of the product using a thoroughly washed sulfonic acid cation-exchange resin in the hydrogen form. Sample sodium ions are exchanged for resin hydrogen ions, reducing the pH of the solution. At pH 3–4 bicarbonate is removed via CO_2 elution. Helium sparging followed by sub-micron filtration removes essentially all of the bicarbonate from the solution. A chromatogram illustrating the determination of fluoride by the procedure is shown in Fig. 3.

Incomplete removal of bicarbonate results in severe early baseline disturbances and a very large system peak. This is the case when the MilliTrap-H^+ is the only form of sample pretreatment. Passing the sample solution through a MilliTrap-H^+ cartridge did not remove enough of the bicarbonate to allow for the determination of fluoride under the specified conditions. Due to the very weak eluent strength, essentially all of the bicarbonate must be removed from the sample solution for the baseline to appear as shown in Fig. 3.

Although excellent results can be obtained with the above procedure, sample preparation is slow and labor-intensive. An easier and more rapid alternative is to use the same column under conditions typical for anion analysis using chemical suppression. If the Hamilton PRP-X100 column is used with the Dionex series 40000i system, sample preparation is simplified and sensitivity is enhanced. Sample preparation consists of a 0.5% aqueous solution in plastic labware followed by sub-micron filtration, (see Fig. 4).

FLUORIDE/MONOFLUOROPHOSPHATE

Disodium monofluorophosphate (MFP) is used as the active anti-caries agent in many toothpastes. MFP can undergo hydrolysis, however, forming fluoride and

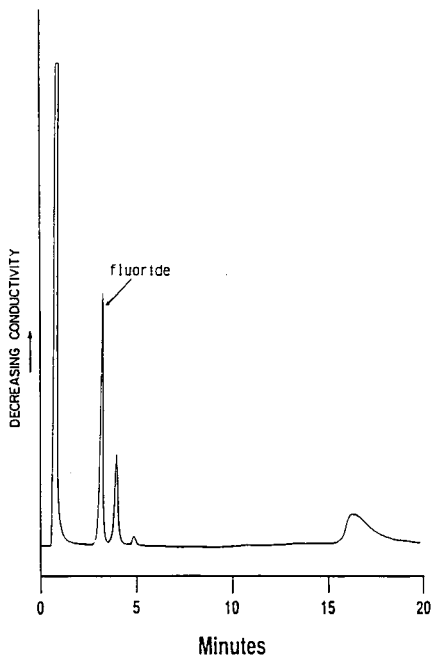

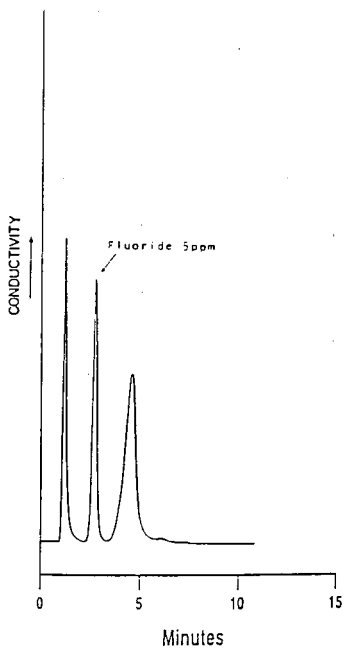

Fig. 3. Fluoride in a bicarbonate-based dentifrice using non-suppressed conductivity detection. PRP-X100 column is used with 3.5 m*M* NaOH–0.5 m*M* sodium benzoate eluent. Flow is 2.5 ml/min. Indirect conductivity detection at 10 μS f.s. is used.

Fig. 4. Fluoride in a bicarbonate-based dentifrice using suppressed conductivity detection. PRP-X100 column is used with a 2.2 m*M* Na_2CO_3–0.75 m*M* $NaHCO_3$ eluent. Flow is 2 ml/min. Range is 10 μS f.s. Regenerant is 6.25 m*M* H_2SO_4 at 3–4 ml/min.

orthophosphate. Once hydrolyzed, the fluoride can react with other ingredients in the sample, such as calcium, thereby rendering it insoluble or "inactive". Therapeutically, there is a minimum level of fluoride a dentifrice may contain below which it is not considered clinically effective. With products containing MFP, it is important to measure the soluble fluoride species to determine the active fluoride level. Although other methods have been previously described [5–7], a new method is now illustrated.

An SCIC system with an HNO_3 eluent with additional NO_3^- driving ion, separates fluoride, orthophosphate and monofluorophosphate. A low pH is necessary to determine MFP as a monovalent ion. Under basic conditions, MFP is divalent and too strongly retained to be determined with the weakly retained fluoride. Sample preparation is designed to keep the extractant/sample ratio as low as practically possible to mimic the actual process a consumer would use while brushing. An example of the chromatography is given in Fig. 5.

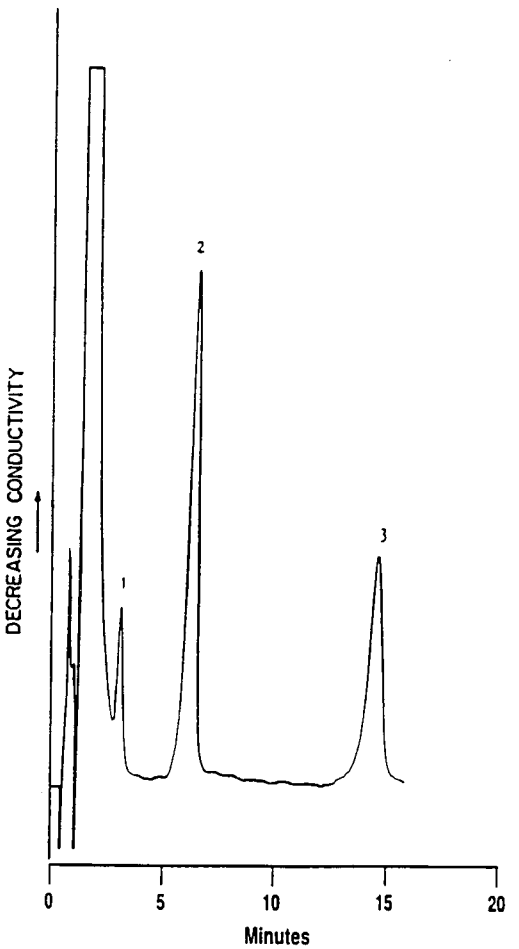

Fig. 5. Fluoride and monofluorophosphate in toothpaste. Sample preparation is 2 g sample with 10 ml water ; mix vigorously for 1–2 min; centrifuge; dilute 2.0 ml to 20 ml; filter through 0.45-μm filter. Conditions as in Fig. 2. Peaks: 1 = fluoride; 2 = orthophosphate; 3 = monofluorophosphate.

PYROPHOSPHATE IN TARTAR CONTROL DENTIFRICES

Pyrophosphate is an excellent hard surface cleaner. The sodium and potassium salts of pyrophosphate are used in a variety of products, such as multipurpose cleaners and automatic dishwasher detergents. In toothpaste, pyrophosphate functions as a tartar control agent.

Since multivalent phosphate species require strong eluents to elute them in a reasonable time, conductivity detectors are not always useful due to the high eluent conductivity [8,9]. For some phosphate species, conductivity detection can be used if the level of the phosphate to be determined is sufficiently large. For our purposes, the simplest system seemed to work adequately. To lower the valency of the pyrophosphate [10], an acidic mobile phase is used, 0.03 *M* HNO_3. With an enormously high conductivity of over 7000 μS, this eluent would seem inappropriate for SCIC. However, because inverse conductivity is used and the level of pyrophosphate in the sample is high enough, excellent results can be obtained without the need for a post column reaction. Fig. 6 illustrates the determination of pyrophosphate in a commer-

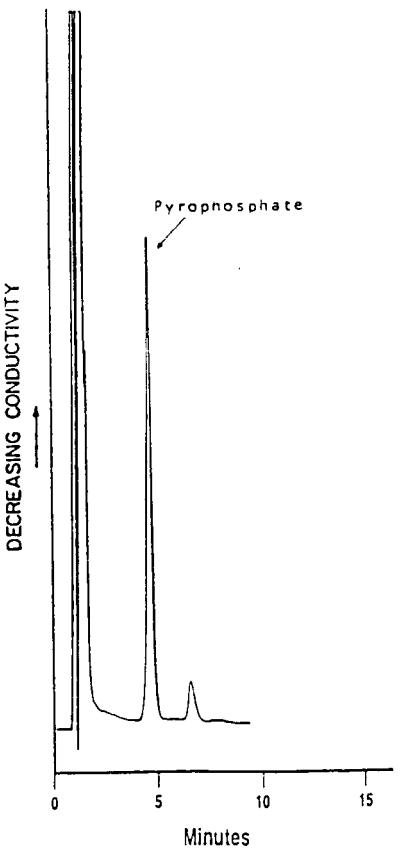

Fig. 6. Pyrophosphate in tartar control toothpaste. PRP-X100 column is used with 0.03 *M* HNO_3 eluent. Flow is 2 ml/min. Indirect conductivity detection is used at 100 μS f.s. Sample is 3% (w/v) solution of toothpaste through 0.45-μm filter.

cially available toothpaste. Sample preparation is simple and the run time is under 10 min.

This scheme will work for tartar control dentifrices containing bicarbonate as well. The sample solution must be slightly less concentrated, approximately 1.0–1.5% (w/v) solution, to minimize the effect of the bicarbonate. Unless additional sensitivity is required, sample pretreatment to completely remove the bicarbonate is not necessary due to the strength of the eluent and the strong retention of the pyrophosphate. If increased sensitivity is a requirement, a more concentrated solution of a bicarbonate-based dentifrice can be prepared and passed through a MilliTrap-H^+ cartridge prior to injection. This is contrary to the determination of fluoride, which necessitated the complete removal of bicarbonate due to the weakness of the fluoride retention and the corresponding eluent strength necessary to determine the weakly retained species.

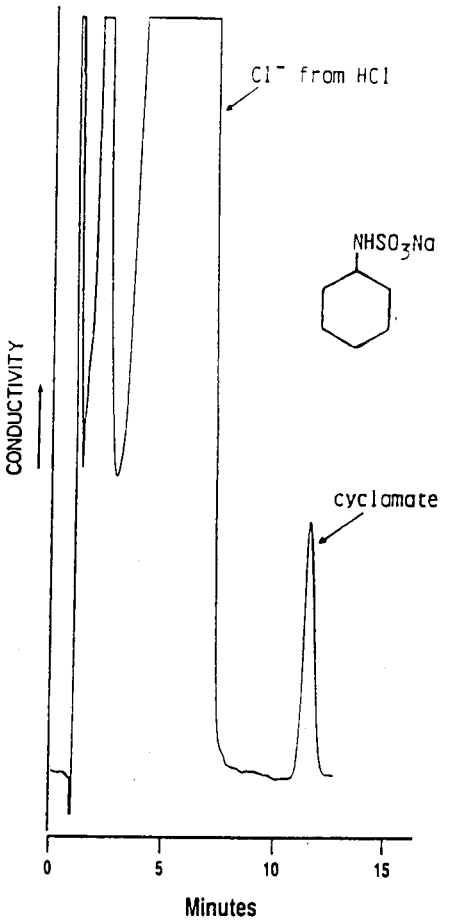

Fig. 7. Cyclamate in dentifrice manufactured in Canada. Vydac 302IC4.6 column with 5 m*M* phthalic acid–methanol (90:10) eluent. Flow is 2 ml/min with direct conductivity detection at 10 μS f.s.

CYCLAMATE IN CANADIAN DENTAL CARE PRODUCTS

Sodium cyclamate is widely used as a sweetener in dentifrices sold in Canada. Unlike its chromophoric counterparts, sodium saccharin and aspartame, it has no appreciable UV absorbance. Being anionic, a sodium salt of a sulfamic acid, it is amenable to ion chromatography and detectable using a conductivity detector. A silica-based anion exchanger, a Vydac 302IC4.6, is used with a phthalic acid–methanol mobile phase. For most products, sample preparation is simply a 1% (w/v) aqueous slurry, filtering any insolubles prior to injection. For bicarbonate-based products, additional sample preparation is necessary. In this particular case, lowering the pH to 2–3 with a minimum amount of 6 *M* HCl proved to be rapid and effective. Though this works well for cyclamate, it will not work for weakly retained anions. Adding an acid to reduce pH inevitably adds a huge amount of the acid anion, in this case, chloride. Most often this will obscure the analyte peak. Cyclamate is strongly retained in this system and the chloride peak, though extremely large, returns to baseline well before the elution of the analyte (see Fig. 7). If HNO_3 or H_2SO_4 were used instead of HCl, the cyclamate peak would be obscured due to the stronger retention and subsequent later elution of nitrate and sulfate.

LAUNDRY DETERGENTS

Ethanolamines are added to liquid laundry detergents as buffering agents. They can be determined by gas chromatography or IC, each method having its own advantages and disadvantages. For our purposes, it was found that ethanolamines can be determined under conditions typical for monovalent cation analysis using the Wescan Cation S column and inverse conductivity detection. Additionally, an entire monovalent cation profile is obtained, giving valuable information as to product formulation. Figs. 8 and 9 illustrate the differences in product composition between competitive brands of liquid laundry detergent. A mixture of ethanolamines was apparently used in the product shown in Fig. 8. Triethanolamine (TEA) is the predominant species, although small amounts of diethanolamine (DEA) and monoethanolamine (MEA) can be detected. The product illustrated in Fig. 9 contains only MEA. Potassium in the formulation can be determined as well. Its presence is due to the use of potassium citrate as a sequestrant.

SILICATE/FORMATE IN LIQUID LAUNDRY DETERGENTS

Silicate is also used as a buffering agent in liquid laundry detergents. Formate is used as an enzyme stabilizer. Both can be determined under similar conditions using a sodium hydroxide–sodium benzoate eluent with the Hamilton PRP-X100 column. Figs. 10 and 11 illustrate the determination of silicate and formate, respectively, in liquid laundry detergents. In each case, sample preparation is simple, requiring only a 0.5% (w/v) dilution in deionized water followed by filtration.

CITRATE IN LAUNDRY DETERGENTS

Citrate is used as a sequestrant in both powdered and liquid laundry detergents.

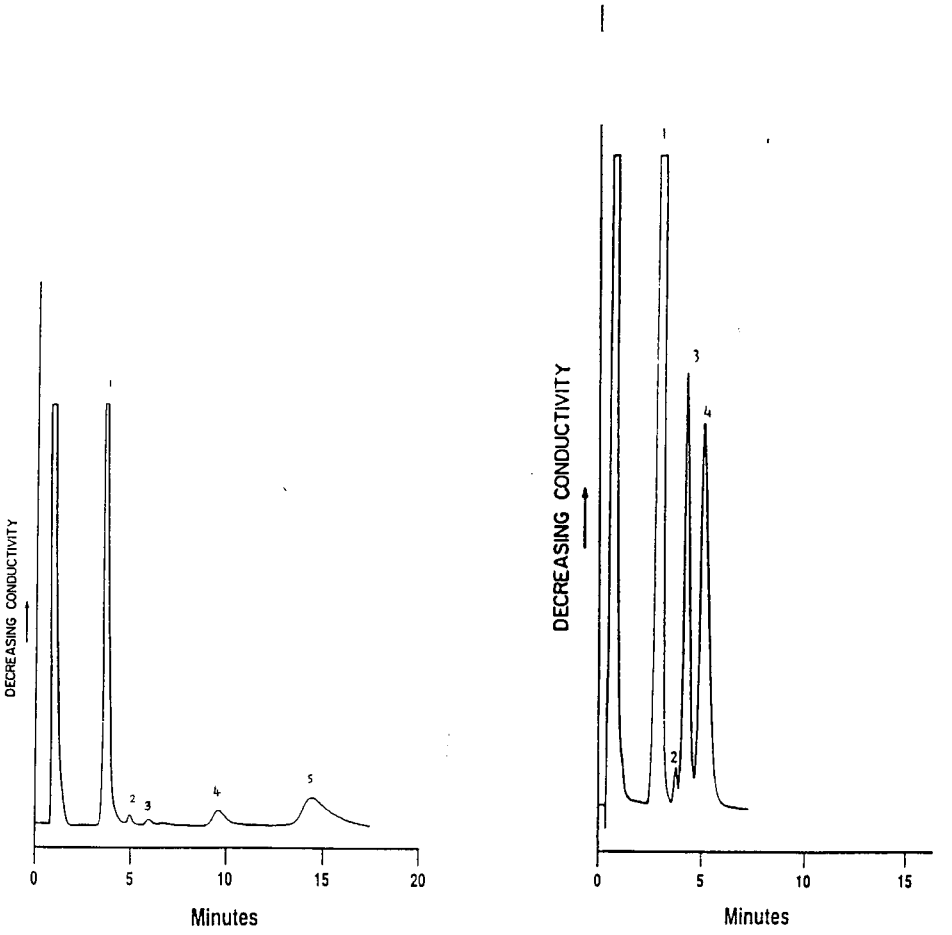

Fig. 8. Ethanolamines in liquid laundry detergent. Wescan Cation S column is used with 3 mM HNO_3 eluent. Flow is 1.5 ml/min. Indirect conductivity detection at 10 μS f.s. is used. Sample is 0.1% (w/v) solution. Peaks: 1 = Na^+; 2 = NH_4^+; 3 = MEA; 4 = DEA; 5 = TEA.

Fig. 9. Ethanolamines in liquid laundry detergent. Conditions as in Fig. 8. Peaks: 1 = Na^+; 2 = NH_4^+; 3 = K^+; 4 = MEA.

It can be determined by many methods including ion exclusion and ion exchange. Of the methods we have evaluated, the following has the distinct benefits of easy sample preparation, good resolution and excellent sensitivity [11]. Fig. 12 illustrates the determination of citrate in powdered laundry detergent using the Vydac 302IC4.6 anion column. A phosphate buffer is used as eluent along with UV detection at 220 nm.

SODIUM LAURATE IN LIQUID LAUNDRY DETERGENTS

Sodium laurate, $C_{12}H_{23}O_2Na$, is a relatively large organic anion added to a brand of liquid laundry detergent as a hardness control agent. It can be determined by

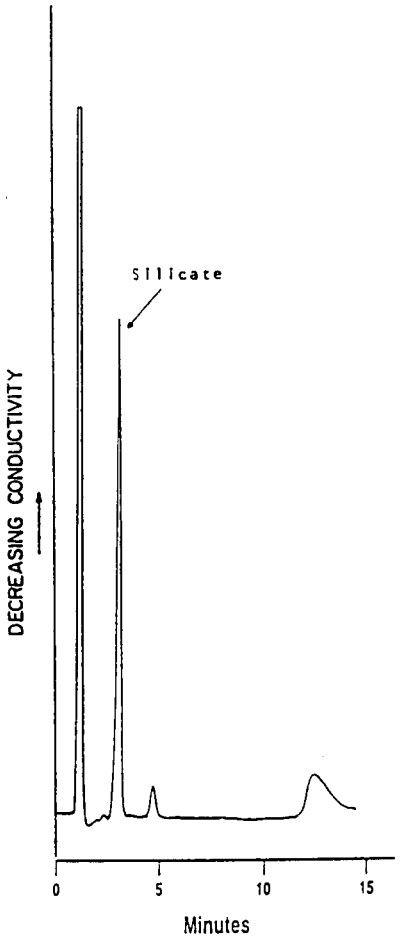

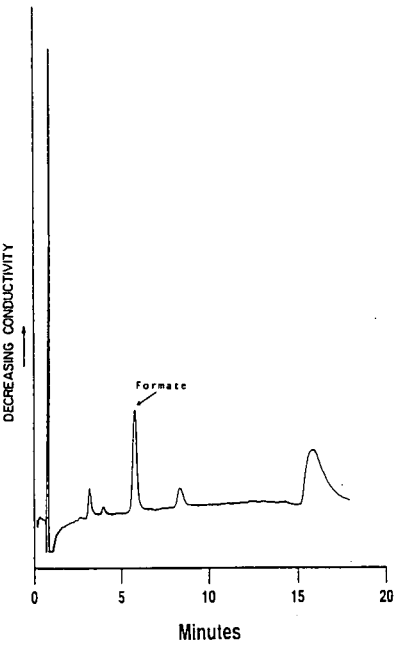

Fig. 10. Silicate in liquid laundry detergent. PRP-X100 column is used with 3.5 m*M* NaOH–0.5 m*M* sodium benzoate eluent. Flow is 2 ml/min with indirect conductivity detection at 10 μS f.s.

Fig. 11. Formate in liquid laundry detergent. Conditions as in Fig. 10.

gas chromatography as well as liquid chromatography. Gas chromatography requires more sample handling, however, as the sodium salt must first be converted to the fatty acid prior to analysis. Attempts at determining sodium laurate on a low-capacity anion exchanger were unsuccessful. Due to its hydrophobic character and low charge to size ratio, reversed-phase ion pairing was chosen. A Supelco LC-C8 reversed-phase column was used along with an eluent of methanol and water. Ammonium acetate was used as the ion pairing agent. Conductivity detection was used due to the lack of UV absorbance of the laurate. Fig. 13 illustrates this procedure.

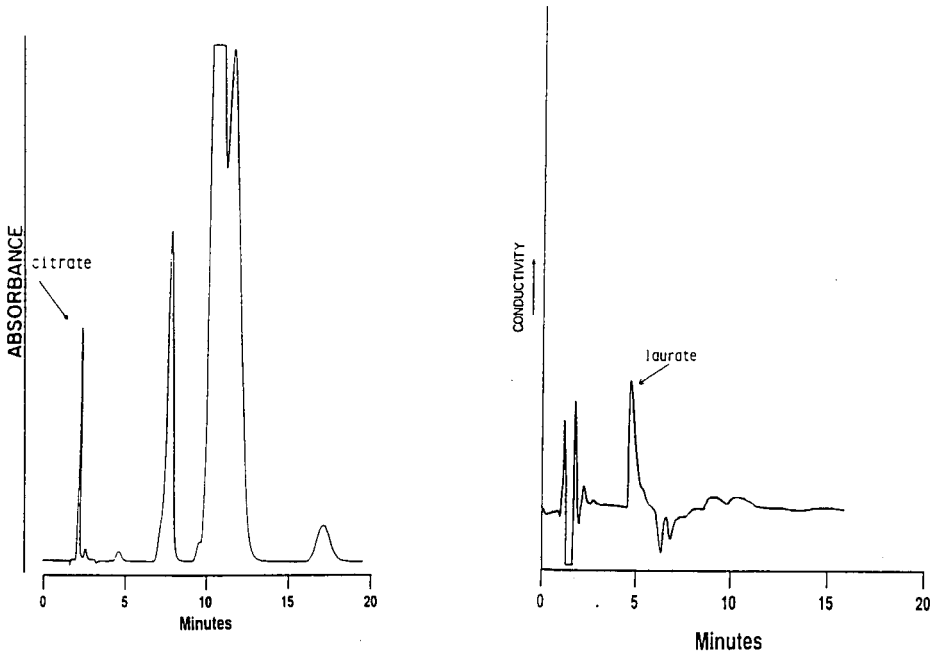

Fig. 12. Citrate in laundry detergent. Vydac 302IC4.6 column is used with 0.1 *M* KH_2PO_4–acetonitrile (90:10), pH 3.2 at 2 ml/min. UV detection at 220 nm is used. Sample is 1% (w/v) solution.

Fig. 13. Sodium laurate in liquid laundry detergent. A Supelco LC-C8 column is used with methanol–water (60:40) and 0.01% ammonium acetate eluent at 1 ml/min. Conductivity detection at 10 μS f.s. is used. Sample is 0.1% (w/v) solution.

ETHANOL AND GLYCERINE IN MOUTHWASH

Both ethanol and glycerine are major ingredients in almost all of the leading brands of mouthwash. Both can be determined by gas chromatography using a suitable thermal gradient. Ion-exclusion chromatography is another alternative, if an anion-exchange precolumn is added in-line immediately prior to the ion-exclusion column. This is done to eliminate an unknown matrix interference found in the mouthwash samples. Without this precolumn, a substantial negative peak appears close to the retention time of glycerine. Quantitative determination is not possible with this interference. The anion precolumn removes this interference.

As discussed earlier, dilute HNO_3 eluents can be useful in determining certain anions with the Hamilton PRP-X100 column. Since the Wescan Anion/R guard column has the same basic chemistry as the PRP-X100, being a resin-based anion exchanger, it was thought that a different retention mechanism in addition to ion exclusion may alter the retention time of these interfering components. Such was found to be the case as these compounds are apparently strongly bound or completely adsorbed by the precolumn. An illustration of the separation is found in Fig. 14.

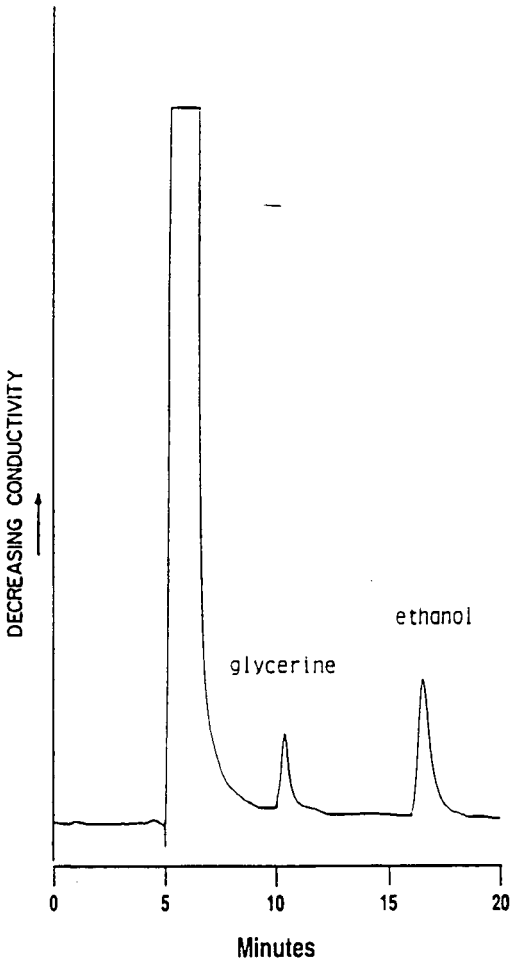

Fig. 14. Glycerine and ethanol in mouthwash using ion-exclusion chromatography. Wescan anion exclusion column No. 269006 with Anion/R Guard precolumn with 4 mM HNO_3 eluent at 0.75 ml/min. Indirect conductivity detection at 10 μS f.s. is used. Sample is 5% (w/v) solution.

CETYLPYRIDINIUM CHLORIDE IN MOUTHWASH

Cetylpyridinium chloride (CPC) is an antibacterial agent added to mouthwash at approximately 0.05%. It is a large organic cation, as shown in Fig. 15. Though opposite in charge, it is similar to sodium laurate in that the charge to molecular size ratio is small, and the large alkyl group adds significant hydrophobic character. Attempts at determining this species using a low capacity cation exchanger were unsuccessful. Instead, an ion-pairing reversed-phase separation was found to work extremely well [12]. Retention of CPC using a C_{18} or C_8 column was found to be too great for short run times even when a large percentage of organic modifier was used in the eluent. A less hydrophobic column, a cyano column was used (Supelco LC-CN,

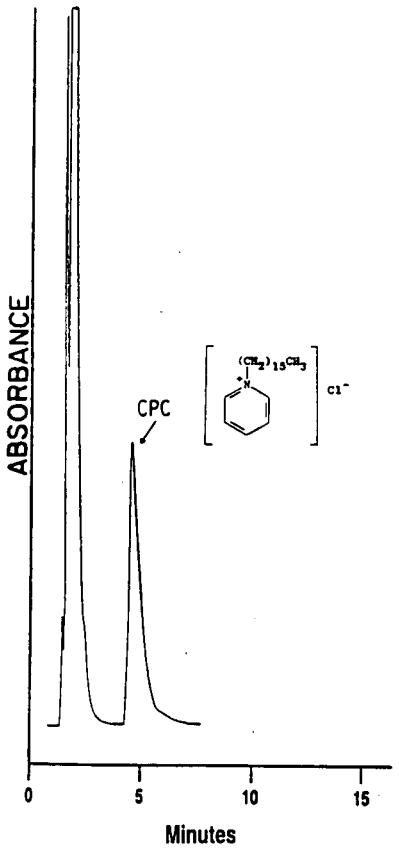

Fig. 15. Cetylpyridinium chloride in mouthwash. Supelco LC-CN column with methanol–water (90:10) and 0.065 *M* acetate (pH 6) is used at 1 ml/min. UV detection at 254 nm is used.

150 × 4.6 mm). This column still required the use of 90% methanol for short analysis time. Sample preparation is simple, a 10% (w/v) solution in methanol–water (90:10). Sensitivity is excellent due to the strong UV absorbance of the CPC cation. Accuracy is more than adequate. Some products contain CPC at 500 ppm, others at 450 ppm. With this method one can quickly and easily distinguish between the two.

NICOTINIC ACID AND NIACINAMIDE

Both nicotinic acid and niacinamide are B complex vitamins. They are used as enriching agents in flour and rice, as nutritional supplements and are even found in at least one commercially available shampoo.

Both have been determined by high-peformance liquid chromatography, although resolution between the two peaks is sometimes difficult to attain and both species respond similarly to changes in organic modifier concentration in the mobile phase. Nicotinic acid can be determined using ion chromatography under a variety of conditions. If niacinamide is present, hydrolysis to nicotinic acid is accomplished

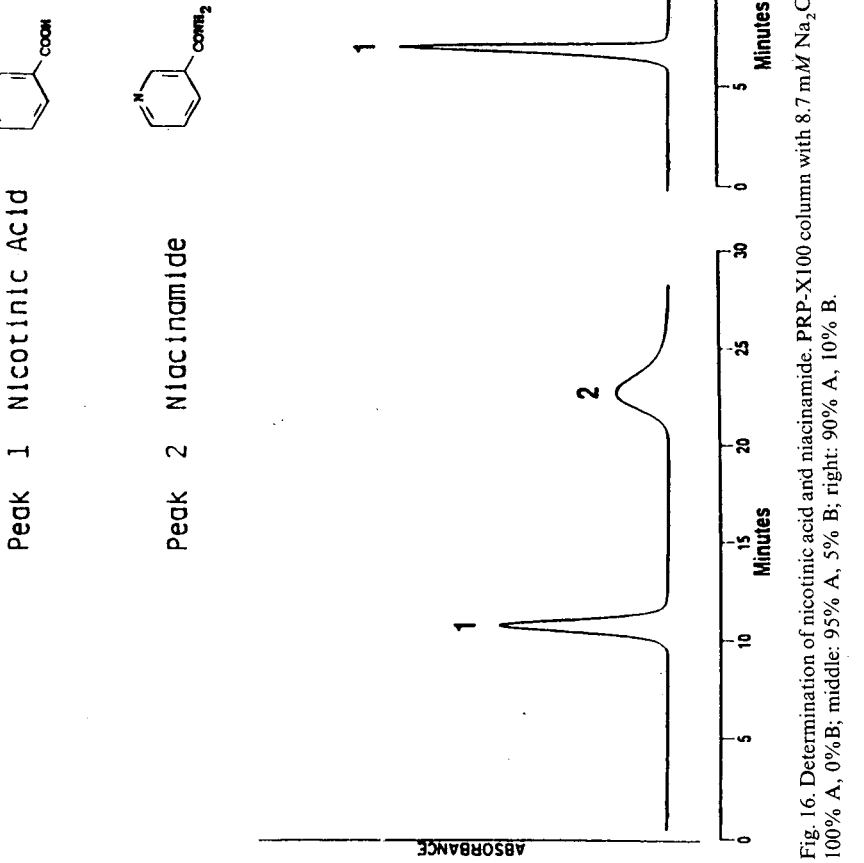

Fig. 16. Determination of nicotinic acid and niacinamide. PRP-X100 column with 8.7 m*M* Na_2CO_3–2.7 m*M* $NaHCO_3$ (eluent A) and methanol (eluent B). Left: 100% A, 0%B; middle: 95% A, 5% B; right: 90% A, 10% B.

using HCl and heat. For our determination, a Hamilton PRP-X100 column was used along with a bicarbonate–carbonate eluent typically used with chemically suppressed detection. Background eluent suppression was unnecessary, however, since UV detection at 263 nm was used.

Upon trying to determine conditions for the complete hydrolysis of the amide to the acid, two peaks were observed in the chromatogram: the first at 10 min, the second at 22 min. The first was easily identified as nicotinic acid using a standard solution. As more severe hydrolysis conditions were used, the nicotinic acid peak grew larger, the second peak smaller. Injection of a niacinamide standard revealed the second peak to be, in fact, niacinamide. The novelty of this separation lies in the fact that under the specified conditions, nicotinic acid is an anion, whereas niacinamide is a neutral species. It was thought that the retention of the amide was due to a hydrophobic interaction with the polymeric support of the column. This was later confirmed by adding an organic modifier (methanol) to the eluent. The addition of 10% methanol to the mobile phase resulted in a threefold decrease in the retention time of niacinamide. At the same time, a similar though less dramatic decrease in retention was observed for the nicotinic acid peak. The retention time of the acid was halved with the addition of 10% methanol to the eluent. Fig. 16 illustrates the effect of the methanol addition to the mobile phase.

A dual mechanism of ion exchange and adsorption is apparently responsible for the retention of the nicotinic acid. This has been observed previously with other organic acids under similar conditions [13]. Organic acids that have a hydrophobic center will exhibit retention due to adsorption with the polymeric support of the column [2]. The retention mechanism of the niacinamide is apparently solely due to adsorption. This method gives the chromatographer a great deal of control in the separation of these two species. Since UV detection is used, it is as sensitive as other high-performance liquid chromatography techniques using the same detection mode, yet affords the analyst great flexibility as to how the final chromatogram will appear.

CONCLUSIONS

Ion chromatography is an extremely useful and flexible tool for the analysis of household consumer products. Many species can be determined in very diverse sample matrices using IC, reversed-phase ion-pairing or ion-exclusion chromatography (IEC). Matrices containing bicarbonate or carbonate pose an additional challenge to the analyst. These products can generally be analyzed using: (1) chemically suppressed IC, (2) sample pretreatment with ion-exchange resin, MilliTrap-H^+, or acidification, (3) an appropriate dilution of the sample if strongly retained analytes of sufficient detectability are to be determined.

The Hamilton PRP-X100 column with a bicarbonate–carbonate eluent provides some interesting separations, including the separation of a neutral species due to a hydrophobic interaction of that compound with the polymeric support of the column.

ACKNOWLEDGEMENT

The author wishes to thank Laura Doskoczynski for her valuable contributions to the development of the method for nicotinic acid and niacinamide.

REFERENCES

1 D. T. Gjerde, in P. Jandik and R. M. Cassidy (Editors), *Advances in Ion Chromatography*, Vol. 2, Century International, Franklin, MA, 1990, p. 171.
2 F. F. Cantwell and S. Puon, *Anal. Chem.*, 51 (1979) 623.
3 *U.S. Pharmacopeia (USP) XXII*, United States Pharmacopeial Convention, Rockville, MD, 1990, p. 1252.
4 H. Small, *Ion Chromatography*, Plenum Press, New York, 1989, p. 139.
5 J. J. Potter, A. E. Hilliker and G. J. Breen, *J. Chromatogr.*, 367 (1986) 423.
6 S. S. Chen, H. Lulla, F. J. Sena and V. Reynoso, *J. Chromatogr. Sci.*, 23 (1985) 355.
7 J. S. Fritz, D. L. DuVal, L. Dean and R. E. Barron, *Anal. Chem.*, 56 (1984) 1177.
8 A. W. Fitchett and A. Woodruff, *LC Mag.*, 1 (1983) 48.
9 T. L. Chester, C. A. Smith and S. Culshaw, *J. Chromatogr.*, 287 (1984) 447.
10 H. Small, *Ion Chromatography*, Plenum Press, New York, 1989, p. 226.
11 D. R. Jenke, *Anal. Chem.*, 56 (1984) 2468.
12 R. C. Meyer and L. T. Takahashi, *J. Chromatogr.*, 280 (1983) 159.
13 T. A. Walker, T. V. Ho and N. Akbari, in P. Jandik and R. M. Cassidy (Editors), *Advances in Ion Chromatography*, Vol. 2, Century International, Franklin, MA, 1990, p. 271.

Journal of Chromatography, 546 (1991) 369–380
Elsevier Science Publishers B.V., Amsterdam

CHROMSYMP. 2238

Ion chromatography in the manufacture of multilayer circuit boards

ROBERT E. SMITH
Allied-Signal Inc., Kansas City Division[a], *Department 838/SC-3, P.O. Box 419159, Kansas City, MO 64141 (U.S.A.)*

ABSTRACT

Ion chromatography (IC) has proven useful in analyzing chemical solutions used in the manufacture of multilayer circuit boards. The manufacturing process is described briefly and previously published IC methods are reviewed. Then, methods are described for determining chlorate and chlorite in a brown oxide solution; salicylic acid in an epoxy cure agent; formate, sulfate and tartrate in an electroless copper bath; anionic detergents in a tin–lead brightener and in a cleaning solution; and aqueous photoresist and non-ionic brightener in a tin–lead bath. Anion exchange, reversed-phase high-performance liquid chromatography on a poly(styrene–divinylbenzene) column and two-dimensional liquid chromatography are described. Chemically suppressed conductivity and photometric detection are used.

INTRODUCTION

Manufacturing process

Multilayer printed wiring boards are manufactured in a multi-step procedure. One starting material is usually a polyimide/glass covered with a copper foil. This is treated with a brown oxide solution, which contains sodium hydroxide and sodium chlorite, which can be converted to sodium chlorate in time. When making rigid circuit boards, the other starting materials are an epoxy pre-polymer, which usually consists mostly of the diglycidyl ether of bisphenol A (DGEBA) and a cure agent consisting of a tetraethyl methylene dianiline plus about 1% salicylic acid. After polymerization, the copper foil is laminated onto the epoxy, which is put on a polyimide-based flexible cable, which is put onto another layer of epoxy/copper foil/polyimide/glass. This pattern is repeated until the desired number of layers are obtained.

Next, holes are drilled in the laminate and the surface is cleaned and prepared for copper plating. If an epoxy laminate is used, the process starts with a chromic acid etchback. The surface is then lightly roughened by wet-blasting. Next, the conductive copper layer is electrodeposited. Initially, 20 microinches are deposited using an electroless copper bath which contains a strong reducing agent, formaldehyde. After

[a] Prepared for the United States Department of Energy by Allied-Signal Inc., Kansas City Division, under contract number DE-AC04-76-DP00613.

0021-9673/91/$03.50

applying this copper strike, a 0.001-in. layer of ductile copper is electrodeposited using an acid copper tank.

Next, photoimaging is performed. A negative photoresist is added and a photographic image of the desired circuitry is applied. Exposure to UV light induces the production of a reactive nitrene which cross-links the three components of the resist to form a polymer. The areas of the circuit boards which were not exposed to light are soluble in aqueous sodium carbonate developing solution, and is so removed. The photochemically reacted photoresist now covers selected regions of the copper conductor.

The exposed, undesired copper is removed in an acid etch, exposing the epoxy, which acts as a dielectric. The cross-linked photoresist is then removed using an aqueous sodium hydroxide stripping solution, leaving the desired bare copper circuitry on an epoxy substrate. When panel plating, the finished board is dipped into molten solder, then a hot air leveler is used to evenly distribute the solder. When pattern plating, a tin–lead bath is used. In either case, there is a solderable alloy to which other devices can be attached.

Solution analysis

Ion chromatography has been used to monitor the concentrations of anions in many of the tanks used in the manufacturing process. Chromic acid was analyzed for chloride and sulfate [1], water rinses for chloride and sulfate, alkaline cleaners for chloride, phosphate and sulfate [2], ammonium bifluoride–HCl etchback tanks for fluoride and chloride and electrolytic acid copper for trace chloride [3].

The anion-exchange columns used are made of surface sulfonated poly(styrene–divinylbenzene), or PS–DVB, to which aminated latex beads have been attached. This polymeric core is resistant to extremes of pH, enabling the analysis of corrosive baths. Fluoride, chloride and sulfate have been separated on older columns such as the AS-1, AS-3 and AS-4 (Dionex, Sunnyvale, CA, U.S.A.). The more efficient columns, AS-4A and AS-5A, are now available and can be used for these separations. To minimize analysis time, there is even a fast run anion separator (for samples with few anions), but to obtain maximum column efficiency, the AS-5A can be used. Chromate, though, is strongly retained on the AS-1, AS-3, AS-4 and AS-5A columns. In the original report, the AS-5 column was recommended because it has a lower selectivity coefficient for chromate, which can be eluted using the standard 3 m*M* sodium bicarbonate plus 2.4 m*M* sodium carbonate eluent [1]. Since the publication of this report, the AS-4A column became available, and chromate can be eluted from it also. When analyzing a plating bath (or any other sample) for a trace anion in the presence of another anion (such as ppm levels of chloride in chromic acid etchback bath), it is important to prepare the standards in the same matrix as exists in the sample [1]. It is important also to use a PS–DVB-based column because it is resistant to damage by low (or high) pH and by corrosive samples such as chromic acid, which can partly hydrolyze silica-based columns.

In addition, mobile phase ion chromatography (MPIC) can be used to monitor the non-ionic organic brightener content in plating baths [4]. Using automated procedures, applied labor can be minimized and sample throughput maximized.

Transition metals

The concentration of the major metal in a bath (copper or tin and lead) can be determined using a cation-exchange column and an eluent containing a mild chelating agent such as oxalate or citrate, followed by post-column reaction and visible detection [5–7]. The metals are converted to a chromophore by post-column reaction with 4-(2-pyridylazo)resorcinol (PAR). In the original reports, the CS-2 cation-exchange column was used, and the technique was capable of separating and detecting ppm levels of divalent copper, lead, cadmium, cobalt, zinc and nickel; it could also differentiate between ferrous and ferric ions [5,6]. Since then, a more efficient cation-exchange column, the CS-5, has become available. This, together with advances in post-column reaction, has enabled the determination of stannous and stannic ions in samples including the tin–lead alloy bath [7]. In addition, low ppm levels of zinc and nickel were determined in acid copper baths [5]. Thus, the transition metals can be routinely determined.

EXPERIMENTAL

Chromatograms were obtained with an automated Dionex Model 4000 ion chromatograph equipped with a Hewlett-Packard 9000 computer and AI-300 software from Dionex. Chemically suppressed conductivity detection was accomplished using an anion micromembrane suppressor (AMMS-II) which was continuously regenerated with 0.0125 *M* sulfuric acid.

Salicylic acid was determined in the amine cure agent by dissolving about 0.5 g of the sample in 25 ml of methylene chloride, then extracting this with 40 ml of 17 m*M* 4-cyanophenolate, pH 9.1. The aqueous extract was transferred to a 50-ml volumetric flask, then diluted to mark. The 50-ml sample was diluted 1/10 with 17 m*M* 4-cyanophenolate, pH 9.1, then injected on an AG-4A plus AS-4A column pre-equilibrated with the same 17 m*M* 4-cyanophenolate, pH 9.1, flowing at 1.6 ml/min. Detection was accomplished by chemically suppressed conductivity using an AMMS-II. Quantitation was done by injecting five different standards of salicylic acid, also dissolved in the eluent, integrating peak areas, then plotting areas *vs.* concentration. Data were fitted to a straight line using linear regression analysis (correlation coefficient was at least 0.999). Peak areas of samples were substituted into the straight line equation to obtain sample concentrations.

Chlorite and chlorate in brown oxide were determined by diluting the sample 1:1000, then injecting it on an AG-4A plus AS-4A pre-equilibrated with 1.9 m*M* sodium carbonate plus 1.5 m*M* sodium carbonate at 2.0 ml/min. Detection and quantitation were performed as in salicylic acid determination, except that standards contained chlorite plus chlorate and calibration lines were calculated for both.

Formate, sulfate and tartrate were determined in electroless copper by diluting the sample 1/1000 then injecting it onto an AG-4A plus AS-4A pre-equilibrated with 2.4 m*M* sodium bicarbonate plus 1.9 m*M* sodium carbonate flowing at 2.0 ml/min. Detection and quantitation were performed as described above, except that standards contained formate, sulfate and tartrate and three calibration lines were calculated.

Aqueous photoresist was determined in a tin–lead bath by diluting the sample 10:25 and injecting it onto a PS–DVB-based MPIC 5 μm column pre-equilibrated with acetonitrile–water (9:1, v/v) at 1.0 ml/min. A Model 1040M diode array detector

(Hewlett-Packard, Kansas City, MO, U.S.A.) had one channel set at 252 nm. The area of the photoresist peak observed was compared to that of photoresist standards (linear regression analysis) to obtain concentrations in tin–lead baths.

Brightener in a tin–lead bath was determined by injecting a 10:25 diluted sample onto a MPIC 5 μm column pre-equilibrated with 77 m*M* NaOH in methanol–water (2:8) at 1.0 ml/min. Chemically suppressed conductivity detection was used.

Retention of ethano-, propano-, butano-, pentano- and hexanophenones on an MPIC 5 μm, PAX-500 and an octadecylsilica (ODS) column was measured using different proportions of acetonitrile in water at 1.0 ml/min. Diode array detection at 246 nm was used. The capacity factor, k', was calculated as follows [8]:

$$k' = (V_r - V_0) / V_0 \quad (1)$$

where V_r is the retention volume of the alkylphenone and V_0 is the column void volume.

Detergent-containing cleaner used to prepare printed wiring boards for copper plating was analyzed by diluting the sample 2:1000 into 0.96 *M* sodium hydroxide in acetonitrile–water (18:82, v/v) and injecting it onto a PAX-100 column pre-equilibrated with the same 0.96 *M* sodium hydroxide in acetonitrile–water (18:82, v/v). Diode array detection at 227 nm was used.

RESULTS AND DISCUSSION

The amine cure agent used to react with DGEBA-containing epoxy must contain the proper amount of salicylic acid to enable proper reaction kinetics. The salicylic acid is ionized at pH 9.1, so it is selectively extracted into the aqueous solution containing 4-cyanophenolate. Salicylate elutes at 2.69 min, as shown in Fig. 1. Any tetraethyl methylene dianiline extracted into the aqueous phase is removed by the suppressor and is not detected. In a single blind experiment, seven samples were submitted for analysis, and the results (Table I) showed an average percent error of 3.99%. This was calculated by first computing the percent difference (or error) between the observed and expected values. The absolute values of the percent differences for each sample were added together, then divided by seven to get the average percent error.

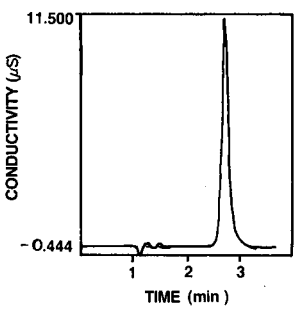

Fig. 1. Salicylic acid determination. Column: AG-4A plus AS-4A. Eluent: 17 m*M* 4-cyanophenol, pH 9.1, 1.6 ml/min. Detection: chemically suppressed conductivity.

TABLE I

PERCENT SALICYLIC ACID

Column: AS-4A; eluent: 17 m*M* 4-cyanophenolate, pH 9.1; detection: chemically suppressed conductivity.

Added	Found
1.77	1.68
2.06	2.14
2.53	2.49
2.53	2.45
2.53	2.39
2.72	2.60
3.10	2.97

The diluted brown oxide sample produced four peaks (Fig. 2). Chlorite (at 1.2 min) is the active ingredient, as it promotes a strong bond between the internal copper circuitry and the epoxy layer. It is easily quantitated, together with chlorate (at 3.2 min) using computerized data analysis in which the chromatograph can be expanded and baselines drawn using menu-driven software. Monitoring chlorite and chlorate informs the electroplator about the strength and age of the bath.

An electroless copper tank deposits 20 microinches of copper on the holes drilled through the multi-layer boards. It uses formaldehyde to reduce the cupric ion to the elemental copper electrodeposit. In the process, the formaldehyde is oxidized to

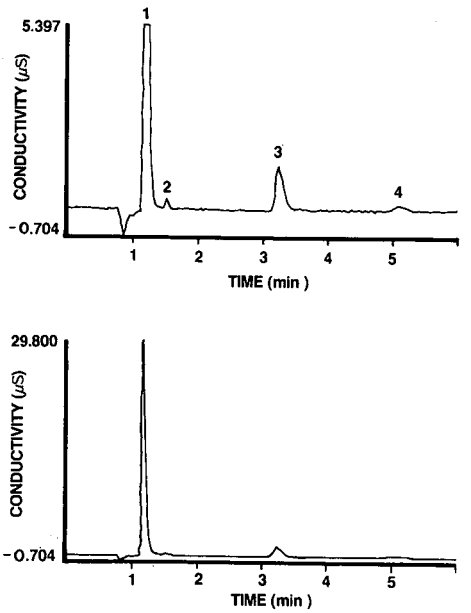

Fig. 2. Brown oxide anion analysis. Column: AG-4A plus AS-4A. Eluent: 1.95 m*M* $NaHCO_3$ + 1.56 m*M* Na_2CO_3, 2.0 ml/min. Detection: chemically suppressed conductivity. Peaks: 1 = chlorite, 2 = chloride, 3 = chlorate, 4 = phosphate. The top is a re-plot of the bottom chromatograph in which the conductivity scale is expanded.

formic acid. In addition, the bath contains sodium tartrate, which forms a slightly dissociated complex with the cupric ion, keeping it in solution despite the high pH of the bath. Tartrate, sulfate and formate can be separated by using the AS-4A column and a 2.4 m*M* sodium bicarbonate plus 1.9 m*M* sodium carbonate eluent as shown in Fig. 3. As the electroless copper tank is used, the formate concentration increases. This can be monitored, so the age of the bath can be observed and bath performance predicted.

Recently, there has been an emphasis on decreasing the use of chlorinated hydrocarbons, so new aqueous-processable photoresists have been developed. Though one wants to protect the environment, it is still important to produce good circuit boards. Thus, a method was developed to measure leaching of an aqueous photoresist.

The material being evaluated is a negative photoresist, meaning that when it is exposed to light, it becomes insoluble in the developing solution. A major manufacturer of photoresists, Hunt Chemical Company, published a report stating that all negative photoresists contain a bis azide compound as a photoinitiator [9]. UV light causes the formation of a reactive nitrene, which can abstract a proton from a carbon in the polymeric component of the photoresist, causing the formation of a covalent bond, as shown below. Hydrogen abstraction:

$$\xrightarrow{\text{UV}}$$

$$R\text{–}N_3 \rightarrow R\text{–}N\text{:} + N_2 \text{ (gas)}$$

$$R\text{–}N\text{:} + H\text{–}C\lesseqgtr \rightarrow N\text{–}C\lesseqgtr$$

where $R\text{–}N_3$ is the photoinitiator and $H\text{–}C\lesseqgtr$ is an acrylate polymer.

In previous negative photoresists, the polymer was a poly(isoprene) which was soluble in chlorinated solvents; these solvents were used to develop the resist after exposure to UV light. On the other hand, the new aqueous processable photoresist contains a water soluble acrylate-based polymer, eliminating the need for hazardous chlorinated solvents.

In pattern plating, a subsequent step after developing the photoresist and washing the circuit board is tin–lead electroplating. Thus, it was necessary to develop a

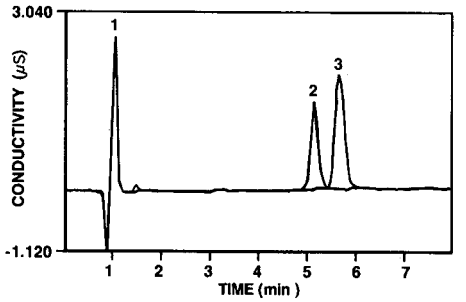

Fig. 3. Ion chromatograph of two week old electroless copper bath. Column: AG-4A plus AS-4A. Eluent: 2.4 m*M* $NaHCO_3$ + 1.9 m*M* Na_2CO_3, 2.0 ml/min. Detection: chemically suppressed conductivity. Peaks: 1 = formate, 2 = sulfate, 3 = tartrate.

method to measure leaching of this aqueous photoresist in the fluoroboric acid-based bath. Because of the low pH of the sample, it was necessary to use the corrosion-resistant MPIC column, which is based on PS–DVB, as opposed to standard reversed-phase HPLC silica-based columns. Using an eluent consisting of acetonitrile–water (9:1, v/v) flowing at 1.0 ml/min, the photoresist can be separated from the other chemicals in the tin–lead bath as shown in Fig. 4. In this case, UV detection was used. Diode array detection provides an UV spectrum of each peak, which helps to confirm its identification. It should be noted that no photoresist was detected in the tin–lead bath after plating 24 circuit boards.

To obtain this chromatogram, the sample was spiked with a solution of UV-curved photoresist in tetrahydrofuran. In addition, the plating performance was mea-

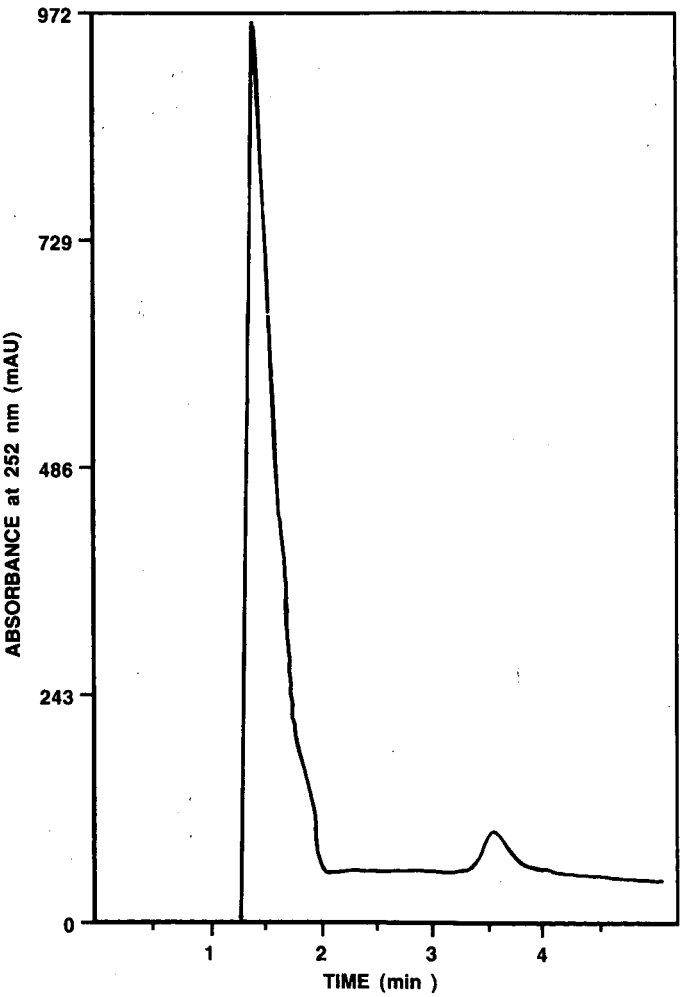

Fig. 4. Analysis of photoresist solubility in 2:5 diluted tin–lead bath. Column: MPIC 5 μm. Eluent: acetonitrile–water (9:1, v/v), 1.0 ml/min. Detection: diode array set at 252 nm. The peak at 3.5 min is due to aqueous photoresist.

sured using a Hull cell test for brightness, and it was found that baths spiked with up to 8 g/ml of photoresist still had the desired matte-gray appearance. X-Ray fluorescence of the Hull cell panel indicated an acceptable plating thickness (minimum of 300 microinches) and composition (63% Sn and 37% Pb) at current densities between 20–30 A/ft.^{2}. Thus, it was demonstrated that not only did normal production operations fail to produce measureable photoresist leaching, but that even if there was photoresist contamination in the tin–lead bath, it did not harm the product. Thus, circuit board manufacture now utilizes this aqueous photoresist.

In addition, surface active organics are added to the acid copper and tin–lead tanks to reduce the particle size of the electrodeposited metals, brightening their appearance. Quite often poly(ethylene glycols) or alkyl phenol poly(ethoxylates) of the Triton or Igepal class are used. These organic materials are non-ionic, so they cannot be detected by conductivity. Instead, a UV detector is used. Conventional reversed-phase HPLC techniques using silica-based columns cannot be used to analyze the highly acidic bath samples. Instead, an acid-resistant PS–DVB-based column is recommended. The non-ionic organics are retained on this column based on non-ionic interactions with the PS-DVB. As shown in Figs. 5–7, the MPIC column was

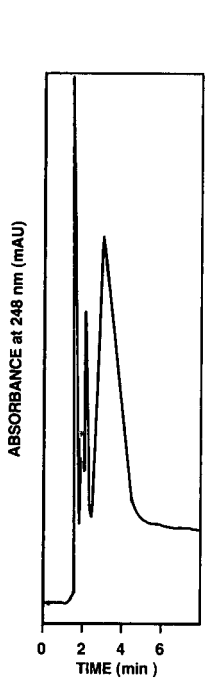

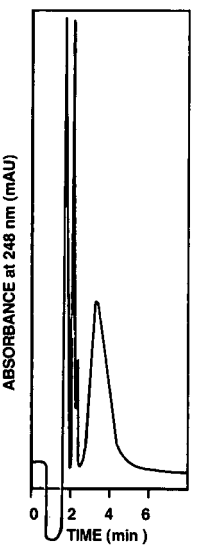

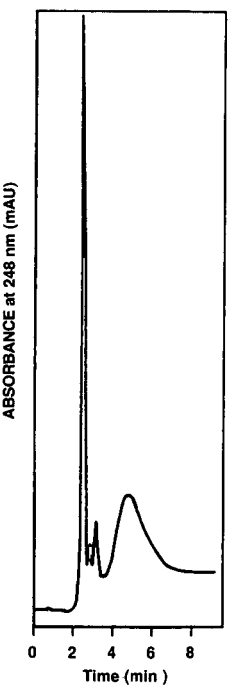

Fig. 5. MPIC of two week old tin–lead bath. Note the comparative sizes of the peaks at 1.8, 2.0 and 3.2 min. The peak at 1.8 min is a breakdown product.

Fig. 6. MPIC of three month old tin–lead bath. Note the increased size of the breakdown product's peak at 1.8 min.

Fig. 7. MPIC of three month old tin–lead bath after carbon treatment. Note the decrease in breakdown product at 1.8 min.

used to monitor the concentration of brightener in the tin–lead tank. After 2 weeks, little break-down product (the peak at 2.0 min) is seen, but after 3 months, it becomes the predominant peak. Carbon treatment removes this break-down product and some of the alkyl phenol poly(ethoxylate) detergent brightener (the peak at 3.5 min). Using MPIC, the electroplator can determine how much of the original brightener solution to add after carbon treatment. Thus, MPIC can monitor the concentration of non-ionic organics in highly corrosive plating tanks.

There is no reason to assume that all brighteners contain only non-ionic organics. Spectroscopic methods such as ^{13}C NMR can identify ethoxylates, alkyl phenols and other organics, but they cannot easily distinguish between non-ionic and ionic compounds. Ion chromatography should be the ideal method for doing this. In the past, though, anion-exchange columns would strongly retain ionic detergents.

Because the detergents were not eluted, they could poison the column. Recently, new polymeric anion-exchange (PAX) columns have become available. These columns are based on surface sulfonated poly(ethylvinylbenzene–divinylbenzene), or EVB–DVB, to which aminated latex beads are covalently attached, so they are also resistant to extremes of pH. Unlike the older anion-exchange columns, though, the covalently attached anion-exchange sites enable the use of 100% organic solvents, which would destroy an AS-4A, AS-5A and other anion separators.

In the past, when attempting to characterize a new brightener, ^{13}C NMR would identify the types of carbons present. Injection of a diluted brightener sample on an AS-4A column would identify the presence of low levels of chloride or perhaps other inorganic anions. Analysis by MPIC would show that there was an organic component that would bind with the non-ionic PS–DVB. Many anionic detergents, though, contain a large non-ionic tail and a small ionic head group. This would have little effect on the MPIC chromatogram or NMR spectrum of the detergent, but the physical properties of an anionic detergent are quite different from a non-ionic detergent.

To distinguish between them, an anion-exchange column compatible with organic solvents is needed. There are two such columns available now [10,11], a PAX-100 and PAX-500. They both contain the same quaternary ammonium anion-exchange sites present in the AS-5A column, but they are attached to latex beads which are covalently attached to the EVB–DVB core particle, making them solvent compatible. The EVB–DVB in the PAX-500 has 60 Å pores with 300 m^2/g adsorption surface area, enabling retention of analytes by the same non-ionic interactions as in MPIC. The EVB–DVB in the PAX-100 is microporous, though, so there is little such interaction with non-ionic compounds. However, anionic organic compounds can interact with the poly(vinylbenzylchloride–divinylbenzene) of the latex beads.

The PAX-500 column can be used exactly as the MPIC column for separating non-ionic compounds. One set of compounds often used to characterize a reversed-phase HPLC column is the alkylphenones. Ethano-, propano-, butano-, pentano- and hexanophenone can be separated on an octadecylsilica (ODS) column and an MPIC column using an acetonitrile–water eluent. Reversed-phase HPLC retention is often described by the equation [12]:

$$k' = k'_0 c^{-m} \tag{2}$$

where c is the concentration of organic solvent in the eluent and k' and m are con-

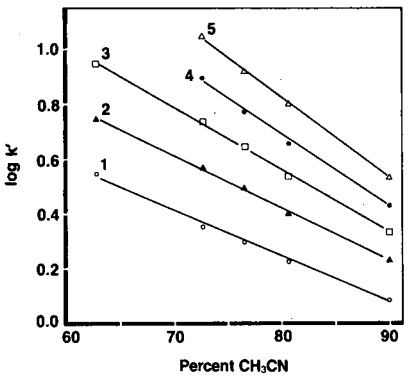

Fig. 8. Plots of log k' of different alkylphenones *vs.* percent acetonitrile in the eluent. The column was a PAX-500. Data were fit to straight lines using linear regression analysis. 1 = Ethanophenone, 2 = propanophenone, 3 = butanophenone, 4 = pentanophenone, 5 = hexanophenone.

stants. Thus, a plot of the log k' *vs.* percent acetonitrile produces a straight line for a wide variety of analytes on the ODS and PS–DVB-based columns. The PAX-500 column produces a similar straigth line, as shown in Fig. 8. However, anions are not retained on an ODS or MPIC column without an ion pair reagent in the eluent, but they are retained and separated on a PAX-100 or PAX-500. With the PAX-100, if an organic compound has a negative charge, its retention can be controlled by varying the concentration of organic solvent as described by eqn. 2.

With a PAX column, then, anionic detergents can be easily identified. One such brightener produced a ^{13}C NMR spectrum similar to most brighteners; that is, it had ethoxylate carbons, phenyl groups and some alkyls. Analysis on an AS-4A indicated low levels of chloride, nitrate, phosphate and sulfate. This provided little useful information, and most likely, the main constituent, the organic detergent, was strongly

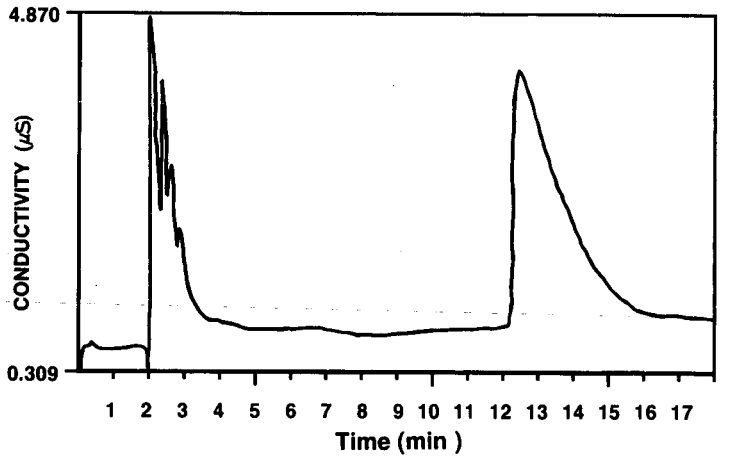

Fig. 9. Analysis of a tin–lead brightener used in pattern plating and infrared reflow. Column: PAX-100. Eluent: 77 mM NaOH in methanol–water (2:8) at 1.0 ml/min. Detection: chemically suppressed conductivity.

retained on the AS-4A. This same brightener was injected on a PAX-100 and 65% of the total peak area (chemically suppressed conductivity detection) was due to a peak eluting much later than the inorganic anions, as shown in Fig. 9. This detergent has an anionic head group, making it more water soluble and causing retention by anion exchange on the PAX-100. As is the case with other anions, increasing the concentration of sodium hydroxide in the eluent causes this detergent to elute sooner.

A cleaning solution used to prepare boards for copper plating was found to contain phosphate using an AS-4A column with 2.4 m*M* sodium bicarbonate plus 1.9 m*M* sodium carbonate eluent and chemically suppressed conductivity detection. The cleaner also contains detergents which were not eluted off the AS-4A column. Using an ODS column with 54% aq. acetonitrile eluent and diode array detection at 227 nm, one peak with a k' value of 0.9 was obtained. Using an MPIC column and acetonitrile–water (18:82, v/v) eluent, three partly resolved peaks were obtained. Using the PAX-100, though, with 0.96 *M* NaOH in 18% aq. acetonitrile as eluent, six different peaks were resolved as shown in Fig. 10. The concentration of sodium hydroxide in the eluent was lowered to 0.80 *M*, then 0.70, then 0.60 *M* and k' values for the first four peaks were measured. Plots of the log k' *vs.* log NaOH concentration produced straight lines for the peaks that appeared at 1.994, 3.715 and 6.182 min in Fig. 10. Slopes were -0.82, -0.83 and -1.73, suggesting that the peaks are due to anions with a charge of -1, -1 and -2, respectively as predicted by the equation [13]:

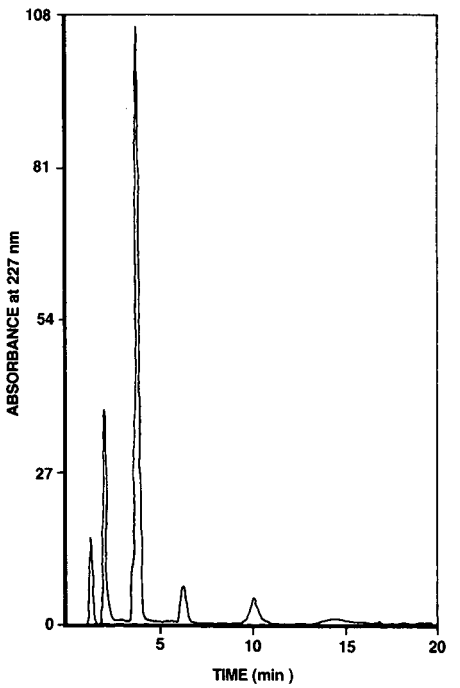

Fig. 10. Analysis of a cleaning solution. Column: PAX-100. Eluent: 0.96 *M* NaOH in acetonitrile–water (18:82) at 1.0 ml/min. Detection: diode array at 227 nm.

$$\log k' = (-Z/E)\log C + \log I$$

where E is the charge on the eluent (-1 for NaOH), I is an isocratic constant and Z is the effective charge (or Z number) of the analyte. The first peak remained in the void volume, indicating that it is due to a non-ionic compound.

Thus, the PAX columns enable two-dimensional chromatography with one column and one injection, whereas older two-dimensional techniques required columns switching or (as in thin-layer chromatography) two completely different runs. With the PAX columns, one can take advantage of retention based on non-ionic interactions by varying the concentration of organic solvent in the eluent, just as one does with reversed-phase HPLC or MPIC. At the same time, one can take advantage of retention based on anion exchange by varying the concentration of ionic (sodium hydroxide, sodium carbonate, etc.) in the eluent, and from the slope of plots of log k' *vs.* log NaOH (or other ionic eluent) one can estimate the charge on the analyte. This promises to be a powerful new tool in helping control the manufacture of high quality circuit boards.

The chromatographic methods have been partly validated. The determination of salicylic acid had an average percent error of 3.99%, obtained in a single blind experiment using seven samples. The absolute value of the percent error for each sample was divided by seven to get the average percent error. Reproducibility was evaluated in each method by injecting at least five replicate samples and calculating the percent relative standard deviation, which varied from 0.95% for salicylic acid to 5.6% for photoresist determination.

An AG-4A guard column will last for about 50 analyses before it needs to be replaced. An MPIC guard column also lasts for about 50 analyses. The AG-4A and MPIC 5 μm separator columns will last for about 200 analyses, and the PAX columns have not degraded after about 100 analyses. It should be noted that the PAX columns should always have at least 10% organic solvent on them (especially during storage), but that the AS-4A (and other AS separator columns) should never have more than 5% organic solvent, and function quite well with no organic solvent. The AS-4A and AG-4A are routinely stored in dilute aqueous sodium hydroxide.

REFERENCES

1 R. E. Smith and W. R. Davis, *Plating Surf. Finish.*, 71 (1984) 60.
2 P. L. Annable and R. E. Smith, *Plating Surf. Finish.*, 73 (1986) 126.
3 R. E. Smith and C. H. Smith, *LC·GC*, 3 (1985) 578.
4 W. R. Davis, R. E. Smith and D. Yourtee, *Metal Finish.*, Sept. (1986) 63.
5 K. K. Haak, *Product Finish.*, 37 (1984) 9.
6 K. K. Haak, *Plating Surf. Finish.*, 70 (1983) 34.
7 R. B. Rubin and S. S. Heberling, *Am. Lab.*, 39 (1987) 46.
8 R. E. Smith, *Ion Chromatography Applications*, CRC Press, Boca Raton, FL, 1988.
9 A. Stein, *The Chemistry and Technology of Negative Photoresists*, Philip A. Hunt Chemical Corporation, Palisades Park, NJ, 1978.
10 J. R. Stillian and C. A. Pohl, *J. Chromatogr.*, 499 (1990) 249.
11 R. W. Slingsby and M. Rey, *J. Liq. Chromatogr.*, 13 (1990) 107.
12 P. Jandera and J. Churáček, *Gradient Elution in Column Liquid Chromatography* (*Journal of Chromatography Library*, Vol. 31), Elsevier, Amsterdam, 1985, p. 11.
13 R. E. Smith and R. A. MacQuarrie, *Anal. Biochem.*, 170 (1988) 308.

Journal of Chromatography, 546 (1991) 381–385
Elsevier Science Publishers B.V., Amsterdam

CHROMSYMP. 2311

Improved determination of alkanolamines by liquid chromatography with electrochemical detection

DANIEL L. CAMPBELL* and STEVE CARSON
Dionex Corporation, 1228 Titan Way, Sunnyvale, CA 94086 (U.S.A.)
and
DONNA VAN BRAMER
Boeing Commercial Airplane Group, Seattle, WA 98124 (U.S.A.)

ABSTRACT

The determination of alkanolamines has traditionally been difficult due to the complexity of the detection methods and the difficulty of the separation. Wet chemistry, gas chromatography and high-performance liquid chromatography methods all require time-consuming, complex sample treatments which are prone to numerous interferences.

This paper will describe the use of a liquid chromatography method using a polymer based reversed-phase column coupled to a pulsed amperometric detector. This method provides simple, direct quantitation of triethanolamine. Evaluation of this method for linearity, reproducibility and detection limits in an alkaline etch process will be presented.

INTRODUCTION

The determination of alkanolamines is currently of great interest, as these compounds are used widely in chemical and pharmaceutical industries. Alkanolamines are used in the production of emulsifying agents, the manufacturing of laundry additives and dyes, and are commonly used in metal surface finishing [1]. The analysis of alkanolamines is important in the purification of gases and in waste water effluents [2].

Several traditional methods have been used for the determination of alkanolamines. These include wet chemistry, high-performance liquid chromatography with spectroscopic detection, ion chromatography with conductivity detection and gas chromatography. Gas chromatography (GC) is almost eliminated as an analytical technique because of the high polarity which alkanolamines exhibit. Precolumn derivatization is required prior to analysis to achieve an acceptable separation. The GC columns tend to degrade rapidly resulting in poor performance [3]. Ion chromatography has worked well for the separation of individual alkanolamines. Still, the sensitivity by suppressed conductivity detection is poor due to the low equivalent conductance of alkanolamines relative to the hydrogen ion [4]. Liquid chromatography

0021-9673/91/$03.50

techniques for amines have shown highly efficient separations, however, the effect of the amine functionality on some silica-based gels can result in serious tailing of the chromatographic peak. Because the alkanolamines lack natural chromophores or fluorophores, derivatization of these compounds with nitroaromatic chromophors is required prior to spectroscopic detection. The reagents available for derivatization result in poor sensitivities and have been shown to be unreliable due to numerous interferences [5].

This paper will describe the use of a polymeric column coupled with pulsed amperometric detection (PAD) for the determination of alkanolamines. Specifically, triethanolamine (TEA) in an aluminum and aluminum alloy chemical etching process will be presented.

The original work for this paper began as a joint project with the Boeing Commercial Airplane Group, Seattle, WA, U.S.A. In an effort to improve the quality control and production performance of their aluminum products for commercial airplanes, Boeing identified the need for improved monitoring of important chemical additives and bath constituents in their Aluminum Finishing Process Line. TEA was identified as a primary additive responsible for maintaining proper operation of the alkaline etch bath. A properly controlled TEA alkaline etch bath is maintained at 4.2–5.3 oz/l sodium hydroxide, 0.4–1.3 oz/l sodium sulfide, 1.1–2.1 oz/l TEA and 0.7–2.6 oz/l dissolved aluminum at an operational temperature of 60–90°F [6]. Improved monitoring of the TEA may allow for the development of tighter specifications in control and product integrity. The data generated and reported in this paper is believed to be accurate and correct for the conditions and processes developed at Boeing.

EXPERIMENTAL

All chromatography was performed on a Dionex system 4000i ion chromatograph consisting of a pump, a chromatography module and a pulsed amperometric detector. A gold working electrode, a stainless-steel counterelectrode and a silver/silver chloride (1 *M* NaCl) reference electrode were used in the amperometric flow-through detector cell. The applied potentials (V) and pulse durations (ms) were the following: $E1(t1)$, 0.08(540); $E2(t2)$, 1.0(420); $E3(t3)$, −0.80(420). The sample volume for all injections was 50 μl unless otherwise noted. The column was a Dionex OmniPac PAX-500 with the anion-exchange resin in the hydroxide form. The eluent was 150 m*M* NaOH and 5% (v/v) acetonitrile at a flow-rate of 1 ml/min. All chemicals used in methods development were reagent grade.

RESULTS AND DISCUSSION

Pulsed amperometric detection

In 1981, Hughes *et al.* introduced pulsed amperometric detection [7]. By using strongly basic solutions, alkanolamines could be detected [8]. Pulsed amperometric detection uses an automated repeating sequence of three potentials. The analyte molecules are oxidized at the first potential ($E1$), and the current is measured. The potential is then stepped to a more positive value ($E2$), and a gold oxide layer is formed on the electrode surface. The third potential ($E3$) is a negative potential at which the

oxide layer is reduced to produce the bare metal. This sequence is repeated several times per second and one point on the chromatogram is acquired during each cycle. The pulsed sequence is an advantage since the electrode is cleaned during the alternating positive and negative pulsing. When only a single potential is used, peak response from a series of injections will quickly decrease as the electrode becomes coated by the products of the oxidation reaction.

Separation

Pulsed amperometric detection at a gold electrode in a basic solution is specific for small oxidizable molecules. These include alkanolamines, sulfides and metals. Detecting these individual species in a complex matrix such as an aluminum etch solution can be a difficult task. Therefore the selectivity for the quantitative analysis must be provided for by the chromatography. Separation was achieved on a Dionex OmniPac PAX-500 using a sodium hydroxide–acetonitrile eluent. The PAX-500 is a solvent-compatible anion exchange, reversed-phase column. The core is a macroporous polymer substrate. Attached to this surface is a cationic latex coating upon which a layer of anion-exchange material is covalently bonded.

A chromatogram of a standard solution of TEA is shown in Fig. 1. Complete baseline separation occurs between diethanolamine and TEA. Other oxidizable species do not interfere. Alkanolamines at the pH of the eluent, pH = 3, have little or no ion-exchange characteristics and their retention is unaffected by the anion-exchange portion of the PAX-500 column. The alkanolamines, therefore, are retained and separated by the reversed-phase mechanisms on the PAX-500 analytical column. The acetonitrile present in the eluent controls the retention mechanisms of the alkanolamines.

Acetonitrile in high pH solutions is decomposed to acetic acid and other nitrogen containing compounds [9]. These decomposition products interfere with the electrochemical detector's response and stability as the contaminates build up with time.

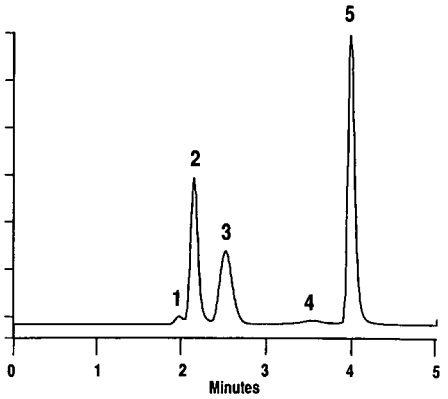

Fig. 1. TEA determination in an operational alkaline etch solution. Column, PAX-500 guard and analytical; eluent, 150 m*M* NaOH–acetonitrile (95:5, v/v); detector, pulsed amperometric detection, range 30 μA; loop, 50 μl; sample preparation, 1/1000 in 150 m*M* NaOH. Peaks: 1 = unknown; 2 = unknown; 3 = diethanolamine; 4 = unknown; 5 = triethanolamine (54 ppm).

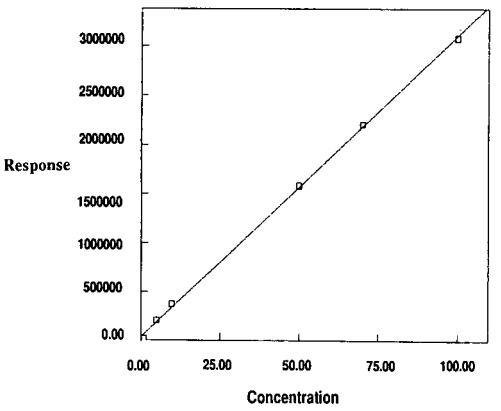

Fig. 2. Linearity of TEA. Correlation coefficient r = 0.9996. TEA range, 1.0–100 ppm (50 μl injection).

The reaction of acetonitrile in sodium hydroxide is not rapid, and the breakdown components have no immediate effects upon the analysis. Eluents should be made fresh every 8 h to ensure optimum performance of the instrument. It is not recommended to store the sodium hydroxide and the acetonitrile in the same bottle.

One way to ensure optimum eluent performance would be the use of a proportioning pump for blending two or more separate solutions together. Individual sodium hydroxide and acetonitrile solutions can be metered together by on-line mixing at the proportioning valve in the eluent pump. This ensures that no degradative chemical reaction takes place prior to the analysis of the alkanolamines and results in reliable long term stability of the analysis.

Low concentrations of alkanolamines are not stable in neutral or low pH matrices. It is recommended that all standards and samples be prepared and stored in 150 mM NaOH. When the standards and samples are diluted in the sodium hydroxide, no stability problems were observed over normal sampling times of 8 h.

The alkanolamines were quantified by automatic measurements of peak areas. A comparison of peak height *vs.* peak area data showed better linearity and reproducibilities by peak area calculations. All calculations in this paper are based upon peak area calculations and not peak height.

TABLE I

REPRODUCIBILITY OF TEA IN A SINGLE ALKALINE ETCH SAMPLE SOLUTION BY PEAK AREAS

	Dionex	Boeing
Observations	374	44
Minimum (ppm)		37.8
Maximum (ppm)		42.1
Mean (ppm)	71.2	40.1
Standard deviation (ppm)	0.954	0.937
Relative standard deviation (%)	1.34	2.3

Fig. 2 shows the linearity of TEA in a standard alkaline etch bath. Standards of TEA were prepared at the 1, 10, 50, 75, and 100 ppm levels. Seven duplicate measurements were made for each standard and the resultant average plotted. The linearity for TEA over the range of 1–100 ppm showed a coefficient of determination (r^2) equal to 0.9992. No overloading of the analytical column was observed over this entire analytical range. Detection limits are approximately 1 part-per-billion for TEA and the other alkanolamines.

Reproducibility data, reported in Table I, was studied under similar conditions at both Dionex and Boeing. At Dionex the relative standard deviation (R.S.D.) for 374 replicate analyses of TEA in a diluted single-concentration alkaline etch sample at the 70 ppm level was 1.34%. A similar sample analyzed at Boeing provided similar reproducibility results. Forty-four replicate analyses of TEA in a diluted single-concentration alkaline etch sample at the 40 ppm level showed a 2.3% R.S.D. All samples were diluted 1 to 1000 for this study.

CONCLUSION

In summary, liquid chromatography using a polymer resin coupled to pulsed amperometric detection is a sensitive and selective technique for the simultaneous determination of TEA and other alkanolamines. This new technique has been adopted as the standard method for the determination of TEA at Boeing. It is believed to be a more rapid, reliable and accurate method for alkanolamines than former wet chemistry or spectroscopic methods. The choice of an OmniPac PAX-500 analytical column and electrochemical detection results in a rugged, simple and reliable method for the analysis of alkanolamines in complex matrices and environmental samples.

REFERENCES

1 *The Merck Index*, Merck, Rahway, NJ, 10th ed., 1983, p. 541.
2 K. F. Butwell, D. J. Kubek and P. W. Sigmund, *Hydrocarbon Processing*, March, 1982, Gulf Publishing Co., pp. 108–116.
3 R. B. Rubin and T. J. Ward, Update Report: *The Determination of Alkanolamine Scrubbers by Ion Chromatography*, presented at the *Gulf Coast Conference, Houston, TX, Oct. 1, 1987*, unpublished.
4 D. T. Gjerde and J. S. Fritz, *Ion Chromatography*, Hüthig, Heidelberg, 2nd ed., 1987, p. 212.
5 W. R. LaCourse, W. A. Jackson and D. C. Johnson, *Anal. Chem.*, 61 (1989) 2466–2471.
6 *Process Specification, BAC 5786, Rev. G*, Boeing, Seattle, WA, Aug. 1988.
7 S. Hughes, P. L. Meschi and D. C. Johnson, *Anal. Chim. Acta*, 132 (1981) 1.
8 D. C. Johnson and W. R. LaCourse, *Anal. Chem.*, 61 (1990) 598A–597A.
9 R. T. Morrison and R. N. Boyd, *Organic Chemistry*, Allyn & Bacon, Boston, MA, 2nd ed., 1966, p. 588.

Journal of Chromatography, 546 (1991) 387–394
Elsevier Science Publishers B.V., Amsterdam

CHROM. 2196

Review

Use of ion chromatography in agricultural research

AHMED A. HAFEZ, SHAM S. GOYAL* and D. WILLIAM RAINS
Department of Agronomy and Range Science, College of Agricultural and Environmental Sciences, University of California, Davis, CA 95616 (U.S.A.)

ABSTRACT

During the last decade ion chromatography developed into a powerful analytical technique. Versatility, speed of operation, simultaneous multi-ion analysis, small sample size requirements and reasonable cost are some of the factors that have contributed to its popularity. One of the unique features of this technique has been the quantitative determination of various species of an ion (*e.g.*, different oxidation states) that may exist in a sample. This paper describes the applications of ion chromatography technology in the agricultural research and some future directions.

CONTENTS

1. INTRODUCTION

In the past decade ion chromatography (IC) techniques have become an increasingly important analytical methodology. Its versatility, simultaneous multi-ion analysis, speed of operation and reasonable cost contributed to its popularity. It is an analytical technique that can separate ionic species, in discrete bands in a liquid moving phase, using different separation modes and different detection technology. The modes of separation are: high-performance ion chromatography (HPIC), mobile phase ion chromatography (MPIC) and mobile phase ion chromatography exclusion (MPICE) [1]. The ionic species of interest are detected by proper selection of one of

0021-9673/91/$03.50

these detection modes: conductivity with and without suppression, amperometric or pulsed amperometric, ultraviolet–visible light absorption, fluorescence and other appropriate systems.

IC has been utilized by many agricultural scientists and soil, water and plant analysis commercial laboratories. There have been significant improvements in different areas of IC including, but not limited to, development of new stationary phases, use of different mobile phases, pre-injection sample concentration, advanced suppressor technology, use of highly sensitive detectors and column-switching techniques [2]. The impact of these progressive improvements will make IC a method of choice now and in the future. The objective of this paper is to describe some of the applications of this technique that have been used in agricultural research.

2. INORGANIC ANION ANALYSIS

Fluoride, chloride, nitrite, bromide, nitrate, sulfate and phosphate in rain, sewer water, soil pore-water and plant and soil extracts have been analyzed by several investigators using IC [3–11]. They have used single-column IC with low-conductivity eluent [12] (Fig. 1) or dual columns in which the second column suppresses the background conductivity [4,10] (Fig. 2). Some investigators used conductivity as a mode of detection [9–11] while others used direct UV detection [5]. Indirect UV detection, in which the eluent includes an ionic species that absorbs in the appropriate region and that is soluble in the eluent, has also been used. Inorganic anions which do not absorb in that region appear as throughs in the baseline [3].

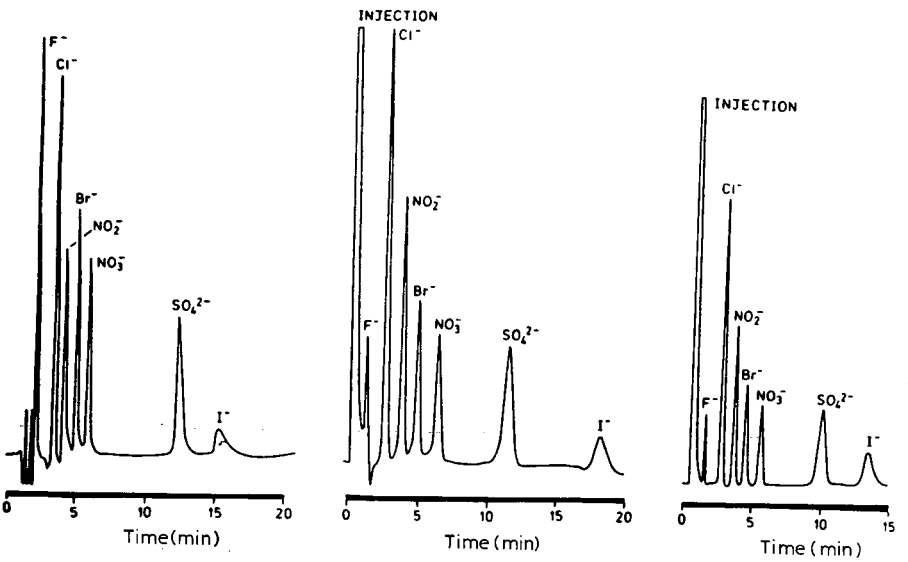

Fig. 1. Non-suppressed (single-column) IC of inorganic anions using different columns. (Left) Hamilton PRP-X100, with 1 m*M* phthalate eluent pH 5.5 at a flow-rate of 2 ml/min. (Middle) Bio-Gel TSK IC Anion PW, with 1 m*M* phthalate eluent pH 5.3 at a flow-rate of 1.2 ml/min. (Right) Waters IC Pak A, with 1 m*M* phthalate eluent pH 7.0 at a flow-rate of 1.2 ml/min. Sample, 10 μl of a mixture containing 100 ppm of the indicated anions. From ref 6.

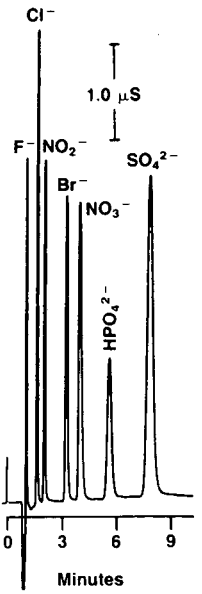

Fig. 2. Typical suppressed (dual-column) IC for inorganic anions. Column: HPIC-AS4A; eluent: 2 m*M* Na_2CO_3, 0.75 m*M* $NaHCO_3$; flow-rate: 2 ml/min; sample: anion standard; F^- (0.5 ppm), Cl^- (1.5 ppm), NO_2^- (2.5 ppm), Br^- (5.0 ppm), NO_3^- (5.0 ppm), HPO_4^{4-} (7.5 ppm) and SO_4^{2-} (7.5 ppm). Reproduced from document No. LPN 32629, Dionex Corporation, Sunnyvale, CA, November 1985.

Tabatabai and Dick [11] compared IC methods for measuring nitrate, chloride, sulfate and phosphate in natural water and soil extracts with currently available wet chemistry methods. They used steam distillation for nitrate, mercuric thiocyanate and ferric ammonium sulfate, colorimetric method for chloride, reduction and colorimetric determination using methylene blue for sulfate and colorimetric molybdenum blue method for phosphate. In all instances there was a close agreement between both techniques (Fig. 3), with the added advantage that IC was rapid and sensitive, required microgram levels of sample size, and all anions were determined in one assay rather than four separate assays.

Nitrate analysis of soil and plant extracts by directly measuring UV absorption at 210 nm suffers from the background interferences by organic compounds. Thayer and Huffaker [13] developed a method for separation of nitrate from the interfering compounds, using an anion-exchange column and then its determination by UV absorbance at 210 nm. Schroeder [14] proposed the use of a reversed-phase separation on an octadecyl column with aqueous phosphoric acid–dihydrogenphosphate as mobile phase. Both methods separated nitrate from organic chromophores. In another approach using MPIC, nitrate was separated using 2 m*M* tetrabutylammonium hydroxide in 0.05 m*M* Na_2CO_3, 10% acetonitrile [1] as mobile phase, and detected with a conductivity detector.

Poulson and Borg [15] used single-column IC for the analysis of sulfide, sulfite, thiosulfate and thiocyanate in water samples. The system used a resin-based anion-exchange column, a gluconate–borate eluent and electrochemical and UV detectors.

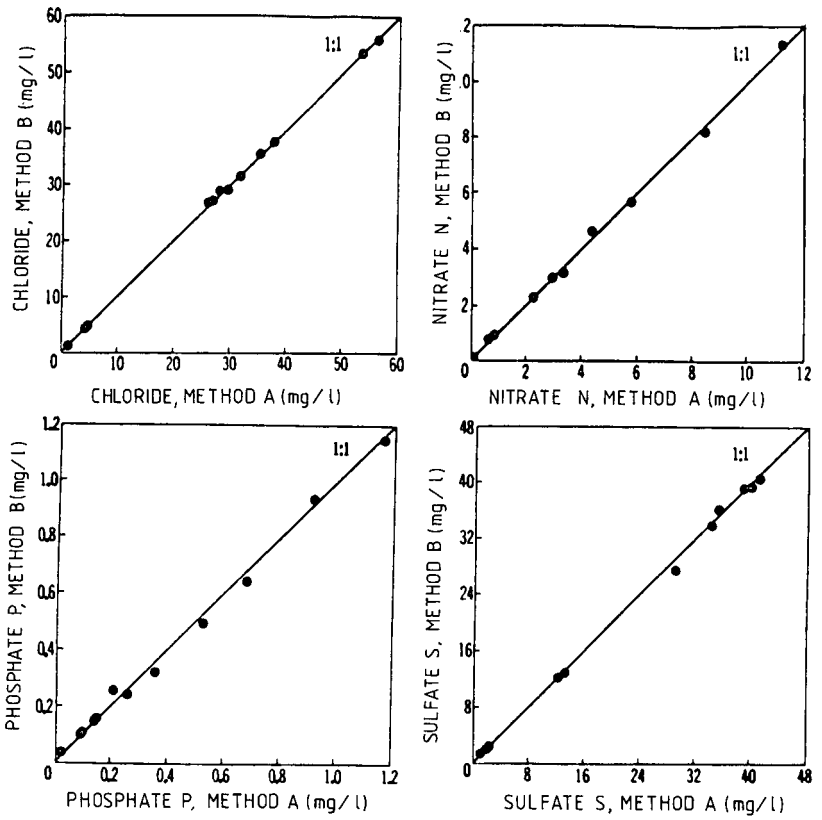

Fig. 3. Reliability of IC method as compared to wet chemistry methods. The *x*-axis (method A) refer to IC values and the *y*-axis (method B) are (I) $Hg(CNS)_2$–Fe^{3+} colorimetric method for chloride, (II) steam distillation method for nitrate, (III) molybdenum blue method for phosphate and (IV) methylene blue method for sulfate. From ref. 11.

Determination of total sulfur in plant material or soil requires conversion of all sulfur forms to SO_4^{2-} by wet digestion or to S^{2-} by reduction. Neither approach yields a sample suitable for IC because of high background ion concentration. Both Hern *et al.* [3] and Busman *et al.* [16] resorted to combustion of sample in oxygen atmosphere with no excess of ionic material. However, combustion of samples in an oxygen flask is cumbersome, time-consuming and difficult to automate. Recently, Hafez *et al.* [17] used IC for the determination of total sulfur (as sulfate) in plant materials digested with nitric and perchloric acids. The sample matrix problem (high ionic background) was solved by evaporating the acid digests to dryness. The separation of sulfate was accomplished on a multisubstrate column (Omni Pac-PAX 500) developed by Dionex [18]. The column substrate has a polymeric hydrophobic surface core with an ion-exchange polymeric colloid attached on it. This created a stationary phase suitable for simultaneous ion-exchange and reversed-phase modes of separation. It took a much longer time for perchlorate ions (relative to sulfate) to elute from a low-capacity anion-exchange column. This would make the assay time

long and render the method impractical. With simultaneous ion-exchange and reversed-phase separation, however, perchlorate ions rapidly eluted while fully separated from sulfate (perchlorate ions are less polar than other inorganic ions). Using this column with 25 m*M* sodium hydroxyde–acetonitrile (45%) as mobile phase at a flow-rate of 0.8 ml/min, the analysis time was only 10 min per sample (Fig. 4) compared to as much as 60 min on a single-mode ion-exchange separation. With this method about 98.2–101% of total sulfur was recovered from several different reference plant materials with and without addition of different sulfur compounds.

Selenite, selenate and arsenate have been measured in soil extracts using single-column IC [19–21]. For selenite analysis, interfering chloride ions were removed by treating the sample with silver-saturated cation-exchange resin [19]. The concentration limit above which there was interference of sulfate on selenate analysis was 40 mg/l, while that of phosphate on arsenate analysis was 30 mg/l. The United States Environmental Protection Agency report [22], investigating the IC technique for determining selenium species in ground water, found that for suitable selenate analysis the sample must be pretreated with $Ba(OH)_2$ to lower the sulfate interference. For lower detection limits (sub-ppb, 10^9) of selenium analysis free from sulfate interference, Yamada *et al.* [23] measured selenite in soils after derivatization with 2,3-diaminonaphthalene (DAN). The derivative, 4,5-benzopiazselenol, was extracted in cyclohexane, separated on a Cosmosil 5 SL silica gel column and detected fluorometrically at 380 nm for excitation and 525 nm for emission. Selenate can be mea-

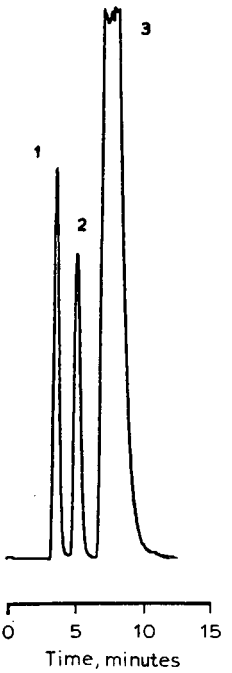

Fig. 4. Determination of sulfate in nitric, perchloric acids plant digest. Peaks: 1 = chloride; 2 = sulfate; 3 = perchlorate from ref. 17.

sured after its reduction to selenite with hydrochloric acid. Recently, Goyal *et al.* [24] reported an IC method using photometric detection for the simultaneous determination of arsenite, arsenate, selenite and selenate in water samples. A background sulfate concentration of up to 2000 mg/l did not affect the selenate analysis. However, arsenate analysis was affected by sulfate concentrations greater than 1400 mg/l.

3. INORGANIC CATION ANALYSIS

Total K, Na, Ca and Mg in plant materials have been measured after dry ashing and extraction in 5 m*M* HCl, with supressed IC and conductivity detection [25]. Exchangeable bases in soils were extracted by 1 *M* ammonium acetate followed by evaporation of the extract and ignition of the residue at 400°C to remove the ammonium acetate background. The clean residue was extracted in 5 m*M* HCl and exchangeable Na, K, Ca and Mg were measured by IC [26]. Fritz *et al.* [27] using single-column IC analyzed drinking water for Li, Na, K, NH_4, Rb and Cs ions using nitric acid as eluent. They also measured Ba, Sr, Ca and Mg ions using ethylene diammonium dinitrate as eluent.

An IC method for the simultaneous determination of urea and ammonium nitrogen in soil extracts has been available [28]. The method used a cation-exchange which retarded the migration of ammonium ions while urea molecules were not retained. An in-line catalytic solid-phase urease reactor, placed after the cation-exchange column, hydrolyzed the urea to ammonium ions. Thus, both ammonium and urea peaks were detected fluorometrically as ammonium after post-column derivatization with *o*-phthalaldehyde (OPA) and mercaptoethanol [29].

An anion- and cation-exchange column, HPIC-CS5 (Dionex) has been shown to separate NO_2^-, NO_3^- and NH_4^+ simultaneously. Nitrite and nitrate are detected by direct UV, while NH_4^+ is post-column-derivatized by OPA and detected by a fluorescence detector. The minimum detection limit was 1 ppm in 10% KCl [30].

4. HEAVY METAL ANALYSIS

Methods for heavy metal analysis such as atomic absorption or inductively coupled plasma atomic emission spectroscopy are based on total mass and do no distinghuish between the ionic species. Speciation of the ionic form is important in studying heavy metals in the environment. For instance some metals can exist in more than one oxidation form. They can also exist in both cationic or anionic form such as Cr(III) or chromate, Cr(VI). IC can be used to separate ionic species and molecules with different oxidation states. In general, separation of metals has been done through on-line metal chelating using an eluent containing complexing agent. The chelating ligands react with the coloring agent to form UV–visible-absorbing derivatives in a wide variety of metal cations including Hg, Pb, Co, Cr, Cu, Fe, Al and Zn [31]. Post-column reaction with 4-(2-pyridylazo)resorcinol results in derivatives of Fe^{2+}, Fe^{3+}, Pb^{2+}, Cd^{2+}, Ni^{2+}, Zn^{2+} and Co^{2+} that can be detected at 520 nm [32]. Heavy metals such as Cu, Zn, Ni, Co and Cd can also be measured by a coulometric detector [33].

5. ORGANIC COMPOUNDS ANALYSIS

Organic acids such as maleic, malonic, lactic, formic and propionic acids were successfully separated by an HPICE-Asl (Dionex) column using suppressed IC with conductivity detection. Amines, carbohydrates, amino acids, sugars and polysaccharides can be measured with IC using a suitable mode of separation (column) and a proper detector. For instance ion-exchange columns with pulsed amperometric detection have been used to measure organic compounds like mono- di- and tri-saccharides, alcohols and primary and secondary amines. Amino acids can be separated on an ion-exchange column and detected fluorometrically or spectrophotometrically after post-column derivatization with OPA or ninhydrin, respectively [34].

6. RECENT DEVELOPMENTS

6.1 New stationary phases

Brown and Pietrzyk [35] demonstrated the use of mixed-bed ion-exchange columns containing alumina and silica for simultaneous separation of anion and cation analytes. Manipulation of the alumina to silica ratio, pH of the mobile phase, eluent counter ions and their concentration were the major factors to improve resolution and shifting retention order. Such stationary phases can separate mono- and divalent anions and cations in single-sample injection with a single column and a single detector.

The Dionex column Omnipac-PAX500 [18] (PCX 500 for cation exchange) combines ion-exchange, reversed-phase and ion-pair separation modes on the same column. These modes of separation can be performed either simultaneously or in series depending on the composition of the mobile phase. This gives a great flexibility to the analyst to choose the best separation conditions.

6.2 Sample pre-concentration

Concentrator columns are used to trap trace levels of solutes and insure interference-free analysis. However, careful selection of eluent and concentrator substrate must be exercised to insure quantitative retention of ions of interest and their subsequent transfer to the analytical column [36].

6.3 Supressor column technology

The use of a micromembrane suppressor, to lower the background conductivity as well as enhancing the conductivity of the analytes, is based on the Donnan equilibrium. Thus in anion analysis, a satisfactory replacement of eluent cation by H ions requires a thin-wall membrane plus continuous-flowing regenerate acid. Higher operation cost due to the flowing acid can now be minimized by regenerating the acid. Tian *et al.* [37] developed an electrochemical supressor with anode and cathode made of platinum-plated titanium. For a 5 m*M* Na_2CO_3 eluent with a flow-rate of 1 ml/min, a constant current of 50 mA is applied and the voltage across the suppressor electrodes is 4 V. For such low voltage, the heating effect on the eluent solution is acceptable. The advantage of the electrochemical supressor is the elimination of the acid, and the back pressure of the suppressor is lowered. The technique shows promise and could simplify supressed IC in the future. However, the suppression efficiency of both systems appears to be similar.

6.4 Column switching

It is either a simple on-line mobile phase direction change or a chromatographic mode change which provides more resolving power as multidimensional chromatography [2]. A single-mode column with mobile phase direction switching can be used to reduce analysis time and eliminate gradient elution when using the same eluent.

Continuous development of techniques in IC for better sensitivity, matrix-free interferences, new separation modes, in-line pre- and post-column treatments and new detection techniques will increase the scope of its utilization in agricultural research.

REFERENCES

1 E. L. Johnson and K. K. Haak, in J. F. Lawrence (Editor), *Liquid Chromatography in Environmental Analysis*, Humana Press, Clifton, NJ, 1984, pp. 263–300.
2 J. G. Dorsey, J. P. Foley, W. T. Cooper, R. A. Barford and H. G. Barth, *Anal. Chem.*, 62 (1990) 324R–356R.
3 J. R. Hern, G. K. Rutherford and G. W. Vanloon, *Talanta* 30 (1983) 677–682.
4 H. Small, T. S. Stevens and W. C. Bauman, *Anal. Chem.* 47 (1975) 1801–1809.
5 R. J. Williams, *Anal. Chem.*, 55 (1983) 851–854.
6 P. R. Haddad, P. E. Jackson and A. L. Heckenberg, *J. Chromatogr.*, 346 (1985) 139–148.
7 M. Dreux and M. Lafosse, *J. High Resolut. Chromatogr. Chromatogr. Commun.*, 9 (1986) 122–124.
8 P. Bark and Y. Chen, *Soil Sci. Soc. Am. J.*, 51 (1987) 257–258.
9 K. F. Nieto and W. T. Frankenberger, Jr., *Soil Sci. Soc. Am. J.*, 49 (1985) 587–592.
10 W. A. Dick and M. A. Tabatabai, *Soil Sci. Soc. Am. J.*, 43 (1979) 899–904.
11 M. A. Tabatabai and W. A. Dick, *J. Environ. Qual.*, 12 (1983) 209–213.
12 D. T. Gjerde, G. Schmuckler and S. Fritz, *J. Chromatogr.*, 187 (1980) 35–45.
13 J. R. Thayer and R. C. Huffaker, *Anal. Biochem.*, 102 (1980) 110–119.
14 D. C. Schroeder, *J. Chromatogr. Sci.*, 25 (1987) 405–408.
15 R. E. Poulson and H. M. Borg, *J. Chromatogr. Sci.*, 25 (1987) 409–414.
16 L. M. Busman, R. P. Dick and M. A. Tabatabai, *Soil Sci. Soc. Am. J.*, 47 (1983) 1167–1170.
17 A. A. Hafez, S. S. Goyal and D. W. Rains, *Agron. J.*, 83 (1991) 148–153.
18 *Document No. 034217*, Dionex Corporation, Sunnyvale, CA, May 1989.
19 U. Karlson and W. T. Frankenberger, Jr., *Anal. Chem.*, 58 (1986) 2704-2708.
20 U. Karlson and W. T. Frankenberger, Jr., *J. Chromatogr.*, 368 (1986) 153–161.
21 H. C. Mehra and W. T. Frankenberger, Jr., *Soil Sci. Soc. Am. J.*, 52 (1988) 1603–1606.
22 J. A. Oppenheimer, A. D. Eaton and P. H. Kreft, *Report No. EPA-600/2-84-190*, U.S. Environmental Protection Agency, Washington, DC, November 1984.
23 H. Yamada, T. Hattori, S. Matuda and Y. Kang, *Bunseki Kagaku*, 36 (1987) 542–546.
24 S. S. Goyal, A. Hafez and D. W. Rains, *J. Chromatogr.*, 537 (1991) 269–276.
25 N. T. Basta and M. A. Tabatabai, *Soil Sci. Soc. Am. J.*, 49 (1985) 79–81.
26 N. T. Basta and M. A. Tabatabai, *Soil Sci. Soc. Am. J.*, 49 (1985) 84–89.
27 J. S. Fritz, D. T. Gjerde and R. M. Becker, *Anal. Chem.*, 52 (1980) 1519–1522.
28 A. Abshahi, S. S. Goyal and D. S. Mikkelsen, *Soil Sci. Soc. Am. J.*, 52 (1988) 969–973.
29 S. S. Goyal, D. W. Rains and R. C. Huffaker, *Anal. Chem.*, 60 (1988) 175–179.
30 *LPN 032992*, Dionex Corporation, Sunnyvale CA, November 1987.
31 I. S. Krull, in J. F. Lawrence (Editor), *Liquid Chromatography in Environmental Analysis*, Humana Press, Clifton, NJ, 1984, pp. 169–262.
32 *LPN 32557*, Dionex Corporation, Sunnyvale, CA, January 1985.
33 J. E. Girard, *Anal. Chem.*, 51 (1979) 836-839.
34 *LPN 32403R*, Dionex Corporation, Sunnyvale, CA, September 1985.
35 D. M. Brown and D. J. Pietrzyk, *J. Chromatogr.*, 466 (1989) 291–300.
36 P. E. Jackson and P. R. Haddad, *J. Chromatogr.*, 439 (1988) 37–48.
37 Z. W. Tian, R. Z. Hu, H. S. Lin and J. T. Wu, *J. Chromatogr.*, 439 (1988) 159–163.

Journal of Chromatography, 546 (1991) 395–403
Elsevier Science Publishers B.V., Amsterdam

CHROMSYMP. 2187

Separation and detection of non-chromophoric, anionic surfactants

J. B. LI* and P. JANDIK
Ion Analysis Department, Waters Chromatography Division of Millipore, 34 Maple Street, Milford, MA 01757 (U.S.A.)

ABSTRACT

The newly developed Solid Phase Reagent (SPR) permits the conductivity detection of various alkylsulfonates and alkylsulfates. In its present version, SPR is an aqueous suspension of submicron particles of a polymeric cation exchange material in the hydrogen form. The SPR is pumped into the eluent stream coming from the separation column. The post-column reaction transforms the tetrabutylammonium alkyl sulfate or sulfonate into the corresponding free acid. This changes the analytes into more conductive species. At the same time the tetrabutylammonium borate eluent is converted to the low conducting boric acid. Both types of post-column reactions greatly increase the sensitivity of detection by conductivity. The conductivity detection method with the help of SPR also makes it possible to employ gradient elution for separations of complex mixtures of alkylsulfates or sulfonates. Such gradient separations are preferably carried out on silica based reversed-phase columns, rather than on polymeric based reversed-phase columns. The latter type of columns shows better tolerance to increased levels of the organic solvents as well as higher separation efficiency.

INTRODUCTION

Solid Phase Reagent (SPR) has been introduced recently as a new method of post-column conductivity enhancement [1,2]. In its most common version, it is used as a highly dilute aqueous suspension (1% and less) of sulfonated submicron polymeric beads. SPR is capable of removing highly conductive countercations from the ion chromatographic eluents on their way from the separator column to a conductivity detector. The removal of alkaline cations from carbonate, borate or hydroxide solutions and the formation of non-conductive carbonic acid, boric acid and water leads to pronounced decrease of background conductivity contributed by the eluent. At the same time, the mostly strongly acidic analyte anions are converted from a salt form into a fully dissociated acid. Both types of ion-exchange reactions occurring on the surface of SPR beads have been shown to increase the sensitivity of detection for low-molecular-weight anionic species [3,4].

Low-molecular-weight anions, such as the anionic surfactants carrying sulfate or sulfonate functional groups have traditionally presented a great challenge to analytical chemists. These types of compounds, used in a large number of personal care products and in a variety of industrial processes are usually synthesized in rather

0021-9673/91/$03.50

complicated reaction mixtures. Correspondingly, there is a great need to determine the composition of synthetic mixtures and the purity of commercial products.

Most anionic surfactant mixtures can be separated on liquid chromatographic (LC) reversed-phase columns using an ion pairing agent and an organic solvent (acetonitrile, methanol tetrahydrofuran)–water gradient. The chromophoric components of such mixtures can then be easily monitored by UV detection. This approach has been shown to be applicable for example to the determination of alkyl chain distribution of alkylbenzenesulfonates [5]. Highly sensitive detection of linear alkylsulfonates was also demonstrated using fluorescence detection [6].

Post-column derivatization followed by UV detection was reported for some non-chromophoric anionic surfactants [7,8]. Simultaneous detection of chromophoric and non-chromophoric surfactants was shown to be feasible with the help of a newly developed evaporative light scattering detector [9]. Other approaches to the universal detection of surfactants included conductivity [10] and indirect UV [11].

The post-column addition of SPR discussed in this article converts the alkylammonium borate eluent into nearly non-conducting boric acid and the anionic surfactants from low conducting alkylammonium salts to highly conductive alkylsulfuric and alkylsulfonic acids. This type of conversion for the enhancement of conductivity signals can be carried out without difficulty in gradient mobile phases containing high levels of an organic solvent. Use of silica based reversed-phase columns also allows a greater range of concentrations of an organic solvent in gradient separations.

EXPERIMENTAL

Instrumentation

The LC system used in our experiments consisted of Waters Action Analyzer (Waters Chromatography Division of Millipore, Milford, MA, U.S.A.), the Waters Novapak C_{18} separation column and Waters Reagent Delivery Module (RDM) for the post-column addition of aqueous suspension of the Solid Phase Reagent (SPR). Waters 431 conductivity and programmable 490 UV detectors were connected in series for most of the experiments. The UV detector was placed between the column outlet and the mixing tee for the addition of SPR.

Chemicals

The eluents were: (A) Milli Q water (used also to prepare all other aqueous solution for this investigation; Millipore, Bedford, MA, U.S.A.) containing 0.5 m*M* tetrabutylammonium borate (TBAB), and (B) acetonitrile (HPLC grade, J. T. Baker, Philipsburg, NJ, U.S.A.) containing 0.5 m*M* TBAB. A concentrate containing 25 m*M* TBAB was used for the preparation of eluents. This concentrate was prepared by neutralizing a 40% aqueous solution of tetrabutylammonium hydroxide (Aldrich Chemical Company, Milwaukee, WI, U.S.A.) with a dilute reagent grade boric acid (J. T. Baker) and by final dilution to 25 m*M* using the Milli Q water.

Standards of alkyl and arylsulfonates were obtained from the following sources: Chem Service, West Chester, PA, U.S.A.; Eastman-Kodak, Rochester, NY, U.S.A.; Fluka Chemie, Buchs, Switzerland; and Aldrich.

Solid Phase Reagent[a]

The SPR was obtained from Waters as a concentrate containing *ca.* 12% solids ($SPR–H^+$) and diluted for use to contain *ca.* 1% solids and a cation-exchange capacity of not less than *ca.* 50 mequiv./l. A complete description of various applications of this new reagent is given elsewhere [1–3]. The efficient removal of tetrabutylammonium ions by SPR was verified by ^1H NMR. After the addition of the same volume of 1% SPR suspension in ^2H_2O to 5 m*M* solutions of TBAB in ^2H_2O, corresponding proton signals (between 0.9 and 3.3 ppm) decreased below the detection limit of the NMR method.

The enhancement of the conductivity signal by SPR was confirmed by the series of measurements shown in Table I.

TABLE I

ENHANCEMENT OF CONDUCTIVITY SIGNAL BY SPR

Solution		Conductance (μS)	Δμ S	% Change
a	Water	0.68		
b	SPR–water (1:9)	12.0		
c	0.5 m*M* TBAB	29.4		
d	b + c (1:3)	6.99		
	d − c		22.41	−76.2
e	d containing 1μg/ml $C_{12}SO_3Na$	8.64		
	e − d		1.65	23.6
f	c containing 1μg/ml $C_{12}SO_3Na$	30.4		
	f − c		1.0	3.4

The concentration of dodecylsulfonate in solutions e and f was chosen to correspond approximately to an average concentration in a peak zone after a 500-ng injection (10 ppm in 50 μl). The expected reduction of the conductivity background due to eluent and the enhancement of the analyte signal (from 3 to 23% for dodecylsulfonate) are thus confirmed.

RESULTS AND DISCUSSION

Separations of standard mixtures of alkyl and arylsulfonates

The separation of a standard mixture of linear alkyl sulfonates is shown in Fig. 1. The gradient curves have been overlaid on this and the following chromatogram. The concentration of acetonitrile in the eluent is increased linearly from 15 to 60%, while the concentration of the tetrabutylammonium borate remains unchanged. The two unknown peaks occurring around 5 min and between the pentane and hexane sulfonates in Fig. 1 were combined impurities stemming from one batch of tetrabutylammonium hydroxide.

Without the employment of the post-column reaction replacing the tetrabutylammonium cation by hydronium ions by means of ion-exchange groups on the surface of SPR, the conductivity detector would register only high background signal

[a] Patent pending.

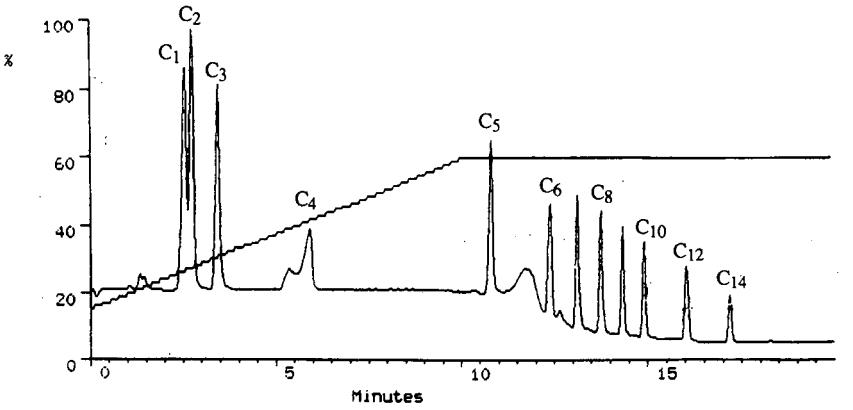

Fig. 1. Linear alkylsulfonate standards [methanesulfonate-(C_1)to tetradecylsulfonate(C_{14})]. The gradient curve is overlaid on the chromatogram. Initial conditions: 85% A–15% B, A: aqueous 0.5 m*M* tetrabutylammonium borate (TBAB), B: 0.5 m*M* TBAB in acetonitrile. Column: Novapak C_{18}. Flow-rates: 1 ml/min A + B, 0.3 ml/min SPR diluted to 50 mequiv./l. Detection by conductivity. Injection: 100 μl standard solution containing *ca.* 10 ppm of sulfonates.

due to borate, and the separated peak zones due to 5–10 ppm alkylsulfonates would remain undetected. The submicroscopic particles of SPR (*ca.* 0.2 μm) are too large to participate to any extent in the transport of electric charge that would affect the conductivity of the solution. After the attachment of the tetrabutylammonium ions to the surface functionalities on the beads, both the beads and the alkylammonium cations pass through the conductivity cell undetected. By exchanging the alkylammonium cations for hydronium ions, the conductivity background of borate is lowered to a level enabling a sensitive detection at ppm concentrations. At the same time, the sulfonates are converted by SPR to their more readily detectable free acid form.

A simultaneous separation of alkylsulfates and alkylsulfonates is presented in Fig. 2. The sulfates were added at a lower concentration than the sulfonates for ease

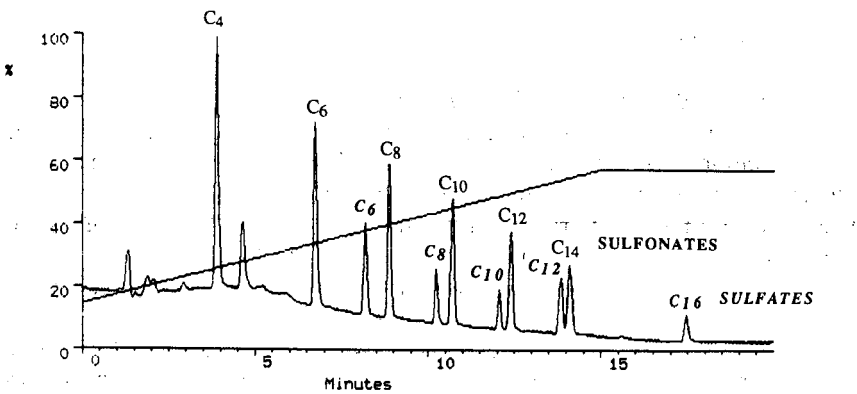

Fig. 2. Mixture of linear alkylsulfonates and alkylsulfates. Injection: 100 μl of standard solution containing 5 ppm sulfates and 10 ppm sulfonates. The gradient curve is overlaid on the chromatogram. Other conditions were as indicated in Fig. 1.

of identification. The gradient range remained the same as in Fig. 1 (15 to 60%), but the gradient curve is not as steep as in the previous chromatogram: the composition of 60% acetonitrile is reached after 15 min, not in 10 min as in Fig. 1. This change of gradient conditions makes it possible to improve the resolution of the three closely eluting peak pairs in the standard mixture of sulfates and sulfonates. It can be noted that all sulfonates included in the standard mixture show a weaker retention than the corresponding homologous sulfates. This is directly attributable to their relatively higher polarity and to their lower tendency to ion pair with the tetrabutylammonium cation. The peak eluting after the butanesulfonate is an unidentified impurity.

Figs. 1 and 2 illustrate both, the capabilities and limitations of chromatographic separations of anionic surfactant mixtures. Organic chemistry describes a multitude of ways by which polarity and ion pairing behavior of compounds containing an identical number of carbon atoms can be broadly modified. Even the least significant of these modifications will have a pronounced influence on the retention behavior on chromatographic columns.

The separation in Fig. 3 which was obtained by using UV and SPR–conductivity detection simultaneously, is another example of varying retention times for sulfo-

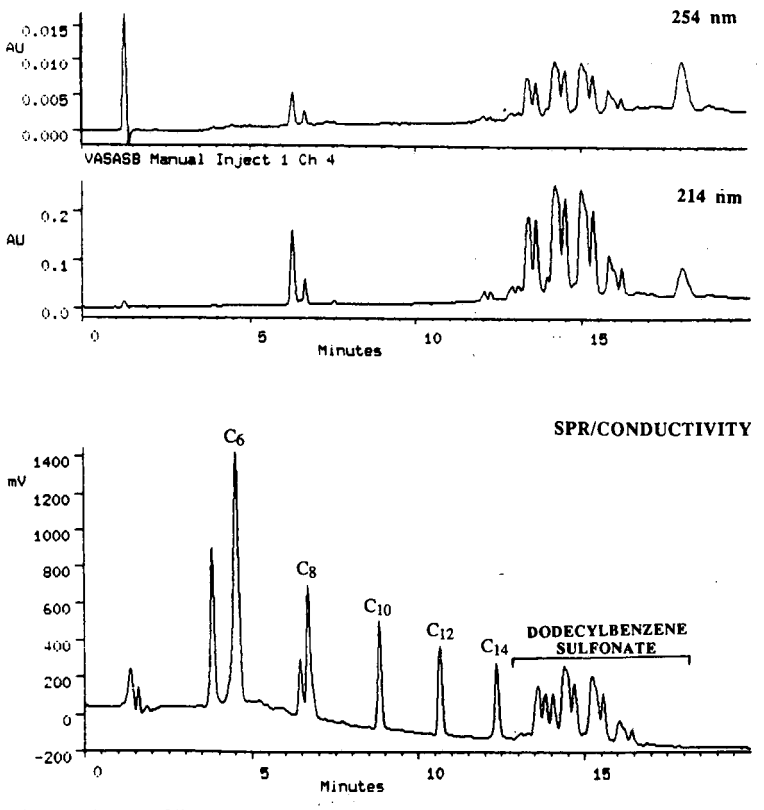

Fig. 3. Mixture of linear alkylsulfonate with dodecylbenzenesulfonate standards. The upper two chromatograms were obtained with UV detection at 254 and 214 nm. Linear gradient from 15%B to 60%B. Injection: 100 μl standard with all components at 10 ppm. Other conditions as in Fig. 1.

nates having the same number of carbon atoms. The dodecylbenzenesulfonate which was added to the mixture of alkylsulfonates is not a single compound as indicated by its manufacturer, but rather a mixture of at least eight different structural isomers.

The simultaneous use of SPR–conductivity and UV detection offers several advantages in the analysis of complex mixtures of organic sulfates and sulfonates. It is possible by this approach to distinguish between the aromatic and non-aromatic

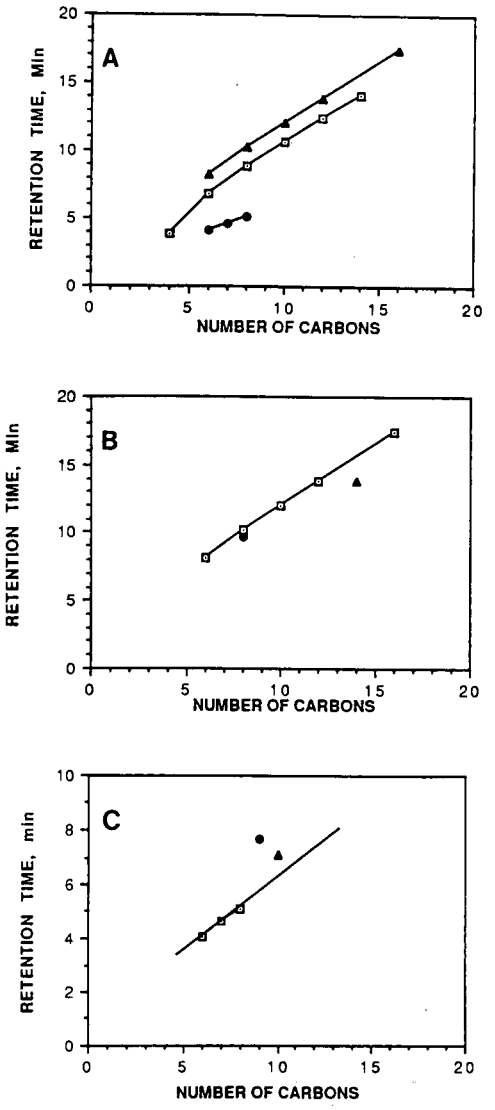

Fig. 4. (A) Methyl group addition to alkylsulfonates (□), alkylsulfates (▲) and arylsulfonates (●). (B) Effect of chain branching of alkylsulfates (□) on retention behaviour (● = 2-ethylhexylsulfate; ▲ = *sec.*-tetradecylsulfate). (C) Effect of carbon addition to benzenesulfonate (□) on retention behaviour (● = cumenesulfonate; ▲ = naphthalensulfonate). Chromatographic conditions as in Fig. 2.

components. Comparisons of UV and conductivity recordings can also reveal the presence of impurities that would otherwise remain undetected. Furthermore, the two different detection modes provide useful information about the possible composition of unknown impurities. Consider for example, the unknown peak preceding the peak of hexanesulfonate in the conductivity trace in Fig. 3. Its absence in the UV recordings, together with the relatively short observed retention time, can be taken as a first indication of the possibility, that this signal may be due to an isomeric alkylsulfonate.

Additional results summarizing the influence of isomeric modifications on the retention behavior are listed in Fig. 4A–B,C. Fig. 4A compares the homologous series of alkylsulfates and sulfonates from Fig. 2 with benzene, toluene and xylenesulfonates. The Fig. 4B compares the influence of two different types of branching of alkyl chains on the retention behavior of corresponding alkylsulfates. It appears from this limited experimental data, that the relative position of secondary carbon atoms in respect to the sulfate group plays an important role. The secondary tetradecylsulfates is observed to deviate more from the homologous series than the 2-ethylhexylsulfate. As seen in Fig. 4C both, naphthalenesulfonate and cumenesulfonate have longer retention times than the benzenesulfonate indicating two other possible types of homologous series influencing the retention behavior of arylsulfonates.

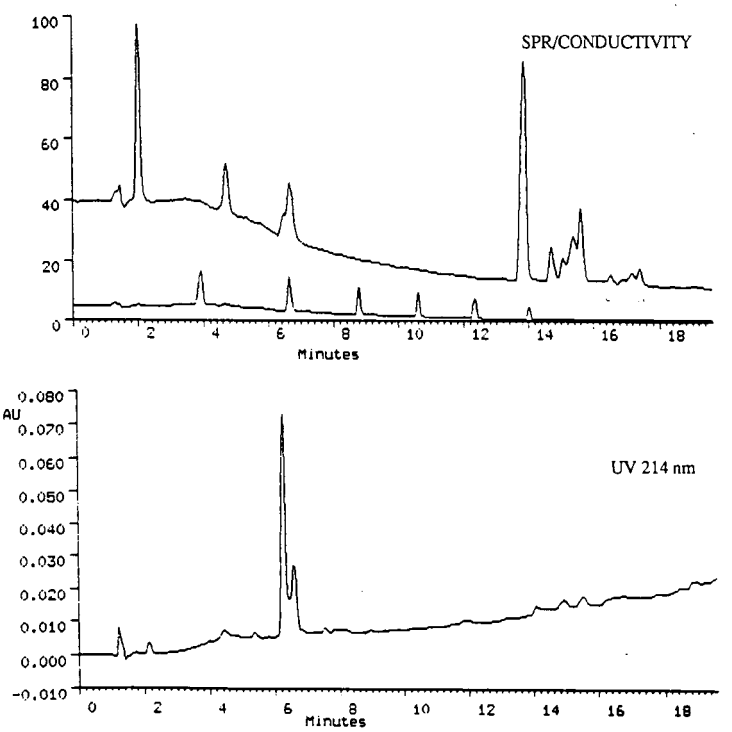

Fig. 5. Separation of components of a commercial shampoo (1:1000 dilution, 100 μl injected). Both UV and SPR–conductivity were used for detection. The overlaid standard shows the peaks for C_4, C_6, C_8, C_{10}, C_{12} and C_{14} linear alkylsulfonates. Chromatographic conditions as in Fig. 2.

There are 3314 possible structural isomers for the homologous series of alkylsulfonates (C_4 to C_{14}) separated in Fig. 2. This number, perhaps better than anything else, shows why the retention times from a LC method can not be used as the only proof of identity of unknown peaks.

Synthetic mixtures of organic sulfonates

The next two chromatograms show separations of two different types of commercial surfactant mixtures —a hair shampoo (Fig. 5) and a common laundry detergent (Fig. 6). The high resolving power of the discussed method can be put to a good use in the quality control and other assays carried out by industrial laboratories. "Good" production results could possibly be correlated to a certain shape of the "finger print" separations. Possible fluctuations of quality of production could then be easily detected by an observed emergence of additional peaks or by shifts in the concentration ratios among the existing peaks.

Simultaneous use of SPR–conductivity and UV detection generates additional information for the analysis of unknown mixtures. Non-aromatic or aromatic components can be easily recognized from the relative signal intensities by conductivity and UV. Overlaid separations of homologous alkyl series (C_4 to C_{14}) make it possible

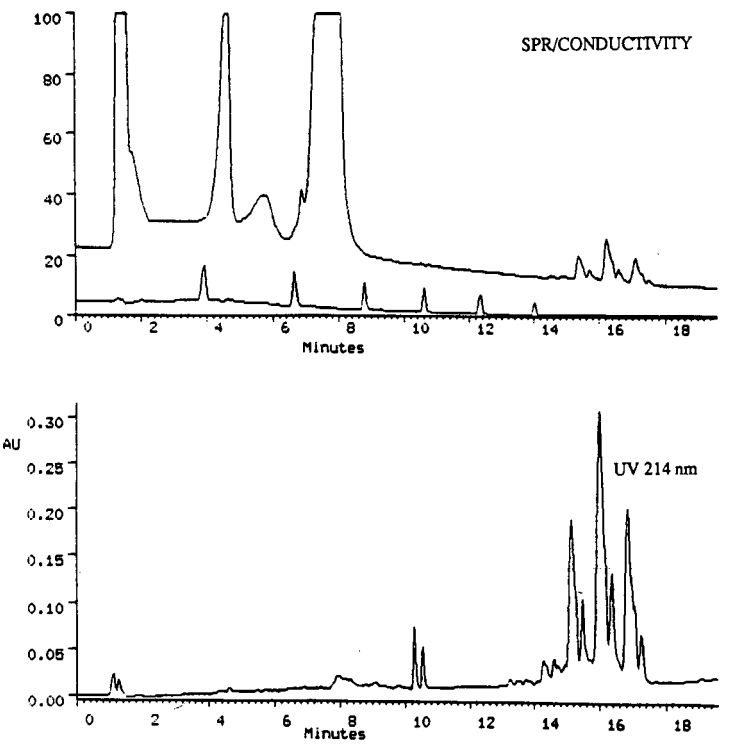

Fig. 6. Common laundry detergent after 1:1000 dilution with UV and SPR–conductivity detection. The overlaid standard shows the peaks for C_4, C_6, C_8, C_{10}, C_{12} and C_{14} linear alkylsulfonates. Chromatographic conditions as in Fig. 2.

to estimate the approximate molecular weight of the unknown components in the reaction mixture.

CONCLUSIONS

Combined use of solvent gradients on silica based reversed-phase columns and SPR–conductivity detection provide a new approach to the analysis of complicated organic sulfonate and sulfate mixtures. Additional information can be gained by a simultaneous utilization of UV detection in series with the SPR–conductivity detection.

The nearly limitless number of structural parameters influencing the retention behavior makes it very difficult to utilize this method for positive identification of unknown components in complex mixtures. However, the technique can be highly useful in the fingerprinting of synthetic mixtures and in the assay of commercial detergent products.

REFERENCES

1 D. T. Gjerde and J. V. Benson, *Anal. Chem.*, 62 (1990) 1801.
2 D. T. Gjerde in P. Jandik and R. M. Cassidy (Editors), *Advances in Ion Chromatography*, Century International, Medfield, MA, 1990, Vol. 2, pp. 1.
3 P. Jandik, L. B. Li, W. R. Jones and D. T. Gjerde, *Chromatographia*, 30 (1990) 509.
4 D. T. Gjerde, D. J. Cox, P. Jandik and J. B. Li, *J. Chromatogr.*, 546 (1991) 151.
5 G. R. Bear, *J. Chromatogr.*, 371 (1986) 387.
6 M. A. Castles, B. L. Moore and S. R. Ward, *Anal. Chem.*, 61 (1989) 2534.
7 M. Kudoh and K. Tsuji, *J. Chromatogr.*, 294 (1984) 456.
8 M. Benning, H. Locke and R. Iannielo, *J. Liq. Chromatogr.*, 12 (1989) 757.
9 G. R. Bear, *J. Chromatogr.*, 459 (1988) 91.
10 J. Weiss, *Handbuch der Ionenchromatographie*, VCH Verlag, Weinheim, 1985, pp. 163.
11 D. J. Pietrzyk, in P. Jandik and R. M. Cassidy (Editors), *Advances in Ion Chromatography*, Century International, Medfield, MA, 1990, Vol. 2, pp. 88.

Journal of Chromatography, 546 (1991) 405–410
Elsevier Science Publishers B.V., Amsterdam

CHROMSYMP. 2159

Determination of total nitrogen in food, environmental and other samples by ion chromatography after Kjeldahl digestion

PETER E. JACKSON*[a], JIM KROL and ALLAN L. HECKENBERG
Waters Chromatography Division, Millipore Corporation, 34 Maple Street, Milford, MA 01757 (U.S.A.)
and
MARINA MIENTJES and WIM STAAL
Millipore BV, Penningweg 33, Postbus 166, 4870 AD Etten-Leur (The Netherlands)

ABSTRACT

Total nitrogen in food, environmental and many other matrices is usually determined by Kjeldahl digestion–distillation followed by titration. The use of ion chromatography to determine total nitrogen as ammonium ion after sample digestion significantly improves the speed of the analysis compared with the conventional method. A poly(styrene–divinylbenzene) cation-exchange column with dilute nitric acid as eluent and indirect conductivity detection was used for the ion chromatographic determination of ammonium in the presence of the elevated levels of sulfuric acid found in the digested sample. The peak-area precision for ten replicate injections of an ammonium standard was 0.6% [relative standard deviation (R.S.D.)] and the retention time precision was 0.3% (R.S.D.). The determination of ammonium was linear from 15 ppb (10^9) up to 25 ppm. The results obtained by the ion chromatographic method were compared with those for the conventional distillation and titration approach for the determination of total nitrogen in animal feeds. The application of the ion chromatographic method is also demonstrated for a variety of other sample matrices.

INTRODUCTION

The determination of total nitrogen in food, environmental and many other sample types is typically carried out using Kjeldahl digestion–distillation followed by titration [1,2]. This well established procedure involves digesting the sample in an acid mixture in the presence of a catalyst, distillation of ammonia in the digest into a dilute acid solution, followed by back-titration with base. Several alternatives to the classical approach for total nitrogen have recently been suggested, including the use of microwave digestion [3] and combustion methods [4,5].

Ion chromatography (IC) has become a well established technique for the determination of ammonium ion [6,7]. The use of ion chromatography to determine total nitrogen as ammonium ion after Kjeldahl digestion can significantly improve the speed of the analysis compared with the conventional method by eliminating the need

[a] Present address: Millipore Pty. Ltd., Private Bag 18, Lane Cove, NSW 2066, Australia.

0021-9673/91/$03.50

for the distillation step. As only microliter volumes of sample are required for analysis, the weight of sample required for the digestion can be reduced, minimizing the amount of catalyst [*e.g.*, mercury(II) oxide or sulfate] that needs to be used, and hence also disposed of. In this work, the use of IC for the determination of total nitrogen in grain samples, organic compounds and sewage sludges after Kjeldahl digestion was investigated. The selection of appropriate analytical conditions is discussed and the results obtained by the digestion–IC method are compared with those obtained by the classical digestion–distillation technique.

EXPERIMENTAL

Instrumentation

The liquid chromatograph consisted of a Waters (Milford, MA, U.S.A.) Model 510 pump, a U6K injector, a Model 431 conductivity detector and a Waters Model 820 data station. The analytical column used was either a Waters IC-Pak Cation (50 × 4.6 mm I.D.) or a Waters Protein-Pak SP-5PW (75 × 4.6 mm I.D.). The eluents used were 2.0 m*M* nitric acid at 1.2 ml/min or 25 m*M* nitric acid–5% acetone at 2.4 ml/min with the IC-Pak Cation or the Protein-Pak SP-5PW column, respectively. The eluents were prepared daily, filtered and degassed with a Waters solvent clarification kit before use.

Reagents

Water (18 MΩ) purified using a Milli-Q water purification system (Millipore, Bedford, MA, U.S.A.) was used to prepare all solutions. Ultrex nitric acid and acetone and analytical-reagents grade chloride salts used for the preparation of the cation standards were obtained from J. T. Baker (Phillipsburg, NJ, U.S.A.).

Kjeldahl digestion

Two different sample digestion procedures were carried out using standard Kjeldahl methods. Organic compounds and sewage sludges were digested using a potassium sulfate–sulfuric acid mixture with a mercury(II) oxide [or mercury(II) sulfate] catalyst [1] and animal feed (grain) samples were digested using an acetic acid–sulfuric acid mixture with hydrogen peroxide as the catalyst [2].

RESULTS AND DISCUSSION

Selection of chromatographic conditions

The chromatographic conditions selected for the determination of ammonium ion depended on the actual digestion precedure employed. The determination of ammonium ion in the grain samples digested using the acetic acid–sulfuric acid procedure was relatively straightforward and could be carried out, after dilution, using 2 m*M* nitric acid as eluent, a low-capacity cation-exchange column (IC-Pak Cation) and indirect conductivity detection. The determination of low ppm levels of ammonium in samples digested using the potassium sulfate–sulfuric acid mixture could not be accomplished using the IC-Pak Cation column owing to the presence of *ca.* 20 000 ppm of potassium in the final digest. This analysis was carried out using a significantly higher cation-exchange capacity column (Protein-Pak SP-5PW) to ensure resolu-

tion of the ammonium peak from the adjacent potassium peak. This column was also suitable for the determination of ammonium in the acetic acid–sulfuric acid–digested samples. The solution obtained from either digestion procedure typically contained ammonium in the range 100–500 ppm and was very acidic (pH < 1). This solution was simply diluted 100–1000-fold before injection into the chromatograph; no other sample pretreatment was necessary.

The retention time and peak-area precision, detection limits and linearity for the ion chromatographic determination of ammonium ion were then established using the IC-Pak Cation column. The retention time precision of ten replicate injections of a 5 ppm ammonium standard was 0.3% [relative standard deviation (R.S.D.)] and the peak-area precision from the ten replicate injections was 0.6% (R.S.D.). The detection limit (three times the signal-to-noise ratio) for ammonium was 15.7 ppb (10^9) using a 100-μl injection and the determination of ammonium was linear up to 25 ppm. A chromatogram of a cation standard containing lithium, sodium, ammonium and potassium obtained using the IC-Pak Cation column and 2 m*M* nitric acid as eluent is shown in Fig. 1.

Application to digested samples

A chromatogram of a 125-fold dilution of an acetic acid–sulfuric acid-digested grain sample using the IC-Pak Cation column and nitric acid as eluent is shown in Fig. 2. The chromatogram shows a large negative void peak due to the low pH of the sample and 3.5 ppm of ammonium in the presence of traces of sodium and potassium. The grain samples typically contained 5–15% total nitrogen, hence the ammonium level in the digest was relatively high. Fig. 3 shows a chromatogram of a 1000-fold dilution of a potassium sulfate–sulfuric acid–digested organic compound (caprolactam) containing *ca.* 2% of total nitrogen obtained using the Protein-Pak SP-5PW column and 25 m*M* nitric acid–5% acetone as eluent. The potassium was typically present in a 50–100-fold excess over ammonium in such samples, hence the need for

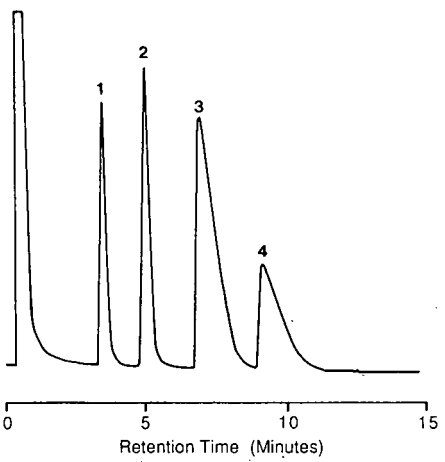

Fig. 1. Chromatogram of a monovalent cation standard using the IC-Pak Cation column. Eluent, 2 m*M* nitric acid; flow-rate: 1.2 ml/min; injection, 100 μl. Solutes: 1 = lithium (1.0 ppm); 2 = sodium (5.0 ppm); 3 = ammonium (10.0 ppm); 4 = potassium (10.0 ppm).

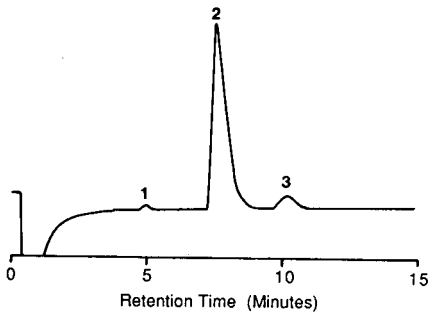

Fig. 2. Chromatogram of an acetic acid–sulfuric acid-digested grain sample using the IC-Pak Cation column. Conditions as in Fig. 1 except sample preparation: 125-fold dilution of acetic acid–sulfuric acid-digested grain. Solutes: 1 = sodium; 2 = ammonium (3.55 ppm); 3 = potassium.

the use of the higher ion-exchange capacity column. Blank digests were processed for both Kjeldahl digestion procedures and no detectable ammonium was found. No decrease in the performance of either column was observed as a result of injecting *ca.* 200 digested samples during the course of this work.

The results for total nitrogen obtained by the classical Kjeldahl and the digestion–IC methods were compared for ten acetic acid–sulfuric acid-digested grain samples. The results obtained by the two methods were normalized to account for differences in sample weights and are given in Table I. The two methods showed reasonably good agreement. A paired comparison Student's *t*-test [8] indicated no significant difference between the two sets of results at the 95% confidence limit. The average difference between the two sets of data pairs was 5.1%.

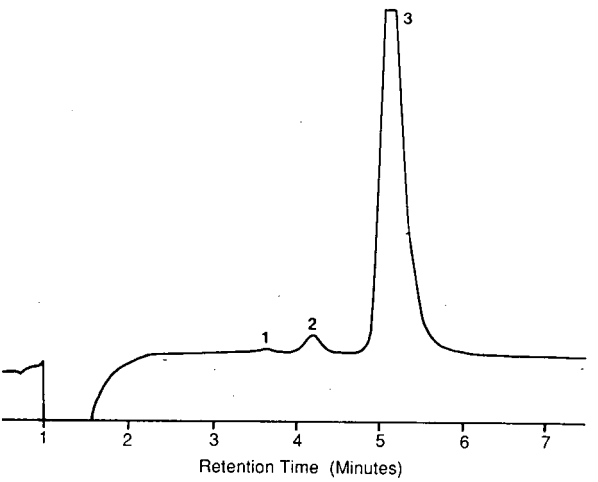

Fig. 3. Chromatogram of a potassium sulfate–sulfuric acid-digested sample of caprolactam using the Protein-Pak SP-5PW column. Eluent, 25 m*M* nitric acid–5% acetone; flow-rate, 2.4 ml/min; injection, 100 µl; sample preparation, 1000-fold dilution of potassium sulfate–sulfuric acid-digested caprolactam. Solutes: 1 = sodium, 2 = ammonium (0.45 ppm); 3 = potassium.

TABLE I

COMPARISON OF RESULTS FOR TOTAL NITROGEN OBTAINED BY THE CLASSICAL KJELDAHL METHOD AND BY THE DIGESTION–IC METHOD[a] FOR TEN ACETIC ACID–SULFURIC ACID-DIGESTED GRAIN SAMPLES

Sample No.	NH_4 in digest (classical method) (ppm)	Total N (classical method) (%)	NH_4 in digest[a] (IC method) (ppm)	Total N (IC method) (%)
1	302.7	12.33	338.1	13.77
2	141.9	5.76	137.2	5.57
3	322.5	13.0	310.9	12.53
4	305.9	12.15	297.6	11.82
5	140.7	5.76	136.6	5.50
6	182.2	7.40	199.8	8.12
7	306.7	12.33	281.7	11.32
8	319.2	13.00	306.8	12.50
9	303.8	12.15	292.8	11.71
10	182.5	7.40	175.3	7.10

[a] Average of triplicate determinations.

The results obtained by the classical Kjeldahl digestion–distillation–titration procedure for four caprolactam samples digested using the potassium sulfate–sulfuric acid method were compared with those obtained by the digestion–IC method. The average difference between the two set of results was 10.4%. The method was also applied to the determination of total nitrogen in sewage sludges digested using a potassium sulfate–sulfuric acid mixture with a mercury(II) oxide catalyst. The results of the digestion–IC method showed an average difference of *ca.* 14% compared with those obtained by the classical Kjeldahl digestion–distillation–titration procedure.

CONCLUSIONS

The use of ion chromatography to determine total nitrogen as ammonium ion after sample digestion improves the speed of the analysis compared with the conventional Kjeldahl method by eliminating the need for the distillation step. As only very small volumes of samples are required for analysis, the weight of sample required for the digestion can be reduced, minimizing the amount of catalyst required, hence also reducing disposal costs. The modified ion chromatographic–Kjeldahl method showed reasonable agreement with the results obtained by conventional methods for total nitrogen analysis; the variation was between 5 and 14% depending on the sample type and digestion procedure used. The method was applied to the determination of total nitrogen in foods, organic compounds and sewage sludges and should also be applicable to a wide variety of other sample types.

ACKNOWLEDGEMENTS

The authors thank Gerard Bondoux, John Morawski and Mike Kennedy for helpful discussions.

REFERENCES

1 K. Helrich (Editor), *Official Methods of Analysis of the Association of Official Analytical Chemists*, AOAC, Arlington, VA, 15th ed., 1990, p. 72.
2 L. S. Clesceri, A. E. Greenberg and R. R. Trussell (Editors), *Standard Methods for the Examination of Water and Wastewater*, American Public Health Association, Washington, DC, 17th ed., 1989, pp. 4–144.
3 D. Mathe and C. Balas, *Proc. 104th A.O.A.C. Ann. Int. Meet. Exp., New Orleans, LA, 1990*, p. 188.
4 R. C. Bicsak, *Proc. 104th A.O.A.C. Ann. Int. Meet. Exp., New Orleans, LA, 1990*, p. 185.
5 S. Hughes, H. Kupka, H. P. Sieper and S. Hughes, *Proc. I.F.T. Annu. Meet., Anaheim, CA, 1990*, p. 107.
6 P. R. Haddad and P. E. Jackson, *Ion Chromatography–Principles and Applications (Journal of Chromatography Library*, Vol. 46), Elsevier, Amsterdam, 1990.
7 D. T. Gjerde and J. S. Fritz, *Ion Chromatography*, Hüthig, Heidelberg, 2nd ed., 1987.
8 G. E. P. Box, W. G. Hunter and J. S. Hunter, *Statistics for Experimenters: an Introduction to Design, Data Analysis and Model Building*, Wiley, New York, 1978, p. 97.

Journal of Chromatography, 546 (1991) 411–421
Elsevier Science Publishers B.V., Amsterdam

CHROMSYMP. 2108

Optimization of inorganic capillary electrophoresis for the analysis of anionic solutes in real samples

JOE ROMANO, PETR JANDIK, WILLIAM R. JONES and PETER E. JACKSON*[a]
Waters Chromatography Division of Millipore, 34 Maple Street, Milford, MA 01757 (U.S.A.)

ABSTRACT

Inorganic capillary electrophoresis (ICE) is a separation technique which offers many advantages for the analysis of anionic solutes in real samples. Parameters which influence ICE separations such as system configuration, choice of electrolyte anion, electrolyte pH and the addition of electroosmotic flow modifier were investigated and a number of electrolytes of varying mobilities were studied. Optimized conditions were established for the separation of inorganic anions, organic acids and alkylsulfonates and the technique was applied to the analysis of a variety of anionic solutes in several complex sample matrices.

INTRODUCTION

Ion chromatography (IC) has seen remarkable growth since the introduction of the technique in 1975 [1]. Perhaps the greatest reason for this growth has been the ability to provide rapid and simple solutions to a large number of analytical problems, particularly the determination of inorganic anions and short-chained carboxylic acids. The technique of IC has expanded significantly to encompass a wide variety of separation and detection methods and is now extensively used in application areas such as water, environmental, industrial, food and clinical analysis [2].

Capillary zone electrophoresis (CZE) is a relatively new separation technique which has also been demonstrated to be applicable to the quantitation of inorganic anions and short-chained carboxylic acids. This technology utilizes narrow diameter capillaries (typically polyimide-coated, 50–100 μm fused-silica) and ionic species are separated according to their mobility under the influence of an applied potential (usually 10–30 kV). In CZE, the direction and magnitude of the bulk fluid flow, or electroosmotic flow (EOF), is dictated by the charge on the inner wall of the capillary [3]. In conventional CZE using a fused-silica capillary, the direction of the EOF is toward the negative electrode at most pH values, hence detection is carried out at this end. Under the influence of an applied potential, inorganic anions migrate rapidly toward the positive (non-detection) electrode and are typically not quantitated as they have excessive migration times or are not eluted at all. Only anions with a mobility less than that of the EOF can be determined using this approach. However, the addition of

[a] Present address: Millipore Pty. Ltd., Private Bag 18, Lane Cove, NSW 2066, Australia.

0021-9673/91/$03.50

a cationic surfactant such as cetyltrimethylammonium bromide to the electrolyte has been demonstrated to significantly reduce migration times for small anionic species by the reducing or reversing the electroosmotic flow [3–5]. Detection of inorganic anions and short-chained carboxylic acids in CZE is carried out using similar strategies to those employed in ion chromatography for solutes which are typically non-UV absorbing. Conductivity [5,6] and both indirect fluorescence [7,8] and indirect UV absorbance [9,10] have all been used for the CZE determination of low-molecular-weight anionic species.

The combination of using a fused-silica capillary with an electrolyte containing a UV absorbing anion plus an electroosmotic flow modifier and indirect photometric detection has recently been termed "inorganic capillary electrophoresis" or ICE [11]. Determination of complex ionic mixtures with analysis times under five minutes and separation efficiences greater than 250 000 plates have been demonstrated using this analytical approach. There are a number of advantages of this approach for anion analysis. Ions are separated according to their mobilities resulting in different selectivities when compared to IC. Extremely efficient separations give more peak information from nanoliter sample volumes with ultra fast analysis times. Also, the instrumentation is very simple and allows rapid methods development.

This study is primarily concerned with parameters that influence the separation in ICE in order to optimize the analysis of anionic solutes in complex sample matrices. The differences (and similarities) between inorganic capillary electrophoresis and ion chromatography will be also discussed.

EXPERIMENTAL

Instrumentation

The capillary electrophoresis instrument used was a Quanta 4000 (Waters Chromatography Division of Millipore, Milford, MA, U.S.A.) with either a Waters 840 or 820 data station. It proved necessary to collect data at 20 points per second due to the very narrow peak widths resulting in ICE. The separations were carried out using a conventional fused-silica capillary (60 cm × 75 μm I.D.) obtained from Waters. While the Quanta 4000 is capable of both hydrostatic and electromigration injections, hydrostatic injection was used as the sample introduction mode for all this work. Typically the sample was elevated at 10 cm for 30 s. Electrolytes were prepared daily, filtered and degassed with a Waters solvent clarification kit. Detection was carried out using indirect photometry at 254 nm. Specific operating conditions are provided as captions to the figures.

Reagents

Purified (18 MΩ) water using a Millipore Milli-Q water purification system (Bedford, MA, U.S.A.) was used for all solutions. Sodium chromate tetrahydrate and the alkylsulphonate standards were obtained from Aldrich; potassium hydrogen phthalate and benzoic acid were obtained from Sigma and 1-naphthalenesulphonic acid (technical grade) was obtained from Kodak. Acetonitrile (HPLC grade) was obtained from J. T. Baker, as were the analytical-grade sodium salts used for the preparation of all the anion standards. C_{18} Sep-Pak cartridges were obtained from Waters and the electroosmotic flow modifier, Nice-Pak OFM Anion BT, is a propriety chemical obtained from Waters.

RESULTS AND DISCUSSION

Instrumental configuration for ICE

The system configuration for the analysis of anionic species by ICE differs from the approach taken in conventional CZE in that detection is carried out at the anodic (positive) electrode and injection is carried out at the cathodic (negative) electrode. The instrumentation for ICE has been described previously [11]. Sample introduction into the capillary differs from that used in IC or HPLC in that no injection valve is used. The most common mode is a hydrostatic (or gravity) injection as this mode, unlike electromigration, introduces a representative sample to the capillary. Electromigration injection involves applying a voltage to the sample in order to force the ions to migrate into the capillary. This injection mode is selectively biased toward faster migrating ions [12]. Hydrostatic injection was used as the sample introduction mode for all this work. As a matter of convention throughout this paper, the power supply used in the ICE configuration (*i.e.*, detection at the anodic electrode) will be referred to as negative. Unless otherwise indicated, the separations in this work were carried out with a cationic surfactant, Nice-Pak OFM Anion BT (patent applied for), added to the electrolyte in order to reverse the direction of the EOF [11]. The high mobility of inorganic anions in the same direction as the EOF (toward the negative electrode) enables very rapid, high efficiency separations to be obtained in ICE. As detection for all the separations was carried out by indirect photometry at 254 nm, electrolytes were chosen on the basis of both mobility and detection properties.

Anion selectivity by ICE

The selectivity for anion separations using ICE differs significantly from that obtained using conventional anion-exchange columns in IC. In an anion-exchange separation, cations and neutral species elute at the void volume of the column. Short-chained monocarboxylic acids and weakly retained anions, such as fluoride and methanesulphonate, are all eluted early and tend to be poorly resolved in many instances. Also, the presence of elevated carbonate and/or high levels of sample cations may further complicate the early portion of the chromatogram. The use of gradient [13] or coupled [14] IC can often overcome these resolution problems, however, both of these approaches are somewhat complex. A separation of inorganic anions and short-chained carboxylic acids obtained using ICE exhibits several significant differences from that obtained using an anion-exchange separation in IC. First, cations do not participate in the separation since they travel in the opposite direction to the anions. As the inorganic anions have high charge-to-ionic radii ratios, they tend to migrate much faster than weak acid anions and are well resolved from these species. Neutral solutes are carried along by the EOF and have appreciably longer migration times, however, these can be simply purged from the capillary once the desired separation is obtained. Fig. 1 shows an electropherogram of low ppm levels of the seven inorganic anions most commonly analyzed in IC [2] obtained using ICE with an electrolyte containing electroosmotic flow modifier (Nice-Pak OFM Anion BT) and the highly mobile chromate anion. All peaks are well resolved in under four minutes with this electrolyte. The retention order for these anions using an ion-exchange separation and an eluent at a pH of 8.5 would be fluoride, chloride, nitrite, bromide, nitrate, phosphate and sulphate. The "tailing" of the fluoride and phosphate peaks

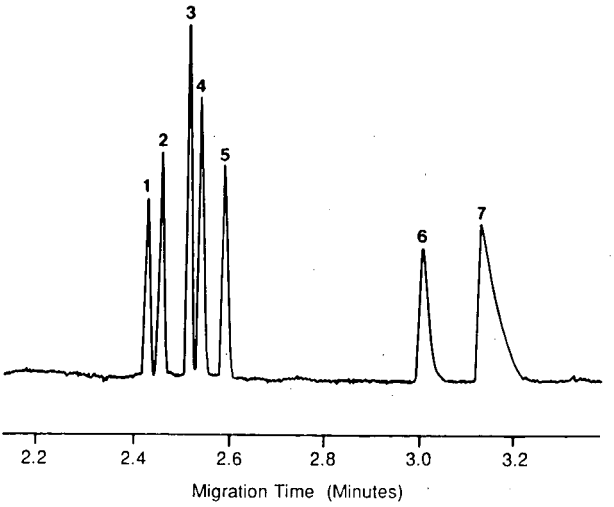

Fig. 1. Electropherogram of standard anions. Conditions, capillary: 60 cm × 75 μm I.D. fused-silica; power supply: negative; electrolyte: 5 m*M* chromate with Nice-Pak OFM Anion BT (patent applied for) at pH 8.0; injection: hydrostatic for 30 s; detection: indirect UV at 254 nm; solutes: 1 = bromide (4 ppm); 2 = chloride (2 ppm); 3 = sulphate (4 ppm); 4 = nitrite (4 ppm); 5 = nitrate (4 ppm); 6 = fluoride (1 ppm); 7 = phosphate (6 ppm).

occurs as a result of these peaks having a lower mobility than the electrolyte (chromate) anion. Solute anions with a higher mobility than the electrolyte anion exhibit "fronting" while solutes with a lower mobility than the electrolyte anion show tailing, as predicted by Mikkers *et al.* [9]. Optimal peak shape results if the electrolyte and solute anions have equivalent mobilities. The chromate anion has a mobility similar to that of bromide as indicated by peak shapes shown in Fig. 1 and is sufficiently absorbing at 254 nm to allow sensitive indirect photometric detection. These selectivity differences, along with rapid run times, high efficiencies and low sample and reagent consumption make ICE an ideal tool for practical analyses.

Practical applications using ICE

Fig. 2 shows a standard separation of chloride, sulphate, citrate, C_1–C_4 carboxylic acids and carbonate obtained using the same chromate electrolyte as above. This particular combination of solutes would be impossible to separate isocratically by IC as citrate is generally very strongly retained while the carboxylic acids are all weakly retained. Typically, a strong eluent species such as phthalate [15] is required to elute citrate in IC and such an eluent would result in poor resolution of the carboxylic acids.

Kraft black liquor is a complex sample from the pulp and paper industry which contains high concentrations of anions and organic acids in a high pH matrix. This sample is difficult to analyze by IC as the species of interest range from weakly retained organic acids such as formate and acetate to very strongly retained anions such as thiosulphate. Two isocratic separations (anion-exchange and ion exclusion) are typically used to quantitate the anions and organic acids in black liquor by IC [16]. Fig. 3 shows an ICE separation of a black liquor sample (diluted 1:1000 followed by

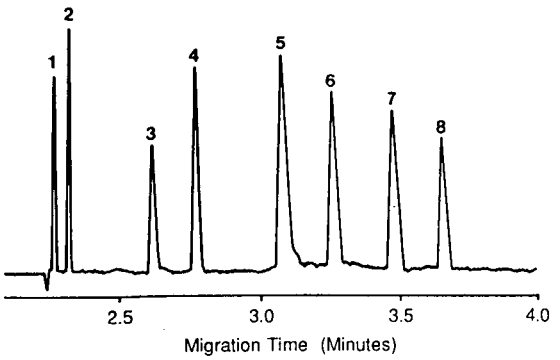

Fig. 2. Electropherogram of standard anions and organic acids. Conditions as for Fig. 1 except, solutes: 1 = chloride (2 ppm) and 4 ppm each of 2 = sulphate; 3 = citrate; 4 = formate; 5 = carbonate; 6 = acetate; 7 = propionate; 8 = butyrate.

C_{18} Sep-Pak clean-up) using the high mobility chromate electrolyte at pH 10.0. Thiosulphate, chloride, sulphate, oxalate, formate, carbonate, acetate, propionate and butyrate were present in the sample, along with several unidentified peaks. The less mobile species (formate, acetate, etc.) all show peak tailing as expected when using a chromate electrolyte. Sulphite, which also may be of interest in such samples, can be stabilized by the addition of mannitol and is well resolved from both oxalate and formate under these conditions.

The high mobility chromate electrolyte is of limited utility for the separation of lower mobility anions and organic acids. A lower mobility electrolyte anion, phthalate, was then employed in an attempt to better resolve a wider range of organic acids. An example of an electropherogram using a phthalate electrolyte at pH 5.6 is shown in Fig. 4. Formic, succinic, acetic, lactic, propionic and butyric acids (and phosphate) are well separated at this electrolyte pH. Variation of the electrolyte pH can be used to readily alter the migration times of weak acids, especially polyprotic acid anions such as phosphate. The higher the electrolyte pH, the more "ionized" is the solute, hence the greater its mobility. The determination of the organic acids shown in Fig. 4a in plaque is of interest in tooth decay research. Fig. 4b shows a electropherogram of a dental

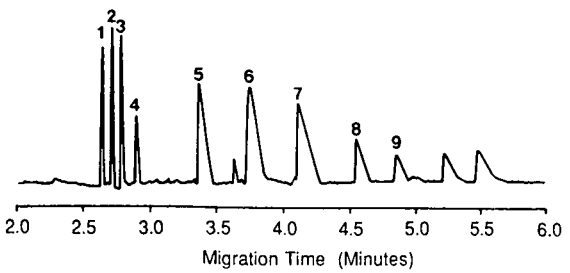

Fig. 3. Electropherogram of Kraft black liquor. Conditions as for Fig. 1 except, electrolyte: 5 m*M* chromate with Nice-Pak OFM Anion BT at pH 10.0; injection: hydrostatic for 20 s; sample preparation: 1000 × dilution in deionized water, solutes: 1 = thiosulphate; 2 = chloride; 3 = sulphate; 4 = oxalate; 5 = formate; 6 = carbonate; 7 = acetate; 8 = propionate; 9 = butyrate.

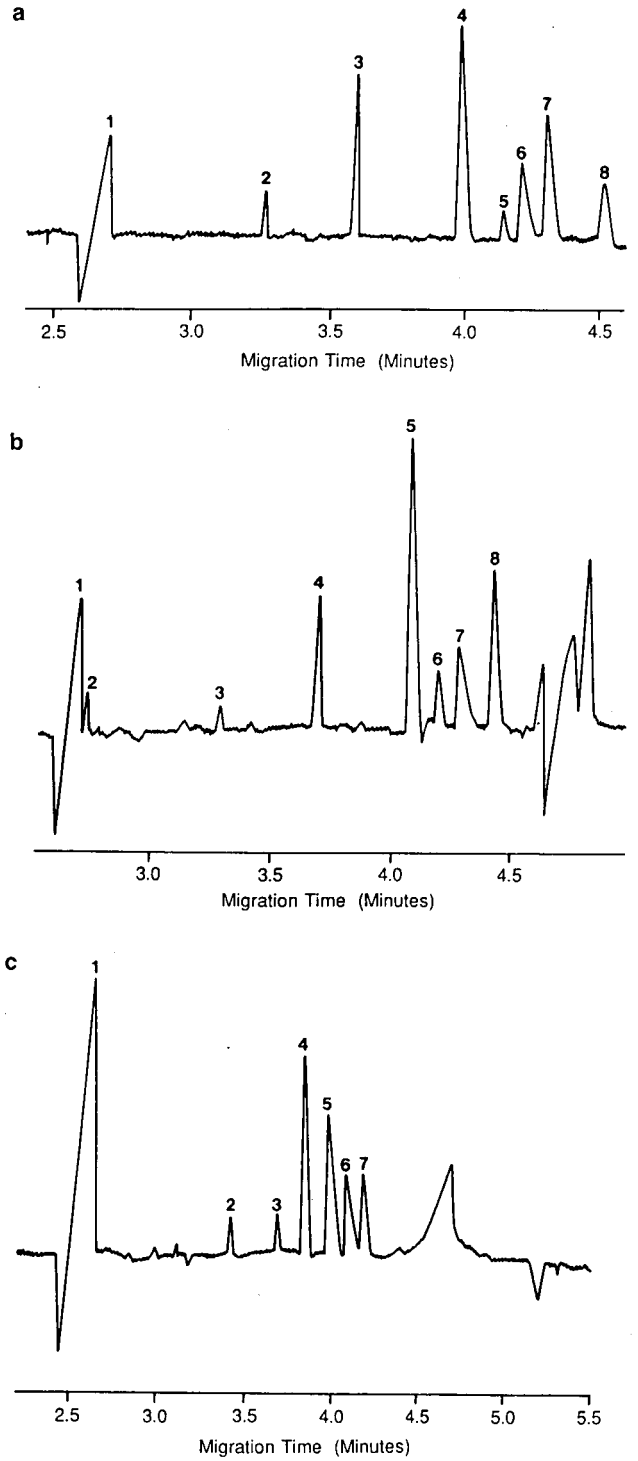
a
1
2
3
4
5
6
7
8
2.5
3.0
3.5
4.0
4.5
Migration Time (Minutes)
b
1
2
3
4
5
6
7
8
3.0
3.5
4.0
4.5
Migration Time (Minutes)
c
1
2
3
4
5
6
7
2.5
3.0
3.5
4.0
4.5
5.0
5.5
Migration Time (Minutes)

Fig. 4.

plaque extract run under the same conditions as the above standard. While similar separations can be achieved using ion-exclusion chromatography [17] or gradient IC [14], ICE is particularly appropriate for this analysis as the volume of sample obtained is limited to approximately 1 μl per patient. Injection volumes in ICE are usually in the order of 10–50 nl. A similar group of organic acids can also be found in saliva, Fig. 4c shows a electropherogram of a 1:10 dilution of a saliva sample using the phthalate electrolyte. The negative peaks in the sample electropherograms are anionic species (unidentified) which must absorb more than phthalate at 254 nm.

The peak shape of the later migrating solutes in Fig. 4a–c can be improved by selecting a still less mobile electrolyte anion. Fig. 5a shows a separation of a similar group of organic acids to those shown in Fig. 4a using a low mobility benzoate electrolyte. Acids such as butyric and caproic give Gaussian peak shapes with this electrolyte while the (relatively) more mobile acids such as formate exhibit fronting. The ICE separation of any group of solutes can be readily optimized by selecting an electrolyte anion with a mobility closely matched to the ions of interest. If a sample contains ions of widely varying mobilities, it can simply be analyzed using more than one electrolyte as the run times in ICE are so short and there is only a two-minute purge required between changing electrolytes. As the same concentration of the electro-osmotic flow modifier is used in the different mobility electrolytes, migration time stability is established within one run when changing between electrolytes. Fig. 5b shows an electropherogram of a diluted butyric acid extract of an air (filter) sample using the benzoate electrolyte; glycolate, acetate and valerate were present, along with two unidentified organic acids and a large butyric acid peak.

The same low mobility electrolyte (benzoate) can be used for the separation of short (C_1–C_7) chained linear alkylsulphonates as shown in the electropherogram in Fig. 6a. This analysis can be used for the determination of alkylsulphonates in a 0.1% dilution of an isopropyl alcohol process extract from a petroleum refinery as shown in Fig. 6b. The large peak at the start of the electropherogram is sulphate as the undiluted sample contained 60% sulphuric acid along with various crude petroleum fractions. A simple dilution and filtration was all the sample preparation necessary for this relatively complex matrix. ICE separations are less affected by sample pH than IC, however, resolution (and migration times) are somewhat dependent upon sample loading. High ionic strength samples will cause a shift in migration times, *e.g.*, compare the migration times of butanesulphonate in Fig. 6a (peak 4) and Fig. 6b (peak 2). Calibration curves in ICE are linear up to approximately 200 ppm [18] depending upon the analyte and the electrolyte being used.

Fig. 4. (a) Electropherogram of organic acid (and phosphate) standard with phthalate electrolyte. Conditions as for Fig. 1 except, electrolyte: 5 m*M* phthalate with Nice-Pak OFM Anion BT at pH 5.6; solutes: 1 = chloride; 2 = formate (0.167 μM); 3 = succinate (0.167 μM); 4 = acetate (0.178 μM); 5 = lactate (0.167 μM); 6 = phosphate (0.167 μM); 7 = propionate (0.175 μM); 8 = butyrate (0.175 μM). (b) Electropherogram of dental plaque extract. Conditions as above except, solutes: 1 = chloride; 2 = sulphate; 3 = formate (0.015 μM); 4 = succinate (0.042 μM); 5 = acetate (0.441 μM); 6 = lactate (0.021 μM); 7 = phosphate (0.081 μM); 8 = propionate (0.164 μM). (c) Electropherogram of human saliva. Conditions as above except, sample preparation: 10 × dilution in deionized water; solutes: 1 = chloride; 2 = formate (0.023 μM); 3 = succinate (0.013 μM); 4 = acetate (0.427 μM); 5 = lactate (0.167 μM); 6 = phosphate (0.101 μM); 7 = propionate (0.115 μM).

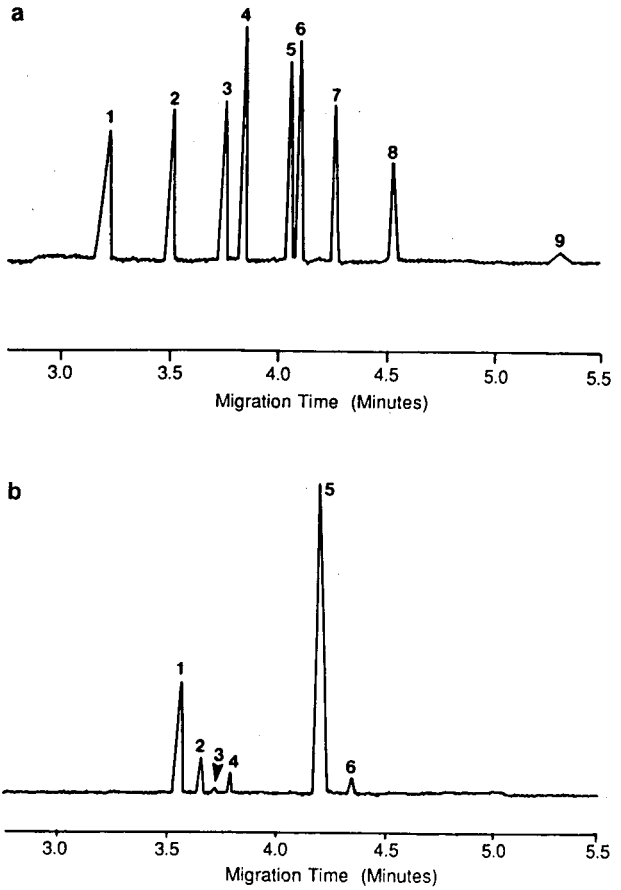

Fig. 5. (a) Electropherogram of organic acid (and phosphate) standard with benzoate electrolyte. Conditions as for Fig. 1 except, electrolyte: 10 m*M* benzoate with Nice-Pak OFM Anion BT at pH 6.0; solutes: 10 ppm each of 1 = formate; 2 = succinate; 3 = glycolate; 4 = acetate; 5 = phosphate; 6 = propionate; 7 = butyrate; 8 = caproate; 9 = caprylate. (b) Electropherogram of butyric acid extract of an air (filter) sample. Conditions as above except, sample preparation: 5000 × dilution in deionized water; solutes: 1 = unknown; 2 = unknown; 3 = glycolate (0.4 ppm); 4 = acetate (1.1 ppm); 5 = butyrate (55.1 ppm); 6 = unknown.

The last peak in the standard pherogram shown in Fig. 6a, a C_7 sulphonate, is poorly shaped with the benzoate electrolyte while C_8 sulphonate is not eluted at all under these electrolyte conditions. Attempts to use a still lower mobility electrolyte anion than benzoate for longer chain alkylsulphonates proved unsuccessful as resolution was limited by poor peak shape. The approach taken for such low mobility solutes was to use a conventional CZE configuration, *i.e.*, a positive polarity power supply and no electroosmotic flow modifier added to the electrolyte. The use of a very low mobility, UV absorbing electrolyte anion such as naphthalenesulphonate permits the analysis of anionic alkylsulphonates because their migration toward the (positive) anode due to the applied potential is less than the mobility of the bulk electroosmotic

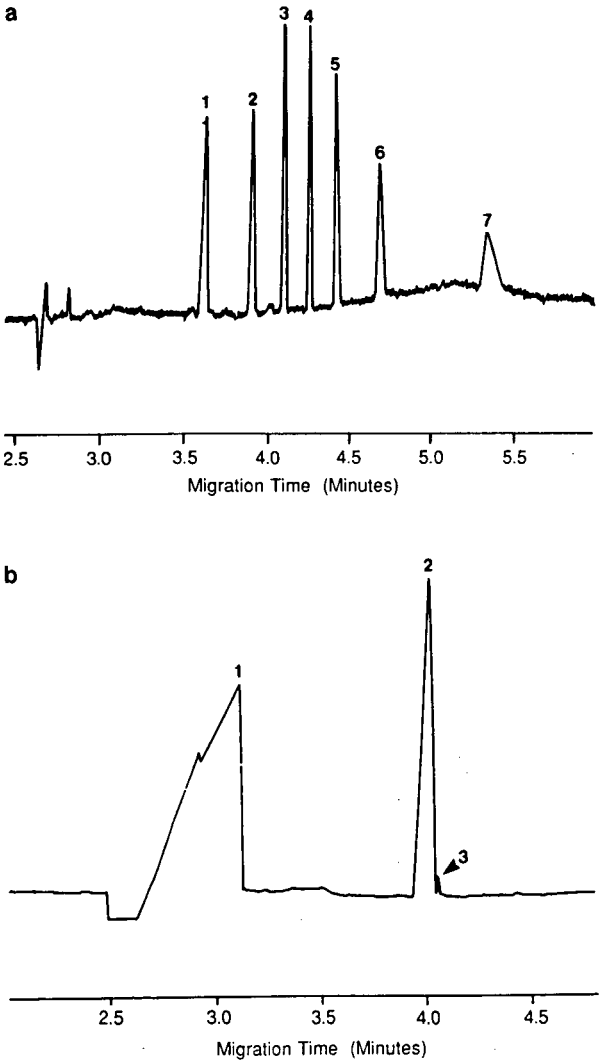

Fig. 6. (a) Electropherogram of C_1–C_7 alkylsulphonate standard with benzoate electrolyte. Conditions as for Fig. 5 except, solutes: 10 ppm each of 1 = methanesulphonate; 2 = ethanesulphonate; 3 = propanesulphonate; 4 = butanesulphonate; 5 = pentanesulphonate; 6 = hexanesulphonate; 7 = heptanesulphonate. (b) Electropherogram of an isopropyl alcohol process extract from a petroleum refinery. Conditions as above except, sample preparation: 1000 × dilution in deionized water; solutes: 1 = sulphate; 2 = propanesulphonate (137.7 ppm); 3 = butanesulphonate (2.4 ppm).

flow toward the (negative) cathode. Hence they can be detected by indirect photometry at the cathodic end of the capillary. A electropherogram of a standard separation of C_4–C_{12} alkylsulphonates obtained using this approach is shown in Fig. 7a. Note that the less mobile anionic species are eluted first under these conditions as they are carried further toward the cathode than more mobile anionic species. Very mobile anions such

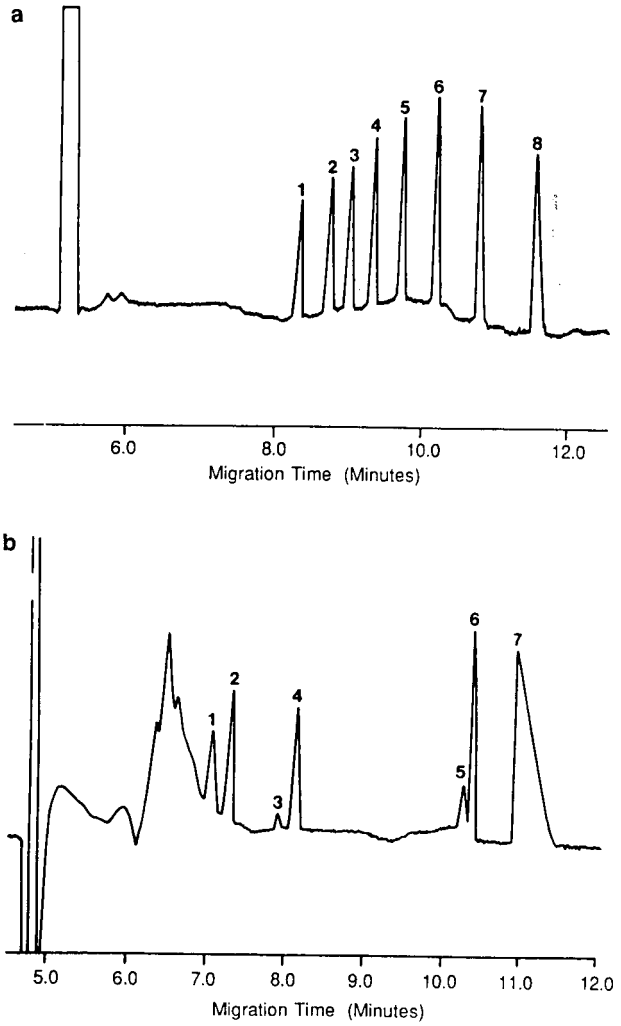

Fig. 7. (a) Electropherogram of C_4–C_{12} alkylsulphonate standard with naphthalenesulphonate electrolyte. Conditions as for Fig. 1 except, power supply: positive; electrolyte: 10 m*M* naphthalenesulphonate with 30% acetonitrile at pH 10.0; solutes: 25 ppm each of 1 = C_{12}-sulphonate; 2 = C_{10}-sulphonate; 3 = C_9-sulphonate; 4 = C_8-sulphonate; 5 = C_7-sulphonate; 6 = C_6-sulphonate; 7 = C_5-sulphonate; 8 = C_4-sulphonate. (b) Electropherogram of an alkylamido glycinate shampoo base. Conditions as above except, sample preparation: 200 × dilution in deionized water; solutes: 1 = C_{10}-sulphonate (27.7 ppm); 2 = C_9-sulphonate (37.0 ppm); 3 = C_7-sulphonate (3.4 ppm); 4 = C_6-sulphonate (25.6 ppm); 5–7 = unknowns.

as chloride do not appear in the electropherogram as their mobility exceeds that of the EOF, hence they are not detected at the cathode. This method can be applied to the determination of several alkylsulphonates in a glycinate shampoo base as shown in Fig. 7b. No sample pretreatment other than dilution was required.

CONCLUSIONS

Inorganic capillary electrophoresis is an powerful separation technique which offers many advantages for the analysis of inorganic and organic acid anions in real samples. Rapid, highly efficient separations with different selectivities (compared to ion chromatography) are obtained from nanoliter sample volumes. A separation can be readily optimized for a particular analysis by choosing an electrolyte anion with a mobility similar to the analytes of interest and changing electrolytes is simply a matter of purging the capillary between successive samples. The utility of the technique was demonstrated by analyzing anionic species such as inorganic anions, organic acids and alkylsulphonates in several complex sample matrices.

REFERENCES

1 H. Small, T. Stevens and W. Bauman, *Anal. Chem.*, 47 (1975) 1801.
2 P. R. Haddad and P. E. Jackson, *Ion Chromatography: Principles and Applications* (*Journal of Chromatography Library*, Vol. 46), Elsevier, Amsterdam, 1990.
3 T. Tsuda, *J. High Resolut. Chromatogr. Chromatogr. Commun.*, 10 (1987) 622.
4 K. D. Altria and C. F. Simpson, *Chromatographia*, 24 (1987) 527.
5 X. Huang, J. A. Luckey, M. J. Gordon and R. N. Zare, *Anal. Chem.*, 61 (1989) 766.
6 X. Huang, M. J. Gordon and R. N. Zare, *J. Chromatogr.*, 480 (1989) 285.
7 L. Gross and E. S. Yeung, *J. Chromatogr.*, 480 (1989) 169.
8 W. G. Kuhr and E. S. Yeung, *Anal. Chem.*, 60 (1988) 2642.
9 F. E. P. Mikkers, F. M. Everaerts and Th. P. E. M. Verheggen, *J. Chromatogr.*, 169 (1979) 11.
10 F. Foret, S. Fanali, L. Ossicini and P. Bocek, *J. Chromatogr.*, 470 (1989) 299.
11 W. R. Jones and P. Jandik, *Am. Lab.*, June (1990) 51.
12 X. Huang, M. J. Gordon and R. N. Zare, *Anal. Chem.*, 60 (1988) 375.
13 R. D. Rocklin, C. A. Pohl and J. A. Schibler, *J. Chromatogr.*, 411 (1987) 107.
14 W. R. Jones, P. Jandik and M. Swartz, *J. Chromatogr.*, 473 (1989) 171.
15 *Waters ILC Series Application Brief No. 4004*, Waters, Milford, MA, 1985.
16 G. O. Franklin, *Tappi*, 65 (1982) 107.
17 P. Walser, *J. Chromatogr.*, 439 (1988) 71.
18 B. F. Kenney, *J. Chromatogr.*, 546 (1990) 423.

Journal of Chromatography, 546 (1991) 423–430
Elsevier Science Publishers B.V., Amsterdam

CHROMSYMP. 2113

Determination of organic acids in food samples by capillary electrophoresis

BEVERLY F. KENNEY
Waters Chromatography Division, Millipore Corporation, 34 Maple Street, Milford, MA 01757 (U.S.A.)

ABSTRACT

Capillary electrophoresis and a new separation chemistry were investigated for the determination of organic acids in food samples. Features of this approach include minimal sample preparation, excellent specificity, low cost of operation and application to a variety of food matrices. The method is quantitative, with recoveries in the range 97–103%, and linear over more than one order of magnitude, and the precision is better than 2–14% for real samples. The chemistry, with slight modifications, can be applied to other ions in many types of matrices.

INTRODUCTION

Measuring organic acid levels in foods and beverages is important from the standpoint of monitoring the fermentation process, checking product stability, validating the authenticity of juices and concentrates and studying the organoleptic properties of fermented products.

Other methods of analysis can be tedious and cost-ineffective. For example, enzyme assay requires separate kits for each acid, which slows down throughput and increases the cost per test for a multiple acid determination. It had been hoped that simultaneous acid determinations with appropriate instrumentation would be an acceptable solution. However, the current instrumental methods are not without limitations.

For example, high-performance liquid chromatographic (HPLC) separations based on ion-exclusion or ion-suppression columns with UV absorbance (typically at 214 nm) or refractive index detection suffer from carbohydrate and phenolic interferences from the sample. Approaches to minimize this lack of specificity include use of two analytical columns with meticulous data handling [1] or multi-step and multi-device sample preparation [2]. These two solutions add to the cost and tedium of analysis. Another instrumental approach, ion chromatography (IC) with conductivity detection, suffers from inorganic ion interferences, which necessitate the use of a gradient or multiple isocratic separations. Also, organic substances in the matrix need to be removed by sample preparation as a limited column lifetime or complicated chromatogram may result [3]. In addition, with both HPLC and IC, very little can be done to manipulate the selectivity as the analytical columns are used with simple

0021-9673/91/$03.50

buffers or dilute acid only. Therefore, it is difficult to optimize the separation for specific analytes from specific matrices.

The above discussion implies the need for alternative methods for organic acids. Capillary electrophoresis (CE), as a new and powerful separation technique, proved to be a good choice for investigation. Part of the power of CE is its unique selectivity; sample components are separated based on their charge. Therefore, negatively charged species (*e.g.*, organic acids) migrate away from more neutral and positively charged species (*e.g.*, sugars and phenolics). Also, with CE, a large number of theoretical plates is possible for the separation. The separation efficienty, N, is typically in the range 100 000–200 000, compared with 5000–10 000 for HPLC or IC [4].

A new separation chemistry for anion separation by CE has been used for organic acid separations. Known as NICE-Pak™ Chemistry, it separates strongly and weakly charged anions such as inorganics, carboxylic acids and alkylsulfonates.

The NICE-Pak Chemistry includes a fused-silica capillary and an electrolyte which contains an osmotic flow modifier. This modifier serves to direct bulk flow of electrolyte towards the anode for fast detection of the anions. The other chemical component of the electrolyte can vary according to the anionic species and sample matrices of interest. It will, however, contain a UV chromophore which absorbs at 254 nm. This type of detection is indirect, that is, the anions absorb less UV radiation than the electrolyte yielding a negative response in the detector. Positive peaks appear on the electopherogram (comparable to a chromatogram) by reversing the detector signal cables to the data device. Those sample components which absorb more UV light than the electrolyte appear as negative peaks.

Other parameters that can be optimized for the separation include electrolyte pH and voltage applied to the system. A change in pH will affect the mobility of the analytes and therefore their migration. Both efficiency and migration time are affected by a change in applied voltage. Therefore, many variables can be used to enhance the separation of sample components.

Samples are automatically introduced into the capillary hydrostatically, that is, by immersing the injection end of the capillary into the sample and raising both by 10 cm for a user-specified period of time. This results in an injection volume of a few nanoliters. This approach to anion determination is quantitative, with reproducibility, linearity and sensitivity comparable to those of other instrumentation techniques [3].

As described, there is flexibility within NICE-Pak Chemistry, including choice of capillary length, applied voltage, electrolyte pH and UV absorber. The following organic acids separation resulted by optimizing these parameters.

EXPERIMENTAL

Chemicals

All water was provided by a Milli-Q Plus water purification system (Millipore, Bedford, MA, U.S.A.). All standards and phthalic acid, monopotassium salt, were obtained from Sigma (St. Louis, MO, U.S.A.). The OFM™ Anion-BT (Osmotic Flow Modifier Anion-BT) reagent (part of NICE-Pak Chemistry) was provided by Waters Chromatography Division of Millipore (Milford, MA, U.S.A.).

Samples and preparation

Samples were purchased at local grocery and liquor stores. They were diluted to appropriate concentrations with water and, when indicated, mixed with an internal standard, butyric acid (100 μg/ml). The only clean-up necessary was microfiltration through a 0.45-μm Millex HV filter (Millipore) when pulp was present in the sample.

Capillary electrophoresis

The instrument, a Quanta™ 4000 capillary electrophoresis system, was interfaced to an 820 Maxima Workstation via a System Interface Module (all from Waters Chromatography Division). The capillary (100 cm × 75 μm I.D.) was constructed of fused silica. The electrolyte consisted of 0.5 m*M* OFM Anion-BT–5 m*M* potassium phthalate (pH 7.0). The applied voltage was 20 000 V using the negative power supply and the injection time was 45 s.

RESULTS AND DISCUSSION

Separation

The electropherogram of citric, tartaric, malic, succinic, acetic and lactic acid and the internal standard butyric acid is shown in Fig. 1. Other inorganic and organic anions that have been characterized by this method are listed in Table I. The migration times were normalized to that of butyric acid. Also listed are equivalent conductance values, which relate directly to the mobilities of the ions. A general pattern that inversely relates migration time to equivalent conductance is indicated. Therefore, anion migration patterns with CE are reasonably predictable. Also, as the equivalent conductances for malic and succinic acid are identical (58.8), their separation is close. Orotic acid yields a negative peak as it absorbs more UV radiation at 254 nm than does the electrolyte. Fumaric acid does not respond under these specific conditions.

For maximum reproducibility of migration time, the use of an internal standard is necessary. For example, the data in Table II compare migration time reproducibility with a without an internal standard, both on a single day (within-run) and on five

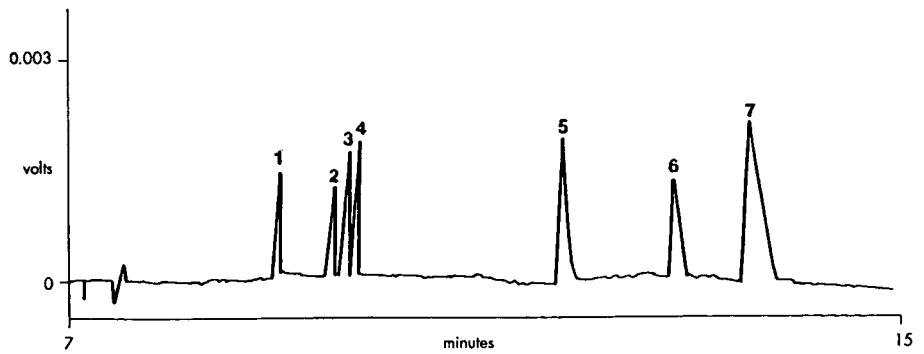

Fig. 1. Electropherogram of a standard mixture. Peaks: 1 = citric acid, monohydrate; 2 = tartaric acid, disodium salt; 3 = malic acid, sodium salt; 4 = succinic acid, calcium salt, monohydrate; 5 = acetic acid; 6 = lactic acid (all 20 μg/ml); 7 = butyric acid (internal standard, 50 μg/ml).

TABLE I

RELATIVE MIGRATION TIMES AND EQUIVALENT CONDUCTANCES

Entries in italics are those from the standard in Fig. 1.

Analyte	Relative migration time[a]	Equivalent conductance[b]
Bromide	0.568	78.1
Chloride	0.577	76.3
Sulfate	0.605	80.0
Nitrite	0.608	71.8
Nitrate	0.617	71.4
Oxalic	0.630	74.1
Sulfite	0.669	79.9
Citric	*0.676*	*70.2*
Tartaric	*0.725*	*59.6*
Fluoride	0.730	55.4
Formic	0.733	54.6
Malic	*0.736*	*58.8*
Succinic	*0.743*	*58.8*
Ketoglutaric	0.743	
Phosphate	0.797	33.0
Carbonate	0.834	69.3
Acetic	*0.868*	*40.9*
Pyruvic	0.877	
Propionic	0.934	35.8
Lactic	*0.950*	*38.8*
Butyric	*1.000*	*32.6*
Orotic[c]	1.023	
Quinic	1.095	
Shikimic	1.095	
Gluconic	1.101	
Fumaric	No response	61.8

[a] Relative to butyric acid.
[b] From ref. 5.
[c] Negative peak.

TABLE II

REPRODUCIBILITY OF MIGRATION TIME WITH AND WITHOUT AN INTERNAL STANDARD (I.S.) AND WITHIN RUN AND BETWEEN RUN (R.S.D., %)

Analyte	Without I.S.	With I.S.
Within-run, n = 10[a]		
Citric acid	0.5	0.3
Succinic acid	0.2	0.3
Lactic acid	0.1	0.1
Between-run, n = 5[b]		
Citric acid	3.1	0.8
Succinic acid	3.2	0.6
Lactic acid	3.6	0.1

[a] Single day, same electrolyte.
[b] Five days, five electrolyte batches.

different days, with five different electrolyte batches (between-run). The relative standard deviation (R.S.D.) is much lower with the internal standard, especially day-to-day. Butyric acid acts as an internal standard as it does not occur naturally in many beverage products.

Linearity of the method was evaluated between 10 and 167 μg/ml with respect to both area and height response. As the correlation coefficient for peak area (0.999) is much better than that for peak height (0.962), the best results are obtained by an area calculation. The detection limit is 1 μg/ml using a signal-to-noise ratio of 3:1.

Sample analysis

Sample preparation, usually a deterrent to the success of an analytical method owing to complexity and cost, appears to be a small issue with this approach. For example, Fig. 2 shows the separation of organic acids in apple juice. The sample is simply diluted with water, internal standard is added and the mixture is injected. Not even filtration is needed. Sugars and phenolics remain in the capillary at the end of the analysis. Programming the autopurge function on the Quanta 4000 cleans the capillary of those compounds prior to the next injection.

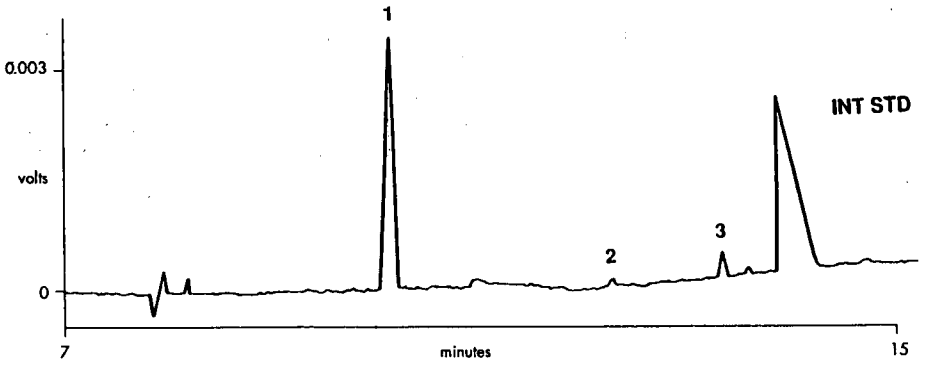

Fig. 2. Electropherogram of apple juice. Sample preparation: dilute and inject. Peaks: 1 = malic acid, 4352 μg/ml; 2 = acetic acid, 48 μg/ml; 3 = lactic acid, 254 μg/ml; INT STD = Internal standard.

Some samples, such as pulp containing large particles. It is then necessary to apply microfiltration to remove such large insolubles from the matrix. This approach works well for orange, grapefruit and tomato juice. The juice is first diluted with water, filtered (0.45-μm Millex HV), then the internal standard is added. Fig. 3 shows an electropherogram of tomato juice, prepared as just described. Chloride in the juice is also identified.

For a few samples, butyric acid is not a good choice of internal standard as it occurs naturally. Fig. 4 shows te separation of acids in soy sauce diluted 1:500 with water. Butyric acid is evident in the electropherogram. Also evident is a huge response for chloride, as would be expected in this sample.

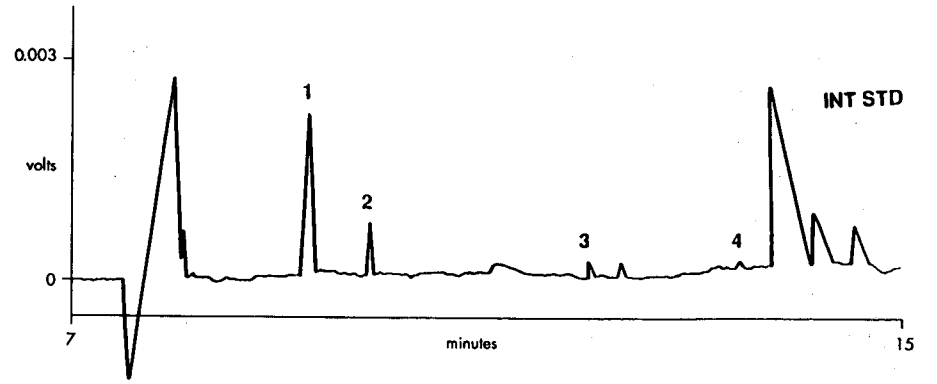

Fig. 3. Electropherogram of tomato juice. Sample preparation: dilute, filter and inject. Peaks: 1 = Citric acid, 3579 μg/ml; 2 = malic acid, 404 μg/ml; 3 = acetic acid, 99 μg/ml; 4 = lactic acid, 69 μg/ml. The large peak on the left is chloride.

Precision and recovery

Results of reproducibility and recovery studies using wine and dark grape juice samples are given in Tables III and IV. Fig. 5 shows an electropherogram for a Chablis wine sample generated after simple dilution. Reproducibility data for ten different analyses of the same wine showed an acceptable R.S.D., especially for tartaric and malic acid (<2%) (Table III). It should be noted that the chosen dilution optimizes the resolution of tartaric, malic and succinic acid and a smaller dilution

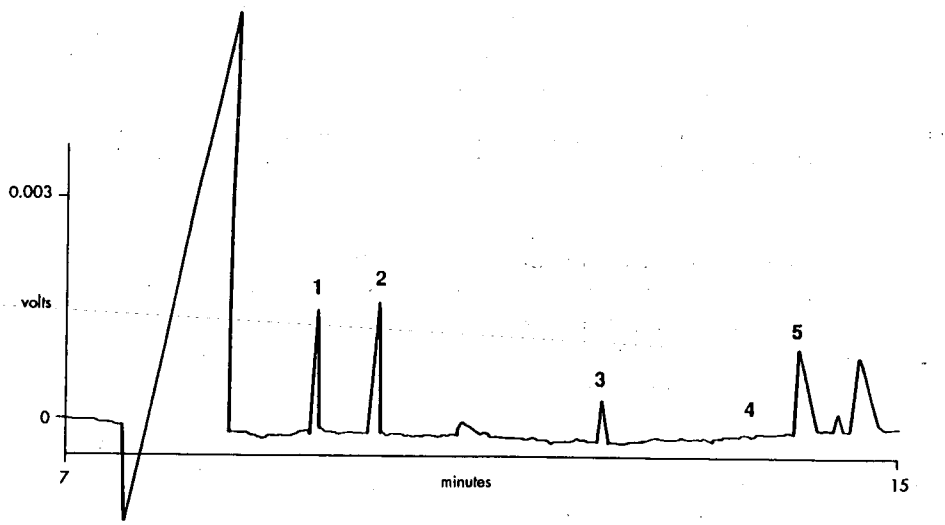

Fig. 4. Electropherogram of soy sauce. Sample preparation: dilute and inject. Peaks: 1 = citric acid; 2 = tartaric acid; 3 = acetic acid 4 = lactic acid; 5 = butyric acid (not added as an internal standard). The large peak on the left is chloride.

TABLE III

RESULTS FOR CHABLIS WINE SAMPLE

Analyte	Concentration (μg/ml)	R.S.D. % ($n=10$)[a]
Citric acid	127	14.1
Tartaric acid	2645	1.9
Malic acid	3291	1.3
Succinic acid	300	2.7
Acetic acid	260	5.4
Lactic acid	296	9.1

[a] Ten different aliquots of sample.

TABLE IV

RECOVERY OF ACIDS FROM GRAPE JUICE

Analyte	Added (μg/ml)	Found (μg/ml)	Recovery (%)
Tartaric acid	0	4330	–
	1160	5525	103
	2319	6703	102
Malic acid	0	3867	–
	1289	5153	100
	2577	6283	94

would increase the response of the other acids. This, in turn, would improve the reproducibility. The recovery from dark grape juice for tartaric and malic acid at two different levels averaged 103% and 97%, respectively (Table IV).

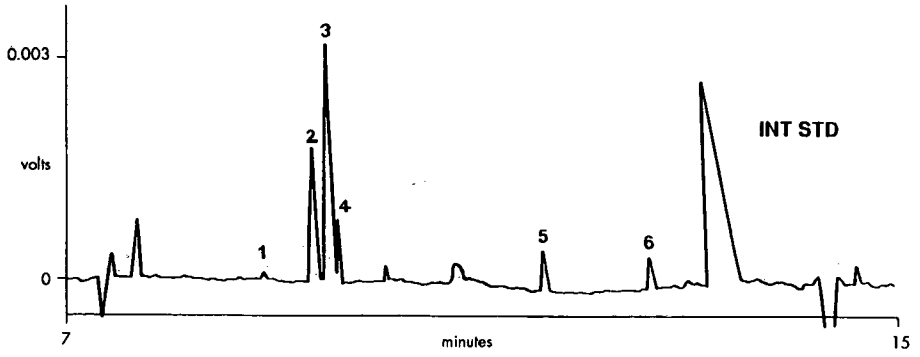

Fig. 5. Electropherogram of Chablis wine. Sample preparation: dilute and inject. Peaks: 1 = citric acid, 127 μg/ml; 2 = tartaric acid, 2645 μg/ml; 3 = malic acid, 3291 μg/ml; 4 = succinic acid, 300 μg/ml; 5 = acetic acid, 260 μg/ml; 6 = lactic acid, 296 μg/ml.

CONCLUSIONS

The determination of organic acids by CE with NICE-Pak Chemistry appears to be a simple alternative to other techniques for many food and beverage matrices. One point not yet stressed is its cost effectiveness. If one compares the cost per test for a six-acid determination in Chablis wine using different techniques, the advantage for CE becomes clear. Enzyme assay, HPLC–IC, and CE were compared with the following results: enzyme assay, US$12.00 (cost of kits divided by number of tests per kit, not including tartaric acid); HPLC–IC, US$ 2.72 (column, filter, mobile phase and vial cost); and CE, US$ 0.39 (capillary, electrolyte and vial cost). On a cost per test basis, CE offers 97% and 86% cost savings over enzyme assay and HPLC–IC, respectively.

Capillary electrophoresis also offers much in terms of automation. Not only are samples introduced into the capillary automatically, if one includes the autopurge function to clean the capillary between injections sample preparation to prevent interferences is also automated.

The flexibility, low cost of operation and automation of CE with the NICE-Pak Chemistry approach should make it an attractive alternative to HPLC–IC for inorganic ion and organic acid determinations.

REFERENCES

1 R. F. Frayne, *Am. J. Enol. Vitic.*, 37 (1986) 281.
2 J. D. McCord, E. Trousdale and D. Y. Ruy Dewey, *Am. J. Enol. Vitic.*, 35 (1984) 28.
3 W. R. Jones and P. Jandik, *Am. Lab.*, June (1990) 51.
4 *Waters Technical Bulletin, Capillary Electrophoresis Analysis of Species Variations in the Tryptic Maps of Cytochrome C*, Waters Assoc., Milford, MA, 1989.
5 J. A. Dean (Editor), *Lange's Handbook of Chemistry*, McGraw-Hill, New York, 1972, p. 6-34.

Journal of Chromatography, 546 (1991) 431–443
Elsevier Science Publishers B.V., Amsterdam

CHROMSYMP. 2138

Optimization of detection sensitivity in the capillary electrophoresis of inorganic anions

P. JANDIK* and W. R. JONES

Ion Analysis Department, Waters Chromatography Division, Millipore Corporation, 34 Maple Street, Milford, MA 01757 (U.S.A.)

ABSTRACT

Published reports describing applications of various capillary electrophoresis methods to the analysis of low-molecular-weight anionic species are reviewed and evaluated. An attempt is made to summarize the parameters relevant to the optimization of detection sensitivity in capillary electrophoresis. Based on a comparison with the results obtained by other techniques, indirect photometry is shown to have a number of important advantages for the detection of anions. For a given carrier electrolyte, the range of linearity can be extended by increasing the concentration of the anion responsible for background UV absorption. With chromate-containing carrier electrolytes the linearity range could be extended over more than three orders of magnitude. Good correlation between the relative molar absorptivities and sensitivity was found for six aromatic carboxylic acids serving as carrier electrolytes. Using optimized conditions for electromigrative sample introduction, the achievable detection limits are found to be in the low nanomolar range. This represents more than a 100-fold increase in sensitivity over the results obtained by hydrodynamic sample introduction. An isotachophoretic steady state occurring during the electromigration is presented as an explanation for the trace enrichment of low levels of analytes during sample introduction by electromigration.

INTRODUCTION

Separations of inorganic anions by capillary electrophoresis (CE) [1–12] are characterized by their unusually high efficiency. Complex ionic mixtures can be separated in less than 10 min. This increased efficiency creates in turn new, challenging requirements for the applications of detection techniques in CE. A detection procedure is expected to be without any negative effects on the separation achieved. In most existing instruments, this is accomplished by placing the translucent separation capillaries directly in the light path of an optical detector. Such an arrangement avoids the necessity to design dead-volume-free connections between the CE capillary and the detection cell. Dictated by the geometry of the capillaries utilized, injection volumes in CE are typically three or four orders of magnitude smaller than those in liquid chromatography [*e.g.*, 100 μl in ion chromatography (IC) *versus* 10 nl in CE]. However, such a limitation in sample size does not necessarily make CE inherently less sensitive than, for example, ion chromatography. The original "handicap" of smaller injection volumes is at least partially compensated for by the considerably higher

0021-9673/91/$03.50

separation efficiency. Peak heights can be expected to increase with the square root of the ratio N_{CE}/N_{IC}, where N_{CE} and N_{IC} are the respective separation efficiencies for CE and IC measured in plate counts [13]. Improved separation efficiencies thus frequently increase mass sensitivities 10–100-fold on going from IC (10^3 theoretical plates) to CE (10^5–10^6 theoretical plates). Such an influence of improved separation efficiency on detectability helps to explain the relatively sensitive levels of CE detection reported in the literature.

REVIEW OF CE APPLICATIONS FOR INORGANIC ANIONS

The first separations of inorganic cations by capillary electrophoresis were reported in 1967 [14] and 1974 [15]. The first reports on applications of CE to inorganic anions began to appear between 1979 and 1990. A brief summary of the applications of CE to inorganic anions is presented in Table I. These accounts mirror the evolution of the CE technique between the end of the 1970s and today. The first two reports (1979, 1983) were generated using isotachophoretic instruments, the only electrokinetic equipment commercially available at that time. The capillaries utilized in the early work were made of PTFE or similar materials. Isotachophoretic potential gradient detectors were adapted to detect the migrating CE zones. Instrumental limitations notwithstanding, an important understanding of fundamental principles was gained and impressive separations were demonstrated by the early workers. Up to sixteen anionic species could be separated in less than 10 min. Over the years, the focus of reports has shifted from PTFE to fused-silica capillaries and from electrochemical (potential gradient, conductivity) to optical (photometric, fluorescence) detection. Detection limits were steadily improved during the same period from sensitivities essentially only in the millimolar range to the micromolar range in the most recent investigations.

The following parameters were shown in the literature to be of great importance to the optimization of detection sensitivity in CE:

(1) Separation efficiency (see Introduction).

(2) Matched ionic mobilities (Excessive peak spreading usually results from a mismatch between the respective mobilities of the analyte and carrier electrolyte anions).

(3) Internal diameter of capillaries (Within a certain range, detection sensitivity increases with increase in diameter).

(4) Method of sample introduction (Electromigration improves sensitivity).

(5) Separation potential (Improved separation efficiency at higher voltages improves sensitivity. Overheating of electrolytes at too high potentials limits the range of available voltages).

(6) Length of capillaries (Generally, the capillaries should be as short as possible).

(7) Cooling (Intensive cooling reduces the thermal noise of baselines and allows higher voltages to be used for a separation).

Two of the latest reports [8,11] demonstrated sensitivity in the micromolar range by means of indirect photometric detection. As all of the state-of-the-art CE instruments are now equipped with photometric detectors, this approach to the CE detection of low-molecular-weight ionic species appears to be more universal than, for

TABLE I

BRIEF SUMMARY OF PUBLISHED CE APPLICATIONS FOR LOW-MOLECULAR-WEIGHT ANIONS

MES = 2-(N-Morpholino)ethanesulphonic acid; HEC = hydroxyethylcellulose; EOF = electroosmotic flow.

Ref.	Year	Detection mode	Carrier electrolyte	Analyte anions	Estimated detection limits
1	1979	Potential gradient	MES–histidine pH 6, 0.1% HEC	Chloride, sulphate, chlorate, chromate, adipate, benzoate, malonate, glutamate, etc.	0.0001 *M*
2	1983	Potential gradient	Cadmium acetate, 0.004 *M*	Nitrate, sulphate, chloride	0.0001 *M*
3	1986	Conductivity	0.01 *M* Butyric acid and creatinine, 1% Triton X-100, pH 4.8	Chloride, sulphate, perchlorate, nitrate, fluoride, phosphate, formate, maleate, glycolate, etc.	0.00001 *M*
4	1988	Conductivity	MES–histidine pH 6, 0.1% HEC	Chloride, formate, acetate, propionate	0.00001 *M*
5	1989	Conductivity	MES–histidine pH 6, 0.05% HEC	Seven alkyl carboxylic acids (C_1 to C_7)	0.00001 *M*
6	1989	Direct UV	20 m*M* Phosphate	Ferro- and ferricyanide, Zn and Cu CN complexes	0.00001 *M*
7	1987	Indirect UV	25 m*M* Sodium veronal pH 8.6	Bromide, cacodylate, four alkyl carboxylic acids (C_1 to C_4)	0.0001 *M*
8	1989	Indirect UV	20 m*M* Benzoate adjusted to pH 6.2 by histidine	Chloride, chlorate, phosphate, various carboxylic acids	10–100 μM
9	1988	Laser-induced fluorescence	250 μM Salicylate pH 7	Bicarbonate, iodate	10–100 μM
10	1989	Laser-induced fluorescence	250 μM Salicylate pH 4.0	Chloride, nitrate, perchlorate, permanganate, chromate, iodate, phosphate	10–100 μM
11	1990	Indirect UV	5 m*M* Chromate, EOF modifier pH 8.1	53 Inorganic and low-molecular-weight organic anions	1–8 μM

example, the applications of laser-induced fluorescence [9,10], which have also been shown to be very promising. From the theory of indirect detection techniques [16], two additional factors are expected to play a role specifically in the indirect photometric detection applied to capillary electrophoresis:

(8) Molar absorptivity coefficient of the carrier electrolyte anion (Optimization of indirect detection is essentially an attempt to increase the dynamic reserve, defined as the ratio of background signal to background noise [16]).

(9) Energy of light source (A higher energy output of a detector lamp increases the dynamic reserve).

Optimization of detection sensitivity in CE frequently follows different rules to those in conventional liquid chromatography. In considerable contrast with ion chromatography (IC), the system peaks stemming from interactions of UV absorber molecules (creating the large background signal required for indirect photometric detection) with the chromatographic stationary phase [17] are completely absent in CE. Owing to considerably decreased or non-existing interactions of UV-absorbing molecules with the capillaries, indirect photometry can be expected to play a more important role in capillary electrophoresis than in IC. CE thus offers a possibility of choice from a much larger number of molecules giving a high UV background. Indirect photometric detection has been shown to give sensitivities in the micromolar range [8,11]. An important contribution to increased sensitivity, unique to capillary electrophoresis, is optimized electrokinetic sample introduction. An isotachophoretic preconcentration step by means of a specially designed precolumn was shown to enhance detectability in CE by several orders of magnitude [18]. As determined by the Kohlrausch regulation function [19], nanomolar concentrations of ionic species from a sample can be concentrated up to millimolar levels inside an optimally designed isotachophoretic device. This paper describes our attempts to combine the detection sensitivities achievable by indirect photometry with the preconcentration capabilities inherent in electromigrative sample introduction.

EXPERIMENTAL

Chemicals

All solutions (carrier electrolytes and standards) were prepared using 18-MΩ water generated by a Milli-Q laboratory water purification system (Millipore, Bedford, MA, U.S.A.). The chromate electrolytes utilized were prepared from two different concentrated stock solutions. The first of the two concentrates contained 100 m*M* analytical-reagent grade Na_2CrO_4 (Mallinckrodt, Paris, KY, U.S.A.) and 0.34 m*M* Ultrex sulfuric acid (J. T. Baker, Phillipsburg, NJ, U.S.A.). The second concentrate was a 20 m*M* solution of OFM-BT electroosmotic flow modifier (proprietary cationic surfactant obtainable from Waters Chromatography Division, Millipore, Milford, MA, U.S.A.). All carrier electrolytes prepared for this investigation contained 0.5 m*M* of the electroosmotic flow modifier. Addition of this chemical reverses the electroosmotic flow, so that the resulting direction is toward the anode [12]. The concentration of chromate differed from experiment to experiment and is specified in the captions to the figures.

Analytical-reagent grade chemicals were obtained as follows: benzoic and trimesic acid from Sigma (St. Louis, MO, U.S.A.), phthalic acid from J. T. Baker,

p-anisic and 1,2,4,5-benzenetetracarboxylic acid from Aldrich (Milwaukee, WI, U.S.A.) and salicylic acid from Mallinckrodt. All aromatic carboxylate carrier electrolytes were prepared as 5 m*M* solutions containing 0.5 m*M* OFM-BT and adjusted to pH 6.0 by an addition of an appropriate volume of 0.1 *M* LiOH. Solutions of carboxylic acids (1 m*M*) for the evaluation of molar absorptivity coefficients were prepared without addition of OFM-BT.

All carrier electrolytes were prepared fresh daily and filtered and degassed using a Millipore solvent clarification kit with a 0.45-μm cellulose acetate filter (Millipore HA) prior to use. All standard mixtures were prepared by diluting 1000 ppm stock solutions containing a single anion. Weighed amounts of salts rather than acids were used for the preparation of stock solutions. Conventional volumetric glassware was utilized for the ppm-level dilutions. However, only polypropylene containers (Nalge, Rochester, NY, U.S.A.) were found to be suitable for storage and handling of solutions at ppb levels.

Instrumentation

A Waters Quanta 4000 CE system equipped with a negative high-voltage power supply was used to generate all electropherograms. Fused-silica capillaries, 75 μm I.D. and length 52 cm from the point of sample introduction to the point where the polyimide coating was removed to permit detection, were obtained from Waters (AccuSep capillaries). In all instances indirect UV detection was accomplished with a mercury lamp and a 254-nm optical filter. Both sample introduction modes (hydrodynamic and electromigration) available with the Quanta 4000 CE system were evaluated. Standard 4-ml Waters Wisp vials made of borosilicate glass were used as containers for the carrier electrolyte and for standards at ppm levels. Only 2-ml polyethylene sample vials (Sun Brokers, Wilmington, NC, U.S.A.) were utilized for the standard solutions of anions at ppb (10^9) levels.

All electropherograms were recorded and evaluated with the help of a Waters Model 840 data station and a Waters SIM interface. The subsequent data processing was done with either Cricket Graph (Cricket Software, Malvern, PA, U.S.A.) or Mathematica (Wolfram Research, Champaign, IL, U.S.A.) using a Macintosh SE personal computer (Apple Computers, Cupertino, CA, U.S.A.).

UV spectra were generated in a flow-injection analysis system consisting of a Waters Model M6000 pump, a Rheodyne (Cotati, CA, U.S.A.) Model 7010 injector and a Waters Model 990 photodiode-array detector. Water pumped at 1 ml/min carried 100-μl samples from the injector to the detector, which was set to acquire UV spectra between 200 and 400 nm.

RESULTS AND DISCUSSION

Indirect UV detection in carrier electrolytes containing chromate

Chromate was chosen as a carrier electrolyte providing a suitable UV absorbance background in a wide range of wavelengths, while at the same time matching the ionic mobility of seven common inorganic anions (fluoride, carbonate, chloride, nitrite, bromide, nitrate, phosphate and sulfate) more closely than, for example, the benzoic acid used in previous investigations [11].

Fig. 1 shows some typical UV spectra of low-molecular-weight anions. All

substances were evaluated as 1 m*M* solutions. Broad UV absorption of the chromate anion in comparison with the narrow absorption by other anionic species is clearly demonstrated by this comparison. One of the principal requirements of the carrier electrolyte is to provide a maximum dynamic reserve for the largest possible number of anions, including those which are themselves UV absorbing. Significant UV absorption of an analyte anion at a wavelength chosen for indirect detection considerably decreases the dynamic reserve. Decreased sensitivity of detection and too narrow linear ranges of calibration are observed as a result of such a mismatch of UV-absorbing properties of analyte and electrolyte anions.

Vanadate is the only other inorganic anion in Fig. 1 having a broader range of UV absorption than the three aromatic carboxylic acids. However, the usefulness of this anion as a carrier electrolyte constituent is limited by its precipitation in 0.5 m*M* solutions of the electroosmotic flow modifier below pH 10.

Typical separation and detection limits for common inorganic anions are shown in Fig. 2. The sensitive detection limits demonstrated here can be seen as a direct result of optimization of the parameters discussed above. The mercury lamp chosen for detection exhibits a high energy output at 254 nm and the UV absorption by chromate sufficiently exceeds that by the analyte anions.

If a calibration graph is generated under the conditions given in Fig. 2 for six different concentrations in the range 2–50 ppm, correlation coefficients in excess of 0.995 are obtained. However, if a more rigorous linearity test, such as the evaluation of the slope of a log (signal) *versus* log (concentration) plot, is employed, the assumption of linearity is not confirmed. As seen for the calibration of sulfate anion in Fig. 3A in the concentration range 2–50 ppm, the slope of the logarithmic plots lies outside the specified linearity range of 0.98–1.02 [20]. It is only within a narrower range of

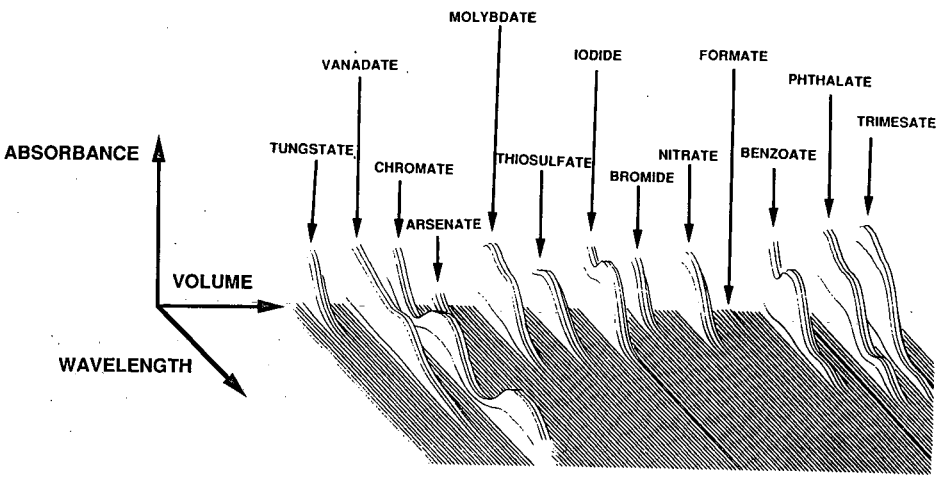

Fig. 1. Typical UV spectra of some inorganic and organic anions. The spectra were recorded between 200 and 400 nm. The range of sensitivity was set at 0–1.1 absorbance units. The volume between any two sample zones was determined by selected time intervals between two injections into the flow-injection analysis (FIA) apparatus and does not represent any separation effect. A more detailed description of the measurement is given under Experimental.

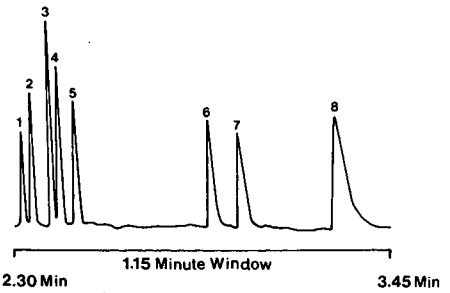

Fig. 2. Separation of inorganic anions using indirect photometric detection at 254 nm. The carrier electrolyte contained 5 mM chromate and 0.5 mM electroosmotic flow modifier and was adjusted to pH 8.1. A fused-silica capillary (75 μm I.D., 52 cm from the point of sample introduction to the detector) was used for the separation. During the analysis the injection side was at -20 kV. Hydrodynamic injection was carried out at a 10-cm height for 30 s. The peak identities, concentrations injected (ppm) and detection limits (three times the noise in μM) were as follows: 1 = bromide, 2 ppm, 4.8 μM; 2 = chloride, 2 ppm, 4.2 μM; 3 = sulfate, 2 ppm, 1.8 μM; 4 = nitrite, 2 ppm, 7.2 μM; 5 = nitrate, 2 ppm, 5.6 μM; 6 = fluoride, 1 ppm, 5.2 μM; 7 = phosphate, 4 ppm, 4 μM; 8 = carbonate, 2 ppm, 2.2 μM.

concentrations (2–30 or 2–15 ppm) where this calibration graph can be considered to be completely linear. According to our experimental results, the linearity range can be extended by increasing the concentration of the carrier electrolyte. In 7 mM chromate the slope of the logarithmic plots for 2–50 ppm standards becomes 0.99–1.00, indicating a reasonable linearity of calibration in that range.

Fig. 3B summarizes the results of another series of linearity tests. At a concentration of 5 mM the chromate electrolyte fails the linearity test in the range between 50 and 200 ppm (slope = 0.80). Even an increase in chromate concentration to 7 mM does not suffice to achieve linearity in this range of higher concentrations (slope = 0.90). If, however, the concentration of chromate is increased to 9 mM, good linearity of calibration can be observed not only between 50 and 200 ppm, but also over more than three orders of magnitude, between 0.5 and 200 ppm of sulfate.

Evaluation of aromatic carboxylic acids for use in carrier electrolytes

The main usefulness of carboxylates as components of carrier electrolytes lies in the CE analysis of less mobile anions (fluoride, carboxylic acids, alkylsulfonates, etc.) producing broadly asymmetric peaks, if analyzed in the chromate electrolyte. On the other hand, because of their relatively low mobilities, aromatic carboxylic acids are not very suitable as electrolytes for the analysis of complex mixtures of highly mobile inorganic anions (bromide, chloride, sulfate, nitrite and nitrate). The requirement of closely matched mobilities between the respective anionic components of a carrier electrolyte and the analyte anions makes it necessary to develop a whole group of highly UV-absorbing carrier electrolytes, covering the range of ionic mobilities of all inorganic anions and other, low-molecular-weight, anionic species such as carboxylic acids, amino acids, carbohydrates and sulfonates. It is therefore of practical interest to compare the molar absorptivity coefficients of common water-soluble aromatic carboxylic acids.

Three aromatic carboxylates in Fig. 1 show sufficiently high levels of UV absorption to be considered useful as carrier electrolyte anions for indirect UV

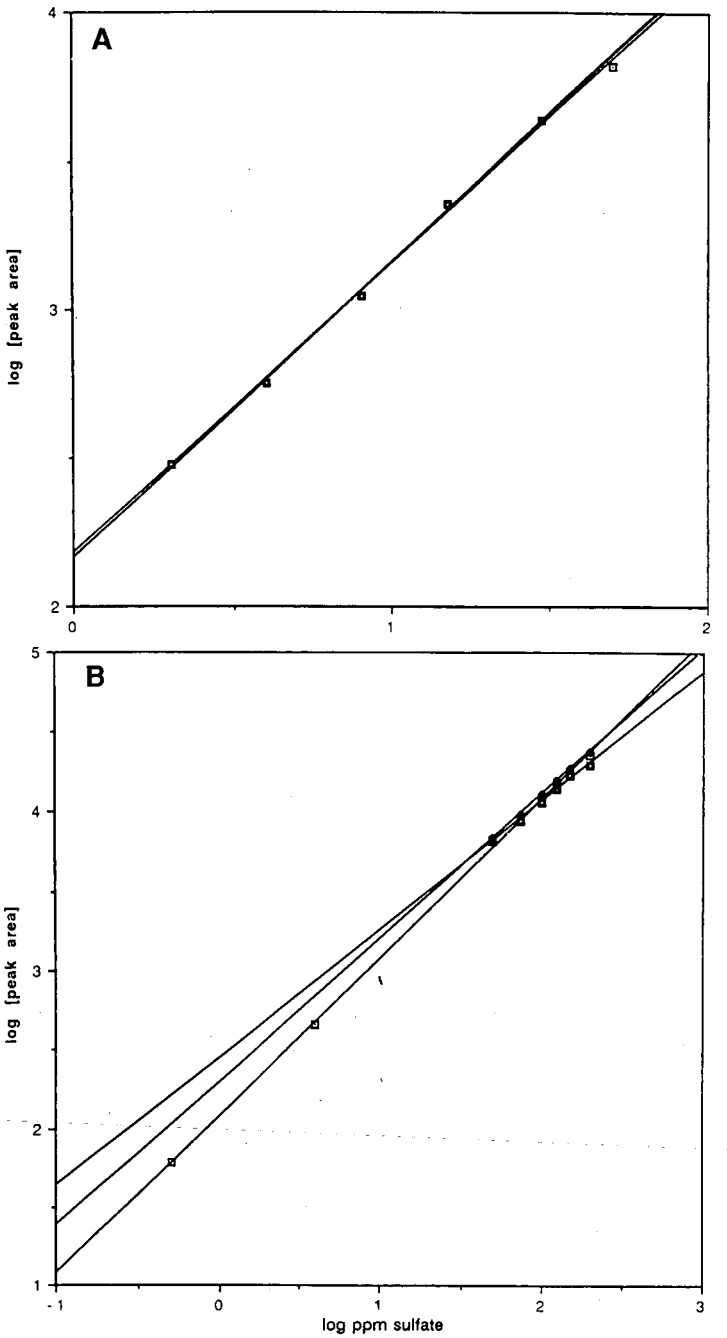

Fig. 3. Linearity tests using logarithmic plots [20]. Calibration graphs are considered linear only for slopes between 0.98 and 1.02. (A) Evaluation of linearity in 5 m*M* chromate electrolyte. Three calibration graphs for three different concentration ranges are overlaid. CE conditions were as specified in Fig. 2. (□) 2–50 ppm, $y = 2.1790 + 0.97848x$; (●) 2–30 ppm, $y = 2.1658 + 0.99799x$; (■) 2–15 ppm, $y = 2.1648 + 0.99956x$. (B) Linearity evaluation between 0.5 and 200 ppm using three different concentrations of chromate electrolyte. Linear regression was calculated only in the range between 50 and 200 ppm for 5 and 7 m*M* electrolytes. CE conditions as specified in Fig. 2, except for the changes in the concentrations of chromate. (□) 9 m*M* chromate, $y = 2.0749 + 1.0013x$; (●) 7 m*M* chromate, $y = 2.2923 + 0.90673x$; (■) 5 m*M* chromate, $y = 2.4419 + 0.80981$x.

detection. The molar absorptivity coefficients of these three carboxylates together with those of several others were evaluated in aqueous solutions of pH 6. The relative molar absorptivity coefficients correlated in Fig. 4 were obtained by dividing the absorbance of a given carboxylate by the absorbance of benzoate at the same wavelength and concentration (254 nm and 1 m*M*, respectively). The relative molar absorptivity of chromate on this scale equals 3.07. As shown, a very good correlation exists between the intensity of UV absorption by the carrier electrolyte molecule and the sensitivity of indirect photometric detection measured as peak area obtained for 10 ppm propionate.

The discussed correlation is also of great practical usefulness in the optimization of detection sensitivity. As seen in Fig. 4, the sensitivity of indirect UV detection can be increased 20-fold on going from salicylate to *p*-anisate. Sensitivity improvements by at least one order of magnitude can be expected by changing from the currently very popular benzoate to other, more suitable UV-absorbing components of carrier electrolytes (*p*-anisate, *p*-hydroxybenzoate, etc.).

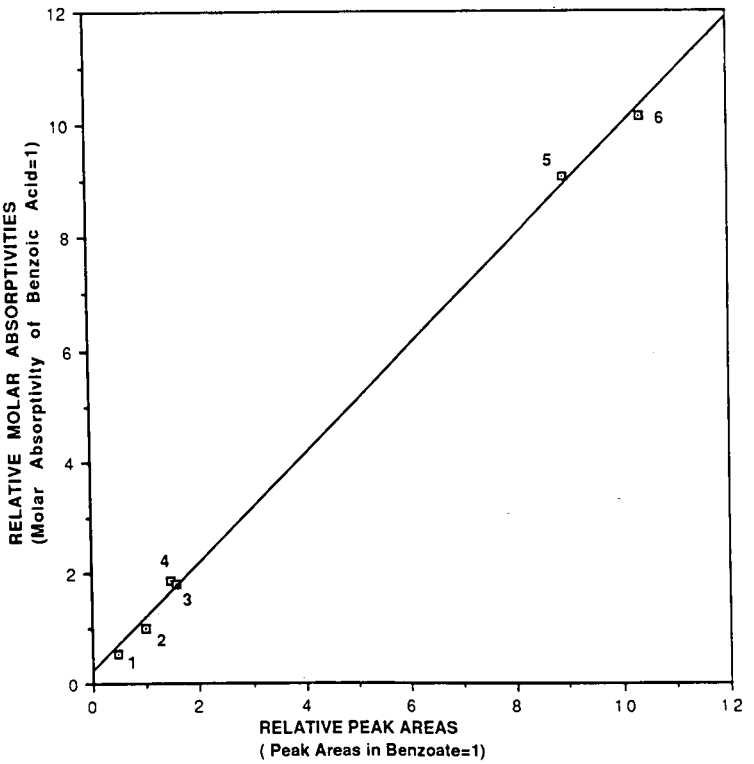

Fig. 4. Correlation of relative molar absorptivities and peak areas for 10 ppm propionic acid introduced by a 15-s hydrodynamic injection. The carrier electrolyte contained 5 m*M* of one of the six aromatic carboxylic acids in a mixture with 0.5 m*M* electroosmotic flow modifier adjusted to pH 6.0. The separations were carried out at −20 kV. 1 = Salicylate; 2 = benzoate; 3 = *o*-phthalate; 4 = trimesate; 5 = benzenetetracarboxylate; 6 = *p*-anisate. $y = 0.19349 + 0.97249x$; $R^2 = 0.998$.

Improving sensitivity by optimized electromigrative sample introduction

Under optimum conditions, an electromigrative sample introduction in CE can be expected to yield an isotachophoretic distribution of ionic concentrations inside the separation capillary [8]. Such a distribution is governed by a relationship introduced by Kohlrausch [19] (Kohlrausch regulation fuction):

$$\frac{c_x}{c_l} = \frac{m_x}{m_x + m_c} \frac{m_l + m_c}{m_l} \tag{1}$$

c_x and c_l are the concentrations of the analyte anion and leading electrolyte anion in their respective isotachophoretic zones and m_x, m_l and m_c are the ionic mobilities of the analyte anion, leading electrolyte anion and the common counter cation, respectively. The ionic mobilities are directly proportional to ionic equivalent conductances. It is therefore possible to generate plots depicting the dependence of the ratio c_x/c_l on the respective ionic equivalent conductances of a common cation and leading electrolyte anion. Fig. 5 was developed using the value of the ionic equivalent conductance of 40 cm^2 $equiv^{-1}$ ohm^{-1} for the analyte anion.

For chromate and other carrier electrolytes fulfilling the requirements placed on leading electrolytes (*i.e.*, higher ionic mobility than that of the analyte anion), it is reasonable to expect the ratio c_x/c_l to lie within the range *ca.* 0.2–1. Even if this applies only to a very narrow zone created during an optimized electromigrative sample introduction, a high enrichment factor can be accomplished, especially in situations where the sample concentration is in the nanomolar range and the concentration of the leading electrolyte anion is adjusted to 5–20 m*M*.

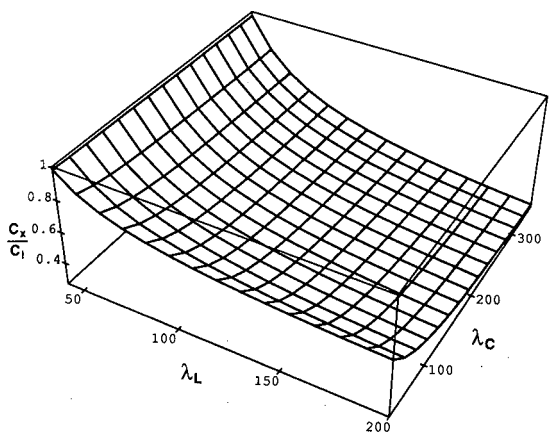

Fig. 5. Kohlrausch regulation function. As direct proportionality exists between the ionic equivalent conductance and ionic mobilities, equivalent conductances are taken directly for calculations of the ratio c_x/c_l of analyte to carrier anion concentrations according to eqn. 1. The range of leading electrolyte equivalent conductances (λ_L) was chosen between 41 and 200 cm^2 $equiv.^{-1}$ Ω^{-1} to cover a large number of possible carrier electrolyte anions, from carboxylates (*ca.* 40) to hydroxide (198). Common cation equivalent conductances (λ_C) are considered in the range 35–350 cm^2 $equiv.^{-1}$ Ω^{-1} to represent the largest possible selection of cations between alkylammonium (*ca.* 30) and hydronium (349.7) ions.

Another important requirement for such a preconcentration effect is the presence of an anion acting as a terminating electrolyte. Its ionic mobility must be smaller than that of any analyte anion. Such terminating electrolyte anions may be added on purpose. In solutions containing total ionic concentrations in the nanomolar range, the sample conductivity becomes too low and has to be adjusted by a suitable additive to permit a sufficient electric charge throughput for ionic transfer from the bulk of the sample solution into the capillary. Four possible stages of such optimized sample introduction by electromigration are represented in Fig. 6.

Chromate, citrate, carbonate and octanesulfonate solutions were evaluated as electromigration additives. In agreement with the rules discussed above, additions of a carrier electrolyte anion to the sample do not lead to the establishment of an isotachophoretic steady state and in consequence do not produce any useful enrichment of low-level analytes by electromigration. This was confirmed in an experimental series with chromate as a carrier electrolyte and chloride as an analyte. Citrate, carbonate and octanesulfonate, on the other hand, do exhibit lower ionic mobilities in comparison with chromate and can thus be used as additives for electromigrative trace enrichment with chromate-containing carrier electrolytes.

Of the remaining three anions, the best results were obtained with sodium octanesulfonate adjusted within the range 15–40 μM in the low ionic content samples. Simultaneously with the preconcentration of analyte anions, it is also possible to observe the enrichment of anions acting as an isotachophoretic terminating electrolyte (see Fig. 6C). In contrast to carbonate and citrate with short CE migration times, addition of relatively excessive concentrations of octanesulfonate does not lead to an interfering comigration with any of the over 50 anionic species analyzable by the CE method under discussion. An additional benefit is that unlike, *e.g.*, citrate, sodium octanesulfonate can be obtained free from common ionic impurities that disturb the determination of common anions such as sulfate and chloride in unknown samples. An example of the determination of common inorganic anions at low ppb levels is shown in Fig. 7. As indicated, the detection limits (calculated as three times the noise in concentration units) are in the low nanomolar range for this separation. This represents approximately a 400-fold increase in sensitivity in comparison with the results achievable in the same carrier electrolyte by hydrodynamic sample introduction.

CONCLUSIONS

Linearity of calibration graphs in CE with indirect photometric detection depends on the total concentration of UV-absorbing molecules in the carrier electrolyte. Linearity across three to four orders of magnitude is possible in chromate electrolytes.

The sensitivity of indirect photometric detection was found to be directly proportional to molar absorptivities for the series of six aromatic carboxylic acids. Application of, *e.g.*, *p*-anisate instead of benzoate or salicylate results in 10–20-fold improvements in sensitivity.

The experimental finding confirm the role of isotachophoretic conditions during the electromigrative sample introduction prior to a separation by capillary electrophoresis. With common inorganic anions, preconcentration can be accomplished

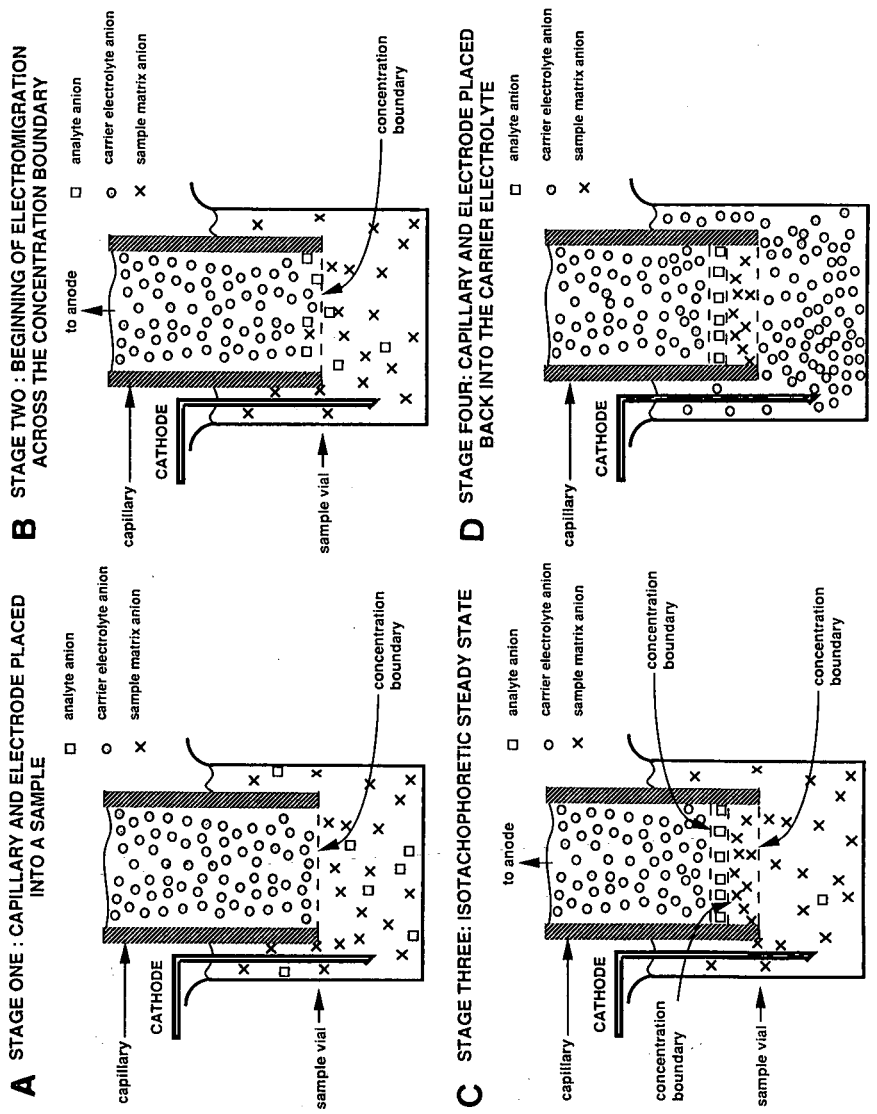

Fig. 6. Four stages of sample introduction by electromigration. Another possible way to describe stage three is as "frontal electrophoresis" [15].

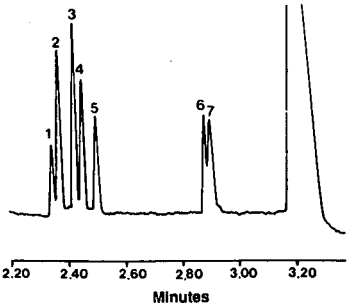

Fig. 7. CE separation after trace enrichment by electromigration. The capillary, carrier electrolyte, separation voltage and detector settings were identical with those in Fig. 2. The electromigrative sample introduction was carried out at 5 kV for 45 s. Sample conductivity was adjusted by addition of octanesulfonate at 18 μM in the sample. The peak identities, concentrations (ppb) and detection limits (nM) (three times the noise) were as follows: 1 = bromide, 4 ppb, 13.6 nM; 2 = chloride, 4 ppb, 13 nM; 3 = sulfate, 4 ppb, 8.4 nM; 4 = nitrite, 4 ppb, 25.4 nM; 5 = nitrate, 4 ppb, 24 nM; 6 = fluoride, 2 ppb, 19.8 nM; 7 = phosphate, 8 ppb, 17.8 nM. The large peak at *ca.* 3.2 min is carbonate. The levels of carbonate were not controlled under the conditions of our experiments.

directly in the separation capillary immersed in a sample containing very low concentrations of analyte anions. One of the requirements for the preconcentration of anions present at very low levels is the addition of a suitable anion capable of acting as an isotachophoretic terminating electrolyte.

REFERENCES

1 F. E. P. Mikkers, F. M. Everaerts and Th. P. M. Verheggen, *J. Chromatogr.*, 169 (1979) 18.
2 P. Gebauer, M. Deml, P. Boček and J. Janak, *J. Chromatogr.*, 267 (1983) 455.
3 F. Foret, M. Deml, V. Kahle and P. Boček, *Electrophoresis*, 7 (1986) 430.
4 J. L. Beckers, Th. P. E. M. Verheggen and F. M. Everaerts, *J. Chromatogr.*, 452 (1988) 591.
5 X. Huang, M. J. Gordon and R. N. Zare, *J. Chromatogr.*, 480 (1989) 285.
6 M. Aquilar, X. Huang and R. N. Zare, *J. Chromatogr.*, 480 (1989) 427.
7 S. Hjerten, K. Elenbring, F. Kilar, J. Liao, A. J. C. Chen, C. J. Siebert and M. Zhu, *J. Chromatogr.*, 403 (1987) 47.
8 F. Foret, S. Fanali, L. Ossicini and P. Boček, *J. Chromatogr.*, 470 (1989) 299.
9 W. G. Kuhr and E. S. Yeung, *Anal. Chem.*, 60 (1988) 2642.
10 L. Gross and E. S. Yeung, *J. Chromatogr.*, 480 (1989) 169.
11 W. R. Jones and P. Jandik, *Am. Lab.*, 22 (1990) 51.
12 W. R. Jones and P. Jandik, *J. Chromatogr.*, 546 (1990) 445.
13 P. Jandik, P. R. Haddad and P. Sturrock, *CRC Crit. Rev. Anal. Chem.*, 20 (1988) 13.
14 S. Hjerten, *Chromatogr. Rev.*, 9 (1967) 122.
15 R. Virtanen, *Acta Polytech. Scand., Chem. Incl. Metall. Ser.*, 123 (1974) 9.
16 E. S. Yeung, *Acc. Chem. Res.*, 22 (1989) 125.
17 P. R. Haddad and P. E. Jackson, *Ion Chromatography* (*Journal of Chromatography Library*, Vol. 46), Elsevier, Amsterdam, 1990.
18 F. Foret, V. Sustacek and P. Boček, *J. Microcolumn Sep.*, 2 (1990) 229.
19 F. Kohlrausch, *Ann. Phys. Chem.*, 62 (1897) 209.
20 R. P. W. Scott, *Liquid Chromatographic Detectors* (*Journal of Chromatography Library*, Vol. 33), Elsevier, Amsterdam, 2nd ed., 1986, pp. 12–14.

Journal of Chromatography, 546 (1991) 445–458
Elsevier Science Publishers B.V., Amsterdam

CHROMSYMP. 2190

Controlled changes of selectivity in the separation of ions by capillary electrophoresis

W. R. JONES* and P. JANDIK
Ion Analysis Department, Waters Chromatography Division of Millipore, 34 Maple Street, Milford, MA 01757 (U.S.A.)

ABSTRACT

The selectivity of low-molecular-weight inorganic and organic anions is evaluated on a capillary electrophoresis system utilizing a negative power supply and indirect UV detection at 254 nm. The background electrolyte chromate was found to be most useful for highly mobile inorganic anions and short chain carboxylates. Incorporated in this electrolyte is an additive that reverses the direction of electroosmotic flow (EOF) in the capillary, so that the EOF augments the mobility of the analytes. This results in exceedingly short analysis times, under 5 min, with efficiencies aproaching 600 000 theoretical plates. From migration time data, a correlation between ionic equivalent conductance and analyte mobility in the electrolyte is established. This empirical correlation equation aids in the prediction of migration order (selectivity) of a separation.

Other parameters evaluated on the chromate electrolyte are ionic strength, pH and EOF modifier concentration. It was found that pH and the EOF modifier provided significant selectivity control over the analytes while the other electrolyte parameters permitted only subtle changes in selectivity.

INTRODUCTION

Currently the most prevalent methodology employed for the analysis of low-molecular-weight inorganic and organic anions is ion chromatography (IC). This technique, introduced in the seventies [1,2], uses low-capacity anion-exchange columns for separation and conductivity as the "universal" mode of detection for ions. Originally developed to analyze several inorganic anions such as fluoride, chloride and sulfate, IC has expanded to encompass a variety of mono-, di- and trivalent inorganic and organic anions. These expanding requirements necessitated an increase in sophistication of IC hardware and chemistry. Specialty columns combined with either gradient elution or coupled separation systems are the most common approaches to maximize the peak capacity of analysis [3,4]. Increased system complexity stems from the limited selectivity and efficiency of anion-exchange columns. For most isocratic anion-exchange separations short-chain monocarboxylic acids coelute with early eluting anions such as fluoride and chloride, while trivalent anions (*e.g.*, citrate) require gradient elution for a reasonable analysis time.

In contrast to that, capillary electrophoresis (CE) separates ions according to their mobility in the electrolyte rather than by an interaction with a stationary phase and correspondingly the early detected anions are small inorganic mono- and divalent

0021-9673/91/$03.50

anions, while the later migrating anions are organic species with a larger Stokes radii. Separation efficiency in a capillary, unlike in a packed column, depends upon the applied field strength (V cm^{-1}) and not on capillary length [5]. It is optimized through use of small-I.D. capillaries for greater dissipation of Joule heating with high running voltages.

Eqn. 1 describes the Giddings [6–8] relationship between the maximum number of peaks that can be resolved (peak capacity n) and the column efficiency as measured by the theoretical plates (N):

$$n = 1 + 0.25 [N^{1/2} \ln (V_x/V_0)] \quad (1)$$

V_0 and V_x are the initial and final volume of an available retention range on any given chromatographic separation device. Eqn. 1 allows us to compare the peak capacity of a commonly used anion-exchange column with that of a fused-silica capillary. Using Fig. 1 for obtaining V_x/V_0 ratio we observe that both IC and CE separations have peaks beginning and ending in the range of 1.4 to 3.1 min. The Waters IC-Pak A column (upper separation trace) yields $N = 1500$ while the average plate count for CE using Waters AccuSep fused-silica capillary (bottom separation) is $N = 300\ 000$. This results in $n = 9$ for IC and 110 for CE. For randomly distributed single analyte peaks (n_r), theory [8] shows that this value never exceeds 18% of n. This leaves a peak capacity of 2 for anion-exchange and 20 for CE. The theoretically obtained n_r values are in good agreement to the 3 and 30 peaks observed for IC and CE, respectively (see Fig. 1). CE thus shows a ten-fold increase in peak capacity over a conventional anion-exchange column. The highest efficiency achieved in the CE separation in Fig. 1 is 568 350 plates by the W_{TAN} method (tangent method) [9] for peak 1 belonging to thiosulfate. Fig. 2 shows peak 1 in an expanded view of a 15-s range together with the first 9 peaks of the

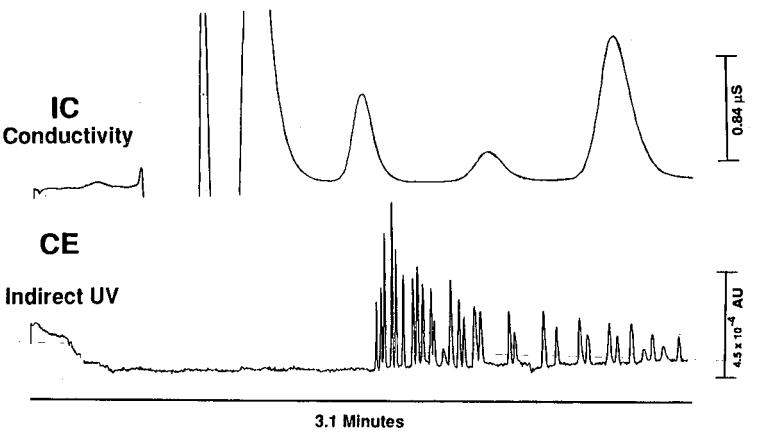

Fig. 1. Comparison of first 3.1 min of an IC separation *vs.* a CE separation. IC chromatogram (top) separates only 3 anions, fluoride, carbonate and chloride (last three peaks) using a Waters IC-Pak A, borate–gluconate eluent at 1.2 ml/min and Waters 431 conductivity detection. A detailed description of this separation system is given in refs. 3, 4 and 10. The negative and positive peaks found prior to the three anions are the water dip and excluded cations, respectively. The electropherogram (bottom) separates 30 anions using Waters AccuSep fused-silica capillary, chromate high-mobility electrolyte at 30 kV and indirect UV detection at 254 nm.

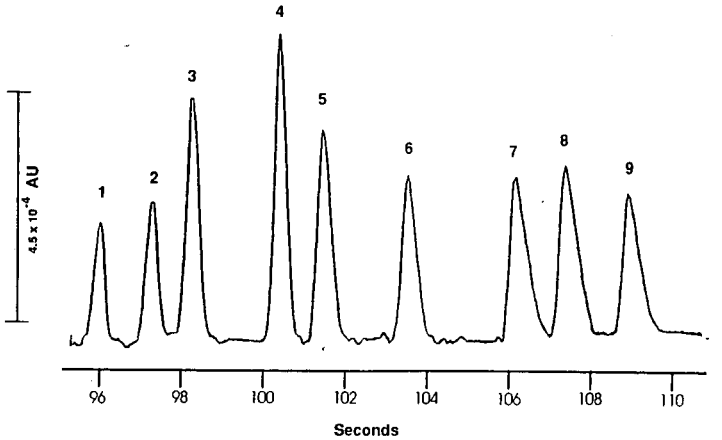

Fig. 2. Close view of the first 9 peaks of the 30-anion electropherogram shown in Fig. 1. High separation efficiency enables baseline resolution of all anions shown in this 15-s electropherographic segment.

30-anion electropherogram. Note that the peaks are baseline resolved with sufficient space for 3 additional peaks of comparable height to be placed in the gaps. CE appears to offer an unprecedented level of analysis power unapproachable by today's IC.

EXPERIMENTAL

Instrumentation

The CE system employed was the Quanta 4000 (Water Chromatography Division of Millipore, Milford, MA, U.S.A.) with a negative power supply and an Hg lamp for 254-nm detection. Waters AccuSep polyimide-coated fused-silica capillaries are used throughout this work. The capillary dimensions were 60 cm total length with 52 cm distance from point of injection to the detector cell. Both 50 and 75 μm I.D. capillaries were used. Data acquisition was carried out with a Waters 840 data station and a System Interface Module (SIM) interface. Detector time constant was set at 0.1 s and data acquisition rate was 20 points/s. Collection of electropherographic data was initiated by a signal cable connection between the Quanta 4000 and the SIM.

Preparation of chromate-based background electrolytes

The chromate electrolytes were prepared from a concentrate containing 100 m*M* Na_2CrO_4 (Mallinckrodt analytical-reagent grade) and 0.69 m*M* H_2SO_4 (J. T. Baker, Ultrex grade, Phillipsburg, NJ, U.S.A.). The dilute sulfuric acid is added to the chromate concentrate to preadjust the electrolyte pH to 8.0 when preparing the carrier electrolyte of 5 m*M* chromate with 0.5 m*M* electroosmotic flow (EOF) modifier. Milli-Q reagent-grade water (Millipore, Bedford, MA, U.S.A.) was used for rinsing and dilution of concentrates. EOF modifier for the reversal of the direction of electroosmotic flow was obtained as a 20 m*M* concentrate from Waters (NICE-Pak OFM Anion-BT[a]). A 100 m*M* NaOH solution was used to adjust the pH of the chromate electrolyte for the pH study.

[a] Patent applied for.

Standard solutions

All standard mixtures were prepared by a dilution of 1000-ppm stock solutions containing a single anion. The stock solutions were prepared fresh every six months and were stored in 200-ml polycarbonate tissue culture flasks (Corning Glass Works, Corning, NY, U.S.A.). All 20-ppm or lower concentration mixed anion standards were prepared freshly for each of the experiments. Milli-Q water and polymethylpentene containers (Nalgene, Rochester, NY, U.S.A.) were used throughout.

System operation

The CE system incorporates two modes of sample entry into the capillary —hydrostatic and by electromigration. All injections for the electrolyte studies were performed in the hydrostatic mode where the capillary was immersed in the sample at a height 10 cm above the running electrolyte level for 30 s. Upon lowering the sample to the 0 cm level the capillary was removed from the sample and the loaded capillary was immersed in the running electrolyte with the voltage ramping up to 20 kV. Electromigration is used only for the electropherogram in Figs. 1–3. Here the cathode and capillary were immersed in the sample at the 0 cm level with an applied voltage of 1 kV for 15 s prior to running the analysis. A 2-min capillary purge is performed prior to all injections. This operation removes the remaining constituents (*i.e.*, water peak) of the last sample from the capillary. The purge is accomplished by a 12 to 15 p.s.i. vacuum applied to the receiving electrolyte vial. Each sample in the carousel has its own electrolyte vial.

RESULTS AND DISCUSSION

Peak capacity

The electropherogram from Figs. 1 and 2 is shown in Fig. 3 as an 89-s segment encompassing the first and last peaks for proper identification. This separation utilizes the same chromate (high mobility) electrolyte described earlier by the authors [10]. However, the previous separation utilized 20 kV and a 75 μm I.D. capillary. The use of a 50 μm I.D. capillary with 30 kV running voltage has improved the plate count in this investigation by a factor of 2. The trade-off for higher efficiency is lower sensitivity. This is due to smaller injection volumes for the same loading time and shorter optical path length of the detector cell which is formed by the capillary. The authors, however, have successfully employed electromigration as a mode of sample enrichment giving detection limits below the ppb (10^9) threshold [11].

Analyte mobility and ionic equivalent conductance

The migration times (T_m) from the electropherogram in Fig. 3 are plotted against the ionic equivalent conductance values obtained from the literature [12,13]. Fig. 4A shows the individual points scattered along the line obtained by a second-order polynomial curve fit with a correlation coefficient $R^2 = 0.967$. A trend does exist but prediction of the actual migration sequence by placing the ionic equivalent conductance values in descending order only approximates the region in which the anions are likely to be found. Fig. 4B shows only the migration times (T_m) of more hydrophilic monovalent anions plotted against their ionic equivalent conductance. Here the curve fit is improved to $R^2 = 0.993$. Plotting and curve fitting the divalent anions as

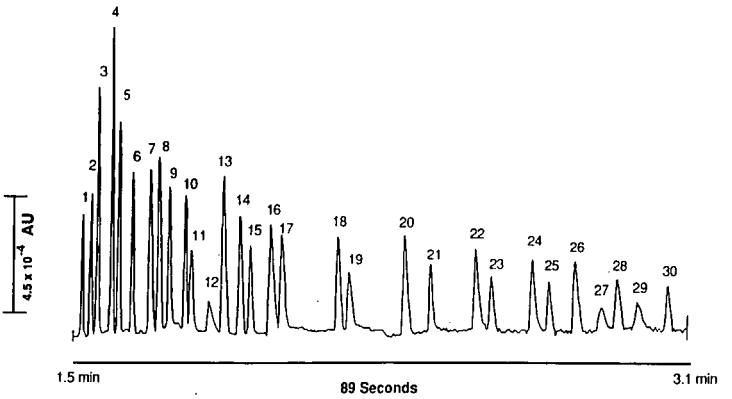

Fig. 3. Peak identity and concentrations (ppm) for 30-anion electropherogram displayed in an 89-s electropherographic segment. Electromigration injection at 1 kV for 15 s. Peaks: 1 = thiosulfate (4); 2 = bromide (4); 3 = chloride (2); 4 = sulfate (4); 5 = nitrite (4); 6 = nitrate (4); 7 = molybdate (10); 8 = azide (4); 9 = tungstate (10); 10 = monofluorophosphate (4); 11 = chlorate (4); 12 = citrate (2); 13 = fluoride (1); 14 = formate (2); 15 = phosphate (4); 16 = phosphite (4); 17 = chlorite (4); 18 = galactarate (5); 19 = carbonate (4); 20 = acetate (4); 21 = ethanesulfonate (4); 22 = propionate (5); 23 = propanesulfonate (4); 24 = butyrate (5); 25 = butanesulfonate (4); 26 = valerate (5); 27 = benzoate (4); 28 = L-glutamate (5); 29 = pentanesulfonate (4); 30 = D-gluconate (5). The electrolyte is a 5 m*M* chromate and 0.5 m*M* EOF modifier adjusted to pH 8.0.

a separate group Fig. 5A, we see that all the divalents are consistently slower than their ionic equivalent conductance values would indicate. The trivalent anion citrate is shifted by approximately an equal amount from the divalents as these are from the monovalent anions. Such dependence upon ionic charge or valence state is very consistent. It indicates that the anions are being slowed down, possibly by wall charge. For this to occur the wall charge must be positive which is apparently the case with the electroosmotic flow modifier in the electrolyte [5]. Reducing the divalent anions ionic equivalent conductance values by 5 S cm^2 equiv.$^{-1}$ and the trivalent anion by 10 S cm^2 equiv.$^{-1}$ helps to eliminate what is assumed to be the wall interaction of the divalent and trivalent anions as shown in Fig. 5B. The correlation coefficient of the second-order polynomial curve fit is now 0.992, an improvement from 0.967. Included in Fig. 5B, but not in the correlation, are the known hydrophobic anions iodide, thiocyanate and perchlorate. These monovalent species have very long retention times on resin based anion exchange columns, far in excess of what their valence charge would indicate. This behavior is usually attributed to the relatively lipophilic character of these anions and to the fact that their retention is mostly due to reversed-phase effects rather than to ion exchange [14]. The lipophilic character of iodide, thiocyanate and perchlorate plays a significant role in CE as well. This is discussed in more detail in one of the following sections of this article. As shown in Fig. 6 for a number of highly mobile anions, the relationship between the ionic equivalent conductance and migration times is essentially linear. The vertical dashed line indicates the projected migration time for hydroxide ions from such linear dependency. At migration times longer than *ca.* 1.8 min the linear relationship no longer applies and is replaced by a second-order exponential curve to approximate the assumed influence of wall

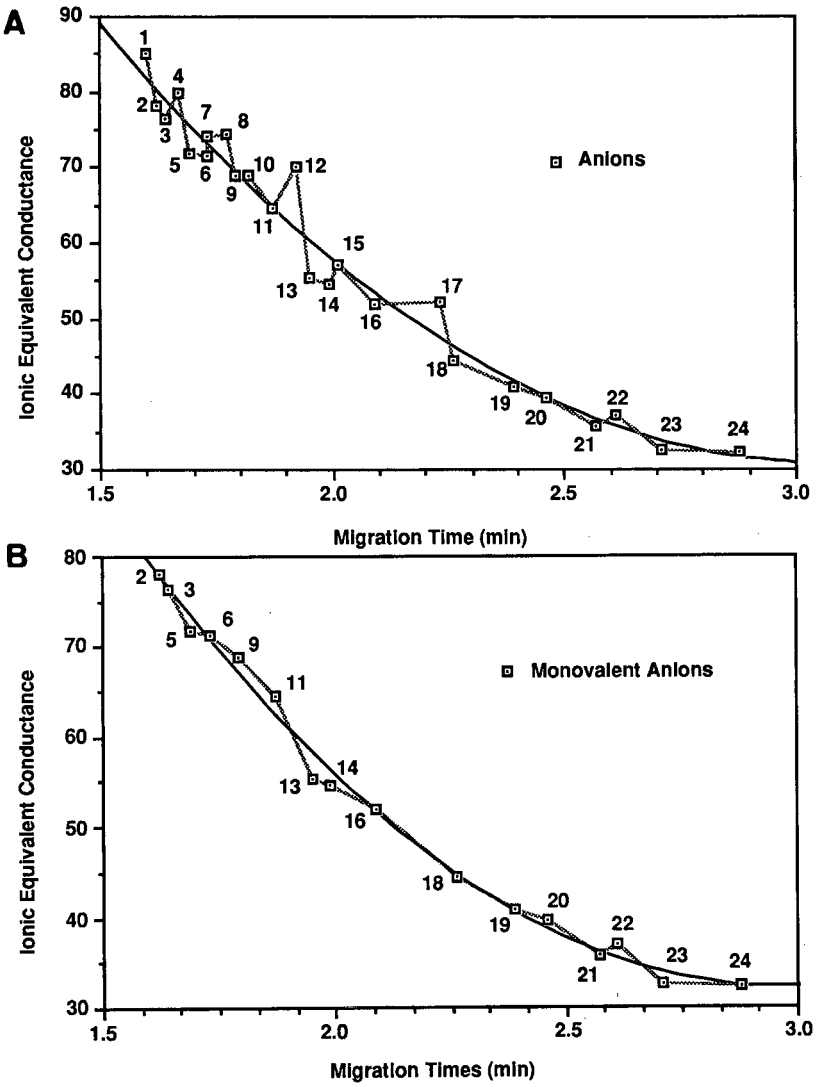

Fig. 4. (A) Migration times of some anions from Fig. 3 plotted against their respective ionic equivalent conductance obtained from the literature [12,13]. The ionic equivalent conductance values for the prevalent ionic form at pH 8 were chosen for this plot (*i.e.*, bicarbonate and not carbonate etc.). $y = 253.91 - 145.48\,x + 23.724\,x^2$; $R^2 = 0.967$. (B) Migration times of the more hydrophilic, monovalent anions separated in Fig. 3 are plotted against ionic equivalent conductance values. Second-order polynomial curve fit is noticeably improved by exclusion of the polyvalent anions. $y = 254.15 - 149.75\,x + 25.270\,x^2$; $R^2 = 0.993$ *versus* 0.967 in (A). 1 = Thiosulfate; 2 = bromide; 3 = chloride; 4 = sulfate; 5 = nitrite; 6 = nitrate; 7 = oxalate; 8 = molybdate; 9 = azide; 10 = tungstate; 11 = chlorate; 12 = citrate; 13 = fluoride; 14 = formate; 15 = phosphate; 16 = chlorite; 17 = phthalate; 18 = carbonate; 19 = acetate; 20 = ethanesulfonate; 21 = propionate; 22 = propanesulfonate; 23 = butyrate; 24 = benzoate.

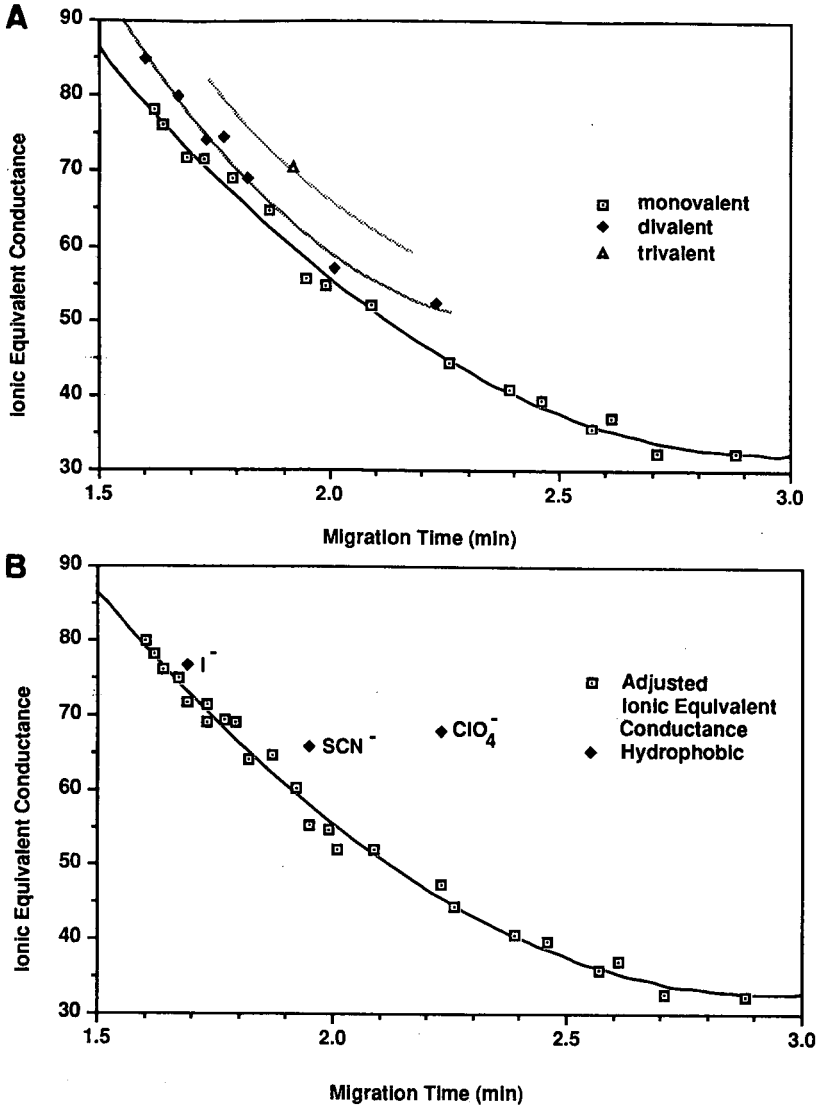

Fig. 5. (A) Migration times of anions plotted against ionic equivalent conductance values with individual second-order polynomial curve fits calculated separately for monovalent and divalent anions. The curve shown for the trivalent anion citrate was chosen to have a similar shape from the behavior of the mono- and divalent anion data. Upper curve: $y = 370.19 - 266.63\ x + 55.532\ x^2$; $R^2 = 0.989$; lower curve: $y = 254.15 - 149.75\ x + 25.270\ x^2$; $R^2 = 0.993$. (B) Migration times of the more hydrophilic mono-, di- and trivalent anions plotted against the adjusted ionic equivalent conductance values (see eqn. 2). $y = 258.79 - 154.26\ x + 26.312\ x^2$; R^2 is improved to 0.992 from the original value of 0.967 obtained from the unadjusted ionic equivalent conductance data found in Fig. 4. The more hydrophobic anions iodide, thiocyanate and perchlorate are also shown, but are not included in the curve fit. A separate ionic equivalent conductance adjustment to account for hydrophobic character is called for to normalize the migration times of lipophilic anions.

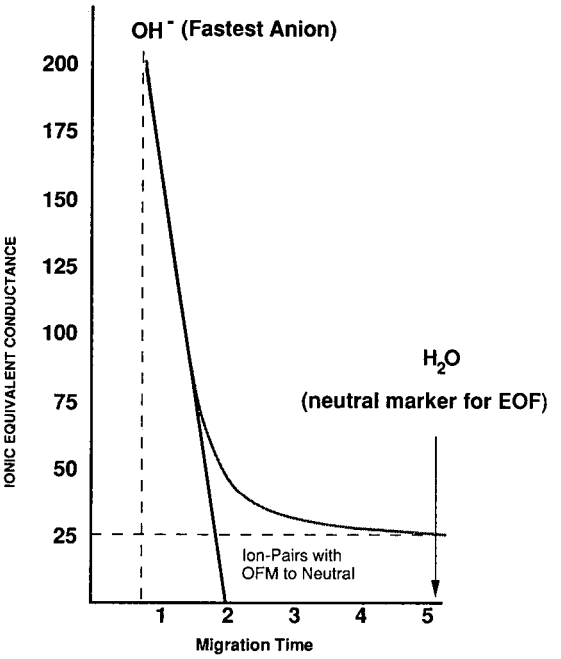

Fig. 6. This graph represents the migration time *vs.* the ionic equivalent conductance values for the entire range of mobilities found for anions in the chromate electrolyte from hydroxide to neutral water. No anion faster than hydroxide will be found to the left of the dashed vertical line and no anion will be found below the dashed horizontal line due to assumed ion pair formation with the electroosmotic flow modifier (OFM). See the corresponding discussion in the text.

interactions and ion pairing. The best fit for complete set of experimental data is given by the empirical eqn. 2:

$$\Lambda_{adj} = 258.79 - 154.26\ T_m + 26.312\ T_m^2, \tag{2}$$

where Λ_{adj} = ionic equivalent conductance $- 5(V - 1)$, V is the ionic charge of an analyte and T_m the migration time. Without polyvalent adjustment (ionic equivalent conductance to Λ_{adj}) the prediction of migration sequence is only 59% correct, with adjustment 78% correct. Individual linear adjustments for ionic equivalent conductance are required for lipophilic interactions to normalize the hydrophobic anions. Practical usefulness of eqn. 2 would be limited without a good precision of migration times. With 15 consecutive hydrostatic injections of an eight-anion standard the T_m relative standard deviation (R.S.D.) ranged from 0.331 to 0.751%. Normalizing T_m with respect to bromide, the first peak of the separation, yields an R.S.D. range of 0 to 0.422% with an average of 0.099%. It can be concluded that the reproducibility of EOF of the electrolyte is quite consistent and comparable to the reproducibility of flow-rates in high-performance liquid chromatography. Note that the EOF for a 50 μm I.D. capillary at 30 kV, using the reference chromate electrolyte (5 mM chromate, 0.5 mM EOF modifier) is 0.2 μl/min with a linear velocity of 10.2 cm/min.

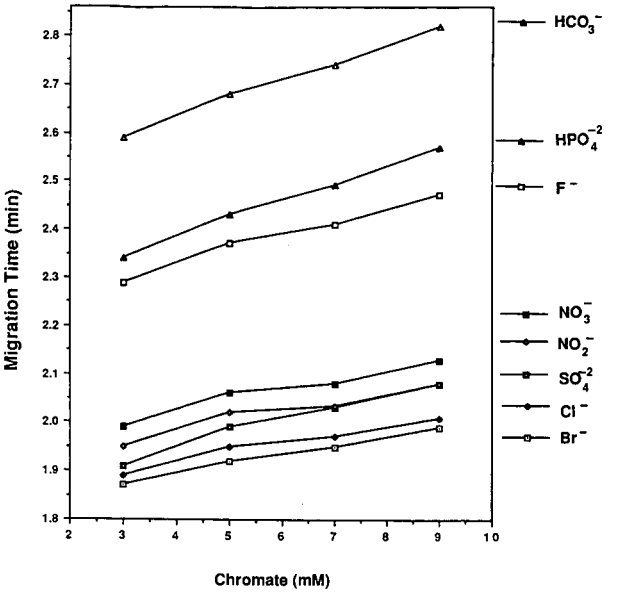

Fig. 7. Increases of chromate concentration in an electrolyte containing 0.5 m*M* EOF modifier *vs.* migration times; pH value is kept constant at 8.0. Plotted are migration times of eight common anions. Sulfate exhibits a subtle selectivity change of increasing migration time as chromate electrolyte concentration increases.

For a 75 μm I.D. capillary at 20 kV using the same electrolyte the EOF is 0.32 μl/min and linear velocity is 7.42 cm/min.

Influence of ionic strength on selectivity in chromate electrolytes

Ionic strength of the background electrolyte plays three different roles in the CE separations. Firstly, increasing concentration of background electrolyte decreases the EOF, secondly it increases efficiency due to higher field strength [5] and thirdly it yields subtle but important selectivity changes as shown in Fig. 7. Here the chromate concentration is varied while keeping the EOF modifier at 0.5 m*M* and pH at 8.0. It is seen that the sulfate anion begins to comigrate with the nitrite anion at higher chromate concentrations.

pH of chromate electrolytes and selectivity

The effect of electrolyte pH on analyte mobility is predictable and most pronounced for weakly acidic anions [15]. Eight anions plus borate were evaluated using a 5 m*M* chromate–0.5 m*M* EOF modifier with a pH starting at 8.0 and increasing in increments of 0.5 pH units to 12. The T_m values of the more strongly acidic anions with pK_a below 8 are unaffected by electrolyte pH changes between pH 8 and 10 (Fig. 8). Borate, carbonate and phosphate, on the other hand, exhibit a gradually increasing mobility (shorter T_m) as the pH of the electrolyte increases. As expected [15], the shape of the dependency (T_m *vs.* pH) resembles a pH titration curve. Fluoride and phosphate are best resolved at pH 8 with a total comigration occurring from 9.5 to

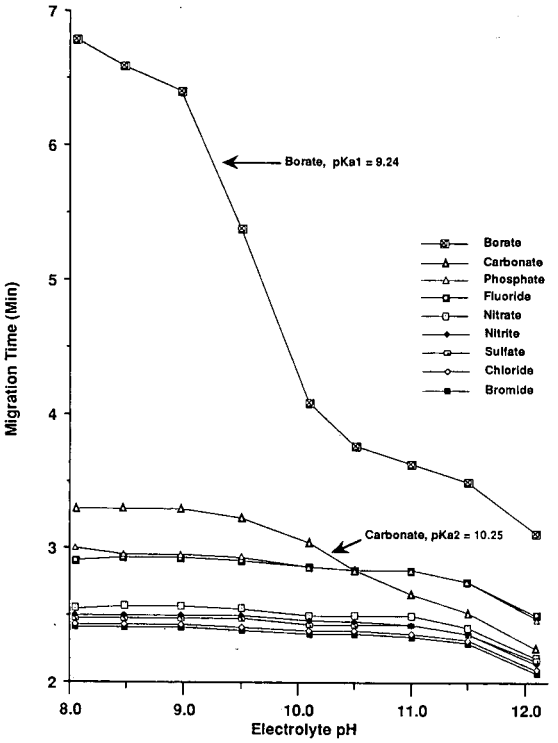

Fig. 8. The migration times of nine anions are plotted against the pH of the electrolyte 5 m*M* chromate–0.5 m*M* EOF modifier. Weak acids such as borate, carbonate and phosphate exhibit increasing ionization as the pH increases and correspondingly the migration times for these weak acids decreases in going from alkaline to more acidic pH values.

11.5. Above pH 11.5 phosphate begins to approach its third pK_a and moves ahead of fluoride. Carbonate comigrates with fluoride and phosphate at pH 10.5. As it converts to its dibasic form above pH 12 it eventually migrates just after nitrate. Interestingly, even a partial ionization is sufficient to give an analyte a higher mobility than that of neutral water peak migrating at 7 min in the chromate electrolyte and 0.5 m*M* EOF modifier. This is exemplified by borate with first pK_a at 9.24. Borate, a Lewis acid [16], is found in mildly alkaline solutions as $B(OH)_4^-/B(OH)_3$ exhibiting anomalous CE peak symmetry contrary to that predicted by Mikkers *et al.* [17]. As long as there is boric acid in the borate–boric acid mixtures (pH 8 to 10.5) the CE peak for borate shows fronting rather than the anticipated tailing. This fronting increases as the electrolyte pH approaches the first pK_a of 9.24. The tailing predicted by theory occurs only at pH values greater than 10.5 (see Fig. 9). The explanation for this unusual behavior can be derived from the fact that the borate anion is in transition between two valence states: at pK_{a1} 50% is $B(OH)_3$ and 50% is $B(OH)_4^-$. To be consistent with the electrophoretic diffusional process described by Mikkers *et al.* [17], the borate must be moving faster than the chromate electrolyte. Since borate is a Lewis acid it forms a polar bond with hydroxide ions which are in a relative surplus as the electrolyte pH is

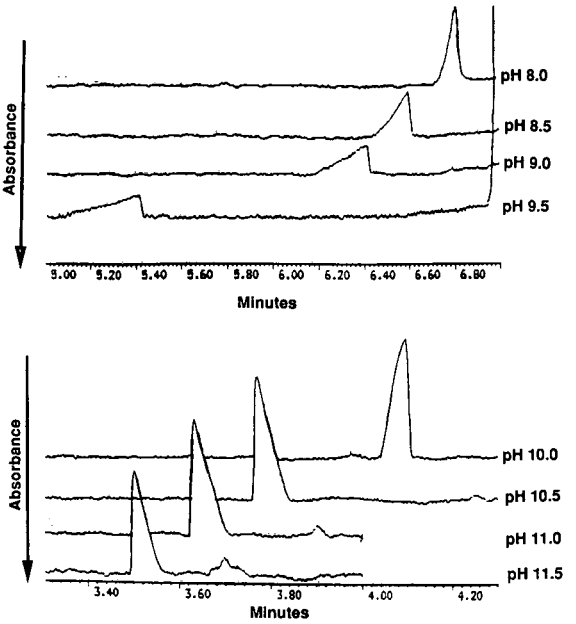

Fig. 9. Borate exhibits "anomalous" peak assymmetries. Fronting is observed as the electrolyte pH approaches the first pK_a. Peak tailing predicted by theory [ionic equivalent conductance (borate) < ionic equivalent conductance (chromate)] occurs only after the electrolyte pH increases beyond the first pK_a of borate.

increased. It is thus likely that borate acquires an increased "apparent" mobility from its association with a hydroxide ion (OH^- is the fastest anion in solution, with an ionic equivalent conductance of 198 S cm^2 $equiv.^{-1}$). Once the pH of the electrolyte is sufficiently higher than pK_{a1} of borate, the predominant form is $B(OH)_4^-$, which is no longer in transition and exhibits peak symmetry consistent with Mikkers *et al.* The relatively long T_m of borate and its unusual peak symmetry behavior make this anion an ideal indicator of electrolyte pH, if spiked into samples where a particular pH is required for resolution of closely migrating analytes.

Unexpectedly, an even weaker acid silicate was identified in the electropherogram (see Fig. 10) at electrolyte pH 11.0. The observed silicate was found to be an extractable from the borosilicate glass vial containing the standard. It is thus important to use polypropylene or polycarbonate vials as sample containers with elevated pH electrolytes.

Selectivity variations due to changing concentrations of EOF modifier

The EOF modifier reverses the natural direction of flow observed in fused-silica capillaries filled with mildly acidic or alkaline electrolytes. The modifier utilized in our experiments is an alkylammonium compound which is electrostatically attracted to the silanol groups on the inner wall of the capillary. It effectively shields these negative charges from the bulk of the electrolyte and creates a net positive wall charge. Without the addition of this modifier it is not possible to analyze highly mobile inorganic and

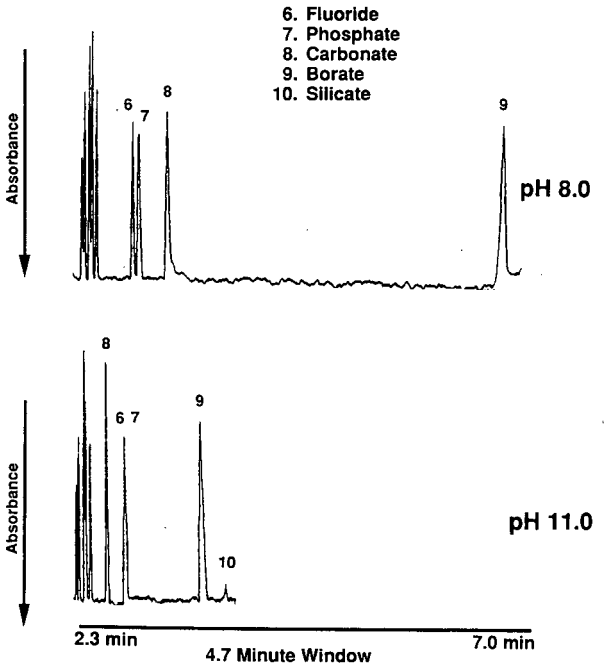

Fig. 10. Significant selectivity differences are observed for borate and carbonate as the electrolyte pH increased from 8 to 11. Peak 10 is due to silicate inadvertantly extracted from the borosilicate glass of the vial containing the sample.

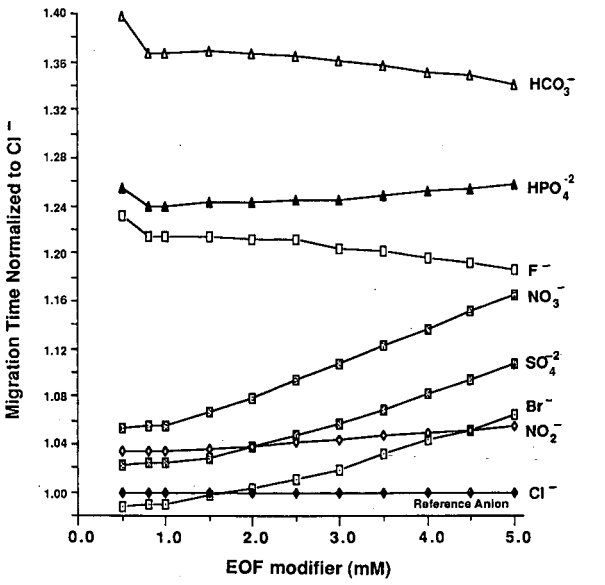

Fig. 11. Increasing EOF modifier concentration *vs.* migration times normalized with respect to chloride. The electrolyte contained 5 m*M* chromate. Bromide, sulfate and nitrate showed decreased mobility with increases EOF modifier concentration, this was attributed to ion pairing between the modifier and the analyte.

less mobile organic anions in a single run. The magnitude of the naturally occurring EOF is greater than the mobility of the majority of organic anions and some inorganic anions. Only the fastest anions such as thiosulfate, bromide and chloride would reach the detector within 30 min using 5 m*M* chromate electrolyte pH 8.0 at 30 kV. The main advantage of the EOF modifier used in this study is its ability to remain in solution with various background electrolytes (chromate included) and to contribute little to the running current of the electrolyte. Most importantly, the EOF modifier provides a stable rate of EOF, as is evident by the R.S.D. of migration times discussed in one of the preceding sections of this report, without any negative effect on the efficiency of the separation. Increasing the concentration of EOF modifier above 0.5 m*M* does not appreciably change the magnitude of the reversed EOF but does change the selectivity for three of the eight anions, namely bromide, sulfate and nitrate. Fig. 11 shows the plot of concentrations of EOF modifier *vs.* the T_m values normalized with respect to chloride.

A possible explanation of this effect involves ion pairing between the three anions and EOF modifier. This is supported by measurements comparing the conductivities of various salt forms of the EOF modifier. As an example, chloride with a lower ionic equivalent conductance than bromide would be expected to give a lower total conductivity in its salt with EOF modifier in comparison with bromide. However, our measurements have shown that in reality chloride salt is significantly more conductive than an equimolar concentration of the bromide form, suggesting that bromide unlike chloride is undergoing ion pairing with the EOF modifier. And correspondingly, the bromide and not chloride exhibits a pronounced dependency of its T_m on the concentration of EOF modifier in carrier electrolytes.

CONCLUSIONS

CE for low-molecular-weight inorganic and organic ions appears to offer a significant improvement over IC in efficiency and analysis time. Also the selectivity of the separation is predictable and can be correlated with the ionic equivalent conductances of the analytes. Variations in selectivity and resolution are achieved by modifications of the electrolyte composition —*i.e.*, the concentration of background electrolyte, pH and concentration of EOF modifiers. To direct EOF in the same direction as the analytes has been recently suggested to be counter productive, if good peak resolution is desired [5]. However, in our own observations, the EOF directed in the opposite direction to that of the analyte ions has resulted in extremely long analysis times. In the work carried out to date, satisfactory resolution was always observed in systems with EOF and analyte ions migrating in the same direction. Moreover, short run times (less than 3 min for 30 anions) and high efficiencies (500 000 plates and higher) make the discussed approach very attractive in applications for mixtures of low-molecular-weight anions. It is these authors belief that for the class of ionic species in question, there is a distinct advantage in the "going with the flow".

ACKNOWLEDGEMENT

The authors wish to acknowledge the assistance of Andrea Weston for her contribution in obtaining the data for the EOF modifier selectivity study.

REFERENCES

1 H. Small, T. Stevens and W. Bauman, *Anal. Chem.*, 47 (1975) 1801.
2 D. T. Gjerde and J. S. Fritz, *J. Chromatogr.*, 176 (1979) 199.
3 W. R. Jones, P. Jandik and M. T. Swartz, *J. Chromatogr.*, 473 (1989) 171.
4 W. R. Jones, P. Jandik and A. L. Heckenberg, *Anal. Chem.*, 60 (1988) 1977.
5 R. Wallingford and A. Ewing, *Adv. Chromatogr.*, 29 (1989) 1–76.
6 J. C. Giddings, *Anal. Chem.*, 56 (1984) 1259A.
7 J. C. Giddings, *J. High Resolut. Chromatogr. Chromatogr. Commun.*, 10 (1987) 319.
8 J. C. Giddings, in H. J. Cortes (Editor), *Multdimensional Chromatography: Techniques and Applications*, Marcel Dekker, New York, 1990, p. 12.
9 B. A. Bidlingmeyer and F. V. Warren, Jr., *Anal. Chem.*, 56 (1984) 1583A.
10 W. R. Jones and P. Jandik, *Am. Lab.*, 22, No. 9 (1990) 51.
11 P. Jandik and W. R. Jones, *J. Chromatogr.*, 546 (1990) 431.
12 R. C. Weast (Editor), *Handbook of Chemistry and Physics*, CRC Press, Boca Raton, FL, 66th ed., 1985, p. D-167.
13 J. A. Dean (Editor), *Lange's Handbook of Chemistry*, McGraw-Hill, New York, 13th ed., 1985, p. 6–45.
14 P. R. Haddad and P. E. Jackson, *Ion Chromatography —Principles and Applications (Journal of Chromatography Library*, Vol. 46), Elsevier, Amsterdam, 1990, pp. 22–25.
15 A. Tiselius, *Nova Acta Regiae Soc. Sci. Uppsaliensis*, 7 (1930) 3.
16 F. A. Cotton and G. Wilkinson, *Advanced Inorganic Chemistry*, Wiley, New York, 1980, p. 289.
17 F. E. P. Mikkers, F. M. Everaerts and Th. P. E. M. Verheggen, *J. Chromatogr.*, 169 (1979) 1.

Journal of Chromatography, 546 (1991) 459–466
Elsevier Science Publishers B.V., Amsterdam

CHROMSYMP. 2254

Analysis of anion constituents of urine by inorganic capillary electrophoresis

BILL J. WILDMAN*, PETER E. JACKSON, WILLIAM R. JONES and PETER G. ALDEN
Waters Chromatography Division of Millipore Corporation, 34 Maple Street, Milford, MA 01757 (U.S.A.)

ABSTRACT

Inorganic capillary electrophoresis (ICE) is a new separations technology which melds the technique of classical electrophoresis with the separations approach of ion chromatography. Matrices which have been difficult to deal with using ion chromatography have proven amenable to analysis by ICE. The simultaneous analysis of weak acid anions, oxalate and citrate and inorganic anions, chloride, sulfate, nitrate, phosphate and carbonate in diluted urine was achieved using ICE. The determination of the oxyanions of arsenic (*i.e.* arsenite and arsenate) in urine was also performed.

INTRODUCTION

The determination of the urinary levels of oxalate has long been recognized as an important factor in the study of renal stone formation. Additionally, citrate in urine can form soluble complexes with calcium oxalate monohydrate for example, which tends to reduce the rate of mineralization of this stone-forming material [1]. There have been a number of papers describing the use of ion chromatography (IC) to analyze oxalate [2–6], citrate [1,7] or nitrate [8] in urine individually.

IC is employed most commonly to analyze strong acid anions such as chloride and sulfate by ion-exchange chromatography. Weak acid anions, such as short-chained organic acids (*e.g.* formate and acetate), are usually separated by ion-exclusion chromatography. Typically, the simultaneous analysis of both weak and strong acid anions must be performed by gradient ion chromatography [9] or coupled techniques [10]. Inorganic capillary electrophoresis (ICE) was recently introduced as an alternative that allows the simultaneous analysis of both groups in a simple and rapid manner [11]. This preliminary investigation was undertaken in an effort to analyze oxalate, citrate and nitrate simultaneously using ICE. This analysis is possible due to the very high efficiency of the separation. Additionally, the separation of chloride, sulfate, phosphate and carbonate occurs within the same analytical run as oxalate, citrate and phosphate. The advantage of ICE with respect to ion chromatography (IC) is that the former results in different selectivities that are predictable based on the charge-to-size ratio of the analyte.

A second aim of this investigation was to examine the possibility of the analysis of the oxyanions arsenite and arsenate in urine. Speciation of these anions is important in the determination of the toxicological effects of each.

0021-9673/91/$03.50

EXPERIMENTAL

Instrumentation

A Waters Chromatography Division of Millipore Corporation Quanta 4000 Capillary Electrophoresis instrument was used with a Model 820 data station. Since the analysis times of the technique are extremely short and very narrow peak widths are obtained, it was necessary to collect the data at 20 points per second. The separations were performed on an Waters AccuSep polyimide-coated, 60 cm × 50 μm I.D. fused-silica capillary. The injection mode used was hydrostatic in which the sample was elevated to constant height (10 cm) for 60 seconds. The electrolyte was prepared daily, filtered and degassed using a Waters Solvent Clarification Kit and Millipore (Bedford, MA, U.S.A.) HATF Membrane filter (0.45 μm). Indirect photometry at 254 nm was used as the detection mode. Operating conditions are provided as captions to the figures.

Reagents

All solutions were prepared using 18 MΩ water purified using a Millipore Milli-Q Water Purification System. ACS grade sodium chromate tetrahydrate, ascorbic acid and boric acid were obtained from Aldrich (Milwaukee, WI, U.S.A.). A 0.5% (w/v) solution of sodium arsenite was obtained from Ricca Chemical (Arlington, TX, U.S.A.). Sodium arsenate was obtained from Mallinckrodt (Paris, KY, U.S.A.). All other anion standards used were prepared from the analytical grade sodium salts purchased from J. T. Baker (Phillipsburg, NJ, U.S.A.). NICE-Pak OFM Anion-BT, the electroosmotic flow modifier, is a proprietary chemical obtained from Waters Chromatography Division of Millipore Corporation.

RESULTS AND DISCUSSION

Instrumental configuration for ICE

In conventional capillary electrophoresis, sample introduction is carried out at the anodic electrode and detection is carried out at the cathodic electrode. There is a bulk fluid flow, referred to as the electroosmotic flow (EOF), toward the cathode at most pH values, that is dependant on the charge on the capillary wall [11]. In ICE, a proprietary compound, NICE-Pak OFM Anion-BT, is used to reverse the electroosmotic flow. Since the EOF, with the osmotic flow modifier present, is toward the anode, injection is carried out at the cathodic electrode and detection at the anodic electrode in ICE.

Migration in capillary electrophoresis is dependant on the charge-to-size ratio of each of the analytes, and the inorganic and organic anions analyzed by ICE are typically low-molecular-weight species, so this ratio is relatively large. Therefore, the anionic species migrate toward the anode preceding the EOF. This results in a very efficient and short analysis. The typical value for theoretical plates is in excess of 250 000 and analysis times are within 6 min.

There are two commonly employed injection modes in capillary electrophoresis. The first, used exclusively in this work, is termed hydrostatic (or gravity) injection. This mode introduces a representative sample of a homogeneous mixture into the capillary. The capillary, immersed in the sample, is raised to a constant height of 10 cm

for a user-specified time. The capillary is then lowered into electrolyte and the voltage is applied. The second mode, electrostatic injection, selects a sample which is biased toward faster-migrating species. The capillary is immersed in sample and a pre-selected sampling voltage is applied which causes anions in the sample to migrate into the capillary. Analysis then occurs as described above. Detection occurs by the process of indirect photometry at 254 nm as the electrolytes chosen have significant absorbance at this wavelength.

Determination of oxalate and citrate in urine

The determination of inorganic anions and short-chained organic acids in urine is a challenging analytical problem. Undiluted urine contains approximately 6000 ppm chloride, 1200 ppm phosphate, 180 ppm sulfate, 100–500 ppm citrate and 10–50 ppm oxalate. These very high levels of inorganic ions can cause severe interferences and quantitation difficulties when analyzing for citrate or oxalate by IC. In all the cited cases, a dilution of the urine was performed before ion chromatographic analysis. A difficult situation exists in that the urine must be diluted sufficiently to prevent overloading of the analytical column but yet not so much as to dilute the oxalate and citrate beyond the detection limits for these species. These IC approaches have yielded analyses for either oxalate or citrate but not both together, nor with the inclusion of the other inorganic ionic species which can also be important in urinary studies.

Fig. 1 shows an electropherogram, henceforth referred to as a pherogram, of eight commonly analyzed anions using ICE with a 50 μm I.D. capillary and a high mobility chromate electrolyte. The very short analysis times allow rapid methods development. It is important to note that a different selectivity is obtained when using this technique as compared to conventional anion-exchange chromatography. The normal elution order using IC is fluoride carbonate, chloride, nitrite, bromide, nitrate, phosphate and sulfate, column efficiencies are on the order of a few thousand plates, and analysis times commonly range from 10 to 15 min. The migration order of these ions using ICE is bromide, chloride, sulfate, nitrite, nitrate, fluoride, phosphate and carbonate, the efficiency of the separation ranges upwards of 250 000 plates, and the analysis time is under 6 min. The combination of selectivity differences, extremely high efficiencies, and fast analysis time make ICE ideal for investigating the analysis of anionic species in urine.

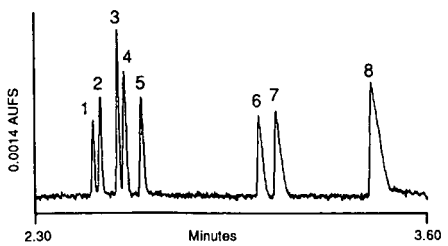

Fig. 1. Pherogram of standard anions. Conditions; Capillary: 60 cm × 50 μm I.D. fused silica. Electrolyte: chromate at pH 8.0 with NICE-Pak OFM Anion-BT (patent applied for); injection: hydrostatic for 60 s; detection: indirect UV at 254 nm; potential: 20 kV. Solutes: 1 = bromide (4 ppm); 2 = chloride (2 ppm); 3 = sulfate (4 ppm); 4 = nitrite (4 ppm); 5 = nitrate (4 ppm); 6 = fluoride (1 ppm); 7 = phosphate (4 ppm); 8 = carbonate (4 ppm).

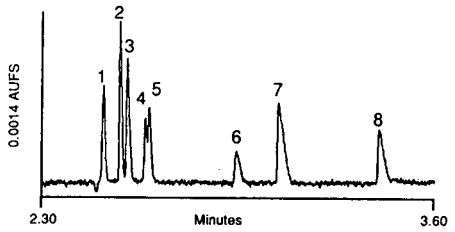

Fig. 2. Pherogram of standard anions expected in urine. Conditions as for Fig. 1 except; solutes: 1 = chloride (2 ppm); 2 = sulfate (4 ppm); 3 = nitrite (4 ppm); 4 = nitrite (2 ppm); 5 = oxalate (2 ppm); 6 = citrate (2 ppm); 7 = phosphate (4 ppm); 8 = carbonate (4 ppm).

A standard was prepared to contain citrate and oxalate (2 ppm each) in addition to other anions expected in diluted urine (*i.e.* chloride, sulfate, nitrite, nitrate, phosphate and carbonate) and then analyzed. The resultant pherogram is shown in Fig. 2. Citrate is well resolved from phosphate but nitrate and oxalate are only partially resolved. Upon closer examination of this pherogram, (Fig. 3) it can be seen, however, that there is sufficient resolution to allow accurate quantitation. The important feature of this separation to note is apparent when contrasted with IC. Oxalate is a strongly retained species using IC and commonly elutes after sulfate. Citrate is so strongly retained that, in most cases, a very strong eluent must be used. Use of such eluents generally sacrifices the ability to analyze for the early-eluting species such as chloride and nitrate. More complex approaches, such as the use of either gradient ion chromatography [9] or a coupled system [10], allow for the analysis of citrate without the loss of resolution of the early eluting anionic species. However, analysis times are significantly lengthened. Figs. 2 and 3 show the advantage of the different selectivity of ICE without the disadvantage of increasing analysis time to incorporate both weak and strong acid anions in one chromatographic run.

A pherogram of a fresh midstream void sample (author), diluted 1:50 in 18 MΩ water, is shown in full-scale view in Fig. 4. Due to the very high efficiency of ICE, the adjacent peaks, chloride and sulfate are well resolved even though present in a 14:1 ratio. A magnification of this pherogram (Fig. 5) shows that in addition to the five peaks seen in Fig. 4, a small peak (0.5 ppm) for nitrate is apparent. For the complexity of this matrix, the pherogram obtained is relatively simple, In IC, cations and water in the sample appear early in the chromatogram at the void volume using anion-exchange

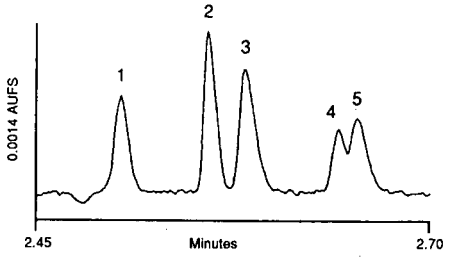

Fig. 3. Expanded view of peaks 1–5 of Fig. 2. Conditions as for Fig. 2.

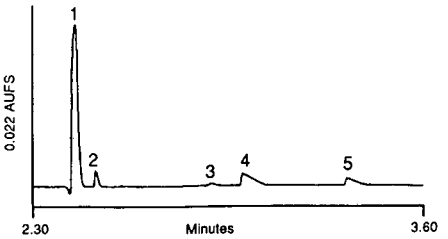

Fig. 4. Pherogram of diluted urine. Conditions as for Fig. 1 except; sample preparation 50× dilution in deionized water; solutes: 1 = chloride (109 ppm); 2 = sulfate (7.9 ppm); 3 = citrate (3.2 ppm); 4 = phosphate (16.2 ppm); 5 = carbonate (12.2 ppm).

separations. This large void peak can interfere in the quantitation of early-eluting anions. An advantage of ICE is that cations in the sample do not appear in the pherogram as they migrate in the opposite direction, toward the cathode hence, do not interfere with the analyte anions. In this particular sample, no oxalate was found so the diluted urine sample was then spiked with 2 ppm oxalate and 2 ppm citrate and reanalyzed (Fig. 6). Nitrate appears as a shoulder on the leading edge of the oxalate peak but it is quantitatively recovered. The recoveries of oxalate (95%) and citrate (94%) are acceptable.

Speciation of arsenite and arsenate in urine

There is some interest in the speciation of arsenic oxyanions in urine to determine the independent toxicological effect of each upon ingestion of contaminated fish. A second aim of this work was to investigate the feasibility of using ICE to analyze for each of these species. Fig. 7 is a pherogram of chloride, sulfate, nitrite, nitrate, phosphate, arsenate, carbonate and arsenite using chromate electrolyte at pH 10. It was necessary to operate the electrolyte at pH 10 to ensure the presence of the anionic form of arsenite as the pK_a of arsenite is 9.22. Good resolution of arsenate, phosphate and carbonate is seen. At pH 10, fluoride and phosphate co-migrate (compare Fig. 1) but this is inconsequential as little or no fluoride is expected in urine. It is important to use plastic sample vials when using electrolytes at elevated pH values rather than the commonly used borosilicate glass vials. When the glass vials were used, a peak identified as the borate anion was found due to a leaching of this anion from the vial wall.

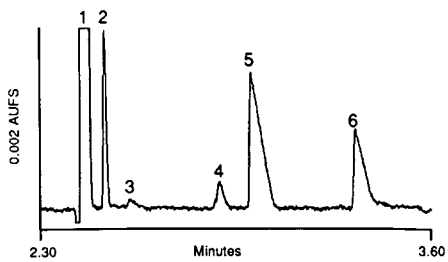

Fig. 5. Expanded view of Fig. 4. Condition as for Fig. 4 except; solutes: 1 = chloride (109 ppm); 2 = sulfate (7.9 ppm); 3 = nitrate (0.5 ppm); 4 = citrate (3.2 ppm); 5 = phosphate (16.2 ppm); 6= carbonate (12.2 ppm).

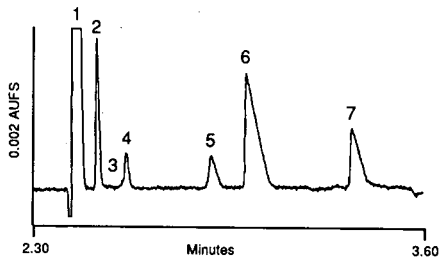

Fig. 6. Pherogram of diluted urine spiked with oxalate and citrate. Conditions as for Fig. 4 except; solutes: 1 = chloride (109 ppm); 2 = sulfate (7.9 ppm); 3 = nitrate (0.5 ppm); 4 = oxalate (1.9 ppm); 5 = citrate (4.9 ppm); 5 = phosphate (16.3 ppm); 6 = carbonate (9.3 ppm).

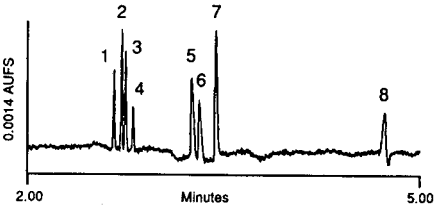

Fig. 7. Pherogram of standard anions and arsenite and arsenate. Conditions as for Fig. 1 except; electrolyte: chromate at pH 10.0 with NICE-Pak OFM Anion-BT; solutes: 1 = chloride (2 ppm); 2 = sulfate (4 ppm); 3 = nitrite (4 ppm); 4 = nitrate (2 ppm); 5 = phosphate (4 ppm); 6 = arsenate (5 ppm); 7 = carbonate (4 ppm); 8 = arsenite (5 ppm).

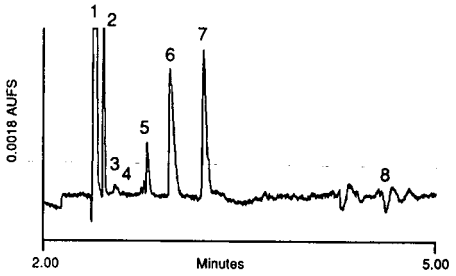

Fig. 8. Pherogram of diluted urine. Conditions as for Fig. 7 except; sample preparation 50× dilution in deionized water, solutes: 1 = chloride (67.7 ppm); 2 = sulfate (9.6 ppm); 3 = nitrate (1.0 ppm); 4 = oxalate (0.6 ppm); 5 = citrate (4.6 ppm); 6 = phosphate (11.5 ppm); 7 = carbonate (7.4 ppm); 8 = ascorbate (0.7 ppm).

A freshly voided midstream sample of urine was collected and diluted 1:50 in 18 MΩ water and analyzed using the conditions above (Fig. 8). Nitrate and oxalate are seen as partially resolved peaks 3 and 4. It was apparent that this sample also contains a small amount of ascorbate (peak 8), which appears as a negative peak (increasing absorbance) as this compound exhibits appreciable absorbance at 254 nm. There are also unidentified peaks appearing before the citrate peak (peak 5). As expected neither arsenite nor arsenate were found. The same urine sample was spiked with 10 ppm each of arsenite and arsenate and reanalyzed. The pherogram (Fig. 9) indicates good resolution between both the arsenic oxyanions and the surrounding peaks.

Future investigations

As this work was undertaken as a feasibility study, non-preserved urines were used. In clinical practice, urine is preserved with acid to approximately pH 2 to prevent precipitation of calcium oxalate species and also to prevent the conversion of urinary ascorbate to oxalate. Continuation of the present work will proceed with several main aims. The first two, improved resolution of nitrate and oxalate and the ability to analyze low-pH-preserved samples may be concurrently solved. At pH 8.0 both oxalate and citrate are totally ionized. There exist a number of alternate electrolytes to chromate which can be used at lower pH values. The use of these electrolytes at pH 3 for example, would allow the analysis of preserved samples and also change the selectivity of both oxalate and citrate since they would each exist as the monovalent species instead of the di- and trivalent species as occurs at pH 8. Since their sizes remain relatively constant, the charge-to-size ratios decrease and both will exhibit increased migration times. Nitrate, being a strong acid remains unaffected so the nitrate–oxalate pair become separated. The third aim is to analyze urine using less dilution to increase the peak size of nitrate and oxalate. Given that oxalate and citrate migrate later using an electrolyte of lower pH, a less-diluted sample may be analyzed without concern for increased resolution problems. A disadvantage however, is the possible loss of the ability to quantitate chloride and sulfate. The fourth aim is to investigate the analysis of two other important urinary anions glyoxalate and glycolate.

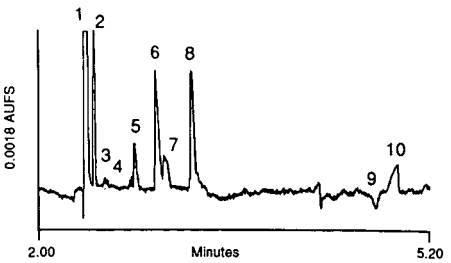

Fig. 9. Pherogram of diluted urine spiked with arsenate and arsenite. Conditions as for Fig. 8 except; solutes: 1 = chloride (67.7 ppm); 2 = sulfate (9.6 ppm); 3 = nitrite (1.0 ppm); 4 = oxalate (0.6 ppm); 5 = citrate (4.6 ppm); 6 = phosphate (11.5 ppm); 7 = arsenate (10.0 ppm); 8 = carbonate (7.4 ppm); 9 = ascorbate (0.7 ppm); 10 = arsenite (10.0 ppm).

CONCLUSIONS

The feasibility of the simultaneous analysis of chloride, sulfate, nitrate, oxalate, citrate, phosphate and carbonate in diluted urine by inorganic capillary electrophoresis has been demonstrated. This technique provides rapid and highly efficient separation of both weak and strong acid anions. The extension of the technique to properly preserved samples with increased resolution between nitrate and oxalate remains the subject of future investigation.

The speciation of the oxyanions of arsenic in diluted urine has also been demonstrated.

ACKNOWLEDGEMENTS

The authors wish to thank Mr. Robert Liedtke of the Nephrology Laboratory at the Mayo Clinic for guidance and several useful conversations and also Dr. David Nixon at the Mayo Clinic for his insight and interst in arsenic speciation in urine.

REFERENCES

1 R. P. Singh and G. H. Nancollas, *Kidney Int.*, 28 (1985) 985.
2 C. J. Mahle and M. Menon, *J. Urol.*, 127 (1982) 159.
3 R. P. Singh and G. H. Nancollas, *Anal. Letters*, 19 (1986) 1487.
4 R. L. Orwell, D. S. Scurr, A. Smith and A. G. Robertson, *Fortschr. Urol. Nephrol.*, 20 (1982) 263.
5 M. Menon and C. J. Mahle, *Clin. Chem.*, 29 (1983) 369.
6 W. G. Robertson, D. S. Scurr, A. Smith and R. L. Orwell, *Clin. Chem. Acta*, 126 (1982) 91.
7 Y. Ogawa, M. Morozumi, T. Tanaka and K. Yamaguchi, *J. Urol.*, 135 (1986) 178.
8 J. P. Witter, S. J. Gatley and E. Balish, *J. Chromatogr.*, 229 (1982) 450.
9 R. D. Rocklin, C. A. Pohl and J. A. Schibler, *J. Chromatogr.*, 411 (1987) 107.
10 W. R. Jones, P. Jandik and M. Swartz, *J. Chromatogr.*, 473 (1989) 171.
11 W. R. Jones and P. Jandik, *Am. Lab.*, June (1990) 51.

Author Index

Vol. 546

journal of chromatography news section

SHORT CONFERENCE REPORT

INTERNATIONAL ION CHROMATOGRAPHY SYMPOSIUM 1990, SAN DIEGO, CA, U.S.A., SEPTEMBER 30–OCTOBER 3, 1990

The International Ion Chromatography Symposium 1990 was held at the Hotel del Coronado in Coronado, CA, U.S.A. Over 250 scientists from 13 countries and 35 states participated in this technical symposium which featured sixty-five podium presentations and twenty posters. Paul R. Haddad, Associate Professor of Chemistry at the University of New South Wales in Australia, served as Program Chairman for the meeting and worked with a Scientific Committee of eleven renowned scientists (Fig. 1) in the field of ion chromatography (IC) to develop a technical program of impressive depth and diversity.

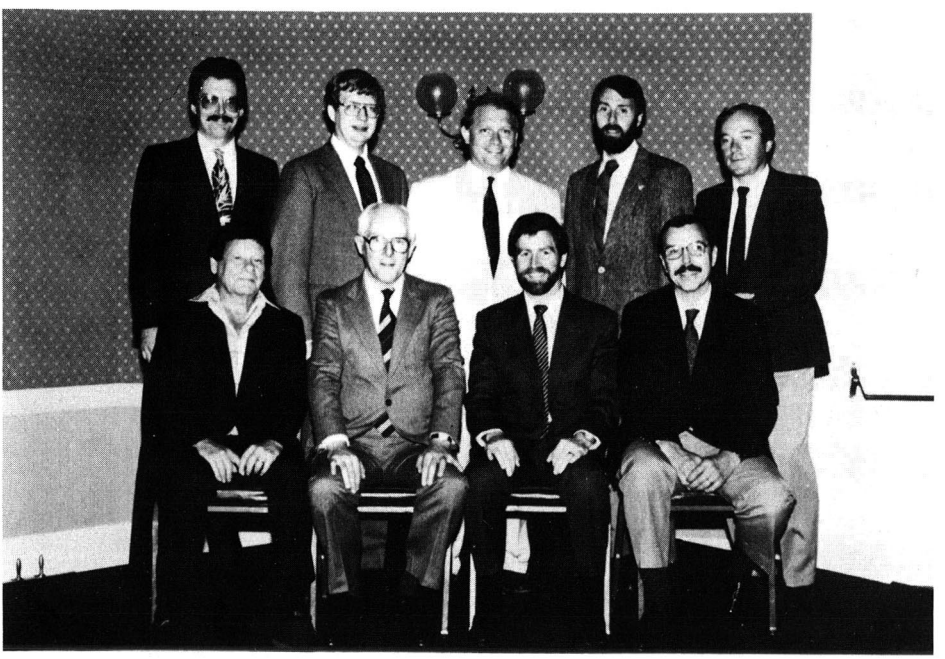

Fig. 1. Scientific committee: front row (left to right), James Fritz, Iowa State University; Hamish Small, consultant; Paul R. Haddad, University of New South Wales; Donald Pietrzyk, University of Iowa; back row (left to right), John Stillian, Dionex Corporation; Doug Gjerde, Sarasep, Inc.; Guenther Bonn, Innsbruck University; Richard Cassidy, University of Saskatchewan and Petr Jandik, Waters Chromatography Division of Millipore Corporation.

Hamish Small, the inventor of suppressed IC while a researcher at Dow Chemical, gave the plenary lecture on "Twenty years of ion chromatography" in which he traced the evolution of IC and gave examples of modern applications and capabilities.

The symposium agenda was organized around nine session topics including: detection, stationary phases and separations, sample handling, applications, ion-exclusion, gradients, post-column reaction detection, general aspects, and inorganic capillary electrophoresis. Each session opened with a review lecture by one of the Scientific Committee. Of particular interest, Donald Pietrzyk, Professor of Chemistry at the University of Iowa, spoke on "Indirect detection in ion chromatography", James Fritz, Distinguished Professor of Chemistry at Iowa State University, presented "Developments in ion-exclusion chromatography", and Richard Cassidy, Professor of Chemistry at the University of Saskatchewan, lectured on "Post-column reaction detection in ion chromatography". The conference was truly international in scope with contributions from scientists from Austria, Mexico, Canada, People's Republic of China, Switzerland, The Netherlands, Germany, Italy, Australia, and the U.S.A.

A highlight of the meeting was the recognition of two scientists for their outstanding contributions in developing the methodology of IC. Award recipients were Petr Jandik, Manager of Ion Analysis R & D at the Waters Chromatography Division of Millipore Corporation, and Christopher A. Pohl, Technical Director of Polymer Chemistry at Dionex Corporation. Jandik presented a keynote lecture on "Optimization of detection sensitivity in the capillary electrophoresis of inorganic ions", and Pohl gave a keynote lecture on "Development of moderate capacity pellicular ion exchange packing materials for ion chromatography" (see Figs. 2 and 3).

The next International Ion Chromatography Symposium will be held in Denver during October 6–9, 1991. John D. Lamb, Associate Professor of Chemistry at Brigham Young University, will serve as Program Chairman. For more information, contact Century International, PO Box 493, Medfield, MA 02052, U.S.A. Tel.: (508) 359-8777; Fax: (508) 359-8778.

Fig. 2. Hamish Small, inventor of IC, plenary lecturer; Christopher Pohl, Dionex Corporation, award recipient; Petr Jandik, Waters Chromatography Division of Millipore Corporation, award recipient; Paul Haddad, University of New South Wales, program chairman.

Fig. 3. Award recipients: Christopher Pohl and Petr Jandik.

ANNOUNCING....

INTERNATIONAL ION CHROMATOGRAPHY SYMPOSIUM 1991

October 6 - 9, 1991
Hyatt Regency Tech Center
Denver, Colorado USA

Program Chairman:

John D. Lamb
Brigham Young University
Provo, Utah USA

Scientific Committee:

Guenther K. Bonn
Innsbruck University
Innsbruck, Austria

Richard M. Cassidy
University of Saskatchewan
Saskatoon, Saskatchewan, Canada

James S. Fritz
Iowa State University
Ames, Iowa USA

Douglas T. Gjerde
Sarasep, Inc.
Santa Clara, California USA

Paul R. Haddad
The University of New South Wales
New South Wales, Australia

Petr Jandik
Waters Chromatography Division
Milford, Massachusetts USA

Donald J. Pietrzyk
University of Iowa
Iowa City, Iowa USA

Gabriella Schmuckler
Technion
Haifa, Israel

Hamish Small
Consultant
Leland, Michigan USA

John Stillian
Dionex Corporation
Sunnyvale, California USA

PLENARY LECTURES:

Ion Chromatography: Quo Vadis Domini?
Purnendu K. "Sandy" Dasgupta
Texas Tech University
Lubbock, Texas

Cold Fusion: What It Is and What It Isn't
Steven E. Jones
Brigham Young University
Provo, Utah

SESSION TOPICS:

- Fundamental Principles and General Aspects of IC
- Separations Using Novel Stationary and Mobile Phases
- Novel Applications
- Sample Handling and Pretreatment
- Industrial Problem-Solving
- Gradient Separations
- Detection and Post-Column Treatment
- Capillary Ion Analysis

For program details and registration information, write or call:

Century International, Inc.
P.O. Box 493
Medfield, MA 02052 USA
508/359-8777 • 508/359-8778 (FAX)

PUBLICATION SCHEDULE FOR 1991

Journal of Chromatography and Journal of Chromatography, Biomedical Applications

MONTH	D 1990–F 1991	M	A	M	J	J	
Journal of Chromatography	Vols. 535–539	540/1 + 2 541/1 + 2 542/1	542/2 543/1	543/2 544/1 + 2 545/1	545/2 546/1 + 2 547/1 + 2	548/1 + 2	The publication schedule for further issues will be published later
Cumulative Indexes, Vols. 501–550							
Bibliography Section		560/1			560/2		
Biomedical Applications	Vols. 562, 563	564/1	564/2 565/1 + 2	566/1 566/2	567/1	567/2	

INFORMATION FOR AUTHORS

(Detailed *Instructions to Authors* were published in Vol. 522, pp. 351–354. A free reprint can be obtained by application to the publisher, Elsevier Science Publishers B.V., P.O. Box 330, 1000 AH Amsterdam, The Netherlands.)

Types of Contributions. The following types of papers are published in the *Journal of Chromatography* and the section on *Biomedical Applications:* Regular research papers (Full-length papers), Review articles and Short Communications. Short Communmications are usually descriptions of short investigations, or they can report minor technical improvements of previously published procedures; they reflect the same quality of research as Full-length papers, but should preferably not exceed six printed pages. For Review articles, see inside front cover under Submission of Papers.

Submission. Every paper must be accompanied by a letter from the senior author, stating that he/she is submitting the paper for publication in the *Journal of Chromatography*.

Manuscripts. Manuscripts should be typed in double spacing on consecutively numbered pages of uniform size. The manuscript should be preceded by a sheet of manuscript paper carrying the title of the paper and the name and full postal address of the person to whom the proofs are to be sent. As a rule, papers should be divided into sections, headed by a caption (*e.g.*, Abstract, Introduction, Experimental, Results, Discussion, etc.). All illustrations, photographs, tables, etc., should be on separate sheets.

Introduction. Every paper must have a concise introduction mentioning what has been done before on the topic described, and stating clearly what is new in the paper now submitted.

Abstract. All articles should have an abstract of 50–100 words which clearly and briefly indicates what is new, different and significant.

Illustrations. The figures should be submitted in a form suitable for reproduction, drawn in Indian ink on drawing or tracing paper. Each illustration should have a legend, all the *legends* being typed (with double spacing) together on a *separate sheet*. If structures are given in the text, the original drawings should be supplied. Coloured illustrations are reproduced at the author's expense, the cost being determined by the number of pages and by the number of colours needed. The written permission of the author and publisher must be obtained for the use of any figure already published. Its source must be indicated in the legend.

References. References should be numbered in the order in which they are cited in the text, and listed in numerical sequence on a separate sheet at the end of the article. Please check a recent issue for the layout of the reference list. Abbreviations for the titles of journals should follow the system used by *Chemical Abstracts*. Articles not yet published should be given as "in press" (journal should be specified), "submitted for publication" (journal should be specified), "in preparation" or "personal communication".

Dispatch. Before sending the manuscript to the Editor please check that the envelope contains four copies of the paper complete with references, legends and figures. One of the sets of figures must be the originals suitable for direct reproduction. Please also ensure that permission to publish has been obtained from your institute.

Proofs. One set of proofs will be sent to the author to be carefully checked for printer's errors. Corrections must be restricted to instances in which the proof is at variance with the manuscript. "Extra corrections" will be inserted at the author's expense.

Reprints. Fifty reprints of Full-length papers and Short Communications will be supplied free of charge. Additional reprints can be ordered by the authors. An order form containing price quotations will be sent to the authors together with the proofs of their article.

Advertisements. Advertisement rates are available from the publisher on request. The Editors of the journal accept no responsibility for the contents of the advertisements.

CHEMOMETRICS AND INTELLIGENT LABORATORY SYSTEMS

An International Journal Sponsored by the Chemometrics Society

which includes **"Laboratory Information Management"**

This international journal publishes articles about new developments on laboratory techniques in chemistry and related disciplines which are characterized by the application of statistical and computer methods. Special attention is given to emerging new technologies and techniques for the building of intelligent laboratory systems, i.e. artificial intelligence and robotics. The journal aims to be interdisciplinary; more particularly it intends to bridge the gap between chemists and scientists from related fields, statisticians and designers of laboratory systems. In order to promote understanding between people from different fields the journal features a special section containing tutorial articles.

The journal deals with the following topics: Chemometrics; Computerized acquisition, processing and evaluation of data: Robotics; Developments in statistical theory and mathematics with application to chemistry; Intelligent laboratory systems; Laboratory information management; Application (case studies) of statistical and computational methods; New software; Imaging techniques and graphical software applied in chemistry. The research papers and tutorials are complemented by the **Monitor Section** which contains news, a calendar of forthcoming meetings, reports on meetings, software reviews, book reviews, news on societies and announcements of courses and meetings. This section also contains the "Chemometrics Newsletter", official bulletin of the Chemometrics Society.

Abstracted/Indexed in:

Analytical Abstracts, ASCA, BioSciences Information Service, Cambridge Scientific Abstracts, Chemical Abstracts, Chromatography Abstracts, Current Contents, Current Index to Statistics, Excerpta Medica, INSPEC, SCISEARCH

Subscription Information:

1991: Vols 10-13 (12 issues) US$ 692.00 / Dfl. 1232.00 including postage

ISSN 0169-7439

A free sample copy of the journal is available on request.

Elsevier Science Publishers

P.O. Box 211, 1000 AE Amsterdam, The Netherlands

P.O. Box 882, Madison Square Station, New York, NY 10159, USA